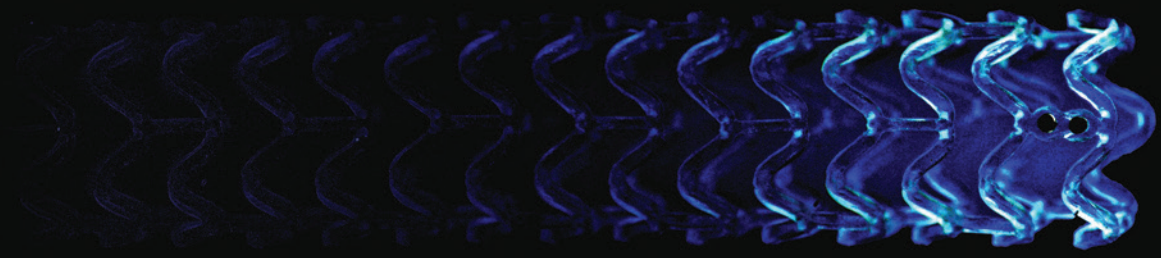

Treatment of Coronary Atherosclerotic Lesions with Bioresorbable Vascular Scaffolds

From early experience to complex scenarios

Roberto Diletti

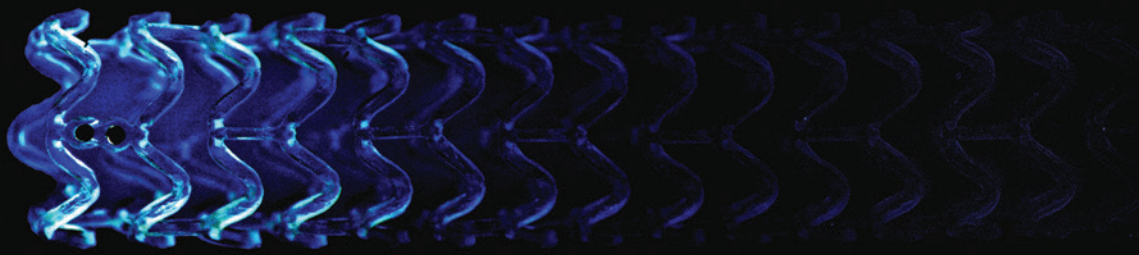

Treatment of Coronary Atherosclerotic Lesions with Bioresorbable Vascular Scaffolds

From early experience to complex scenarios

Roberto Diletti

Printed by: Ridderprint BV, Ridderkerk, the Netherlands
Lay-out by: Ridderprint BV, Ridderkerk, the Netherlands
Cover design by: Sara Manna, Jurgen M.R. Ligthart, Rakesh Ramdhan and Roberto Diletti

ISBN 978-94-6299-341-9

Treatment of Coronary Atherosclerotic Lesions with Bioresorbable Vascular Scaffolds

From early experience to complex scenarios

Behandeling van Coronaire Atherosclerotische Laesies met Bioresorbeerbare Vasculaire Scaffolds

Van de eerste ervaringen tot complexe scenario's

Proefschrift

ter verkrijging van de graad van doctor aan de
Erasmus Universiteit Rotterdam
op gezag van de
rector magnificus

Prof.dr. H.A.P. Pols

en volgens besluit van het College voor Promoties.

De openbare verdediging zal plaatsvinden op
woensdag 25 mei om 9:30 uur.

Door

Roberto Diletti

Geboren te Rieti Italië

Erasmus University Rotterdam

Erasmus

Promotiecommissie

Promotoren:	**Patrick W. Serruys**
	Felix Zijlstra
Overige leden:	**Robert Jan van Geuns**
	Eric Boersma
	Manel Sabatè
Co-promotor:	**Nicolas M. Van Mieghem**

TABLE OF CONTENTS

Chapter 1

Introduction

INTRODUCTION

The field of interventional cardiology was characterized during the last decades by a continuous improvement in terms of materials, techniques and ultimately clinical outcomes. The initial use of bare metal stents enhanced the procedural success rate compared with simple balloon angioplasty[1] and the subsequent introduction of drug-eluting coronary stents (DES) was associated with a remarkable inhibition of neointimal growth, translating into a reduction in in-stent restenosis, lowering the need for repeated revascularizations [2,3]

Second generation DES further improved the clinical results and they are currently considered extremely well performing devices and the gold standard for percutaneous coronary artery interventions.[4-6]

However, metallic stent placement is not devoid of important long-term limitations. The metallic implant results in a permanent caging of the vessel, preventing late lumen enlargement, jailing side branches, precluding non-invasive imaging and further surgical revascularization of stented segments.[7]

Furthermore, beside the beneficial effect of neointimal inhibition, the antiproliferative drug elution could interfere with the vascular healing processes thus providing the background for delayed strut coverage and persistent or acquired malapposition, all possibly related to late and very late stent thrombosis.[8,9]

Given this background bioresorbable vascular scaffolds have been introduced in the attempt to overcome the above-mentioned limitations of the current generation metallic DES.

In addition to the theoretical advantages, of future surgical revascularization and a potential reduction of very late thrombotic events,[7] the implantation of the Absorb BVS has been demonstrated to allow the non-invasive imaging follow-up of the treated arteries [10,11] and the restoration of coronary vasomotion, observed to return already after 1 year post-implantation.

The vasomotor activity plays an important role in the regulation of coronary blood flow, ensuring the maintenance of an appropriate coronary flow pressure, while an impaired vasomotion could be associated with an increased risk of future cardiovascular events. [12-15] Moreover scaffold placement has been associated with the formation of a neointimal layer that may potentially represent a *de novo* circumferential plaque thick cap, with the potential function of plaque stabilization, after scaffold bioresorption. [16]

From a physiological perspective, complete scaffold bioresorption exposes the vessel wall to the cyclical strain of blood pulsatility. Previous studies proposed mechanical stimuli induced by a pulsatile blood flow as a factor increasing the release of nitric oxide (NO) and

prostacyclin [17] and associated with a reduction of monocyte adhesion, thus providing a fundamental atheroprotective effect.[18-21] Biomechanical stimuli also modulate endothelial cell morphology, proliferation, apoptosis, [22,23] elongation and realignment, [24] extracellular matrix production[25] and inflammatory signals.[26] Pulsatile flow and its mechanical action on vessel wall is associated with a down regulation of NADPH oxidase activity, present in the endothelium, vascular smooth muscle cells, fibroblasts, and monocytes [27,28] with a consequent reduction in reactive oxygen species formation. (29,30 Previous reports have demonstrated that reactive oxygen species, such as superoxide and hydrogen peroxide inactivates nitric oxide and provokes the formation of oxidants that induces both low-density lipoprotein (LDL) oxidation and expression of monocyte chemo-attractant proteins on endothelial cells with subsequent monocyte binding and trans-endothelial migration, that are both fundamental processes in atherogenesis. [31-34]
The restoration of the beneficial cyclical strain, [15,35] and the consequent reduction in reactive oxygen species formation may therefore have an impact on both endothelium-dependent vasodilation and atherogenesis.
In the new scenario of a coronary vessel free of metallic caging, the concomitant scaffold drug elution at early stages, [36] and medical therapy in the early and late phase [37-39] may both play a key additional role to facilitate phenomena such as plaque regression, expansive remodeling and late luminal enlargement.
An analysis of vasoreactivity in scaffolded segments at 12- and 24- month follow-up with both endothelial-depend and -independ agents, showed that endothelial dysfunction in those regions is correlated to the amount of plaque burden and necrotic core content. [40] These data support the hypothesis that an improvement of plaque composition and plaque burden could have a beneficial impact also on post scaffolding vasomotion resembling the behaviour of native non-stented segments.
Given this background the concept of bioresorbable device for treatment of coronary atherosclerotic lesions has been rapidly embraced by the scientific community and an initial clinical experience in relatively simple lesions and stable patients showed promising results in terms of restoration of vasomotion already at 1-year post implantation[15] and long-term clinical outcomes[41].
However, at the current state of the art, a profound knowledge of the performance of the bioresorbable technology in real world complex lesions and patents is still lacking. In addition, the higher complexity if the implantation technique and the observation of a slightly higher rate of thrombotic events tempered the initial enthusiasm related to this novel paradigm for treatment of coronary atherosclerosis.

The present thesis represents a journey through our initial experience with the bioresorbable scaffold up to the implementation of this technology in complex scenarios such as unstable patients with acute thrombotic lesions, calcified plaques, coronary bifurcations, and even complex chronic total occlusions thus resembling as much as possible the entire spectrum of our daily clinical practice.

REFERENCES

1. Serruys PW, de Jaegere P, Kiemeneij F et al. A comparison of balloon-expandable-stent implantation with balloon angioplasty in patients with coronary artery disease. Benestent Study Group. The New England journal of medicine 1994;331:489-95.
2. Sousa JE, Costa MA, Abizaid A et al. Lack of neointimal proliferation after implantation of sirolimus-coated stents in human coronary arteries: a quantitative coronary angiography and three-dimensional intravascular ultrasound study. Circulation 2001;103:192-5.
3. Sousa JE, Costa MA, Abizaid AC et al. Sustained suppression of neointimal proliferation by sirolimus-eluting stents: one-year angiographic and intravascular ultrasound follow-up. Circulation 2001;104:2007-11.
4. Stone GW, Rizvi A, Newman W et al. Everolimus-eluting versus paclitaxel-eluting stents in coronary artery disease. The New England journal of medicine 2010;362:1663-74.
5. Serruys PW, Silber S, Garg S et al. Comparison of zotarolimus-eluting and everolimus-eluting coronary stents. The New England journal of medicine 2010;363:136-46.
6. Sabate M, Brugaletta S, Cequier A et al. Clinical outcomes in patients with ST-segment elevation myocardial infarction treated with everolimus-eluting stents versus bare-metal stents (EXAMINATION): 5-year results of a randomised trial. Lancet 2016;387:357-66.
7. Serruys PW, Garcia-Garcia HM, Onuma Y. From metallic cages to transient bioresorbable scaffolds: change in paradigm of coronary revascularization in the upcoming decade? European heart journal 2012;33:16-25b.
8. Finn AV, Joner M, Nakazawa G et al. Pathological correlates of late drug-eluting stent thrombosis: strut coverage as a marker of endothelialization. Circulation 2007;115:2435-41.
9. Joner M, Finn AV, Farb A et al. Pathology of drug-eluting stents in humans: delayed healing and late thrombotic risk. Journal of the American College of Cardiology 2006;48:193-202.
10. Bruining N, Tanimoto S, Otsuka M et al. Quantitative multi-modality imaging analysis of a bioabsorbable poly-L-lactic acid stent design in the acute phase: a comparison between 2- and 3D-QCA, QCU and QMSCT-CA. EuroIntervention : journal of EuroPCR in collaboration with the Working Group on Interventional Cardiology of the European Society of Cardiology 2008;4:285-91.
11. Serruys PW, Ormiston JA, Onuma Y et al. A bioabsorbable everolimus-eluting coronary stent system (ABSORB): 2-year outcomes and results from multiple imaging methods. Lancet 2009;373:897-910.
12. Kitta Y, Obata JE, Nakamura T et al. Persistent impairment of endothelial vasomotor function has a negative impact on outcome in patients with coronary artery disease. Journal of the American College of Cardiology 2009;53:323-30.
13. Vita JA, Treasure CB, Nabel EG et al. Coronary vasomotor response to acetylcholine relates to risk factors for coronary artery disease. Circulation 1990;81:491-7.
14. von Mering GO, Arant CB, Wessel TR et al. Abnormal coronary vasomotion as a prognostic indicator of cardiovascular events in women: results from the National Heart, Lung, and Blood Institute-Sponsored Women's Ischemia Syndrome Evaluation (WISE). Circulation 2004;109:722-5.
15. Serruys PW, Onuma Y, Dudek D et al. Evaluation of the second generation of a bioresorbable everolimus-eluting vascular scaffold for the treatment of de novo coronary artery stenosis: 12-month clinical and imaging outcomes. Journal of the American College of Cardiology 2011;58:1578-88.
16. Brugaletta S, Radu MD, Garcia-Garcia HM et al. Circumferential evaluation of the neointima by optical coherence tomography after ABSORB bioresorbable vascular scaffold implantation: Can the scaffold cap the plaque? Atherosclerosis 2011.

17. Frangos JA, Huang TY, Clark CB. Steady shear and step changes in shear stimulate endothelium via independent mechanisms--superposition of transient and sustained nitric oxide production. Biochemical and biophysical research communications 1996;224:660-5.
18. Hsiai TK, Cho SK, Reddy S et al. Pulsatile flow regulates monocyte adhesion to oxidized lipid-induced endothelial cells. Arteriosclerosis, thrombosis, and vascular biology 2001;21:1770-6.
19. Ross R. Atherosclerosis is an inflammatory disease. American heart journal 1999;138:S419-20.
20. Gerrity RG. The role of the monocyte in atherogenesis: II. Migration of foam cells from atherosclerotic lesions. The American journal of pathology 1981;103:191-200.
21. Gerrity RG. The role of the monocyte in atherogenesis: I. Transition of blood-borne monocytes into foam cells in fatty lesions. The American journal of pathology 1981;103:181-90.
22. Kaiser D, Freyberg MA, Friedl P. Lack of hemodynamic forces triggers apoptosis in vascular endothelial cells. Biochemical and biophysical research communications 1997;231:586-90.
23. Karlon WJ, Hsu PP, Li S, Chien S, McCulloch AD, Omens JH. Measurement of orientation and distribution of cellular alignment and cytoskeletal organization. Annals of biomedical engineering 1999;27:712-20.
24. Hsiai TK, Cho SK, Honda HM et al. Endothelial cell dynamics under pulsating flows: significance of high versus low shear stress slew rates (d(tau)/dt). Annals of biomedical engineering 2002;30:646-56.
25. Galis ZS, Sukhova GK, Lark MW, Libby P. Increased expression of matrix metalloproteinases and matrix degrading activity in vulnerable regions of human atherosclerotic plaques. The Journal of clinical investigation 1994;94:2493-503.
26. Dirksen MT, van der Wal AC, van den Berg FM, van der Loos CM, Becker AE. Distribution of inflammatory cells in atherosclerotic plaques relates to the direction of flow. Circulation 1998;98:2000-3.
27. Hsieh HJ, Cheng CC, Wu ST, Chiu JJ, Wung BS, Wang DL. Increase of reactive oxygen species (ROS) in endothelial cells by shear flow and involvement of ROS in shear-induced c-fos expression. Journal of cellular physiology 1998;175:156-62.
28. Mollnau H, Wendt M, Szocs K et al. Effects of angiotensin II infusion on the expression and function of NAD(P)H oxidase and components of nitric oxide/cGMP signaling. Circulation research 2002;90:E58-65.
29. Irani K. Oxidant signaling in vascular cell growth, death, and survival : a review of the roles of reactive oxygen species in smooth muscle and endothelial cell mitogenic and apoptotic signaling. Circulation research 2000;87:179-83.
30. Hwang J, Ing MH, Salazar A et al. Pulsatile versus oscillatory shear stress regulates NADPH oxidase subunit expression: implication for native LDL oxidation. Circulation research 2003;93:1225-32.
31. Cushing SD, Berliner JA, Valente AJ et al. Minimally modified low density lipoprotein induces monocyte chemotactic protein 1 in human endothelial cells and smooth muscle cells. Proceedings of the National Academy of Sciences of the United States of America 1990;87:5134-8.
32. Berliner JA, Territo MC, Sevanian A et al. Minimally modified low density lipoprotein stimulates monocyte endothelial interactions. The Journal of clinical investigation 1990;85:1260-6.
33. Berliner JA, Navab M, Fogelman AM et al. Atherosclerosis: basic mechanisms. Oxidation, inflammation, and genetics. Circulation 1995;91:2488-96.
34. Sevanian A, Hwang J, Hodis H, Cazzolato G, Avogaro P, Bittolo-Bon G. Contribution of an in vivo oxidized LDL to LDL oxidation and its association with dense LDL subpopulations. Arteriosclerosis, thrombosis, and vascular biology 1996;16:784-93.
35. Resnick N, Yahav H, Shay-Salit A et al. Fluid shear stress and the vascular endothelium: for better and for worse. Progress in biophysics and molecular biology 2003;81:177-99.
36. Mueller MA, Beutner F, Teupser D, Ceglarek U, Thiery J. Prevention of atherosclerosis by the mTOR inhibitor everolimus in LDLR-/- mice despite severe hypercholesterolemia. Atherosclerosis 2008;198:39-48.

37. Serruys PW, Garcia-Garcia HM, Buszman P et al. Effects of the direct lipoprotein-associated phospholipase A(2) inhibitor darapladib on human coronary atherosclerotic plaque. Circulation 2008;118:1172-82.
38. Khera AV, Cuchel M, de la Llera-Moya M et al. Cholesterol efflux capacity, high-density lipoprotein function, and atherosclerosis. The New England journal of medicine 2011;364:127-35.
39. Jensen LO, Thayssen P, Pedersen KE, Stender S, Haghfelt T. Regression of coronary atherosclerosis by simvastatin: a serial intravascular ultrasound study. Circulation 2004;110:265-70.
40. Brugaletta S, Heo JH, Garcia-Garcia HM et al. Endothelial-dependent vasomotion in a coronary segment treated by ABSORB everolimus-eluting bioresorbable vascular scaffold system is related to plaque composition at the time of bioresorption of the polymer: indirect finding of vascular reparative therapy? European heart journal 2012;33:1325-33.
41. Serruys PW, Ormiston J, van Geuns RJ et al. A Polylactide Bioresorbable Scaffold Eluting Everolimus for Treatment of Coronary Stenosis: 5-Year Follow-Up. Journal of the American College of Cardiology 2016;67:766-76.

PART I

ASSESSMENT OF CORONARY ATHEROSCLEROSIS WITH INTRAVASCULAR IMAGING

Chapter 2

Assessment of Coronary Atherosclerosis Progression and Regression at Bifurcations Using Combined IVUS and OCT

Roberto Diletti, MD; Hector M. Garcia-Garcia, MD, PHD; Josep Gomez-Lara, MD; Salvatore Brugaletta, MD; Joanna J. Wykrzykowska, MD; Nienke van Ditzhuijzen, MSC; Robert Jan van Geuns, MD, PHD; Evelyn Regar, MD, PHD; Giuseppe Ambrosio, MD, PHD; Patrick W. Serruys, MD, PHD

JACC Cardiovasc Imaging. 2011 Jul;4(7):774-80.

ABSTRACT

Objectives The aim of this study was to evaluate the progression of atherosclerotic coronary plaques at bifurcations, using combined intravascular ultrasound–virtual histology (IVUS-VH) and optical coherence tomography (OCT).

Background Pathological findings reveal that atherosclerotic plaques characterized by the presence of large necrotic cores (NCs) with fibrous cap thicknesses < 65 μ.m are more prone to rupture. Accuracy in the detection of high-risk plaques could be improved by the combined use of IVUS-VH and OCT.

Methods IVUS-VH and OCT are 2 imaging modalities with different lateral resolutions and different depths of penetration. To provide a precise matching of the images, bifurcations were used as landmarks. IVUS-VH and OCT were performed in 56 bifurcations from 24 patients at baseline and at 6-month follow-up. All patients were treated with standard medical therapy. Bifurcations were studied at the proximal, in-bifurcation, and distal regions. Plaques were classified according to their composition as assessed by IVUS-VH and fibrous cap thickness as quantified by OCT.

Results At baseline, 27 NC-rich plaques were found. At 6-month follow-up, 22 (81%) did not show any significant change. Four new NC-rich lesions developed. At both time points, percent NC was higher and the fibrous cap was thinner at the proximal bifurcation rim compared with the distal. There were no significant changes in percent NC and fibrous cap thickness in the 3 bifurcation regions between baseline and follow-up examinations. No major cardiovascular events due to bifurcation lesion progression were observed.

Conclusions The combined use of IVUS-VH and OCT is a reliable tool to serially assess plaque progression and regression, and in the present study it was demonstrated to be safe and feasible. At 6-month follow-up, in this post–percutaneous coronary intervention patient population, most high-risk plaques remained unchanged, retaining their imaging classifications, nevertheless appearing to have remained clinically silent.

INTRODUCTION

Plaque rupture and subsequent activation of the clotting cascade resulting in sudden intraluminal thrombosis are thought to be the most frequent cause of acute coronary syndromes [1,2]. In pathology, precursor lesions, known as thin-cap fibroatheromas (TCFA), are characterized by a large pool of necrotic core (NC) covered by a thin fibrous cap <65 µ.m [3]. The resolution of current intravascular ultrasound (IVUS) systems (100 to 200 µ.m) constitutes an important limitation of this technique for the measurement of fibrous cap thickness [4]. Optical coherence tomography (OCT), in contrast, has higher resolution (10 to 20 µ.m) but low signal penetration. This can be a source of inaccurate assessment of NC size, especially in plaques with large plaque bur- den and positive remodeling, which is a characteristic of TCFA lesions [5]. Therefore, combining the 2 imaging techniques might provide a more accurate method to investigate TCFAs [6,7]. There are only a few published reports of the combined use of IVUS and OCT in vivo [6,7] and none describing the longitudinal assessment of plaque progression and regression at bifurcations. The aim of the present study was therefore to evaluate serial changes in plaque type and composition at bifurcations of the main coronary arteries using combined IVUS–virtual histology (VH) and OCT.

METHODS

Study population

Fifty-six bifurcations were selected from 24 patients presenting with stable angina, unstable angina, or silent ischemia. All patients were treated at the Thoraxcenter, Erasmus Medical Center (Rotterdam, the Netherlands), and enrolled in 2 different stent studies (ABSORB cohort B and SECRITT). Both studies used IVUS-VH and OCT as part of their protocols. The bifurcations selected for this study were more than 5 mm away from the stented region and had side branch orifice diameters >1.5 mm as measured by OCT. Only bifurcations imaged with both modalities and for which imaging was of high quality were considered. All bifurcations fitting this inclusion criteria were included. All patients re- ceived standard medical therapy, including aspirin, clopidogrel, and statins, for at least 6 months.

IVUS-VH acquisition and analysis

IVUS acquisitions were performed using an Eagle Eye catheter (Volcano Corporation, Rancho Cordova, California) with automatic continuous pullback at a speed of 0.5 mm/s. IVUS grayscale and IVUS-VH analyses were performed offline using dedicated software [8].

OCT acquisition

The OCT M3 (Time Domain- OCT) and C7 (Fourier Domain-OCT) systems were used in this study (LightLab Imaging, Inc., Westford, Massachusetts). For each patient, the same system was used for baseline and follow-up examinations. Measurements were performed offline by 2 independent observers using LightLab imaging software.

OCT analysis

Fibrous cap thickness measurement was performed in each bifurcation frame at the thinnest part of the fibrous cap overlying the pool of NC. The reproducibility of this variable has been previously reported by our group [9].

Bifurcation matching analysis

IVUS-VH and OCT are 2 imaging modalities with different lateral resolutions and different depths of penetration. To provide a precise matching of the images, a strict selection of frames was followed using a method previously described [7]. Only the main branches were analyzed, and for each bifurcation the following frames were considered: 1) the proximal rim of the side branch ostium; 2) the in-bifurcation site (the frame with the largest ostial diameter of the side branch); and 3) the distal rim of the side branch ostium (Fig. 1).

Plaque type classification

Plaques were classified ac- cording to the following previously described [7] hierarchical classification: 1) those with high percents of fibrotic tissue (adaptive intimal thickening, pathological intimal thickening, fibrotic plaque, and fibrocalcific plaque); and 2) NC-rich plaques (those with more than 10% confluent NC) (fibroatheroma and calcified fibroatheroma); if covered by fibrous caps thinner than 65 μ.m, they constitute TCFA and calcified TCFA. These plaque types are reported per location within the bifurcation (at the distal, in-bifurcation, and proximal frames) and per bifurcation, defined as the worst plaque type within the bifurcation detected among the 3 frames considered. In addition, we introduce an IVUS-VH and OCT– derived plaque risk index, defined as the ratio between the sum of NC-rich plaques and the sum of non-NC-rich plaques in a given bifurcation region. This index was calculated for each bifurcation region at both baseline and follow-up.

Statistical analysis

Categorical variables are presented as frequencies and percents. Continuous variables are presented as medians and interquartile ranges and were compared using the Wilcoxon signed rank test. A p value <0.05 was considered statistically significant. The bifurcation

was the unit of analysis, without correction for correlated observations in the same subjects. Statistical analyses were performed using SPSS version 16.0 for Windows (SPSS, Inc., Chicago, Illinois).

RESULTS

Patients' baseline clinical characteristics are reported in Table 1. The median age was 67 years, and most patients were men (79%). At follow-up, all patients were treated with statins: 6 received rosuvastatin (4 received 10 mg and 2 received 20 mg), 9 patients received simvastatin (7 received 20 mg and 2 received 40 mg), and 9 patients received atorvastatin (6 received 40 mg, 2 received 20 mg, and 1 received 10 mg).

Table 1. Baseline Clinical Characteristics (n = 24).

	n=24
Age (yrs)	67 (58–73)
Men	19 (79)
Presentation	
Stable angina	16 (67)
Unstable angina	5 (20)
Silent ischemia	3 (13)
Hypertension	18 (75)
Hypercholesterolemia	17 (71)
Diabetes	4 (17)
Smoking	5 (20)
Family history of CAD	13 (54)
Previous AMI	9 (37)
Previous PCI	10 (42)
Vessel	
LAD	11 (46)
LCX	5 (20)
RCA	8 (33)
Therapy	
Antiplatelet therapy	24 (100)
Beta-blockers	15 (62)
ACE inhibitors/ARBs	13 (54)
Statins	16 (67)
Insulin	1 (4)

Values are median (interquartile range) or n (%). ACE = angiotensin-converting enzyme; AMI = acute myocardial infarction; ARB = angiotensin II receptor blocker; CAD = coronary artery disease; LAD = left anterior descending coronary artery; LCX = left circumflex coronary artery; PCI = percutaneous coronary intervention; RCA = right coronary artery.

Table 2. Geometrical and Compositional Data in Each Region of the Bifurcation at Baseline and Follow-Up.

Variable	Baseline	Follow-Up	p Value
Distal	14.01 (10.75–18.06)	13.52 (10.32–16.49)	0.051
In-bifurcation	15.62 (12.47–20.14)	14.75 (12.11–18.77)	0.543
Proximal	15.84 (12.86–20.85)	14.89 (12.23–20.83)	0.262
Luminal CSA (mm^2)			
Distal	7.23 (6.19–9.27)	7.20 (6.19–9.27)	0.012
In-bifurcation	8.46 (7.25–11.05)	7.93 (7.04–10.68)	0.184
Proximal	7.62 (6.80–9.85)	7.27 (6.00–9.75)	0.005
Plaque CSA (mm^2)			
Distal	5.68 (3.74–8.50)	6.26 (4.07–8.30)	0.231
In-bifurcation	5.79 (3.93–8.23)	6.07 (4.36–8.96)	0.144
Proximal	6.84 (5.11–10.72)	7.54 (6.00–10.86)	0.046
Plaque burden (%)			
Distal	42.74 (33.30–57.12)	49.13 (36.61–57.87)	0.004
In-bifurcation	39.38 (30.30–48.86)	42.76 (34.37–48.42)	0.027
Proximal	48.67 (39.32–58.69)	51.50 (46.39–59.54)	0.008
Minimal luminal diameter (mm)			
Distal	2.80 (2.44–3.24)	2.65 (2.29–3.18)	0.007
In-bifurcation	2.87 (2.56–3.21)	2.77 (2.48–3.29)	0.033
Proximal	2.90 (2.60–3.28)	2.78 (2.47–3.16)	0.039
Minimal vessel diameter (mm)			
Distal	3.95 (3.48–4.54)	3.88 (3.41–4.31)	0.075
In-bifurcation	4.06 (3.77–4.59)	4.06 (3.61–4.45)	0.489
Proximal	4.22 (3.81–4.69)	4.13 (3.71–4.72)	0.194
Fibrous CSA (mm^2)			
Distal	1.33 (0.13–3.23)	1.44 (0.45–2.72)	0.423
In-bifurcation	1.53 (0.52–2.83)	1.48 (0.94–2.96)	0.368
Proximal	1.65 (1.20–4.20)	2.57 (1.31–3.49)	0.329
Fibrous tissue (%)			
Distal	60.36 (40.41–70.90)	61.03 (50.83–68.17)	0.922
In-bifurcation	62.63 (50.21–69.14)	59.68 (52.75–66.83)	0.094
Proximal	58.85 (51.09–69.24)	58.18 (50.65–64.23)	0.150
Fibrofatty CSA (mm^2)			
Distal	0.18 (0.02–0.75)	0.30 (0.03–0.87)	0.498
In-bifurcation	0.26 (0.06–0.68)	0.29 (0.07–0.72)	0.739
Proximal	0.50 (0.18–1.09)	0.45 (0.23–1.16)	0.870
Fibrofatty tissue (%)			
Distal	10.54 (1.56–18.02)	10.47 (6.07–18.88)	0.299
In-bifurcation	10.99 (5.24–16.78)	10.55 (3.79–18.84)	0.504
Proximal	13.12 (6.24–23.88)	10.46 (5.53–18.48)	0.339
NC CSA (mm^2)			
Distal	0.19 (0.02–0.62)	0.39 (0.06–0.82)	0.374
In-bifurcation	0.38 (0.05–0.70)	0.50 (0.12–0.88)	0.089
Proximal	0.44 (0.44–0.13)	0.62 (0.28–1.28)	0.265

Table 2. Continued.

Variable	Baseline	Follow-Up	p Value
NC (%)			
Distal	9.90 (1.79–18.13)	13.95 (7.42–21.94)	0.261
In-bifurcation	12.31 (6.52–18.15)	16.10 (8.81–21.65)	0.199
Proximal	12.44 (5.92–23.15)	16.24 (8.65–20.43)	0.280
Dense calcium CSA (mm^2)			
Distal	0.08 (0.00–0.42)	0.20 (0.00–0.40)	0.021
In-bifurcation	0.10 (0.01–0.48)	0.20 (0.01–0.40)	0.005
Proximal	0.17 (0.02–0.53)	0.30 (0.01–0.70)	0.002
Dense calcium (%)			
Distal	3.29 (0.00–9.52)	4.87 (0.43–15.71)	0.031
In-bifurcation	6.70 (0.46–13.85)	7.62 (1.74–13.30)	0.124
Proximal	3.74 (0.92–9.86)	6.60 (1.89–14.55)	0.003

Values are median (interquartile range). CSA = cross-sectional area; NC = necrotic core.

Results from the geometrical and compositional analysis at the distal rim, in-bifurcation, and proximal rim of the side branch ostium are reported in Table 2. At follow-up, the median vessel cross-sectional area remained unchanged at the distal, in- bifurcation, and proximal frames, while median luminal cross-sectional area decreased slightly, resulting in an increase in plaque burden (Table 2). Fibrous and fibrofatty tissue did not change between baseline and follow-up. Median NC cross-sectional area and percent NC nonsignificantly increased in each region. Dense calcium cross- sectional area significantly increased at the distal, in-bifurcation, and proximal segment (Table 2). In NC-rich plaques (NC > 10% [fibroatheroma, calcified fibroatheroma, TCFA, and calcified TCFA]), the percent of NC nonsignificantly decreased over time at the distal rim (21.65% vs. 18.54%, p = 0.193), in-bifurcation (22.38% vs. 20.25%, p = 0.573), and proximal rim (23.15% vs. 18.06%, p = 0.317).

Distribution of IVUS-VH and OCT– derived plaque types at the 3 bifurcation regions

The distribution of NC-rich and NC-poor plaques is presented in Table 3. There was a gradient of disease from the proximal to the distal rim. NC-rich plaques were more frequently located at the proximal rim. Non– NC-rich plaques showed an inverse gradient. In addition, the highest value of the IVUS-VH and OCT– derived plaque risk index was found in the proximal rim of the bifurcations at both baseline and follow-up. From baseline to follow-up, the index increased in each region, implying that the number of NC regions relative to non-NC regions also increased (Table 3).

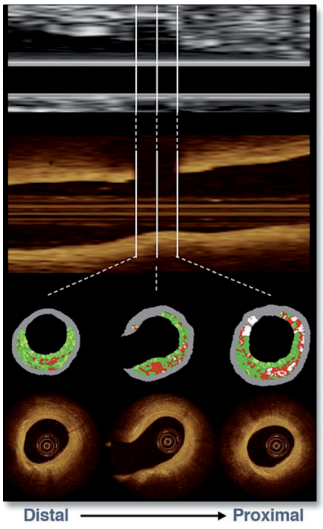

Figure 1. Frame Selection at Bifurcations.
A strict selection of the analyzed cross-sections was followed to provide a correct match between the 2 imaging modalities and between baseline and follow-up. Plaques were analyzed only in the main coronary arteries at the proximal rim of the ostium of the side branch (the first frame proximal to the takeoff of the side branch), at the in-bifurcation site (the frame with the larger ostial diameter of the side branch), and at the distal rim of the ostium of the side branch (the first frame distal to the takeoff of the side branch).

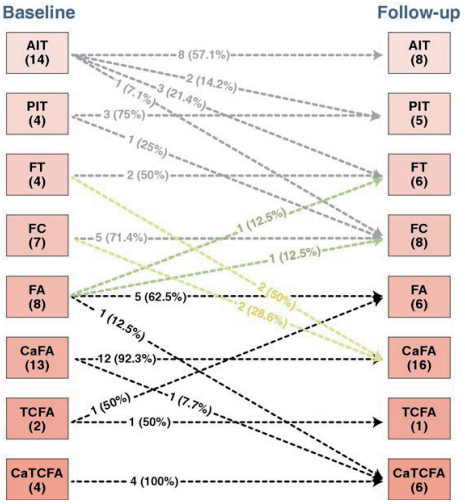

Figure 2. Changes in Bifurcation Plaque Type.
Changes in bifurcation plaque type at 6-month follow-up. For each plaque type, the percent of changes is reported. AIT = adaptive intimal thickening; CaFA = calcified fibroatheroma; CaTCFA = calcified thin-cap fibroatheroma; FA = fibroatheroma; FC = fibrocalcific plaque; FT = fibrotic plaque; PIT = pathological intimal thickening; TCFA = thin-cap fibroatheroma.

Table 3. Plaque Type at Distal Rim, In-Bifurcation, and Proximal Rim at Baseline and Follow-Up and IVUS-VH and OCT–Derived Plaque Risk Index.

	Non–NC-Rich Plaques				NC-Rich Plaques				
Segment	AIT	PIT	FT	FC	FA	CaFA	TCFA	CaTCFA	Plaque Risk Index*
	23 (41)	4 (7.1)	9 (16.1)	3 (5.4)	6 (10.7)	10 (17.9)	0 (0)	1 (1.8)	17/39 = 0.43
In-bifurcation BL	17 (30.4)	4 (7.1)	9 (16.1)	7 (12.5)	7 (12.5)	10 (17.9)	0 (0)	2 (3.6)	19/37 = 0.51
In-bifurcation FU	12 (21.4)	6 (10.7)	8 (14.3)	8 (14.3)	9 (16.1)	10 (17.9)	1 (1.8)	2 (3.6)	22/34 = 0.65
Proximal rim BL	14 (25.0)	5 (8.9)	7 (12.5)	6 (10.7)	6 (10.7)	12 (21.4)	2 (3.6)	4 (7.1)	24/32 = 0.75
Proximal rim FU	8 (14.3)	7 (12.5)	9 (16.1)	5 (8.9)	6 (10.7)	14 (25.0)	1 (1.8)	6 (10.7)	27/29 = 0.93

Values are n (%). *Sum of NC nrich/non-NC-rich plaques. AIT = adaptive intimal thickening; BL = baseline; CaFA = calcified fibroatheroma; CaTCFA = calcified thin-cap fibroatheroma; FA = fibroatheroma; FC = fibrocalcific plaque; FT = fibrotic plaque; FU = follow-up; IVUS = intravascular ultrasound; NC = necrotic core; OCT = optical coherence tomography; PIT = pathological intimal thickening; TCFA = thin-cap fibroatheroma; VH = virtual histology.

Bifurcation plaque types

At baseline, 27 NC-rich plaques were found, of which 6 were classified as thin-cap lesions (TCFA and calcified TCFA). Two fibroatheroma plaques became fibrotic and fibrocalcific (regressed), and 1 TCFA became a fibroatheroma (regressed). Two fibroatheromas became TCFAs (progressed), and 22 (81%) did not change. Four new NC-rich lesions developed from fibrotic and fibrocalcific plaques. Most (83%) thin-cap lesions did not change at 6-month follow-up (Fig. 2).

Fibrous cap thickness, distribution, and changes over time

Fibrous cap thickness significantly decreased from the distal to the proximal region at both baseline and follow-up (Fig. 3). However, no changes in cap thickness were observed from baseline to follow-up within each of the 3 regions (Table 4, Fig. 4). The same held for frames with thin-cap lesions, for which no changes in cap thickness were observed over time (Table 4).

Table 4. Minimal Fibrous Cap Thickness at Distal, In-Bifurcation, and Proximal Segments in All NC-Rich Plaques.

NC-Rich Plaques	Segment	Baseline (m)	Follow-Up (m)	P Value
Non–thin-cap lesions	Distal	100 (80–130)	90 (70–110)	0.206
	In-bifurcation	80 (70–100)	80 (60–100)	0.670
	Proximal	70 (50–90)	70 (60–100)	0.065
Thin-cap lesions	Distal	50 (40–50)	70 (40–90)	0.317
	In-bifurcation	50 (40–60)	50 (40–50)	0.564
	Proximal	50 (40–60)	50 (50–60)	0.084

Values are median (interquartile range). NC = necrotic core.

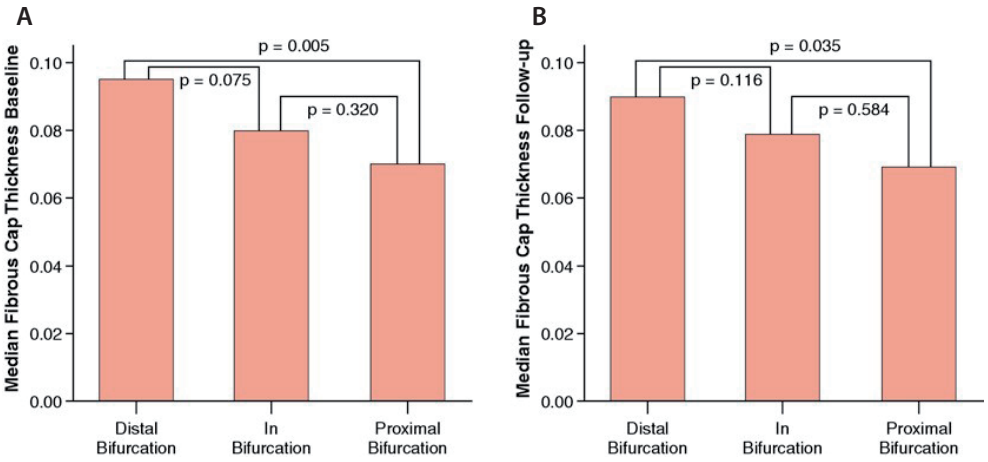

Figure 3. Fibrous Cap Thickness in the Three Regions of the Bifurcation.
The fibrous cap was measured in each frame with a plaque more than 600 µ.m thick assessed by optical coherence tomography and with more than 10% of confluent necrotic core detected by intravascular ultrasound–virtual histology. The fibrous cap showed a progres- sive reduction in thickness from the distal to the proximal frame at baseline (A) and follow-up (B).

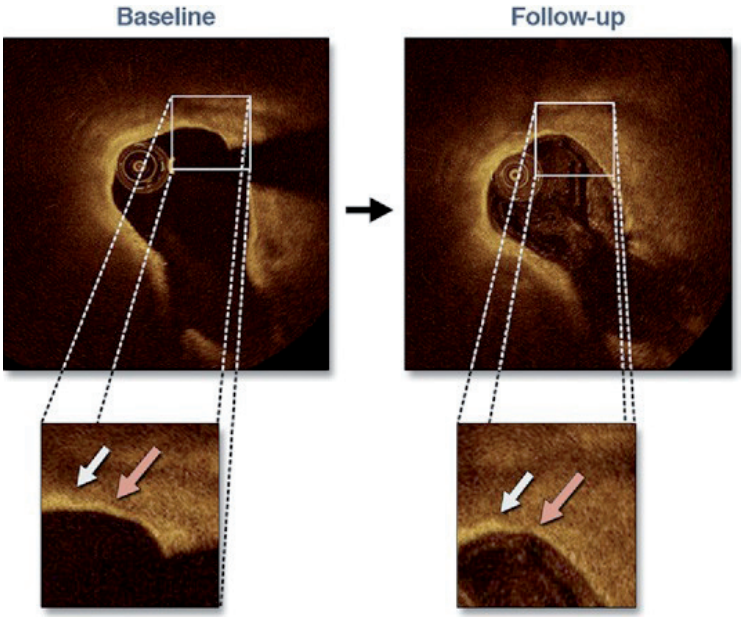

Figure 4. Thin Fibrous Cap at Baseline and Follow-Up.
Thin fibrous cap did not show a statistically significant difference in cap thickness at 6-month follow-up (red arrows). The matching of the frames was done using bifurcations and also microstructures (white arrows) as landmarks.

DISCUSSION

The main findings of our study are as follows: 1) dual-modality acquisition and analysis at 2 different time points for the evaluation of coronary atherosclerosis is feasible, addressing the complementary limitations of the 2 imaging modalities.
2) In a post–percutaneous coronary intervention patient population treated with standard medical therapy, most NC-rich plaques remained unchanged in their composition as measured by IVUS-VH at 6-month follow-up, and most thin-cap lesions remained thin capped (<65 μ.m) as measured by OCT. 3) Although the study population was small, the serial imaging findings of plaque morphology were in line with the clinical outcomes.
Moreover, we observed that the proximal rim of the side branch ostium is more likely to contain a larger amount of NC and the thinnest fibrous cap within the bifurcation. The plaque index, defined as the ratio of NC-rich to non-NC-rich frames, increased, implying a progression of the disease at 6 months. This finding is supported by the observation that in this small series, 4 new NC-rich plaques developed and 2 additional plaques became TCFAs. This progression was due mostly to an increase of NC in non–NC-rich plaques (development of new NC-rich areas). To our knowledge, this is the first in vivo study evaluating longitudinal changes in plaque type and composition using combined plaque assessment with IVUS-VH and OCT.
Sawada et al. [6] recently reported in a small series that 54% of IVUS-VH– derived TCFAs were non- thin-cap lesions by OCT, and 6.3% of OCT-derived TCFAs were not definitively TCFAs. This study strongly supports the combined use of these 2 imaging modalities, which appears to be necessary for the correct detection of high-risk plaques. In addition, Manfrini et al. [5] reported that if used alone, OCT can lead to misinterpretations due to its low signal penetration, which does not allow an accurate detection of signal-poor areas with heterogeneous compositions.
Previously, Kubo et al. [10] reported in a serial population that 75% of TCFAs detected on VH healed at 1-year follow-up. Takarada et al. [11] reported that therapy with statins significantly increased fibrous cap thickness detected with OCT in a population with untreated hypercholesterolemia. However, potentially all single-modality imaging studies could have obtained different results by combining the 2 modalities, virtually increasing accuracy for TCFA detection. Therefore, further investigations are needed to better understand the evolution of high-risk plaques in patients with optimal medical treatment, and the combined use of IVUS-VH and OCT could be a key tool to characterize the coronary model of future events [12].

Study limitations

This study might have been under- powered to detect differences in plaque composition, and the length of follow-up was short, so the study should be considered exploratory and hypothesis generating, without formal statistical hypotheses.

Local endothelial shear stress was not measured. We cannot exclude that different plaque progression and regression might be also associated in the present series to different shear stress conditions. Because the BVS (Abbott Laboratories, Abbott Park, Illinois) is a drug-eluting device, in bifurcations located distally to the scaffold, the drug might have a considerable impact on the progression or regression of atherosclerosis.

CONCLUSIONS

The combined use of IVUS-VH and OCT is a reliable tool to serially assess plaque progression and regression, and in the present study, it was demonstrated to be safe and feasible. At 6-month follow-up, in this post–percutaneous coronary intervention patient population, most high-risk plaques remained unchanged, retaining their imaging classification, nevertheless appearing to have remained clinically silent.

REFERENCES

1. Virmani R, Kolodgie FD, Burke AP, Farb A, Schwartz SM. Lessons from sudden coronary death: a comprehensive morphological classification scheme for atherosclerotic lesions. Ar- terioscler Thromb Vasc Biol 2000;20:1262–75.
2. Burke AP, Farb A, Malcom GT, Li- ang YH, Smialek J, Virmani R. Coronary risk factors and plaque morphology in men with coronary disease who died suddenly. N Engl J Med 1997;336:1276 – 82.
3. Virmani R, Burke AP, Farb A, Kolodgie FD. Pathology of the vulnerable plaque. J Am Coll Cardiol 2006;47:C13– 8.
4. Nair A, Vince DG, Calvetti D. "Blind" data calibration of intravascular ultrasound data for automated tissue characterization. IEEE Ultrason Symp 2004;2:1126 –9.
5. Manfrini O, Mont E, Leone O, et al. Sources of error and interpretation of plaque morphology by optical coher ence tomography. Am J Cardiol 2006; 98:156 –9.
6. Sawada T, Shite J, Garcia-Garcia HM, et al. Feasibility of combined use of intravascular ultrasound radiofrequency data analysis and optical coherence tomography for detecting thin-cap fibroatheroma. Eur Heart J 2008;29:1136 – 46.
7. Gonzalo N, Garcia-Garcia HM, Re- gar E, et al. In vivo assessment of high-risk coronary plaques at bifurcations with combined intravascular ultrasound and optical coherence to- mography. J Am Coll Cardiol Img 2009;2:473– 82.
8. Garcıa-Garcıa HM, Mintz GS, Ler- man A, et al. Tissue characterisation using intravascular radiofrequency data analysis: recommendations for acquisition, analysis, interpretation and reporting. EuroIntervention 2009;5:177– 89.
9. Barlis P, Serruys PW, Gonzalo N, van der Giessen WJ, de Jaegere PJ, Regar E. Assessment of culprit and remote coronary narrowings using optical coherence tomography with long-term outcomes. Am J Cardiol 2008;102:391–5.
10. Kubo T, Maehara A, Mintz GS, et al. The dynamic nature of coronary artery lesion morphology assessed by serial virtual histology intravascular ultrasound tissue characterization. J Am Coll Cardiol;55:1590 –7.
11. Takarada S, Imanishi T, Kubo T, et al. Effect of statin therapy on coronary fibrous-cap thickness in patients with acute coronary syndrome: assessment by optical coherence tomography study. Atherosclerosis 2009;202:491–7.
12. Deliargyris EN. Intravascular ultra- sound virtual histology derived thin cap fibroatheroma: now you see it, now you don't. J Am Coll Cardiol 2010;55:1598 –9.

Chapter 3

Assessment of stenosis structure with intravascular ultrasound

Hector M. Garcia-Garcia; Salvatore Brugaletta; Roberto Diletti;
Gioel Gabrio Secco; Carlo Di Mario; Patrick W. Serruys

Coronary stenosis imaging, structure and physiology 2010

INTRODUCTION

Atherosclerosis is the main cause of coronary heart disease, which is today the leading cause of death worldwide and will continue to be the first in the world in 2030 [1]. In the formation of atherosclerotic coronary lesions, a critical primary step is the accumulation and oxidation of low-density lipoprotein (LDL) particles. Oxidized-LDL favors leukocyte recruitment and their activation, as well as cell death. This leads to generation of complex atherosclerotic plaques [2]. These plaques have a high content of necrotic core, a thin inflamed fibrous cap (intense accumulation of macrophages) and scarce presence of smooth muscle cells (i.e. thin capped fibroatheroma – TCFA).

At early stages of the formation of the atheroma, the remodeling of the vessel wall usually prevent plaque from encroaching the lumen, thereby masking the presence of atheroma on angiography. In contrast, greyscale intravascular ultrasound (IVUS) can fully assess the extension of the disease axially and longitudinally. This intravascular imaging technique has played a vital role in advancing our understanding of the pathophysiology of coronary artery disease, and in the development of novel cardiovascular drugs and device therapies [3, 4]. In the last decade, IVUS based imaging modalities have been introduced such as backscatter data analysis and echogenicity, facilitating characterisation of plaque components and its mechanical properties. This intravascular imaging technology and its clinical and research applications are discussed in detail in the different sections of this chapter.

RATIONALE FOR INTRAVASCULAR IMAGING

Coronary angiography depicts arteries as a planar silhouette of the contrast-filled lumen. Importantly, angiography does not provide visualisation of the vessel wall and is not suitable for assessment of atherosclerosis. Angiographic disease assessment is based on the comparison of the stenotic segment with the adjacent, "normal appearing" coronary, which is often an incorrect assumption due to the diffuse nature of atherosclerosis as shown by pathological and IVUS studies. [7, 8] (Figure 1) . Angiography interpretation is flawed by large inter- and intra-observer variability and usually underestimates the severity of the disease and vessel dimensions. Although quantitative coronary angiography (QCA) has reduced the visual error, the ability of arteries to enlarge to compensate for plaque growth makes angiography an unreliable method to assess atherosclerosis burden [8]. Three-dimensional angiography obtained with systems such as DynaCT (Siemens Medical

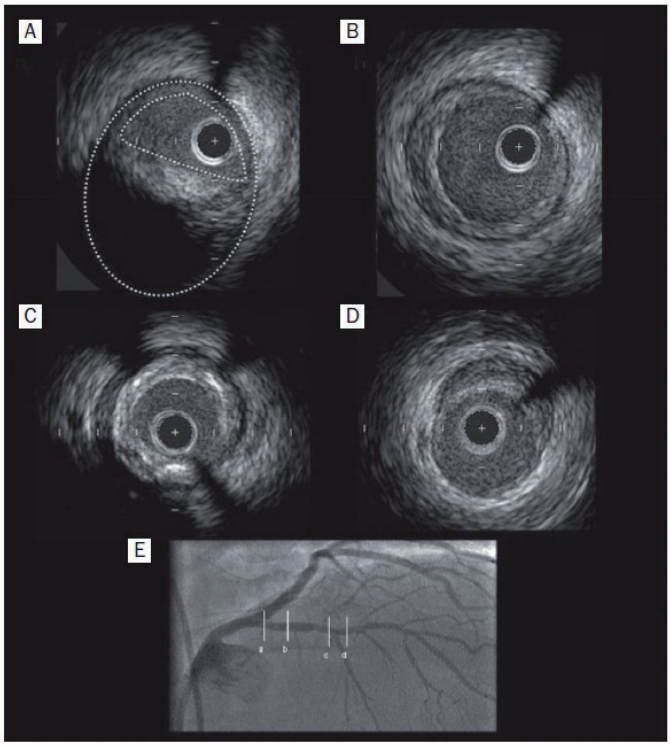

Figure 1. Coronary angiography and IVUS. This figure illustrates the heterogeneity of atherosclerotic disease and the lack of correlation of IVUS findings (Panels A through D) and angiography appearance (Panel E). The patient presented with stable angina and a significant stenosis in the right coronary artery which was stented (not shown). A greyscale IVUS pullback in the left anterior descending (LAD) was performed in order to better characterise the mild stenosis in its mid segment. Panel A shows a large eccentric plaque in the ostium of the LAD that angiographically has minimum lumen compromise. Panel B depicts a soft concentric plaque. Panel C shows a mixed plaque. Panel D depicts an eccentric, soft lesion.

Solutions) at the time of the contrast injection may provide more accurate and precise assessment of the luminogram, addressing some of the limitations of conventional angiography, but it still does not allow visualisation of the arterial wall and plaque burden. These limitations of angiography can be minimised by the intravascular tomographic visualisation of lumen and vessel wall architecture. In addition, IVUS enables assessment of ambiguous disease in vessels with aneurysmal dilatation, ostial stenoses, disease located at branching points or in the left main; tortuous or calcified segments; eccentric disease, complex disease morphology, intraluminal filling defects, thrombus, dissection and lumen dimensions after coronary intervention.

INTRAVASCULAR ULTRASOUND

Basic principles

The IVUS image is the result of reflected ultrasound waves that are converted to electrical signals and sent to an external processing system for amplification, filtering and scan-conversion. After leaving the transducer, the beam remains almost parallel for a short distance ("near field"; better image quality) and then begins to diverge ("far field"). After encountering a transition between different materials, for example the interface between blood and the intimal arterial layer, the beam will be partially reflected and partially transmitted, depending on tissue composition and differences in mechanical impedance between materials. For example, calcium produces nearly complete backscattering of the signal and is displayed as a bright image with a characteristic acoustic shadowing. Ultimately, greyscale IVUS imaging is formed by the envelope (amplitude) of the obtained radiofrequency signal (Figure 2).

The quality of ultrasound images can be described by spatial resolution and contrast resolution. Its axial resolution is approximately 100 microns, while lateral resolution reaches 200-250 microns in conventional IVUS system (20-40 MHz). Contrast resolution is the distribution of the grey scale of the reflected signal, and is often referred to as dynamic range.

An image of low dynamic range appears as black and white with a few levels of grey; images at high dynamic range are often softer.

Catheter designs

The IVUS equipment consists of a catheter incorporating a miniaturised transducer and a console to reconstruct and display the image. (Figure 3) . Lately, IVUS consoles have been incorporated into the cathlab equipment for easier operation. Current catheters range from 2.6 to 3.2 Fr in size and can be introduced through conventional 6 Fr guide catheters. Rotational, mechanical IVUS probes rotate a single piezoelectric transducer at 1800 rpm and operate at frequencies between 30 and 40 Mhz, while electronic phased-array systems operate at a centre-frequency of approximately 20 MHz. Higher ultrasound frequencies are associated with better image resolution, but increasing the frequency beyond 40 MHz has been limited because of decreased tissue penetration [9, 10]. Electronic systems have up to 64 transducer elements in an annular array that are activated sequentially to generate the cross-sectional image [10]. In general, electronic catheter designs are slightly easier to set-up and use, whereas mechanical probes offer superior image quality. Electronic IVUS catheters have the ability to display blood flow in colour to facilitate distinction between lumen and wall boundaries.

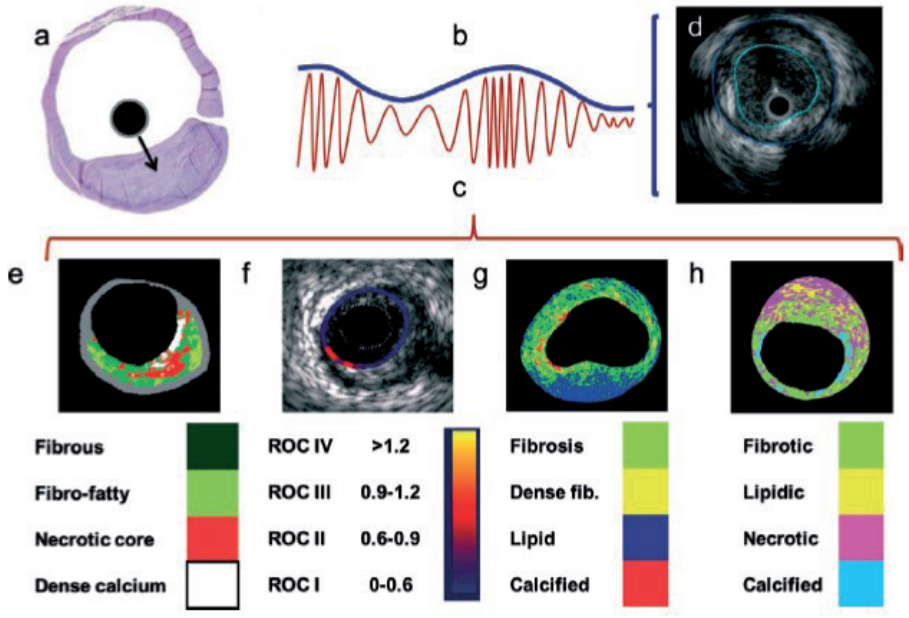

Figure 2. Assessment of atheromatous plaque components with different IVUS modalities.Intravascular ultrasound signal is obtained from the vessel wall (A). Greyscale IIVUS imaging is formed by the envelope (amplitude) (B) of the radiofrequency signal (C). By greyscale, atherosclerotic plaque can be classified into 4 categories: soft, fibrotic, calcified and mixed plaques. Panel D shows a cross-sectional view of a greyscale image. The blue lines limit the actual atheroma. The frequency and power of the signal commonly differ between tissues, regardless of similarities in the amplitude. From the backscatter radiofrequency data different types of information can be retrieved: virtual histology (E), palpography (F), integrated baskscattered (IB), IVUS (G) and iMAP (H). Virtual histology is able to detect four tissue types: necrotic core, fibrous, fibro-fatty and dense calcium. Palpography plaque deformability is reported in strain values, which are subsequently categorized into four grades according to the ROtterdam Classification (ROC). The tissues characterised by integrated baskscattered(IB) IVUS are lipidic, fibrous and calcified; and iMAP detects fibrotic, lipidic, necrotic and calcified.

Autoregressive spectral analysis of IVUS backscattered data has been incorporated into conventional IVUS systems to facilitate image interpretation of different tissue components (i.e., necrotic core in red, dense calcium in white, fibrous in dark green, and fibrofatty in light green) [11]. (Figure 2). In a post mortem validation study, RF analysis demonstrated sensitivity and specificity for detection of necrotic core of 92 % and 97 %, respectively [11]. The first commercially available IVUS backscattering image analysis, named virtual-histology™ (IVUS-VH), was built on the electronic 20 MHz IVUS platform. This system has been utilised in clinical trials to monitor progression of atherosclerosis. Lately rotational mechanical IVUS systems have also integrated a backscattering regression algorithm. (Figure 2). [179]
Another approach is to assess the deformability of coronary plaque using also the analysis

of radiofrequency signals at different diastolic pressure levels, normalised to a pressure difference of 2.5 mmHg per frame. This allows the construction of a "strain" image, in which harder ("low strain") and softer ("high strain") regions of the coronary arteries can be identified, with radial strain values ranging between 0 % and 2 % [12]. (Figure 2). Post mortem coronary arteries were investigated with histology and IVUS palpography. The sensitivity and specificity of palpography to detect vulnerable plaques are 88%, and 89%, respectively. [12]

Examination technique

The IVUS procedure is performed under full anticoagulation with an activated clotting time of > 250 sec. Following intracoronary infusion of intracoronary nitroglycerine (100-200 micrograms) to minimise vasospasm, the rapid exchange IVUS catheters are introduced in the coronary over a standard 0.014" guidewire. Mechanical IVUS systems require infusion of heparinised saline to clear air bubbles inside the sheath covering the transducer before inserting the catheter in the guide catheter. The IVUS catheter should be advanced under fluoroscopy guidance approximately 10 mm distal to an anatomical landmark (i.e., side branch) (Video 1) and retracted slowly to straighten the catheter shaft which may have built some slack during insertion in order minimise non-uniform rotation distortion (NURD) artifacts.

Motorised pullback devices should be used to withdraw the catheter at a constant speed (most frequently at 0.5 mm/sec) to allow proper examination of the entire coronary and calculation of distances. Unless coronary ischaemia ensues, the catheter should be withdrawn up to the aortic coronary junction, as the guide catheter should be retracted slightly to allow imaging of the coronary ostium.

Safety

IVUS imaging has been performed safely in a large number of subjects enrolled in research studies with no apparent increase in the incidence of adverse effects. In general, the rate of complication related to IVUS is small across several studies. In one study, the rate of complications was 2.9 % of patients who experienced transient spasm and 0.4 % of the patients who had acute vessel occlusions, dissections, and/or embolism. The complication rate was higher in patients with unstable angina or acute myocardial infarction, and in patients undergoing intervention compared with diagnostic IVUS [13]. Another group reported a 1.1 % rate of complications, without adverse clinical consequences [14]. In 7,085 IVUS studies from 51 centres [15], vasospasm occurred in 3 %. Major complications (dissection, thrombosis, ventricular fibrillation, and refractory spasm) occurred in 10 (0.14%). There was only one major event.

In 103 patients with acute ST-elevation myocardial infarction (STEMI) undergoing primary PCI, the feasibility of multimodality imaging (with optical coherence tomography and intravascular ultrasound) and the procedural and long-term safety of intracoronary (i.c) imaging for documentary purposes has been reported. [180]These patients underwent serial three-vessel coronary imaging during primary PCI and at 13 months. Clinical outcomes were compared with the results from a cohort of 485 STEMI patients undergoing primary PCI without additional imaging. Imaging of the infarct-related artery at baseline (and follow-up) was successful in 92.2 % (96.6 %) of patients using OCT and in 93.2 % (95.5 %) using IVUS. Imaging of the non-infarct-related vessels was successful in 88.7 % (95.6 %) using OCT and in 90.5 % (93.3 %) using IVUS. Periprocedural complications occurred in 2.0 % of OCT and none during IVUS. There were no differences throughout 2 years between the imaging and control group in terms of MACE (16.7 vs. 13.3 %, adjusted HR1.40, 95 % CI 0.77–2.52, p = 0.27). Authors concluded that multi-modality three-vessel i.c. imaging in STEMI patients undergoing primary PCI can be performed safely without impact on cardiovascular events at long- term follow-up.

The long-term safety of IVUS in transplant recipients has been reported [16]. Subsequent angiographic stenoses were observed in 19.5 % (107/548) of imaged arteries vs. 16.2 % (21/130) of non-imaged arteries (p = 0.4). Another study [17] reported 18-24 months quantitative coronary angiographic analysis comparing IVUS-imaged and non-IVUSimaged arteries in 525 patients. New stenoses lesions occurred in 3.6 % and 3.9 % of IVUS-imaged and non-IVUSimaged arteries, respectively (p = 0.84). When all coronary lesions were considered, the incidence of lesion progression was not significantly different between IVUS-imaged (11.6 %) and non-IVUS-imaged (9.8 %) arteries.

We can conclude that the use of IVUS imaging is safe as confirmed by the low rate of complications and the absence of lesion progression in coronary arteries imaged with this technique.

Limitations in plaque assessment and image artifacts Greyscale IVUS provides a limited insight into atheroma composition. Soft (echolucent) plaques have been related either to high lipid content [18, 19] or presence of smooth muscle cells [20]. While fibrous plaques usually have an intermediate echogenicity, but sometimes very dense fibrous plaques can also appear as calcified lesions [21]. Traditionally, acoustic shadowing has been considered as a sign of calcification, but necrotic tissue can also cause shadowing [20]. In addition, the inter-observer variability in the plaque type assessment by greyscale IVUS reported in the literature varies considerably, with percentages of concordance between observers ranging from 88 % to only 47 % [22, 23, 24].

Most artifacts of IVUS imaging are specific to the construct of each system. NURD is specific to mechanical catheters, and arises from friction of the transducer in the coronary

or guiding catheter or from a poor connection of the IVUS catheter in the motor drive unit, which causes a typical onion skin image appearance. Tortuosity, severely stenotic segments, small guide lumen size, guide catheters with sharp secondary curves or slack in the catheter shaft or tightened haemostatic valve are common causes of NURD.
The ring-down artefact, however, is specific to electronic systems due to transducer oscillations that obscure the near field image [21]. Side lobes artefacts are intense reflections that come from strong reflectors such as calcium and stent struts. These usually follow the circumferential sweep of the beam. The presence of the side lobes may mask the actual lumen edge or may also be taken as tissue prolapse or dissection flaps. Another artefact that is also coming from strong reflectors is the reverberation. Reverberations are concentric repetitions at equidistant locations of the same image.

An eccentric or non perpendicular position of the IVUS catheter produces geometric distortions and an artificially elliptical appearance of the cross-sectional image leading to overestimation of lumen area [21].
The speed of catheter pullback is also prone to errors which may lead to incorrect assessment of the length of the segment of interest [25]. At a difference with non-sheath based catheters (electronic systems), sheath-based, mechanical catheter systems allow more uniform pullbacks during image acquisition and are more precise length measurements [25].
All these factors should be considered when assessing IVUS images to avoid misinterpretation and thereby making erroneous clinical decisions.

Combined intravascular imaging modalities

Another imaging modality able to characterise coronary atherosclerosis invasively is near infrared spectroscopy (NIRS.) [26]. A commercially available catheter employing NIRS to detect lipid core plaque has been developed and combined with simultaneous coregistered IVUS (Infraredx, Inc., Burlington, MA USA). (Figure 4) Unique from all other technologies currently purported to detect lipid core, the system was rigorously prospectively validated and carries specific label claims for the detection of lipid core in multiple countries including the US FDA. [27]. This 3.2 Fr NIRS-IVUS catheter is compatible with a conventional 0.014" guidewire, has a rotating core 960 RPM), and is pulled back by a motor drive unit at 0.5mm/sec. 30. (Video 2) The next generation of the catheter has recently been introduced, which incorporates a novel extended bandwidth transducer centered at 50MHz, tailored detection electronics, and a specialized processing stream. These improvements are expected to result in a best-in-class IVUS resolution and image quality. The system design is intended to gain the finer resolution afforded by higher

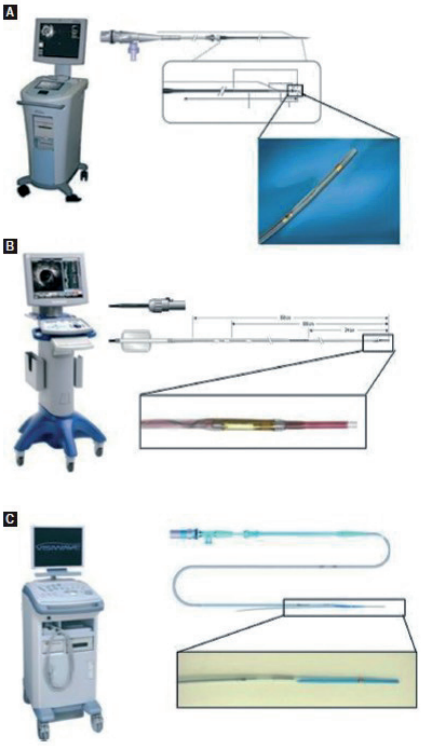

Figure 3. Intravascular ultrasound catheters. The consoles of the Boston Scientific (Natick, MA, USA) iLab® ultrasound imaging system (not shown) and the iCross™, is the coronary imaging catheter (A). The Console of the Volcano's s5™ Ultrasound Imaging System (not shown) and the Eagle Eye™ Gold Coronary Imaging Catheter are shown in Panel B. Panel C shows the IVUS catheter ViewIT (Terumo Corp., Tokyo, Japan) and the console of Terumo Corporation is named Visiwave (not shown).

transducer frequencies, but through the strategic full utilization of a wider bandwidth, avoids the potential drawbacks of increased blood speckle and reduced imaging depth. A number of studies [SPECTACL - NCT00330928 [1402].SAVOIR - NCT00901446, SAVOIR 2 – NCT02154295, COLOR – NCT00831116, CANARY – NCT01268319, Atheroremo – VPS, IBIS-3, YELLOW, YELLOW II – NCT01837823, ORACLE-NIRS – NCT02265146, Lipid Rich Plaque – NCT02033694, PROSPECT II and PROSPECT ABSORB - NCT02171065] have been completed or are in progress to assess the clinical value of NIRS-IVUS. Early studies focused on proof of concept of the technology, reproducibility, comparison to other modalities, prediction of stenting complications, optimization of stenting strategy, monitoring of drug effect, and early indications of major adverse event prediction. Three large events trials are in progress that aim to definitively tie lipid cores found at index catheterization with the risk of subsequent events, both at the patient and plaque level. At least two of those trials

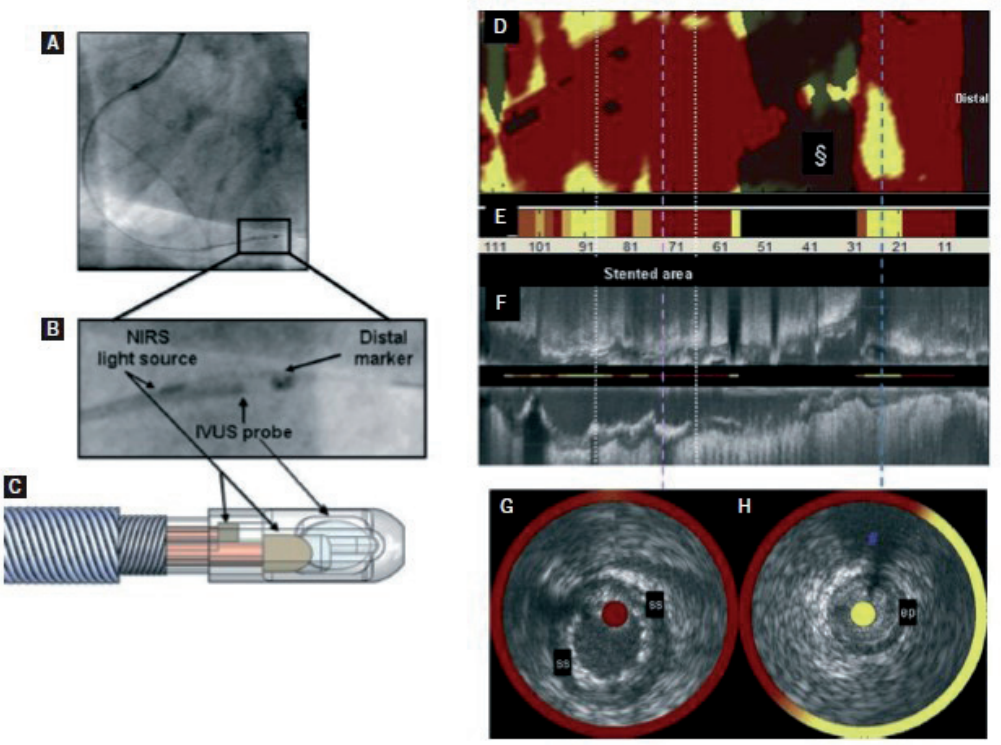

Figure 4. A picture of the Apollo catheter tip indicating the relative positions to each other of the NIRS light source and IVUS probe. (A) The combined intravascular ultrasound images and chemical information from a pullback through the right coronary artery obtained using the Apollo catheter. The chemogram obtained from the Apollo catheter pullback, with the stented area as indicated. (B) The chemogram is a map of the measured probability of lipid core plaque (LCP) from each scanned arterial segment; the yellow regions represent those with the highest probability for the presence of LCP, whilst red regions represent those the lowest. The chemogram displays pullback position against circumferential position of the measurement in degrees. The § represents a region of the coronary artery where insufficient NIRS signals were obtained to generate a chemogram. In this image the proximal end of the stent is located in an area with a high probability of LCP (yellow). The block chemogram provides a summary of the raw data from the chemogram and displays the probability that an LCP is present for all measurements in a 2 mm block of coronary artery. The order of probability for the presence of LCP from highest to lowest is yellow, light brown, brown and red. (C) The longitudinal IVUS pullback, with NIRS overlay. (D) The lilac and blue lines mark the anatomical position on the IVUS, and the corresponding position on the chemogram during pullback, enabling simultaneous assessment of plaque structure and composition. Panel E shows a cross sectional intra-vascular ultrasound image with the chemogram obtained from b, demonstrating well opposed clearly identifiable stent struts (ss), highlighting the ability of the Apollo catheter to be used as a standalone IVUS catheter if required. The corresponding longitudinal IVUS image and chemogram is indicated by the lilac line on b, c and d. The chemogram indicates that there is a low probability of lipid present in the stented plaque. In panel F, cross-sectional IVUS image distal to the stent demonstrating the presence of echolucent plaque between 1 and 7 o'clock. The chemogram displays a high probability of lipid in this plaque. The corresponding longitudinal IVUS image, and chemogram is indicated by the blue line on b, c and d.

(LRP and PIIA) will explore new treatments (i.e. BVS) of non-flow-limiting lesions that show other signs of vulnerability.

CHARACTERISATION OF ATHEROSCLEROSIS

Normal coronary artery structure

Adequate knowledge of the structure of the arterial wall andatheromatous plaques is of paramount importance for the interpretation of IVUS images. The coronary wall is composed of three layers. The innermost tunica intima is in direct contact with the blood and is constituted by an endothelial cell monolayer resting upon a basement membrane. Ageing of human arteries is associated with the presence of smooth muscle cells in the tunica intima.

These cells produce extracellular matrix molecules leading to intimal layer thickening. This process is not necessarily associated with pathological lipid accumulation and atherosclerosis formation. The second layer, tunica media, is separated from the tunica intima by the internal elastic membrane (IEM) and is formed by concentric layers of smooth muscle cells. The adventitia is the outermost arterial layer which is separated from the media by the external elastic membrane (EEM) and contains fibroblasts and mast cells, collagen fibrils, vasa vasorum and nerve endings.

The normal coronary architecture can be assessed using intravascular imaging. The circulating blood elements may assist IVUS image interpretation and differentiate lumen from vessel wall, as these produce characteristic speckles in the image. However, blood speckles are dependent on flow velocity and may have increased intensity in situation of slow blood flow, which may have similar appearance as the vessel wall. The reported normal value for intimal thickness in young subjects is 0.15 ± 0.07 mm. Thus, the thin tunica intima reflects ultrasound poorly and is not visualised as a separate layer. The media is typically less echogenic than the intima, but may appear thick because of signal attenuation and weak reflectivity of the internal elastic membrane. A monolayer appearance is a common finding in normal coronary arteries, while a trilayered appearance suggests the presence of intimal thickening. [29] A trilaminar appearance is dependent not only on the age but also on the histologic characteristics of the vessel. The adventitia has the strongest echo signal which is used a reference to determine plaque components. Importantly, the IVUS beam penetrates beyond the adventitial layer allowing visualisation of perivascular structures, including the cardiac veins and the pericardium. Based on histologic and ultrasound data, coronary vessel wall with an intimal thickness ≥ 0.5 mm is considered to be diseased. [21]

Atheroma

A detailed description of the structure of atheromatous plaques can be found in Chapter 6 of this book. In brief, atheromatous plaques are formed by an intricate sequence of events, not necessarily in a linear chronological order, that involves extracellular lipid accumulation, endothelial dysfunction, leukocyte recruitment, intracellular lipid accumulation (foam cells), smooth muscle cell migration and proliferation, expansion of extracellular matrix, neoangiogenesis, tissue necrosis and mineralisation at later stages. The ultimate characteristic of an atherosclerotic plaque at any given time depends on the relative contribution of each of these features [2]. Thus, the pathologic intimal thickening (PIT) is rich in proteoglycans and lipid pools, but no trace of necrotic core is seen. The earliest lesion with a necrotic core is the fibroatheroma (FA), and this is the precursor lesion that may give rise to symptomatic heart disease. Thin-capped fibroatheroma is a lesion characterised by a large necrotic core containing numerous cholesterol clefts. The overlying fibrous cap is thin and rich in inflammatory cells, macrophages and T-lymphocytes with few smooth muscle cells. A cut-off value for cap thickness of < 65 microns to define a vulnerable coronary plaque has been based on pathology studies [30], but in vivo confirmation of such threshold is lacking. Figure 5 outlines the virtual histology plaque and lesion types that are proposed based on the above pathologic data [31]. Based on tissue echogenicity (i.e., their appearance) and not necessarily histological composition, atheromas have been classified into four categories by greyscale IVUS:

1. soft plaque (lesion echogenicity less than the surrounding adventitia - hypoechoic);
2. fibrous plaque [intermediate echogenicity between soft (echolucent or isoechoic) atheromas and highly echogenic calcified plaques];
3. calcified plaque (echogenicity higher than the adventitia with acoustic shadowing); and
4. mixed plaques (no single acoustical subtype represents > 80% of the plaque) [21]. Figure 1

Another greyscale IVUS classification has been widely used:

1. Echo-attenuated plaques have no ultrasound signal behind plaque. This plaque can be either hypoechoic or isoechoic but contained no bright calcium [181].
2. Echolucent plaque present an intraplaque hypoechoic zone surrounded by tissue of greater echodensity.

Detection of calcification

The mechanisms of coronary calcification are not fully known. Extent of coronary calcification as assessed by computed tomography (CT), has been shown to be a better predictor of future events than the Framingham risk index alone [182] This may be partly due

Lesion type		Brief description
Adaptative Intimal Thickening (AIT)		< 600 µm of intima thickness
Pathological Intimal Thickening (PIT)	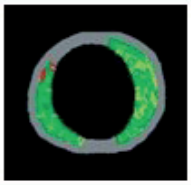	≥ 600 µm thickness for > 20 % of the circumference with FF > 15 %, and no confluent NC or DC
Fibrotic Plaque (FT)	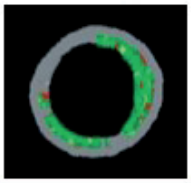	Dominant FT and no confluent NC or DC
Fibrocalcific Plaque (FC)		> 10 % confluent DC with no confluent DC
Fibroatheroma (FA)	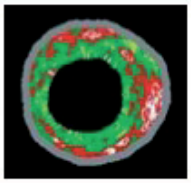	> 10 % confluent NC not at the lumen on three consecutive frames
Thin Cap Fibroatheroma (TCFA)	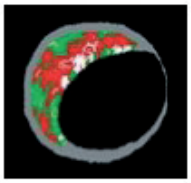	> 10 % confluent NC not at the lumen on three consecutive frames

Figure 5. Virtual histology plaque types. FF: fibrofatty; FT: fibrous tissue; NC: necrotic core and DC: dense calcium.

to the close relationship between the presence of calcium and atherosclerotic coronary plaque burden. [183]

On IVUS, calcium appears as bright echoes that obstruct the penetration of ultrasound (acoustic shadowing). (Figure 1 [C] and Video 3). Therefore, IVUS detects only the leading edge of calcium and cannot determine its thickness. Calcification on IVUS is usually described based on its circumferential angle (arc), longitudinal length and its depth. Calcification can be located deeper in the arterial wall or in the surface of the plaque, in close contact with the lumen wall interface. The presence, depth and circumferential distribution of calcification are not only important factors for selecting the type of interventional device, and estimating the risk of vessel dissection and perforation during PCI [32], but also in designing and conducting studies on progression/regression of coronary atheroma. Plaques with moderate to severe calcification showed not change or progression of atheroma size [33]. Thus, careful selection of coronary segments to evaluate the effect of drugs on coronary atherosclerosis should be considered.

IVUS has shown significantly higher sensitivity than fluoroscopy in the detection of coronary calcification [34]. Virtual histology, in comparison with histology, has a predictive accuracy of 96.7 % for detection of dense calcium [35].

Arterial remodelling

Arterial remodelling refers to a continuous process involving changes in vessel size measured by the EEM crosssectional area (also called vessel cross-sectional area – CSA). "Positive remodelling" occurs when there is an outward increase in EEM. "Negative remodelling" occurs when the EEM decreases in size (shrinkage of the vessel) [21]. The magnitude and direction of remodelling can be expressed by following index: EEM cross-sectional area at the plaque site divided by EEM CSA at the reference "non-diseased" vessel. Positive remodelling will demonstrate an index > 1.0; while negative remodelling has an index < 1.0. Direct evidence of remodelling can only be demonstrated in serial studies showing changes in the EEM CSA over time, since remodelling may also be encountered at the "normal-appearing" reference coronary segment [21].

The limitation of angiography in determining disease burden and stenosis severity is largely due to vessel remodelling. Detection of remodelling is extremely important during PCI to define plaque burden and appropriate size of devices. Pathological studies have also suggested a relationship between positive vessel remodelling and plaque vulnerability. Vessels with positive remodelling showed increased inflammatory marker concentrations, larger lipid cores, paucity of smooth muscle cells and medial thinning [36, 37, 38]. Several IVUS studies have linked positive vessel remodelling with culprit [39] and ruptured coronary plaques [40, 41]. Positive remodelling has been observed more often in

patients with acute coronary syndromes than in those with stable coronary artery disease [42, 43], and has been identified as an independent predictor of major adverse cardiac events in patients with unstable angina [44]. Plaques exhibiting positive remodelling also had more often thrombus and signs of rupture [45]. Pattern of remodelling has also been correlated with plaque composition, soft plaques are associated with positive remodelling while fibrocalcific plaques more often have negative or constrictive remodelling [46]. Similar findings have been observed in studies utilising IVUS radiofrequency data (RFD) analysis, a technique developed specifically for tissue characterisation. Positive remodelling was directly correlated with the presence and size of necrotic core, and inversely associated with fibrotic tissue [47].

Vulnerable plaque and thrombi Acute coronary syndromes are often the first manifestation of coronary atherosclerosis, making the identification of plaques at high-risk of complication an important component of strategies to reduce casualties associated with atherosclerosis. Our current understanding of plaque biology suggests that ~ 60 % of clinically evident plaque rupture originates within an inflamed thin-capped fibroatheroma (TCFA) [48, 49]. Pathological studies demonstrated that ruptured plaques are mainly located in the proximal portions of the LAD and LCX and are more disperse in the RCA [50]. This tendency of advanced plaques to develop preferentially in these locations has been explained by the low shear stress conditions generated in areas with tortuosity or many branches. Low shear stress may induce the migration of lipid and monocytes into the vessel wall leading to the progression of the lesion towards a plaque with high risk of rupture [51].

The definition of an IVUS-derived TCFA is a lesion fulfilling the following criteria in at least 3 frames: 1) plaque burden ≥ 40 % and 2) confluent necrotic core ≥10 % in direct contact with the lumen (i.e., no visible overlying tissue) [52]. Using this refined definition of IVUS-derived TCFA, in patients with ACS who underwent IVUS of all three epicardial coronaries, on average, there were 2 IVUS-derived thin cap fibroatheroma per patient, with half of them showing outward remodelling [52]. Hong et al., reported the frequency and distribution of TCFA identified by virtual histology intravascular ultrasound in acute coronary syndrome (ACS = 105 pts) and stable angina pectoris (SAP = 107 pts) in a 3-vessel IVUS-VH study [53]. There were 2.5 ± 1.5 in ACS and 1.7 ± 1.1 in SAP TCFAs per patient, $p < 0.001$. Presentation of ACS was the only independent predictor for multiple ID-TCFA ($p = 0.011$). Eighty-three percent of ID-TCFAs were located within 40 mm of the coronary.

The potential value of these VH IVUS-derived plaque types in the prediction of adverse coronary events has been evaluated in three trials—Providing Regional Observations to Study Predictors of Events in the Coronary Tree (PROSPECT) [184], VH-IVUS in Vulnerable Atherosclerosis (VIVA) [185], and the European Collaborative Project on Inflammation and

Vascular Wall Remodeling in Atherosclerosis (ATHEROREMO-IVUS) [186] - studied the value of VH in detecting plaque characteristics associated with future events and identifying high-risk prone-to-rupture plaques. In PROSPECT a VH TCFA with a minimum lumen area of ≤4mm^2 and a large plaque burden (≥70%), had a 17.2% likelihood of causing an event within 3 years [HR 10.8, (95%CI 4.3, 27.2), p<0.001]. While in the VIVA study, the presence of a non-calcified TCFA lesion was the only factor that was associated with MACE, which was mainly driven by coronary revascularizations (unadjusted HR 1.79; 95% CI 1.20-2.66, p=0.004). Lastly, in ATHEROREMO IVUS study, the presence of TCFA was an independent predictor for MACE (adjusted HR 1.98, 95% CI 1.09-3.60; p=0.026). Furthermore, the predictive value of TCFA lesions for the occurrence of acute cardiac events (composite of death or ACS only) was even stronger (adjusted HR 2.51, 95% CI 1.15-5.49; p=0.021). These findings emphasize the biological importance of TCFA for plaque rupture.

Although the three trials showed the same association, namely the presence of high-risk plaque characteristics with clinical outcomes, the following should be acknowledged: i. in the PROSPECT trial the total number of events was low, particularly the incidence of myocardial infarction (~1%). Most of MACE were either unstable angina or revascularization; ii. The VIVA study has a limited sample size and; the ATHEROREMO study has performed only one vessel imaging (vs. three-vessel imaging in the PROSPECT and VIVA studies) and associations were performed in a patient-level basis (vs. lesion level in the PROSPECT and VIVA studies).

The transition to plaque rupture has been characterised by the presence of active inflammation (monocyte/macrophage infiltration), thinning of fibrous cap (< 65 μm), development of large lipid necrotic core, endothelial denudation with superficial platelet aggregation and intraplaque haemorrhage [54, 55]. The remaining plaques that cause ACS contain calcium nodules (~ 10 %), or have none of the pathological features described above (~ 20 %). Superficial plaque erosion explains at least a portion of the latter events, particularly in women and diabetics [56]. The lack of cellular or anatomical signature of plaque erosion makes it difficult for existing imaging methods to have high accuracy in predicting ACS events. In addition, most plaque ruptures are silent without clinical manifestation, and repetitive healed ruptures may contribute to stable progression into obstructive disease [57].

Although plaque characteristics do not yet influence current therapeutic guidelines, the available clinical imaging modalities, IVUS and IVUS-based tissue characterisation techniques such as virtual histology, integrated backscattered IVUS and iMap, have the ability to identify some of the pathological atheroma features described above Figure 2. Ruptured plaques may have a variable appearance. Most commonly, IVUS may reveal an “axial”, abrupt ulceration depicted as an echolucent “void” or cavity beginning at the

luminal-intimal border. (Video 4) These features should be distinguished from longitudinal tear of the intima and media associated with spontaneous or iatrogenic dissection. The tear of the rupture in the fibrous cap can be identified in approximately 60 % of the cases and occurs more often at the shoulder of the plaque than in the centre [40, 58, 59]. Due to its relatively poor resolution, IVUS is unsuitable to detect a thin fibrous cap, but IVUS often reveals other features of ruptured plaques which are large in volume, eccentric, have mixed or soft composition and irregular surface, and are associated with positive vessel remodelling [40, 41, 60, 61]. Ruptured plaques have been shown to have quantitatively less calcium, especially superficial calcium, but a larger number of small (< 90º arc) calcium deposits, particularly deep calcium deposits [62]. IVUS can also reveal blood speckles passing through intraplaque channels created by the rupture, which usually produces the typical hazy, complex and non stenotic angiographic appearance of ruptured plaques.

Several IVUS studies have reported the frequency and distribution of plaque ruptures investigating the three coronary epicardial vessels. Rioufol et al. studied 24 patients (72 arteries) with ACS and found a mean prevalence of two ruptured plaques per patient. Interestingly, 12.5 % of these patients had ruptured plaques in the three major coronary arteries. Only 37.5 % of the ruptured plaques were located on the culprit lesion, and 79 % of the patients had also a ruptured plaque somewhere other than on the culprit lesion [63]. In a similar study in 45 patients with acute myocardial infarction (AMI), plaque rupture was observed in 21 patients (47 %) at the culprit site and 17 additional plaque ruptures were found at sites in 11 patients (24 %) [64]. Hong et al. evaluated the incidence of plaque rupture depending on the clinical presentation. They performed 3-vessel IVUS examination in 235 patients (122 AMI and 113 stable angina pectoris – SAP). Plaque rupture of infarct-related or target lesions occurred in 66 % of AMI patients and in 27 % of SAP patients. Non-infarct related or non-target artery plaque ruptures occurred in 17 % AMI patients and 5 % SAP patients. Multiple plaque ruptures were observed in 20 % AMI and 6 % SAP patients [65]. The same authors evaluated the distribution of plaque rupture in native coronary arteries in 392 patients (231 ACS and 161 SAP). Threevessel IVUS imaging showed that plaque ruptures occurred mainly in proximal segments of the LAD (83 % of LAD ruptured plaques), the proximal and distal segments of the RCA (48 % and 32 % of RCA ruptured plaques, respectively), and the entire LCX [66]. These results are in line with another study that included 104 patients and studied 160 ruptured plaques in the LAD, the majority were located within the proximal 30 mm of the artery [67].

A study aiming at characterising plaque ruptures in the left main coronary artery (LMCA) found 16 plaque ruptures in 17 patients (2 AMI, 13 unstable angina and 1 SAP). The ruptures were located in the distal portion and/or bifurcation of the LMCA, often did not compromise the lumen, and had an angiographic complex appearance. When

ruptured plaques involved the bifurcation LAD-LCX, they occurred opposite to the flow divider [68]. This is in line with our findings, lesions involving the bifurcation LAD-LCX were predominantly located in the outer wall of the carina, and such location was associated with larger necrotic core content [69].

Ruptured atherosclerotic plaques in native coronary arteries, but not in saphenous vein grafts (SVGs), have been well described with intravascular ultrasound. In 791 preintervention IVUS SVG studies, 95 ruptured plaques in 76 SVGs (73 patients) were identified (prevalence of 9.7 %). These ruptured plaques were found to be associated with complex angiographic characteristics and positive remodelling [70, 71]. Likewise, in an analysis of 300 ruptured plaques in 254 patients, Maehara et al. described that ruptured plaques detected by IVUS strongly correlated with complex angiographic lesion morphology: ulceration in 81 %, intimal flap in 40 %, thrombus in 7 %, and aneurysm in 7 % [40].

IVUS has also been used to assess the natural evolution of ruptured plaques. IVUS studies have suggested that up to 50 % of the ruptured plaques detected in a first ACS event heals with medical therapy, without significant change in plaque size [72]. One study revealed complete healing of plaque rupture in 29 % of the patients treated with statins and incomplete healing in untreated patients [73].

The ruptured plaque profile in 40 patients referred for cardiac catheterisation has been described [74]. There were 13 with stable angina, 12 with unstable angina and 15 with acute myocardial infarction. Ruptured plaque was identified in 26 patients and, as expected, was more frequent in patients with acute myocardial infarction and unstable angina. Patients with ruptured plaques have larger body mass index when compared with those without plaque rupture and were more likely smokers, patients with ruptures had more diffuse calcification and necrotic core area. Of note, the location of plaque ruptures in this study mirrors the pathological findings [75]. In our study, the proximal left anterior descending coronary artery was the most common site of plaque rupture. In a pathological series of 79 ruptures, Burke et al. [75] have found 74 % in the proximal left anterior descending. Similarly, in the report by Hong et al., the frequency and distribution of ruptured plaques identified by IVUS-VH in acute coronary syndrome (ACS = 105 pts) and stable angina pectoris (SAP = 107 pts) in a 3-vessel IVUS-VH study were reported [53]. There were 76 ruptured plaques (55 in ACS and 21 in SAP). Presentation of ACS was the only independent predictor for multiple ruptured plaques ($p = 0.013$).

Thrombus represents the ultimate pathological feature leading to ACS. Thrombus is usually recognised as an echolucent intraluminal mass, often with a layered or pedunculated appearance by IVUS [21]. Fresh or acute thrombus may appear as an echo-dense intraluminal tissue, which does not follow the circular appearance of the vessel wall, while older, more organised thrombus has a darker ultrasound appearance. However, none of these IVUS

features are a hallmark for thrombus, and one should consider slow flow (fresh thrombus), air, stagnant contrast or black hole, an echolucent neointimal tissue observed after DES and radiation therapy, as differential diagnoses [21].

CLINICAL APPLICATIONS: DIAGNOSTIC

Determination of the severity and extent of atherosclerosis

The determination of the severity and extent of atherosclerosis remains one of the main diagnostic clinical applications of intravascular imaging, as angiography and noninvasive methods lack spatial or temporal resolution for accurate coronary disease assessment. Standards for acquisition, measurement and reporting of IVUS has been proposed in a clinical expert consensus document [21]. Luminal area stenosis describes the relative decrease in luminal cross-sectional area (CSA) at the site of disease, in percentage, compared to lumen CSA in a "normal appearing" reference segment in the same coronary. The lumen area relative to the reference lumen area is analogous to the angiographic definition of diameter stenosis.

Proximal and distal reference lumen areas are calculated at sites with the largest lumen located prior to large side branches, and within 10 mm proximal and distal to the plaque, respectively. The image analyst should be aware of potential post stenotic dilatation of the vessel wall when using these measurements to guide clinical decision.

Minimal lumen area (MLA) describes the smallest lumen CSA area along the length of the target lesion. As most vessels depict an oval rather than a perfect circular shape, maximum lumen diameter and minimal lumen diameters are calculated along a vector passing through the lumen centre at the reference segments. Reference vessel lumen diameter is essential to guide section of interventional devices. Measurements of distances (length) are based on the automated pullback speed during image acquisition. Disease length can be calculated based on number of seconds or frames between the first and last image frames depicting the atherosclerotic plaque.

Intimal thickening

IVUS cannot distinguish between tunica intima and media.

Hence, IVUS-determined "intimal thickening" in non-stented vessels combines the thickness of both layers. Based on histologic and ultrasound data, coronary vessel wall with an intimal thickness ≥0.5 mm is considered to be diseased [21].

Assessment of atheroma burden

Quantification of atheroma or plaque area in cross-sectional IVUS images is performed by subtracting the lumen area from the EEL area. Hence, IVUS defined atheroma area is a combination of plaque plus media area. The atheroma area can be calculated in each frame (cross-sectional image), and total atheroma volume (TAV) can be calculated based on pullback speed during imaging acquisition. Atheroma volume can be reported as the percent of the volume of the external elastic membrane occupied by atheroma namely percent atheroma volume (PAV). Parameters commonly used to report the extent of the coronary atherosclerosis are shown in Figure 6 . Measurements are performed between the inner lumen border and the media, delimited by the IEL, which corresponds to the "true" histological area of the atheroma.

Assessment of ambiguous anatomy

The 3-dimensional and dynamic nature of the coronary vasculature cannot be fully appreciated by planar angiography. Frequently, defining the proper angiographic angulation that provides a straight, non-foreshortened view of the target coronary segment without overlapping of other vessels may be a challenge in the cathlab. As discussed previously, determination of disease severity by angiography is hampered by the diffuse nature of atherosclerosis and its most common eccentric growth in the vessel wall. Hence, lesions can appear more stenotic in one orthogonal view than in the other, making clinical decisions difficult. The so-called "intermediate lesion" is the more

$$TAV = (EEM_{CSA} - LUMEN_{CSA})$$

$$TAV_{norm} = \sum \frac{EEM_{CSA} - LUMEN_{CSA}}{\text{number of analyzed frames per patient}} \times \text{mean/median no. of analyzed frames in the population}$$

$$\%\ \text{change in TAV} = \frac{\text{TAV (follow-up)} - \text{(baseline)}}{\text{TAV (baseline)}} \times 100$$

$$PAV = \frac{\sum (EEM_{CSA} - LUMEN_{CSA})}{\sum EEM_{CSA}} \times 100$$

Figure 6. Parameters commonly used to report the extent of the coronary atherosclerosisare total atheroma volume (TAV) and percent atheroma volume (PAV).EEM: external elastic membrane; CSA: cross-sectional area.

prevalent phenotype in the coronary tree. The American Heart Association/American College of Cardiology/Society for Angiography and Interventions (AHA/ACC/SCAI) guidelines define intermediate coronary lesion as a plaque producing a 30-70 % stenosis between by angiography [76]. These plaques represent a heterogeneous group of coronary lesions, which can be either haemodynamically flow limiting or not. Intravascular imaging, particularly IVUS, was granted a class IIa indication (level of evidence C) for "evaluation of coronary obstruction at a location difficult to image by angiography in a patient with a suspected flow-limiting stenosis" [77].

IVUS minimum luminal cross sectional area (MLA) proved to be a good morphometric surrogate of coronary physiology.

IVUS MLA showed a direct correlation with coronary flow reserve determined by Doppler flow-wire ($r = 0.831$, $p < 0.001$) [77]. In 73 patients studied pre-intervention, a MLA of ≥4.0 mm^2 had a diagnostic accuracy of 89 % in predicting a coronary flow reserve > 2.0. Likewise, IVUS has been correlated with non-invasive single-photon emission computed tomography (SPECT) [79]. A 4 mm^2 MLA by IVUS had 88 % sensitivity and 90 % specificity to discriminate the SPECT (+) group from the SPECT (-) group. This cut-off of 4.0 mm^2 MLA does not apply to small vessels [80] or large segments such as the left main (LM) or venous bypass grafts. In a larger study (FIRST registry [187), 350 patients (367 lesions) were studied. In general, an MLA <3.07 mm^2 (64.0% sensitivity, 64.9% specificity, area under curve [AUC] 0.65) was the best threshold value for identifying FFR <0.8. Yet, stratifying by vessel size, an MLA <2.4 mm^2 (AUC 0.66) was best for reference vessel diameters (RVD) <3.0 mm, an MLA <2.7 mm^2 (AUC 0.71) for RVD of 3.0 to 3.5 mm, and an MLA <3.6 mm^2 (AUC 0.68) for RVD 3.5 mm.

Left main coronary artery

There is no absolute consensus regarding the CSA at which a left main obstruction is considered critical. A study evaluating IVUS assessment of 121 patients with intermediate LM lesions found no significant difference in MACE (death, non-fatal MI and TVR) after 3 years follow-up between patients with MLA < 7.5 mm^2 who underwent revascularisation and those with MLA > 7.5 mm^2 in whom revascularisation was deferred (21 % vs. 12 %). By contrast patients with MLA < 7.5 mm^2 who did not undergo revascularisation had a 3 year MACE rate of 50 % [80]. In another study, an IVUS-determined MLD of 2.8 mm and an MLA of 5.9 mm^2 had the highest sensitivity and specificity (93 % and 98 % for MLD, 93 % and 95 % for MLA, respectively) for detecting haemodynamic significant left main stenosis compared with FFR [82].

FOCUS BOX 1: RECOMMENDATION OF THE USE OF IVUS IN ESC GUIDELINES 2014 [188]	
IVUS should be considered to assess severity and optimize treatment of unprotected left main lesions	IIa/B
IVUS should be considered for optimization of stent implantation	IIa/B
IVUS and/or OCT should be considered to assess mechanisms of stent failure	IIa/C
Repeat Revascularization	
Restenosis: IVUS and/or OCT should be considered to detect stent-related mechanical problems **Stent Thrombosis:** IVUS and/or OCT should be considered to detect stent-related mechanical problems	IIa/C

Ostial and bifurcation disease

The continuous dynamic variation in the three-dimensional anatomical configurations of coronary bifurcations poses significant challenges to planar coronary imaging modalities. Intravascular imaging plays an important role in evaluating severity and distribution of atheroma in the bifurcation segment. IVUS has been also used to identify and characterise aorto-ostial disease. The concept of "plaque shift" to explain side branch occlusion during intervention in the main branch is not supported by IVUS and necropsy studies that have shown plaques most commonly located in the opposite side of side branches origins [69, 83]. The in vivo frequency and distribution of high-risk plaques (i.e., necrotic core rich) at bifurcations using a combined plaque assessment with IVUS virtual histology and optical coherence tomography have been reported. A total of 30 patients (103 bifurcations) were imaged. Twenty-seven fibroatheromas (26.2 %) and 18 thin-cap fibroatheromas (17.4 %) were found. Overall the % of necrotic core decreases from proximal to distal rim (16.8 % vs. 13.5 % respectively $p = 0.01$) while the cap thickness showed an inverse tendency (130 ± 105 vs. 151 ± 68 ìm for proximal and distal rim respectively $p = 0.05$). 44.1 % of the thin caps were located in the proximal rim, 41.2 % followed by the in-bifurcation segment and were less frequent in the distal rim (14.7 %). The proximal rim of the ostium of the side branch has been identified as a region more likely to contain thin fibrous cap and a greater proportion of necrotic core [84].

Cardiac allograft disease

Most clinical adverse events in transplant patients occur after 1 year. Cumulative incidence of cardiac events per patient year was 0.9 % within the first year, increasing to 1.9 % by

5 years. Cardiac events accounted for 3.8 % of the deaths by the end of the first year, rising to 18 % of total mortality by 7 years after heart transplantation. After the first year of transplantation, 36 % (20/55) of the patients died because sequelae of coronary artery disease [85]. Death is usually silent because heart is denervated. Therefore, there is a need for screening in order to early detect coronary atherosclerosis. The presence of obstructive coronary disease in angiography is a predictor of any cardiac event (odds ratio 3.44, $p < 0.05$), as well as a predictor of cardiac death (OR 4.6, $p < 0.05$). However, a pathological study reported 10 patients who died or underwent re-transplantation within 2 months of coronary angiography. One quarter of the patients had intermediate lesions or atheromatous plaques. Fresh or organising thrombus was most often associated with discrete lesions and accounted for all complete occlusions. Authors concluded that transplant coronary artery disease has a heterogeneous histologic and angiographic appearance, with angiographic underestimation of disease in some patients. Accordingly, many active transplant centres incorporated IVUS imaging into their post-transplant surveillance, but there is no consensus on how frequent IVUS should be performed. The predictive value of IVUS has been explored in a study that included 143 patients who underwent 3-vessel IVUS investigation at 1 and 12 months after transplantation. The change in intimal thickness was calculated (≥ 0.5 mm was defined as rapidly progressive vasculopathy). At one year, rapid progression was demonstrated in 37 % of the patients and in 47 % of them a new lesion was found. At 5.9 years, patients with rapid progression died more than their counterparts (26 % vs. 11 %, $p = 0.03$). The combined endpoint of death and MI was also more frequently seen in patients with rapid progression (51 % vs. 16 %, $p < 0.0001$) [86].

IVUS has been also used to assess novel therapies in heart transplantation recipients. Eisen et al., randomised 634 patients to receive 1.5 mg of everolimus per day (209 patients), 3.0 mg of everolimus per day (211 patients), or 1.0 to 3.0 mg of azathioprine per kilogram of body weight per day (214 patients), in combination with cyclosporine, corticosteroids and statins. The primary efficacy endpoint was a composite of death, graft loss or re-transplantation, loss to follow-up, biopsy-proved acute rejection of grade 3A, or rejection with haemodynamic compromise. At 1 year, IVUS showed that the average increase in maximal intimal thickness was significantly smaller in the two everolimus groups than in the azathioprine group [87].

CLINICAL APPLICATIONS: INTERVENTIONAL

The utilisation of intravascular imaging to guide percutaneous coronary interventions (PCI) is heterogeneously distributed across the world, varying from > 60 % of use during PCI in Japan to less than 20 % in Europe and United States. The explanation for such disparity is multifactorial, but likely involves local reimbursement practices for the procedure, differences in clinical practice and training, and a relative lack of scientific evidence.

Pre-interventional imaging

Intravascular imaging provides the only means to accurately determine vessel size, severity, character, extent and location of disease and guide therapeutic decision-making in the catheterisation laboratory. The main limitation of intravascular imaging is that, despite the extreme miniaturisation of IVUS catheters, these probes may occlude vessels with severe stenoses, which may disturb image acquisition and interpretation. The additional information provided by IVUS on lesion composition, eccentricity and length may change treatment strategies in up to 20 % of the cases [88]. As discussed previously, the presence, depth and circumferential distribution of calcification are very important factors for selecting the type of interventional device [89].

Non-stent based percutaneous coronary interventions

Contemporary PCI techniques are essentially based on stents, but balloon angioplasty remains an integral step of the procedure. In addition, atherectomy and plaque modification strategies remain necessary in some procedures. Thus, understanding of mechanisms and the proper utilisation of these techniques remains important in the modern era [90]. The importance of intravascular imaging is likely amplified in non stent-based interventions, with the goal of maximal luminal gain and minimal risk of dissection and vessel perforation. Selection of the device size can be based on measurements of the total vessel (i.e., EEM) diameter, although a more conservative approaches matching balloon size to that of lumen diameter of the distal reference segments is most routinely performed in practice. In the landmark CLOUT study [91], angioplasty was initially performed using angiography-define balloon sizes; then repeat angioplasty was performed guided by IVUS imaging. Even after achieving an "optimal" angiographic result, 73 % of the lesions needed larger sized balloons. These findings have been confirmed in other studies [70, 71, 72]. Modifications of the dilatation strategy based on IVUS results include changes in balloon diameter, length, type and inflation pressure. IVUS is also critical to define circumferential and longitudinal extension of plaque fracture or dissection, and to guide the need for further intervention.

Dissections can be classified into five categories: 1) intimal; 2) medial; 3) adventitial; 4) intramural haematoma (an accumulation of blood within the medial space, displacing the internal elastic membrane inward and EEM outward); and 5) intrastent [21].
The severity of a dissection can be quantified according to: 1) depth; 2) circumferential extent (in of arc); 3) length; 4) size of residual lumen (CSA); and 5) CSA of the luminal dissection [9].
Additional descriptors of a dissection may include the presence of a false lumen, the identification of mobile flap(s), the presence of calcium at the dissection border, and dissections in close proximity to stent edges.
IVUS studies have also been performed to define predictors of restenosis after balloon angioplasty. One of the main contributions of intravascular imaging to this field was the realisation that negative remodelling, not neointimal hyperplasia, was the most important mechanism of long-term failures of non-stented coronary interventions, namely restenosis. This was initially demonstrated in the peripheral vessels [92] and later reported in the coronary circulation [93]. These studies revealed that > 70 % of lumen loss was attributable to the decrease in EEM area, whereas the neointimal area accounted for only 23 % of the loss. Although stand-alone atherectomy coronary intervention is not used in modern practice, these techniques still play a role for plaque modification and facilitate stent deployment. The use of IVUS during atherectomy results in a more aggressive strategy, leading to a greater plaque removal and a larger lumen diameter [94]. The adjunctive use of IVUS-guided directional coronary atherectomy (DCA) prior to stenting was proposed in the SOLD registry [95], but the AMIGO randomised trial failed to show a benefit in terms of angiographic restenosis of DCA followed by coronary stenting compared to coronary stenting alone. While DCA technologies have been removed from the United States market, rotational atherectomy remains a niche technique to facilitate stent delivery in patients with severe coronary lesion calcification. IVUS can detect calcification, define the location and extent of calcification and help define the need for the use of rotational atherectomy in clinical practice. However, vessel calcification impacts delivery of the IVUS catheter and the quality of images, which hinders pre-intervention IVUS utilisation in many cases.

Stent-based percutaneous coronary interventions

Stents have become standard in virtually every percutaneous coronary intervention. IVUS has played a critical role in the establishment of modern stent deployment techniques. IVUS provides cross-sectional views of the stent and its interaction with the vessel wall enabling unique assessment of expansion, apposition, vessel dissection and residual untreated disease that cannot be properly defined by angiography. (Video 5) The pioneer

report of Colombo and co-workers revealing a mean residual stenosis of 51 % percent following angiography guided stent deployment and a high prevalence of incomplete stent apposition significantly altered the understanding of optimal stent deployment and prevention of subacute thrombosis [96]. After balloon inflations at higher pressures (typically 18-20 atm), use of a larger balloon or both, the operators were able to reduce the residual stenosis to 34 % which likely led to a 0.3 % rate of subacute thrombosis without the need for systemic post-procedure anticoagulation [96]. However, restenosis remained an important limitation of bare metal stents (BMS) affecting approximately 20 to 40 % of patients. "The bigger the better" adage which has dominated the interventional cardiology approach for decades [97] derived from angiography assessment of lumen gain and late loss, but it also suggests the importance of IVUS to optimise stent expansion and maximise lumen gain without the risk of vascular complication. The landmark MUSIC registry [5] helped defined IVUS criteria for optimal stenting and was based on 3 variables: 1) complete apposition of the stent over its entire length; 2) symmetric stent expansion defined by the ratio of minimal/maximal lumen diameter ≥ 0.7; 3) in-stent minimal lumen area ≥ 90 % of the average area of distal and proximal references or ≥ 100 % of the lumen area of the reference segment with the smallest lumen area. The subgroup of patients who met the criteria had a record 8 % rate of restenosis after bare metal stent implantation. However, the criteria are difficult to achieve in real practice. In the Optimal Stent Implantation Trial, stent were post-dilatated at 18 atmospheres and only 60 % reached the MUSIC criteria. In the Angiography Versus Intravascular Ultrasound Directed stent placement (AVID) trial, the more liberal goal of in-stent lumen CSA ≥ 90 % of the distal reference area was not achieved in > 70 % of 225 patients [5]. Other adaptations to the criteria have been suggested: a) 80 % average reference area and 90 % lumen area of the reference segment with smallest area, b) minimal in-stent lumen area ≥ 9 mm^2 and c) ratio of stent area to reference EEM area ≥ 0.55. However, these commonly employed IVUS endpoints based on a predefined stent-to-reference ratio are also difficult to achieve.

Several prospective clinical studies were conducted to test the hypothesis that IVUS guidance of stent deployment improves outcomes, but results are conflicting.
CRUISE was a large observational substudy involving 538 patients from the Stent Anticoagulation Regimen Study (STARS) a randomised multicentre trial testing different antithrombotic regimens and compared angiographic versus ultrasound guidance on a centre-by-centre basis. The study showed improvement in the rates of target vessel repeat revascularisation after 9 months in patients treated at centres using the IVUS-guided approach [99]. In the Optimisation with ICUS (OPTICUS) study, IVUS and angiographicguided approaches resulted in similar rates of both angiographic restenosis and need for target

vessel revascularisation [100]. The TULIP study [101] suggested that routine IVUS guidance for stent deployment was likely to be of benefit only in patients with a high risk for restenosis. A large retrospective study including 884 patients compared outcomes of IVUS-guided versus a propensity-score matched population undergoing drug-eluting stent (DES) implantation with angiographic guidance alone [6]. The study showed that IVUS-guidance during DES implantation reduced both DES thrombosis and the need for repeat revascularisation. These considerations may also explain the mortality reduction observed after 3 years in the patients treated with left main stenoses under IVUS guidance in the unpublished MAIN-COMPARE IVUS Registry. For restenoses after both conventional bare metal stents and DES. Knowledge of the initial mechanism of restenosis (under-expansion, hyperplasia, incomplete lesion coverage) is important for selecting the proper length and diameter of stent to be deployed and for guiding its expansion. Table 1 .

The focus of contemporary interventional cardiology has shifted towards improving the safety rather than efficacy of DES, as these devices virtually eliminated the problem of restenosis, but have been associated with late thrombosis.

IVUS studies were important to provide a morphological analysis of the local biological effects of the implantation of DES. Initial IVUS studies [102, 103] were essentially to confirm suppression of neointimal hyperplasia by DES. These studies also revealed the occurrence of new late incomplete stent apposition, which has been anecdotally associated with thrombosis. While no large randomised study has been conducted to support the approach of IVUSguided DES deployment, the use of IVUS has increased over the past decade. [6]. Clinical benefit has been suggested in large metaanalysis (14 studies involving 29,029 patients), with reductions in death (hazard ratio [HR]: 0.66, 95% confidence interval [CI]: 0.55-0.78, p<0.001), stent thrombosis (HR: 0.57, 95% CI: 0.44-0.73, p<0.001), myocardial infarction (MI) (HR: 0.74, 95% CI: 0.62-0.90, p=0.002) [189]; IVUS guidance has been advocated particularly in selected high-risk lesions (i.e. ACS patients as shown in ADAPT DES study-[189]) results from randomised clinical trials are still warranted to justify routine IVUS-guided DES implantation.

Diseased bypass grafts have been a challenge for both interventionists and cardiac surgeons. Intravascular imaging is important to guide stent size selection and define extent of disease. IVUS has also been used to monitor outcomes after treatment of vein grafts with DES. The SECURE study included 76 patients (n = 94 lesions) with graft disease treated with a sirolimus eluting stent, and 14 patients had IVUS follow-up performed at 8 months. Overall, the percentage of intimal hyperplasia was 11.8 ± 16.5 % and half of the patients with graft sirolimus-eluting stent had < 1 % intimal hyperplasia [104]. In the setting of a randomised trial, 75 patients with graft disease (96 lesions) that received

Table 1. IVUS criteria of optimal stent expansion. CSA, cross-sectional area.

Historical milan criteria

Criteria were governed by the principles of optimising stent expansion and covering the full extent of the lesion in order to minimise any potential impairment to flow that could contribute to stent thrombosis,

- Qualitative evaluation of the stent site involving the achievement of good stent apposition to the vessel wall with good plaque compression.
- Achievement of a quantitative assessment of optimal stent expansion.
  - Or 60 % of the average of the proximal and distal reference CSA (used for the majority of lesions, initially chosen to accommodate the compensatory dilatation that occurs with early atheroma deposition).
  - Or an intrastent lumen CSA equal or greater than the distal reference lumen CSA (was adjusted during the course of the investigation in order to simplify the criterion and because of the perceived overriding importance of not leaving the stent with a stenosis relative to the distal lumen rather than achieving a specified percent dilatation relative to the reference vessel).
- The non-stented segments immediately adjacent to the stent (proximal or distal) did not reveal evidence of a significant lesion defined as a CSA stenosis > 60 %.
- Achievement of symmetrical stent expansion (never used alone independently of CSA measurements).

MUSIC (Multicentre Ultrasound guided Stent Implantation in the Coronaries), later adopted and modified in the OPTICUS (OPTimisation with ICUS to reduce stent restenosis) study

Based on a comparison between lumen inside the stent and lumen of the proximal and distal reference segment.

- Complete apposition of the stent over its complete length.
- In-stent minimal lumen area greater or equal to 90 % of the average reference area or greater or equal to 100 % of the lumen area of the reference segment with the smallest lumen area; this criterion was modified because attainable only in a minority of lesions into: 80 % average reference lumen area and 90 % lumen area of the reference segment with the smallest area) if minimal lumen area inside the stent is equal or greater than 9 mm^2
- Symmetric stent expansion defined by the ratio minimal/maximal lumen diameter greater or equal to 0.7.

AVID (Angiography Versus Intravascular ultrasound-Directed stent placement)

- Smallest cross-sectional area within the stent > 90 % of the distal reference vessel lumen cross-sectional area.
- Full apposition of the stent to the vessel wall.
- No major dissections (dissections involving exposure of the media should be covered by stent placement).

PRAVIO (Preliminary Investigation to the Angiographic Versus IVUS Optimisation Trial)

IVUS criteria recently proposed by the Milan group based on vessel remodelling that results in an increment in the final minimum lumen diameter (MLD) compared to angiographic guidance.

- The final stent CSA (cross-sectional area) should be > 70 % of the optimal balloon CSA. The diameter of the optimal balloon was calculated according to the vessel media-to-media diameters at various sites inside the stented segment (proximal, mid lesion, distal, and any other points of interest. These diameters were averaged and this value determined the diameter of the post-dilating balloon).

Optimisation balloon (mm)	Optimisation balloon 100 % (mm^2)	Target CSA = 70 % optimisation balloon cross-sectional area (mm^2)
2.5	4.91	3.43
3	7.07	4.95
3.5	9.62	6.73
4	12.57	8.80
4.5	15.90	11.13

either sirolimus-eluting stents or bare metal stents (RRISC study) were assessed by IVUS at 6 months.
Sirolimus-eluting stents showed smaller neointimal hyperplasia volume compared with BMSs (1.3 vs. 24.5 mm^3, $p < 0.001$). In the sirolimus-eluting stent group, there was a greater intimal hyperplasia at overlapping sites as compared to non-overlapping segments [105].

Assessment of complications after percutaneous coronary intervention thrombosis

Intravascular imaging can play an important role in both prevention and diagnosis of stent thrombosis. Stent underexpansion, incomplete wall apposition and vessel dissection, features easily identified by intravascular imaging, have been associated with increased risk of stent thrombosis [106]. The minimum stent cross-sectional area (4.3 ± 1.6 mm^2 vs. 6.2 ± 1.9 mm^2, $p < 0.001$) and the degree of stent expansion (0.65 ± 0.18 vs. 0.85 ± 0.14, $p < 0.001$) were significantly smaller patients with DES versus those without DES thrombosis [107]. The same study also showed that residual edge, defined as edge lumen CSA < 4 mm^2, and a plaque burden > 70 % was associated with risk of thrombosis. Intravascular imaging is also essential to identify mechanical abnormalities in patient presenting with stent thrombosis. Cook S. et al. [108] reported that very late DES thrombosis is associated with eosinophilic infiltrates and intravascular ultrasound evidence of vessel remodelling. Degree of inflammation correlated with the extent of stent malapposition.
Dedicated studies have been reported in which the use of IVUS is central during index PCI in order to prevent a future stent thrombosis. The Assessment of Dual Antiplatelet Therapy With Drug-Eluting Stents (ADAPT-DES) was a nonrandomized "all-comers" study of 8583 consecutive patients aiming at charaterizing the frequency, timing, and correlates of stent thrombosis and adverse clinical events after DES. IVUS guidance compared with angiography guidance reduced definite/probable stent thrombosis (0.6% [18 events] versus 1.0% [53 events]; adjusted hazard radio, 0.40; 95% confidence interval, 0.21-0.73; P=0.003), myocardial infarction (2.5% versus 3.7%; adjusted hazard radio, 0.66; 95% confidence interval, 0.49-0.88; P=0.004), and composite adjudicated major adverse cardiac events (ie, cardiac death, myocardial infarction, or stent thrombosis) (3.1% versus 4.7%; adjusted hazard radio, 0.70; 95% confidence interval, 0.55-0.88; P=0.002) at 1-year. [190]

Restenosis

Unlike restenosis after balloon angioplasty or atherectomy, IVUS studies have shown that in-stent restenosis is essentially a result of neointimal hyperplasia. (Video 6) Predictors of stent restenosis have been identified by multivariate analyses and include small reference

vessel and lumen size, the larger plaque burden and small in-stent lumen area. While the prevalence of restenosis has decreased dramatically with DES, maximising luminal gain remains an important approach to prevent restenosis. Receiver operating characteristic curves identified a post-stenting minimum stent CSA of 5 mm^2 for sirolimus-eluting stent, 6.5 mm^2 for bare metal stents were associated with lumen CSA > 4 mm^2 at 8-months follow-up [109]. Others have shown that the highest restenosis rate was observed in lesions with stent area < 5.5 mm^2 and stent length > 40 mm after deployment of sirolimus-eluting stents [110].

Intravascular imaging is also essential to guide therapy of in-stent restenosis as mechanical problems related to stent deployment procedures contribute to approximately 25 % of in-stent restenosis [111]. Stent fracture has been reported as a cause of stent restenosis in the modern era of long stent implantation, which can be identified by intravascular imaging [112]. Intravascular imaging has shown that characteristics of neointimal hyperplasia may differ between bare metal and DES. Neointimal hyperplasia in DES may have an echolucent appearance, also known as a black hole [112].

In addition, while diffuse in-stent restenosis is common after bare metal stents, the pattern of restenosis associated with DES is most frequently focal. One of the most common variables used to report restenosis is percentage intimal hyperplasia volume in the stent segment [114]. This variable normalises the intimal hyperplasia to the stent length therefore allowing the comparison of different stent types (BMS vs. DES), as well as different drug types (i.e., SES vs. PES). Table 2 . The percentage of intimal hyperplasia, however, minimises the impact of focal restenosis. A metaanalysis of TAXUS IV, V and VI demonstrated that nearly half of the stent length was free of IH in the Taxus group (48.8 ± 36.0 % vs. 13.4 ± 22.1 % in the control group, $p < 0.0001$) [115]. In another study comparing the paclitaxel stent and sirolimus stent, 46.1 vs. 5.4 % of the stent length had covering, $p < 0.001$, respectively [116]. A similar intimal hyperplasia distribution to the Taxus stent has been reported for the zotarolimus-eluting stent [117]. It has been suggested that the "patchy" distribution of intimal growth associated with DES (i.e., lack of neointimal tissue in the mid-portion of the stent) could be related to a higher concentration of drug in that portion of the stent [118].

The use of IVUS-VH to assess in-stent restenosis in metal stents is hampered by the following factors: lack of validation of the technique in this context, misclassification of the stent struts as "dense calcium" surrounded by necrotic core, and the potential interference of the superficial stent struts on the backscattering of the tissue behind them [119]. On the contrary, IVUS-VH can be used in research protocols evaluating serial changes in plaque type and composition in bioabsorbable stents.

Table 2. Percentage of intimal hyperplasia volume in drug-eluting stent trials assessed by intravascular ultrasoundSES: sirolimus-eluting stents; PES: paclitaxel-eluting stents; ZES: zotarolimus-eluting stent; EES: everolimus-eluting stent.† median (inter-quartile range).‡ percentage of neointimal volume index.Table modified from Mintz G. [111].

Trial	Subgroup	Follow-up	% IH Vol (Mean ± SD)
Sirolimus ES trials			
RAVEL [132]	SES (n = 48) BMS (n = 47)	6 mo	1 ± 3 % 29 ± 20 %
RAVEL [133]	SES, diabetes mellitus (n = 19) SES, no diabetes (n = 25)	9 mo	0.82 ± 1.38 %† 30.2 ± 22.9 %
SIRIUS [134]	SES (n = 23) BMS (n = 20)	9 mo	3.1 %
Sao Paulo registry [135, 137]	SES fast release	1 yr (n = 15) 2 yr (n = 14) 4 yr (n = 13)	2.3 ± 5.5 % 6.3 ± 5.5 % 9.1 ± 5.4 %
Sao Paulo registry	SES slow release	1 yr (n = 15 2 yr (n = 14) 4 yr (n = 13)	2.2 ± 3.4 % 7.5 ± 7.3 % 5.7 ± 4.25 %
SICTO [138]	SES for CTO (n = 25)	6 mo	4.9 ± 6.8 %
Sao Paulo [139]	SES (n = 25) _ radiation (n = 25)	12 mo	6.6 ± 3.0 % 38.0 ± 7.8 %
DIABETES I [140]	SES for diabetics (n = 75) BMS for diabetics (n = 65)	9 mo	1.31 ± 3.5 % 28.4 ± 21.9 %
RIBS II§ [141]	SES (n = 76) Balloon angioplasty (n = 74)	9 mo	279 mm^3 [IQR 227 to 300] 197 mm^3 [IQR 177 to 230]
FIM&RAVEL (Sao Paulo) (TCT 2008-426,p164i)	SES (n = 38)	9 mo 21 mo	1.1 ± 2.2 % 1.8 ± 1.9 %
Paclitaxel ES trials			
TAXUS II [142]	Polymeric PES slow release (n = 131) BMS (n = 136)	6 mo	7.84 ± 9.9 % 23.17 ± 18.19 %
TAXUS II [143]	Polymeric PES moderate release (n = 135) BMS (n = 134)	6 mo	7.84 ± 9.7 % 20.54 ± 16.68 %
TAXUS IV [144]	Polymeric PES slow release (n = 88) BMS (n = 82)	9 mo	12.2 ± 12.4 %
TAXUS V	Polymeric PES (n = 149) BMS (n = 135)	9 mo	10.7 ± 10.8 % 31.8 ± 15.1 %
Meta-analysis of TAXUS IV, TAXUS V, and TAXUS VI [144]	Polymeric PES (n = 45) Overlapping Nonoverlapping BMS (n = 35) Overlapping Nonoverlapping	9 mo	 9.8 ± 12.0 % 11.3 ± 10.9 % 39.0 ± 17.1 % 33.4 ± 16.6 %
Meta-analysis of TAXUS IV, TAXUS V, and TAXUS VI [145]	Patients with diabetes mellitus Polymeric PES (n = 84) BMS (n = 70) Patients without diabetes mellitus Polymeric PES (n = 208) BMS (n = 204)	9 mo 9 mo 	 13.7 % 34.9 % 11.9 % 30.1 %
Meta-analysis of TAXUS IV, TAXUS V, and TAXUS VI [146]	Lesions ≥ 26 mm Polymeric PES (n = 38) BMS (n = 29)	9 mo	 13.4 ± 9.2 % 34.6 ± 15.7 %
TAXUS V ISR i2 Summit 2006. Abstract 2402.	BMS in-stent restenosis Polymeric PES (n = 42) Brachytherapy (n = 41)	9 mo	 12.2 ± 10.3 % 32.4 ± 11.7 %
ASPECT [147]	Low-dose nonpolymeric PES (n = 17) High-dose nonpolymeric PES (n = 19) BMS (n = 17)	6 mo	12.3 ± 8.7 % 9.0 ± 10.4 % 21.6 ± 13.7 %

Table 2. Continued

Trial	Subgroup	Follow-up	% IH Vol (Mean ± SD
ASPECT [147]	Low-dose nonpolymeric PES (n = 17) High-dose nonpolymeric PES (n = 19) BMS (n = 17)	2 yr	15.9 ± 9.0 % 21.9 ± 13.7 % 23.3 ± 16.2 %
DiabeDES [116]†	SES (n = 66) PES (n = 64)	8 mo	0.0 % (0.0-0.0) 7.5 % (0.1-27.0)
Other DES trials			
ENDEAVOR II [148]‡	BMS (n = 165) Polymeric ZES (n = 178)	8 mo	29.4 ± 17.2 % 17.6 ± 10.1 %
ENDEAVOR III [117]	Polymeric ZES (n = 190) Polymeric SES (n = 68)	8 mo	1.1 ± 0.8 mm^3/mm 0.2 ± 0.1 mm^3/mm
ENDEAVOR IV [149]	Polymeric ZES (n = 79) Polymeric PES (n = 86)	8 mo	16.6 ± 12.0 % 9.9 ± 8.9 %
ENDEAVOR in real world (registry) [150]	Polymeric ZES (n = 100)	6 mo	14.4 ± 13.4 %
RESOLUTE FIM [151]	Polymeric ZES (n = 30)	4 mo	2.23 ± 2.43 %
RESOLUTE [152]	Polymeric ZES (n = 130)	9 mo	3.73 ± 4.05 %
NOBORI I [153]	Polymeric Biolimus A9 (n = 36) Polymeric PES (n = 15)	9 mo	2.2 ± 6.0 % 8.9 ± 9.2 %
STEALTH SOLACI 2007 by Abizaid A	Polymeric Biolimus A9 (n = 80) BMS (n = 40)	6 mo	3.2 ± 2.5 % 32 ± 18 %
CUSTOM II &III (TCT 2008-345,p137i)	Polymeric Biolimus A9 long lesion (n = 20) Polymeric Biolimus A9 short lesion (n = 48)	6 mo	5.9 ± 8.0 % 2.6 ± 5.2 %
AXXESS PLUS [154]	Polymeric Biolimus A9 (n = 49)	6 mo	2.3 ± 2.2 %
AXXENT [155]	Polymeric Biolimus A9 (n = 26)	6 mo	3.0 ± 4.1 %
SPIRIT I [156]	Polymeric EES (n = 21) BMS (n = 24)	6 mo	8.0 ± 10.4 % 28.1 ± 14 %
SPIRIT I [157]	Polymeric EES (n = 16) BMS (n = 21)	12 mo	10.0 ± 7.0 % 28.0 ± 12.0 %
SPIRIT II [158]	Polymeric EES (n = 225) Polymeric PES (n = 75) Polymeric EES (n = 64) Polymeric PES (n = 31)	6 mo 24 mo 	2.5 % 7.4 % 5.2 % 5.8 %
SPIRIT III TCT 2008-347,p138i)	Polymeric EES (n = 115) Polymeric PES (n = 45) EES Japan (n = 79)	8 mo	7.0 ± 6.7 % 11.1 ± 10.5 % 3.4 ± 4.1 %
EXCELLA FIM [159]	Novolimus eluting stent (n = 15)	4 mo 8 mo	2.6 ± 2.6 % 6.0 ± 4.4 %
GENESIS [160]	Costar PES (n = 16) SymBio P and Pimecrolimus ES (n = 26) Corio Pimecrolimus ES (n = 16)	6 mo	16.6 ± 12 % 27.1 ± 12.4 % 41.2 ± 11.5 %
Non-polymer SES [161]	Non-polymer Vestasync SES(VES) (nn = 15)	9 mo	4.0 ± 2.2 %
ABSORB [162, 163]	Bioresorbable vascular scaffold (n = 29)	6mo	5.54 % (8.45)

Percentage of intimal hyperplasia volume in drug-eluting stent trials assessed by intravascular ultrasound (continued).

SES: sirolimus-eluting stents; PES: paclitaxel-eluting stents; ZES: zotarolimus-eluting stent; EES: everolimus-eluting stent.
† median (inter-quartile range).
‡ percentage of neointimal volume index.
Table modified from Mintz G. [111].

RESEARCH APPLICATIONS

Intravascular imaging has played an important role in the understanding of atherosclerosis disease in humans and translation of novel therapies to the clinical arena.

Drug effects on atherosclerosis

The initial observations about a positive continuous relationship between coronary heart disease risk and blood cholesterol levels led to the conduction of a number of IVUS-based studies to evaluate the effect of different lipid lowering drugs on atheroma size. Changes in plaque characteristics may be a more relevant endpoint to predict risk of vascular thrombosis than plaque progression or regression of mild to moderate disease, but imaging tools to accurately evaluate plaque characteristics were not available until recently. Other limitations of using conventional greyscale IVUS to assess the natural history of atherosclerosis should be enumerated: 1) catheterisation, which is an invasive procedure, is required for serial imaging; 2) only a segment of the coronary tree can be studied; 3) plaque composition is not obtained; and 4) there is no direct evidence linking changes in coronary plaques and clinical events. The efficacy of lowering LDL-C with inhibitors of hydroxymethylglutaryl coenzyme A reductase (statins) is unequivocal; however the change in atheroma size by statins is not constant across all IVUS studies. There are many potential explanations for these discrepancies in IVUS studies such as drug properties, dose, and duration of treatment. In early studies like the GAIN study [120], atheroma volume was not reduced by atorvastatin despite the reduction in LDL-C (86 vs. 140 mg/dL) at 12 months. In contrast, the REVERSAL study [3] showed that LDL-C levels were further lowered by atorvastatin versus pravastatin (110 mg/dL vs. 79 mg/dL), which was associated with an increased of 2.7 percent of atheroma volume in pravastatin-treated patients, and in a 0.4 percent reduction in atheroma volume in atorvastatin-treated patients. The clinical significance and accuracy of IVUS for such measurements are still debatable, but these results were "statistically significant". The PROVE-IT study [121], showed that the lower the LDL-C and CRP values, the greater the reduction in clinical events and atheroma progression.

The first study showing regression of plaque size was the ASTEROID trial (A Study to Evaluate the Effect of Rosuvastatin on Intravascular Ultrasound-Derived Coronary Atheroma Burden) [4]. At 24 months, treatment with rosuvastatin 40 mg daily resulted in lowering of LDL-C to 60.8 mg/dL and elevation of high-density lipoprotein cholesterol (HDL-C) by 14.7 %. These lipid effects were associated with statistically significant, albeit small reductions in percent atheroma volume (0.79 %) and total atheroma volume (6.8 %).

In another cohort of patients similar to ASTEROID, so called IBIS 4 [191], 103 STEMI patients were imaged with IVUS and radiofrequency ultrasonography (IVUS-VH) of the two non-infarct-related epicardial coronary arteries (non-IRA) after successful primary PCI. Patients received rosuvastatin (40 mg/day) for 13 months and serial intracoronary imaging with the analysis of matched segments was available for 82 patients with 146 non-IRA. After 13 months, PAV of the non-IRA decreased by -0.9% (95% CI: -1.56 to -0.25, P = 0.007). Patients with regression in at least one non-IRA were more common (74%) than those without (26%). Percent necrotic core remained unchanged (-0.05%, 95% CI: -1.05 to 0.96%, P = 0.93) as did the number of RF-IVUS defined thin cap fibroatheromas (124 vs. 116, P = 0.15). IVUS studies have also demonstrated coronary plaque modification in HDL-treated patients. The infusion of synthetic HDL-C particles containing the variant apolipoprotein, apoA-I Milano, complexed with phospholipids (ETC-216) reduced the percent atheroma volume by – 1.06 % (3.17 % p = 0.02 compared with baseline) in the combined ETC-216 group at 5 weeks. On the contrary, in the placebo group, percent atheroma volume increased by 0.14 % (3.09 %; p = 0.97 compared with baseline. In the ERASE study [122], 60 patients were randomly assigned to receive 4 weekly infusions of placebo (saline), 111 to receive 40 mg/kg of reconstituted HDL (CSL-111); and 12 to receive 80 mg/kg of CSL-111. The latter was discontinued due to liver function test abnormalities. Within the treated group, the percentage change in atheroma volume was −3.4 % with CSL-111 (p < 0.001 vs. baseline), whilst for the placebo group was – 1.6 % (P = 0.48 between groups). It is still unclear what the future holds for these therapeutical agents.

Patients with human deficiency of cholesterylester transfer protein (CETP) have elevated circulating levels of HDL-C. This has led to investigation on CETP inhibition as a novel and potentially effective approach to elevate HDL-C. In the ILLUSTRATE trial, the percent atheroma volume (the primary efficacy measure) increased was similarly low in patients receiving atorvastatin monotherapy versus in those receiving the combined torcetrapib–atorvastatin therapy after 24 months (0.19 % vs. 0.12 %, respectively) [123].

The enzyme acyl–coenzyme A:cholesterol acyltransferase (ACAT) esterifies cholesterol in a variety of cells and tissues. Inhibition of ACAT1, by blocking the esterification of cholesterol, could prevent the transformation of macrophages into foam cells and slow the progression of atherosclerosis, while inhibition of ACAT2 would be expected to decrease serum lipid levels. In the ACTIVATE study, the change in percent atheroma volume was similar in the pactimibe (100 mg daily) and placebo groups (0.69 percent and 0.59 percent, respectively; P = 0.77) [124].

Systolic blood pressure has been shown to be an independent predictor of plaque progression by IVUS [124]. A randomised study of patients with CAD and a diastolic blood pressure < 100 mmHg treated with placebo or antihypertensive therapy using either

amlodipine 10 mg daily or enalapril 20 mg daily showed that patients treated with amlodipine had a reduction in plaque size and also a reduction in cardiovascular events as compared to placebo at 24 months [125]. The PERSPECTIVE study [126], a substudy of the EUROPA trial, evaluated the effect of perindopril on coronary plaque progression in 244 patients. There were no differences in changes in IVUS plaque measurements detected between the perindopril and placebo groups. Thiazolidinediones (TZDs) increase insulin sensitivity in peripheral tissues thereby lowering glucose. In addition, TZDs (i.e., rosiglitazone and pioglitazone) lower blood pressure, inflammatory markers, and improve lipid profile, endothelial function, and carotid IMT. TZDs may therefore reduce progression of coronary atherosclerosis compared to other antidiabetic drugs. Two studies have addressed this question. The APPROACH study and the PERISCOPE (Comparison of Pioglitazone vs. Glimepiride on Progression of Coronary Atherosclerosis in Patients With Type 2 Diabetes) trials [127]. Rosiglitazone significantly reduced normalised total atheroma volume (TAV) by 5.1 mm^3 (95 % CI −10.0, −0.3; p = 0.04) when compared to glipizide, whereas pioglitazone just failed to achieve statistically significant in change in total atheroma volume (−5.5 ± 1.6 vs. −1.5 ± 1.5 mm^3, p = 0.06) when compared to glimepiride. Change in PAV in the APPROACH study was not different in patients allocated to glipizide or rosiglitazone (–0.64 %, 95 % CI –1.46, 0.17; p = 0.12), while in the PERISCOPE study pioglitazone vs. glimepiride was associated with favorable effects on change of PAV (–0.16 ± 0.21 vs. 0.73 ± 0.20 %, p = 0.002). Pioglitazone resulted in comparable plaque size reduction as rosiglitazone but this reduction was associated with an almost double reduction in vessel size so that the change in normalised lumen volume was quite comparable. Change in percent atheroma volume with as numerator change in atheroma volume and as denominator change in vessel volume, may mask the specific directional changes in its numerator and denominator when used as primary endpoint to compare two pharmacological agents.

There are several recent reports showing serial changes of plaque composition in patients treated with various statin treatments. In one of them, patients with stable angina pectoris (n = 80) treated with fluvastatin for one year had significant regression of plaque volume, and changes in atherosclerotic plaque composition with a significant reduction of fibrofatty volume ($p < 0.0001$). This change in fibrofatty volume had a significant correlation with change in LDL-cholesterol level ($r = 0.703$, $p < 0.0001$) and change in hsCRP level ($r = 0.357$, $p = 0.006$) [128]. Of note, the necrotic core did not change significantly. In a second study, Hong et al. randomised 100 patients with stable angina and ACS to either rosuvastatin 10 mg or simvastatin 20 mg for 1 year. Overall necrotic core volume significantly decreased ($p = 0.010$) and fibrofatty plaque volume increased ($p = 0.006$) after statin treatments. Particularly, there was a significant decrease in necrotic

core volume (p = 0.015) in rosuvastatin-treated subgroup. By multiple stepwise logistic regression analysis, they showed that the only independent clinical predictor of decrease in necrotic core volume was baseline HDL-cholesterol level (p = 0.040, odds ratio: 1.044, 95 % confidence interval (CI): 1.002 to 1.089) [129].

The IBIS 2 study compared the effects of 12 months of treatment with darapladib (oral Lp-PLA2 inhibitor, 160 mg daily) or placebo in 330 patients [130]. Endpoints included changes in necrotic core size (IVUS-VH), and atheroma size (IVUSgreyscale).

Background therapy was comparable between groups, with no difference in LDL-cholesterol at 12 months (placebo: 88 ± 34 and darapladib: 84 ± 31 mg/dL, p =0.37). In the placebo-treated group, however, necrotic core volume increased significantly, whereas darapladib halted this increase, resulting in a significant treatment difference of –5.2 mm^3 (p = 0.012). These intra-plaque compositional changes occurred without a significant treatment difference in total atheroma volume (Table 3).

Vascular response to endovascular devices

IVUS has been extensively used as surrogate endpoint in stent trials, primarily to assess effectiveness of devices as it relates to neointimal proliferation. IVUS was an essential investigational tool during initial clinical testing of DES [102, 103], confirming the dramatic suppression of neointimal proliferation, revealing new patterns of restenosis and establishing intravascular imaging metrics of stent optimisation as described above.

Recently, the feasibility and safety of a bioabsorbable everolimus-eluting vascular scaffold (BVS) was also assessed with intravascular imaging. In a prospective, open label study, 30 patients with a single de novo lesion that was suitable for treatment with a single BVS were enrolled. At 6-month follow-up, the angiographic in-stent late loss was 0.44 (0.35) mm and was mainly due to a reduction of the stent area (-11.8%) as measured by intravascular ultrasound. The neointimal area was small (0.30 [SD 0.44] mm^2), with a minimal area obstruction of 5.5% [192]. At 2 years, intravascular ultrasound showed a significant increase in minimal luminal area and average luminal area and volume, together with a significant decrease in plaque area and volume between 6 months and 2 years [193]. At 5 years, some patients were re-imaged and the complete IVUS findings are shown in figure 15 [194].

In the backscatter radiofrequency analysis, stent struts are classified as dense calcium (DC) and necrotic core (NC) by IVUS-VH. IVUS-VH changes at 6 months suggest alteration of the BVS with reduction of RF backscattering by polymeric struts. [119].

Table 3. Intravascular ultrasound progression/regression studies.IVUS: intravascular ultrasound; IB: integrated backscatter; VH: vir tual histology.

Study	Design	Year	Treatment	n	FU	Primary endpoint	Results (mean ± SD)
Statin trials							
GAIN [120]	RCT	2001	atorvastatin	48	12 months	Plaque volume	2.5 ± 24.9 mm^3
			control	51			11.8 ± 31 mm^3
ESTABLISH [164]	RCT	2004	atorvastatin	24	6 months	% change in plaque volume	13.1 ± 12.8 %
			control	24			± 14.9 % 8.7
REVERSAL [3]	RCT	2004	atorvastatin	253	18 months	% change in plaque volume	4.1 ± 29.6 %
			pravastatin	249			5.4 ± 20.1 %
Jensen [165]	Observational	2004	simvastatin	40	12 months	% change in plaque volume	6.30 %
Petronio [166]	RCT	2005	simvastatin	36	12 months	Plaque volume	–2.5 ± 3.0 mm^3/mm
			control	35			1.0 ± 3.0 mm^3/mm
Nishioka [167]	Observational	2004	pravastatin, atorvastati, simvastatin and fluvastatin	22	6 months	Plaque volume	30.9 ± 15.6 mm^3
			control	26			35.5 ± 12.7 mm^3
Tani [168]	RCT	2005	pravastatin	52	6 months	% change in plaque volume	–14.4 ± 23 %
			control	23			1.1 ± 4.6 %
ASTEROID [169]	Observational	2006	rosuvastatin	349	24 months	Change in PAV	–0.98 ± 3.15 %
Takashima [170]	Observational	2007	pitavastatin	41	6 months	% change in plaque volume	–10.6 ± 9.4 %
			control	41			8.1 ± 14.0 %
COSMOS [171]	Observational	2009	rosuvastatin	126	18 months	Change in PAV	–5.1 ± 14.1 %
JAPAN-ACS [172]	RCT	2009	atorvastatin	127	8-12 months	% change in plaque volume	–18.1 ± 14.2 %
			pitavastatin	125			–16.9 ± 13.9 %
Hirayama	Observational	2009	atorvastatin	28	28 weeks	% change in plaque volume	–9.4 ± 10.3 %
					80 weeks		–18.9 ± 14.1 %
ACAT (acyl coenzyme A:cholesterol acyltransferase) inhibitor trials							
A-PLUS [173]	RCT	2004	avasimibe 50 mg	108	24 months	Change in PAV	0.7 ± 0.4 %
			avasimibe 250 mg	98			0.8 ± 0.4 %
			avasimibe 750 mg	117			1.0 ± 0.3 %
			placebo	109			0.4 ± 0.4 %
ACTIVATE [124]	RCT	2006	pactimibe	206	18 months	Change in PAV	0.69 ± 0.25 %
			placebo	202			-0.59 ± 0.25 %
Increasing high-density lipoprotein therapies							
ApoA-I Milano [174]	RCT	2003	ApoA-I Milano 15mg/kg	21	5 weeks	Change in PAV	–1.29 ± 3.5 %
			ApoA-I Milano 45mg/kg	15			–0.73 ± 2.8 %
			Placebo	11			0.14 ± 3.09 %
ERASE [122]	RCT	2007	CSL-111 (reconstituted HDL infusion)	89	4 weeks	% change in plaque volume	–3.41 (IQR, –6.55 to 2.25)
			placebo	47			–1.62 (IQR, -5.95 to 1.94)
CART-2 [175]	RCT	2008	Succinobucol (AGI-1067)	183	12 months	Absolute change in plaque volume	–3.4 ± 14.5 mm^3
			placebo	49			–0.6 ± 13.4 mm^3
Other therapies							
CAMELOT [125]	RCT	2004	amlodipine	91	24 months	Change in PAV	0.5 ± 3.9 %
			enalapril	88			0.8 ± 3.7 %
Waseda	Observational	2006	losartan	41	7 months	Change in plaque area	–9.9 ± 3.1 mm^2
			non ARB	23	7 months		–9.1 ± 2.7 mm^2

Table 3. Continued

Study	Design	Year	Treatment	n	FU	Primary endpoint	Results (mean ± SD)
ILLUSTRATE [123]	RCT	2007	torcetrapib + atorvastatin	464	24 months	Change in PAV	0.12 ± 2.99 %
			atorvastatin	446			0.19 ± 2.83 %
PERSPECTIVE [126]	RTC	2007	perindopril	75	36 months	Change in plaque area	−0.2 ± 1.6 mm^2
			placebo	69			−0.1 ± 1.2 mm^2
PERISCOPE [127]	RCT	2008	pioglitazone	179	18 months	Change in PAV	−0.16 % (9 5 % CI, −0.57 % to 0.25 %)
			glimepiride	181			0.73 % (95 % CI, 0.33 % to 1.12 %)
STRADIVARIUS [176]	RCT	2008	rimonabant	335	18 months	Change in PAV	0.25 % (95 % CI, −0.04 % to 0.54 %)
			placebo	341			0.51 % (95 % CI, 0.22 % to 0.80 %)
ENCORE II [177]	RCT	2009	nifedipine	97	18-24 months	% change in plaque volume	5.0 (95 % CI, −1.3, 11.2)
			placebo	96			3.2 (95 % CI,-1.9, 8.3)
APPROACH	RCT	2010	rosiglitazone	233	18 months	Change in PAV	−0.21 (95 % CI, −0.86, 0.44)
			glipizide	229			0.43 (95 % CI, −0.22, 1.08)
IVUS-based tissue characterisation studies							
Yokoyama	RCT	2005	atorvastatin	25	6 months	Overall plaque size and tissue characterisation by IB IVUS	Atorvastatin reduced plaque size and changed plaque composition
			control	25			
Kawasaki [178]	RCT	2005	pravastatin	17	6 months	Overall tissue characterisation by IB IVUS	Statins reduced lipid without changes in plaque size
			atorvastatin	18			
			diet	17			
IBIS 2 [130]	RCT	2008	darapladib	175	12 months	Necrotic core vol by IVUS VH	Darapladid reduced significantly necrotic core
			placebo	155			
Nasu [128]	Observational	2009	fluvastatin	40	12 months	Overall tissue characterisation by IVUS VH	Fluvastatin reduced plaque volume and fibro-fatty
			control	40			
Hong [129	RTC	2009	simvastatin	50	12 months	Overall tissue characterisation by IVUS VH	Both reduced necrotic core and increased in fibrofatty volume
			rosuvastatin	50			
Toi	RCT	2009	atorvastatin	80	2-3 weeks	Overall tissue characterisation by IVUS VH	Pitavastatin reduced plaque volume and fibrofatty
			pivastatin	80			
Miyagi	Observational	2009	statin (pravastatin, pitavastatin, atorvastatin, fluvastatin, simvastatin) non statin	44	6 months	Overall tissue characterisation by IB IVUS	Statins reduced lipid and increased fibrous

IVUS: intravascular ultrasound; IB: integrated backscatter; VH: vir tual histology.

FUTURE DIRECTIONS

In the future, integration of multiple image technologies in a single catheter is likely to provide a more comprehensive assessment of the coronary vasculature. The combined use of IVUS-VH analysis and OCT seems to improve the accuracy for TCFA detection [83, 131]. Another potential combination is NIR spectroscopy and OCT; both imaging techniques are light-based, which may facilitate their combination in one single catheter. Using NIRS, an accurate characterisation of necrotic core can be achieved, while OCT will provide morphological information about the relationship of the necrotic core and lumen, as well as information on the fibrous cap overlying the pool of necrotic core.

IVUS guidance during some interventional procedures may increase the likelihood of a greater success rate. Specifically, in the context of the treatment of chronic total occlusions, in which the most exacting parts of the procedure are to enter into the proximal part of the occlusion and to keep the guidewire within the limits of the vessel to avoid coronary perforations. Forward-looking intravascular ultrasound (FL-IVUS) holds promise because it is able to visualise the vessel, plaque morphology, and true and false lumens in front of the imaging catheter. The Preview catheter is currently undergoing preclinical and early clinical evaluation. It is a single-use, over-the-wire imaging catheter, and the distal imaging tip is shown in Figure 7. This catheter is advanced over a conventional 0.014-inch guidewire to the site of occlusion. It rotates at a rate of 3 to 5 revolutions per a second at a frame rate of 3 to 5 frames per second. The current generation of this catheter has a 45 MHz transducer at the tip and is compatible with a 7 Fr guide.

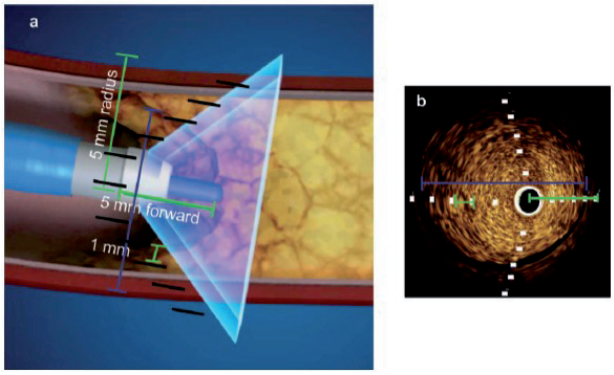

Figure 7. Forward-looking intravascular ultrasound (FL-IVUS; Volcano Corp., Rancho Cordova, CA, USA) is a 45-MHz transducer oriented at a 45º angle at the tip of the catheter, which rotates providing a forward-looking cone of visualisation (A). A 0.014-inch chronic total occlusion (CTO) dedicated guidewire can be advanced through the catheter. Thus, a true lumen position can be maintained under FL-IVUS guidance while treating CTO via antegrade. An FL-IVUS view of the proximal end of CTO phantom model (B), and directed in real time to maintain a true lumen position.

REFERENCES

1. World Health Statistics 2008. World Health Organization. http:// www.who.int/whosis/whostat/EN_WHS08_Full.pdf. Last access July 18,2010.
2. Virmani R., Kolodgie F.D., Burke A.P., Farb A., Schwartz S.M. Lessons from sudden coronary death: a comprehensive morphological classification scheme for atherosclerotic lesions. Arterioscler Thromb Vasc Biol 2000;20:1262-75.
3. Nissen S.E., Tuzcu E.M., Schoenhagen P., Brown B.G., Ganz P., Vogel RA, Crowe T., Howard G., Cooper C.J., Brodie B., Grines C.L., DeMaria A.N. Effect of intensive compared with moderate lipidlowering therapy on progression of coronary atherosclerosis: A randomized controlled trial. JAMA 2004;291:1071-80.
4. Nissen S.E., Nicholls S.J., Sipahi I., Libby P., Raichlen J.S., Ballantyne C.M., Davignon J., Erbel R., Fruchart J.C., Tardif J.C., Schoenhagen P., Crowe T., Cain V., Wolski K., Goormastic M., Tuzcu E.M. Effect of very high-intensity statin therapy on regression of coronary atherosclerosis: The asteroid trial. JAMA 2006;295:1556-1565.
5. De Jaegere P., Mudra H., Figulla H., Almagor Y., Doucet S., Penn I., Colombo A., Hamm C., Bartorelli A., Rothman M., Nobuyoshi M., Yamaguchi T., Voudris V., DiMario C., Makovski S., Hausmann D., Rowe S., Rabinovich S., Sunamura M., van Es G.A. Intravascular ultrasound-guided optimized stent deployment. Immediate and 6 months clinical and angiographic results from the multicenter ultrasound stenting in coronaries study (music study). Eur Heart J 1998; 19:1214-1223.
6. Roy P., Steinberg D.H., Sushinsky S.J., Okabe T., Pinto Slottow T.L., Kaneshige K., Xue Z., Satler L.F., Kent K.M., Suddath W.O., Pichard A.D., Weissman N.J., Lindsay J., Waksman R. The potential clinical utility of intravascular ultrasound guidance in patients undergoing percutaneous coronary intervention with drug-eluting stents. Eur Heart J 2008;29:1851-1857.
7. Roberts W.C., Jones A.A. Quantitation of coronary arterial narrowing at necropsy in sudden coronary death: Analysis of 31 patients and comparison with 25 control subjects. Am J Cardiol 1979;44:39-45.
8. Escaned J., Baptista J., Di Mario C., Haase J., Ozaki Y., Linker D.T., de Feyter P.J., Roelandt J.R., Serruys P.W. Significance of automated stenosis detection during quantitative angiography. Insights gained from intracoronary ultrasound imaging. Circulation 1996;94:966-972.
9. Lockwood G.R., Ryan L.K., Hunt J.W., Foster F.S. Measurement of the ultrasonic properties of vascular tissues and blood from 35- 65 mHz. Ultrasound Med Biol 1991;17:653-66.
10. Bridal S.L., Fornes P., Bruneval P., Berger G. Parametric (integrated backscatter and attenuation) images constructed using backscattered radio frequency signals (25-56 mHz) from human aortae in vitro. Ultrasound Med Biol 1997;23:215-29.
11. Nair A., Margolis M.P., Kuban B.D., Vince D.G. Automated coronary plaque characterisation with intravascular ultrasound backscatter: Ex vivo validation. EuroIntervention 2007;3:113-20.
12. Schaar J.A., De Korte C.L., Mastik F., Strijder C., Pasterkamp G., Boersma E., Serruys P.W., Van Der Steen A.F. Characterizing vulnerable plaque features with intravascular elastography. Circulation 2003;108:2636-2641.
13. Hausmann D., Erbel R., Alibelli-Chemarin M.J., Boksch W., Caracciolo E., Cohn J.M., Culp S.C., Daniel W.G., De Scheerder I., DiMario C., et al. The safety of intracoronary ultrasound. A multicenter survey of 2207 examinations. Circulation 1995;91:623-630.
14. Batkoff B.W., Linker D.T. Safety of intracoronary ultrasound: Data from a multicenter european registry. Cathet Cardiovasc Diagn 1996;38:238- 241.
15. Gorge G., Peters R., Pinto F., Distante A., Visser C., Fraser A., Erbel R. Intravascular ultrasound: Safety and indications for use in 7085 consecutive patients studied in 32 centers in europe and israel. J Am Coll Cardiol 1996;27:155A (abstract).

16. Ramasubbu K., Schoenhagen P., Balghith M.A., Brechtken J., Ziada K.M., Kapadia S.R., Hobbs R.E., Rincon G., Nissen S.E., Tuzcu E.M. Repeated intravascular ultrasound imaging in cardiac transplant recipients does not accelerate transplant coronary artery disease. J Am Coll Cardiol 2003;41:1739-1743.
17. Guedes A., Keller P.F., L'Allier P.L., Lesperance J., Gregoire J., Tardif J.C. Long-term safety of intravascular ultrasound in nontransplant, nonintervened, atherosclerotic coronary arteries. J Am Coll Cardiol 2005;45:559-564.
18. Honda O., Sugiyama S., Kugiyama K., Fukushima H., Nakamura S., Koide S., Kojima S., Hirai N., Kawano H., Soejima H., Sakamoto T., Yoshimura M, Ogawa H. Echolucent carotid plaques predict future coronary events in patients with coronary artery disease. J Am Coll Cardiol 2004;43:1177-1184.
19. Gronholdt M.L., Nordestgaard B.G., Schroeder T.V., Vorstrup S., Sillesen H. Ultrasonic echolucent carotid plaques predict future strokes. Circulation 2001;104:68-73.
20. Bruining N., Verheye S., Knaapen M., Somers P., Roelandt J.R., Regar.E, Heller I., de Winter S., Ligthart J., Van Langenhove G., de Feijter P.J., Serruys P.W., Hamers R. Three-dimensional and quantitative analysis of atherosclerotic plaque composition by automated differential echogenicity. Catheter Cardiovasc Interv 2007;70:968-978.
21. Mintz G.S., Nissen S.E., Anderson W.D., Bailey S.R., Erbel R., Fitzgerald P.J., Pinto F.J., Rosenfield K., Siegel R.J., Tuzcu E.M., Yock P.G. American college of cardiology clinical expert consensus document on standards for acquisition, measurement and reporting of Intravascular ultrasound studies (IVUS). A report of the american college of cardiology task force on clinical expert consensus documents. J Am Coll Cardiol 2001;37:1478-1492.
22. Palmer N.D., Northridge D., Lessells A., McDicken W.N., Fox K.A. In vitro analysis of coronary atheromatous lesions by intravascular ultrasound; reproducibility and histological correlation of lesion morphology. Eur Heart J 1999;20:1701-1706.
23. Hiro T., Leung C.Y., Russo R.J., Moussa I., Karimi H., Farvid A.R., Tobis J.M. Variability in tissue characterization of atherosclerotic plaque by intravascular ultrasound: A comparison of four intravascular ultrasound systems. Am J Card Imaging 1996;10:209-218.
24. Hodgson J.M., Reddy K.G., Suneja R., Nair R.N., Lesnefsky E.J., Sheehan H.M. Intracoronary ultrasound imaging: Correlation of plaque morphology with angiography, clinical syndrome and procedural results in patients undergoing coronary angioplasty. J Am Coll Cardiol 1993;21:35-44.
25. Tanaka K., Carlier S.G., Mintz G.S., Sano K., Liu X., Fujii K., de Ribamar Costa J. Jr, Lui J., Moses J.W., Stone G.W., Leon M.B. The accuracy of length measurements using different intravascular ultrasound motorized transducer pullback systems. Int J Cardiovasc Imaging 2007;23:733-738.
26. Gardner C.M. T.H., Hull E.L., Lisauskas J.B., Sum S.T., Meese T.M., Jiang C., Madden S.P., Caplan J.D., Burke A.P., Virmani R., Goldstein J., Muller J.E. Detection of lipid core coronary plaques in autopsy specimens with a novel catheter based near-infrared spectroscopy system. Am Coll Cardiol Img 2008;1:638-648.
27. Gardner C.M., Tan H., Hull E.L., Lisauskas J.B., Sum S.T., Meese T.M., Jiang C., Madden S.P., Caplan J.D., Burke A.P., Virmani R., Goldstein J., Muller J.E. Detection of lipid core coronary plaques in autopsy specimens with a novel catheter-based near-infrared spectroscopy system. JACC Cardiovasc Imaging 2008;1:638-648.
28. Waxman S., Dixon S.R., L'Allier P., Moses J.W., Petersen J.L., Cutlip D., Tardif J.C., Nesto R.W., Muller J.E., Hendricks M.J., Sum S.T., Gardner C.M., Goldstein J.A., Stone G.W., Krucoff M.W. In vivo validation of a catheter-based near-infrared spectroscopy system for detection of lipid core coronary plaques: Initial results of the spectacl study. JACC Cardiovasc Imaging 2009;2:858-868.
29. Davies M.J. Anatomic features in victims of sudden coronary death. Coronary artery pathology. Circulation 1992;85:I19-24.
30. Burke A.P., Farb A., Malcom G.T., Liang Y.H., Smialek J., Virmani R. Coronary risk factors and plaque morphology in men with coronary disease who died suddenly. N Engl J Med 1997;336:1276-1282.

31. García-García H.M. M.G., Lerman A., Vince D.G., Margolis M.P., van Es G.A., Morel M.A., Nair A., Virmani R., Burke A.P. S.G., Serruys P.W. Tissue characterisation using intravascular radiofrequency data analysis: Recommendations for acquisition, analysis, interpretation and reporting. Eurointervention 2009;5:177.
32. Silber S., Albertsson P., Aviles F.F., Camici P.G., Colombo A., Hamm C., Jorgensen E., Marco J., Nordrehaug J.E., Ruzyllo W., Urban P., Stone G.W., Wijns W. Guidelines for percutaneous coronary interventions. The task force for percutaneous coronary interventions of the european society of cardiology. Eur Heart J 2005;26:804-847.
33. Bruining N., de Winter S., Roelandt J.R., Rodriguez-Granillo G.A., Heller I., van Domburg R.T., Hamers R., de Feijter P.J. Coronary calcium significantly affects quantitative analysis of coronary ultrasound: Importance for atherosclerosis progression/regression studies. Coron Artery Dis 2009;20:409-414.
34. Mintz G.S., Popma J.J., Pichard A.D., Kent K.M., Satler L.F., Chuang Y.C., Ditrano C.J., Leon M.B. Patterns of calcification in coronary artery disease. A statistical analysis of intravascular ultrasound and coronary angiography in 1155 lesions. Circulation 1995;91:1959- 1965.
35. Nair A. M.P., Kuban B.D., Vince D.G. Automated coronary plaque characterization with intravascular ultrasound backscatter: Ex vivo validation. Eurointervention 2007;3:113-130.
36. Pasterkamp G., Schoneveld A.H., van der Wal A.C., Haudenschild C.C., Clarijs R.J., Becker A.E., Hillen B., Borst C. Relation of arterial geometry to luminal narrowing and histologic markers for plaque vulnerability: The remodeling paradox. J Am Coll Cardiol 1998;32: 655-662.
37. Varnava A.M., Mills P.G., Davies M.J. Relationship between coronary artery remodeling and plaque vulnerability. Circulation 2002;105: 939-943.
38. Burke A.P., Kolodgie F.D., Farb A., Weber D., Virmani R. Morphological predictors of arterial remodeling in coronary atherosclerosis. Circulation 2002;105:297-303.
39. Kotani J., Mintz G.S., Castagna M.T., Pinnow E., Berzingi C.O., Bui A.B., Pichard A.D., Satler L.F., Suddath W.O., Waksman R., Laird J.R. Jr, Kent K.M., Weissman N.J. Intravascular ultrasound analysis of infarct-related and non-infarct-related arteries in patients who presented with an acute myocardial infarction. Circulation 2003; 107:2889-2893.
40. Maehara A., Mintz G.S., Bui A.B., Walter O.R., Castagna M.T., Canos D., Pichard A.D., Satler L.F., Waksman R., Suddath W.O., Laird J.R. Jr, Kent K.M., Weissman N.J. Morphologic and angiographic features of coronary plaque rupture detected by intravascular ultrasound. J Am Coll Cardiol 2002;40:904-910.
41. Von Birgelen C., Klinkhart W., Mintz G.S., Papatheodorou A., Herrmann J., Baumgart D., Haude M., Wieneke H., Ge J., Erbel R. Plaque distribution and vascular remodeling of ruptured and nonruptured coronary plaques in the same vessel: An intravascular ultrasound study in vivo. J Am Coll Cardiol 2001;37:1864-1870.
42. Jeremias A., Spies C., Herity N.A., Pomerantsev E., Yock P.G., Fitzgerald P.J., Yeung A.C. Coronary artery compliance and adaptive vessel remodelling in patients with stable and unstable coronary artery disease. Heart 2000;84:314-319.
43. Nakamura M., Nishikawa H., Mukai S., Setsuda M., Nakajima K., Tamada H., Suzuki H., Ohnishi T., Kakuta Y., Nakano T., Yeung A.C. Impact of coronary artery remodeling on clinical presentation of coronary artery disease: An intravascular ultrasound study. J Am Coll Cardiol 2001;37:63-69.
44. Gyongyosi M., Yang P., Hassan A., Domanovits H., Laggner A., Weidinger F., Glogar D. Intravascular ultrasound predictors of major adverse cardiac events in patients with unstable angina. Clin Cardiol 2000;23:507-515.
45. Gyongyosi M., Yang P., Hassan A., Weidinger F., Domanovits H., Laggner A., Glogar D. Arterial remodelling of native human coronary arteries in patients with unstable angina pectoris: A prospective intravascular ultrasound study. Heart 1999;82:68-74.
46. Tauth J., Pinnow E., Sullebarger J.T., Basta L., Gursoy S., Lindsay J. Jr, Matar F. Predictors of coronary arterial remodeling patterns in patients with myocardial ischemia. Am J Cardiol 1997;80:1352-1355.

47. Rodriguez-Granillo G.A., Serruys P.W., Garcia-Garcia H.M., Aoki J., Valgimigli M., van Mieghem C.A., McFadden E., de Jaegere P.P., de Feyter P. Coronary artery remodelling is related to plaque composition. Heart 2006;92:388-391.
48. Virmani R., Burke A.P., Farb A., Kolodgie F.D. Pathology of the vulnerable plaque. J Am Coll Cardiol 2006;47:C13-18.
49. Schaar J.A., Muller J.E., Falk E., Virmani R., Fuster V., Serruys P.W., Colombo A., Stefanadis C., Ward Casscells S., Moreno P.R., Maseri A., van der Steen A.F. Terminology for high-risk and vulnerable coronary artery plaques. Report of a meeting on the vulnerable plaque, june 17 and 18, 2003, santorini, greece. Eur Heart J 2004;25: 1077-1082.
50. Cheruvu P.K., Finn A.V., Gardner C., Caplan J., Goldstein J., Stone G.W., Virmani R., Muller J.E. Frequency and distribution of thin-cap fibroatheroma and ruptured plaques in human coronary arteries: A pathologic study. J Am Coll Cardiol 2007;50:940-949.
51. Cunningham K.S., Gotlieb A.I. The role of shear stress in the pathogenesis of atherosclerosis. Lab Invest 2005;85:9-23.
52. Garcia-Garcia H.M., Goedhart D., Schuurbiers J.C., Kukreja N., Tanimoto S., Daemen J., Morel M.A., Bressers M., van Es G.A., Wentzel J., Gijsen F., van der Steen A.F., Serruys P.W. Virtual histology and remodeling index allow in vivo identification of allegedly high risk coronary plaques in patients with acute coronary syndromes: A three vessel intravascular ultrasound radiofrequency data analysis. Eurointervention 2006;2:338-344.
53. Hong M.K., Mintz G.S., Lee C.W., Lee J.W., Park J.H., Park D.W., Lee S.W., Kim Y.H., Cheong S.S., Kim J.J., Park S.W., Park S.J. A threevessel virtual histology intravascular ultrasound analysis of frequency and distribution of thin-cap fibroatheromas in patients with acute coronary syndrome or stable angina pectoris. Am J Cardiol 2008;101:568-572.
54. Fujii K., Mintz G.S., Carlier S.G., Costa J.R. Jr., Kimura M., Sano K., Tanaka K., Costa R.A., Lui J., Stone G.W., Moses J.W., Leon M.B. Intravascular ultrasound profile analysis of ruptured coronary plaques. Am J Cardiol 2006;98:429-435.
55. Kolodgie F.D., Gold H.K., Burke AP, Fowler D.R., Kruth H.S., Weber D.K., Farb A., Guerrero L.J., Hayase M., Kutys R., Narula J., Finn A.V., Virmani R. Intraplaque hemorrhage and progression of coronary atheroma. N Engl J Med 2003;349:2316-2325.
56. Kruk M., Pregowski J., Mintz G.S., Maehara A., Tyczynski P., Witkowski A., Kalinczuk L., Hong Y.J., Pichard A.D., Satler L.F., Kent K.M., Suddath W.O., Waksman R., Weissman N.J. Intravascular ultrasonic study of gender differences in ruptured coronary plaque morphology and its associated clinical presentation. Am J Cardiol 2007;100: 185-189.
57. Burke A.P., Kolodgie F.D., Farb A., Weber D.K., Malcom G.T., Smialek J., Virmani R. Healed plaque ruptures and sudden coronary death: Evidence that subclinical rupture has a role in plaque progression. Circulation 2001;103:934-940.
58. Jensen L.O., Mintz G.S., Carlier S.G., Fujii K., Moussa I., Dangas G., Mehran R., Stone G.W., Leon M.B., Moses J.W. Intravascular ultrasound assessment of fibrous cap remnants after coronary plaque rupture. Am Heart J 2006;152:327-332.
59. Ge J., Chirillo F., Schwedtmann J., Gorge G., Haude M., Baumgart D., Shah V., von Birgelen C., Sack S., Boudoulas H., Erbel R. Screening of ruptured plaques in patients with coronary artery disease by intravascular ultrasound. Heart 1999;81:621-627.
60. von Birgelen C., Klinkhart W., Mintz G.S., Wieneke H., Baumgart D., Haude M., Bartel T., Sack S., Ge J., Erbel R. Size of emptied plaque cavity following spontaneous rupture is related to coronary dimensions, not to the degree of lumen narrowing. A study with intravascular ultrasound in vivo. Heart 2000;84:483-488.

61. Fujii K, Kobayashi Y., Mintz G.S., Takebayashi H., Dangas G., Moussa I., Mehran R., Lansky A.J., Kreps E., Collins M., Colombo A., Stone G.W., Leon M.B., Moses J.W. IIntravascular ultrasound assessment of ulcerated ruptured plaques: A comparison of culprit and nonculprit lesions of patients with acute coronary syndromes and lesions in patients without acute coronary syndromes. Circulation 2003;108:2473-2478.
62. Fujii K., Carlier S.G., Mintz G.S., Takebayashi H., Yasuda T., Costa R.A., Moussa I., Dangas G., Mehran R., Lansky A.J., Kreps E.M., Collins M., Stone G.W., Moses J.W., Leon M.B. Intravascular ultrasound study of patterns of calcium in ruptured coronary plaques. Am J Cardiol 2005;96:352-357.
63. Rioufol G., Finet G., Ginon I., Andre-Fouet X., Rossi R., Vialle E., Desjoyaux E., Convert G., Huret J.F., Tabib A. Multiple atherosclerotic plaque rupture in acute coronary syndrome: A three-vessel intravascular ultrasound study. Circulation 2002;106:804-808.
64. Tanaka A., Shimada K., Sano T., Namba M., Sakamoto T., Nishida Y., Kawarabayashi T., Fukuda D., Yoshikawa J. Multiple plaque rupture and c-reactive protein in acute myocardial infarction. J Am Coll Cardiol 2005;45:1594-1599.
65. Hong M.K., Mintz G.S., Lee C.W., Kim Y.H., Lee S.W., Song J.M., Han K.H., Kang D.H., Song J.K., Kim J.J., Park S.W., Park S.J. Comparison of coronary plaque rupture between stable angina and acute myocardial infarction: A three-vessel intravascular ultrasound study in 235 patients. Circulation 2004;110:928-933.
66. Hong M.K., Mintz G.S., Lee C.W., Lee B.K., Yang T.H., Kim Y.H., Song J.M., Han K.H., Kang D.H., Cheong S.S., Song J.K., Kim J.J., Park S.W., Park S.J. The site of plaque rupture in native coronary arteries: A. three-vessel intravascular ultrasound analysis. J Am Coll Cardiol 2005;46:261-265.
67. Pregowski J., Tyczynski P., Mintz G.S., Kim S.W., Witkowski A., Satler L., Kruk M., Waksman R., Maehara A., Weissman N.J. Intravascular ultrasound assessment of the spatial distribution of ruptured coronary plaques in the left anterior descending coronary artery. Am Heart J 2006;151:898-901.
68. Tyczynski P., Pregowski J., Mintz G.S., Witkowski A., Kim S.W., Waksman R., Satler L., Pichard A., Kalinczuk L., Maehara A., Weissman N.J. Intravascular ultrasound assessment of ruptured atherosclerotic plaques in left main coronary arteries. Am J Cardiol 2005;96:794- 798.
69. Rodriguez-Granillo G.A., Garcia-Garcia H.M., Wentzel J., Valgimigli M., Tsuchida K., van der Giessen W., de Jaegere P., Regar E., de Feyter P.J., Serruys P.W. Plaque composition and its relationship with acknowledged shear stress patterns in coronary arteries. J Am Coll Cardiol 2006;47:884-885.
70. Pregowski J., Tyczynski P., Mintz G.S., Kim S.W., Witkowski A., Waksman R., Pichard A., Satler L., Kent K., Kruk M., Bieganski S., Ohlmann P., Weissman N.J. Incidence and clinical correlates of ruptured plaques in saphenous vein grafts: An intravascular ultrasound study. J Am Coll Cardiol 2005;45:1974-1979.
71. Pregowski J., Tyczynski P., Mintz G.S., Kim S.W., Witkowski A., Waksman R., Pichard A., Satler L., Kent K., Kalinczuk L., Bieganski S., Ohlmann P., Maehara A., Weissman N.J. Comparison of ruptured plaques in native coronary arteries and in saphenous vein grafts: An intravascular ultrasound study. Am J Cardiol 2006;97:593-597.
72. Rioufol G., Gilard M., Finet G., Ginon I., Boschat J., Andre-Fouet X. Evolution of spontaneous atherosclerotic plaque rupture with medical therapy: Long-term follow-up with intravascular ultrasound. Circulation 2004;110:2875-2880.
73. Hong M.K., Mintz G.S., Lee C.W., Suh I.W., Hwang E.S., Jeong Y.H., Park D.W., Kim Y.H., Han K.H., Cheong S.S., Kim J.J., Park S.W., Park S.J. Serial intravascular ultrasound evidence of both plaque stabilization and lesion progression in patients with ruptured coronary plaques: Effects of statin therapy on ruptured coronary plaque. Atherosclerosis 2007;191:107-114.
74. Rodriguez-Granillo G.A., Garcia-Garcia H.M., Valgimigli M., Vaina S., van Mieghem C., van Geuns R.J., van der Ent M., Regar E., de Jaegere P., van der Giessen W., de Feyter P., Serruys P.W. Global characterization of coronary plaque rupture phenotype using three-vessel intravascular ultrasound radiofrequency data analysis. Eur Heart J 2006.

75. Burke A.P., Joner M., Virmani R. Ivus-vh: A. predictor of plaque morphology? Eur Heart J 2006;27:1889-1890.

76. Smith S.C. Jr, Feldman T.E., Hirshfeld J.W. Jr, Jacobs A.K., Kern M.J., King S.B. 3rd, Morrison D.A., O'Neill W.W., Schaff H.V., Whitlow P.L., Williams D.O., Antman E.M., Adams C.D., Anderson J.L., Faxon D.P., Fuster V., Halperin J.L., Hiratzka L.F., Hunt S.A., Nishimura R., Ornato J.P., Page R.L., Riegel B. Acc/aha/scai 2005 guideline update for percutaneous coronary intervention--summary article: A. report of the american college of cardiology/american heart association task force on practice guidelines (acc/aha/scai writing committee to update the 2001 guidelines for percutaneous coronary intervention). Circulation 2006;113:156-175.

77. Smith S.C. Jr, Feldman T.E., Hirshfeld J.W. Jr, Jacobs A.K., Kern M.J., King S.B., 3rd, Morrison D.A., O'Neill WW, Schaff H.V., Whitlow P.L., Williams D.O., Antman E.M., Adams C.D., Anderson J.L., Faxon D.P., Fuster V., Halperin J.L., Hiratzka L.F., Hunt S.A., Nishimura R., Ornato J.P., Page R.L., Riegel B. Acc/aha/scai 2005 guideline update for percutaneous coronary intervention a report of the american college of cardiology/american heart association task force on practice guidelines (acc/aha/scai writing committee to update the 2001 guidelines for percutaneous coronary intervention). J Am Coll Cardiol 2006;47:e1-121.

78. Abizaid A., Mintz G.S., Pichard A.D., Kent K.M., Satler L.F., Walsh C.L., Popma J.J., Leon M.B. Clinical, intravascular ultrasound, and quantitative angiographic determinants of the coronary flow reserve before and after percutaneous transluminal coronary angioplasty. Am J Cardiol 1998;82:423-428.

79. Nishioka T., Amanullah A.M., Luo H., Berglund H., Kim C.J., Nagai T., Hakamata N., Katsushika S., Uehata A., Takase B., Isojima K., Berman D.S., Siegel R.J. Clinical validation of intravascular ultrasound imaging for assessment of coronary stenosis severity: Comparison with stress myocardial perfusion imaging. J Am Coll Cardiol 1999; 33:1870-1878.

80. Costa M.A., Sabate M., Staico R., Alfonso F., Seixas A.C., Albertal M., Crossman A., Angiolillo D.J., Zenni M., Sousa J.E., Macaya C., Bass T.A. Anatomical and physiologic assessments in patients with small coronary artery disease: Final results of the physiologic and anatomical evaluation prior to and after stent implantation in small coronary vessels (phantom) trial. Am Heart J 2007;153:296 e291-297.

81. Fassa A.A., Wagatsuma K., Higano S.T., Mathew V., Barsness G.W., Lennon R.J., Holmes D.R. Jr, Lerman A. Intravascular ultrasoundguided treatment for angiographically indeterminate left main coronary artery disease: A long-term follow-up study. J Am Coll Cardiol 2005;45:204-211.

82. Jasti V., Ivan E., Yalamanchili V., Wongpraparut N., Leesar M.A. Correlations between fractional flow reserve and intravascular ultrasound in patients with an ambiguous left main coronary artery stenosis. Circulation 2004;110:2831-2836.

83. Gonzalo N., Garcia-Garcia H.M., Regar E., Barlis P., Wentzel J., Onuma Y., Ligthart J., Serruys P.W. In vivo assessment of high-risk coronary plaques at bifurcations with combined intravascular ultrasound and optical coherence tomography. JACC Cardiovasc Imaging 2009;2:473-482.

84. Gonzalo N. G-GH., Regar E., Barlis P., Wentzel J., Onuma Y., Ligthart J., Serruys P.W. In vivo assessment of high-risk coronary plaques at bifurcations with combined intravascular ultrasound virtual histology and loptical coherence tomography. JIMG 2009: In press.

85. Uretsky B.F., Kormos R.L., Zerbe T.R., Lee A., Tokarczyk T.R., Murali S., Reddy P.S., Denys B.G., Griffith BP, Hardesty RL, et al. Cardiac events after heart transplantation: Incidence and predictive value of coronary arteriography. J Heart Lung Transplant 1992;11:S45-51.

86. Tuzcu E.M., Kapadia S.R., Sachar R., Ziada K.M., Crowe T.D., Feng J., Magyar W.A., Hobbs R.E., Starling R.C., Young J.B., McCarthy P., Nissen S.E. Intravascular ultrasound evidence of angiographically silent progression in coronary atherosclerosis predicts long-term morbidity and mortality after cardiac transplantation. J Am Coll Cardiol 2005;45:1538-1542.

87. Eisen H.J., Tuzcu E.M., Dorent R., Kobashigawa J., Mancini D., Valantine- von Kaeppler H.A., Starling R.C., Sorensen K., Hummel M., Lind J.M., Abeywickrama K.H., Bernhardt P. Everolimus for the prevention of allograft rejection and vasculopathy in cardiac-transplant recipients. N Engl J Med 2003;349:847-858.

88. Mintz G.S., Pichard A.D., Kovach J.A., Kent K.M., Satler L.F., Javier SP, Popma J.J., Leon M.B. Impact of preintervention iintravascular ultrasound imaging on transcatheter treatment strategies in coronary artery disease. Am J Cardiol 1994;73:423-430.

89. Fitzgerald P.J., Ports T.A., Yock P.G. Contribution of localized calcium deposits to dissection after angioplasty. An observational study using intravascular ultrasound. Circulation 1992;86:64-70.

90. Honye J., Mahon D.J., Jain A., White C.J., Ramee S.R., Wallis J.B., al-Zarka A., Tobis J.M. Morphological effects of coronary balloon angioplasty in vivo assessed by iintravascular ultrasound imaging. Circulation 1992;85:1012-1025.

91. Stone G.W., Hodgson J.M., St Goar F.G., Frey A., Mudra H., Sheehan H., Linnemeier T.J. Improved procedural results of coronary angioplasty with intravascular ultrasound-guided balloon sizing: The clout pilot trial. Clinical outcomes with ultrasound trial (clout) investigators. Circulation 1997;95:2044-2052.

92. Pasterkamp G., Borst C., Gussenhoven E.J., Mali W.P., Post M.J., The S.H., Reekers J.A., van den Berg F.G. Remodeling of de novo atherosclerotic lesions in femoral arteries: Impact on mechanism of balloon angioplasty. J Am Coll Cardiol 1995;26:422-428.

93. Kimura T., Kaburagi S., Tamura T., Yokoi H., Nakagawa Y., Hamasaki N., Nosaka H., Nobuyoshi M., Mintz G.S., Popma J.J., Leon M.B. Remodeling of human coronary arteries undergoing coronary angioplasty or atherectomy. Circulation 1997;96:475-483.

94. Baptista J., Umans V.A., di Mario C., Escaned J., de Feyter P., Serruys P.W. Mechanisms of luminal enlargement and quantification of vessel wall trauma following balloon coronary angioplasty and directional atherectomy. Eur Heart J 1995;16:1603-1612.

95. Moussa I., Moses J., Di Mario C., Busi G., Reimers B., Kobayashi Y., Albiero R., Ferraro M., Colombo A. Stenting after optimal lesion debulking (sold) registry. Angiographic and clinical outcome. Circulation 1998;98:1604-1609.

96. Colombo A., Hall P., Nakamura S., Almagor Y., Maiello L., Martini G., Gaglione A., Goldberg S.L., Tobis J.M. Intracoronary stenting without anticoagulation accomplished with iintravascular ultrasound guidance. Circulation 1995;91:1676-1688.

97. Kuntz R.E., Baim D.S., Safian R.D. Pursuit of large lumen dimensions after coronary intervention {editorial}. J Interv Cardiol 1993;6:287-291.

98. Russo R.J., Silva P.D., Teirstein P.S., Attubato M.J., Davidson C.J., DeFranco A.C., Fitzgerald P.J., Goldberg S.L., Hermiller J.B., Leon M.B., Ling F.S., Lucisano J.E., Schatz R.A., Wong S.C., Weissman N.J., Zientek D.M. A randomized controlled trial of angiography versus intravascular ultrasound-directed bare-metal coronary stent placement (the avid trial). Circ Cardiovasc Interv 2009;2:113-123.

99. Fitzgerald P.J., Oshima A., Hayase M., Metz J.A., Bailey S.R., Baim D.S., Cleman M.W., Deutsch E., Diver D.J., Leon M.B., Moses J.W., Oesterle S.N., Overlie P.A., Pepine C.J., Safian R.D., Shani J., Simonton C.A., Smalling R.W., Teirstein P.S., Zidar J.P., Yeung A.C., Kuntz R.E., Yock P.G. Final results of the can routine ultrasound influence stent expansion (cruise) study. Circulation 2000;102:523- 530.

100. Mudra H., di Mario C., de Jaegere P., Figulla H.R., Macaya C., Zahn R., Wennerblom B., Rutsch W., Voudris V., Regar E., Henneke K.H., Schachinger V., Zeiher A. Randomized comparison of coronary stent implantation under ultrasound or angiographic guidance to reduce stent restenosis (opticus study). Circulation 2001;104:1343-1349.

101. Oemrawsingh P.V., Mintz G.S., Schalij M.J., Zwinderman A.H., Jukema J.W., van der Wall E.E. Intravascular ultrasound guidance improves angiographic and clinical outcome of stent implantation for long coronary artery stenoses: Final results of a randomized comparison with angiographic guidance (tulip study). Circulation 2003;107:62-67.

102. Sousa J.E., Costa M.A., Abizaid A., Abizaid A.S., Feres F., Pinto I.M., Seixas A.C., Staico R., Mattos L.A., Sousa A.G., Falotico R., Jaeger J., Popma J.J., Serruys P.W. Lack of neointimal proliferation after implantation of sirolimus-coated stents in human coronary arteries: A quantitative coronary angiography and three-dimensional intravascular ultrasound study. Circulation 2001;103:192-195.
103. Morice M.C., Serruys P.W., Sousa J.E., Fajadet J., Ban Hayashi E., Perin M., Colombo A., Schuler G., Barragan P., Guagliumi G., Molnar F., Falotico R. A randomized comparison of a sirolimus-eluting stent with a standard stent for coronary revascularization. N Engl J Med 2002;346:1773-1780.
104. Costa M., Angiolillo D.J., Teirstein P., Gilmore P., Leon M., Moses J., Yakubov S., Carter A., Fischell T., Zenni M., Bass T. Sirolimus-eluting stents for treatment of complex bypass graft disease: Insights from the secure registry. J Invasive Cardiol 2005;17:396-398.
105. Agostoni P., Vermeersch P., Semeraro O., Verheye S., Van Langenhove G., Van den Heuvel P., Convens C., Van den Branden F., Bruining N. Intravascular ultrasound comparison of sirolimus-eluting stent versus bare metal stent implantation in diseased saphenous vein grafts (from the rrisc [reduction of restenosis in saphenous vein grafts with cypher sirolimus-eluting stent] trial). Am J Cardiol 2007; 100:52-58.
106. Cheneau E., Leborgne L., Mintz G.S., Kotani J., Pichard A.D., Satler L.F., Canos D., Castagna M., Weissman N.J., Waksman R. Predictors of subacute stent thrombosis: Results of a systematic intravascular ultrasound study. Circulation 2003;108:43-47.
107. Fujii K., Carlier S.G., Mintz G.S., Yang Y.M., Moussa I., Weisz G., Dangas G., Mehran R., Lansky A.J., Kreps E.M., Collins M., Stone G.W., Moses J.W., Leon M.B. Stent underexpansion and residual reference segment stenosis are related to stent thrombosis after sirolimus-eluting stent implantation: An intravascular ultrasound study. J Am Coll Cardiol 2005;45:995-998.
108. Cook S., Ladich E., Nakazawa G., Eshtehardi P., Neidhart M., Vogel R., Togni M., Wenaweser P., Billinger M., Seiler C., Gay S., Meier B., Pichler W.J., Juni P., Virmani R., Windecker S. Correlation of intravascular ultrasound findings with histopathological analysis of thrombus aspirates in patients with very late drug-eluting stent thrombosis. Circulation 2009;120:391-399.
109. Sonoda S., Morino Y., Ako J., Terashima M., Hassan A.H., Bonneau H.N., Leon M.B., Moses J.W., Yock P.G., Honda Y., Kuntz R.E., Fitzgerald P.J. Impact of final stent dimensions on long-term results following sirolimus-eluting stent implantation: Serial intravascular ultrasound analysis from the sirius trial. J Am Coll Cardiol 2004;43: 1959-1963.
110. Hong M.K., Mintz G.S., Lee C.W., Park D.W., Choi B.R., Park K.H., Kim Y.H., Cheong S.S., Song J.K., Kim J.J., Park S.W., Park S.J. Intravascular ultrasound predictors of angiographic restenosis after sirolimus-eluting stent implantation. Eur Heart J 2006;27:1305-1310.
111. Castagna M.T., Mintz G.S., Leiboff B.O., Ahmed J.M., Mehran R., Satler L.F., Kent K.M., Pichard A.D., Weissman N.J. The contribution of "Mechanical" Problems to in-stent restenosis: An intravascular ultrasonographic analysis of 1090 consecutive in-stent restenosis lesions. Am Heart J 2001;142:970-974.
112. Shaikh F., Maddikunta R., Djelmami-Hani M., Solis J., Allaqaband S., Bajwa T. Stent fracture, an incidental finding or a significant marker of clinical in-stent restenosis? Catheter Cardiovasc Interv 2008;71: 614-618.
113. Costa M.A., Sabate M., Angiolillo D.J., Jimenez-Quevedo P., Teirstein P., Carter A., Leon M.B., Moses J., Zenni M., Yakubov S., Guzman L.A., Gilmore P., Macaya C., Bass T.A. Intravascular ultrasound characterization of the "Black hole" Phenomenon after drugeluting stent implantation. Am J Cardiol 2006;97:203-206.
114. Mintz G.S. Features and parameters of drug-eluting stent deployment discoverable by intravascular ultrasound. Am J Cardiol 2007;100: 26M-35M.
115. Escolar E., Mintz G.S., Popma J., Michalek A., Kim S.W., Mandinov L., Koglin J., Stone G., Ellis S.G., Grube E., Dawkins K.D., Weissman N.J. Meta-analysis of angiographic versus intravascular ultrasound parameters of drug-eluting stent efficacy (from taxus iv, v, and vi). Am J Cardiol 2007;100:621-626.

116. Jensen L.O., Maeng M., Thayssen P., Christiansen E.H., Hansen K.N., Galloe A., Kelbaek H., Lassen J.F., Thuesen L. Neointimal hyperplasia after sirolimus-eluting and paclitaxel-eluting stent implantation in diabetic patients: The randomized diabetes and drug-eluting stent (diabedes) intravascular ultrasound trial. Eur Heart J 2008;29:2733- 2741.
117. Miyazawa A., Ako J., Hongo Y., Hur S.H., Tsujino I., Courtney B.K., Hassan A.H., Kandzari D.E., Honda Y., Fitzgerald P.J. Comparison of vascular response to zotarolimus-eluting stent versus sirolimuseluting stent: Intravascular ultrasound results from endeavor iii. Am Heart J 2008;155:108-113.
118. Finn A.V., Nakazawa G., Joner M., Kolodgie F.D., Mont E.K., Gold H.K., Virmani R. Vascular responses to drug eluting stents: Importance of delayed healing. Arterioscler Thromb Vasc Biol 2007;27:1500-1510.
119. Garcia-Garcia H.M., Gonzalo N., Pawar R., Kukreja N., Dudek D., Thuesen L., Ormiston J.A., Regar E., Serruys P.W.: Assesment of the absorption process following bioabsorbable everolimus-eluting stent implantation: Temporal changes in strain values and tissue composition using intravascular ultrasound radiofrequency data analysis. A substudy of the absorb clinical trial. Eurointervention 2009:443-448.
120. Schartl M., Bocksch W., Koschyk D.H., Voelker W., Karsch K.R., Kreuzer J., Hausmann D., Beckmann S., Gross M. Use of intravascular ultrasound to compare effects of different strategies of lipidlowering therapy on plaque volume and composition in patients with coronary artery disease. Circulation 2001;104:387-392.
121. Cannon C.P., Braunwald E., McCabe C.H., Rader D.J., Rouleau J.L., Belder R., Joyal S.V., Hill K.A., Pfeffer M.A., Skene A.M. Intensive versus moderate lipid lowering with statins after acute coronary syndromes. N Engl J Med 2004;350:1495-1504.
122. Tardif J.C., Gregoire J., L'Allier P.L., Ibrahim R., Lesperance J., Heinonen T.M., Kouz S., Berry C., Basser R., Lavoie M.A., Guertin M.C., Rodes-Cabau J. Effects of reconstituted high-density lipoprotein infusions on coronary atherosclerosis: a randomized controlled trial. JAMA 2007;297:1675-82.
123. Nissen S.E., Tardif J.C., Nicholls S.J., Revkin J.H., Shear C.L., Duggan W.T., Ruzyllo W., Bachinsky W.B., Lasala G.P., Tuzcu E.M. Effect of torcetrapib on the progression of coronary atherosclerosis. N Engl J Med 2007;356:1304-16.
124. Nissen S.E., Tuzcu E.M., Brewer H.B., Sipahi I., Nicholls S.J., Ganz P., Schoenhagen P., Waters D.D., Pepine C.J., Crowe T.D., Davidson M.H., Deanfield J.E., Wisniewski L.M., Hanyok J.J., Kassalow L.M. Effect of ACAT inhibition on the progression of coronary atherosclerosis. N Engl J Med 2006;354: 1253-63.
125. Nissen S.E., Tuzcu E.M., Libby P., Thompson P.D., Ghali M., Garza D., Berman L., Shi H., Buebendorf E., Topol E.J. Effect of antihypertensive agents on cardiovascular events in patients with coronary disease and normal blood pressure: the CAMELOT study: a randomized controlled trial. Jama 2004;292:2217-25.
126. Rodriguez-Granillo G.A., Vos J., Bruining N., Garcia-Garcia H.M., de Winter S., Ligthart J.M., Deckers J.W., Bertrand M., Simoons M.L., Ferrari R., Fox K.M., Remme W., De Feyter P.J. Long-term effect of perindopril on coronary atherosclerosis progression (from the perindopril's prospective effect on coronary atherosclerosis by angiography and intravascular ultrasound evaluation [PERSPECTIVE] study). Am J Cardiol 2007;100:159-63.
127. Nissen S.E., Nicholls S.J., Wolski K., Nesto R., Kupfer S., Perez A., Jure H., De Larochelliere R., Staniloae C.S., Mavromatis K., Saw J., Hu B., Lincoff A.M., Tuzcu E.M. Comparison of pioglitazone vs glimepiride on progression of coronary atherosclerosis in patients with type 2 diabetes: the PERISCOPE randomized controlled trial. JAMA 2008;299:1561-73.
128. Nasu K., Tsuchikane E., Katoh O., Tanaka N., Kimura M., Ehara M., Kinoshita Y., Matsubara T., Matsuo H., Asakura K., Asakura Y., Terashima M., Takayama T., Honye J., Hirayama A., Saito S., Suzuki T. Effect of fluvastatin on progression of coronary atherosclerotic plaque evaluated by virtual histology intravascular ultrasound. JACC Cardiovasc Interv 2009;2:689-96.
129. Hong M.K., Park D.W., Lee C.W., Lee S.W., Kim Y.H., Kang D.H., Song J.K., Kim J.J., Park S.W., Park S.J. Effects of statin treatments on coronary plaques assessed by volumetric virtual histology intravascular ultrasound analysis. JACC Cardiovasc Interv 2009;2:679-88.

130. Serruys P.W., Garcia-Garcia H.M., Buszman P., Erne P., Verheye S., Aschermann M., Duckers H., Bleie O., Dudek D., Botker H.E., von Birgelen C., D'Amico D., Hutchinson T., Zambanini A., Mastik F., van Es G.A., van der Steen A.F., Vince D.G., Ganz P., Hamm C.W., Wijns W., Zalewski A. Effects of the direct lipoprotein-associated phospholipase A(2) inhibitor darapladib on human coronary atherosclerotic plaque. Circulation 2008;118:1172-82.

131. Sawada T., Shite J., Garcia-Garcia H.M., Shinke T., Watanabe S., Otake H., Matsumoto D., Tanino Y., Ogasawara D., Kawamori H., Kato H., Miyoshi N., Yokoyama M., Serruys P.W., Hirata K. Feasibility of combined use of intravascular ultrasound radiofrequency data analysis and optical coherence tomography for detecting thin-cap fibroatheroma. Eur Heart J 2008;29:1136-46.

132. Serruys P.W., Degertekin M., Tanabe K., Abizaid A., Sousa J.E., Colombo A., Guagliumi G., Wijns W., Lindeboom W.K., Ligthart J., de Feyter P.J., Morice M.C. Intravascular ultrasound findings in the multicenter, randomized, double-blind RAVEL (RAndomized study with the sirolimus-eluting VElocity balloon-expandable stent in the treatment of patients with de novo native coronary artery Lesions) trial. Circulation 2002;106:798-803.

133. Abizaid A., Costa M.A., Blanchard D., Albertal M., Eltchaninoff H., Guagliumi G., Geert-Jan L., Abizaid A.S., Sousa A.G., Wuelfert E., Wietze L., Sousa J.E., Serruys P.W., Morice M.C. Sirolimus-eluting stents inhibit neointimal hyperplasia in diabetic patients. Insights from the RAVEL Trial. Eur Heart J 2004;25:107-12.

134. Moses J.W., Leon M.B., Popma J.J., Fitzgerald P.J., Holmes D.R., O'Shaughnessy C., Caputo R.P., Kereiakes D.J., Williams D.O., Teirstein P.S., Jaeger J.L., Kuntz R.E. Sirolimus-eluting stents versus standard stents in patients with stenosis in a native coronary artery. N Engl J Med 2003;349:1315-23.

135. Sousa J.E., Costa M.A., Abizaid A.C., Rensing B.J., Abizaid A.S., Tanajura L.F., Kozuma K., Van Langenhove G., Sousa A.G., Falotico R., Jaeger J., Popma J.J., Serruys P.W. Sustained suppression of neointimal proliferation by sirolimus-eluting stents: one-year angiographic and intravascular ultrasound follow-up. Circulation 2001;104:2007- 11.

136. Sousa J.E., Costa M.A., Abizaid A., Feres F., Seixas A.C., Tanajura L.F., Mattos L.A., Falotico R., Jaeger J., Popma J.J., Serruys P.W., Sousa A.G. Four-year angiographic and intravascular ultrasound followup of patients treated with sirolimus-eluting stents. Circulation 2005;111:2326-9.

137. Aoki J., Abizaid A.C., Serruys P.W., Ong A.T., Boersma E., Sousa J.E., Bruining N. Evaluation of four-year coronary artery response after sirolimus-eluting stent implantation using serial quantitative intravascular ultrasound and computer-assisted greyscale value analysis for plaque composition in event-free patients. J Am Coll Cardiol 2005; 46:1670-6.

138. Lotan C., Almagor Y., Kuiper K., Suttorp M.J., Wijns W. Sirolimuseluting stent in chronic total occlusion: the SICTO study. J Interv Cardiol 2006;19:307-12.

139. Feres F., Munoz J.S., Abizaid A., Albertal M., Mintz G.S., Staico R., Centemero M., Mattos L.A., Maldonado G., Tanajura L.F., Chaves A., Pinto I., Abizaid A.S., Seixas A.C., Vaz V.D., Sousa A., Sousa J.E. Comparison between sirolimus-eluting stents and intracoronary catheter-based beta radiation for the treatment of in-stent restenosis. Am J Cardiol 2005;96:1656-62.

140. Jimenez-Quevedo P., Sabate M., Angiolillo D.J., Costa M.A., Alfonso F., Gomez-Hospital J.A., Hernandez-Antolin R., Banuelos C., Goicolea J., Fernandez-Aviles F., Bass T., Escaned J., Moreno R., Fernandez C., Macaya C. Vascular effects of sirolimus-eluting versus bare-metal stents in diabetic patients: three-dimensional ultrasound results of the Diabetes and Sirolimus-Eluting Stent (DIABETES) Trial. J Am Coll Cardiol 2006;47:2172-9.

141. Alfonso F., Perez-Vizcayno M.J., Hernandez R., Bethencourt A., Marti V., Lopez-Minguez J.R., Angel J., Mantilla R., Moris C., Cequier A., Sabate M., Escaned J., Moreno R., Banuelos C., Suarez A., Macaya C. A randomized comparison of sirolimus-eluting stent with balloon angioplasty in patients with in-stent restenosis: results of the Restenosis Intrastent: Balloon Angioplasty Versus Elective Sirolimus- Eluting Stenting (RIBS-II) trial. J Am Coll Cardiol 2006;47:2152-60.

142. Colombo A., Drzewiecki J., Banning A., Grube E., Hauptmann K., Silber S., Dudek D., Fort S., Schiele F., Zmudka K., Guagliumi G., Russell M.E. Randomized study to assess the effectiveness of slow- and moderate-release polymer-based paclitaxel-eluting stents for coronary artery lesions. Circulation 2003;108:788-94.

143. Weissman N.J., Koglin J., Cox D.A., Hermiller J., O'Shaughnessy C., Mann J.T., Turco M., Caputo R., Bergin P., Greenberg J., Kutcher M., Wong S.C., Strickland W., Mooney M., Russell M.E., Ellis S.G., Stone G.W. Polymer-based paclitaxel-eluting stents reduce in-stent neointimal tissue proliferation: a serial volumetric intravascular ultrasound analysis from the TAXUS-IV trial. J Am Coll Cardiol 2005; 45:1201-5.

144. Weissman N.J., Ellis S.G., Grube E., Dawkins K.D., Greenberg J.D., Mann T., Cannon L.A., Cambier P.A., Fernandez S., Mintz G.S., Mandinov L., Koglin J., Stone G.W. Effect of the polymer-based, paclitaxel- eluting TAXUS Express stent on vascular tissue responses: a volumetric intravascular ultrasound integrated analysis from the TAXUS IV, V, and VI trials. Eur Heart 2007;J 28:1574-82.

145. Kimura M., Mintz G.S., Weissman N.J., Dawkins K.D., Grube E., Ellis SG, Cannon L.A., Masud Z., Mandinov L., Baim D., Stone G.W. Meta-analysis of the effects of paclitaxel-eluting stents versus bare metal stents on volumetric intravascular ultrasound in patients with versus without diabetes mellitus. Am J Cardiol 2008;101:1263-8.

146. Doi H., Maehara A., Mintz G.S., Yu A., Wang H., Mandinov L., Popma J.J., Ellis S.G., Grube E., Dawkins K.D., Weissman N.J., Turco M.A., Ormiston J.A., Stone G.W. Impact of Post-Intervention Minimal Stent Area on 9-Month Follow-Up Patency of Paclitaxel-Eluting Stents An Integrated Intravascular Ultrasound Analysis From the TAXUS IV, V, and VI and TAXUS ATLAS Workhorse, Long Lesion, and Direct Stent Trials. JACC Cardiovasc Interv 2009;2:1269-75.

147. Park D.W., Hong M.K., Mintz G.S., Lee C.W., Song J.M., Han K.H., Kang D.H., Cheong S.S., Song J.K., Kim J.J., Weissman N.J., Park S.W., Park S.J. Two-year follow-up of the quantitative angiographic and volumetric intravascular ultrasound analysis after nonpolymeric paclitaxel-eluting stent implantation: late "catch-up" phenomenon from ASPECT Study.i 2006;48:2432-9.

148. Sakurai R., Hongo Y., Yamasaki M., Honda Y., Bonneau H.N., Yock P.G., Cutlip D., Popma J.J., Zimetbaum P., Fajadet J., Kuntz R.E., Wijns W., Fitzgerald P.J. Detailed intravascular ultrasound analysis of Zotarolimus-eluting phosphorylcholine-coated cobalt-chromium alloy stent in de novo coronary lesions (results from the ENDEAVOR II trial). Am J Cardiol 2007;100:818-23.

149. Waseda K., Miyazawa A., Ako J., Hasegawa T., Tsujino I., Sakurai R., Yock P.G., Honda Y., Kandzari D.E., Leon M.B., Fitzgerald P.J. Intra-vascular ultrasound results from the ENDEAVOR IV trial: randomized comparison between zotarolimus- and paclitaxel-eluting stents in patients with coronary artery disease. JACC Cardiovasc Interv 2009; 2:779-84.

150. Feres F., Andrade P.B., Costa R.A., de Ribamar Costa J. Jr, Abizaid A., Staico R., Tanajura L.F., Siqueira D., Maia J.P., Lasave L., Sousa A.G., Sousa J.E. Angiographic and intravascular ultrasound findings following implantation of the Endeavor zotarolimus-eluting stents in patients from the real-world clinical practice. EuroIntervention 2009; 5:355-62.

151. Meredith I.T. W.S., Whitbourn R., Walters D., Popma J., Cutlip D., Fitzgerald P. The next-generation Endeavor Resolute stent: 4-month clinical and angiographic results from the Endeavor Resolute first-inman trial. Eurointervention 2007;3:50-3.

152. Meredith I.T., Worthley S., Whitbourn R., Walters D.L., McClean D., Horrigan M., Popma J.J., Cutlip D.E., DePaoli A., Negoita M., Fitzgerald P.J. Clinical and angiographic results with the next-generation resolute stent system: a prospective, multicenter, first-in-human trial. JACC Cardiovasc Interv 2009;2:977-85.

153. Chevalier B., Silber S., Park S.J., Garcia E., Schuler G., Suryapranata H., Koolen J., Hauptmann K.E., Wijns W., Morice M.C., Carrie D., van Es G.A., Nagai H., Detiege D., Paunovic D., Serruys P.W. Randomized comparison of the Nobori Biolimus A9-eluting coronary stent with the Taxus Liberte paclitaxel-eluting coronary stent in patients with stenosis in native coronary arteries: the NOBORI 1 trial--Phase 2. Circ Cardiovasc Interv 2009;2:188-95.

154. Miyazawa A., Ako J., Hassan A., Hasegawa T., Abizaid A., Verheye S., McClean D., Neumann F.J., Grube E., Honda Y., Fitzgerald P.J. Analysis of bifurcation lesions treated with novel drug-eluting dedicated bifurcation stent system: intravascular ultrasound results of the AXXESS PLUS trial. Catheter Cardiovasc Interv 2007;70:952-7.

155. Hasegawa T., Ako J., Koo B.K., Miyazawa A., Sakurai R., Chang H., Dens J., Verheye S., Grube E., Honda Y., Fitzgerald P.J. Analysis of left main coronary artery bifurcation lesions treated with biolimuseluting DEVAX AXXESS plus nitinol self-expanding stent: intravascular ultrasound results of the AXXENT trial. Catheter Cardiovasc Interv 2009;73:34-41.

156. Serruys P.W. O.T., Piek J.J., Neumann F.J., van der Giessen W.J., Wiemer M., Zeiher A., Grube E., Haase J., Thuesen L., Hamm C. O-T.P. A randomized comparison of a durable polymer Everolimus-eluting stent with a bare metal coronary stent: The SPIRIT first trial. Eurointervention 2005;1:58-65.

157. Tsuchida K., Piek J.J., Neumann F.J., van der Giessen W.J., Wiemer M., Zeiher A., Grube E., Haase J., Thuesen L., Hamm C. V.S., Dorange C., Serruys P.W. One year results of a durable polymer everolimus-eluting stent in de novo coronary narrowings (The Spirit First Trial). Eurointervention 2005;1:266-72.

158. Serruys P.W., Ruygrok P., Neuzner J., Piek J., Seth A., Schofer J., Richardt G., Wiemer M., Carrie D., Thuesen L., Boone E., Miquel- Herbert K., Daemen J. A randomised comparison of an everolimuseluting coronary stent with a paclitaxel-eluting coronary stent: the SPIRIT II trial. Eurointervention 2006;2:286-94.

159. Costa J.R. Jr, Abizaid A., Feres F., Costa R., Seixas A.C., Maia F., Tanajura L.F., Staico R., Siqueira D., Meredith L., Bhat V., Yan J., Ormiston J., Sousa A.G., Fitzgerald P., Sousa J.E. EXCELLA First-in- Man (FIM) study: safety and efficacy of novolimus-eluting stent in de novo coronary lesions. EuroIntervention 2008;4:53-8.

160. Verheye S., Agostoni P., Dawkins K.D., Dens J., Rutsch W., Carrie D., Schofer J., Lotan C., Dubois C.L., Cohen S.A., Fitzgerald P.J., Lansky A.J. The GENESIS (Randomized, Multicenter Study of the Pimecrolimus-Eluting and Pimecrolimus/Paclitaxel-Eluting Coronary Stent System in Patients with De Novo Lesions of the Native Coronary Arteries) trial. JACC Cardiovasc Interv 2009;2:205-14.

161. Costa J.R. Jr, Abizaid A., Costa R., Feres F., Tanajura L.F., Maldonado G., Staico R., Siqueira D., Sousa A.G., Bonan R., Sousa J.E. 1-year results of the hydroxyapatite polymer-free sirolimus-eluting stent for the treatment of single de novo coronary lesions: the VESTASYNC I trial. JACC Cardiovasc Interv 2009;2:422-7.

162. Ormiston J.A., Serruys P.W., Regar E., Dudek D., Thuesen L., Webster M.W.I., Onuma Y., Garcia-Garcia H.M., McGreevy R., Veldhof S. A bioabsorbable everolimus-eluting coronary stent system for patients with single de-novo coronary artery lesions (ABSORB): a prospective open-label trial. Lancet 371:899-907.

163. Serruys P.W., Ormiston J.A., Onuma Y., Regar E., Gonzalo N., Garcia- Garcia H.M., Nieman K., Bruining N., Dorange C., Miquel-Hebert K., Veldhof S., Webster M., Thuesen L., Dudek D. A bioabsorbable everolimus-eluting coronary stent system (ABSORB): 2-year outcomes and results from multiple imaging methods. Lancet 2009;373:897- 910.

164. Okazaki S., Yokoyama T., Miyauchi K., Shimada K., Kurata T., Sato H., Daida H. Early statin treatment in patients with acute coronary syndrome: demonstration of the beneficial effect on atherosclerotic lesions by serial volumetric intravascular ultrasound analysis during half a year after coronary event: the ESTABLISH Study. Circulation 2004;110:1061-8.

165. Jensen L.O., Thayssen P., Pedersen K.E., Stender S., Haghfelt T. Regression of coronary atherosclerosis by simvastatin: a serial intravascular ultrasound study. Circulation 2004;110:265-70.

166. Petronio A.S., Amoroso G., Limbruno U., Papini B., De Carlo M., Micheli A., Ciabatti N., Mariani M. Simvastatin does not inhibit intimal hyperplasia and restenosis but promotes plaque regression in normocholesterolemic patients undergoing coronary stenting: a randomized study with intravascular ultrasound. Am Heart J 2005; 149:520-6.

167. Nishioka H., Shimada K., Kataoka T., Hirose M., Asawa K., Hasegawa T., Yamashita H., Ehara S., Kamimori K., Sakamoto T., Kobayashi Y., Yoshimura T., Yoshiyama M., Takeuchi K., Yoshikawa J. Impact of HMG-CoA reductase inhibitors for non-treated coronary segments. Osaka City Med J 2004;50:61-8.

168. Tani S., Watanabe I., Anazawa T., Kawamata H., Tachibana E., Furukawa K., Sato Y., Nagao K., Kanmatsuse K., Kushiro T. Effect of pravastatin on malondialdehyde-modified low-density lipoprotein levels and coronary plaque regression as determined by threedimensional intravascular ultrasound. Am J Cardiol 2005;96:1089- 94.

169. Nissen S.E., Nicholls S.J., Sipahi I., Libby P., Raichlen J.S., Ballantyne C.M., Davignon J., Erbel R., Fruchart J.C., Tardif J.-C., Schoenhagen P., Crowe T., Cain V., Wolski K., Goormastic M., Tuzcu E.M., for the ASTEROID Investigators. Effect of Very High-Intensity Statin Therapy on Regression of Coronary Atherosclerosis: The ASTEROID Trial. JAMA 2006;295:1556-65.

170. Takashima H., Ozaki Y., Yasukawa T., Waseda K., Asai K., Wakita Y., Kuroda Y., Kosaka T., Kuhara Y., Ito T. Impact of lipid-lowering therapy with pitavastatin, a new HMG-CoA reductase inhibitor, on regression of coronary atherosclerotic plaque. Circ J 2007;71:1678-84.

171. Takayama T., Hiro T., Yamagishi M., Daida H., Hirayama A., Saito S., Yamaguchi T., Matsuzaki M. Effect of rosuvastatin on coronary atheroma in stable coronary artery disease: multicenter coronary atherosclerosis study measuring effects of rosuvastatin using intravascular ultrasound in Japanese subjects (COSMOS). Circ J 2009; 73:2110-7.

172. Hiro T., Kimura T., Morimoto T., Miyauchi K., Nakagawa Y., Yamagishi M., Ozaki Y., Kimura K., Saito S., Yamaguchi T., Daida H., Matsuzaki M. Effect of intensive statin therapy on regression of coronary atherosclerosis in patients with acute coronary syndrome: a multicenter randomized trial evaluated by volumetric intravascular ultrasound using pitavastatin versus atorvastatin (JAPAN-ACS [Japan assessment of pitavastatin and atorvastatin in acute coronary syndrome] study). J Am Coll Cardiol 2009;54:293-302.

173. Tardif J.C., Gregoire J., L'Allier P.L., Anderson T.J., Bertrand O., Reeves F., Title L.M., Alfonso F., Schampaert E., Hassan A., McLain R., Pressler M.L., Ibrahim R., Lesperance J., Blue J., Heinonen T., 03-14_Garcia.fm Page 210 Mardi, 17. août 2010 5:34 17 Rodes-Cabau J. Effects of the acyl coenzyme A:cholesterol acyltransferase inhibitor avasimibe on human atherosclerotic lesions. Circulation 2004;110:3372-7.

174. Nissen S.E., Tsunoda T., Tuzcu E.M., Schoenhagen P., Cooper C.J., Yasin M., Eaton G.M., Lauer M.A., Sheldon W.S., Grines C.L., Halpern S., Crowe T., Blankenship J.C., Kerensky R. Effect of recombinant ApoA-I Milano on coronary atherosclerosis in patients with acute coronary syndromes: a randomized controlled trial. Jama 2003;290: 2292-300.

175. Tardif J.C., Gregoire J., L'Allier P.L., Ibrahim R., Anderson T.J., Reeves F., Title L.M., Schampaert E., LeMay M., Lesperance J., Scott R., Guertin M.C., Brennan M.L., Hazen S.L., Bertrand O.F. Effects of the antioxidant succinobucol (AGI-1067) on human atherosclerosis in a randomized clinical trial. Atherosclerosis 2008;197: 480-6.

176. Nissen S.E., Nicholls S.J., Wolski K., Rodes-Cabau J., Cannon C.P., Deanfield J.E., Despres J.P., Kastelein J.J., Steinhubl S.R., Kapadia S., Yasin M., Ruzyllo W., Gaudin C., Job B., Hu B., Bhatt D.L., Lincoff A.M., Tuzcu E.M. Effect of rimonabant on progression of atherosclerosis in patients with abdominal obesity and coronary artery disease: the STRADIVARIUS randomized controlled trial. JAMA 2008; 299:1547-60.

177. Luscher T.F., Pieper M., Tendera M., Vrolix M., Rutsch W., van den Branden F., Gil R., Bischoff K.O., Haude M., Fischer D., Meinertz T., Munzel T. A randomized placebo-controlled study on the effect of nifedipine on coronary endothelial function and plaque formation in patients with coronary artery disease: the ENCORE II study. Eur Heart J 2009;30:1590-7.

178. Kawasaki M., Sano K., Okubo M., Yokoyama H., Ito Y., Murata I., Tsuchiya K., Minatoguchi S., Zhou X., Fujita H., Fujiwara H. Volumetric quantitative analysis of tissue characteristics of coronary plaques after statin therapy using three-dimensional integrated backscatter intravascular ultrasound. J Am Coll Cardiol 2005;45:1946-53.

179. 179. Taniwaki M, Radu MD, Garcia-Garcia HM, Heg D, Kelbaek H, Holmvang L, Moschovitis A, Noble S, Pedrazzini G, Saunamaki K, Dijkstra J, Landmesser U, Wenaweser P, Meier B, Stefanini GG, Roffi M, Luscher TF, Windecker S, Raber L. Long-term safety and feasibility of three-vessel multimodality intravascular imaging in patients with st-elevation myocardial infarction: The ibis-4 (integrated biomarker and imaging study) substudy. The international journal of cardiovascular imaging. 2015

180. Taniwaki M, Radu MD, Garcia-Garcia HM, Heg D, Kelbaek H, Holmvang L, Moschovitis A, Noble S, Pedrazzini G, Saunamaki K, Dijkstra J, Landmesser U, Wenaweser P, Meier B, Stefanini GG, Roffi M, Luscher TF, Windecker S, Raber L. Long-term safety and feasibility of three-vessel multimodality intravascular imaging in patients with st-elevation myocardial infarction: The ibis-4 (integrated biomarker and imaging study) substudy. The international journal of cardiovascular imaging. 2015

181. Pu J, Mintz GS, Biro S, Lee JB, Sum ST, Madden SP, Burke AP, Zhang P, He B, Goldstein JA, Stone GW, Muller JE, Virmani R, Maehara A. Insights into echo-attenuated plaques, echolucent plaques, and plaques with spotty calcification: Novel findings from comparisons among intravascular ultrasound, near-infrared spectroscopy, and pathological histology in 2,294 human coronary artery segments. J Am Coll Cardiol. 2014;63:2220-2233

182. Pletcher MJ, Sibley CT, Pignone M, Vittinghoff E, Greenland P. Interpretation of the coronary artery calcium score in combination with conventional cardiovascular risk factors: the Multi-Ethnic Study of Atherosclerosis (MESA). Circulation. 2013;128:1076–1084

183. Sangiorgi G, Rumberger JA, Severson A, Edwards WD, Gregoire J, Fitzpatrick LA, Schwartz RS. Arterial calcification and not lumen stenosis is highly correlated with atherosclerotic plaque burden in humans: a histologic study of 723 coronary artery segments using nondecalcifying methodology. J Am Coll Cardiol. 1998;31:126–133.

184. Stone GW, Maehara A, Lansky AJ, de Bruyne B, Cristea E, Mintz GS, Mehran R, McPherson J, Farhat N, Marso SP, Parise H, Templin B, White R, Zhang Z, Serruys PW. A prospective natural-history study of coronary atherosclerosis. The New England journal of medicine. 2011;364:226-235

185. Calvert PA, Obaid DR, O'Sullivan M, Shapiro LM, McNab D, Densem CG, Schofield PM, Braganza D, Clarke SC, Ray KK, West NE, Bennett MR. Association between ivus findings and adverse outcomes in patients with coronary artery disease the viva (vh-ivus in vulnerable atherosclerosis) study. JACC. Cardiovascular imaging. 2011;4:894-901

186. Cheng JM, Garcia-Garcia HM, de Boer SP, Kardys I, Heo JH, Akkerhuis KM, Oemrawsingh RM, van Domburg RT, Ligthart J, Witberg KT, Regar E, Serruys PW, van Geuns RJ, Boersma E. In vivo detection of high-risk coronary plaques by radiofrequency intravascular ultrasound and cardiovascular outcome: Results of the atheroremo-ivus study. European heart journal. 2014;35:639-647 http://www.ncbi.nlm.nih.gov/pubmed?term=Clin Ther. 2009; 31(1): 64-73.

187. Waksman R, Legutko J, Singh J, Orlando Q, Marso S, Schloss T, Tugaoen J, DeVries J, Palmer N, Haude M, Swymelar S, Torguson R. First: Fractional flow reserve and intravascular ultrasound relationship study. J Am Coll Cardiol. 2013;61:917-923

188. Authors/Task Force m, Windecker S, Kolh P, Alfonso F, Collet JP, Cremer J, Falk V, Filippatos G, Hamm C, Head SJ, Juni P, Kappetein AP, Kastrati A, Knuuti J, Landmesser U, Laufer G, Neumann FJ, Richter DJ, Schauerte P, Sousa Uva M, Stefanini GG, Taggart DP, Torracca L, Valgimigli M, Wijns W, Witkowski A. 2014 esc/eacts guidelines on myocardial revascularization: The task force on myocardial revascularization of the european society of cardiology (esc) and the european association for cardio-thoracic surgery (eacts) developed with the special contribution of the european association of percutaneous cardiovascular interventions (eapci). European heart journal. 2014;35:2541-2619

189. Zhang YJ, Garcia-Garcia HM, Farooq V, Bourantas CV, Serruys PW, Chen SL. Revisiting: "Comparison of intravascular ultrasound versus angiography-guided drug-eluting stent implantation: A meta-analysis of one randomised trial and ten observational studies involving 19,619 patients". EuroIntervention : journal of EuroPCR in collaboration with the Working Group on Interventional Cardiology of the European Society of Cardiology. 2013;9:891-892

190. Witzenbichler B, Maehara A, Weisz G, Neumann FJ, Rinaldi MJ, Metzger DC, Henry TD, Cox DA, Duffy PL, Brodie BR, Stuckey TD, Mazzaferri EL, Jr., Xu K, Parise H, Mehran R, Mintz GS, Stone GW. Relationship between intravascular ultrasound guidance and clinical outcomes after drug-eluting stents: The assessment of dual antiplatelet therapy with drug-eluting stents (adapt-des) study. Circulation. 2014;129:463-470

191. Raber L, Taniwaki M, Zaugg S, Kelbaek H, Roffi M, Holmvang L, Noble S, Pedrazzini G, Moschovitis A, Luscher TF, Matter CM, Serruys PW, Juni P, Garcia-Garcia HM, Windecker S, Investigators IT. Effect of high-intensity statin therapy on atherosclerosis in non-infarct-related coronary arteries (ibis-4): A serial intravascular ultrasonography study. European heart journal. 2015;36:490-500

192. Ormiston JA, Serruys PW, Regar E, Dudek D, Thuesen L, Webster MW, Onuma Y, Garcia-Garcia HM, McGreevy R, Veldhof S. A bioabsorbable everolimuseluting coronary stent system for patients with single de-novo coronary artery lesions (ABSORB): a prospective open-label trial. Lancet. 2008; 371(9616): 899-907. http://www.ncbi.nlm.nih.gov/pubmed?term=Ormiston JA, Serruys PW, Regar E, Dudek D, Thuesen L, Webster MW, Onuma Y, Garcia-Garcia HM, McGreevy R, Veldhof S. A bioabsorbable everolimuseluting coronary stent system for patients with single de-novo coronary a

193. Serruys PW, Ormiston JA, Onuma Y, Regar E, Gonzalo N, Garcia-Garcia HM, Nieman K, Bruining N, Dorange C, Miquel-Hébert K, Veldhof S, Webster M, Thuesen L, Dudek D. A bioabsorbable everolimus-eluting coronary stent system (ABSORB): 2-year outcomes and results from multiple imaging methods. Lancet. 2009; 373(9667): 897-910.

194. Simsek C, Karanasos A, Magro M, Garcia-Garcia HM, Onuma Y, Regar E, Boersma E, Serruys PW, van Geuns RJ. Long-term invasive follow-up of the everolimus-eluting bioresorbable vascular scaffold: Five-year results of multiple invasive imaging modalities. EuroIntervention : journal of EuroPCR in collaboration with the Working Group on Interventional Cardiology of the European Society of Cardiology. EuroIntervention. 2014 Oct 28. pii: 20130724-03. doi: 10.4244/EIJY14M10_12. [Epub ahead of print]

195. Nicholls SJ, Ballantyne CM, Barter PJ, Chapman MJ, Erbel RM, Libby P, Raichlen JS, Uno K, Borgman M, Wolski K, Nissen SE. Effect of two intensive statin regimens on progression of coronary disease. The New England journal of medicine. 2011;365:2078-2087

196. Nicholls SJ, Bakris GL, Kastelein JJ, Menon V, Williams B, Armbrecht J, Brunel P, Nicolaides M, Hsu A, Hu B, Fang H, Puri R, Uno K, Kataoka Y, Bash D, Nissen SE. Effect of aliskiren on progression of coronary disease in patients with prehypertension: The aquarius randomized clinical trial. JAMA. 2013;310:1135-1144

197. Tardif JC, Ballantyne CM, Barter P, Dasseux JL, Fayad ZA, Guertin MC, Kastelein JJ, Keyserling C, Klepp H, Koenig W, L'Allier PL, Lesperance J, Luscher TF, Paolini JF, Tawakol A, Waters DD, Can HDLISQARI. Effects of the high-density lipoprotein mimetic agent cer-001 on coronary atherosclerosis in patients with acute coronary syndromes: A randomized trial. European heart journal. 2014;35:3277-3286

198. Kini AS, Baber U, Kovacic JC, Limaye A, Ali ZA, Sweeny J, Maehara A, Mehran R, Dangas G, Mintz GS, Fuster V, Narula J, Sharma SK, Moreno PR. Changes in plaque lipid content after short-term intensive versus standard statin therapy: The yellow trial (reduction in yellow plaque by aggressive lipid-lowering therapy). J Am Coll Cardiol. 2013;62:21-29

Chapter 4

Early detection and invasive passivation of future culprit lesions: a future potential or an unrealistic pursuit of chimeras?

Christos V. Bourantas, MD, PhD; Hector M. Garcia-Garcia, MD, PhD; Roberto Diletti, MD; Takashi Muramatsu, MD, PhD; Patrick W. Serruys, MD, PhD

Am Heart J. 2013 Jun;165(6):869-881.

ABSTRACT

New advances in image and signal processing have allowed the development of numerous invasive and noninvasive imaging modalities that have revealed details of plaque pathology and allowed us to study in vivo the atherosclerotic evolution. Recent natural history of atherosclerosis studies permitted us to evaluate changes in the compositional and morphological characteristics of the plaque and identify predictors of future events. The idea of being able to identify future culprit lesions and passivate these plaques has gradually matured, and small scale studies have provided proofs about the feasibility of this concept. This review article summarizes the recent advances in the study of atherosclerosis, cites the current evidence, highlights our limitations in understanding the evolution of the plaque and in predicting plaque destabilization, and discusses the potentiality of an early invasive sealing of future culprit lesions.

INTRODUCTION

The miniaturization of medical devices, technological innovations, new developments in image and signal processing, and advances in biological and molecular imaging have provided us with a variety of imaging modalities that permit detection of local inflammation and detailed evaluation of changes in atheroma burden and its composition. These techniques demonstrated that coronary atherosclerosis has focal and eccentric manifestations that evolve in an independent manner, which is affected by the composition of the plaque, the presence of inflammation, and the local hemodynamic environment. Prospective natural history of atherosclerosis studies shed light into the mechanisms involved in this process and allowed us to identify predictors of future culprit lesions. [1-3]

The idea of being able to predict plaque development has gradually evolved and recently the Shield Evaluated at Cardiac Hospital in Rotterdam for Investigation and Treatment of TCFA study has been reported, which examined the feasibility of sealing non– flow-limiting lesions that have features associated with increased vulnerability (Figure 1).[4]

The aim of this review article is to summarize the technological advances in the study of atherosclerosis, cite the current evidence, and discuss the potentiality of an invasive passivation of future culprit lesions.

EFFECT OF THE COMPOSITION OF THE PLAQUE ON THE NATURAL COURSE OF ATHEROSCLEROSIS

Even before the development of intravascular imaging, it was apparent that the composition of the atheroma has significant prognostic implications and affects its natural course. Pathology-based studies have shown that the type of the plaque is associated with the final act of atherosclerosis and allowed identification of plaque characteristics associated with acute coronary events.[5]

Today, it is known that most of the acute myocardial infractions (MIs) are due to plaque rupture, which occurs in lesions referred as thin-capped fibroatheromas (TCFAs). These plaques exhibit positive remodeling, have a large lipid core that is covered by a thin fibrous cap, and are rich in macrophages. [6,7]

Other features associated with increased vulnerability are the presence of microcalcifications and neoangiogenesis.[8,9] The introduction of intravascular imaging permitted in vivo visualization of these characteristics and opened new horizons in the study of plaque growth.

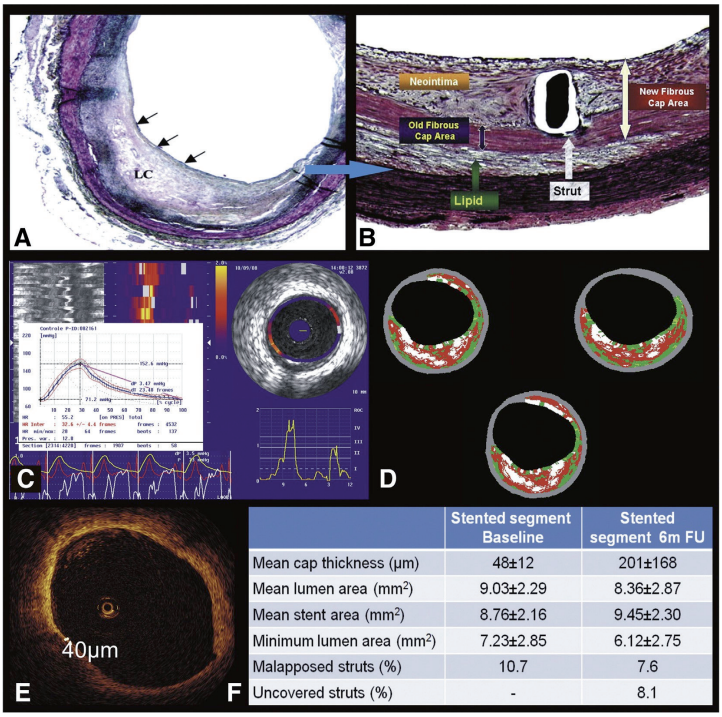

	Stented segment Baseline	Stented segment 6m FU
Mean cap thickness (µm)	48±12	201±168
Mean lumen area (mm^2)	9.03±2.29	8.36±2.87
Mean stent area (mm^2)	8.76±2.16	9.45±2.30
Minimum lumen area (mm^2)	7.23±2.85	6.12±2.75
Malapposed struts (%)	10.7	7.6
Uncovered struts (%)	-	8.1

Figure 1. Stent implantation in a high-risk plaque leads to neointimal formation and increases the thickness of the tissue that covers a lipid core (LC) (A) resulting in the potential passivation of the plaque (B). Imaging data acquired at baseline from a patient recruited in the SECRITT study: palpography demonstrated high strain (C), radiofrequency analysis of the backscattered intravascular ultrasound signal showed a lipid-rich plaque, which, however, did not cause luminal obstruction (D), whereas optical coherence tomography demonstrated a TCFA (cap thickness 40 µm) (E). The results of the study are summarized in panel (F): at 6-month follow-up, the thickness of the fibrous cap was increased by 170 µm, there was a minor reduction in the mean lumen area, minimal malapposition, and most of the struts were fully covered. Panel A and B were obtained with permission from Moreno.[73]

IVUS-VH and OCT of Coronary Bifurcations

Intravascular ultrasound

Intravascular ultrasound (IVUS) was the first invasive modality that allowed imaging of the lumen and vessel wall, quantification of plaque burden, and characterization of its composition. The analysis of the radiofrequency backscatter IVUS signal (RF-IVUS) permitted more reliable detection of the type of the plaque and has been extensively implemented to quantify and assess changes in the composition of the atheroma.[10-12] Numerous studies used RF-IVUS at 1 time point to assess the distribution of the atheroma and evaluate differences in the composition of the plaque in patients with different clinical presentations, whereas others implemented serial RF-IVUS to evaluate atherosclerotic

process and the effect of medical treatment on plaque growth.[11-13] The most recent study with serial assessment was reported by Kubo et al[13] and included 99 patients who had RF-IVUS examination at baseline and at 12-month follow-up. Two hundred sixteen lesions were examined at these 2 time points. At baseline, 20 TCFAs were identified, 5 of which were unchanged at follow-up, whereas 15 regressed to more stable forms. On the other hand, 12 new TCFAs appeared at the follow-up examination.

These findings demonstrated the dynamic nature of atherosclerosis and the value of RF-IVUS in assessing this process.[13]

The PROSPECT trial was the largest natural history of atherosclerosis study and used RF-IVUS to detect anatomical and compositional features associated with an increased risk for a plaque to evolve to a culprit lesion.[1] Six hundred ninety-seven patients treated for an acute coronary syndrome underwent RF-IVUS post intervention at the 3 epicardial coronary arteries. At 3- year follow-up, 104 new symptomatic lesions became manifest in the non-treated segments. Multivariable analysis demonstrated that the presence of TCFA, a minimum lumen area ≤4 mm^2, and a plaque burden ≥70% were associated with future events. Similar results were reported by the VH-IVUS in Vulnerable Atherosclerosis Study study that had a similar design. [3] The PROSPECT trial not only showed the potential predictive value of intravascular imaging but also highlighted its limited prognostic accuracy as only 4% of the detected TCFA evolved to culprit lesions. This should be attributed to the fact that the included patients were on optimal treatment and to the inherited limitations of IVUS imaging.[14]

Optical coherence tomography

Optical coherence tomography (OCT) is the light-based analogous of IVUS. It provides high-resolution cross-sectional images and permits visualization of details, which cannot be imaged by other intravascular techniques such as evaluation of the thickness of the fibrous cap, detection of macro- phages, and neovascularization and identification of plaque erosion. [15] Optical coherence tomography is the method of choice for characterizing the superficial plaque and detecting culprit lesions, and it has been used to assess the distribution of different plaque types in patients with different clinical presentations.[16-18] A limitation of OCT is its poor penetration, which often does not allow complete visualization of the vessel wall and assessment of vessel remodeling. In addition, OCT signal cannot penetrate lipid tissue, and thus, it is unable to quantify the lipid component. To overcome these pitfalls, multimodality imaging has been proposed, and currently, the Integrated Biomarkers and Imaging Study (IBIS) 4 is underway that implements serial IVUS and OCT examination to investigate the effect of pharmaceutical treatment on plaque burden and characteristics in patients who have sustained an acute coronary event.[18,19]

Other invasive imaging techniques — Upcoming hybrid imaging modalities

Angioscopy and intravascular magnetic spectroscopy have been used in the past in the study of atherosclerosis, but today, they have limited use. On the other hand, near-infrared spectroscopy (NIRS) is a relatively new modality, introduced to provide more accurate identification of lipid component, and has already applications in research arena. Furthermore, intravascular magnetic imaging, photoacoustic imaging, Raman spectroscopy, and time-resolved fluorescence spectroscopy are emerging techniques, which are currently under evaluation and are expected to provide additional information about plaque evolution (online Appendix Supplementary Table I).

In parallel, an effort is being made to overcome the limitations of the prominent intravascular imaging modalities either by developing new methodologies that would allow better processing of the acquired data (eg, focused acoustic computed tomography, micro-OCT, polarized OCT) or by creating hybrid catheters that would permit multimodality intravascular imaging, pro- vide complete visualization of coronary pathology, and more accurate detection of future culprit lesions.[20,21] A hybrid catheter that combines an IVUS and a NIRS probe (TVC, MC 7 system; InfraRedx, Burlington, MA) is currently available and being used in research arena, whereas catheters that permit fusion of IVUS with OCT, photoacoustic imaging, or time resolved fluorescence spectroscopy are under evaluation. [22] Initial experimental studies have shown promising results. [23-25] However, the large dimensions of the available catheters, the concerns regarding the safety of the new techniques, and the low image acquisition rate as well as the moderate image quality that they provide have not allow their implementation in humans yet.

Noninvasive imaging modalities

Advances in computed tomographic imaging (eg, the use of dual x-ray sources, the increased number of detectors, the decreased slice thickness, and the faster rotation gantry) have permitted imaging of coronary anatomy and pathology and reduced the radiation dose. Several studies used intravascular imaging techniques as criterion standard to validate computed tomographic coronary angiography (CTCA) and demonstrated that it can accurately measure the luminal and vessel wall dimensions, identify the presence of vessel wall remodeling, and discriminate calcified from non-calcified plaques. [26,27] On the other hand, CTCA has limited capability in differentiating lipid-rich from fibrotic plaques and has low resolution, which does not permit visualization of plaque characteristics associated with increased vulnerability. [28]

Although CTCA has considerable limitations, it seems that it provides useful prognostic information. A study conducted by Motayama et al[29] that included N 1,000 patients who underwent CTCA because of suspected coronary artery disease (CAD) demonstrated

that the detected by CTCA vessel wall remodeling and the low- attenuated plaques were independent predictors of cardiac morbidity. Moreover, the Coronary CT Angiography Evaluation for Clinical Outcomes: An International Multicenter registry showed that in symptomatic patients the combination of the Morise risk score and the CTCA derived data—in particular, the number of the epicardial vessels with obstructive (≥50%) stenoses—allowed more accurate prediction of the 2-year major adverse cardiac events (all-cause mortality, nonfatal myocardial infarction, and revascularization) than the Morise score (accuracy 0.83 vs 0.68, respectively).[30] In view of these findings, an ambitious prospective study commenced, the BioImage trial that aims to include N6,000 asymptomatic subjects who will undergo noninvasive imaging (including CTCA if they have a high-risk cardiovascular profile) to identify new imaging-based predictors of future cardiovascular events.[31]

Magnetic resonance imaging (MRI) appears to be able to detect the composition of the plaque and has been used to study the atherosclerotic process in the aorta and the carotids, but it has a limited value in assessing coronary pathology, as it requires prolonged acquisition time and has poor spatial resolution.[32] Further improvements in external coils as well as the development of contrast agents that will allow more accurate plaque characterization are required so as this modality to be useful in this setting.

ROLE OF INFLAMMATION ON PLAQUE DEVELOPMENT AND DESTABILIZATION

Cumulative evidence has demonstrated that inflammation plays an important role in atherogenesis as it regulates the expression of mediators associated with plaque development. Several metabolic pathways triggered by increased inflammation appear to contribute to plaque destabilization and promote thrombus formation and collagen breakdown, which increase the fragility of the fibrous cap. [33,34] Appreciating the prominent role of inflammation on plaque rupture research focused on developing methodologies to detect and quantify its presence on vessel wall.

Invasive techniques for the detection of inflammation

Thermography

Thermography is the first invasive imaging technique developed to identify vessel wall inflammation and relies on the measurement of plaque heat. High temperatures indicate increased inflammatory activity and vulnerability of the plaque. Initial reports

demonstrated the efficacy of thermography in detecting high-risk plaques, but recent studies have raised concerns about its effectiveness in patent coronaries suggesting that blood flow obstruction is necessary to obtain accurate estimations, fact that has limited its current applications. [35,36]

Near-infrared fluorescence molecular imaging

Near-infrared fluorescence (NIRF) imaging is a novel technique introduced to detect vascular activity. It involves injection of agents that bind molecules related to plaque's inflammation and have the ability to fluoresce after being irradiated with near-infrared light emitted by a specially designed catheter. Experimental studies demonstrated the feasibility and the potential of thistechnology.[37] Recently, a hybrid NIRF-OCT catheter (diameter 2.4F) has been designed that allows simultaneous molecular functional imaging (provided by NIRF) and visualization of vessel pathology (given by OCT).[38] The feasibility of this approach has been tested ex vivo and in vivo in animal models and the first results appear promising. However, the safety of this technique has to be proven before being implemented in humans.[39]

Noninvasive imaging of vessel wall inflammation

Nuclear imaging

Nuclear imaging constitutes the leading noninvasive modality for the evaluation of vascular activity. Initial positron emission tomography (PET) studies, conducted to detect malignant tumors, demonstrated an increased 18F-fluorodeoxyglucose (18F- FDG) uptake in large arteries and later reports confirmed a correlation between 18F-FDG and vessel wall inflammation.[40] Recent reports demonstrated the feasibility of the combined CTCA-18F-FDG imaging for the identification of inflamed plaques on the coronary tree.[41,42] The concept of fusing 2 noninvasive modalities that provide anatomical (derived from CTCA) and biological (given by PET) information constitutes a breakthrough in the study of atherosclerosis as it will allow detailed imaging of plaque pathology in larger populations and it is expected to provide additional information about the distribution of plaque inflammation and its association with different plaque components.

Apart from 18F-FDG, several other tracers have been developed to assess vascular activity, such as the 99mTc- AA5, which binds phosphatidylserine produced by apoptotic cells; the 99mTc matrix metalloproteinase inhibitor that binds active metalloproteinases; and the IK17 tracer, which is labeled with 125I and is able to detect the presence of oxidized low density lipoprotein, without however being used in clinical setting yet.[43-45]

Other noninvasive techniques

A significant limitation of nuclear imaging is the increased radiation dose required, which restricts its research applications. Therefore, an effort has been made toward the development of alternative imaging techniques, which would be able to evaluate vessel wall inflammation. Injection of iodinate nanoparticles has been recently proposed to detect the presence of macrophages with CTCA.[46] Initial validation of this methodology in rabbit models using histology as criterion standard showed that it is accurate and that it compares favorably to the estimations of PET.[47]

The current value of MRI in assessing vascular activity is limited as most of the paramagnetic contrast agents are not able to deliver the necessary amount of gadolinium ions that would permit MRI detection. Moreover, most of the MRI contrast agents have large dimensions, which do not allow them to access to biochemical epitopes within the vessel wall.[32]

ROLE OF BLOOD FLOW ON THE ATHEROSCLEROTIC EVOLUTION AND PLAQUE DESTABILIZATION

The implications of blood flow on plaque development have been observed several years ago by Caro et al[48] who speculated the athero-promoting effect of low endothelial shear stress (ESS). This observation was supported later by studies conducted in cadaver specimens and experimental models. Recent advances in invasive and noninvasive imaging permitted in vivo reconstruction of coronary anatomy and allowed detailed assessment of the role of the hemodynamic forces on atherosclerotic evolution.

Blood flow simulation in models derived from invasive and noninvasive imaging modalities

Several small scale studies fused IVUS and coronary angiographic data to reconstruct coronary anatomy and showed that low or oscillating ESS promotes plaque growth and neointimal formation and alters the composition of the plaque.[49-51] Recently, the PREDICTION study examined prospectively in a large number of patients the implications of ESS on plaque development.[2] This trial included 506 patients who were admitted for an acute coronary event and underwent 3-vessel IVUS examination at baseline and at 6- to 10-month follow-up. The baseline IVUS and angiographic data were used to reconstruct coronary anatomy and evaluate the ESS distribution. It was found that low ESS promoted plaque growth and was independent predictor of future revascularizations.

Although today there are robust data to support the effect of the hemodynamic environment on plaque progression, there is little evidence about its role on plaque

destabilization.[52,53] It has been speculated that high ESS and increased axial tensile stress may cause plaque deformation and disruption of the fibrous cap leading to rupture.[54] However, further research is required toward this direction to test the validity of this hypothesis.

Computed tomographic coronary angiography and MRI have limited resolution and cannot provide meticulous visualization of luminal morphology. This limitation has raised concerns about the value of CTCA- and MRI-derived models in the assessment of ESS distribution. However, recent experimental studies demonstrated that noninvasive imaging reconstructions allow reliable blood flow simulation supporting their applications in research.[55]

Initial reports have confirmed the potential use of CTCA patient-derived models for the evaluation of ESS distribution and provided the substrate for the conduction of large scale prospective trials, which will examine the impact of the hemodynamic milieu on plaque growth.[56]

FUTURE TRENDS IN THE STUDY OF ATHEROSCLEROSIS

Today, our ability to predict plaque rupture is limited.

In the PROSPECT study, the quantitative and qualitative information provided by RF-IVUS predicted future culprit lesions with a positive predictive value of 18%, whereas in the PREDICTION study, the positive predic- tive value of the ESS and IVUS-derived measurements for identifying future significant stenoses was 42%.[1,2] It worth to be mentioned that, in both studies, only few of the reported events/revascularizations were related to acute coronary syndromes. The aforementioned results highlight the potential value of multimodality imaging in the identification of future culprit lesions among high-risk plaques. Today, it is impossible to perform a complete study of the coronary tree using multiple intravascular imaging catheters that would permit evaluation of vessel morphology (given by IVUS or OCT), composition (obtained by RF-IVUS, OCT, or NIRS), and inflammation (derived by OCT or NIRF) and provide reliable reconstruction of coronary anatomy for blood flow simulation. This, however, is likely to become feasible in the near future with the development of hybrid catheters that will allow simultaneous data acquisition (eg, a combined IVUS— intravascular photoacoustic catheter would permit assessment of the plaque burden, characterization of the type of the plaque, and detection of vessel wall inflammation) and a thorough assessment of coronary pathology (Figure 2).

Similarly, the integration of CTCA, nuclear imaging, and computational fluid dynamics

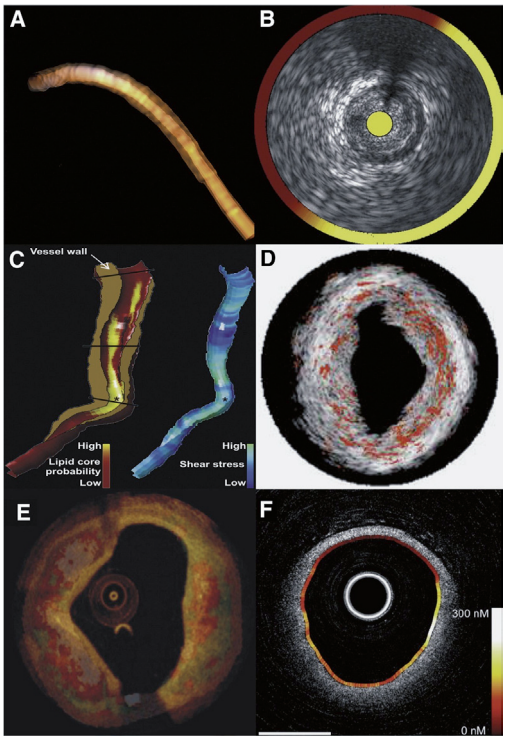

Figure 2. Output of hybrid imaging techniques. A, Fusion of coronary angiography and IVUS imaging. In the obtained model, the outer vessel wall is portrayed in a semitransparent fashion. B, Output of a dual-modality IVUS-NIRS catheter. Intravascular ultrasound permits visualization of the lumen, plaque, and outer vessel wall, whereas NIRS allows detection of the lipid tissue. C, Fusion of computed tomography, IVUS, and NIRS. The obtained models provide information about vessel geometry, and the distribution of the lipid tissue on the plaque and can be used to simulate blood flow and evaluate the endothelial shear stress. D, Combination of IVUS and intravascular photoacoustic imaging. Intravascular photoacoustic imaging allows detection of the lipid tissue (portrayed in an orange color), whereas IVUS provides visualization of the luminal morphology and the plaque. E, Fusion of OCT and IVUS radiofrequency backscatter images. The integration of different information acquired by these techniques permits more accurate characterization of the plaque. F, Output of a dual-modality catheter that allows simultaneous acquisition and coregistration of OCT and near-infrared fluorescence data. Optical coherence tomography provides information about the luminal morphology and the composition of the plaque, whereas near-infrared fluorescence allows identification of vessel wall inflammation portrayed in a color-coded map with the white-yellow color corresponding to increased inflammation. Images were obtained with permission from Bourantas et al, Wentzel et al, Wang et al, Raber et al, and Yoo et al.[38,74-77]

is expected to provide a holistic noninvasive evaluation of the plaque, whereas the introduction of nanoparticles for the detection of inflammation is anticipated to reduce the radiation dose and allow the conduction of large scale studies that will enhance our understanding about atherosclerotic evolution (Figure 3).

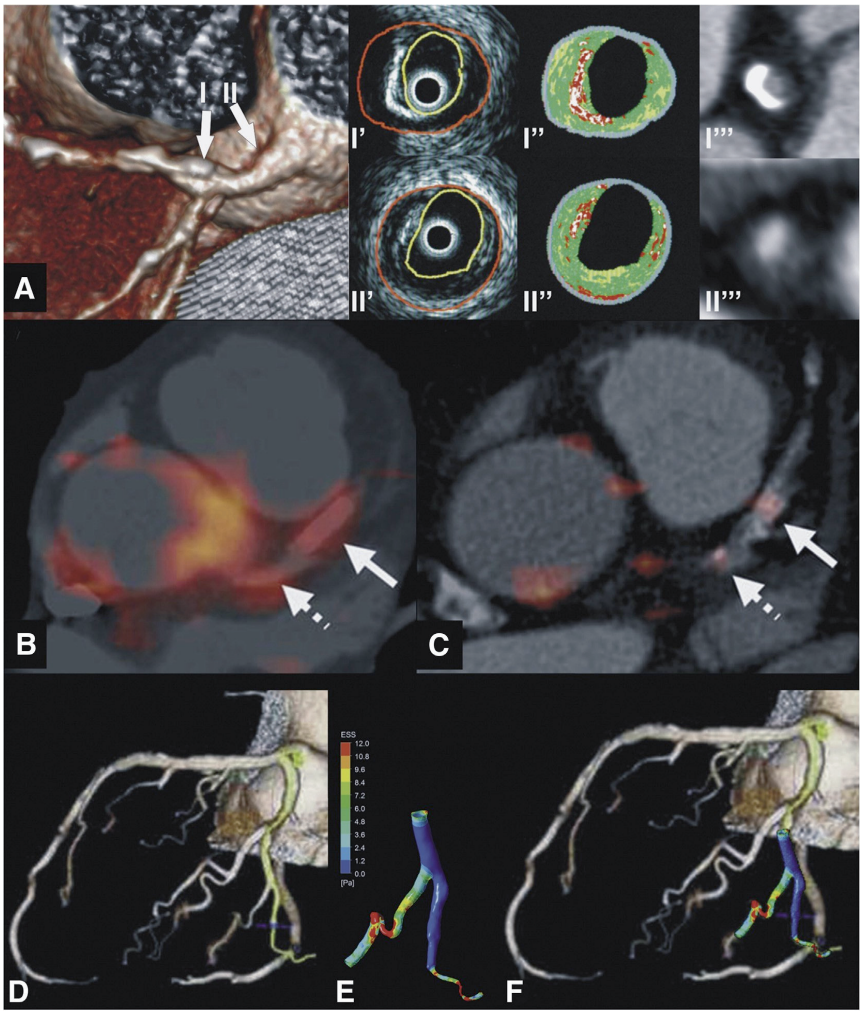

Figure 3. Implications of CTCA in the study of atherosclerosis. A, Ability of CTCA to detect the composition of the plaque. The arrows indicate the location of the IVUS and CTCA cross-sectional images. Panels (I'-I''') portray IVUS, IVUS radiofrequency backscatter analysis, and CTCA cross-sections for the distal calcified plaque, whereas the panels (II'-II'''), the corresponding cross-sections for the proximal plaque. The luminal morphology and the distribution of the plaque are similar in the CTCA and IVUS images. CTCA appears to allow accurate differentiation between calcified from noncalcified plaques. B, Fusion of CTCA and positron emission computed tomography. Increased ^{18}F-FDG uptake was noted in the aorta, left main stem, and left anterior descending artery (arrows) of a patient admitted with an acute coronary syndrome. C, On the other hand, minor inflammation was detected in the aorta and coronary tree of a patient with stable angina. D, Reconstruction of coronary tree from CTCA. E, These data were used to model the distal circumflex, simulate blood flow, and evaluate the shear stress distribution (portrayed in a color-coded map). F, Superimposition of the reconstructed model onto the coronary tree provided by CTCA. Panels B and C were obtained with permission from Rogers et al, whereas panels D to F were provided by Sakellarios AI and Fotiadis DI.[41]

CONSIDERATIONS THAT NEED TO BE ADDRESSED BEFORE ADVOCATING AN INVASIVE TREATMENT OF VULNERABLE PLAQUES

How accurate can we predict an upcoming event in patients with known coronary artery disease?

Although our knowledge about plaque vulnerability has increased over the last few years, our ability to predict the time of a future event remains low. The traditional risk models appear to predict with a moderate accuracy the short-term cardiovascular morbidity and mortality (cardiac death, MI, and repeat revascularization) in patients who have sustained an acute coronary syndrome (range 0.26-0.84) (online Appendix Supplementary Table II). To improve the performance of these scores, several new variables have been added such as the SYNergy between PCI with TAXUS and Cardiac Surgery (SYNTAX) score or biomarkers related with worse outcomes (eg, activated protein C, N-terminal pro-brain natriuretic peptide, glucose, cardiac troponin T). However, the information regarding coronary anatomy, given by the SYNTAX score, has only slightly increased the accuracy of these models, whereas the scores that included biomarkers were designed to predict all-cause mortality and not to estimate the risk of future cardiac events (online Appendix Supplementary Table II).

How accurately can we predict a future event in an asymptomatic population?

Most of the conventional models, designed for asymptomatic populations, focus on the prediction of the long-term cardiac outcomes (death, MI, coronary revascularization), and have low predictive accuracy. The new risk models that include bio- markers or genetic information have a slightly better predictive accuracy, whereas the ones that include CTCA data appear to allow accurate prediction of major adverse cardiovascular events but focus on the long-term outcomes (range 3.9-10 years) (online Appendix Supplementary Table III).

Over the last few years, several new markers associated with increased vulnerability have been identified (eg, patient genotype, myeloperoxidase, A2 phospholipase, blood monocytes subsets count, pregnancy associated plasma protein A, etc), and in a recent report, Brennan et al [57] combined the traditional with new risk factors, provided by patients' hematology profile (including leukocyte peroxidase-, erythrocyte- and platelet-related parameters), into a model that permitted prediction of 1-year MI and death with an accuracy of almost 80%.[57-60] Further research is required toward this direction to find new predictors and construct novel models that would give precise short- term risk stratification and potentially reliable estimation of upcoming coronary events.

Should we always treat a ruptured plaque?

Even if we were able to foresee which plaque and when this will rupture, it would be still debatable whether we should seal it. Several intravascular imaging studies have demonstrated the presence of ruptured plaque in the coronary tree of asymptomatic patients and of patients with CAD indicating that plaque rupture does not always cause an acute coronary event (Figure 4).[61,62]

Furthermore, chronically ruptured plaques appear clinically silent and do not require an interventional treatment.[63] Which of the ruptured plaques will cause MI and which will heal are still unclear. A small study that compared culprit and nonculprit ruptured plaques demonstrated that the culprit lesions had increased length, plaque burden, and remodeling index and exhibited a smaller luminal area comparing with the asymptomatic ulcerated plaques.[64] Apart from the morphological characteristics of the plaque, systemic factors and more specifically blood viscosity, platelet activity, fibrinogen levels, von Willebrand factor, and the interplay between coagulation and fibrinolytic system seem also to determine the final clinical consequences of plaque rupture.[65-67] Therefore, further effort should be made to identify predictors associated with extensive thrombus formation, blood flow obstruction, and the clinical manifestation of an acute coronary syndrome.

Should we focus only on thin capped fibroatheromas?

Histology-based studies have demonstrated that one- third of the acute coronary syndromes are due to plaque erosion occurring in plaques, which do not have the typical characteristics of a high-risk lesion. These plaques have the histologic appearance of pathologic intimal thickening or fibroatheroma and are rich in proteoglycan and smooth muscle cells.[68] The underlying mechanism of plaque erosion is poorly understood, and it has been speculated that it can be due to coronary vasospasm. Today, it is impossible to predict which of these stable-looking plaques will erode and cause MI.

Is there an ideal device to seal future culprit lesions?

The invasive treatment of a potential culprit lesion in asymptomatic patients can be justified only if stent implantation is safe. Initial reports demonstrated an unacceptable high risk of complications in non–flow- limiting lesions treated with balloon angioplasty or bare metal stents, whereas the new developments in stent design may have reduced the risk of complications, but they have not eradicated them.[69]The distortion of vessel wall physiology as well as the risk of neoatherosclerosis and of an inflammatory reaction to a permanent foreign body remains considerable pitfalls of metallic stents. Bioresorbable scaffold is a recent technology introduced to address the abovementioned drawbacks.

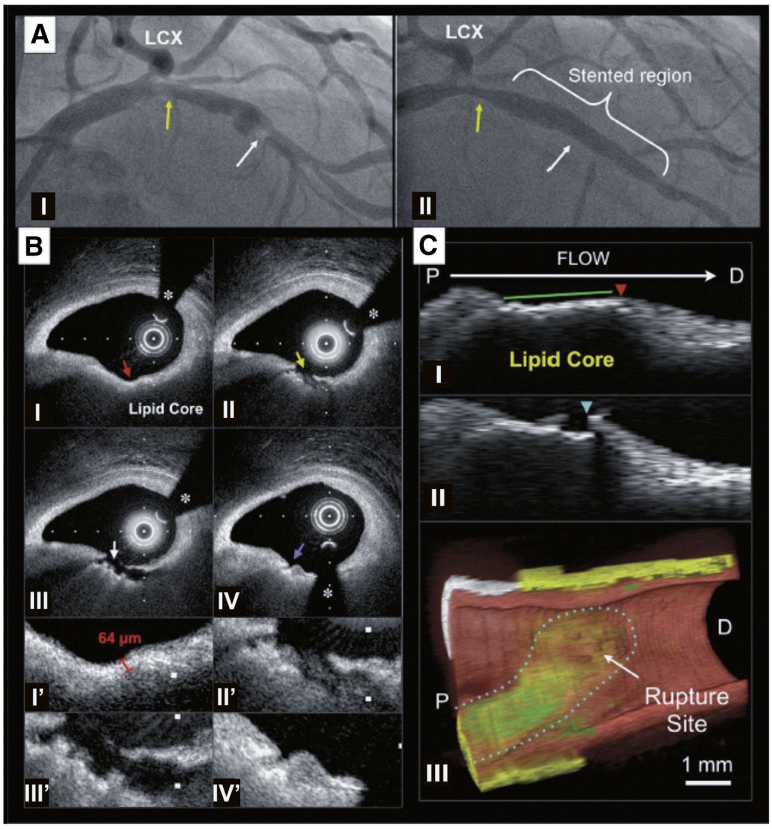

Figure 4. In vivo OCT imaging of an asymptomatic plaque rupture. Angiographic images showing 2 lesions, a distal (white arrow), which was stented successfully and a proximal (yellow arrow) that was left untreated (AI-AII). Optical coherence tomographic examination revealed a TCFA at the proximal lesion (red arrow) (BI, BI'). Repeat imaging few minutes later demonstrated plaque disruption (yellow arrow) (BII, BII') and an intimal flap (BIII, BIII'). Thrombus was gradually formed, which covered the created crater (BIV, BIV'). Longitudinal images (CI, CII) and 3-dimensional reconstruction of the OCT data (CIII) showed increased macrophages accumulation (indicated with a green color) at the ruptured plaque (arrow), which was located at the distal site of the lipid core.

These devices have the ability to dissolve after restoring the patency of the vessel allowing the coronary artery to maintain its physiologic integrity.[70] Recent reports demonstrated that the neointimal tissue developed postimplantation of a bioresorbable scaffold can seal the underlying plaques, whereas studies in animal models showed that the neotissue has features associated with plaque stability.[71,72]

These initial reports may support the use of bioresorbable scaffolds for paving diseased coronary segments with vulnerable plaques, but long-term follow-up data are required to elucidate this prospective (Figure 5).

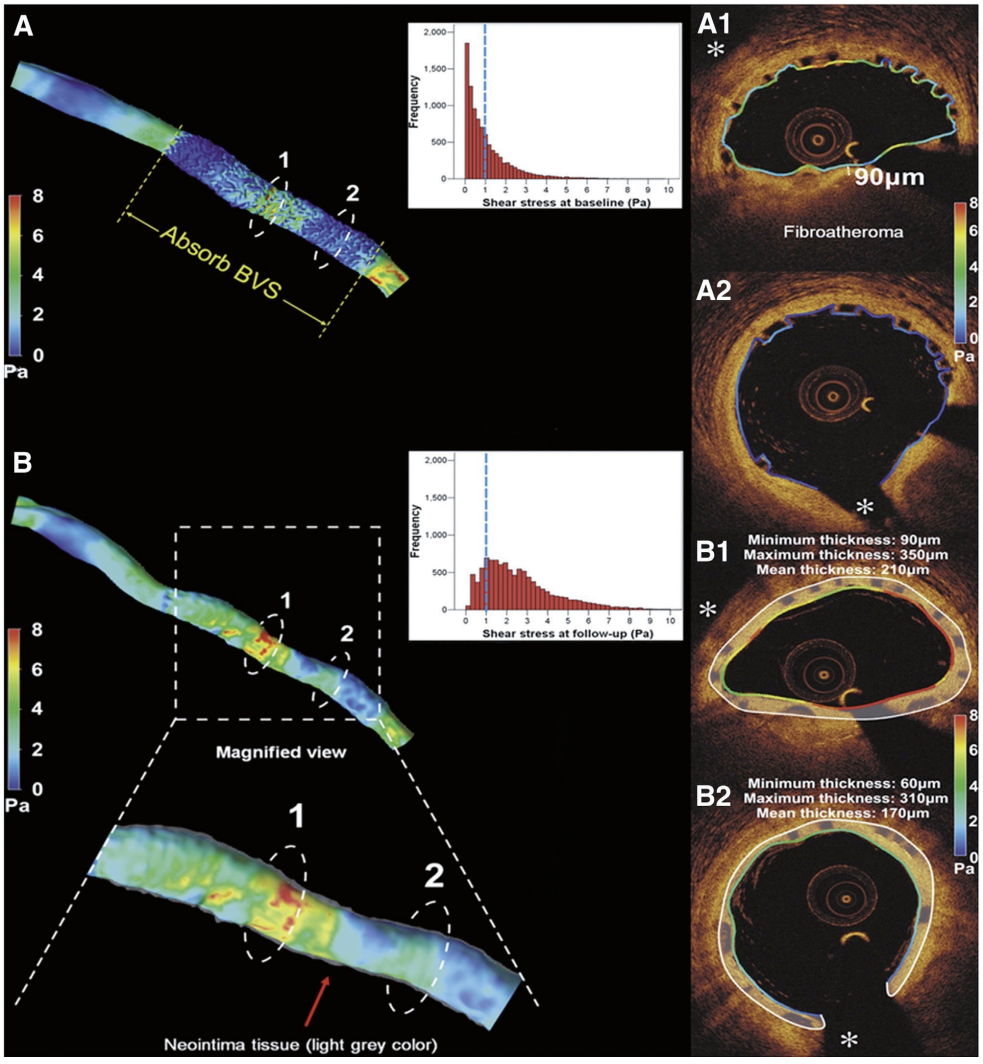

Figure 5. A, Three-dimensional reconstruction of a left anterior descending coronary artery from coronary angiographic and OCT data acquired immediate after an Absorb bioresorbable vascular scaffold implantation. The ESS is portrayed in the reconstructed surface with the use of a color-coded map. low ESS in noted in the scaffolded segment with 61% of the ESS being <I Pa. Panels AI and A2 illustrate 2 OCT cross-sectional images and the estimated ESS along the luminal circumference. The asterisk indicates a side branch. A fibroatheroma is shown al panel AI with a cap thickness of 90 IJm. Panel **B** portrays the reconstructed vessel al 2-year follow-up. The ESS in the scaffolded segment (B, B2) is normalized (only 17% of the ESS estimations are <17%) al follow-up creating an atheroprotective for the vessel environment. In addition, as it is shown in the magnified view, a thin layer of neointimal tissue is developed with a mean thickness of 160 IJm that covers the vessel wall and the fibroatheroma detected al baseline (BI). Image was obtained modified and used with permission from Bourantas et al.[78]

SUMMARY

New developments in invasive and noninvasive imaging have allowed detailed visualization of coronary pathology and have considerably increased our knowledge about plaque growth and rupture. Prospective natural history of atherosclerosis studies permitted evaluation of changes in plaque composition and assessment of the complexity of plaque evolution. Our inability to accurately predict which of the detected vulnerable plaques will rupture, when this will occur, and whether this event will have clinical implications cannot justify an invasive sealing of potential culprit lesions. However, this is likely to change in the future. The revolution occurring in invasive and noninvasive imaging and the advances in molecular biology are expected to provide additional information about atherosclerotic disease progression/regression, allow us to study this process in larger populations, and probably predict with a higher accuracy events and plaque ruptures. Although, few years ago, the early detection and invasive passivation of future culprit lesions appeared as an unrealistic dream, nowadays, it is regarded as a future potentiality.

REFERENCES

1. Stone GW, Maehara A, Lansky AJ, et al. A prospective natural- history study of coronary atherosclerosis. N Engl J Med 2011;364(3):226-35.
2. Stone PH, Saito S, Takahashi S, et al. Prediction of progression of coronary artery disease and clinical outcomes using vascular profiling of endothelial shear stress and arterial plaque characteristics: The PREDICTION Study. Circulation 2012;126(2):172-81.
3. Calvert PA, Obaid DR, O'Sullivan M, et al. Association between IVUS findings and adverse outcomes in patients with coronary artery disease: the VIVA (VH-IVUS in Vulnerable Atherosclerosis) Study. JACC Cardiovasc Imaging 2011;4(8):894-901.
4. Wykrzykowska JJ, Diletti R, Gutierrez-Chico JL, et al. Plaque sealing and passivation with a mechanical self-expanding low outward force nitinol vShield device for the treatment of IVUS and OCT-derived thin cap fibroatheromas (TCFAs) in native coronary arteries: report of the pilot study vShield Evaluated at Cardiac hospital in Rotterdam for Investigation and Treatment of TCFA (SECRITT). EuroIntervention 2012;8:945-54.
5. Kragel AH, Reddy SG, WittesJT, et al. Morphometric analysis of the composition of atherosclerotic plaques in the four major epicardial coronary arteries in acute myocardial infarction and in sudden coronary death. Circulation 1989;80(6):1747-56.
6. Moreno PR, BernardiVH, Lopez-CuellarJ, et al. Macrophages, smooth muscle cells, and tissue factor in unstable angina. Implications for cell-mediated thrombogenicity in acute coronary syndromes. Circulation 1996;94(12):3090-7.
7. Burke AP, Farb A, Malcom GT, et al. Coronary risk factors and plaque morphology in men with coronary disease who died suddenly. N EngIJ Med 1997;336(18):1276-82.
8. Ehara S, Kobayashi Y, Yoshiyama M, et al. Coronary artery calcification revisited. J Atheroscler Thromb 2006;13(1):31-7.
9. Virmani R, KolodgieFD, Burke AP, et al. Atherosclerotic plaque progression and vulnerability to rupture: angiogenesis as a source of intraplaquehemorrhage. Arterioscler Thromb Vasc Biol 2005; 25(10):2054-61.
10. Garcia-Garcia HM, Mintz GS, Lerman A, et al. Tissue characterisation using intravascular radiofrequency data analysis: recommendations for acquisition, analysis, interpretation and reporting. EuroIntervention 2009;5(2):177-89.
11. Marso SP, Frutkin AD, Mehta SK, et al. Intravascular ultrasound measures of coronary atherosclerosis are associated with the Framingham risk score: an analysis from a global IVUS registry. EuroIntervention 2009;5(2):212-8.
12. Serruys PW, Garcia-Garcia HM, Buszman P, et al. Effects of the direct lipoprotein-associated phospholipase A(2) inhibitor darapladib on human coronary atherosclerotic plaque. Circulation 2008;118(11):1172-82.
13. Kubo T, Maehara A, Mintz GS, et al. The dynamic nature of coronary artery lesion morphology assessed by serial virtual histology intravascular ultrasound tissue characterization. J Am Coll Cardiol 2010;55(15):1590-7.
14. Thim T, Hagensen MK, Wallace-Bradley D, et al. Unreliable assessment of necrotic core by virtual histology intravascular ultrasound in porcine coronary artery disease. Circ Cardiovasc Imaging 2010;3(4):384-91.
15. Tearney GJ, Regar E, Akasaka T, et al. Consensus standards for acquisition, measurement, and reporting of intravascular optical coherence tomography studies: a report from the International Working Group for Intravascular Optical Coherence Tomography Standardization and Validation. J Am Coll Cardiol 2012;59(12):1058-72.
16. Kang SJ, Mintz GS, Akasaka T, et al. Optical coherence tomographic analysis of in-stent neoatherosclerosis after drug-eluting stent implantation. Circulation 2011;123(25):2954-63.

17. Fujii K, Kawasaki D, Masutani M, et al. OCT assessment of thin-cap fibroatheroma distribution in native coronary arteries. JACC Cardiovasc Imaging 2010;3(2):168-75.
18. Gonzalo N, Garcia-Garcia HM, Regar E, et al. In vivo assessment of high-risk coronary plaques at bifurcations with combined intravascular ultrasound and optical coherence tomography. JACC Cardiovasc Imaging 2009;2(4):473-82.
19. Sawada T, Shite J, Garcia-Garcia HM, et al. Feasibility of combined use of intravascular ultrasound radiofrequency data analysis and optical coherence tomography for detecting thin-cap fibroatheroma. Eur Heart J 2008;29(9):1136-46.
20. Giattina SD, Courtney BK, Herz PR, et al. Assessment of coronary plaque collagen with polarization sensitive optical coherence tomography (PS-OCT). Int J Cardiol 2006;107(3):400-9.
21. Liu L, Gardecki JA, Nadkarni SK, et al. Imaging the subcellular structure of human coronary atherosclerosis using micro-optical coherence tomography. Nat Med 2011;17(8):1010-4.
22. Simsek C, Garcia-Garcia HM, van Geuns RJ, et al. The ability of high dosage rosuvastatin to improve plaque composition and decrease necrotic core in non-intervened coronary arteries: rationale and design of the integrated biomarker and imaging study-3 (IBIS-3). EuroIntervention 2012;8:235-41.
23. Karpiouk AB, Wang B, Emelianov SY. Development of a catheter for combined intravascular ultrasound and photoacoustic imaging. Rev Sci Instrum 2010;81(1):014901.
24. Li BH, Leung AS, Soong A, et al. Hybrid intravascular ultrasound and optical coherence tomography catheter for imaging of coronary atherosclerosis. Catheter Cardiovasc Interv 2013;81:494-507.
25. Stephens DN, Park J, Sun Y, et al. Intraluminal fluorescence spectroscopy catheter with ultrasound guidance. J Biomed Opt 2009;14(3):030505.
26. Papadopoulou SL, Neefjes LA, Schaap M, et al. Detection and quantification of coronary atherosclerotic plaque by 64-slice multidetector CT: a systematic head-to-head comparison with intravascular ultrasound. Atherosclerosis 2011;219(1):163-70.
27. Gauss S, Achenbach S, Pflederer T, et al. Assessment of coronary artery remodelling by dual-source CT: a head-to-head comparison with intravascular ultrasound. Heart 2011;97(12):991-7.
28. Voros S, Rinehart S, Qian Z, et al. Prospective validation of standardized, 3-dimensional, quantitative coronary computed tomographic plaque measurements using radiofrequency backscatter intravascular ultrasound as reference standard in intermediate coronary arterial lesions: results from the ATLANTA (assessment of tissue characteristics, lesion morphology, and hemodynamics by angiography with fractional flow reserve, intravascular ultrasound and virtual histology, and noninvasive computed tomography in atherosclerotic plaques) I study. JACC Cardiovasc Interv 2011;4(2):198-208.
29. Motoyama S, Sarai M, Harigaya H, et al. Computed tomographic angiography characteristics of atherosclerotic plaques subsequently resulting in acute coronary syndrome. J Am Coll Cardiol 2009;54(1): 49-57.
30 Villines TC, Hulten EA, Shaw LJ, et al. Prevalence and severity of coronary artery disease and adverse events among symptomatic patients with coronary artery calcification scores of zero undergoing coronary computed tomography angiography: results from the CONFIRM (Coronary CT Angiography Evaluation for Clinical Outcomes: An International Multicenter) registry. J Am Coll Cardiol 2011;58(24):2533-40.
31. Muntendam P, McCall C, Sanz J, et al. The BioImage Study: novel approaches to risk assessment in the primary prevention of atherosclerotic cardiovascular disease—study design and objectives. Am Heart J 2010;160(1):49 e1-57 e1.
32. Corti R, Fuster V. Imaging of atherosclerosis: magnetic resonance imaging. Eur Heart J 2011;32(14):1709-1719b.
33. Mach F, Schonbeck U, Bonnefoy JY, et al. Activation of monocyte/macrophage functions related to acute atheroma complication by ligation of CD40: induction of collagenase, stromelysin, and tissue factor. Circulation 1997;96(2):396-9.

34. Amento EP, Ehsani N, Palmer H, et al. Cytokines and growth factors positively and negatively regulate interstitial collagen gene expression in human vascular smooth muscle cells. Arterioscler Thromb 1991;11(5):1223-30.
35. Rzeszutko L, Legutko J, Kaluza GL, et al. Assessment of culprit plaque temperature by intracoronary thermography appears inconclusive in patients with acute coronary syndromes. Arterioscler Thromb Vasc Biol 2006;26(8):1889-94.
36. Stefanadis C, Diamantopoulos L, Vlachopoulos C, et al. Thermal heterogeneity within human atherosclerotic coronary arteries detected in vivo: A new method of detection by application of a special thermography catheter. Circulation 1999;99(15):1965-71.
37. Jaffer FA, Calfon MA, Rosenthal A, et al. Two-dimensional intravascular near-infrared fluorescence molecular imaging of inflammation in atherosclerosis and stent-induced vascular injury. J Am Coll Cardiol 2011;57(25):2516-26.
38. Yoo H, Kim JW, Shishkov M, et al. Intra-arterial catheter for simultaneous microstructural and molecular imaging in vivo. Nat Med 2011;17(12):1680-4.
39. Tearney GJ, Yabushita H, Houser SL, et al. Quantification of macrophage content in atherosclerotic plaques by optical coherence tomography. Circulation 2003;107(1):113-9.
40. Tawakol A, Migrino RQ, Bashian GG, et al. In vivo 18F-fluorodeoxyglucose positron emission tomography imaging provides a noninvasive measure of carotid plaque inflammation in patients. J Am Coll Cardiol 2006;48(9):1818-24.
41. Rogers IS, Nasir K, Figueroa AL, et al. Feasibility of FDG imaging of the coronary arteries: comparison between acute coronary syndrome and stable angina. JACC Cardiovasc Imaging 2010;3(4):388-97.
42. Wykrzykowska J, Lehman S, Williams G, et al. Imaging of inflamed and vulnerable plaque in coronary arteries with 18F-FDG PET/CT in patients with suppression of myocardial uptake using a low-carbohydrate, high-fat preparation. J Nucl Med 2009;50(4):563-8.
43. Fujimoto S, Hartung D, Ohshima S, et al. Molecular imaging of matrix metalloproteinase in atherosclerotic lesions: resolution with dietary modification and statin therapy. J Am Coll Cardiol 2008;52(23):1847-57.
44. Kietselaer BL, Reutelingsperger CP, Heidendal GA, et al. Noninvasive detection of plaque instability with use of radiolabeled annexin A5 in patients with carotid-artery atherosclerosis. N EnglJ Med 2004;350(14):1472-3.
45. Tsimikas S. Noninvasive imaging of oxidized low-density lipoprotein in atherosclerotic plaques with tagged oxidation-specific antibodies. Am J Cardiol 2002;90(10C):22L-7L.
46. Hyafil F, Cornily JC, Feig JE, et al. Noninvasive detection of macrophages using a nanoparticulate contrast agent for computed tomography. Nat Med 2007;13(5):636-41.
47. Hyafil F, Cornily JC, Rudd JH, et al. Quantification of inflammation within rabbit atherosclerotic plaques using the macrophage-specific CT contrast agent N1177: a comparison with 18F-FDG PET/CT and histology. J Nucl Med 2009;50(6):959-65.
48. Caro CG, Fitz-Gerald JM, Schroter RC. Arterial wall shear and distribution of early atheroma in man. Nature 1969;223(5211):1159-60.
49. Samady H, Eshtehardi P, McDaniel MC, et al. Coronary artery wall shear stress is associated with progression and transformation of atherosclerotic plaque and arterial remodeling in patients with coronary artery disease. Circulation 2011;124(7):779-88.
50. Wentzel JJ, Krams R, Schuurbiers JC, et al. Relationship between neointimal thickness and shear stress after Wallstent implantation in human coronary arteries. Circulation 2001;103(13):1740-5.
51. Stone PH, Coskun AU, Kinlay S, et al. Regions of low endothelial shear stress are the sites where coronary plaque progresses and vascular remodelling occurs in humans: an in vivo serial study. Eur Heart J 2007;28(6):705-10.

52. Bourantas CV, Papafaklis MI, Naka KK, et al. Fusion of optical coherence tomography and coronary angiography—in vivo assessment of shear stress in plaque rupture. Int J Cardiol 2012;155(2):e24-6.
53. Fukumoto Y, Hiro T, Fujii T, et al. Localized elevation of shear stress is related to coronary plaque rupture: a 3-dimensional intravascular ultrasound study with in-vivo color mapping of shear stress distribution. J Am Coll Cardiol 2008;51(6):645-50.
54. Slager CJ, Wentzel JJ, Gijsen FJ, et al. The role of shear stress in the destabilization of vulnerable plaques and related therapeutic implications. Nat Clin Pract Cardiovasc Med 2005;2(9):456-64.
55. Goubergrits L, Kertzscher U, Schoneberg B, et al. CFD analysis in an anatomically realistic coronary artery model based on non-invasive 3D imaging: comparison of magnetic resonance imaging with computed tomography.Int J Cardiovasc Imaging 2008;24(4):411-21.
56. van der Giessen AG, Wentzel JJ, Meijboom WB, et al. Plaque and shear stress distribution in human coronary bifurcations: a multislice computed tomography study. EuroIntervention 2009;4(5):654-61.
57. Brennan ML, Reddy A, Tang WH, et al. Comprehensive peroxidase-based hematologic profiling for the prediction of 1-year myocardial infarction and death. Circulation 2010;122(1):70-9.
58. Elesber AA, Conover CA, Denktas AE, et al. Prognostic value of circulating pregnancy-associated plasma protein levels in patients with chronic stable angina. Eur Heart J 2006;27(14):1678-84.
59. Prins BP, Lagou V, Asselbergs FW, Snieder H, Fu J. Genetics of coronary artery disease: genome-wide association studies and beyond. Atherosclerosis 2012;225:1-10.
60. Thompson A, Gao P, Orfei L, et al. Lipoprotein-associated phospholipase A(2) and risk of coronary disease, stroke, and mortality: collaborative analysis of 32 prospective studies. Lancet 2010;375(9725):1536-44.
61. Maehara A, Mintz GS, Bui AB, et al. Morphologic and angiographic features of coronary plaque rupture detected by intravascular ultrasound. J Am Coll Cardiol 2002;40(5):904-10.
62. Tanaka A, Imanishi T, Kitabata H, et al. Distribution and frequency of thin-capped fibroatheromas and ruptured plaques in the entire culprit coronary artery in patients with acute coronary syndrome as determined by optical coherence tomography. Am J Cardiol 2008;102(8):975-9.
63. Rioufol G, Gilard M, Finet G, et al. Evolution of spontaneous atherosclerotic plaque rupture with medical therapy: long-term follow-up with intravascular ultrasound. Circulation 2004;110(18):2875-80.
64. Fujii K, Kobayashi Y, Mintz GS, et al. Intravascular ultrasound assessment of ulcerated ruptured plaques: a comparison of culprit and nonculprit lesions of patients with acute coronary syndromes and lesions in patients without acute coronary syndromes. Circulation 2003;108(20):2473-8.
65. Cecchi E, Liotta AA, Gori AM, et al. Comparison of hemorheological variables in ST-elevation myocardial infarction versus those in non-ST-elevation myocardial infarction or unstable angina pectoris. Am J Cardiol 2008;102(2):125-8.
66. Smyth SS, Monroe III DM, Wysokinski WE, et al. Platelet activation and its patient-specific consequences. Thromb Res 2008;122(4):435-41.
67. Spiel AO, Gilbert JC, Jilma B. von Willebrand factor in cardiovascular disease: focus on acute coronary syndromes. Circulation 2008;117(11):1449-59.
68. Farb A, Burke AP, Tang AL, et al. Coronary plaque erosion without rupture into a lipid core. A frequent cause of coronary thrombosis in sudden coronary death. Circulation 1996;93(7):1354-63.
69. Mercado N, Maier W, Boersma E, et al. Clinical and angiographic outcome of patients with mild coronary lesions treated with balloon angioplasty or coronary stenting. Implications for mechanical plaque sealing. Eur Heart J 2003;24(6):541-51.
70. Serruys PW, Garcia-Garcia HM, Onuma Y. From metallic cages to transient bioresorbable scaffolds: change in paradigm of coronary revascularization in the upcoming decade? Eur Heart J 2012;33(1):16-25b.

71. Onuma Y, Serruys PW, Perkins LE, et al. Intracoronary optical coherence tomography and histology at 1 month and 2, 3, and 4 years after implantation of everolimus-eluting bioresorbable vascular scaffolds in a porcine coronary artery model: an attempt to decipher the human optical coherence tomography images in the ABSORB trial. Circulation 2010;122(22):2288-300.
72. Brugaletta S, Radu MD, Garcia-Garcia HM, et al. Circumferential evaluation of the neointima by optical coherence tomography after ABSORB bioresorbable vascular scaffold implantation: can the scaffold cap the plaque? Atherosclerosis 2012;221(1):106-12.
73. Moreno PR. Vulnerable plaque: definition, diagnosis, and treatment. Cardiol Clin 2010;28(1):1-30.
74. Raber L, Heo JH, Radu MD, et al. Offline fusion of co-registered intravascular ultrasound and frequency domain optical coherence tomography images for the analysis of human atherosclerotic plaques. EuroIntervention 2012;8(1):98-108.
75. Wang B, Su JL, Amirian J, et al. Detection of lipid in atherosclerotic vessels using ultrasound-guided spectroscopic intravascular photoacoustic imaging. Opt Express 2010;18(5):4889-97.
76. Bourantas CV, Kalatzis FG, Papafaklis MI, et al. ANGIOCARE: an automated system for fast three-dimensional coronary reconstruction by integrating angiographic and intracoronary ultrasound data. Catheter Cardiovasc Interv 2008;72(2):166-75.
77. Wentzel JJ, van der Giessen AG, Garg S, et al. In vivo 3D distribution of lipid-core plaque in human coronary artery as assessed by fusion of near infrared spectroscopy-intravascular ultrasound and multislice computed tomography scan. Circ Cardiovasc Imaging 2010;3(6):e6-7.
78. Bourantas CV, Papafaklis MI, Garcia-Garcia HM, et al. Short- and long-term implications of a bioresorbable vascular scaffold implantation on the local endothelial shear stress patterns. JACC Cardiovasc Interv 2013 In press.

PART II

INITIAL EXPERIENCE WITH BIORESORBABLE SCAFFOLDS

Chapter 5

A comparative assessment by optical coherence tomography of the performance of the first and second generation of the everolimus-eluting bioresorbable vascular scaffolds

Josep Gomez-Lara; Salvatore Brugaletta; Roberto Diletti; Scot Garg; Yoshinobu Onuma; Bill D. Gogas; Robert Jan van Geuns; Cécile Dorange; Susan Veldhof; Richard Rapoza; Robert Whitbourn; Stephan Windecker; Hector M. Garcia-Garcia; Evelyn Regar; Patrick W. Serruys

Eur Heart J. (2011) 32, 294–304

ABSTRACT

Aims The first generation of the everolimus-eluting bioresorbable vascular scaffold (BVS 1.0) showed an angiographic late loss higher than the metallic everolimus-eluting stent Xience V due to scaffold shrinkage. The new generation (BVS 1.1) presents a different design and manufacturing process than the BVS 1.0. This study sought to evaluate the differ- ences in late shrinkage, neointimal response, and bioresorption process between these two scaffold generations using optical coherence tomography (OCT).

Methods and results A total of 12 lesions treated with the BVS 1.0 and 12 selected lesions treated with the revised BVS 1.1 were imaged at baseline and 6-month follow-up with OCT. Late shrinkage and neointimal area (NIA) were derived from OCT area measurements. Neointimal thickness was measured in each strut. Strut appearance has been classified as previously described. Baseline clinical, angiographic, and OCT characteristics were mainly similar in the two groups. At 6 months, absolute and relative shrinkages were significantly larger for the BVS 1.0 than for the BVS 1.1 (0.98 vs. 0.07 mm^2 and 13.0 vs. 1.0%, respectively; $P = 0.01$). Neointimal area was significantly higher in the BVS 1.0 than in the BVS 1.1 (in-scaffold area obstruction of 23.6 vs. 12.3%; $P < 0.01$). Neointimal thickness was also larger in the BVS 1.0 than in the BVS 1.1 (166.0 vs. 76.4 mm; $P < 0.01$). Consequently, OCT, intravascular ultrasound, and angio- graphic luminal losses were higher with the BVS 1.0 than with the BVS 1.1. At 6 months, strut appearance was pre- served in only 2.9% of the BVS 1.0 struts, but remained unchanged with the BVS 1.1 indicating different state of strut microstucture and/or their reflectivity.

Conclusion The BVS 1.1 has less late shrinkage and less neointimal growth at 6-month follow-up compared with the BVS 1.0. A difference in polymer degradation leading to changes in microstructure and reflectivity is the most plausible explanation for this finding.

BACKGROUND

The first generation of the everolimus-eluting bioresorbable vascu lar scaffold (BVS 1.0) was tested in 30 patients enrolled in the ABSORB Cohort A study. At 6-month follow-up, this device showed a late shrinkage of the scaffold area of 11.8% as assessed by intravascular ultrasound (IVUS) and rapid changes in strut appearance, documented by multiple imaging modalities.[1]

At variance with metallic stents, which do not exhibit late shrink- age,[2] the reduction of the BVS 1.0 scaffold area was the main component of late luminal loss at 6 months.

The BVS 1.1 represents a new generation of bioresorbable devices. It utilizes a novel platform design and polymer processing different than the previous BVS 1.0. This new generation is designed to improve the radial force and to slow-down the loss in mechanical integrity, without substantially affecting the bioresorption process.[3] It has been investigated in 101 patients enrolled in the ABSORB cohort B trial. Forty-five of these patients were scheduled for a 6-month control with conventional angiography and multiple intravascular imaging techniques.

Optical coherence tomography (OCT) is a high resolution imaging technique capable of an accurate assessment of the polymeric struts, changes in luminal and scaffold dimensions, and the quantification of neointimal hyperplasia.[4–6]

Our aim is to compare the late shrinkage and neointimal response of the two polymeric devices using OCT imaging and to assess the qualitative changes in strut appearance as a marker of bioresorption at 6-month follow-up.

MATERIALS AND METHODS

Study design and population

The ABSORB trial is a non-randomized, multicentre, single-arm, efficacy – safety study. The first Cohort (A) included 30 patients treated with the BVS 1.0; the trial design and results up to 3-year follow-up have been already published.[1,4,7] The second Cohort (B) included 101 patients with 102 lesions treated with a single size 3 × 18 mm of the BVS 1.1 design; the study design is available at clinicaltrials.gov (NCT00856856).

The inclusion criteria were similar in both studies: patients aged 18 years or older diagnosed with stable, unstable, or silent ischaemia, with a de novo lesion in a native coronary artery between 50 and 99% of the luminal diameter and a Thrombolysis In Myocardial Infarction (TIMI) flow grade of 1 or more. Exclusions included patients with an evolving myocardial infarction, stenosis of an unprotected left main or ostial right coronary artery

(RCA), presence of intracoronary thrombus or heavy calcification. Excessive tortuosity and lesions involving a side branch more than 2 mm in diameter were also exclusion criteria. The ethics committee at each participating institution approved the protocol and each patient gave written informed consent before inclusion.

Four centres (Auckland, Aarhus, Krakow, and Rotterdam) participated in the Absorb Cohort A in 2006 using the BVS 1.0.1 In this first-in-man study, angiography and IVUS were mandatory investigations at 6 and 24 months of follow-up. Optical coherence tomography was an optional investigation that was only executed and performed in Rotterdam with the available system at that time (M2 Light Lab). Subsequently, the Rotterdam group performed OCT follow-up of their patients at 6 and 24 months. As a result, 13 patients in Cohort A had sequential OCT investigation at baseline and 6 months.4 The Cohort B study was started during 2009 using the BVS 1.1. In this study, 7 of the 12 participating centres performed OCT at baseline and follow-up and three of them (Rotterdam = 9, Melbourne = 2, and Bern = 1) used the most advanced system (C7 Light Lab). As a result, 12 patients in Cohort B have been imaged with the OCT C7 system. This limited but almost equal number of patients represents a unique opportunity to analyse, with the high resolution of OCT, the mechanical behavior of the first and second generation of everolimus-eluting BVS at baseline and at 6-month follow-up.

Devices

The BVS 1.0 (Abbott Vascular, Santa Clara, CA, USA) is a balloon expandable device built on a backbone of semi-crystalline poly-L-lactide (PLLA) polymer. The polymer consists of crystalline and amorphous domains. The balance between the crystalline and amorphous fractions and the molecular orientation state of these phases depends on their thermal and deformation history. The plat- form is coated with the poly-D,L-lactide (PDLLA) copolymer that contains and controls the release of the antiproliferative everolimus (Novartis, Switzerland). Both PLLA and PDLLA are fully bioresorbable. The strut thickness is 150 mm and the struts are distributed as circumferential out-of-phase zigzag hoops linked together by three longitudinal bridges between each hoop. The BVS 1.0 design is shown in Figure 1.

The manufacturing process the BVS 1.1 (Abbott Vascular, Santa Clara, CA, USA) has been modified to enhance the mechanical strength and mechanical durability of the struts. Moreover, the new design has in-phase zigzag hoops linked by bridges that allow for a more uniform strut distribution, reduce maximum circular unsupported surface area, and provide more uniform vessel wall support and drug transfer.3 The polymer mass, coating content, amount of drug, and the strut thickness remain the same. The BVS 1.1 design is also shown in Figure 1.

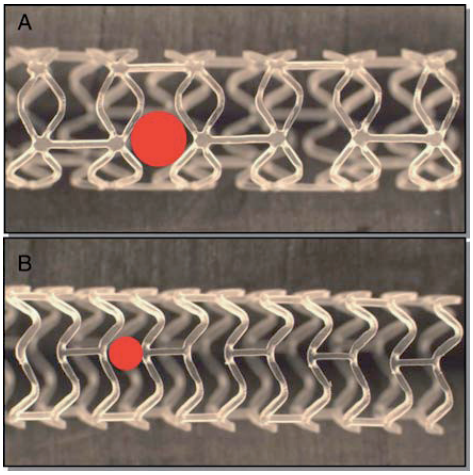

Figure 1. Design of the different bioresorbable vascular scaffold (BVS). (A) BVS 1.0 design. The struts are distributed as circumfer- ential out-of-phase zigzag hoops linked together by three longi- tudinal bridges between each hoop. The maximal circular unsupported surface area is drawn as a red circle. (B) BVS 1.1 design. The struts are arranged as in-phase zigzag hoops linked together by three longitudinal bridges. The strut distribution is more uniform and allows the maximal circular unsupported surface area (red circle) to be smaller than in the BVS 1.0.

Treatment procedure

All procedures were performed electively. Lesions were treated with routine interventional techniques that included mandatory pre- dilatation. The study protocol forbade the use of pre-dilatation bal- loons longer than the pre-specified length of the device (18 mm), and recommended using balloons 0.5 mm smaller in diameter than the reference vessel diameter (RVD). The BVS had to be implanted at a pressure not exceeding the rated burst pressure (16 atmospheres). Post-dilation was allowed at the operator's discretion with shorter balloons than the BVS length and inflated at diameters that fit within the boundaries of the scaffold. Bail-out stenting was also allowed at operator's discretion.

Quantitative angiography analysis

The 2D angiograms were stored in DICOM format and analysed offline by the core lab (Cardialysis, Rotterdam, The Netherlands) using the CASS II analysis system (Pie Medical BV, Maastricht, The Netherlands). In each patient, the treated region and the peri-treated regions (defined by a length of 5 mm proximal and distal to the device edge) were analysed. The following quantitative coronary angiography (QCA) analysis parameters were measured: computer-defined minimal luminal diameter (MLD), RVD obtained by an interpolated method, and percentage of diameter stenosis (DS). Late loss was defined as the difference between MLD post-procedure and MLD at follow-up.[8]

Optical coherence tomography acquisition

In the ABSORB Cohort A, baseline and follow-up OCT acquisition was executed with an M2 Time-Domain System (LightLab Imaging, West- ford, MA, USA) using the balloon occlusion method. The occlusion balloon Helios (Goodman, Japan) was advanced distal to the treated region over a conventional angioplasty guidewire of 0.014" . Then, the conventional guidewire was replaced by the OCT ImageWire (LightLab Imaging, Westford, MA, USA) and the occlusion balloon catheter was positioned proximal to the segment of interest. Pullback of the ImageWire was performed with automated pullback at 1 mm/s and 15.6 frames/s during the occlusion of the artery by the balloon at low pressure (0.5 – 0.7 atm), and during simultaneous flushing of the vessel distal to the occlusion with lactated Ringer's solution at 378C (flow rate 0.8 mL/s).

In ABSORB Cohort B, the baseline and follow-up OCT acquisitions were performed with the C7 XR Fourier-Domain System (LightLab Imaging, Westford, MA, USA) without occluding the coronary artery. In these cases, a conventional wire was placed distal to the segment of interest. Then the OCT imaging catheter (RX ImageWire II; LightLab Imaging, Westford, MA, USA) was advanced distally to the treated region. Removal of the conventional wire was left to the operator's discretion. The pullback was performed during a continuous injection of 3 mL/s of contrast medium (Iodixanol 370, Visipaque, GE Health Care, Cork, Ireland) injected at a maximum pressure of 300 psi through the guiding catheter using an injection pump. In this case, the automated pullback rate was 20 mm/s and the frame rate was 100 images/s. The resolution of both OCT systems is exactly the same (15 – 20 mm of lateral resolution and 15 – 20 mm of axial resolution).[9]

Optical coherence tomography analysis

The OCT measurements were performed with proprietary software for offline analysis (LightLab Imaging, Westford, MA, USA). Adjusting for the pullback speed, the analysis of contiguous cross-sections was performed at each 1 mm longitudinal intervals within the treated segment.

The monochromatic peak wavelength of the OCT is differently reflected, refracted, and absorbed by the polymeric or metallic struts. A great deal of the OCT light energy is transmitted through the polymeric struts, such that only part of it is reflected at the endoluminal and abluminal sides of the struts generating a visible optical frame border; the core of the polymeric struts is imaged as a black square at baseline. As a consequence, the vessel wall is easily imaged through the struts without any major signs of shadowing (Figure 2). Thus, OCT analysis of the BVS has several advantages over that of metallic stents. First, at baseline, the vessel wall/lumen and its luminal area can be readily measured behind the polymeric struts. At follow-up, most of the struts are fully covered

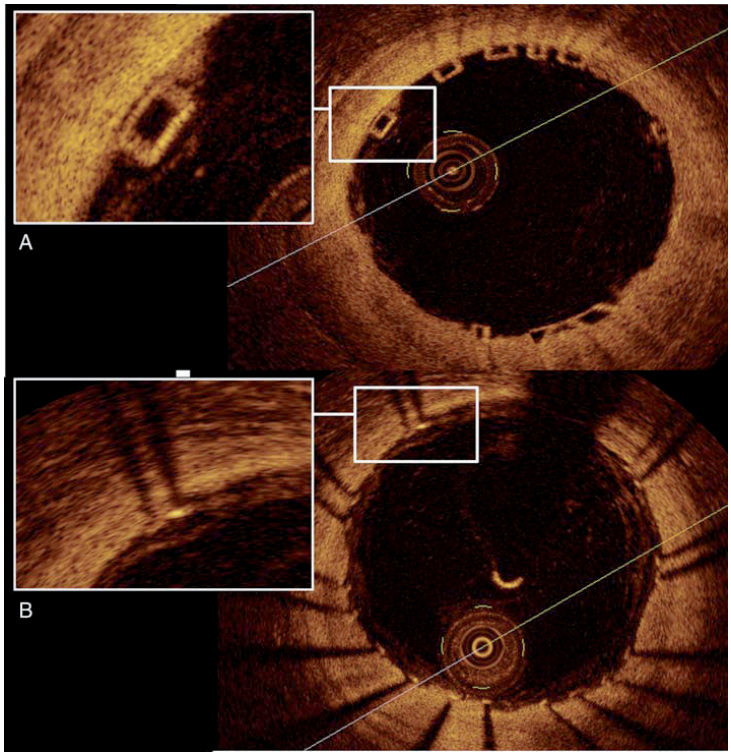

Figure 2. Optical coherence tomography (OCT) imaging of the bioresorbable scaffolds and metallic platform stents. (A) Bioresorbable vascular scaffold imaged with OCT. The strut appearance is translucent and allows a perfect imaging of the vessel wall. (B) Metallic platform stent imaged with OCT. The metallic struts are opaque to the OCT light and produce the typical shadow into the vessel wall.

and embedded in the vessel wall and the luminal area can be drawn with an automated detection algorithm available in the Light Lab proprietary software; manual corrections are performed if necessary. Second, since polymeric struts are accurately imaged at baseline, the device area can be obtained manually by joining the middle point of each consecutive strut around the circumference. In frames with only a few struts, the BVS area was adjusted to follow the lumen area in the regions where its contour was outside the lumen area. At follow-up, the BVS area was also measured by joining the middle point of the struts (Figure 3).

Device shrinkage is defined as the decrease over time of the device area with respect to the area measured immediately after the deployment. [10,11]

Absolute late shrinkage has been measured as the difference between the mean BVS area at baseline minus the mean BVS area at follow-up. Relative late shrinkage has been

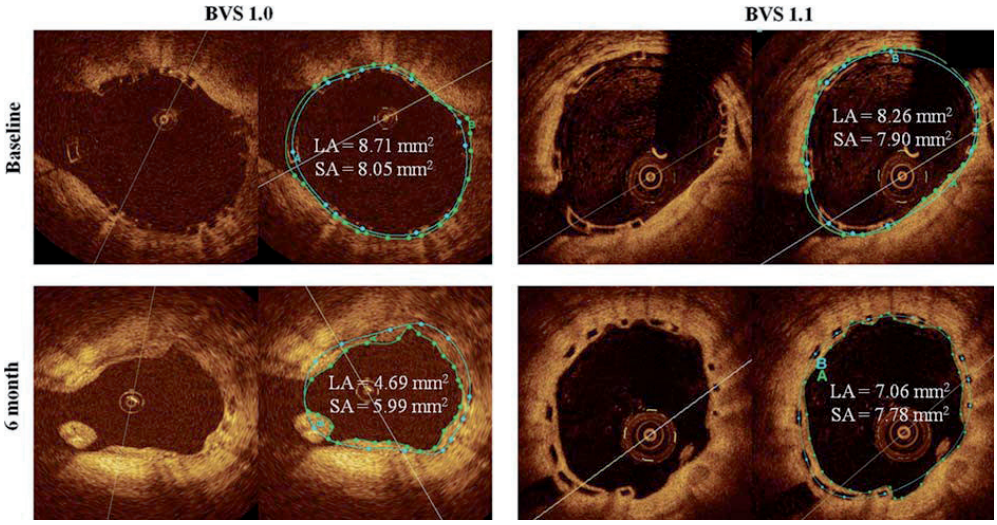

Figure 3. Late shrinkage assessment. Optical coherence tomography (OCT) imaging of the BVS 1.0 and 1.1. At baseline, the scaffold area (SA; blue line) is usually drawn into the luminal area (LA; green line). At follow-up, the neointima covers the polymeric struts and then, the scaffold area usually is drawn outside of the luminal area. The absolute late shrinkage for the BVS 1.0 is 2.06 mm^2 (relative shrinkage of 25.6%) and for the BVS 1.1 is 0.12 mm^2 (relative shrinkage of 1.5%).

measured as: [(absolute late shrinkage)/baseline mean BVS area] × 100 (Figure 3).

In case of incomplete scaffold/strut apposition (ISA), the area between the backside of the struts and the vessel wall has been measured as ISA area. The neointimal area (NIA) has been measured at follow-up as: BVS area – (Lumen Area – ISA area). The neointimal thickness (NIT) has been measured at follow-up with the 'thickness ruler' tool from the endoluminal border of the black strut core to the lumen.

Moreover, a qualitative assessment of the appearance of polymeric struts has been obtained at follow-up. Basically, the struts were classi- fied as preserved box, open box, dissolved bright box, and dissolved black box in order of decreasing reflectivity (Figure 4).[1] The kappa index to detect the four types of strut appearance was 0.58.[12] Strut tissue coverage was assessed qualitatively when clear neointimal tissue covered the polymeric strut.

Intra-vascular ultrasound acquisition and analysis

The scaffolded segments were examined with phased array IVUS cath- eters (EagleEye; Volcano Corporation, Rancho Cordova, CA, USA) with an automated pullback at 0.5 mm/s. Lumen area was measured with a validated computer-based contour detection

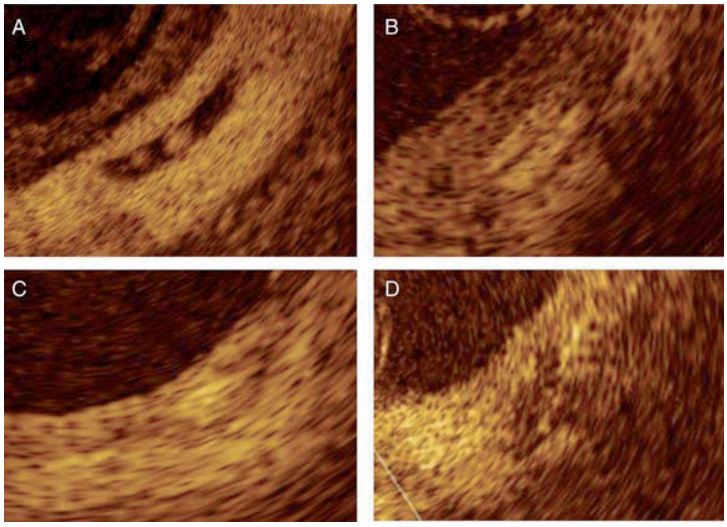

Figure 4. Strut appearance of the bioresorbable vascular scaffold at follow-up. (A) Preserved box appearance: sharp defined, bright reflection borders with preserved box-shaped appearance; strut body shows low reflection; (B) open box: luminal and abluminal long-axis borders thickened bright reflection; short-axis borders not visible; (C) dissolved bright box: partially visible bright spot, contours poorly defined; no box-shaped appearance; (D) dissolved black box: black spot, contours poorly defined, often confluent; no box-shaped appearance.

programme (CURAD BV, Wijk bij Duurstede, The Netherlands) that allows for semi-automatic detection of lumen.[13]

Statistical analysis

Normality distribution of continuous variables was explored with the Kolmogorov – Smirnov test. All continuous variables had normal distribution and have been expressed as means and 1 standard deviation (SD). Categorical variables are presented as counts (%). Paired comparisons of continuous variables within groups between the different time points were done by the Wilcoxon's signed rank test. Comparison of continuous variables between Cohorts A and B has been made using the U-Mann – Whitney test. Comparisons of absolute differences between baseline and follow-up have also been made with the U-Mann – Whitney test. Comparisons of categorical variables between groups have been made using the Chi-square test or the Fisher test when one of the cells had less than five events. A two-sided P-value ≤ 0.05 was considered statistically significant. All the statistics have been per- formed with the SPSS 15.0 version for Windows (IL, US).

RESULTS

Study population

A total of 13 lesions in 13 patients had baseline and follow-up OCT imaging in the ABSORB Cohort A study.[1] One of these patients underwent a non-ischaemia driven target lesion revascularization treated with a metallic platform stent at Day 42. The OCT imaging at that time showed strut discontinuation with attached thrombi probably due to overstretching of the BVS during implantation.[7] This patient has not been included in the present study. In the ABSORB Cohort B study, 28 patients with scheduled imaging control at 6-month follow-up were studied with OCT at baseline. Two of them were excluded due to the sub-optimal quality of the imaging, and of the remaining 26 patients, 13 were imaged with the M3 OCT system and 13 were imaged with the OCT C7. None of the 13 patients imaged with the M3 system needed an unscheduled angiography and all of them were studied with OCT at 6 months. One patient imaged with the C7 system presented with a symptomatic peri-procedural myocardial infarction at the index procedure secondary to an occlusion of a small diagonal after the implantation of the BVS in the left anterior descending. This patient refused invasive imaging at 6-month follow-up. Finally, 24 patients were included in the present study: 12 were treated with the BVS 1.0 and 12 were treated with the BVS 1.1. None of those patients had BVS fractures at baseline or 6-month follow-up. The baseline clinical characteristics are shown in Table 1. Both groups were similar in gender and age. There was a trend toward lower percentage of hypercholesterolaemia (72.7 vs. 100.0%; P = 0.06) and prior acute myocardial infarction (8.3 vs.41.7%; P = 0.06) in the BVS 1.0 than in the BVS 1.1 group, respectively. There was a significant difference in the smoking status favouring the BVS 1.1 group (33 vs. 0%, respectively; P = 0.03). A total of 11 patients in ABSORB Cohort A were treated with a BVS 1.0 of 3 × 12 mm and 1 was treated with a BVS 1.0 of 3 × 18 mm. All patients of the ABSORB Cohort B were treated with a BVS 1.1 of 3 × 18 mm.

Quantitative coronary angiography results

Baseline and follow-up angiographic parameters are shown in Table 2. Both groups had similar angiographic characteristics at pre-implantation. Patients treated with the BVS 1.0 tended to have a larger RVD than patients treated with the BVS 1.1 (2.95 vs. 2.69 mm; P = 0.14). At 6-month follow-up, patients treated with the BVS 1.0 had a significant decrease in MLD (angiographic late loss) of 0.43 mm (P = 0.01), whereas a non-significant 0.08 mm decrease was seen in those treated with the BVS 1.1. The difference in late loss between the BVS 1.0 and 1.1, although numerically appreciable, failed to reach statistical significance at 6 months (P = 0.07). The serial individual changes in MLD between baseline and follow-up are shown in Figure 5.

Table 1. Baseline clinical and angiographic characteristics.

	BVS 1.0 (n = 12)	BVS 1.1 (n = 12)	P-value
Male	8 (66.7)	9 (75.0)	0.65
Age (years + SD)	59.5 + 8.3	61.2 + 9.6	0.76
Hypertension	6 (50.0)	7 (58.3)	0.68
Hypercholesterolaemia	8 (72.7)	12 (100.0)	0.06
Diabetes mellitus	1 (8.3)	1 (8.3)	1.00
Smoke	4 (33.3)	0	0.03
Prior MI	1 (8.3)	5 (41.7)	0.06
Prior PCI	2 (16.7)	3 (25.0)	0.62
Clinical indication			0.27
Stable or silent angina	11 (91.7)	9 (75.0)	
Unstable angina	1 (8.3)	3 (25.0)	
Number of vessel disease			0.14
One	12 (100.0)	10 (83.3)	
Two	0	2 (16.7)	
Culprit vessel			0.22
LAD	4 (33.3)	6 (50.0)	
LCX	6 (50.0)	2 (16.7)	
RCA	2 (16.7)	4 (33.3)	
BVS size			< 0.01
3 × 12 mm	11 (91.7)	0	
3 × 18 mm	1 (8.3)	12 (100.0)	

Values are expressed as count (%), except for age.
MI, myocardial infarction; PCI, percutaneous coronary intervention; LAD, left anterior descending; LCX, left circumflex; RCA, right coronary artery; BVS, bioresorbable vascular scaffold.

Optical coherence tomography results

Baseline and follow-up quantitative OCT and IVUS findings are shown in Table 3. Both groups had similar OCT findings at baseline after the deployment of the BVS. At 6 months, the BVS 1.0 had a significantly higher late shrinkage than the BVS 1.1 (absolute shrinkage of 0.98 vs. 0.07 mm^2 and relative shrinkage of 13.0 vs. 1.0%, respectively; P = 0.01). Neointimal area was significantly higher with the BVS 1.0 when compared with the BVS 1.1 (1.44 vs. 0.87 mm^2, respectively; P < 0.01). NIH was also larger in the findings at 6 months caused a significantly higher reduction in mean lumen area (relative difference of 35.1 vs. 16.1%; P < 0.01) and in minimal luminal area (47.0 vs. 20.7%; P < 0.01) with the BVS 1.0 than with the BVS 1.1 as assessed by OCT. Serial individual changes of the BVS area and

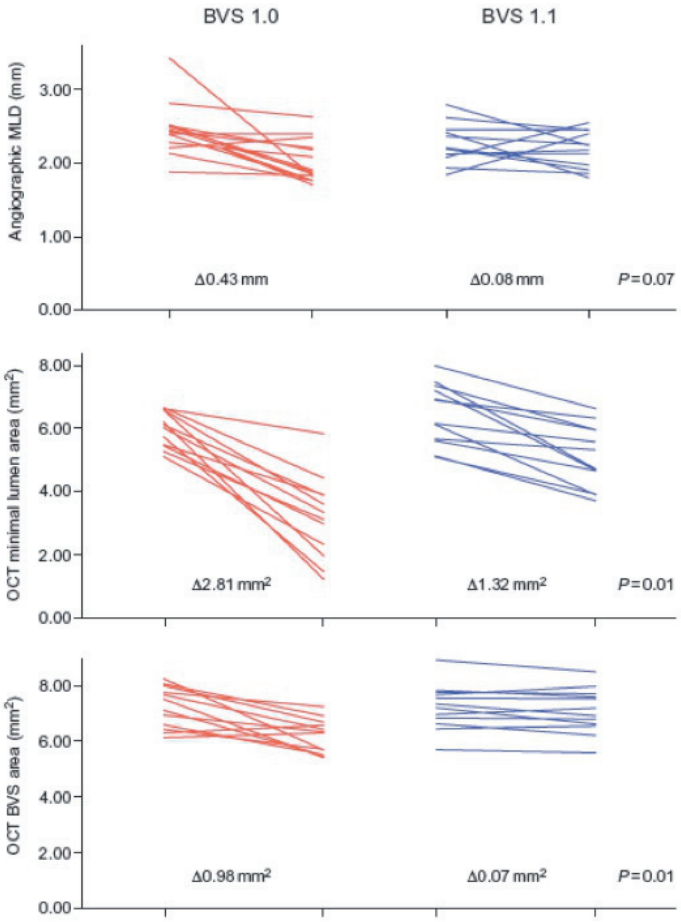

Figure 5. Serial changes in angiographic late lumen loss, BVS area (late shrinkage) and minimal lumen area as assessed by optical coherence tomography.

of the minimal lumen area as assessed by OCT are shown in Figure 5. The ISA area of the BVS 1.0 at 6 months increased significantly with respect to the baseline (0.10 mm^2; CI 95%: from 20.02 to 0.21 mm^2; P = 0.04), while the ISA area of the BVS 1.1 remained unchanged (0.02 mm^2; 20.18 to 0.22 mm^2; P = 0.26). A total of 662 struts of the BVS 1.0 and 1575 of the BVS 1.1 were detected at baseline. After deployment, all struts appear as preserved box in both BVS devices. At follow-up, 620 struts and 1639 struts were analysed. The strut appearance of the BVS 1.0 showed substantial changes in appearance: at 6 months struts had changed from 100% preserved black box to 29.7% open box, 51.4% dissolved bright

Table 2. Quantitative coronary angiography findings at baseline and 6-month follow-up.

BVS	Pre-deployment	Post-deployment	6-month FU	Difference post –pre (CI 95%)	P-value*	Difference post – 6 m FU (CI 95%)	P-value**	P-value†
QCA								
Lesion length (mm)a								
BVS 1.0	9.86 (3.46)	10.34 (1.70)	10.17 (2.20)	-0.48 (-2.90 to 1.94)	0.18	0.18 (-0.26 to 0.61)	0.64	0.93
BVS 1.1	8.99 (2.89)	17.08 (1.12)	16.08 (1.48)	-8.09 (-9.82 to -6.35)	<0.01	1.00 (-0.16 to 2.16)	0.13	
RVD (mm)								
BVS 1.0	2.95 (0.38)	3.03 (0.39)	2.87 (0.41)	0.08 (-0.10 to 0.26)	0.31	0.16 (0.01 to 0.31)	0.04	0.24
BVS 1.1	2.69 (0.35)	2.64 (0.23)	2.53 (0.22)	-0.05 (-0.21 to 0.11)	0.70	0.11 (0.02 to 0.20)	0.03	
MLD (mm)								
BVS 1.0	1.13 (0.30)	2.46 (0.38)	2.03 (0.30)	1.32 (1.03 to 1.62)	<0.01	0.43 (0.13 to 0.73)	0.01	0.07
BVS 1.1	1.23 (0.44)	2.26 (0.28)	2.18 (0.25)	1.03 (0.69 to 1.37)	<0.01	0.08 (-0.14 to 0.30)	0.24	
DS (%)								
BVS 1.0	60.8 (13.4)	18.6 (9.4)	27.8 (16.0)	-42.3 (-50.8 to -33.7)	<0.01	-9.3 (-18.7 to 0.2)	0.07	0.24
BVS 1.1	57.6 (13.1)	14.7 (7.5)	15.7 (9.3)	-42.9 (-50.9 to -35.0)	<0.01	-1.0 (-5.5 to 3.5)	0.66	

Data are expressed as mean (SD).
QCA, quantitative coronary angiography; BVS, bioresorbable vascular scaffold; FU, follow-up; RVD, reference vessel diameter; MLD, minimal lumen diameter; DS, diameter
stenosis.
aLesion length at post-procedure and at follow-up has been measured between the platinum markers of the BVS.
*Paired comparison between pre- and post-deployment within each group.
**Paired comparison between post-deployment and follow-up within each group.
†Comparison of the difference post-deployment—follow-up between the two groups. Comparison between groups at pre-deployment and post-deployment were non-significant (P = 0.10).

Table 3. Quantitative optical coherence tomography and intravascular ultrasound findings at baseline and 6-month follow-up.

BVS (n 5 12 vs. 12)	Baseline (post-deployment)	6-month FU	Absolute difference between BL and FU (CI 95%)	Relative difference between BL and FU (%)	P-value*	P-value**
OCT						
Mean luminal area (mm^2)						
1.0 BVS	7.63 (0.79)	4.94 (1.10)	2.69 (1.99–3.39)	35.07 (13.31)	<0.01	<0.01
1.1 BVS	7.67 (0.94)	6.44 (0.93)	1.23 (0.89–1.57)	16.09 (6.48)	0.01	
Minimal luminal area (mm^2)						
1.0 BVS	5.99 (0.57)	3.19 (1.28)	2.81 (2.03–3.59)	46.97 (19.67)	<0.01	<0.01
1.1 BVS	6.32 (0.96)	5.01 (0.97)	1.32 (0.83–1.80)	20.65 (10.94)	<0.01	
Mean BVS area (mm^2)						
1.0 BVS	7.18 (0.73)	6.20 (0.64)	0.98 (0.42–1.54)	12.95 (11.70)	0.01	0.01
1.1 BVS	7.21 (0.82)	7.14 (0.84)	0.07 (-0.10 to 0.24)	0.97 (3.73)	0.37	
Minimal BVS area (mm^2)						
1.0 BVS	5.82 (0.60)	4.75 (0.83)	1.07 (0.49 – 1.66)	17.90 (14.26)	<0.01	0.01
1.1 BVS	6.21 (0.98)	6.00 (0.85)	0.21 (-0.14 to 0.56)	2.81 (8.11)	0.29	
ISA area (mm^2)						
1.0 BVS	0.14 (0.25)	0.22 (0.31)	-0.10 (-0.21 to 0.02)	-36.36 (10.33)	0.04	0.88
1.1 BVS	0.15 (0.30)	0.17 (0.18)	-0.02 (-0.22 to 0.18)	-11.76 (15.35)	0.26	
NIA (mm^2)						
1.0 BVS	NA	1.44 (0.32)	NA	NA	NA	<0.01[a]
1.1 BVS	NA	0.87 (0.22)	NA	NA	NA	
NIT (mm)						
1.0 BVS	NA	0.17 (0.04)	NA	NA	NA	<0.01[a]
1.1 BVS	NA	0.08 (0.02)	NA	NA	NA	
In-device area obstruction (%)						
1.0 BVS	NA	23.62 (6.55)	NA	NA	NA	<0.01[a]
1.1 BVS	NA	12.28 (3.38)	NA	NA	NA	
IVUS						
Mean luminal area (mm^2)						
1.0 BVS	6.84 (0.74)	5.94 (0.67)	0.90 (0.43–1.37)	12.71 (9.89)	<0.01	0.17
1.1 BVS	6.69 (0.81)	6.20 (0.76)	0.47 (0.24–0.69)	6.93 (4.68)	<0.01	
Minimal luminal area (mm^2)						
1.0 BVS	5.75 (0.52)	4.41 (0.70)	1.34 (0.83–1.84)	22.83 (12.73)	<0.01	<0.01
1.1 BVS	5.51 (0.78)	5.15 (0.73)	0.28 (-0.01 to 0.57)	4.81 (7.20)	0.09	

Data are expressed as mean (SD).
QCA, quantitative coronary angiography; BVS, bioresorbable vascular scaffold; FU, follow-up; RVD, reference vessel diameter; MLD, minimal lumen diameter; DS, diameter stenosis.
aLesion length at post-procedure and at follow-up has been measured between the platinum markers of the BVS.
*Paired comparison between pre- and post-deployment within each group.
**Paired comparison between post-deployment and follow-up within each group.
†Comparison of the difference post-deployment follow-up between the two groups. Comparison between groups at pre-deployment and post-deployment were non-significant (P> 0.10).

box, 16.0% dissolved black box, and only 2.9% were preserved black box. For the BVS 1.1, all struts maintained a preserved black box appearance at 6 months (P < 0.01). Uncovered struts were less frequent in the BVS 1.0 (1.1%) than in the BVS 1.1 (5.3%) (P = 0.01).

Intravascular-ultrasound results

IVUS results are shown in Table 3. The reduction in mean lumen area was larger with the BVS 1.0 than with the BVS 1.1 (12.71 vs. 6.93%), but this difference was not statistically significant (P = 0.17). The reduction in minimal lumen area was significantly larger with the BVS 1.0 than with the BVS 1.1 (22.83 vs. 4.81%; P<0.01).

Reproducibility of optical coherence tomography measurements

The scaffold area reproducibility using our method has been assessed specifically for our study. Two independent analysts measured the scaffold area in 100 images at follow-up. After 1 week, one of the analysts re-analysed the same frames. The inter- observer R2 for repeated measures was 0.88 and the intraobserver R2 was 0.98.

DISCUSSION

The main findings of our study are: (i) the BVS 1.1 does not show late shrinkage at 6 months with respect to the baseline scaffold area; (ii) the BVS 1.0 has higher neointimal response and higher in-scaffold area obstruction than the BVS 1.1; (iii) these changes resulted in a higher OCT and IVUS luminal losses and angiographic late loss in the BVS 1.0 than in the BVS 1.1; (iv) the overall strut appearance at 6-month follow-up is dramatically different between the two generations of BVS, which may reflect differences in the polymer's interaction with light, arising from differences in microstructure and its degradation. A pre-clinical animal study involving histological samples at differing time points divided the evolution process of the BVS into two parts:12 first, the BVS resorption process, which consists of the disappearance of the polymeric PLA and the subsequent filling of the strut voids with proteoglycan material; second, the BVS integration process, which consists of the formation of organized tissue with connective cells and connective extracellular matrices replacing the polymeric and the proteoglycan material. In the same study, the strut appearance as assessed by OCT was compared with matched histological sections.[12] At 24 months, all the struts were discernible by OCT and 80.4% of them were classified as having the preserved box appearance (similar to the BVS 1.1 at 6 months). At that point of time, matched histological samples showed that almost all the strut footprints were occupied by proteoglycans and the analysis with gel permeation chromatography did

not find traces of the polymeric material. This demonstrated that the polymer was already resorbed at that time, and therefore OCT imaging was not able to assess the resorption process. At 3- and 4-year follow-up, almost all the struts were not discernible and the few observed struts were classified as a dissolved bright or dissolved black box (similar to the BVS 1.0 at 6 months). There was poor correlation of these types of OCT strut appearance with the particular patterns observed on histology. But, the indiscernible struts and the dissolved black box appearance as assessed by OCT were observed as circumscribed regions of dense connective tissue with low cellularity on histology.

Therefore, as assessed by OCT, the most advanced resorption/ integration states were characterized as: (i) observation of other types of strut appearance rather than the preserved box; and (ii) the reduction of discernible struts over time jointly with the observation of a dissolved black box strut appearance.[12]

In our study, the number of discernible struts of the BVS 1.1 was slightly lower at baseline than at follow-up (1575 vs. 1639, respectively; P = 0.06). At 6 months, the strut appearance was 'preserved' in all the patients. In contrast, the number of discernible struts of the BVS 1.0 was higher at baseline than at follow-up (662 vs. 620, respectively; P = 0.05) and at 6 months, only 2.9% of the discernible struts had a preserved box appearance. The correlation of our findings with the animal study shows that the BVS 1.0 had a more advanced resorption/integration state than the BVS 1.1 at 6 months. Our hypothesis is that this faster resorption/integration state is the main cause of the higher late shrinkage and greater neointimal response of the BVS 1.0 compared with the BVS 1.1.

Late shrinkage is a phenomenon resulting from the loss of structural integrity of the polymeric scaffold in conjunction with fatigue and constrictive remodelling of the vessel in the first months following the vessel injury. Loss of structural integrity is an inevitable part of the resorption process of these polymeric devices. The poly-L-lactic acid (PLLA) polymer has a lifecycle which can be divided in five phases.[14] First, immediately after the deployment, the polymer absorbs water from blood and surrounding tissues. Second, the long chains of PLLA degrade by hydrolysis into smaller chains without affecting the device's structure. Third, the hydrolysis process continues and causes a loss in integrity, with fragmentation of the struts and loss of radial strength. Fourth, soluble monomeric anions dissolve into the intercellular fluid and microparticles of less than 2 mm may be phagocyted by the macrophages; manifesting in mass loss and bioresorption. Finally, the soluble L-lactate is converted into pyruvate, which enters the Krebs cycle, being eventually converted into carbon dioxide and water. The initial degradation process of the PLLA semi-crystalline polymer depends on the length of the polymers chain (molecular weight), the hydrophilicity, and the degree of crystallinitiy. In BVS 1.1, initial degradation rate (i.e. losses in molecular weight leading to structural degradation) has been reduced through

changes in the manufacturing process. This slower degradation allows for maintenance of the radial strength over months following the implantation.

The second cause of late shrinkage is the constrictive remodel- ling of the treated vessel in the first few months after implantation. In the era of balloon angioplasty, more than 70% of the restenotic process was attributed to negative remodelling of the vessel in the treated segment, and less than 30% was done to neointimal growth.[15] In the metallic stent era, late lumen loss within the stent correlated strongly with tissue growth (r = 0.975), eliminating negative remodelling as the common cause of restenosis.[16,17]

Thus, the key question for intracoronary bioresorbable scaffolds is for how long radial strength (i.e. scaffolding) must be maintained to avoid constrictive remodelling. In a cohort of patients consecutively re-catheterizated at 1, 2, 3, and 4 months, Serruys et al.18 demonstrated that the restenotic process after balloon angioplasty ceases to progress after 4 months. It is possible that after this time, scaffolding is no longer needed, and the structural degradation and bioresorption processes can commence. It is uncertain whether the constrictive remodelling is more focused in the regions of the vessel with more plaque burden or is equally distributed. This can affect the results of our study due to the differences in the BVS lengths according to the lesion length. The lesion length prior to the implantation was similar in both groups (around 9 – 10 mm), but the device length as assessed by QCA at post-deployment was significantly higher in the BVS 1.1 than in the BVS 1.0 (17.08 vs. 10.34 mm; $P < 0.01$). This difference resulted from the fact that all patients treated in the ABSORB Cohort B study received a single size device (3 × 18 mm), while in the ABSORB Cohort A there were two different sizes (3 × 12 and 3 × 18 mm). A sub-analysis of the 12 central millimeter of the scaffold imaged by OCT (that part of the scaffold is more likely to be located at the nadir of the narrowing) in the patients treated with a 3 × 18 mm showed that the mean scaffold area at baseline and at 6-month follow-up was 7.18 and 6.19 mm^2 with the BVS 1.0 (relative shrinkage of 13.09%) and 7.14 and 7.10 mm^2 with the BVS 1.1 (relative shrinkage of 0.50%); $P = 0.01$.

Until now, four different fully bioresorbable scaffolds have been tested in humans. The polymeric PLLA non-drug-eluting Igaki-Tamai device was the first fully bioresorbable scaffold used in humans. The IVUS analysis did not show bioresorption of the polymeric struts at 6 months and this absence of ultrasonic changes in struts was parallel to the absence of scaffold shrinkage. This device presented a target vessel revascularization of 6.7% at 6 months and a low rate of major cardiac events at 10 years.[19,20]

Conversely, the PROGRESS-AMS magnesium platform non-drug-eluting bioresorbable scaffold had a rapid resorption which was complete at 4-month follow-up. This swift resorption produced an important reduction of the lumen (60% of the late lumen loss) and a high incidence of restenosis (47.5% assessed by QCA).[21] The REVA device is a poly

(iodinated desaminotyrosyltyrosine ethyl ester) carbonate non-drug-eluting scaffold. The closed design and the lifecycle of the carbonate provide enough radial strength during the first 3 months following the implantation without appreciable shrinkage. However, focal mechanical failures driven by polymer embrittlement led to a high rate of TLR (66.7%) between 4- and 6-month follow-up.[22] Finally, the IDEALTM Poly (Anhydride Ester) Salicylic acid sirolimus-eluting device has been tested in only 11 patients.[23]

The shrinkage phenomenon observed in the BVS 1.0 was linked to a significant increase of the ISA area with respect to baseline and with higher neointimal response with respect to the BVS 1.1. The increasing of the ISA area with the BVS 1.0 can be explained by the scaffold shrinkage itself. At baseline, 95% of the struts were apposed or aligned, while in the follow-up only 93% of the struts were apposed to the vessel wall. Moreover, less than 10% of the malapposed struts at baseline were resolved at follow-up.1 The NIA measured in this population was significantly different between the two generations of BVS (1.44 mm^2 for the BVS 1.0 vs. 0.87 mm^2 for the BVS 1.1). In-scaffold area obstruction was also different between BVS 1.0 and 1.1 (23.6 vs. 12.3%, respectively). The significantly lower neointimal response of the BVS 1.1 with respect to the BVS 1.0 has no clear explanation. Both generations of BVS are built with the same polymer mass, strut thickness, drug, and coating elution and the same amount of drug. One hypothesis is that the loss in scaffold area leads to a decreased efficiency in drug transfer to the vessel wall and thus, a reduction in antiproliferative efficacy. Another hypothesis is that the more accelerated resorption/ integration process of the BVS 1.0 com- pared with the BVS 1.1 could generate a larger neointimal response. Unfortunately, this cannot be assessed by OCT due to the lack of correlation between the different types of strut appear- ance and the histological findings based on animal studies.12 An exploratory analysis of the patients treated with the BVS 1.0 in our study relating the NIT measured above the preserved box appearance (0.15 ± 0.04 mm) with the NIT measured above the other types of strut appearance (0.18 ± 0.06) failed to be significant ($P = 0.27$). The same patients treated with the BVS 1.0 studied with OCT at 2 years showed few discernible struts with no measurable neointima. Nevertheless, the mean lumen area increased up to 19% from 6-month to 2-year follow-up.4 This fact may be a sign of vessel remodelling at the neointimal level but the low number of patients are a clear limitation to this conclusion. This hypothesis will be examined further when the strut appearance of patients treated with the BVS 1.1 changes in future scheduled imaging controls.

The OCT performance of the BVS 1.1 can be compared with some drug-eluting stents (DES). The NIT observed in the BVS 1.1 (0.08 mm) is similar to that seen with the sirolimus-DES (from 0.05 to 0.12 mm) at 6-month follow-up.[24,25] Paclitaxel-DES and zotarolimus-DES showed an NIT of 0.20 and 0.33 mm, respectively.[24] The late shrinkage of metallic DES

has not been yet explored with OCT. Using IVUS, the everolimus-DES showed a relative difference in mean stent area of 0.3% at 6-month follow-up.[26] This value is similar to the 1.0% found in our study with the BVS 1.1. Based on this information, the BVS 1.1 presents a similar profile as the metallic DES as assessed by OCT.

In summary, our study represents the first comparison of two generations of bioresorbable devices in terms of late shrinkage, neointimal response, and bioresorption state using the most sophisticated intravascular imaging technique (OCT) and the same methodology for both devices. The OCT findings at 6 months show the improvement of the new generation of BVS with respect to the previous generation. The slower bioresorption process of the BVS 1.1, compared with the BVS 1.0, is the most plausible explanation for the near elimination of the late shrinkage and for the higher inhibition of the neointimal response. Further investigations will be required to assess the preservation of these results after 6-month follow-up for the BVS 1.1. A more advanced bioresorption state can contribute to a very late shrinkage of the device or later neointimal responses studied with OCT at 2 years showed few discernible struts with no measurable neointima. Nevertheless, the mean lumen area increased up to 19% from 6-month to 2-year follow-up.4 This fact may be a sign of vessel remodelling at the neointimal level but the low number of patients are a clear limitation to this conclusion. This hypothesis will be examined further when the strut appearance of patients treated with the BVS 1.1 changes in future scheduled imaging controls.

Limitations

The result of the present analysis must be interpreted with caution as a major limitation of our study is the small number of patients who have been enrolled in a non-randomized comparison. Figure 5 shows that there is a homogeneous trend of higher late shrinkage and higher loss in minimal lumen area in the BVS 1.0 than in the BVS 1.1. The histogram distribution of the NIA in the two populations also shows this trend of higher neointimal growth in the BVS 1.0 than in the BVS 1.1 (data not shown). This trend, however, is not observed with the angiographic late lumen loss in which one outlier can be influencing the higher late lumen loss in the BVS 1.0. Moreover, two eligible patients imaged at baseline and scheduled for an invasive follow-up at 6 months did not undergo repeat invasive imaging. It is uncertain how this lack of serial imaging in those patients affects the global results of our study. Although the small number of patients, we have used the maximal number of 'historical' cases performed with the BVS 1.0 and imaged with the best available OCT system M2 at that time and compared with the same number of patients of the BVS 1.1 imaged with the best available system nowadays (OCT C7 system).

These differences in OCT systems are inherent to the fact that the ABSORB Cohort A trial was conducted in 2006, when a balloon occlusive technique was needed due to the lower frame/ rate and acquisition speed of the available systems at that time. One in vitro study showed less accuracy in the lumen area measurement with lower frame rate and acquisition speed than with higher frame/rate and speed.[27] An in vivo study, comparing the non- occlusive and the occlusive technique in the same non-scaffolded native coronary artery, showed systematically smaller mean and minimal lumen areas with the occlusive technique than with the non-occlusive technique (relative differences of 13.2 and 28.2%, respectively).[28] These differences were probably produced by the lack of physiological pressurization of the vessel during the occlusive technique imaging and/ or the over-pressurization of the vessel during the contrast infusion of the non-occlusive tech- nique.[28] These differences represent an important limitation of our study because the two different devices were imaged with different OCT techniques (occlusive for the BVS 1.0 and non- occlusive for the BVS 1.1). However, in our study, the baseline and follow-up acquisition were performed using the same imaging technique in each cohort of patients and also, the analysed region is scaffolded by the BVS. The scaffolded region is probably less susceptible to changes in volumetric parameters according to the intravascular pressure. Unfortunately, there is no current information comparing the changes in lumen areas within the scaffolded regions with the two different OCT techniques. The method of analysis used in our study is slightly different from the current method of OCT measurement of polymeric scaffold. The strut appearance of the BVS 1.0 at 6 months (and probably the appearance of the BVS 1.1 in later controls) does not permit the delineation of the strut contour at the front or backside of the strut. Using the central part of the strut as landmark for measurement is the most reliable method to assess the scaffold area. However, it must be recognized that the neointima area as such determined is an arbitrary entity resulting from the difference between the luminal area and the scaffold area, and does not depict accurately the neointimal tissue that has grown between, on the top and behind the struts either biologically altered in the case of the BVS 1.0 or almost intact in the case of the BVS 1.1. Finally, the differences in device lengths in the two groups may be favourable to the BVS 1.1 due to a better anchoring in the healthy part of the vessel that can be subjected to a less constrictive modelling of the vessel.

CONCLUSION

The two generations of the everolimus-eluting bioresorbable vascular scaffold have different OCT findings at 6-month follow-up. The BVS 1.1 has less late shrinkage and less neointimal growth at 6-month follow-up compared with the BVS 1.0. Consequently, less angiographic late loss and less OCT and IVUS luminal losses were observed with the BVS 1.1. A difference in polymer degradation leading to changes in microstructure and reflectivity is the most plausible explanation for this finding.

REFERENCES

1. Ormiston JA, Serruys PW, Regar E, Dudek D, Thuesen L, Webster MW, Onuma Y, Garcia-Garcia HM, McGreevy R, Veldhof S. A bioabsorbable everolimus-eluting coronary stent system for patients with single de-novo coronary artery lesions (ABSORB): a prospective open-label trial. Lancet 2008;371:899–907.
2. Painter JA, Mintz GS, Wong SC, Popma JJ, Pichard AD, Kent KM, Satler LF,Leon MB. Serial intravascular ultrasound studies fail to show evidence of chronic Palmaz-Schatz stent recoil. Am J Cardiol 1995;75:398–400.
3. Okamura T, Garg S, Gutierrez-Chico JL, Shin ES, Onuma Y, Garcia-Garcia HM, Rapoza R, Sudhir K, Regar E, Serruys PW. In vivo evalution of stent strut distribution patterns in the bioabsorbable everolimus-eluting device: an OCT ad hoc analysis of the revision 1.0 and revision 1.1 stent design in the ABSORB clinical trial. EuroIntervention 2010;5:932–938.
4. Serruys PW, Ormiston JA, Onuma Y, Regar E, Gonzalo N, Garcia-Garcia HM,Nieman K, Bruining N, Dorange C, Miquel-Hebert K, Veldhof S, Webster M,Thuesen L, Dudek D. A bioabsorbable everolimus-eluting coronary stent system (ABSORB): 2-year outcomes and results from multiple imaging methods. Lancet 2009;373:897–910.
5. Kawase Y, Hoshino K, Yoneyama R, McGregor J, Hajjar RJ, Jang IK, Hayase M. In vivo volumetric analysis of coronary stent using optical coherence tomography with a novel balloon occlusion-flushing catheter: a comparison with intravascular ultrasound. Ultrasound Med Biol 2005;31:1343–1349.
6. Suzuki Y, Ikeno F, Koizumi T, Tio F, Yeung AC, Yock PG, Fitzgerald PJ, Fearon WF. In vivo comparison between optical coherence tomography and intravascular ultrasound for detecting small degrees of in-stent neointima after stent implantation. JACC Cardiovasc Interv 2008;1:168–173.
7. Onuma Y, Serruys PW, Ormiston JA, Regar E, Webster M, Thuesen L, Dudek D, Veldhof S, Rapoza R. Three-year results of clinical follow-up after a bioresorbable everolimus-eluting scaffold in patients with de novo coronary artery disease: the ABSORB trial. EuroInterv 2010;6:447–453.
8. Reiber JH, Serruys PW, Kooijman CJ, Wijns W, Slager CJ, Gerbrands JJ, Schuurbiers JC, den Boer A, Hugenholtz PG. Assessment of short-, medium-,and long-term variations in arterial dimensions from computer-assisted quantitation of coronary cineangiograms. Circulation 1985;71:280–288.
9. Takarada S, Imanishi T, Liu Y, Ikejima H, Tsujioka H, Kuroi A, Ishibashi K, Komukai K, Tanimoto T, Ino Y, Kitabata H, Kubo T, Nakamura N, Hirata K, Tanaka A, Mizukoshi M, Akasaka T. Advantage of next-generation frequencydomain optical coherence tomography compared with conventional time-domain system in the assessment of coronary lesion. Catheter Cardiovasc Interv 2009;75:202–206.
10. Tanimoto S, Serruys PW, Thuesen L, Dudek D, de Bruyne B, Chevalier B, Ormiston JA. Comparison of in vivo acute stent recoil between the bioabsorbable everolimus-eluting coronary stent and the everolimus-eluting cobalt chromium coronary stent: insights from the ABSORB and SPIRIT trials. Catheter Cardiovasc Interv 2007;70:515–523.
11. Tanimoto S, Bruining N, van Domburg RT, Rotger D, Radeva P, Ligthart JM, Serruys PW. Late stent recoil of the bioabsorbable everolimus-eluting coronary stent and its relationship with plaque morphology. J Am Coll Cardiol 2008;52:1616–1620.
12. Onuma Y, Serruys P, Perkins L, Okamura T, Gonzalo N, Garcia-Garcia HM, Regar E, Kamberi M, Powers JC, Rapoza R, van Beusekom H, van der Giessen W, Virmani R. Intracoronary optical coherence tomography (OCT) and histology at 1 month, at 2, 3 and 4 years after implantation of everolimus-eluting bioresorbable vascular scaffolds in a porcine coronary artery model: An attempt to decipher the human OCT images in the ABSORB trial. Circulation 2010; Published online ahead of print 25 October 2010.

13. von Birgelen C, de Vrey EA, Mintz GS, Nicosia A, Bruining N, Li W, Slager CJ, Roelandt JR, Serruys PW, de Feyter PJ. ECG-gated three-dimensional intravascular ultrasound: feasibility and reproducibility of the automated analysis of coronary lumen and atherosclerotic plaque dimensions in humans. Circulation 1997;96:2944–2952.
14. Aalst M, Eenink M, Kruft M, van Tuil R. ABC's of bioabsorption: application of lactide based polymers in fully resorbable cardiovascular stents. Eurointervention 2009;5(Suppl. F):F23–F27.
15. Mintz GS, Popma JJ, Pichard AD, Kent KM, Satler LF, Wong C, Hong MK, Kovach JA, Leon MB. Arterial remodeling after coronary angioplasty: a serial intravascular ultrasound study. Circulation 1996;94:35–43.
16. Hoffmann R, Mintz GS, Dussaillant GR, Popma JJ, Pichard AD, Satler LF, Kent KM, Griffin J, Leon MB. Patterns and mechanisms of in-stent restenosis. A serial intravascular ultrasound study. Circulation 1996;94:1247–1254.
17. Nakamura M, Yock PG, Bonneau HN, Kitamura K, Aizawa T, Tamai H, Fitzgerald PJ, Honda Y. Impact of peri-stent remodeling on restenosis: a volumetric intravascular ultrasound study. Circulation 2001;103:2130–2132.
18. Serruys PW, Luijten HE, Beatt KJ, Geuskens R, de Feyter PJ, van den Brand M, Reiber JH, ten Katen HJ, van Es GA, Hugenholtz PG. Incidence of restenosis after successful coronary angioplasty: a time-related phenomenon. A quantitative angiographic study in 342 consecutive patients at 1, 2, 3, and 4 months. Circulation 1988;77:361–371.
19. Tamai H, Igaki K, Kyo E, Kosuga K, Kawashima A, Matsui S, Komori H, Tsuji T, Motohara S, Uehata H. Initial and 6-month results of biodegradable poly-l-lactic acid coronary stents in humans. Circulation 2000;102:399–404.
20. Nishio S, Kosuga K, Okada M, Harita T, Ishii M, Kawata Y, Takeda S, Takeuchi Y, Hata T, Ikeguchi S. Long term (.10 years) clinical outcomes of the first-in-man biodegradable poly-L-lactic acid coronary stents. Oral presentation. Paris:EuroPCR; 2010.
21. Erbel R, Di Mario C, Bartunek J, Bonnier J, de Bruyne B, Eberli FR, Erne P, Haude M, Heublein B, Horrigan M, Ilsley C, Bose D, Koolen J, Luscher TF, Weissman N, Waksman R. Temporary scaffolding of coronary arteries with bioabsorbable magnesium stents: a prospective, non-randomised multicentre trial. Lancet 2007;369:1869–1875.
22. Pollman M. Engineering a bioresorbable stent: the REVA programme update. Euro-Intervention 2009;5(Suppl. F):F54–F57.
23. Jabara R. Poly-anhydridre Basic on Salicylic Acid and Adipic Acid Anhydridre. Barcelona:EuroPCR; 2009.
24 Guagliumi G, Musumeci G, Sirbu V, Bezerra HG, Suzuki N, Fiocca L, Matiashvili A, Lortkipanidze N, Trivisonno A, Valsecchi O, Biondi-Zoccai G, Costa MA. Optical coherence tomography assessment of in vivo vascular response after implantation of overlapping bare-metal and drug-eluting stents. JACC Cardiovasc Interv 2010;3:531–539.
25. Matsumoto D, Shite J, Shinke T, Otake H, Tanino Y, Ogasawara D, Sawada T, Paredes OL, Hirata K, Yokoyama M. Neointimal coverage of sirolimus-eluting stents at 6-month follow-up: evaluated by optical coherence tomography. Eur Heart J 2007;28:961–967.
26. Serruys PW, Ong AT, Piek JJ, Neumann FJ, van der Giessen WJ, Wiemer M, Zeiher A, Grube E, Haase J, Thuesen L, Hamm C, Otto-Terlouw PC. A randomized comparison of a durable polymer Everolimus-eluting stent with a bare metal coronary stent: The SPIRIT first trial. EuroIntervention 2005;1:58–65.
27. Sawada T, Shite J, Negi N, Shinke T, Tanino Y, Ogasawara D, Kawamori H, Kato H, Miyoshi N, Yoshino N, Kozuki A, Koto M, Hirata K. Factors that influence measurements and accurate evaluation of stent apposition by optical coherence tomography. Assessment using a phantom model. Circ J 2009;73:1841–1847.
28. Gonzalo N, Serruys PW, Garcia-Garcia HM, van Soest G, Okamura T, Ligthart J, Knaapen M, Verheye S, Bruining N, Regar E. Quantitative ex vivo and in vivo comparison of lumen dimensions measured by optical coherence tomography and intravascular ultrasound in human coronary arteries. Rev Esp Cardiol 2009;62:615–624.

Chapter 6

Comparison between the first and second generation bioresorbable vascular scaffolds: a six month virtual histology study

Salvatore Brugaletta, MD; Hector M. Garcia-Garcia, MD, PhD; Roberto Diletti, MD; Josep Gomez- Lara, MD; Scot Garg, MBChB, MRCP; Yoshinobu Onuma, MD; Eun-Seok Shin, MD, PhD; Robert Jan van Geuns, MD, PhD; Bernard de Bruyne, MD; Dariusz Dudek, MD; Leif Thuesen, MD; Bernard Chevalier, MD; Dougal McClean, MD; Stephan Windecker, MD, PhD; Robert Whitbourn, MD; Cecile Dorange, MSc; Susan Veldhof, RN; Richard Rapoza, PhD; Krishnankutty Sudhir, MD, PhD; Nico Bruining, PhD; John A. Ormiston, MBChB, PhD; Patrick W. Serruys, MD, PhD, FACC, FESC

EuroIntervention 2011 Apr;6(9):1110-6

ABSTRACT

Aims To compare the intravascular ultrasound virtual histology (IVUS-VH) appearance of the polymeric struts of the first (Revision 1.0) and the second (Revision 1.1) generation bioresorbable vascular scaffold (BVS).

Methods and results IVUS-VH misrepresents polymeric struts as dense calcium (DC) and necrotic core (NC) so that their presence and disappearance could be used as potential artifactual surrogate of bioresorption. DC and NC were assessed in both revisions of the BVS by analysing IVUS-VH from all patients in the ABSORB cohort A (Revision 1.0) and cohort B (Revision 1.1) study who had an IVUS-VH post-treatment and at 6-month follow-up. Post-treatment and 6-month follow-up IVUS-VH results, available in 60 patients (BVS 1.0 n=28; BVS 1.1 n=32), indicated an insignificant rise in DC+NC area compared to baseline with Revision 1.1 ($0.10\pm0.46 mm^2$, p=0.2), whilst a significant reduction was seen with Revision 1.0 ($-0.57\pm1.3 mm^2$, p=0.02). A significant correlation has been found between the change in the DC+NC area and the change in external elastic membrane area ($y=0.68\times-0.1$; r=0.58, p=0.03).

Conclusions Based on 6-months IVUS-VH analysis, the BVS 1.1 appears to have a different backscattering signal compared to the BVS 1.0, which may reflect differences in the speed of chemical and structural alteration.

INTRODUCTION

The bioresorption process of new bioresorbable vascular scaffolds (BVS) is crucial in the determination of their performance at medium and long-term. A BVS should have enough radial strength to counteract acute vessel recoil following angioplasty and should also be able to maintain its mechanical integrity until late recoil forces subside. The fully resorbable BVS (Abbott Vascular, Santa Clara, CA, USA) has been tested in 30-patient in the first-in-man ABSORB cohort A study and demonstrated excellent long-term clinical results up to two years with a major adverse cardiac event rate of 3.6%.[1] However, due to faster degradation, the first generation BVS showed higher late recoil than conventional metallic platform stents.[1-3] To prolong the mechanical strength of the scaffold and reduce late recoil, a second generation BVS –Revision 1.1– has recently been introduced, and this is currently undergoing clinical evaluation in the ABSORB cohort B study.[4] Compared to the Revision 1.0 which was used in the ABSORB cohort A study, the Revision 1.1 has a smaller maximum circular unsupported surface area,[5] a more uniform strut distribution and improved stent retention. Importantly, these changes have not resulted in an increased amount of polymeric material or an increase in strut thickness. Proprietary process changes have been implemented to increase radial strength. In addition, these changes have reduced polymer degradation rates at early time points and thus prolonged mechanical integrity of the scaffold throughout the first few months following implantation. Intravascular ultrasound virtual histology (IVUS-VH), a tool developed to assess tissue composition of intact native coronary arteries, misclassifies polymeric stent struts as "dense calcium" and "necrotic core" (white and red in the VH colour code).[6] This could potentially be used as surrogate marker of alteration of the polymeric struts and to assess in vivo the degradation process of a BVS.[7,8] Shin's method, for IVUS-VH analysis, allows a more accurate detection of dense calcium and necrotic core so that the bioresorption process can be better explored.[9] The aim of this study was; 1) to evaluate temporal changes in the IVUS-VH signal of the BVS 1.1 and BVS 1.0; 2) to assess the correlation between the changes in IVUS-VH signal for BVS 1.1 and 1.0, and the change in external elastic membrane (EEM) area.

METHODS

Study design

All patients from cohort A and cohort B of the ABSORB trial with paired post-BVS implantation and 6-month follow-up IVUS-VH data were included. The ABSORB cohort A study is described elsewhere.[1] In brief, for cohort A and cohort B, patients were suitable

for inclusion if they were older than 18 years, with adiagnosis of stable, unstable or silent ischaemia. All treated lesions were *de novo* lesions in a native coronary artery with a reference vessel diameter of 3.0 mm, with a percent diameter stenosis ≥50% and <100% and a thrombolysis in myocardial infarction (TIMI) flow grade of ≥1. The BVS 1.0 was used in patients in cohort A, whilst Revision 1.1 was used in cohort B.[4] Major exclusion criteria were: patients presenting with an acute myocardial infarction, unstable arrhythmias or patients who had left ventricular ejection fraction ≤30%, restenotic lesions, lesions located in the left main coronary artery, lesions involving a side branch >2 mm in diameter, and the presence of thrombus or another clinically significant stenosis in the target vessel. Both ABSORB trials were approved by ethics committee at each participating institution and each patient gave written informed consent before inclusion.

Study device

The BVS has an amorphous poly-DL-lactide (PDLLA) coating that contains and controls the release of the anti-proliferative drug everolimus. The scaffold body is made of semi-crystalline poly-L-lactide (PLLA). PLA is completely degraded via hydrolysis and bioresorbed via the lactate shuttle. There are no differences in polymeric material, drug dose, drug release or strut thickness between BVS Revisions 1.0 and 1.1. Of note, the BVS Revision 1.1 has a smaller maximum circular unsupported surface area compared to Revision 1.0.[5] Processing changes in Revision 1.1 have resulted in higher and prolonged mechanical strength and stability post implantation. (Figure 1) the lactate shuttle.

BVS implantation procedure

In both cohorts, lesions were treated with routine interventional techniques that included mandatory pre-dilatation using a balloon shorter than the study device and 0.5 mm less in diameter. All patients were pre-treated with aspirin and a loading dose of at least 300 mg of clopidogrel was administered according to local hospital practise. After the procedure, all patients received aspirin ≥75 mg for the study duration (five years) and clopidogrel 75 mg daily for a minimum of six months. Anticoagulation and glycoprotein IIb/IIIa use was according to local hospital practice.

Imaging procedure and acquisition

IVUS-VH post-BVS implantation and at 6-month follow-up were obtained from patients from both cohorts. Imaging techniques were acquired simultaneously with a phased array 20MHz intravascular ultrasound catheter (EagleEye™; Volcano Corporation, Rancho Cordova, CA, USA) using an automated pullback of 0.5 mm per second. Four tissue components (necrotic core – red; dense calcium – white; fibrous – green; and fibrofatty –

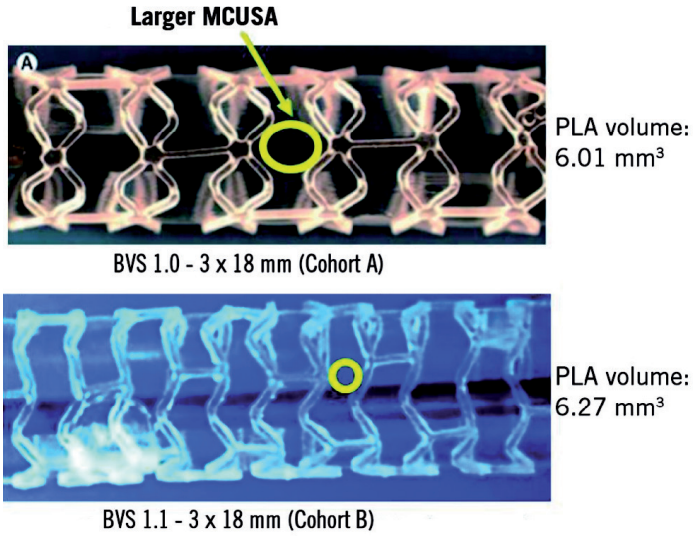

Figure 1. Although the scaffold design is different between revision 1.0 and revision 1.1, the content of polymer is nearly the same. MCUSA: maximum circular unsupported surface area; BVS: bioresorbable vascular scaffold; PLA: polylactide

light green) were identified with autoregressive classification systems.[10,11] Each individual tissue component was quantified and colour coded in all IVUS cross sections as previously described.10 All IVUS-VH analyses were performed offline using pcVH 2.1 (Volcano Corporation, Rancho Cordova, CA, USA). We carefully matched the region received BVS implantation using anatomical markers to compare the post implantation and 6-month follow-up IVUS-VH images. Regions received non-BVS stent implantation were not analysed. For each cross section, polymeric struts were detected as areas of apparent "dense calcium" and "necrotic core". The quantitative changes in dense calcium (DC) and necrotic core (NC) content were used as a surrogate marker of alteration of the polymeric struts, as previously described.[1,7,12,13] Only changes in DC and NC, which can be seen as the fingerprint of the BVS, were required, therefore the lumen contour was drawn around the IVUS catheter without following the leading edge of the interface lumen intima, as previously described by Shin et al.[9] Using this approach, the BVS struts closest to the lumen were better detected and recognised as DC and NC by the VH software and the ones overlying small plaques (thinner side of an eccentric plaque) were not obscured by the imposed grey medial stripe seen with IVUS-VH. (Figure 2) We also recorded in all patients the interface between plaque+media and the adventitia (EEM area). Lumen area and plaque area cannot be recorded using this method.

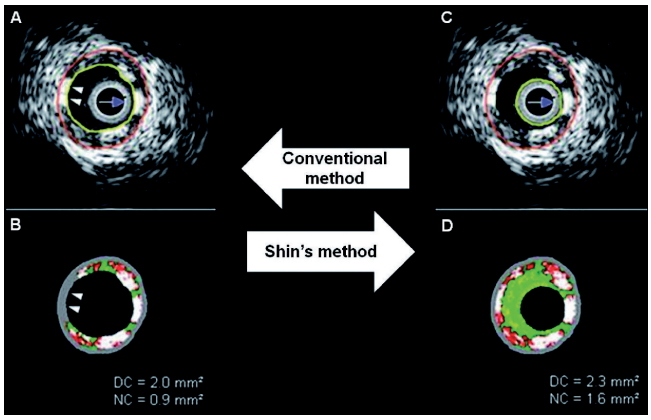

Figure 2. The conventional method (A and B) does not show some necrotic core and dense calcium (two white arrow heads), hidden by the grey medial stripe (two white arrow heads), that are showed by the Shin's method (C and D). DC: dense calcium, NC: necrotic core

Statistical analysis

Discrete variables are presented as counts and percentages. Continuous variables are presented as mean ± standard deviation (SD). The DC and NC values have been statistically tested separately post-procedure and 6-month follow-up. The VH fingerprint of the BVS in the artery was defined as the sum of the changes in DC and NC, as IVUS-VH detects stent struts as dense calcium surrounded by necrotic core halo.[6] The calculation of the changes between post-treatment and six months was as follows: mean six month area minus mean post-procedure area for both NC and DC. Paired comparisons between post-procedure and 6-month follow-up were performed using the Wilcoxon signed rank test. Comparisons between groups were assessed using non parametric tests, whilst correlations between parameters were performed by using a Spearman test. A two-side p-value of less than 0.05 indicated statistical significance. Statistical analyses were performed with use of SPSS 13.0 software (SPSS Inc., Chicago IL, USA).

RESULTS

The comparison between post-procedure and 6-month follow-up IVUS-VH included 28 patients from cohort A and 32 patients from cohort B. (Figure 3). Table 1 shows clinical and angiographic data in both cohorts. Compositional changes from post-treatment to six month follow-up by IVUS-VH (Table 2). In cohort A, there was a relative 20% decrease in both DC and NC (p=0.08 and p=0.02) between post-procedure and 6-month follow-up.

Table 1. Baseline demographics, risk factors and lesion characteristics.

	Cohort A (N=28) (Lesions=28)	Cohort B (N=32) (Lesions=32)	P-Value
Age (years)			
Mean±SD	62.03±9.00	62.83±10.01	0.67[1]
Men,% (n)	57.1% (16)	65.6% (21)	0.43[2]
Smokers, % (n)	21.4% (6)	12.5% (4)	0.49[2]
Diabetes, % (n)	3.6% (1)	15.6% (5)	0.19[2]
Hypertension requiring medication, % (n)	57.1% (16)	59.3% (19)	0.79[2]
Hyperlipidaemia requiring medication, % (n)	63.0% (17)	87.5% (28)	0.02[2]
Previous target vessel intervention, % (n)	3.6% (1)	6.2% (2)	1.00[2]
Previous myocardial infarction, % (n)	3.5% (1)	37.5% (12)	<0.01[2]
Stable angina, % (n)	67.9% (19)	68.7% (22)	1.00[2]
Unstable angina, % (n)	28.6% (8)	15.6% (5)	0.34[2]
Silent ischaemia, % (n)	3.6% (1)	0.0% (0)	0.47[2]
Target vessel, % (n)			
Left anterior descending	50.0% (14)	37.5% (12)	0.30[2]
Left circumflex	28.6% (8)	25.0% (8)	1.00[2]
Right coronary artery	21.4% (6)	37.5% (12)	0.17[2]
AHA/ACC lesion classification, % (n)			
A	0.0% (0)	3.1% (1)	1.00[2]
B1	64.3% (18)	43.8% (14)	0.19[2]
B2	35.7% (10)	50.0% (16)	0.43[2]
C	0.0% (0)	3.1% (1)	1.00[2]
Mean reference vessel diameter (mm), Mean±SD (n)	2.70±0.47 (28)	2.60±0.45 (32)	0.39[1]
Minimum luminal diameter (mm), Mean±SD (n)	1.08±0.25 (28)	1.08±0.31 (32)	0.77[1]
Diameter stenosis (%), Mean±SD (n)	59.13±11.28 (28))	57.81±12.60 (32	0.87[1]
Lesion length (mm), Mean±SD (n)	8.79±3.67 (28)	10.08±3.50 (32)	0.09[1]

1. from Wilcoxon's rank sum test; 2. from Fisher's exact test; AHA/ACC: American Heart Association/American College of Cardiology; SD: standard deviation

Conversely, over the same time period in cohort B, a small relative increase in DC and NC of 9% (p=0.2) and of 4% (p=0.1) respectively, was observed. (Figure 4) At 6-month follow-up, while in cohort A there was regression in the calcified pattern in 16 out of 27 patients (59%) and in the necrotic pattern in 20 out of 27 patients (74%), in cohort B there was regression in the calcified pattern in 11 out of 26 patients (42%) and in necrotic pattern

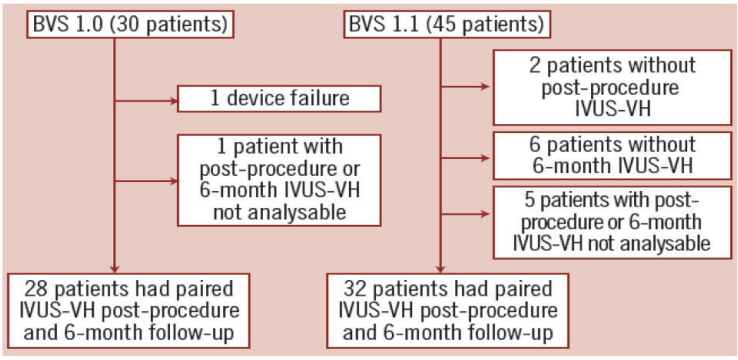

Figure 3. Flow chart of paired IVUS-VH data available for both cohorts

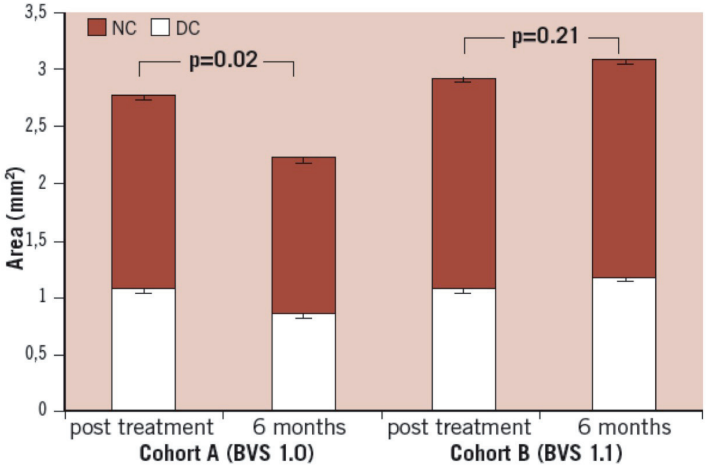

Figure 4. DC and NC area at six months compared to post-treatment in BVS 1.0 and BVS 1.1. Error bars portray standard error of the mean. DC: dense calcium; NC: necrotic core

in seven out of 26 patients (27%). Overall, the absolute DC+NC decrease was significantly larger in cohort A than cohort B, suggesting an earlier IVUS-VH alteration of the polymeric struts with the BVS 1.0 as compared to the BVS 1.1.

Grey-scale intravascular ultrasound data and correlation with IVUS-VH alteration of BVS 1.0 and 1.1

On average, at six month follow-up, the EEM area did not significantly differ from post-treatment status in both cohorts (Table 2). Classifying patients according to reduction in the EEM area at 6- month follow-up, we analysed changes in absolute area of DC and NC

Table 2. IVUS-VH data between post-procedure and 6-month follow-up.

	Cohort A (BVS 1.0), n=28			Cohort B (BVS 1.1), n=32			P value Cohort A vs. Cohort B	
	Post-procedure	6-month follow-up	*p* value	Post-procedure	6-month follow-up	p value	Post-procedure	6-month follow-up
DC area (mm^2)	1.07±0.55	0.85±0.54	0.08	1.08±0.69	1.18±0.66	0.2	0.9	0.01
DC (%)	7.73±3.70	6.21±3.69	0.1	8.87±4.58	10.39±5.64	0.09	0.2	<0.001
NC area (mm^2)	1.71±1.03	1.36±0.91	0.02	1.84±1.14	1.91±0.93	0.1	0.5	0.001
NC (%)	11.35±4.78	9.44±4.84	0.001	15.3±6.81	16.04±6.69	0.2	0.01	<0.001
NC+DC area (mm^2)	2.78±1.42	2.21±1.29	0.02	2.91±1.76	3.08±1.47	0.2	0.7	0.003
NC+DC (%)	19.08±6.89	15.65±7.34	0.03	23.90±10.71	26.43±11.28	0.2	0.05	<0.001
EEM area (mm^2)	14.13±3.53	13.96±3.38	0.4	14.1±3.7	14.25±3.72	0.1	0.5	0.3
Absolute DC change (mm^2)		−0.22±0.62			0.10±0.46		0.06	
Absolute NC change (mm^2)		−0.35±0.79			0.07±0.79		0.007	
Absolute DC+NC change (mm^2)		−0.57±1.3			0.16±1.16		0.013	

Data are expressed as mean±SD; DC: dense calcium; NC: necrotic core; BVS: bioresorbable vascular scaffold

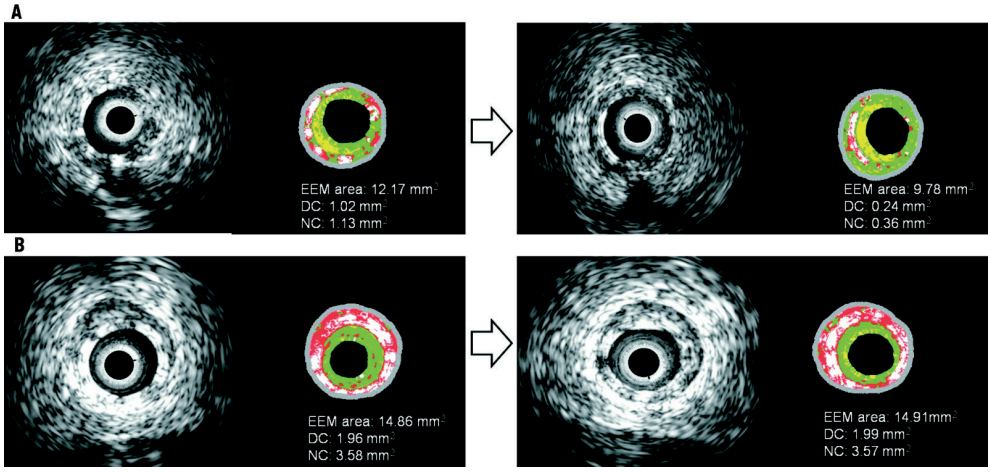

Figure 5. In the A panels, an extreme example of bioresorption at 6-months correlated with EEM area reduction. In the B panels, the persistence of the stent at six months is not associated with EEM area reduction. With the Shin method, blood surrounding ultrasound catheter is detected as fibrous and fibrous-fatty tissues. The boundaries of the lumen area are not depicted or superimposed on the figures. EEM: external elastic membrane; DC: dense calcium; NC: necrotic core

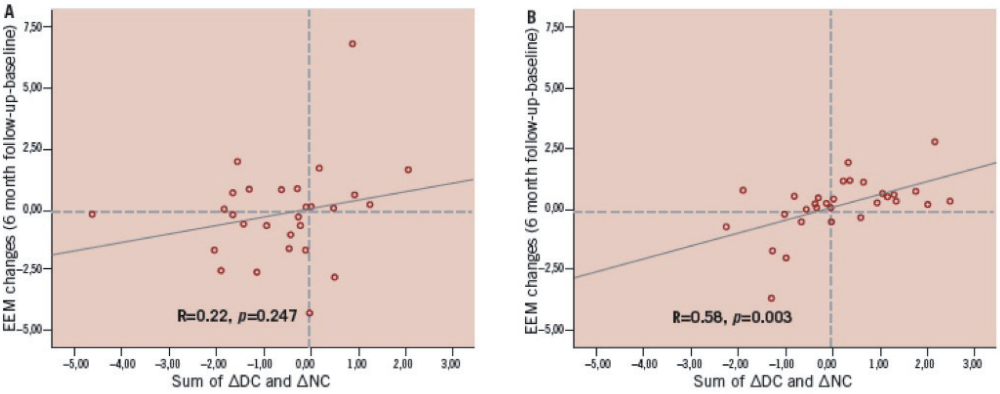

Figure 6. Bioresorption of the scaffold, measured by sum of absolute change in dense calcium and necrotic core area is significantly correlated with change of EEM area in cohort B (Panel B), but not in cohort A (Panel A). In the lower left quadrant of both panels, patients with bioresorption of BVS and reduction of EEM area are shown. EEM: external elastic membrane; DC: dense calcium, NC: necrotic core; BVS: bioresorbable vascular scaffold

core in both cohorts. In patients from cohort A, those with reduction of the EEM area at 6-month (n=15) showed a significantly lower absolute area change of NC compared to other patients (n=13) (-0.69±0.73 mm^2 vs. 0.05±0.68 mm^2, p=0.017) (Figure 5). Reduction of DC was no different (-0.40±0.63 mm^2 vs. –0.02±0.56 mm^2, p=0.1). Overall no correlation

was found between changes in EEM area and the sum of absolute change in DC+NC area (Figure 6A).On the other hand, in patients from cohort B with a reduction in the EEM area (n=16), there was a significantly lower change in absolute area of DC and NC at follow-up compared to other patients (n=16) (respectively for DC –0.12±0.41 mm^2 vs. 0.30±0.42 mm^2, p=0.007; for NC –0.38±0.84 mm^2 vs. 0.50±0.45 mm^2, p<0.001). In the overall population, the change in DC+NC area correlated significantly with the change in EEM area. (R=0.58, p=0.003). (Figure 6B).

DISCUSSION

The major findings of our study are: 1) the changes in design, degradation rate and mechanical durability of the BVS 1.1 compared to BVS 1.0 significantly influenced its IVUS-VH changes over a period of six months (i.e., less reduction in DC and NC at six months); 2) a relationship exists between change overtime in EEM area and in DC+NC area. Kim et al. have previously shown that metallic stents eluting sirolimus and paclitaxel introduce artifacts in IVUS-VH images, that interfere with the classification of plaque behind the struts.[6] Normally struts of drugeluting stents appear as DC, surrounded by a red halo. Although the BVS is made of non-metallic materials, it was also recognised by IVUS-VH software as DC and NC. For this scaffold, the presence of "pseudo"DC and NC could be used as surrogate marker of alteration of the polymeric struts.[1,7,8,12-14] Garcia-Garcia et al have already shown in a sub-study of ABSORB cohort A trial that polymeric struts are identified with radiofrequency backscattering as calcific structures. Using IVUS-VH, it has been shown that there was an important increase in DC and NC immediately after BVS implantation.[7] This sudden change in DC and NC has been attributed to the introduction of polymeric struts and might represent their VH fingerprint. Our data confirm that polymeric struts appear as DC and NC and that IVUS-VH is a potential approach to semi-quantify or state the presence of the polymer. The ability of IVUS-VH to recognise polymeric struts is important also to potentially follow the mechanical support or bioresorption process. Our study demonstrated that while for the BVS Revision 1.0 there is a reduction in DC and NC after six months,[7] for the BVS Revision 1.1 the IVUS-VH signature appears to be unchanged over the same period. This stable backscattering signal with the BVS 1.1 suggests unchanging polymeric structure and/or stable mechanical properties due to slower degradation *in vivo*, as intended. The first revision of the BVS showed slightly higher acute recoil than conventional metallic platform stents[2] and at six months an 11.7% reduction in scaffold area of the BVS 1.0 area was documented.[3] Of note, the longer-lasting mechanical integrity of the BVS Revision 1.1, – as suggested by unaltered IVUS-VH signature over a period of

six months, may prevent this loss in structural integrity and reduction in scaffold area.1,15 This observation of constancy in radiofrequency backscattering of BVS 1.1 is largely confirmed by the absence of qualitative alterations of the appearance of the polymeric struts of BVS 1.1 with optical coherence tomography (OCT).4 They uniformly keep their "preserved box" appearance, whereas with the BVS 1.0 only 3% of preserved box were present at six months follow-up.[12] Our data also showed that the change in DC+NC area detected by IVUS-VH may be associated with shrinkage of the EEM area. For Revision 1.1, we found a significant correlation between the reduction of the EEM area at follow-up and changes in the sum of DC and NC. In particular, it seems to be a trend between the EEM shrinkage and the positive/negative value of sum of changes in DC and NC. In the case of Revision 1.0, the absence of any relationship between the change in IVUS-VH and the change in EEM area may be the result of a different phenomenon, or it may relate to a broader biological and/or sample variability; in particular looking at Figure 6, the two lines for both the cohorts seem similar and one is significant but not the other probably because of less variability. It is interesting to note that for both scaffolds the IVUS-VH changes (and potentially the bioresorption process) are not uniform in all patients. It depends not only on the hydrolysis of the scaffold, but probably also on the nature of the underlying plaque (composition and inflammatory state), and the further recruitment of macrophages to the site of the scaffold implantation. OCT of the presence of macrophages surrounding the scaffold, and the analysis of plaque composition behind the scaffold will enhance the understanding of the bioresorption process of the BVS. In conclusion, IVUS-VH is a clinical method that can detect differences in behaviour between BVS Revision 1.0 and 1.1. Their IVUS-VH fingerprints may be influenced by changes in mechanical design or in product processing. Stability in the IVUS-VH signal of the BVS 1.1 through to 6-months follow-up might suggest a more durable mechanical integrity than the BVS 1.0.

Limitations

We acknowledge that the classification tree of IVUS radiofrequency analysis has not been validated for polymeric struts. We did not collect data about change in fibrous tissue, because it is known that polymeric struts only appear as dense calcium and necrotic core on IVUS-VH. At the same time, using Shin's method, we did not collect data on changes to the lumen area and plaque burden. Changes in DC and NC at follow-up are probably not only related to the BVS, but also to the natural history of the atherosclerotic disease.

REFERENCES

1. Serruys PW, Ormiston JA, Onuma Y, Regar E, Gonzalo N, Garcia-Garcia HM, Nieman K, Bruining N, Dorange C, Miquel-Hebert K, Veldhof S, Webster M, Thuesen L, Dudek D. A bioabsorbable everolimus-eluting coronary stent system (ABSORB): 2-year outcomes and results from multipleimaging methods. Lancet 2009; 373:897-910.
2. Tanimoto S, Serruys PW, Thuesen L, Dudek D, de Bruyne B, Chevalier B, Ormiston JA. Comparison of in vivo acute stent recoil between the bioabsorbable everolimus-eluting coronary stent and the everolimus eluting cobalt chromium coronary stent: insights from the ABSORB and SPIRIT trials. Catheter Cardiovasc Interv 2007;70:515-523.
3. Tanimoto S, Bruining N, van Domburg RT, Rotger D, Radeva P,Ligthart JM, Serruys PW. Late stent recoil of the bioabsorbable everolimuseluting coronary stent and its relationship with plaque morphology. J Am Coll Cardiol 2008; 52:1616-1620.
4. Serruys PW, Onuma Y, Ormiston JA, De Bruyne B, Regar E, Dudek D, Thuesen L, Smith P, Chevalier B, McClean D, Koolen J, Windecker S, Whitbourn R, Meredith I, Dorange C, Veldhof S, Miquel-Hebert K, Rapoza R, Garcia Garcia HM. Evaluation of the second generation of a bioresorbable everolimus drug-eluting vascular scaffold for treatment of de novo coronary artery stenosis:6-month clinical and imaging outcomes. Circulation, 2010;122:2301-12.
5. Okamura T, Garg S, Gutierrez-Chico JL, Shin ES, Onuma Y, Garcia HM, Rapoza R, Sudhir K, Regar E, Serruys PW. In-vivo evaluation of stent strut distribution patterns in the bioabsorbable everolimus-eluting device: An OCT ad hoc analysis of the Revision 1.0 and Revision 1.1 stent design in the ABSORB clinical trial. EuroIntervention 2010;:932-938.
6. Kim SW, Mintz GS, Hong YJ, Pakala R, Park KS, Pichard AD, Satler LF, Kent KM, Suddath WO, Waksman R, Weissman NJ. The virtual histology intravascular ultrasound appearance of newly placed drug-eluting stents. Am J Cardiol 2008; 102:1182-1186.
7. Garcia-Garcia HM, Gonzalo N, Pawar R, Kukreja N, Dudek D, Thuesen L, Ormiston JA, Regar E, Serruys PW. Assessment of the absorption process following bioabsorbable everolimus-eluting stent implantation: temporal changes in strain values and tissue composition using intravascular ultrasound radiofrequency data analysis. A substudy of the ABSORB clinical trial. EuroIntervention 2009;4:443-448.
8. Sarno G, Onuma Y, Garcia Garcia HM, Garg S, Regar E, Thuesen L, Dudek D, Veldhof S, Dorange C, Ormiston JA, Serruys PW. IVUS radiofrequency analysis in the evaluation of the polymeric struts of the bioabsorbable everolimus-eluting device during the bioabsorption process. Catheter Cardiovasc Interv. 2010;75:914-918.
9. Shin ES, Garcia-Garcia HM, Serruys PW. A new method to measure necrotic core and calcium content in coronary plaques using intravascular ultrasound radiofrequency-based analysis. Int J Cardiovasc Imaging 2010;26:387-396.
10. Nair A, Kuban BD, Tuzcu EM, Schoenhagen P, Nissen SE, Vince DG. Coronary plaque classification with intravascular ultrasound radiofrequency data analysis. Circulation 2002;106:2200-2206.
11. Nasu K, Tsuchikane E, Katoh O, Vince DG, Virmani R, Surmely JF, Murata A, Takeda Y, Ito T, Ehara M, Matsubara T, Terashima M, Suzuki T. Accuracy of in vivo coronary plaque morphology assessment: a validation study of in vivo virtual histology compared with in vitro histopathology. J Am Coll Cardiol 2006;47:2405-2412.
12. Ormiston JA, Serruys PW, Regar E, Dudek D, Thuesen L, Webster MW,Onuma Y, Garcia-Garcia HM, McGreevy R, Veldhof S. A bioabsorbable everolimus-eluting coronary stent system for patients with single de-novo coronary artery lesions (ABSORB): a prospective open-label trial. Lancet 2008; 371:899-907.

13. Ormiston JA, Webster MW, Armstrong G. First-in-human implantation of a fully bioabsorbable drug-eluting stent: the BVS poly-L-lactic acid everolimus-eluting coronary stent. Catheter Cardiovasc Interv 2007;69:128-131.
14. Bruining N, de Winter S, Roelandt JR, Regar E, Heller I, van Domburg RT, Hamers R, Onuma Y, Dudek D, Webster MW, Thuesen L, Ormiston JA, Cheong WF, Miquel-Hebert K, Veldhof S, Serruys PW. Monitoring in vivo absorption of a drug-eluting bioabsorbable stent with intravascular ultrasound-derived parameters a feasibility study. JACC Cardiovasc Interv. 2010;3:449-456.
15. Mintz GS, Popma JJ, Pichard AD, Kent KM, Satler LF, Wong C, Hong MK, Kovach JA, Leon MB. Arterial remodeling after coronary angioplasty: a serial intravascular ultrasound study. Circulation 1996;94:35-43.

PART
II

Chapter 7

Angiographic maximal luminal diameter and appropriate deployment of the everolimus-eluting bioresorbable vascular scaffold as assessed by optical coherence tomography: an ABSORB cohort B trial sub-study

Josep Gomez-Lara, MD; Roberto Diletti, MD; Salvatore Brugaletta, MD; Yoshinobu Onuma, MD; Vasim Farooq, MB, ChB, MRCP; Leif Thuesen, MD; Dougal McClean, MD; Jacques Koolen, MD, PhD; John A Ormiston, MB,ChB, PhD; Stefan Windecker, MD; Robert Whitbourn, MD; Dariusz Dudek, MD; Cécile Dorange, MSc; Susan Veldhof, RN; Richard Rapoza, PhD; Evelyn Regar, MD, PhD; Hector M. Garcia-Garcia, MD, PhD; Patrick W. Serruys, MD, PhD

EuroIntervention. 2012 Jun 20;8(2):214-24

ABSTRACT

Aims Bioresorbable vascular scaffolds (BVS) present different mechanical properties as compared to metallic platform stents. Therefore, the standard procedural technique to achieve appropriate deployment may differ.

Methods and results Fifty-two lesions treated with a 3x18 mm BVS were imaged with optical coherence tomography (OCT) post-implantation and screened for parameters suggesting non-optimal deployment. These included minimal scaffold area (minSA)<5 mm2, residual area stenosis (RAS)>20%, edge dissections, incomplete scaffold/strut apposition (ISA)>5% and scaffold pattern irregularities. The angiographic proximal and distal maximal lumen diameters (DMAX) were measured by quantitative coronary angiography. Based on the DMAX values, the population was divided into three groups: DMAX <2.5 mm (n=13), DMAX between 2.5-3.3 mm (n=30) and DMAX >3.3 mm (n=9). All three groups presented with similar pre-implantation angiographic characteristics except for the vessel size and were treated with similar balloon/artery ratios. The group with a DMAX <2.5 mm presented with a higher percentage of lesions with minSA <5 mm2 (30.8% vs. 10.0% vs. 0%; p=0.08) and edge dissections (61.5% vs. 33.3% vs. 11.1%; p=0.05). Lesions with >5% of ISA were significantly higher in the group with DMAX >3.3 mm (7.7% vs. 36.7% vs. 66.7%; p=0.02). RAS >20% was similar between all groups (46.2 vs. 53.3 vs. 77.8%; p=0.47) and scaffold pattern irregularities were only documented in three cases.

Conclusions BVS implantation guided with quantitative angiography may improve the OCT findings of optimal deployment. The clinical significance of these angiographic and OCT findings warranted long term follow-up of larger cohort of patients.

INTRODUCTION

Everolimus-eluting bioresorbable vascular scaffolds (BVS) are a promising new generation of intravascular devices that may potentially circumvent many of the drawbacks of permanently implanted metallic coronary stents[1,2]. The mechanical properties of the polymeric platforms undoubtedly differ from the features of metallic platform stents and should be taken into account during the procedure for appropriate deployment of the BVS.

Previous studies using intravascular ultrasound (IVUS)-guided percutaneous coronary intervention (PCI) reported that the presence of minimal scaffold area (minSA) <5 mm^2, residual area stenosis >20%, edge dissections, incomplete scaffold/strut apposition (ISA) and scaffold pattern disruptions have an impact on the short and long-term outcomes[3-8]. Optical coherence tomography (OCT) is a high resolution imaging technique that allows more accurate assessment of these parameters as compared to IVUS[9], although the prognostic value of these refined observations measured or documented by OCT are so far unknown.

The ABSORB cohort B study used a single size BVS (3x18 mm). The study protocol did not allow the inclusion of patients with an interpolated reference diameter (RVD) <2.5 mm or >3.3 mm, although it was not mandatory to perform quantitative coronary angiography (QCA) prior to the implantation.

The interpolated-RVD, as indicated by its name, is the virtual reference diameter measured at the site of the minimal lumen diameter (MLD) prior to the implantation. The interpolated-RVD can differ from any reference diameter arbitrary selected and measured in the segment located either proximal or distal to the MLD[10]. Amongst the multiple values of reference diameters measured in the proximal or distal segments to the MLD, the DMAX values (proximal or distal) represented the two single largest values of reference diameters observed in the segments proximal or distal to the lesions (Figure 1).

The aim of this study is to describe the angiographic DMAX prior to BVS implantation and to relate these angiographic measurements to the OCT criteria of appropriate BVS deployment. In addition, we report the inappropriate adverse events at medium term follow-up of 180 days potentially associated with the non-respect of the angiographic exclusion criteria and the consequent impact on scaffold deployment as documented by OCT.

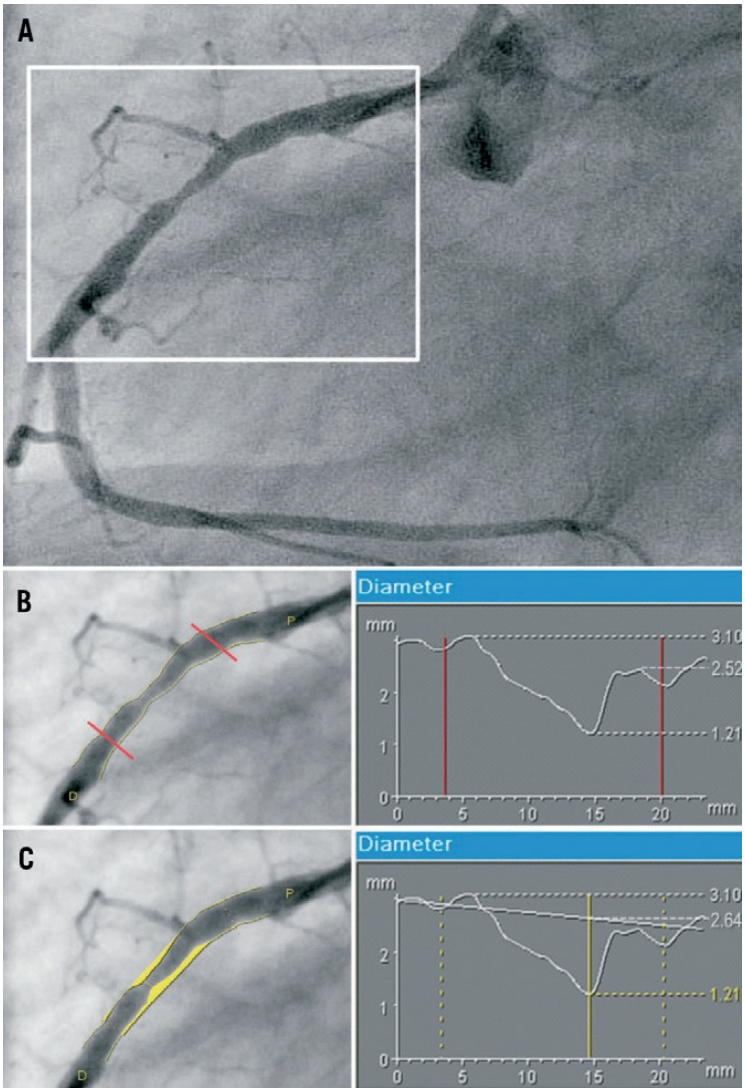

Figure 1. Assessment of the DMAX and interpolated-RVD values. Panel A shows a lesion in the mid right coronary artery at pre- treatment. The length of the region "to be scaffolded" is super- imposed on the pre-treatment angiogram (Panels B and C) with the corresponding diameter function obtained with quantitative coronary angiography. Image B shows the DMAX assessment. The three non-ambiguous points of the diameter function are: the proximal DMAX (3.10 mm), the MLD (1.21 mm) and the distal DMAX (2.52 mm). Panel C shows the interpolated-RVD assessment. According to the diameter function of the proximal and distal segments to the BVS edges an interpolated diameter line is generated. The "predicted" diameter at the site of the MLD (2.64 mm) defines the interpolated-RVD. DMAX: maximal lumen diameter; MLD: minimal lumen diameter; RVD: reference vessel diameter..

MATERIAL AND METHODS

Study design and population

The ABSORB Cohort B trial was a non-randomised, multicentre, single arm, efficacy-safety study that included 101 patients with 102 lesions treated with BVS. All the implanted devices were 3.0 mm in diameter and 18 mm in length. OCT imaging was an optional investigation performed in selected participating centers. The study design of the ABSORB Cohort B is available at clinicaltrials.gov (NCT00856856).

In brief, the common inclusion criteria were patients aged 18 years or older, with a diagnosis of stable, unstable or silent ischaemia, which presented with a *de novo* stenosis in a native coronary artery.

Exclusion criteria included patients with stenosis of an unprotected left main or ostial right coronary artery (RCA), presence of intracoronary thrombus or heavy calcification.

The present study is a *post hoc* analysis of the subset of patients included in the ABSORB Cohort B trial who had optical coherence tomography (OCT) imaging performed post-BVS implantation.

The population included in the present study was divided in three groups based on the proximal and distal DMAX prior to the BVS implantation: group 1 included those patients with proximal or distal DMAX <2.5 mm; group 2 included those patients with proximal and distal DMAX between 2.5-3.3 mm; group 3 included those patients with proximal or distal DMAX >3.3 mm.

Bioresorbable Vascular Scaffold

The BVS 1.1 revision (Abbott Vascular, Santa Clara, CA, USA) is a balloon expandable device, consisting of a polymer backbone of Poly-L lactide (PLLA) coated with a thin layer of a 1:1 mixture of an amorphous matrix of Poly-D, L lactide (PDLLA) polymer containing 100 micrograms/cm^2 of the antiproliferative drug everolimus. The implant is radiolucent, but has two platinum markers at each edge, that allow visualization on angiography and other imaging modalities. Physically, the scaffold has struts with an approximate thickness of 150 μm arranged in-phase zigzag hoops linked together by three longitudinal bridges.

Treatment Procedure

Lesions were treated with routine interventional techniques that included mandatory pre-dilation. The operator was requested to select an angiographic view with minimal foreshortening of the lesion and limited overlap with other vessels. This view was used for all phases of the treatment, including the inflation of the delivery system balloon or the post-dilation balloons at the highest pressures. The study protocol forbade the use

of pre-dilation balloons longer than the pre-specified length of the device. According to the protocol, the BVS had to be implanted at a pressure not exceeding the rated burst pressure (16 atmospheres) corresponding to a predicted diameter of 3.3 mm as per the manufacturer's chart. Post-dilatation with a balloon shorter than the implanted device and a maximum diameter of 3.25 mm was allowed at the operator's discretion, as was post-dilatation balloon size, use of non-compliant balloons or bailout treatment. During the BVS implantation or the post-dilatation with other balloons, the highest inflated pressure of the largest balloon was used to calculate the "predicted device diameter" according to the manufacturer's BVS or post-dilatation balloon charts, which describes the theoretical diameter of the BVS achieved at the end of the procedure.

Quantitative coronary angiography analysis

The 2D angiograms were stored in DICOM format and analysed by the core lab (Cardialysis, Rotterdam, The Netherlands) using the CASS II analysis system (Pie Medical BV, Maastricht, The Netherlands). In each patient, the treated region and the peri-treated regions (defined by a length of 5 mm proximal and distal to the device edge) were analyzed. The following QCA analysis parameters were computed: MLD, interpolated-RVD and percentage of diameter stenosis (DS). The DMAX was measured as previously described (Figure 1).
During the BVS implantation or post-dilation with other balloons, the highest inflated pressure of the largest balloon was quantitatively measured as the 'mean inflated-balloon diameter'. Balloon / artery ratio (B:A ratio) was estimated as: (mean inflated-balloon diameter/interpolated-RVD).

Optical coherence tomography acquisition

OCT imaging was performed using two different OCT systems (M3 Time-Domain System and C7XR Fourier-Domain System; LightLab Imaging, Westford, MA, USA) with the non-occlusive technique. The imaging was performed after the last dilatation and after a nitroglycerine infusion. The acquisition method of both systems has been previously described[11].

Optical coherence tomography analysis

Offline quantitative and qualitative OCT data analysis was carried out by the core laboratory (Cardialysis BV, Rotterdam, The Netherlands) with proprietary software for offline analysis (LightLab Imaging, Westford, MA, USA).
Adjusting for the pullback speed, the analysis of contiguous cross-sections was performed at each 1 mm longitudinal intervals within the treated segment. The BVS demonstrated important differences as compared to metallic stents when imaged by OCT[1]. The optically

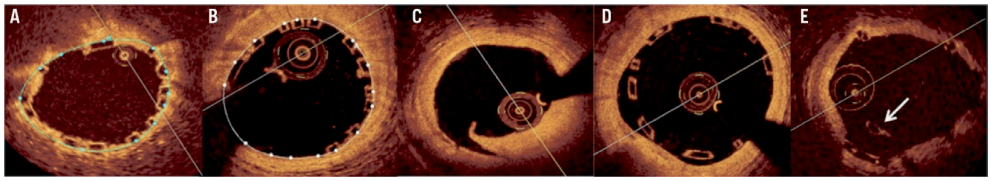

Figure 2. Optical coherence tomography optimal deployment criteria. A) Minimal scaffold area <5 mm2. This picture shows a scaffold area (blue line) of 4.2 mm2 in (minimum scaffold area of the BVS); B) Residual area stenosis >20%. This patient presents a minimal scaffold area of 5.7 mm2 (white line) and a reference vessel area of 7.9 mm2. The estimated residual area stenosis is 27.8%; C) Edge dissection distally to the BVS; D) Incomplete scaffold/strut apposition; E) Scaffold pattern irregularity with an overhanging strut (arrow) at the centre of the vessel without obvious connection to the expected/adjacent strut pattern.

translucent polymeric struts did not shadow the vessel wall thereby allowing complete imaging of the struts and the lumen vessel wall contours.

Qualitative assessments of strut apposition, scaffold pattern continuity and edge dissections could therefore easily be performed (Figure 2). Incomplete strut apposition (ISA) was diagnosed when the back-side of the polymeric strut was separated from the vessel wall. The scaffold pattern was assessed for irregularities such as two struts overhanging each other in the same angular sector of the lumen perimeter, with or without malapposition, or for isolated struts located more or less at the centre of the vessel without obvious connection to the expected adjacent strut pattern[12]. An endoluminal flap at the BVS edge was reported as an edge dissection.

Quantitative assessment of the scaffold area was measured at the back-side of the apposed struts. In the case of two consecutive frames with ISA, the area between the lumen and the scaffold was measured as the ISA area. Reference vessel area (RVA) was estimated as the mean between the two largest luminal areas in the outer 5 mm proximal and distal segments to the edges of the BVS11. In the cases of absence of any of the proximal or distal segments due to ostial lesions or the presence of near side branches the opposite segment was instead used as the RVA. Residual area stenosis (RAS) was calculated as: (1-[minSA / RVA])×100.

The corelab reproducibility for ISA, scaffold area and edge dissection assessment has been previously reported and showed an excellent inter and intra-observer agreement using OCT[13].

The detection of scaffold pattern irregularities was performed by two experienced analysts who analyzed qualitatively the full length of the device in all the frames.

Non-optimal deployment endpoints

Non-optimal deployment endpoints were: presence of minSA <5 mm^2, presence of RAS >20%, presence of edge dissections as assessed by OCT, presence of ISA per scaffold >5% and presence of any scaffold pattern irregularities[3-8].

Statistical analysis

The Kolmogorov-Smirnov test was used to evaluate the normality assumptions of all continuous variables. Continuous variables were expressed as a mean ± standard deviation and categorical variables were presented as counts (%). Comparisons of continuous variables at lesion level and frame level analysis were estimated with the non-parametric Mann-Whitney test when comparing two groups or Kruskall-Wallis test when comparing three groups. Categorical variables were compared with the chi-square test. All measurements were obtained by SPSS 15 software version (SPSS Inc, Chicago IL, USA).

RESULTS

Population

A total of 54 out of the 101 lesions included in the ABSORB cohort B trial were imaged by OCT after BVS deployment in 53 patients. Two of the pullbacks were not included because lack of visualization of the full length and size of the device. Finally, 52 lesions in 51 patients are therefore reported in this study. A C7 OCT system was used in 36 lesions (69.2%) and a M3 system in 16 (30.8%). According to the baseline DMAX, either proximal or distal, 13 lesions were included in group 1 (DMAX <2.5 mm), 30 in group 2 (DMAX between 2.5 and 3.3 mm) and nine lesions in group 3 (DMAX >3.3 mm). The interpolated-RVD, the proximal and distal DMAX distribution values are shown in Figure 3.

Baseline clinical, angiographic and procedural characteristics

Baseline clinical characteristics are shown in Table 1. Briefly, 37 patients (72.5%) were males, mean age was 62.1±10.0 years, 88.2% of patients presented with stable angina as an indication for the procedure and only seven patients (13.8%) had more than single vessel disease.

Angiographic and procedural characteristics are summarised in Table 2. The treated vessel was similar between all groups. Prior to BVS implantation, the interpolated-RVD value rose incrementally according to the DMAX subgroups (2.44 mm vs. 2.61 mm vs. 2.87 mm; p=0.02). The use of post-dilatation with other balloons was similar in all groups (53.8% vs. 56.7% vs. 66.7%; p=0.82) with no differences in balloon length or nominal sizes.

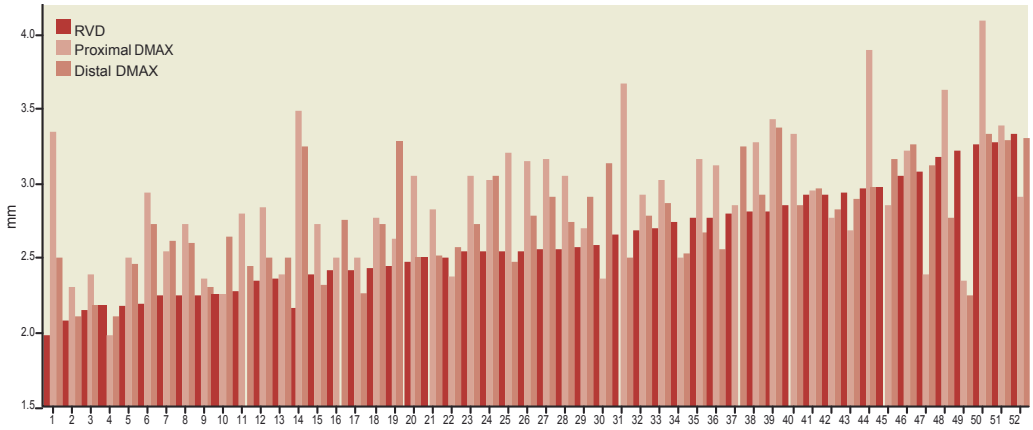

Figure 3. Distribution of the interpolated-reference vessel diameter and the proximal and distal DMAX in the global population.

Table 1. Baseline clinical characteristics (n=51).

Age*	**62.1±10.0**
Males	37 (72.5)
Hypertension	31 (60.8)
Hypercholesterolaemia	44 (86.3)
Diabetes mellitus	4 (7.8)
Smoking status	12 (23.5)
Previous MI	16 (31.4)
Previous PCI	12 (23.5)
Unstable angina	6 (11.8)
Number vessel disease:	
One	44 (86.2)
Two	6 (11.8)
Three	1 (2.0)

Values are expressed as n (%). *Age is reported as mean±SD

However, the mean balloon-inflated diameter of the largest balloon inflated at highest pressure tend to be larger in group 3 (2.66 mm vs. 2.76 mm vs. 2.88 mm; p=0.22). The balloon/artery ratios were similar in all groups (1.07 vs. 1.07 vs. 1.02; p=0.53). Quantitative analysis of the final result showed larger MLD, interpolated-RVD and DMAX in group 3.

Table 2. Angiographical and procedural characteristics.

n=52	DMAX <2.5 mm (n=13)	DMAX 2.5 to 3.3 mm (n=30)	DMAX >3.3 mm (n=9)	All p
Target vessel, n (%)				0.99
LAD	7 (53.8)	15 (50.0)	5 (55.6)	
LCX	3 (23.1)	6 (20.0)	2 (22.2)	
RCA	3 (23.1)	9 (30.0)	2 (22.2)	
QCA Pre-treatment				
D max proximal	2.40±0.20	2.91±0.24	3.54±0.34	<0.01
Interpolate RVD (mm)	2.44±0.35	2.61±0.24	2.87±0.47	0.02
Dmax distal	2.46±0.34	2.79±0.24	3.03±0.36	<0.01
MLD (mm)	1.07±0.32	1.19±0.39	1.17±0.40	0.66
DS (%)	54.4±9.9	57.4±10.4	63.8±10.7	0.16
Post-dilatation with other balloon, n (%):	7 (53.8)	17 (56.7)	6 (66.7)	0.82
Length of the largest post-dilatation balloon (mm)	14.3±4.2	14.8±3.7	13.4±4.2	0.63
Nominal diameter (mm)	3.1±0.2	3.1±0.1	3.2±0.2	0.20
Predicted device diameter (mm)	3.32±0.10	3.30±0.15	3.50±0.21	0.01
QCA mean - inflated balloon diameter (mm)	2.66±0.20	2.76±0.21	2.88±0.36	0.22
Balloon / artery ratio	1.07±0.14	1.07±0.12	1.02±0.14	0.53
Bail-out stenting for edge dissection, n (%)	1 (7.7)	2 (6.7)	0	0.71
QCA Post-treatment				
RVD (mm)	2.44±0.33	2.55±0.30	2.81±0.42	0.13
MLD (mm)	2.01±0.28	2.23±0.30	2.48±0.32	0.01
DS (%)	13.1±4.7	14.4±4.6	16.2±6.7	0.62
Dmax post (mm)	2.90±0.24	3.07±0.27	3.31±0.46	<0.01

All values are expressed as mean±SD; LAD: left anterior descending; LCX: left circumflex; RCA: right coronary artery; QCA: quantitative coronary angiography; DMAX: maximal lumen diameter; RVD: reference vessel diameter; MLD: minimal lumen diameter; DS: diameter stenosis.

Optical coherence tomography findings

OCT findings are summarised in Table 3. A total of 1,001 frames and 8,634 struts were analyzed. The lumen area, scaffold area, RVA, minSA and RAS were increasingly larger amongst the three subgroups.

ISA analysis at lesion level showed a slight trend towards higher percentages of ISA struts in groups 2 and 3 (2.2% vs. 5.5% vs. 14.4%; p=0.16). At frame level analysis, the percentage of frames with malapposed struts was significantly higher in group 3 (15.4% vs. 21.5% vs. 26.9%; p=0.02) and the percentage of ISA struts per frame was significantly higher in group 3 (2.4% vs. 5.4% vs. 10.9%; p<0.01).

Table 3. Optical coherence tomography findings.

n=52	DMAX <2.5 m (n=13)	DMAX 2.5 to 3.3 mm (n=30)	DMAX >3.3 mm (n=9)	All *p*	1 vs. 2 *p*	2 vs. 3 *p*
Lesion level						
Average lumen area (mm^2)	6.9±1.2	7.5±0.9	8.9±1.6	0.01	0.12	0.01
minLA (mm^2)	5.6±1.3	6.2±1.0	6.7±1.0	0.07	0.12	0.18
Scaffold area (mm^2)	7.1±1.3	7.6±0.8	8.6±1.0	0.01	0.18	0.01
minSA (mm^2)	5.8±1.4	6.3±0.9	6.8±1.3	0.18	0.20	0.22
ISA area (mm^2)*	0.2±0.5	0.2±0.4	0.5±0.8	0.69	0.56	0.76
RVA (mm^2)	7.0±1.2	8.2±1.6	10.3±3.1	0.01	0.02	0.05
RAS (%)	16.1±12.1	20.9±12.8	27.9±22.8	0.34	0.38	0.42
Lesion level (ISA analysis)						
Lesions with at least 1 ISA, n (%)	10 (76.9)	23 (76.7)	7 (77.8)	0.82	0.99	0.55
Percentage of ISA per lesion, mean	2.2±2.5	5.5±6.5	14.4±15.0	0.16	0.14	0.27
ISA frames per lesion,%	15.0±15.4	21.9±20.2	29.4±27.3	0.44	0.33	0.52
Frame level (ISA analysis)						
Frames with ISA,%	15.4	21.5	26.9	0.02	0.05	0.15
ISA struts per frame,%	2.4±7.1	5.4±13.0	10.9±22.5	<0.01	0.02	0.05

Values are expressed as mean ± SD; DMAX: maximal lumen diameter; minLA: minimal lumen area; BVS: bioresorbable vascular scaffold; minSA: minimal scaffold area; RVA: reference vessel area; ISA: incomplete scaffold/strut apposition; Percentage of ISA per lesion: number of ISA/total number of struts per lesion *ISA area has been estimated only in patients with ISA.

Table 4. Non-optimal deployment endpoints (lesion level analysis).

n=52	DMAX <2.5 mm (n=13)	DMAX 2.5 to 3.3 mm (n=30)	DMAX >3.3 mm (n=9)	All p	1 vs. 2 p	2 vs. 3 p
minSA <5 mm^2	4 (30.8)	3 (10.0)	0	0.08	0.09	0.32
RAS >20%	6 (46.2)	16 (53.3)	7 (77.8)	0.31	0.67	0.19
Edge dissections¶	8 (61.5)	10 (33.3)	1 (11.1)	0.05	0.08	0.19
ISA struts >5%	1 (7.7)	11 (36.7)	6 (66.7)	0.02	0.05	0.11
Structural discontinuities	0	2 (6.7)	1 (11.1)	0.52	–	–

Values are expressed as count (%). minSA: minimal scaffold area; RAS: residual area stenosis; ISA: incomplete scaffold/strut apposition. ¶ Edge dissections detected by OCT including the three cases of dissection, detected by angiography and treated with bail-out stent.

Non-optimal deployment endpoints

Non-optimal deployment endpoints are showed in Table 4. Lesions with minSA<5 mm^2 were more frequent in group 1 (30.8% vs. 10.0% vs. 0%; p=0.08). Edge dissections as assessed by OCT were more frequently observed in group 1 (61.5% vs. 33.3% vs. 11.1%; p=0.05). Lesions with >5% of ISA struts were found in greater percentage in group 3 (7.7% vs. 36.7% vs. 66.7%; p=0.02). Lesions with RAS >20% were not related with DMAX and scaffold pattern irregularities were only documented in three cases at baseline.

DISCUSSION

The main findings of our study are: 1) DMAX measured prior to the implantation has some bearing on the appropriate deployment of the BVS as assessed by OCT criteria; 2) Lesions with DMAX <2.5 mm showed a trend toward higher incidence of minSA <5 mm^2 and presented with higher rates of edge dissections; 3) Lesions with DMAX >3.3 mm presented with a higher incidence of malapposed struts.

The assessment of the lumen size using QCA has been extensively used since the beginning of the interventional cardiology field. There are different methods to assess the lumen size taking into account different regions of the vessel10. The interpolated-RVD predicts the "expected lumen diameter" at the site of the MLD taking as a reference the proximal and distal segments to the stenotic region. However, the interpolated-RVD does not assume the actual lumen dimensions of the predicted "landing zone" and is highly influenced by proximal or distal side branches not included in the scaffolded segment. The Dmax estimation is an interactive measurement that helps the investigator to select the appropriate "landing zone", especially in the setting of a single size device study (Figure 1). Figure 3 shows that in the majority of occasions the interpolated-RVD underestimated the maximal lumen diameter within the scaffolded region.

Since there are no widely accepted OCT criteria for optimal stent deployment, our OCT endpoints have been directly inferred from the IVUS criteria previously used for the evaluation of metallic platform stents. IVUS criteria of non-optimal deployment have been validated with 1-year clinical outcomes as previously described in the literature[5-9].

Minimal scaffold area: Baseline minSA<5 mm^2 imaged after the implantation of sirolimus-eluting stents resulted on average in a minSA <4 mm^2 at eight months follow-up as assessed by IVUS[6]; this threshold has been associated with adverse events, especially with restenosis[14,15]. In our study, seven lesions (13.5%) did not achieve a minSA ≥5 mm^2 at the end of the procedure and one of them (1.9%) presented with a minSA <4 mm^2. These percentages are similar to those reported for metallic platform stents (29% had minimal

stent area <5 mm^2 and 4% had <4 mm^2)[15]. However, in our series, none of those patients presented with clinical events in the first 180 days.

Residual area stenosis: IVUS studies measured the RAS as the expansion index (minimal stent area/reference vessel area)[5,15]. In the setting of metallic platform stents, which do not suffer from acute or late recoil, this index reflects the grade of the device expansion at the site of the minimum area with respect to the normal vessel area. This value is commonly higher than one when the final procedure result shows the typical angiographic image of "step-up / step-down". An expansion index below 0.80 (that corresponds to a RAS >20%) was previously related with acute/subacute stent thrombosis[3,5]. In these studies, the mean expansion index and the rate of patients with a RAS >20% at the end of the procedure in the group of patients without adverse events were 0.85 and 23%, respectively[3,5]. In our study, the mean expansion index was 0.79 (RAS=21%), but 29 patients (56%) presented with a residual area stenosis ≥20%, independently from the DMAX subgroups. We hypothesise that this slightly higher incidence of underexpansion compared to the metallic stents is the result of weaker radial forces of the BVS as compared to metallic stents16. However, this moderate level of under-expansion does not seem to have any acute or subacute thrombosis as well as restenosis implications in these patients.

Edge dissections: Non-treated edge dissections, as assessed by IVUS, is a controvert topic in the current literature. Nishida et al did not find different acute clinical outcomes in 97 patients with edge dissection compared to 100 patients without IVUS-detected edge dissections[17]. On the other hand, Cheneau et al demonstrated that non-obstructive edge dissections were related to subacute stent thromboses5. The incidence of edge dissection reported in these studies was around 9.2%[17,18]. Since the resolution of OCT is 10 times higher than IVUS, OCT has better accuracy in detecting edge dissections9; and indeed, the reported incidence of edge dissections higher (25-40%)[19,20]. Our study found 19 edge dissections (36.5%) with only one patient (5.3%) presenting with an adverse event (periprocedural myocardial infarction). This patient belonged to the group with DMAX <2.5 mm and presented with an angiographically-detected dissection that caused slow-flow and required bail-out treatment with a metallic stent. Apparently, the higher rate of edge dissections in group 1 was not related with the balloon/artery ratio, which was very similar in the three groups. (1.07 vs. 1.07 vs. 1.02; p=0.53). However, the predicted device diameter achieved at the end of the procedure as assessed by the manufacture's chart was similar between groups 1 and 2, showing that the group with DMAX <2.5 mm was treated more aggressively according to the reference vessel size. A correct assessment of the vessel size prior to the BVS implantation can potentially discourage the operator from performing additional aggressive post-dilatation in under-sized vessels, possibly avoiding edge dissection in these undersized vessels. Nevertheless, there is little information

regarding the clinical implications of OCT-detected dissections. Two reports even failed to relate these findings to acute clinical events[19,20]. Incomplete scaffold/strut apposition: Despite angiographic and IVUS-guided PCI procedures, acute ISA as assessed by IVUS is still common following the deployment of metallic platform stents. In elective patients, IVUS-studies have reported rates of stents with at least one ISA ranging between 2.6 to 11.6%8,[21]; and more than 30% in patients with ST-elevation myocardial infarction[22]. OCT imaging has a considerably higher resolution and sensitivity in detecting ISA as compared to IVUS and therefore, detects higher rates of malapposed struts[9]. Translucency of the BVS struts enhances this detection capability. Recent OCT studies have reported a percentage of lesions with at least one ISA of 88% and a percentage of malapposed struts between 4.5 to 9.1%23,[24]. Our study reports 39 lesions (75.0%) with at least one malapposed strut and a mean percentage of ISA of 6.2%.

The clinical impact of acute ISA is not completely understood, considering the small rate of adverse events observed with drug-eluting stents. IVUS studies with baseline and 6 month follow-up imaging showed that the presence of post-procedural and follow-up ISA were not related to death, myocardial infarction, target vessel revascularisation or stent thrombosis[21,25.] Nevertheless, around 40-70% of the acute ISA persisted at follow-up[25]. The presence of late ISA has been clearly related with a delay in or lack of neointimal coverage at follow-up[26]; and patients who had sustained late or very late stent thromboses presented with higher rates of ISA and a lack of neointimal coverage[27,28]. In our study, two out of four patients with adverse events in the firsts 180 days presented with ISA >5% after the deployment. In one patient the ISA was related to significant disruption of the scaffold at deployment. At day 33, the patient presented with chest pain with documented exercise induced ischaemia. Although angiographically patent, the patient underwent target lesion revascularisation. A second patient suffered a periprocedural acute myocardial infarction due to the occlusion of a diagonal branch.

Due to the high rate of lesions with at least one ISA imaged by OCT, the same IVUS criteria to define optimal deployment cannot be applied to OCT. Therefore, we defined a 5% of malapposed struts in each device as one of the criteria of non-optimal BVS deployment. This value is arbitrary but corresponds to the highest tertile of our population with malapposed struts and has been reported in previous studies as a widely accepted cut-off[29].

Scaffold pattern irregularities: Metallic stent fractures have been related to metal fatigue, mostly detected at follow-up. Stent fractures were more frequently found in overlapping stents, hinging points, angulated vessels and with some specific types of drug-eluting stents[30,31]. Moreover, stent fractures were also related with adverse events, especially with target lesion revascularisation[32]. The incidence of stent fracture ranged from 1.3% to 28.8%, and it depended on the used imaging technique[30,33].

In our study, BVS pattern irregularities were observed with OCT at baseline. These irregularities ranged from local overhanging single struts shifted out of their expected pattern position during deployment, to complete pattern disruptions possibly involving structural discontinuities. We report three cases of scaffold pattern irregularities at baseline (5.8%). All of them were associated with the use of post-dilatation balloons that over-stretched the polymeric device beyond 3.3 mm (as assessed by the balloons charts). Post-dilatation with other balloons was needed in two cases due to a sub-optimal residual stenosis after the BVS deployment and in one case because of the presence of severe ISA as assessed by OCT. The last one was observed in a patient with a DMAX >3.3 mm and required target lesion revascularisation after 33 days.

Clinical outcomes: A total of four out of 51 patients (7.8%) included in the present study had an adverse cardiac event at follow-up in the first 180 days after the procedure. Two patients presented with adverse events not related to mismatch of the vessel / device size: one patient suffered a periprocedural myocardial infarction without further complications due to the occlusion of a small side branch and the other patient presented a myocardial infarction during an unscheduled angiogram not related with the device. The adverse event of the first patient with vessel / device mismatch was caused by a periprocedural myocardial infarction during the BVS implantation (the troponin value raised 2.5 times after the procedure without any further complications). The patient presented with a mild lesion (DS 52%) of a small second marginal (proximal and distal DMAX of 2.4 and 2.2 mm, respectively). After the predilation with a 2.75×10.00 mm compliance balloon a flow-limiting dissection was observed. The BVS implantation was not enough to seal the dissection and the patient did not recover the TIMI flow 3. Finally, a bail-out stenting with a metallic stent was implanted successfully and the patient recovered TIMI flow 3. The second patient presented with a moderate lesion in a large obtuse marginal (Figure 4). After the 3×18 mm BVS implantation the OCT imaging showed severe ISA in the proximal part of the device and the patient was treated with a 3.5×9 mm post-dilatation compliance balloon. The predicted device diameter at the end of the procedure was 3.96 mm. After the post-dilatation, a new OCT pullback showed scaffold pattern irregularities that were not treated and the patient was discharged the day after. At day 33, the patient complained of chest pain with documented exercise induced ischaemia. The angiography showed a patent coronary vessel with a diameter stenosis of 23% by QCA. However, OCT confirmed multiple signs of scaffold pattern irregularities. It was decided to treat with a metallic stent. After the procedure, the troponin value raised three times the upper limit of normality.[34]

For all these reasons it seems advisable to perform BVS implantation using precise measurements for accurate vessel sizing. We recommend a mandatory predilatation in

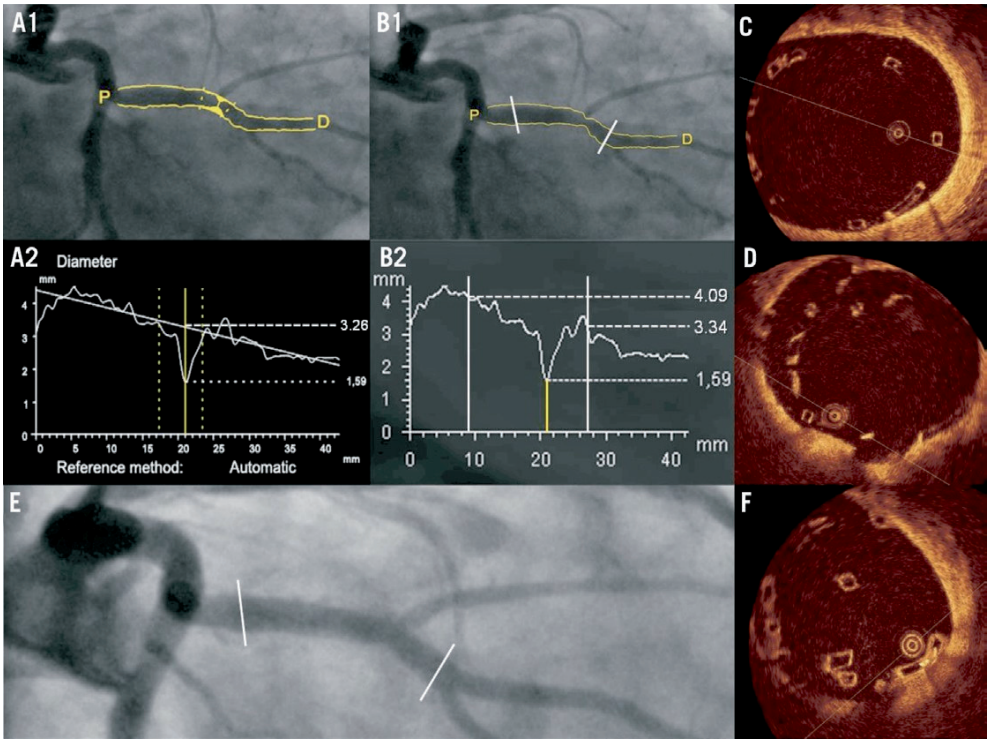

Figure 4. Coronary angiography and OCT of a patient with scaffold pattern irregularity at post-implantation. Patient affected of a moderate lesion in the obtuse marginal. The interpolated-RVD was 3.26 mm (A) and the proximal and distal Dmax of the scaffolded segment (prior to the implantation) were 4.09 and 3.34 mm respectively (B). After the BVS implantation the OCT imaging showed severe malapposition of the scaffold (C); and the operator decided to post-dilate with a compliance balloon up to 3.96 mm of predicted diameter. A second OCT pullback showed scaffold pattern irregularities highly suggestive of fracture (D) that were untreated. At day 33, the patient presented with ischaemia and was re-catheterised (E). A new OCT (F) showed scaffold pattern irregularities with attached thrombi (arrow).

all patients ensuring an optimal expansion of the balloon. The quantification of the maximal lumen diameter (DMAX) in the proximal and distal segments of the MLD is currently viewed as one of the preventative measures used to ensure accurate sizing of the BVS with respect to the target vessel dimensions (Figure 1). According to the DMAX results, an appropriate device size and inflated balloon pressure should be chosen to achieve optimal device apposition and expansion. Post-dilation can be performed but without over-stretching the BVS beyond 3.3 mm. Consequently, in the on-going ABSORB EXTEND single-arm study, currently recruiting more than 1000 patients, the operator is requested to assess the DMAX prior to BVS implantation. In the case of DMAX <2.5 mm or >3.3 mm the patient should not be included in the study. A third generation of the device with a

slightly modified pattern is intended to raise the current upper limit of deployment of the 3.0 mm (nominal diameter) device to 3.8 mm.

Limitations

The first limitation is the few number of patients included in our study, despite the data representing one of the largest studies ever made with baseline optical coherence tomography. The second limitation refers to the OCT endpoints of non-optimal deployment. Due to a lack of expert consensus we decided to infer the IVUS definitions to the OCT technology; these criteria have however not yet been validated with clinical outcomes in formal randomised controlled trials. Third, this study is a description of the OCT findings observed in the ABSORB Cohort B study. The selected DMAX cut-offs of 2.5 and 3.3 mm are arbitrary and not evidence-based. They are however inferred from the knowledge of the mechanical properties of the polymeric BVS device. The BVS chart of the 3.0 mm nominal size diameter sets the burst pressure at 16 atmospheres, which corresponds to a predicted device diameter of 3.35 mm. The expansion of the device exceeding this boundary can potentially fracture the polymeric struts. On the other hand, when the BVS is under-expanded below 2.5 mm, the actual diameter may potentially be even smaller than 2.2 mm since the 150 µm thickness of the apposed struts to each side of the lumen (2×150 µm=0.3 mm) has to be subtracted from the scaffold diameter of 2.5 mm.

CONCLUSIONS

Appropriate deployment of the bioresorbable vascular scaffold as assessed by optical coherence tomography is related to the quantitative angiographic assessment of the maximal lumen diameter prior to the implantation. Lesions between 2.5 to 3.3 mm of maximal lumen diameter achieved better deployment criteria than those with a maximal lumen diameter <2.5 mm and >3.3 mm. Further investigations are warranted to correlate the angiographic guidelines with the OCT findings and clinical outcomes at short, medium and long-term follow-up.

REFERENCES

1. Ormiston JA, Serruys PW, Regar E, Dudek D, Thuesen L, Webster MW, Onuma Y, Garcia-Garcia HM, McGreevy R, Veldhof S. A bioabsorbable everolimus-eluting coronary stent system for patients with single de-novo coronary artery lesions (ABSORB): a prospective open-label trial. *Lancet*. 2008;371:899-907.
2. Serruys PW, Ormiston JA, Onuma Y, Regar E, Gonzalo N, Garcia-Garcia HM, Nieman K, Bruining N, Dorange C, Miquel- Hebert K, Veldhof S, Webster M, Thuesen L, Dudek D. A bioabsorbable everolimus-eluting coronary stent system (ABSORB): 2-year outcomes and results from multiple imaging methods. *Lancet*. 2009;373:897-910.
3. Uren NG, Schwarzacher SP, Metz JA, Lee DP, Honda Y, Yeung AC, Fitzgerald PJ, Yock PG. Predictors and outcomes of stent thrombosis: an intravascular ultrasound registry. *Eur Heart J*. 2002;23: 124-132.
4. Costa MA, Angiolillo DJ, Tannenbaum M, Driesman M, Chu A, Patterson J, Kuehl W, Battaglia J, Dabbons S, Shamoon F, Flieshman B, Niederman A, Bass TA. Impact of stent deployment procedural factors on long-term effectiveness and safety of sirolimus-eluting stents (final results of the multicenter prospective STLLR trial). *Am J Cardiol*. 2008;101:1704-1711.
5. Cheneau E, Leborgne L, Mintz GS, Kotani J, Pichard AD, Satler LF, Canos D, Castagna M, Weissman NJ, Waksman R. Predictors of subacute stent thrombosis: results of a systematic intravascular ultrasound study. *Circulation*. 2003;108:43-47.
6. Sonoda S, Morino Y, Ako J, Terashima M, Hassan AH, Bonneau HN, Leon MB, Moses JW, Yock PG, Honda Y, Kuntz RE, Fitzgerald PJ. Impact of final stent dimensions on long-term results following sirolimus-eluting stent implantation: serial intravascular ultrasound analysis from the sirius trial. *J Am Coll Cardiol*. 2004;43: 1959-1963.
7. de Jaegere P, Mudra H, Figulla H, Almagor Y, Doucet S, Penn I, Colombo A, Hamm C, Bartorelli A, Rothman M, Nobuyoshi M, Yamaguchi T, Voudris V, DiMario C, Makovski S, Hausmann D, Rowe S, Rabinovich S, Sunamura M, van Es GA. Intravascular ultrasound-guided optimized stent deployment. Immediate and 6 months clinical and angiographic results from the Multicenter Ultrasound Stenting in Coronaries Study (MUSIC Study). *Eur Heart J*. 1998;19:1214-1223.
8. Russo RJ, Silva PD, Teirstein PS, Attubato MJ, Davidson CJ, DeFranco AC, Fitzgerald PJ, Goldberg SL, Hermiller JB, Leon MB, Ling FS, Lucisano JE, Schatz RA, Wong SC, Weissman NJ, Zientek DM. A randomized controlled trial of angiography versus intravascular ultrasound-directed bare-metal coronary stent placement (the AVID Trial). *Circ Cardiovasc Interv*. 2009;2:113-123.
9. Bouma BE, Tearney GJ, Yabushita H, Shishkov M, Kauffman CR, DeJoseph Gauthier D, MacNeill BD, Houser SL, Aretz HT, Halpern EF, Jang IK. Evaluation of intracoronary stenting by intravascular optical coherence tomography. *Heart*. 2003;89:317-320.
10. Reiber JH, Serruys PJ. Quantitative Coronary Angiography: Methodologies. Quantitative Coronary Angiography. Dordrecht, The Netherlands: Kluwer Academic Publishers; 1991. p. 98-102.
11. Prati F, Regar E, Mintz GS, Arbustini E, Di Mario C, Jang IK, Akasaka T, Costa M, Guagliumi G, Grube E, Ozaki Y, Pinto F, Serruys PW. Expert review document on methodology, terminology, and clinical applications of optical coherence tomography: physical principles, methodology of image acquisition, and clinical application for assessment of coronary arteries and atherosclerosis. *Eur Heart J*. 2010;31:401-415.
12. Onuma Y, Serruys PW, Ormiston JA, Regar E, Mark Webster, Thuesen L, Dudek D, Veldhof S, Rapoza R. Three-year results of clinical follow-up after a bioresorbable everolimus-eluting scaffold in patients with de novo coronary artery disease: the ABSORB trial. *EuroIntervention*. 2010;6:447-53.
13. Gonzalo N, Garcia-Garcia HM, Serruys PW, Commissaris KH, Bezerra H, Gobbens P, Costa M, Regar E. Reproducibility of quantitative optical coherence tomography for stent analysis. *EuroIntervention*. 2009;5:224-232.

14. Abizaid AS, Mintz GS, Mehran R, Abizaid A, Lansky AJ, Pichard AD, Satler LF, Wu H, Pappas C, Kent KM, Leon MB. Long-term follow-up after percutaneous transluminal coronary angioplasty was not performed based on intravascular ultrasound findings: importance of lumen dimensions. *Circulation.* 1999;100: 256-261.
15. Fujii K, Carlier SG, Mintz GS, Yang YM, Moussa I, Weisz G, Dangas G, Mehran R, Lansky AJ, Kreps EM, Collins M, Stone GW, Moses JW, Leon MB. Stent underexpansion and residual reference segment stenosis are related to stent thrombosis after sirolimus-eluting stent implantation: an intravascular ultrasound study. *J Am Coll Cardiol.* 2005;45:995-998.
16. Tanimoto S, Serruys PW, Thuesen L, Dudek D, de Bruyne B, Chevalier B, Ormiston JA. Comparison of in vivo acute stent recoil between the bioabsorbable everolimus-eluting coronary stent and the everolimus-eluting cobalt chromium coronary stent: insights from the ABSORB and SPIRIT trials. *Catheter Cardiovasc Interv.* 2007;70:515-523.
17. Nishida T, Colombo A, Briguori C, Stankovic G, Albiero R, Corvaja N, Finci L, Di Mario C, Tobis JM. Outcome of nonobstructive residual dissections detected by intravascular ultrasound following percutaneous coronary intervention. *Am J Cardiol.* 2002;89: 1257-1262.
18. Liu X, Tsujita K, Maehara A, Mintz GS, Weisz G, Dangas GD, Lansky AJ, Kreps EM, Rabbani LE, Collins M, Stone GW, Moses JW, Mehran R, Leon MB. Intravascular ultrasound assessment of the incidence and predictors of edge dissections after drug-eluting stent implantation. *JACC Cardiovasc Interv.* 2009;2:997-1004.
19. Gonzalo N, Serruys PW, Okamura T, Shen ZJ, Onuma Y, Garcia-Garcia HM, Sarno G, Schultz C, van Geuns RJ, Ligthart J, Regar E. Optical coherence tomography assessment of the acute effects of stent implantation on the vessel wall: a systematic quantitative approach. *Heart.* 2009;95:1913-1919.
20. Kubo T, Imanishi T, Kitabata H, Kuroi A, Ueno S, Yamano T, Tanimoto T, Matsuo Y, Masho T, Takarada S, Tanaka A, Nakamura N, Mizukoshi M, Tomobuchi Y, Akasaka T. Comparison of vascular response after sirolimus-eluting stent implantation between patients with unstable and stable angina pectoris: a serial optical coherence tomography study. *JACC Cardiovasc Imaging.* 2008;1:475-484.
21. Tanabe K, Serruys PW, Degertekin M, Grube E, Guagliumi G, Urbaszek W, Bonnier J, Lablanche JM, Siminiak T, Nordrehaug J, Figulla H, Drzewiecki J, Banning A, Hauptmann K, Dudek D, Bruining N, Hamers R, Hoye A, Ligthart JM, Disco C, Koglin J, Russell ME, Colombo A. Incomplete stent apposition after implantation of paclitaxel-eluting stents or bare metal stents: insights from the randomized TAXUS II trial. *Circulation.* 2005; 111:900-905.
22. Maehara A, Mintz GS, Lansky AJ, Witzenbichler B, Guagliumi G, Brodie B, Kellett MA, Jr., Parise H, Mehran R, Stone GW. Volumetric intravascular ultrasound analysis of Paclitaxel-eluting and bare metal stents in acute myocardial infarction: the harmonizing outcomes with revascularization and stents in acute myocardial infarction intravascular ultrasound substudy. *Circulation.* 2009;120:1875-1882.
23. Tanigawa J, Barlis P, Dimopoulos K, Dalby M, Moore P, Di Mario C. The influence of strut thickness and cell design on immediate apposition of drug-eluting stents assessed by optical coherence tomography. *Int J Cardiol.* 2009;134:180-188.
24. Kim JS, Jang IK, Fan C, Kim TH, Park SM, Choi EY, Lee SH, Ko YG, Choi D, Hong MK, Jang Y. Evaluation in 3 months duration of neointimal coverage after zotarolimus-eluting stent implantation by optical coherence tomography: the ENDEAVOR OCT trial. *JACC Cardiovasc Interv.* 2009;2:1240-1247.
25. Kimura M, Mintz GS, Carlier S, Takebayashi H, Fujii K, Sano K, Yasuda T, Costa RA, Costa JR, Jr., Quen J, Tanaka K, Lui J, Weisz G, Moussa I, Dangas G, Mehran R, Lansky AJ, Kreps EM, Collins M, Stone GW, Moses JW, Leon MB. Outcome after acute incomplete sirolimus-eluting stent apposition as assessed by serial intravascular ultrasound. *Am J Cardiol.* 2006;98:436-442.

26. Finn AV, Nakazawa G, Joner M, Kolodgie FD, Mont EK, Gold HK, Virmani R. Vascular responses to drug eluting stents: importance of delayed healing. *Arterioscler Thromb Vasc Biol.* 2007; 27:1500-1510.
27. Cook S, Wenaweser P, Togni M, Billinger M, Morger C, Seiler C, Vogel R, Hess O, Meier B, Windecker S. Incomplete stent apposition and very late stent thrombosis after drug-eluting stent implantation. *Circulation.* 2007;115:2426-2434.
28. Finn AV, Joner M, Nakazawa G, Kolodgie F, Newell J, John MC, Gold HK, Virmani R. Pathological correlates of late drug-eluting stent thrombosis: strut coverage as a marker of endothelialization. *Circulation.* 2007;115:2435-2441.
29. Barlis P, Regar E, Serruys PW, Dimopoulos K, van der Giessen WJ, van Geuns RJ, Ferrante G, Wandel S, Windecker S, van Es GA, Eerdmans P, Juni P, di Mario C. An optical coherence tomography study of a biodegradable vs. durable polymer-coated limus-eluting stent: a LEADERS trial sub-study. *Eur Heart J.* 2010;31:165-176.
30. Nakazawa G, Finn AV, Vorpahl M, Ladich E, Kutys R, Balazs I, Kolodgie FD, Virmani R. Incidence and predictors of drug-eluting stent fracture in human coronary artery a pathologic analysis. *J Am Coll Cardiol.* 2009;54:1924-1931.
31. Ino Y, Toyoda Y, Tanaka A, Ishii S, Kusuyama Y, Kubo T, Takarada S, Kitabata H, Tanimoto T, Mizukoshi M, Imanishi T, Akasaka T. Predictors and prognosis of stent fracture after sirolimus-eluting stent implantation. *Circ J.* 2009;73:2036-2041.
32. Lee SH, Park JS, Shin DG, Kim YJ, Hong GR, Kim W, Shim BS. Frequency of stent fracture as a cause of coronary restenosis after sirolimus-eluting stent implantation. *Am J Cardiol.* 2007;100: 627-630.
33. Popma JJ, Tiroch K, Almonacid A, Cohen S, Kandzari DE, Leon MB. A qualitative and quantitative angiographic analysis of stent fracture late following sirolimus-eluting stent implantation. A*m J Cardiol.* 2009;103:923-929.
34. Ormiston JA, De Vroey F, Serruys PW, Webster MW. Bioresorbable polymeric vascular scaffolds: a cautionary tale. *Circ Cardiovasc Interv*. 2011;4:535-8.

PART
II

Chapter 8

Comparison of In Vivo Eccentricity and Symmetry Indices Between Metallic Stents and Bioresorbable Vascular Scaffolds: Insights From the ABSORB and SPIRIT Trials

Salvatore Brugaletta, MD; Josep Gomez-Lara, MD; Robert Diletti, MD; Vasim Farooq, MBChB, MRCP; Robert Jan van Geuns, MD; Bernard de Bruyne, MD; Dariusz Dudek, MD; Hector M. Garcia-Garcia, MD; PhD, John A. Ormiston, MBChB, PhD and Patrick W. Serruys, MD, PhD

Catheter Cardiovasc Interv 2012 Feb 1;79(2):219-28

ABSTRACT

Objective To compare the geometrical parameters of a bioresorbable vascular scaffold (BVS) with a standard metallic stent. Background: The introduction of polymeric bioresorbable materials in the design of novel coronary scaffolds may affect some geometrical parameters, such as eccentricity and symmetry indices, previously introduced as IVUS criteria for optimal metallic stent deployment.

Methods From ABSORB Cohort A, ABSORB Cohort B, SPIRIT I, and SPIRIT II, all patients implanted with BVS 1.0, BVS 1.1, or XIENCE V, respectively and intravascular ultrasound analyses post-implantation were selected. The eccentricity index was calculated frame by frame and expressed as an average per device (minimum diameter/maximum diameter). The symmetry index of the device was reported as ([maximum diameter 2 minimum diameter]/maximum diameter). Six months major adverse cardiac events (MACE) were analyzed.

Results A total of 242 patients were selected (BVS 1.0: n = 28, BVS 1.1: n = 94, XIENCE V: n = 120). The BVS exhibited a significantly lower eccentricity index (BVS 1.0: 0.83 ± 0.09; BVS 1.1: 0.85 ± 0.08; XIENCE V: 0.90 ± 0.06; $P < 0.01$) and a significantly higher symmetry index (BVS 1.0: 0.30 ± 0.07; BVS 1.1: 0.31 ± 0.06, XIENCE V 0.26 ± 0.07; $P < 0.01$) as compared to the XIENCE V. An inverse correlation was found between the symmetry and eccentricity indices for both (BVS $r = -0.69$, $P < 0.01$; XIENCE V $r = -0.61$, $P < 0.01$). No differences in MACE were detected between the groups according to their geometrical parameters.

Conclusions The introduction of a new polymeric material in the design of BVS resulted in a lower eccentricity index and a higher symmetry index as compared to metallic stents, without detectable impact in MACE, at 6 months.

INTRODUCTION

The introduction of intravascular ultrasound (IVUS) and high pressure implantation of coronary stents in interventional cardiology practice have had a significant impact on stent deployment [1,2]. The MUSIC trial showed how the use of IVUS criteria (such as complete apposition of the stent against the vessel wall; in-stent minimal lumen area ≥90% of the average reference lumen area; eccentricity index
≥0.7), may positively contribute to the immediate and 6-month clinical and angiographic outcomes [3]. A meta-analysis from the BENESTENT and MUSIC trials further confirmed how the IVUS guidance is responsible for reduction in restenosis rate [4,5].

Some geometrical stent parameters, such as eccentricity and symmetry, easily detectable by IVUS, have previously been demonstrated to be related to either favorable or adverse clinical outcomes [3,6]. With the transition from a metallic stent to a polymeric bioresorbable platform, the need for the re-evaluation of these geometrical parameters is required at short and long term.

In the present analysis, we evaluated the eccentricity and symmetry indices of the bioresorbable vascular scaffold (BVS) in the ABSORB trials and compared these to the XIENCE V stent from the SPIRIT trials.

METHODS

Study Population

For the present analysis, we screened all patients from ABSORB (Cohort A and B) and SPIRIT I [7] and II [8] trials, and selected all the patients with available IVUS data post-device implantation. These patients were then subdivided into three groups according to the device implanted (BVS 1.0, BVS 1.1 and XIENCE V, all Abbott Vascular, Santa Clara, CA). The design of the ABSORB studies has been previously described [9–11]. Briefly, in the ABSORB Cohort A trial (NCT00300131), patients with a diagnosis of stable or unstable angina or silent ischemia, were enrolled. All treated lesions were single and de novo in a native coronary artery of 3.0 mm diameter, shorter than 8 mm for the 12-mm stent and shorter than 14 mm for the 18-mm stent, with a diameter stenosis greater than 50% and less than 100%, and with a thrombolysis in myocardial infarction (TIMI) flow grade more than 1. All lesions were treated by implantation of BVS 1.0 (3.0 x 12 mm and 3.0 x 18 mm). The ABSORB Cohort B trial (NCT00856856) enrolled patients with the same clinical profile and lesion type. All lesions were treated by implantation of a BVS 1.1 (3.0 x 18 mm) [11].

The SPIRIT trials were planned to assess the safety and efficacy of the everolimus eluting

stent (XIENCE V) in patients with coronary artery disease. SPIRIT I and II were prospective, multicenter, single-blinded, randomized-controlled clinical investigations which compared XIENCE V with either the bare Multi-Link VISION metal (Abbott Vascular, Santa Clara, CA, SPIRIT I trial, NCT00180453) or paclitaxel-eluting (Boston Scientific, Natick, MA, SPIRIT II trial, NCT00180310) stents [7,8]. The exclusion criteria of the two SPIRIT trials were similar to those of the ABSORB trials. All the trials had previously been approved by the ethics committee at each participating institution with written informed consent obtained for each patient before inclusion.

Quantitative Coronary Angiography Analysis of Vessels Pretreatment

Quantitative coronary angiography (QCA) pre-treatment was performed by an independent core laboratory (Cardialysis BV, Rotterdam, The Netherlands), using the CAAS II analysis system (Pie Medical BV, Maastricht, Netherlands). For each pre-treatment angiogram, the treated and the peri-treated regions (defined by a length of 5-mm proximal and distal to the device edge) were analyzed. The following QCA parameters were computed: computer-defined minimum lumen diameter (MLD), reference vessel diameter (RVD), obtained by the interpolate method, and percentage diameter stenosis [12].

Study Devices

The BVS has an amorphous poly-DL-lactide (PDLLA) coating that contains and controls the release of the anti- proliferative drug everolimus (Figure 1). The scaffold body is made of semi-crystalline poly-L-lactide (PLLA). PLLA is completely degraded via hydrolysis and bioresorbed via the Krebs cycle [9,10]. Physically, the scaffold has struts with an approximate thickness of 150 lm. There are no differences in polymeric material, drug dose, drug release, or strut thickness between BVS revisions 1.0 and 1.1. Of note, the BVS revision 1.1 has a smaller maximum circular unsupported surface area compared to revision 1.0, with the struts arranged as in- phase zigzag hoops linked together by three longitudinal links, similar to the XIENCE V design [13].

The XIENCE V stent is an everolimus-eluting, cobalt chromium alloy device with a platform consisting of serpentine rings connected by links fabricated from a single piece. The strut thickness is 81 μm with the polymer and drug coating adding a further thickness of 7 μm to the overall thickness.

Lesions were treated with standard interventional techniques, with mandatory pre-dilatation, using a balloon shorter and 0.5 mm smaller in diameter than the study device. The study device was implanted at a pressure not exceeding the rated burst pressure. Post- dilatation with a balloon shorter than the implanted device was allowed at the operator's discretion, as was bailout treatment.

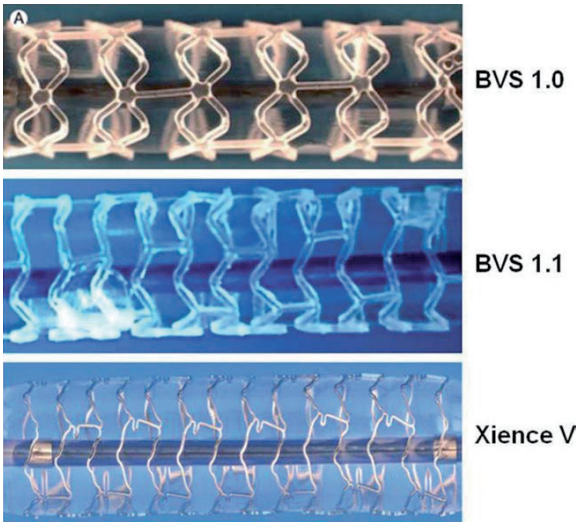

Figure 1. Pictures of BVS 1.0, BVS 1.1, and XIENCE V. [Color figure can be viewed in the online issue, which is available at wileyonlinelibrary.com.]

Intravascular Ultrasound Analysis

Post-procedure treated vessel segments were examined with mechanical (Atlantis, Boston Scientific, Natick, MA) or phased array (Eagle-eye Volcano, Rancho Cordova, CA) intravascular ultrasound (IVUS), using automated pullbacks at 0.5 mm per second after administration of 0.2 mg intracoronary nitroglycerin. IVUS analyses were performed by an independent core laboratory (Cardialysis BV, Rotterdam, The Netherlands). Only the lesions implanted with a BVS 1.0, BVS 1.1, or a XIENCE V were included in the analysis. A computer-based contour detection program was used for automated 2D reconstruction of the treated segment. The lumen, stent/scaffold boundaries and external elastic membrane (vessel boundaries) were detected using a minimum cost algorithm [14].

For each treated vessel segment, we analyzed frame by frame the lumen, device implanted (stent/ scaffold), plaque, and vessel area and upfront selected the site (single frame) of minimum stent/ scaffold area (MSA). The MSA is classically described as the flow-limiting area and has been previously related to angiographic and clinical outcomes [15,16]. In each frame, we obtained the "projected" diameters of the stent/scaffold, as previously described and validated [17].

For each device implanted we therefore calculated:

- Eccentricity index at the MSA frame, as a ratio between the minimum and maximum diameters in that frame; [3,18]

- Eccentricity index, as the average of all eccentricity indices of each frame; [3,18]
- Symmetry index as [maximum stent/scaffold diameter in a single frame minus minimum stent/scaffold diameter in a single frame] divided by the maximum stent/scaffold diameter [19]. Note that the maximum and the minimum stent/scaffold diameters in this calculation were possibly located in two different frames over the length of the device implanted (Figure 2).

Intravascular Ultrasound Assessment of Lesion Calcification

The MSA frames selected upfront for each lesion were also assessed by two experienced cardiologists to quantify calcium, as previously described [19–22]. Calcium produced bright echoes (using the adventitia as reference) with acoustic shadowing (attenuation) of deeper arterial structures. The extent and distribution of lesion calcification were assessed as follows:

- The location of the calcium was defined as superficial (calcium at the intimal/lumen interface or closer to the lumen than to the adventitia), deep (calcium at the media/adventitia border or closer to the adventitia than to the lumen), or both.
- The largest arc of calcium was measured in degrees with a protractor centered on the lumen. If there was more than one deposit of calcium in the frame, the total arc of calcium for that frame was obtained by adding up the arcs of each individual deposit. Calcification was then classified an none, one-quadrant (≤90°), two- quadrant (91° to 180°), three-quadrant (181° to 270°), or four-quadrant (271° to 360°) calcification.

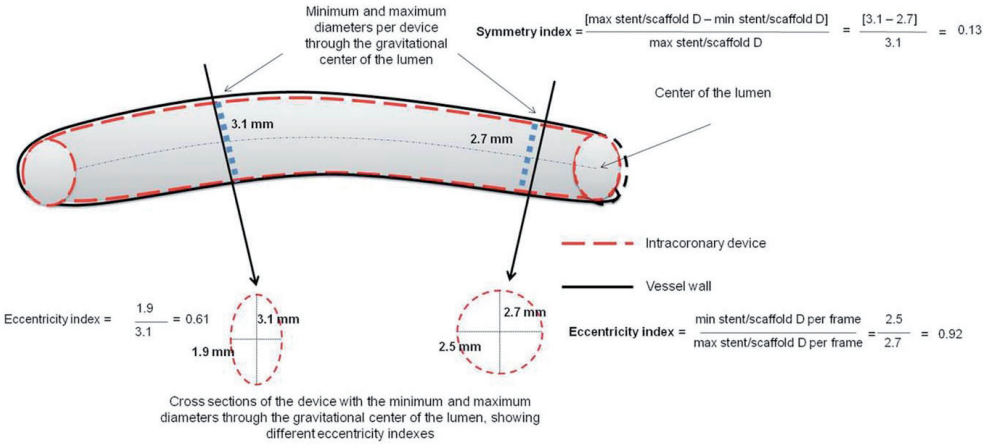

Figure 2. Relationship between the symmetry and eccentricity indices of a intracoronary device. Minimum and maximum diameters over the length of the device are shown. Two cross-sections with different eccentricity indices are also shown. [Color figure can be viewed in the online issue, which is available at wileyonlinelibrary.com.]

Statistical Analysis

Categorical variables are presented as counts and percentages and compared by means of the Chi-square test. Continuous variables are presented as means ± standard deviation (SD). The distribution of the variables was tested as normal or non normal by Kolmogorov-Smirnov test. Depending on the distribution of the data, comparison between groups was made with the ANOVA test with Bonferroni correction or with the Kruskal-Wallis test with Dunn correction for multiple comparisons. Correlation between parameters was performed by Pearson or Spearman test, depending on their distribution. Cardiac death, any acute myocardial infarction and ischemia-driven target lesion revascularization at 6-month follow-up were considered as major cardiac events (MACE), according to the original protocol of ABSORB A and B trials, and SPIRIT I and II trials [7,8,10]. The threshold between the considered normal and non normal value for the eccentricity index was ≥0.7, as previously described [3,11]. A multivariate linear regression analysis was tested for the independent predictors of eccentricity index: symmetry index, type of lesion according to AHA/ACC classification, target vessel, size of the device as a categorical variable (size of 3.0 x 18 mm or not) and device implanted (BVS vs. XIENCE V) were introduced in the model. A two side P-value <0.05 was considered as significant. Statistical analyses were performed with use of SPSS 13.0 software (SPSS, Chicago, IL).

RESULTS

Baseline Clinical and Angiographic Characteristics

We studied 242 patients (249 lesions) with available post-stent/scaffold implantation IVUS analyses and subdivided these into three groups according to the device implanted. Group 1 (28 patients): ABSORB Cohort A trial, BVS 1.0; group 2 (94 patients): ABSORB Cohort B trial, BVS 1.1, and group 3 (120 patients/127 lesions): SPIRIT I and II trials, XIENCE V stent. Table 1 shows the baseline clinical characteristics.

No significant differences were found between the groups in the pre-treatment QCA analysis. The diameter and the length of the stents/scaffold implanted were significantly different between the groups (both $P < 0.0001$). In particular, only two (7.1%) patients from group 1 received a BVS 1.0 3.0 x 18 mm, while all the patients (100%) from group 2 received a BVS 1.1 3.0 x 18 mm, and 37 patients (31%) from group 3 received a XIENCE V 3.0 x 18 mm. Six-month follow-up data were available in 225 patients (92.9%). A total of 7 MACE were recorded: 1 (3.5%) MACE was recorded for BVS 1.0 [9], 4 (4.2%) MACE for BVS 1.1 [11], and 2 (1.9%) MACE for XIENCE V [7,8].

Table 1. Clinical and Angiographic Baseline Characteristics.

	BVS 1.0 (patients/lesions = 28)	BVS 1.1 (patients/lesions = 94)	XIENCE V (patients = 120; lesions = 127)	P-value
Age, mean ± SD	62.0 ± 9.0	60.7 ± 8.9	61.6 ± 10.5	0.90
Male, % (n)	57.1 (16)	61.7 (58)	76.6 (92)	0.23
Hypertension requiring medication, % (n)	57.1 (16)	56.3 (53)	68.3 (82)	0.49
Hyperlipidaemia requiring medication, % (n)	60.7 (17)	65.9 (62)	77.5 (93)	0.57
Smokers, % (n)	21.4 (6)	15.9 (15)	36.6 (44)	0.05
Diabetes, % (n)	3.5 (1)	15.9 (15)	20 (24)	0.20
Previous PCI, % (n)	3.5 (1)	4.2 (4)	6.6 (8)	0.82
Previous AMI, % (n)	7.1 (2)	17.0 (16)	40 (48)	0.04
Renal Impairment, % (n)	3.5 (1)	2.1 (2)	1.6 (2)	0.71
Stable angina, % (n)	71.4 (20)	63.8 (60)	64.1 (77)	0.41
Unstable angina, % (n)	25.1 (7)	31.9 (30)	33.3 (40)	0.01
Silent ischaemia, % (n)	3.5 (1)	4.3 (4)	2.6 (3)	0.48
Target vessel, % (n)				
Left anterior descending	53.5 (15)	44.6 (42)	48.8 (62)	0.83
Left Circumflex	25.0 (7)	22.3 (21)	22.8 (29)	0.69
Right coronary artery	21.5 (6)	33.1 (31)	28.4 (36)	0.78
AHA/ACC lesion classification, % (n)				
A	0 (0)	1 (1.1)	2 (1.5)	0.46
B1	18 (64.3)	52 (55.3)	34 (26.7)	0.01
B2	10 (35.7)	8 (40.4)	76 (59.8)	0.01
C	0 (0)	3 (3.2)	15 (12)	0.01
Diameter of stent implanted (mean ± SD, mm)	3.0 ± 0.0	3.0 ± 0.0	3.17 ± 0.3	0.01
Length of stent implanted (mean ± SD, mm)	12.2 ± 1.1	18.0 ± 0.0	22.8 ± 8.5	0.01
QCA analysis pre-treatment				
RVD (mean ± SD, mm)	2.69 ± 0.47	2.61 ± 0.37	2.66 ± 0.44	0.71
MLD (mean ± SD, mm)	1.05 ± 0.26	1.06 ± 0.28	1.10 ± 0.30	0.67
Diameter stenosis (mean ± SD, %)	60 ± 11	58 ±9	58 ± 8	0.83

PCI = percutaneous coronary interventions; AMI = acute myocardial infarction; AHA/ACC = American heart association/American college of Cardiology; QCA = quantitative coronary angiography; RVD = reference vessel diameter; MLD = minimum lumen diameter.

Table 2. Intravascular Ultrasound Postprocedure Data.

	BVS 1.0 (28 lesions)	BVS 1.1 (94 lesions)	XIENCE V (127 lesions)	P-value between the groups	P-value XIENCE V vs. BVS 1.0 and BVS 1.1
Mean vessel area (mm^2)	13.22 ± 3.65	14.13 ± 3.38	14.84 ± 3.91	0.113	0.151 vs. BVS 1.0 0.632 vs. BVS 1.1
Mean lumen area (mm^2)	6.01 ± 1.09	6.42 ± 1.03	7.22 ± 1.65	<0.001	<0.001 for both
Mean plaque area (mm^2)	7.21 ± 2.78	7.68 ± 2.64	7.65 ± 2.72	0.726	1.000 for both
Minimum stent/scaffold area (mm^2)	5.04 ± 1.00	5.28 ± 0.99	5.96 ± 1.52	<0.001	<0.001 for both
Eccentricity index	0.86 ± 0.05	0.88 ± 0.03	0.92 ± 0.03	<0.001	<0.001 for both
Eccentricity index at MSA frame	0.83 ± 0.09	0.85 ± 0.08	0.90 ± 0.06	<0.001	<0.001 for both
Stent/scaffold symmetry index	0.30 ± 0.07	0.31 ± 0.06	0.26 ± 0.07	<0.001	<0.001 for both

Data are expressed as mean ± SD. BVS: bioresorbable vascular scaffold; MSA: Minimum stent/scaffold area.

Intravascular Ultrasound Analysis After Implantation

Both the mean lumen area and the MSA were significantly lower for the BVS 1.0 and 1.1 compared to XIENCE V (P < 0.001; Table 2). However, in a further sub-analysis, including only the stents with the same size (3.0 x 18 mm), no significant differences were found between the groups in terms of mean lumen area (P = 0.368) and post-procedural MSA (P = 0.268).

Eccentricity and Symmetry Index After Implantation

The eccentricity index, either average-of-all-frames or at the MSA, was significantly lower for BVS 1.0 and 1.1 as compared to XIENCE V (both P < 0.001). Conversely, the symmetry index was significantly lower for XIENCE V compared to BVS 1.0 and BVS 1.1 (P < 0.001) (Figure 3). Analyzing the 3.0 x 18 mm stents alone, the BVS maintained a lower eccentricity index and a higher symmetry index compared to XIENCE V (both P < 0.001). No significant differences were found, in terms of eccentricity and symmetry index, when comparing the 3.0 x 18 mm devices against other sizes (Table 3).

Whilst no patients demonstrated an average eccentricity index per stent below the threshold of 0.7, 10 patients (4.1%) exhibited an eccentricity index at the MSA below 0.7: two (7.1%) of these had a BVS 1.0, seven (7.4%) a BVS 1.1, and one (0.8%) a XIENCE V (P = 0.023). Only one MACE (10%) occurred in the patients with a value <0.7 (n = 10), whilst the remaining six MACE (2.5%) occurred in those patients with a value > 0.7 (n = 239) (log rank test P = 0.283).

There was an inverse correlation between the symmetry and eccentricity indices for the XIENCE V (r = -0.61, P < 001) and BVS (r =-0.69, P < 0.001) (Figure 4).

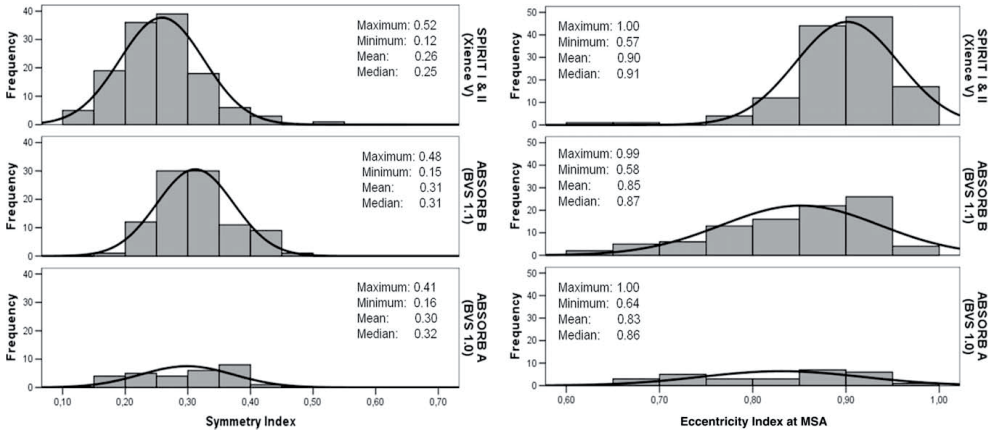

Figure 3. Distribution of symmetry (left panel) and eccentricity index at MSA (right panel) between the groups. XIENCE V shows the lowest symmetry index and highest eccentricity index, significantly different compared to that of BVS 1.0 and BVS 1.1 (P < 0.001 in the comparison between all the groups, and P < 0.001 in post-hoc statistical analysis between XIENCE V vs. BVS 1.0 and BVS 1.1). MSA 5 minimum stent/scaffold area.

Table 3. Eccentricity and Symmetry Index According to the Size of the Device.

	3.0 x 18 mm	Other sizes	P-value
Eccentricity index XIENCE V	0.91 ± 0.03	0.92 ± 0.03	0.256
Symmetry index XIENCE V	0.27 ± 0.07	0.25 ± 0.07	0.101
Eccentricity index BVS	0.88 ± 0.03	0.86 ± 0.05	0.126
Symmetry index BVS	0.31 ± 0.06	0.30 ± 0.07	0.759

Data are expressed as mean ± SD. BVS: bioresorbable vascular scaffold.

Table 4. Frequency and Distribution of Calcium Between the Groups.

	BVS 1.0 (28 lesions)	BVS 1.1 (94 lesions)	XIENCE V (127 lesions)	P value between the groups
Presence and location of calcium, n (%)				
No calcium	16 (57)	48 (51)	56 (44)	0.151
Only superficial	1 (3)	16 (17)	27 (21)	0.032
Only deep	9 (32)	20 (21)	28 (22)	0.346
Both superficial and deep	2 (8)	10 (11)	16 (13)	0.335
Distribution of the maximum arc, n (%)				
One quadrant (≤90°)	10 (83)	34 (74)	32 (45)	0.041
Two-quadrant (91°–180°)	2 (17)	11 (24)	28 (39)	0.038
Three-quadrant (181°–270°)	0 (0)	1 (2)	11 (16)	0.061
Four-quadrant (271°–360°)	0 (0)	0 (0)	0 (0)	na

BVS: bioresorbable vascular scaffold.

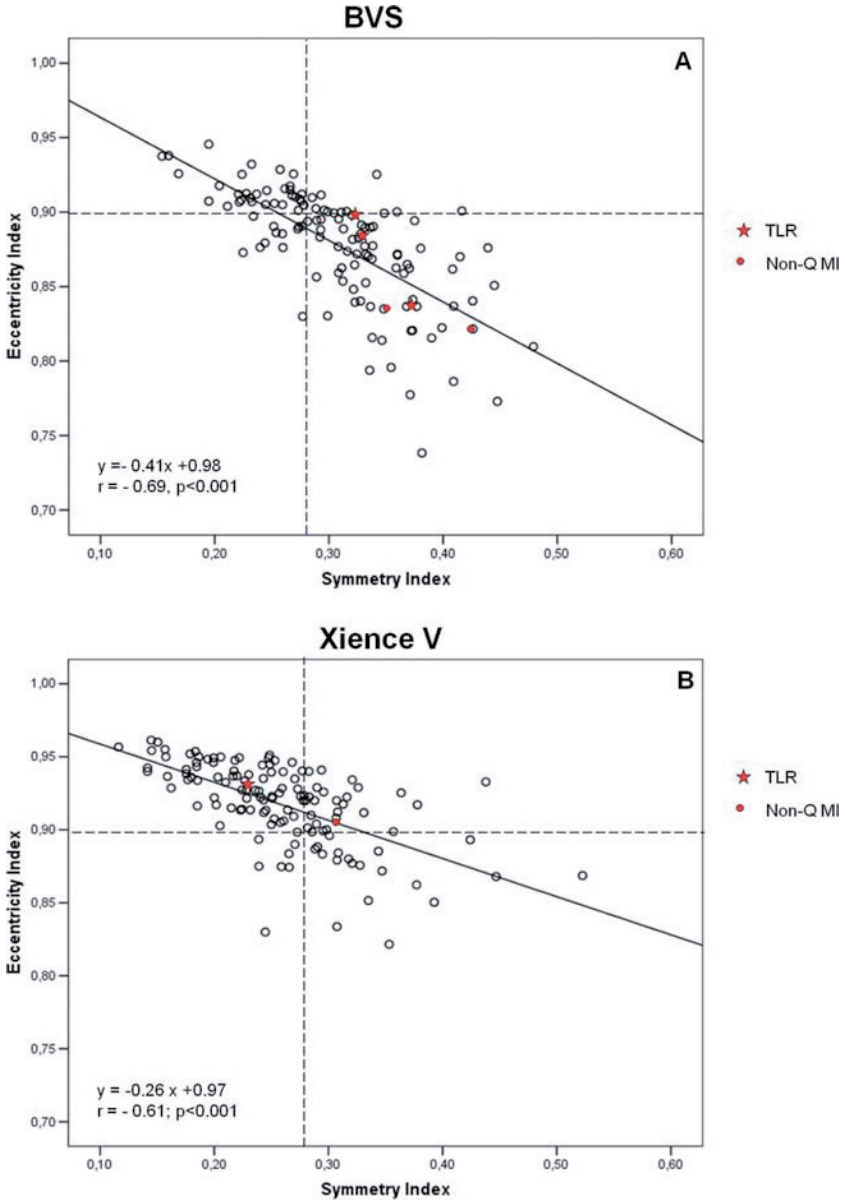

Figure 4. Correlation between the symmetry and the eccentricity indices for BVS (Panel A) and XIENCE V (Panel B). Dotted lines represent the median value of symmetry and eccentricity indices in the overall population. Full dots and stars represent the patients who developed a MACE during the 6-month follow-up. Note that the majority of the BVS are distributed in the quadrant lower/right, while the XIENCE V in the quadrant upper/left. TLR 5 ischemia-driven target lesion revascularization; non-Q MI 5 non-Q myocardial infarction. [Color figure can be viewed in the online issue, which is available at wileyonlinelibrary.com.]

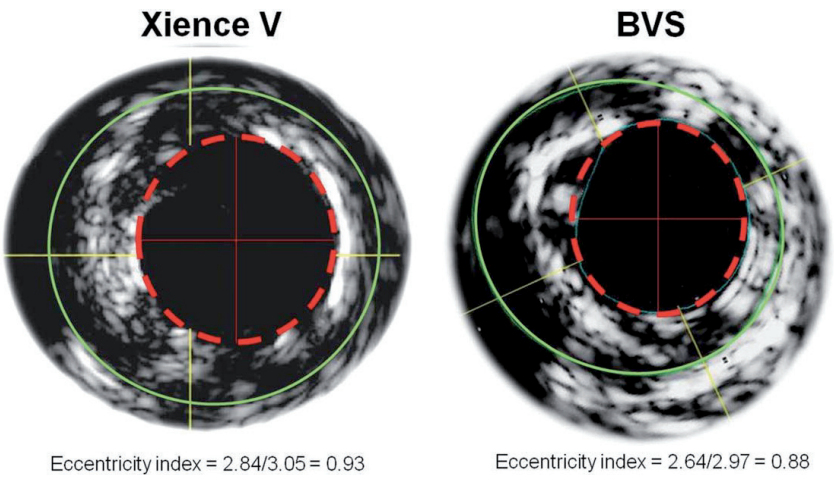

Figure 5. Two examples of eccentricity index of XIENCE V and BVS in MSA frames in presence of calcium (from 7 to 11 o'clock). Red circles with dotted lines represent the stent/scaffold contours; the minimum and maximum diameters are drawn inside as continuous red line. Green lines represent the external elastic membrane. Note that the polymeric struts of the BVS are brighter and thicker than struts of XIENCE. [Color figure can be viewed in the online issue, which is available at wileyonlinelibrary.com.]

Multivariate analysis demonstrated that independent predictors of eccentricity index were the symmetry index ($P < 0.001$) and the implanted device ($P < 0.001$).

Eccentricity Index at MSA According to Lesion Calcification

By IVUS, calcium was identified at MSA in 129 frames (52%). When present, it was only superficial in 44 (34%), only deep in 57 (44%) and both superficial and deep in 28 (22%). The maximum arc of calcium measured was 42° ± 57°. The distribution of the maximum arc of calcium was one-quadrant in 76 (59%), two-quadrant in 41 (32%), three-quadrant in 12 (9%).

Table 4 shows the frequency and distribution of calcium between the groups.

Both BVS (0.82 ± 0.09 vs. 0.87 ± 0.08, $P < 0.01$) and XIENCE V (0.89 ± 0.04 vs.0.92 ± 0.04, $P < 0.01$) exhibited a significantly lower eccentricity index at the MSA in presence of calcium compared to its absence. The eccentricity index at the MSA of BVS was significantly lower compared to XIENCE V, either with or without the presence of calcium, (both $P < 0.01$) (Figure 5). No difference in eccentricity index was found between the groups according to the localization of calcium (deep, superficial or both). We observed that when there was a maximum arc of calcium in two or three quadrants, the eccentricity indices for both BVS (one-quadrant 0.85 ± 0.08, two-quadrant 0.81± 0.08, three-quadrant 0.72, $P = 0.101$) and Xience V (one quadrant 0.91 ± 0.05, two-quadrant 0.87 ± 0.06, three-quadrant 0.87 ± 0.05,

P = 0.005) were lower as compared to the maximum arc of calcium being present in only one quadrant.

DISCUSSION

The major findings of our analysis are: (1) BVS exhibits a lower eccentricity index when compared to a metallic stent; (2) BVS tends to have a higher symmetry index compared to a metallic stent; nevertheless (3) these differences in geometrical parameters did not seem to generate clinical events in the small cohort of patients studied at 6 months.

Some properties influenced by stent material and design, such as conformability and flexibility, have previously been studied in various metallic stent platforms [23–25]. However, these geometrical parameters seen in the metallic stent era have to be re-evaluated with the recent introduction of the polymeric bioresorbable scaffolds [26,27].

The BVS 1.0 and 1.1 have different geometrical designs, but are manufactured from the same material. The BVS 1.1 and the XIENCE V have similar designs, but are made from differing materials. Our study shows that different values of eccentricity and symmetry are observed when comparing BVS with conventional metallic stents. We found that while an everolimus-eluting metallic stent tends to exhibit a symmetrical shape and a high eccentricity index after deployment, the everolimus-eluting BVS tends to have a less symmetrical shape and a low eccentricity index (Fig. 5). The relationship between these two parameters is inversely correlated for both devices, but the slope of this correlation is different (Fig. 3). Thus, device symmetry and eccentricity seem to be related to the material rather to the device design itself. The size of the device, and in particular its length, do not seem to have any significant influence on the eccentricity and symmetry of the devices, but—as expected—differences in device sizes appear to have an impact on the mean lumen area and the MSA after implantation. The characteristics of the lesion treated, evaluated by the ACC/AHA classification, do not seem to influence the eccentricity index, although they were differently distributed between the groups. Multivariate analysis, indeed, demonstrated symmetry index and type of the device implanted (BVS vs. XIENCE V) to be the only independent predictors of the eccentricity index.

We explored also the influence of lesion's calcification, estimated by IVUS, on the eccentricity index in the MSA frame. As not all the patients included in the analysis received an intravascular ultrasound virtual histology (VH) imaging, we used a validated greyscale IVUS methodology for calcium quantification [22]. In addition use of greyscale IVUS data overcomes the problem of VH dense calcium overestimation in the presence of a BVS or metallic stent, as the stent/scaffold struts are recognized as dense calcium

by the VH [28,29]. We found that in presence of calcium the eccentricity at MSA frame for both devices is lower, confirming that BVS exhibits a lower eccentricity index compared to XIENCE V (Figure 5).
It is noteworthy to consider that despite these differences in geometrical properties, BVS has previously been shown to have an acute recoil only slightly higher, but insignificantly different, from that of theXIENCE V, implying for both devices a sufficient radial strength to counteract the recoil of the vessel [26].
The different grade of eccentricity and symmetry of the BVS does not seem to generate clinical events, although our study was obviously underpowered to demonstrate this. An eccentricity value of 0.7 has previously been shown to be an acceptable cut-off in the evaluation of good stent expansion in the MUSIC trial, with favorable angiographic results seen at 6-month follow-up [3]. Otake et al. found that a low eccentricity index may be associated with thrombus formation after sirolimus-eluting stent implantation [6]. Alfonso et al., analyzing the IVUS data of 12 consecutive patients with stent thrombosis, found that MUSIC criteria were not fulfilled in any patient [30]. Nevertheless, closer analysis of the single MUSIC criteria in each patient showed that the eccentricity index was above 0.7 in every case. Stent under-expansion or malapposition, inflow/outflow disease or edge dissections were suggested to be more important. These findings have also been confirmed in larger IVUS studies [31–33].

Limitations

The low risk nature of these patients may have contributed to their favorable outcomes and lower rate of MACE during follow-up. Therefore, the results may be difficult to generalize or to apply to a less selected patient population treated in different settings. A more complex type of lesions and patients are currently recruited in the ABSORB EXTEND registry that will enroll 1,000 patients.

CONCLUSION

The bioresorbable vascular scaffold appears to have reduced eccentricity index and increased symmetry index, when compared to conventional metallic stents, without detectable impact on 6-month MACE. Long term IVUS follow-up is required to assess the geometrical outcome of these devices and to ascertain the impact of these peri-procedural IVUS parameters on the long-term outcome.

REFERENCES

1. Goldberg SL, Colombo A, Nakamura S, Almagor Y, Maiello L, Tobis JM. Benefit of intracoronary ultrasound in the deployment of Palmaz-Schatz stents. J Am Coll Cardiol 1994;24:996–1003.
2. Serruys PW, Emanuelsson H, van der Giessen W, Lunn AC, Kiemeney F, Macaya C, Rutsch W, Heyndrickx G, Suryapra- nata H, Legrand V, et al. Heparin-coated Palmaz-Schatz stents in human coronary arteries. Early outcome of the Benestent-II Pilot Study. Circulation 1996;93:412–422.
3. de Jaegere P, Mudra H, Figulla H, Almagor Y, Doucet S, Penn I, Colombo A, Hamm C, Bartorelli A, Rothman M, et al. Intra- vascular ultrasound-guided optimized stent deployment. Immediate and 6 months clinical and angiographic results from the multicenter ultrasound stenting in coronaries study (MUSIC Study). Eur Heart J 1998;19:1214–1223.
4. Serruys PW, Kay IP, Disco C, Deshpande NV, de Feyter PJ. Periprocedural quantitative coronary angiography after Palmaz- Schatz stent implantation predicts the restenosis rate at six months: Results of a meta-analysis of the BElgian NEtherlands Stent study (BENESTENT) I. BENESTENT II Pilot, BENESTENT II, and MUSIC trials. Multicenter ultrasound stent in coronaries. J Am Coll Cardiol 1999;34:1067–1074.
5. de Feyter PJ, Kay P, Disco C, Serruys PW. Reference chart derived from post-stent-implantation intravascular ultrasound predictors of 6-month expected restenosis on quantitative coronary angiography. Circulation 1999;100:1777–1783.
6. Otake H, Shite J, Ako J, Shinke T, Tanino Y, Ogasawara D, Sawada T, Miyoshi N, Kato H, Koo BK, et al. Local determinants of thrombus formation following sirolimus-eluting stent implantation assessed by optical coherence tomography. JACC Cardiovasc Interv 2009;2:459–466.
7. Serruys PW, Ong AT, Piek JJ, Neumann FJ, van der Giessen WJ, Wiemer M, Zeiher A, Grube E, Haase J, Thuesen L, et al. A randomized comparison of a durable polymer Everolimus- eluting stent with a bare metal coronary stent: The SPIRIT I trial. EuroIntervention 2005;1:58–65.
8. Serruys PW, Ruygrok P, Neuzner J, Piek JJ, Seth A, Schofer JJ, Richardt G, Wiemer M, Carrie D, Thuesen L, et al. A rando- mised comparison of an everolimus-eluting coronary stent with a paclitaxel-eluting coronary stent: The SPIRIT II trial. EuroIntervention 2006;2:286–294.
9. Ormiston JA, Serruys PW, Regar E, Dudek D, Thuesen L, Web- ster MW, Onuma Y, Garcia-Garcia HM, McGreevy R, Veldhof S. A bioabsorbable everolimus-eluting coronary stent system for patients with single de-novo coronary artery lesions (ABSORB): A prospective open-label trial. Lancet 2008;371:899–907.
10. Serruys PW, Ormiston JA, Onuma Y, Regar E, Gonzalo N, Garcia-Garcia HM, Nieman K, Bruining N, Dorange C, Miquel- Hebert K, et al. A bioabsorbable everolimus-eluting coronary stent system (ABSORB): 2-year outcomes and results from multiple imaging methods. Lancet 2009;373:897–910.
11. Serruys PW, Onuma Y, Ormiston JA, de Bruyne B, Regar E, Dudek D, Thuesen L, Smits PC, Chevalier B, McClean D, et al. Evaluation of the second generation of a bioresorbable everolimus drug-eluting vascular scaffold for treatment of de novo coronary artery stenosis: Six-month clinical and imaging outcomes. Circulation 2010;122:2301–2312.
12. Reiber JH, Serruys PW. Quantitative Coronary Angiography: Methodologies. Quantitative Coronary Angiography. Dordrecht, The Netherlands: Kluwer Academic Publishers; 1991, Vol. 98. p 102.
13. Okamura T, Garg S, Gutierrez-Chico JL, Shin ES, Onuma Y, Garcia HM, Rapoza R, Sudhir K, Regar E, Serruys PW. In-vivo evaluation of stent strut distribution patterns in the bioabsorbable everolimus-eluting device: An OCT ad hoc analysis of the Revision 1.0 and Revision 1.1 stent design in the ABSORB clinical trial. EuroIntervention 2010:932–938.
14. Hamers R, Bruining N, Knook M, Sabate M. A novel approach to quantitative analysis of intravascular ultrasound images. Computers Cardiol 2008;28:589–592.

15. Doi H, Maehara A, Mintz GS, Yu A, Wang H, Mandinov L, Popma JJ, Ellis SG, Grube E, Dawkins KD, et al. Impact of post-intervention minimal stent area on 9-month follow-up patency of paclitaxel-eluting stents: An integrated intravascular ultrasound analysis from the TAXUS IV, V, and VI and TAXUS ATLAS workhorse, long lesion, and direct stent trials. JACC Cardiovasc Interv 2009;2:1269–1275.
16. Sonoda S, Morino Y, Ako J, Terashima M, Hassan AH, Bonneau, HN, Leon MB, Moses JW, Yock PG, Honda Y, et al. Impact of final stent dimensions on long-term results following sirolimus- eluting stent implantation: Serial intravascular ultrasound analysis from the sirius trial. J Am Coll Cardiol 2004;43:1959–1963.
17. Tsuchida K, Garcia-Garcia HM, Ong AT, Valgimigli M, Aoki J, Rademaker TA, Morel MA, van Es GA, Bruining N, Serruys PW. Revisiting late loss and neointimal volumetric measurements in a drug-eluting stent trial: Analysis from the SPIRIT I trial. Catheter Cardiovasc Interv 2006;67:188–197.
18. Costa MA, Sabate M, Kay IP, de Feyter PJ, Kozuma K, Serrano P, de Valk V, Albertal M, Ligthart JM, Disco C, et al. Three- dimensional intravascular ultrasonic volumetric quantification of stent recoil and neointimal formation of two new generation tubular stents. Am J Cardiol 2000;85:135–139.
19. Mintz GS, Nissen SE, Anderson WD, Bailey SR, Erbel R, Fitzgerald PJ, Pinto FJ, Rosenfield K, Siegel RJ, Tuzcu EM, et al. American college of cardiology clinical expert consensus document on standards for acquisition, measurement and reporting of intravascular ultrasound studies (IVUS). A report of the American college of cardiology task force on clinical expert consensus documents. J Am Coll Cardiol 2001;37:1478–1492.
20. Mintz GS, Pichard AD, Popma JJ, Kent KM, Satler LF, Bucher TA, Leon MB. Determinants and correlates of target lesion calcium in coronary artery disease: A clinical, angiographic and intravascular ultrasound study. J Am Coll Cardiol 1997;29:268–274.
21. Kostamaa H, Donovan J, Kasaoka S, Tobis J, Fitzpatrick L. Calcified plaque cross-sectional area in human arteries: Correlation between intravascular ultrasound and undecalcified histology. Am Heart J 1999;137:482–488.
22. Mintz GS, Popma JJ, Pichard AD, Kent KM, Satler LF, Chuang YC, Ditrano CJ, Leon MB. Patterns of calcification in coronary artery disease. A statistical analysis of intravascular ultrasound and coronary angiography in 1155 lesions. Circulation 1995;91:1959–1965.
23. Schmidt W, Lanzer P, Behrens P, Topoleski LD, Schmitz KP. A comparison of the mechanical performance characteristics of seven drug-eluting stent systems. Catheter Cardiovasc Interv 2009;73:350–360.
24. Sangiorgi G, Melzi G, Agostoni P, Cola C, Clementi F, Romitelli P, Virmani R, Colombo A. Engineering aspects of stents design and their translation into clinical practice. Ann Ist Super Sanita 2007;43:89–100.
25. Rieu R, Barragan P, Garitey V, Roquebert PO, Fuseri J, Commeau P, Sainsous J. Assessment of the trackability, flexibility, and conformability of coronary stents: A comparative analysis. Catheter Cardiovasc Interv 2003;59:496–503.
26. Tanimoto S, Serruys PW, Thuesen L, Dudek D, de Bruyne B, Chevalier B, Ormiston JA. Comparison of in vivo acute stent recoil between the bioabsorbable everolimus-eluting coronary stent and the everolimus-eluting cobalt chromium coronary stent: Insights from the ABSORB and SPIRIT trials. Catheter Cardiovasc Interv 2007;70:515–523.
27. Gomez-Lara J, Garcia-Garcia HM, Onuma Y, Garg S, Regar E, De Bruyne B, Windecker S, McClean D, Thuesen L, Dudek D, et al. A comparison of the conformability of everolimus-eluting bioresorbable vascular scaffolds to metal platform coronary stents. JACC Cardiovasc Interv 2010;3:1190–1198.
28. Kim SW, Mintz GS, Hong YJ, Pakala R, Park KS, Pichard AD, Satler LF, Kent KM, Suddath WO, Waksman R, et al. The virtual histology intravascular ultrasound appearance of newly placed drug-eluting stents. Am J Cardiol 2008;102:1182–1186.

29. Brugaletta S, Garcia-Garcia HM, Garg SJ, G-L, Diletti R, Onuma Y, Van Geuns RJ, McClean D, Dudek D, Thuesen L, Chevalier B, Windecker S, Whitbourn R, Dorange C, Miquel- Hebert K, Sudhir K, Ormiston JA, Serruys PW. Temporal changes of coronary artery plaque located behind the struts of the everolimus eluting bioresorbable vascular scaffold. Int J Cardiovasc Imaging 2010, Oct 13 [epub ahead of print] (in press).
30. Alfonso F, Suarez A, Perez-Vizcayno MJ, Moreno R, Escaned J, Banuelos C, Jimenez P, Bernardo E, Angiolillo DJ, Hernan- dez R, et al. Intravascular ultrasound findings during episodes of drug-eluting stent thrombosis. J Am Coll Cardiol 2007;50:2095–2097.
31. Uren NG, Schwarzacher SP, Metz JA, Lee DP, Honda Y, Yeung AC, Fitzgerald PJ, Yock PG. Predictors and outcomes of stent thrombosis: An intravascular ultrasound registry. Eur Heart J 2002;23:124–132.
32. Cheneau E, Leborgne L, Mintz GS, Kotani J, Pichard AD, Satler LF, Canos D, Castagna M, Weissman NJ, Waksman R. Predictors of subacute stent thrombosis: Results of a systematic intravascular ultrasound study. Circulation 2003;108:43–47.
33. Alfonso F, Suarez A, Angiolillo DJ, Sabate M, Escaned J, Moreno R, Hernandez R, Banuelos C, Macaya C. Findings of intra- vascular ultrasound during acute stent thrombosis. Heart 2004;90:1455–1459.

Chapter 9

In vivo characterisation of bioresorbable vascular scaffold strut interfaces using optical coherence tomography with Gaussian line spread function analysis

Alexander Sheehy, MSc; Juan Luis Gutiérrez-Chico, MD, PhD, FESC, FACC; Roberto Diletti, MD ; James P. Oberhauser, PhD; Thierry Glauser, PhD; Joel Harrington, PhD; Mary Beth Kossuth, PhD; Richard J. Rapoza, PhD; Yoshinobu Onuma, MD; Patrick W. Serruys, MD, PhD, FESC, FACC

EuroIntervention. 2012 Feb;7(10):1227-35.

ABSTRACT

Aims Optical coherence tomography (OCT) of a bioresorbable vascular scaffold (BVS) produces a highly reflective signal outlining struts. This signal interferes with the measurement of strut thickness, as the boundaries cannot be accurately identified, and with the assessment of coverage, because the neointimal backscattering convolutes that of the polymer, frequently making them indistinguishable from one another. We hypothesise that Gaussian line spread functions (LSFs) can facilitate identification of strut boundaries, improving the accuracy of strut thickness measurements and coverage assessment.

Methods and results Forty-eight randomly selected BVS struts from 12 patients in the ABSORB Cohort B clinical study and four Yucatan minipigs were analysed at baseline and follow-up (six months in humans, 28 days in pigs). Signal intensities from the raw OCT backscattering were fit to Gaussian LSFs for each inter- face, from which peak intensity and full-width-at-half-maximum (FWHM) were calculated. Neointimal coverage resulted in significantly different LSFs and higher FWHM values relative to uncovered struts at baseline ($p<0.0001$). Abluminal polymer-tissue interfaces were also significantly different between baseline and follow-up ($p =0.0004$ in humans, $p <0.0001$ in pigs). Using the location of the half-max of the LSF as the polymer tissue boundary, the average strut thickness was 158±11 μm at baseline and 152±20 μm at six months ($p=0.886$), not significantly different from nominal strut thickness.

Conclusions Fitting the raw OCT backscattering signal to a Gaussian LSF facilitates identification of the interfaces between BVS polymer and lumen or tissue. Such analysis enables more precise measurement of the strut thickness and an objective assessment of coverage.

INTRODUCTION

The ABSORB™ bioresorbable vascular scaffold (BVS) (Abbott Vascular, Santa Clara, CA, USA) consists of a semi-crystalline poly(L-lactide) (PLLA) backbone and conformal coating of amorphous poly(D,L-lactide) (PDLLA) and the antiproliferative agent everolimus. The ABSORB BVS struts are fully resorbed approximately two years after implantation,[1,2] following a process in which the long chains of PLLA and PDLLA are progressively shortened as the ester bonds present in each lactic acid repeat unit are hydrolysed. Ultimately, PLLA and PDLLA degrade to lactic acid, which is metabolised via the Krebs' cycle.[3] ABSORB has exhibited excel- lent clinical and angiographic results up to two years follow-up.[1,4]

A BVS is particularly suitable for optical coherence tomography (OCT) imaging, given the translucency of the polymers from which it is manufactured. The transmitted light can readily penetrate the material and any backscattering stems from changes in refractive index on a length scale greater than or equal to the wavelength of the light. Immediately post-implantation, backscattering associated with the BVS is only significant at the borders of the strut, and changes in backscattering at later time points suggest an evolution in polymer microstructure on the length scale described above. Struts imaged with OCT post-implantation typically appear as a box-shaped highly reflective frame that marks the refractive index change at the lumen-polymer and polymer-tissue interfaces.[1,4] However, measuring the strut thickness from leading-edge to leading-edge of the adluminal and abluminal boundaries of this frame results in values greater than the nominal 158 μm value characteristic of the backbone and coating of the ABSORB BVS strut. This discrepancy highlights a lack of precision in the measurement and the need to develop a methodology by which OCT signals may be used to accurately discern the true edges of BVS struts. Even histological assessment may not provide accurate strut measurements at all-time points due to processing artifacts,[2] reinforcing the importance of improving the accuracy of OCT measurements.

OCT is an experimental tool for the evaluation of neointimal coverage after implantation of metallic stents[5-10] and translucent polymeric scaffolds.[2] Coverage assessed by OCT *in vivo* correlates well with neointimal coverage assessed by histology in experimental animal models.[2,5-10] Unlike metallic stents, the assessment of coverage in the ABSORB BVS is more challenging, because the backscattering from thin neointimal layers mixes with that from the polymer interface and can be difficult to discern in a conventional analysis of the log-transformed OCT signal.

The basic principles of light and its interaction with matter provide the means by which these challenges may be addressed. A point-spread function (PSF) describes the

response of an imaging system to a point source or point object. Similarly, the spreading of light along a perfect line or slit has been called the line spread function (LSF).[11] Because OCT is a measurement of backscattering intensity, the edge of a BVS strut forms a relatively uniform line from which a LSF can be measured. However, when tissue or other backscattering media are present, the uniformity of the optical response at the edge may vary. By smoothing the edge response variance due to backscattering tissue, the LSF may facilitate the definition of BVS strut edges and provide an objective criterion for the measurement of strut thickness and tissue coverage.

METHODS

Clinical study

The ABSORB Cohort B study (NCT00856856) design has been published elsewhere.[12] It enrolled patients older than 18 years with diagnosis of stable or unstable angina pectoris or silent ischaemia and *de novo* lesions in native coronary arteries amenable to percutaneous treatment with the ABSORB BVS. Target lesions were required to be characterised by percent diameter stenosis greater than or equal to 50% by visual estimation and reference vessel diameter of 2.5-3.5 mm. Major exclusion criteria were: acute myocardial infarction, unstable arrhythmias, left ventricular ejection fraction less than or equal to 30%, restenotic lesions, lesions located in the left main coronary artery or in bifurcations involving a side branch greater than 2 mm, a second clinically or haemodynamically significant lesion in the target vessel, documentation of intracoronary thrombus, or initial TIMI 0 flow. All the study lesions were treated with the ABSORB BVS revision 1.1 (3.0×18 mm). Fifty percent of the cohort underwent scheduled invasive follow-up six months after the implantation, including OCT study whenever available at the participating site. The registry was approved by the ethics committee at each participating site, and each patient gave written informed consent before inclusion in the study.

Preclinical (Porcine) study

All experimentation conformed with the Animal Welfare Act, the Guide for Care and Use of Laboratory Animals (NIH Publication 85-23, 1996), and the Canadian Council on Animal Care regulations. All procedures were performed at AccelLab, Inc. (Montreal, Quebec, Canada), accredited by the Association for Assessment and Accreditation of Laboratory Animal Care (AAALAC) and in accordance with the protocol approved by the institutions animal care and use committee (IACUC).

Four Yucatan mini-swine implanted with BVS were used in this analysis. Animals were

administered oral acetylsalicylic acid (325 mg initial dose, 81 mg daily subsequently) and clopidogrel (300 mg initial dose and 75 mg daily subsequently) beginning three days prior to BVS implantation. Animals were tranquilised with ketamine (0.04 mg/kg), azaperone (4.0 mg/kg), and atropine (25 mg/kg) intramuscularly. Anaesthesia was achieved with propofol, (1.66 mg/kg IV), and maintained with inhaled isofluorane (1-3%) throughout the procedure. A vascular access sheath was placed in the femoral artery percutaneously. Before catheterisation, heparin (5,000 to 10,000 U) was injected to maintain an activated clotting time greater than 250 s. For each BVS deployment, an arterial segment was chosen so as to achieve a balloon-to-artery ratio of 1.1:1, ensuring full apposition based on angiographic assessment. Each animal received a single BVS revision 1.1 in one of the three main coronary arteries. Although a 3.0×12 mm BVS was used in the animal studies, the design was the same as that used in the clinical study. Animals recovered from anaesthesia under veterinary care for future time point analysis following the procedure. All the devices were imaged by OCT immediately after implantation and at 28-day follow-up.

Oct Image acquisition and analysis

In both animal and human procedures, OCT pullbacks were obtained at baseline and follow-up with a Fourier-domain C7 system using a Dragonfly™ catheter (St. Jude Medical Inc., Saint Paul, MN, USA) 10-15 µm axial and 20-40 µm lateral resolution[13] at a rotation speed of 100 frames/s with non-occlusive technique.[14]

After infusion of intracoronary nitroglycerine, the imaging wire was withdrawn by a motorised pullback at a constant speed of 20 mm/s, while Iodixanol 320 contrast (Visipaque™, GE Health Care, Cork, Ireland) was infused through the guiding catheter at a continuous rate of 2-4 mL/min.

A random sampling of 12 struts at each time point from both the animal and the human studies was selected using the following criteria: (1) OCT images were obtained with a Fourier-domain C7 system at both baseline and follow-up; (2) the luminal edge of the strut was perpendicular to the light source in order to minimise the effect of wire eccentricity and vessel-catheter misalignment; and (3) the strut was well-apposed.

Light intensity analysis was performed in the region surrounding the selected struts using ImageJ 1.43 u software (Wayne Rasband, National Institutes of Health, USA). The raw polar image was used to ensure that interpolation, dynamic range compression, or other image processing did not alter the signal and bias the analysis. Because the strut boundaries are expected to be found within the reflective frame, an intensity profile was created by averaging consecutive pixels aligned parallel to the frame boundary and spanning the whole reflective frame orthogonally through the frame boundaries beginning on the

adluminal side. Since the C7 system displays 500 A-lines per frame, 976 pixels per line, and a depth of field 5 mm, the axial dimension of a single pixel in raw polar coordinates is ca. 5.12 µm for *in vivo* coronary imaging with this OCT catheter. Using the catheter dimensions as a standard (0.89 mm), we measured the pixel/µm conversion factor at 5.05 µm and used this for the measurements herein. The result is a two-dimensional profile plot of intensity versus distance through the centre of the strut. The following interfaces were analysed (Figure 1): lumen-polymer, defined as the optical signal generated by the adluminal border of the strut at baseline (LP-bl); lumen-neointima-polymer, defined as the optical signal generated by the adluminal border of the strut at follow-up (LNP-fu); polymer-vessel wall, defined as the optical signal generated by the abluminal border of the well-apposed strut at baseline or follow-up (PV-bl; PV-fu); lumen-vessel wall, defined as the optical signal generated by the vessel wall of a strut-free sec- tor at baseline or follow-up (LV-bl; LV-fu).
The data corresponding to each interface were individually summarised in plots of optical intensity versus distance, where the origin of the plot was located at the point corresponding to the strut centre and zero optical intensity (Figure 2). The centre of the strut was determined as the point equidistant from the points at which the intensity signal exceeded a consistent threshold value at the strut interior side of the adluminal and abluminal interfaces.

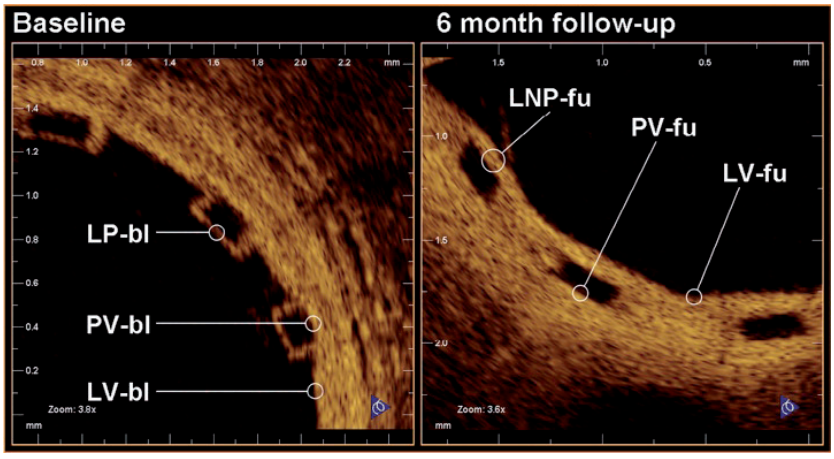

Figure 1. Denomination of the different optical interfaces analyzed.
LNP-fu: Lumen-neointima-polymer at follow-up; LP-bl: Lumen-polymer at baseline; LV-bl: Lumen-vessel at baseline; LV-fu: Lumen-vessel at follow-up; PV-bl: Polymer-vessel at baseline; PV-fu: Polymer-vessel at follow-up.

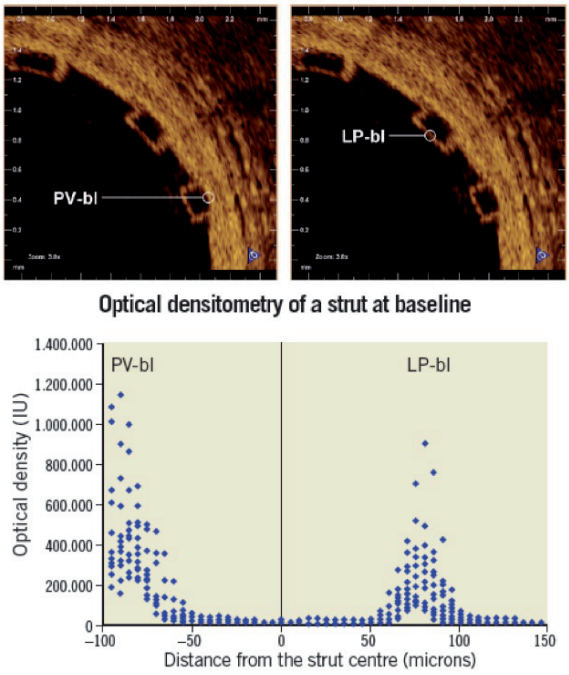

Figure 2. Graphic representation of the 12 struts analyzed at baseline.
The coordinate system origin is located at the calculated center of the strut (x-axis) and zero optical intensity (y-axis). The strut center is defined as the point equidistant to the rises of the adluminal (LP-bl interface) and abluminal (PV-bl interface) strut borders.
LP-bl: Lumen-polymer interface at baseline; PV-bl: Polymer-vessel interface at baseline.

The curves for each type of interface were fit to a Gaussian form given by:

$$f(x) = a\exp^{-(x-b)^2/2c^2},$$

where a is the maximum intensity of the curve, b is the midpoint of the Gaussian curve, and c is a function of the full-width-at-half-maximum (FWHM), namely $c = \mathrm{FWHM}/2\sqrt{2\ln(2)}$. Coefficients for the Gaussian curve fits were determined using an iterative least squares minimisation process (Figure 3). Gaussian curves were chosen to remain consistent with the practice commonly used for PSFs. Because the LSF differs from the PSF and includes scattering components, other functions commonly used to describe optical profiles, Lorentzian and exponential functions[15-17], were also evalu- ated and found inferior to the Gaussian fits (data not shown). Where tissue was present, the LSF was derived through

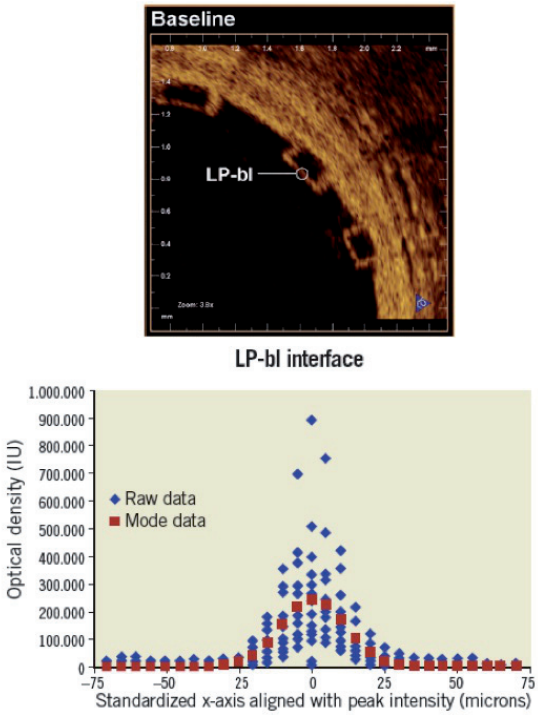

Figure 3. Lumen-polymer interface curve fit.
LP-bl: Lumen-polymer interface at baseline.

symmetry of a one-tailed Gaussian fit with the first peak defining the peak of the Gaussian function. Though the transition between polymer and tissue appears to be sigmoidal or step-like, mirroring a one-sided Gaussian function enabled comparison with the Gaussian fit of the uncovered strut. Additionally, the convolution of two Gaussian functions is a Gaussian function, and thus this best represented the optics of the system.

Two approaches were used to determine the location of strut interfaces. For struts without tissue coverage (e.g., LP-bl), the strut interface was assigned to the location of the peak of the signal intensity. The justification is that the high signal contrast of the LP interface represents an ideal LSF example, and the peak of the LSF defines the line. Alternatively, for interfaces adjacent to tissue (e.g., LNP-fu, PV-bl, PV-fu, LV-bl, LV-fu), the location of the half-max was assigned to the interface to represent the spatial location of intensity halfway between the low polymer intensity and high tissue intensity[18]. Because there was no normalisation of the intensity signal, the half-max was chosen to enable objective threshold based filtering. All strut width measurements were performed according to these definitions.

Statistical analysis

Non-linear least squares curve fits were compared with a Snedecor F-test using sum of squares for two separate curves and sum of squares of a single curve generated from combined data. Strut width measurements were compared using a two tailed Fisher's student t-test. All the analysis was performed with Microsoft Excel 2003, SP3 with solver toolkit.

RESULTS

Results in human

Twenty-four patients in the ABSORB Cohort B study received OCT at baseline and 6-month follow-up. In only 12 of these cases were the images acquired with a Fourier-domain C7 system. One strut meeting the selection criteria of the study was randomly selected for each OCT pullback (12 at baseline, 12 at follow-up).Across all types of interface, the FWHM of the signal was greatest for LV-fu (56.91 μm) and least for LP-bl at baseline (25.86 μm). Table 1 summarises the curve fit parameters for each interface type (Figures 4 and 5). Neointimal coverage of struts resulted in an increase of the FWHM, and the curves corresponding to LP-bl and LNP-fu interfaces differed significantly ($p<0.0001$, Table 2). There was no significant difference between LNP-fu and PV-fu interfaces (LNP-fu vs. PV-fu, $p=0.347$). However, the PV-bl interface differed significantly from the PV-fu interface (PV-bl vs. PV-fu, $p=0.0004$) as well as the LV-bl, LV-fu, and LPN-fu interfaces (PV-bl vs. LV-bl, $p<0.0001$; PV-bl vs. LV-fu, $p<0.0001$; PV-bl vs. LPN-fu, $p<0.0001$). Measuring from peak to half-max (PV-bl to PV-bl) and half-max to half-max (LNP-fu to PV-fu) for baseline and follow-up, respectively (Figure 6), the average strut thickness was 158±11 μm at baseline and 152±20 μm at the 6-month follow-up ($p=0.41$), both of which are similar to the nominal BVS strut thickness (ca. 152 μm for the backbone only and ca. 158 μm for the backbone and coating).

Table 1. Parameters characterizing the curve fit for each type of interface.

	Swine		Human	
Interface	Max Intensity	FWHM (μm)	Max Intensity	FWHM (μm)
LP-bl	303.33	22.24	244.78	25.86
PV-bl	1118.22	50.69	544.32	45.32
LV-bl	801.67	49.42	338.71	52.00
LNP-fu	635.54	60.71	475.06	38.89
PV-fu	542.40	54.37	490.91	42.97
LV-fu	681.54	54.00	739.27	56.91

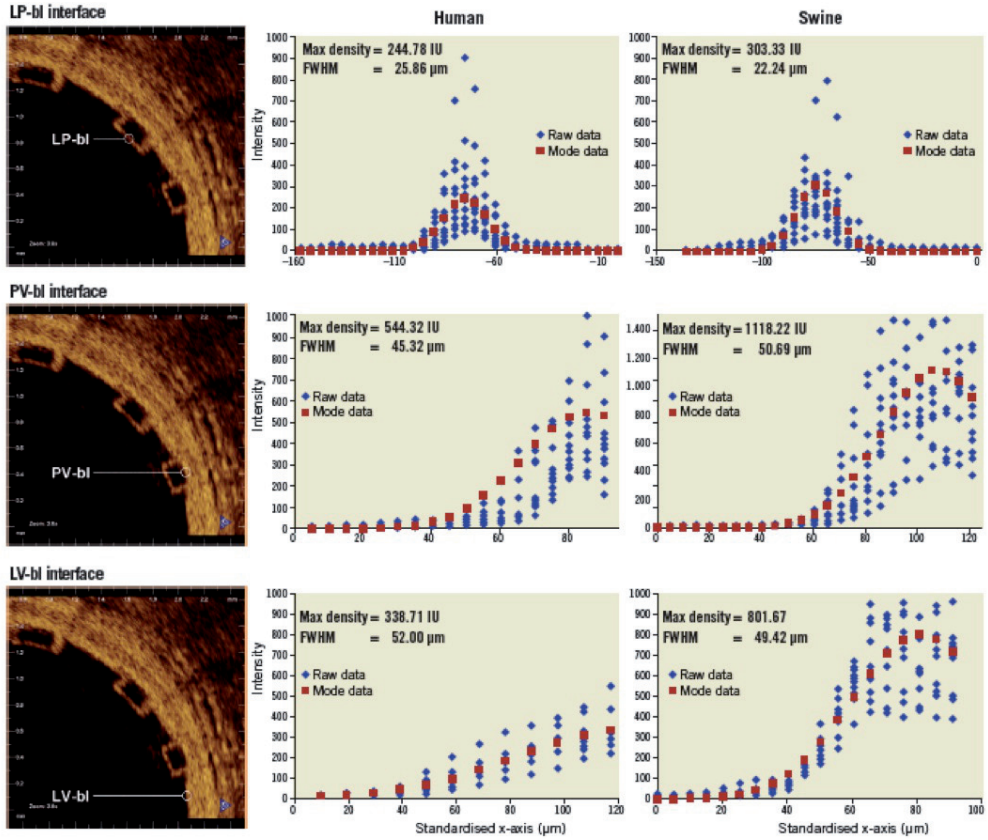

Figure 4. Fitting curves characterizing the different interfaces at baseline in human and swine studies.
FWHM: Full width at half max; LP-bl: Lumen-polymer at baseline; LV-bl: Lumen-vessel at baseline; PV-bl: Polymer-vessel at baseline.

Results In the swine Model

Three struts meeting the same selection criteria defined for the clinical sample were randomly selected in each of the four animals (12 at baseline, 12 at follow-up). The curve fit parameters for each interface had absolute values different than the ones reported in humans, but the same trends were observed.

Similar to the clinical samples, the FWHM increased when tissue was present. In swine samples, LNP-fu had the greatest FWHM at 60.71 µm, while LP-bl had the smallest FWHM

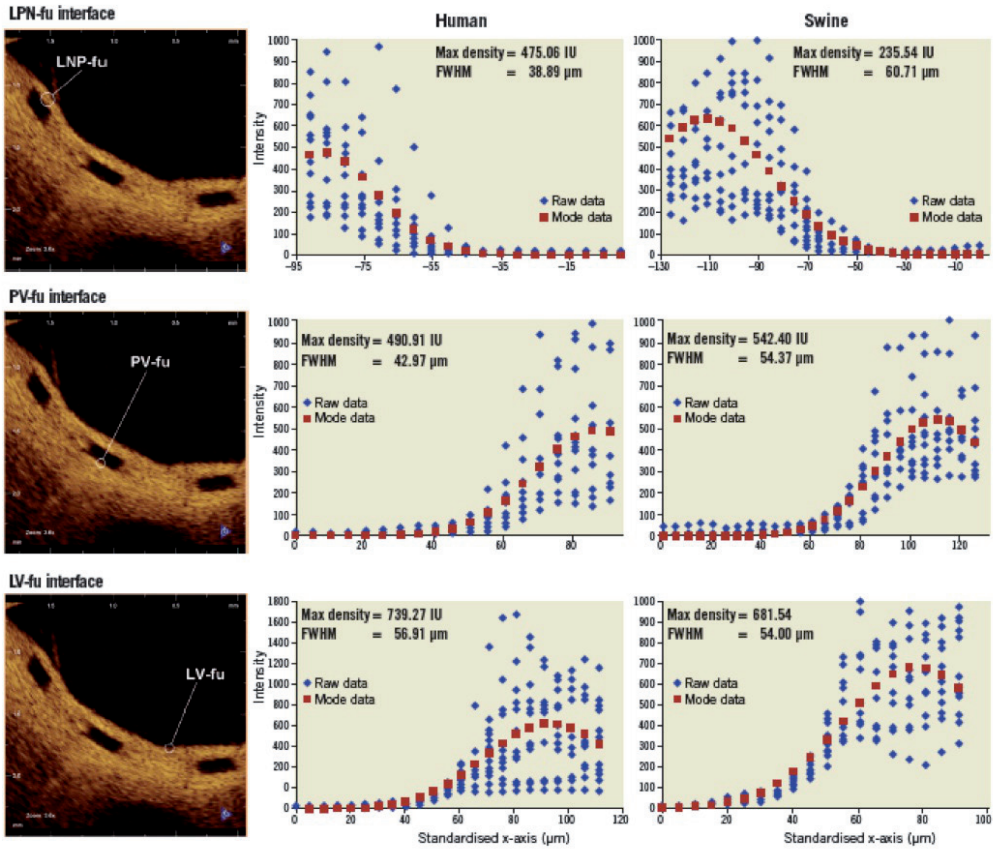

Figure 5. Fitting curves characterizing the different interfaces at follow-up in human (6 months) and swine (28 days) studies.
FWHM: Full width at half max; LNP-fu: Lumen-neointima-polymer at follow-up; LV-fu: Lumen-vessel at follow-up; PV-fu: Polymer-vessel at follow-up.

at 22.24. Table 1 summarises the curve fit parameters for each interface (Figures 4 and 5). Neointimal coverage of struts resulted in an increase of the FWHM when going from LP-bl to LNP-fu ($p<0.0001$, Table 2). Paralleling the human results, the LNP and PV interfaces had similar FHWM at the 28-day follow-up. All other curves were significantly different from each other with p values less than 0.01.

Based upon the previously defined edge detection algorithm, the average strut thickness was 164±14 µm at baseline and 172±16 µm at the 6-month follow-up ($p=0.28$).

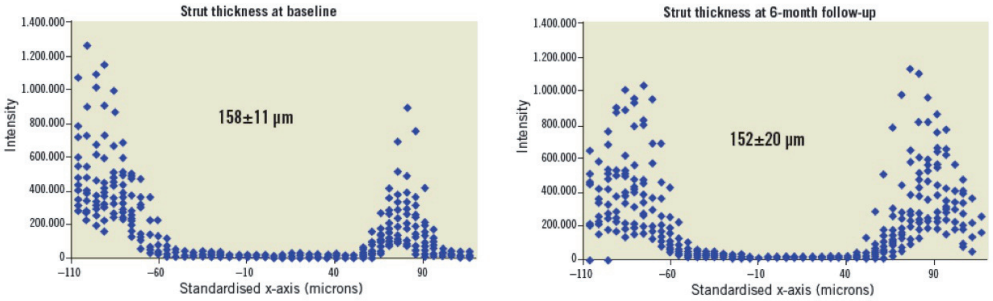

Figure 6. (a) Strut thickness measured from the peak intensity of the fitting curve for the adluminal interface to the half-max of the fitting curve for the abluminal interface at baseline, and (b) Strut thickness measured from the half-max of the fitting curve for the adluminal interface to the half-max of the fitting curve for the abluminal interface at follow-up (human data).

Table 2. Statistical comparison of curve fit: p-values from Snedecor F-tests.

Swine interface	LP-bl	PV-bl	LV-bl	LNP-fu	PV-fu	LV-fu
LP-bl	--	<0.0001	<0.0001	<0.0001	<0.0001	<0.0001
PV-bl		--	<0.0001	<0.0001	<0.0001	<0.0001
LV-bl			--	<0.0001	<0.0001	0.005
LNP-fu				--	0.99	<0.0001
PV-fu					--	<0.0001
LV-fu						--
Human interface	**LP-bl**	**PV-bl**	**LV-bl**	**LNP-fu**	**PV-fu**	**LV-fu**
LP-bl	--	<0.0001	<0.0001	<0.0001	<0.0001	<0.0001
PV-bl		--	<0.0001	<0.0001	0.0004	<0.0001
LV-bl			--	<0.0001	<0.0001	0.073
LNP-fu				--	0.347	<0.0001
PV-fu					--	<0.0001
LV-fu						--

DISCUSSION

The main findings of this study are: 1) the different interfaces between lumen, polymer, and vessel can be characterised *in vivo* according to the peak intensity and the FWHM of the Gaussian fit of the raw OCT intensity signal; 2) considering the half-max of the LSF as the strut boundary when it is adjacent to tissue, the strut thickness remains the same at all-time points and consistent with the nominal thickness of BVS struts given the resolution intrinsic to the OCT equipment.

To the best of our knowledge, this study is the first attempt to differentiate the interface between a translucent polymer and tissue on the basis of optical properties *in vivo*. It describes a methodology by which these interfaces may be defined that utilises LSFs to fit the raw OCT intensity signal and FWHM analysis to compensate for the convolution of polymer and tissue reflectivity.

The intensity of the OCT signal is a measurement of the back- scattering intensity of infrared light. The magnitude of changes in the refractive index on length scales greater than the wavelength of that light determines the backscattering intensity. In the case of a polymeric implant like the ABSORB BVS, a signal is produced at the boundary of the BVS strut, but there is no signal in the centre of the strut due to the homogeneity of the refractive index of the polymer.1,12 The FWHM of the axial reflectance at an interface has been reported as the true image resolution19. Though methodologies differ slightly from previous reports, the FHWM measurement for LP-bl reported here (22.24-25.86) may be consistent with the practical resolution of OCT *in vivo* for measurements of BVS struts. The absolute difference in the measured FWHM between human and swine is within the resolution of OCT. Additionally, slight variability in imaging catheters and the ability of the edge of the scaffold to be a perfect line could contribute to slight differences in the measured FWHM.

The LSF characterising the LP-bl interface is significantly different from that for interfaces where polymer is adjacent to tissue, because tissue increases backscattering in proximity to the interface and broadens the resulting backscattering signal. Hence, the FWHM increases. On the abluminal side of struts, the LSF also changes over time, as evidenced by the fact that the FWHM of the PV-bl and PV-fu interfaces differ significantly for both humans and swine.

Several factors may contribute to this result, including changes in the optical properties of the BVS near the interface or changes in the optical properties of the tissue due to pharmacological activity or foreign body response.Further bench and animal investigations will be needed to interrogate the mechanisms behind these observations.

As expected, the FWHM of the LNP-fu and PV-fu interfaces were not significantly different,

suggesting that optical changes at the BVS interface occur consistently in both locations over time.

Quantification of strut dimensions over time has been difficult due to the similarity of OCT backscattering signal from tissue and polymer. Utilisation of the LSF to characterise the OCT signal offers an objective tool by which the interface between tissue and polymer may be defined, resulting in a more consistent measurement of strut thickness.

According to the results reported here, no significant change in strut thickness is observed between baseline and six months, as the baseline measurements (158±11 μm) were similar to the reported thickness of the device (ca. 158 μm). The finding that the strut thickness remains stable over this time scale is also consistent with the previous OCT results where a gross estimate of "mean strut core area" did not change significantly between baseline and six months in a cohort of 25 patients.[12] Future investigation at longer time points will be required to evaluate changes in optical properties following further degradation and mass loss from the scaffold.

The second potential application of the LSF methodology applies to the objective assessment of tissue coverage of a BVS. Incomplete neointimal coverage of struts and incomplete endothelialisation are the morphologic features most strongly associated with stent thrombosis.[20] Although OCT has been validated for the assessment of neointimal coverage after stenting in animal models,[5-8] the inability to discriminate between neointima and fibrin/thrombus and the inability to detect endothelial rims thinner than the axial resolution of the equipment limit the specificity and the sensitivity of this technology, respectively. In metallic stents, the hyper-intense backscattering at the luminal edge of struts caused by the profound refractive index contrast between metal and tissue facilitates identification and accurate measurement of very thin layers of tissue covering the struts. Conversely, the assessment of tissue coverage of BVS is more challenging, because the refractive index contrast is less. For thin layers of tissue, the signal displayed is often indistinguishable from that generated by the LP interface alone, requiring more sophisticated signal processing to detect. In considering this issue, it is important to revisit the various length scales that frame the problem. Although OCT reflectivity can theoretically be caused by refractive index changes on a length scale as small as that of the wavelength of the OCT light (1.3 μm), the axial resolution of OCT is reported to be 10-15 μm[13], and the FWHM of the LP-bl signal was measured at 22-26 μm in the current study, The latter may rep- resent the practical resolution of OCT applied to polymeric materials. However, the presence of even thin layers of tissue broadens the FWHM, as reported herein, and consequently the LSF FWHM methodology might permit detection of tissue coverage even when the thickness of that coverage cannot be directly measured. A recent study demonstrated the potential of OCT analysis to discern between

tissue and fibrin/thrombus (i.e., specificity) in metallic stents.[10] The LSF FWHM approach may constitute a step forward in improving sensitivity and provide an objective criterion for the assessment of neointimal coverage of BVS struts.

Besides the objective assessment of neointimal coverage and the differential diagnosis between neointima and fibrin[10], the analysis of the raw linear OCT signal has been used to detect inflammation and to quantify the density of macrophages in the vessel wall[21,22]. An ongoing study is also using this technology to evaluate cardiac allograft vasculopathy (NCT01403142). All these fields constitute potential future applications for the hereby described LSF analysis, after adjusting the methodology. However, the diagnostic efficiency of LSF analysis is maximal when there exists a normal reference to compare: this uses to be readily available for study of intracoronary devices (post-implant study), but it can be substantially more problematic for the study of the non-stented vessel wall. Sub-cellular OCT appears as a more attractive alternative for the study of vessel inflammation and atherosclerosis in a near future[23].

Limitations

Contrary to previous optical intensity analysis,[10] the current study does not perform any normalisation of the signal intensity due to the lack of a reliable reference in the tissue or polymer. Therefore, the absolute intensity values are not directly comparable. The analysis was focused on the shape of the curves, represented by the LSF curve fit and FWHM calculation, which could explain the differences in absolute peak intensity between the human and swine results.

This study was performed on a random sampling of struts meeting specific inclusion criteria. This was necessary to circumvent challenging *in vivo* problems, such as signal attenuation due to eccentricity of the imaging catheter and differences in interpolation as a function of distance from the light source. The described methodology cannot be directly applied to struts not meeting these criteria, e.g., struts lying oblique to the light beam, which are in fact the majority of struts, but further investigations to adapt this methodology for more general use are underway. The LSF analysis of raw linear OCT signal can be performed on any conventional commercially available OCT system, using simple specific software, but this analysis is still experimental and must be performed offline manually by experienced investigators. The assessment of oblique struts will require alignment of measurements perpendicularly to the adluminal strut surface, calculation of the angle of this adluminal surface with the light beam, and eventually deriving a correction factor. Automation of the analysis protocol will be essential before it can be used more broadly. Future validation studies to identify cut-off values, sensitivity, specificity, and predictive capability are still unknown.

CONCLUSIONS

Fitting the raw OCT backscattering signal to a Gaussian LSF facilitates identification of the interfaces between BVS struts and lumen or tissue. The resulting analysis enables more precise and consistent measurement of BVS strut thickness, which for the ABSORB Cohort B BVS remains unchanged from baseline to the 6-month follow-up and not different from the nominal value. It may also allow inferential detection of neointimal coverage that might not be detected with- out the benefit of this more sophisticated signal processing.

REFERENCES

1. Serruys PW, Ormiston JA, Onuma Y, Regar E, Gonzalo N, Garcia-Garcia HM, Nieman K, Bruining N, Dorange C, Miquel-Hebert K, Veldhof S, Webster M, Thuesen L, Dudek D. A bioabsorbable everolimus-eluting coronary stent system (ABSORB): 2-year outcomes and results from multiple imaging methods. *Lancet*. 2009;373:897-910.
2. Onuma Y, Serruys PW, Perkins LE, Okamura T, Gonzalo N, Garcia-Garcia HM, Regar E, Kamberi M, Powers JC, Rapoza R, van Beusekom H, van der Giessen WJ, Virmani R. Intracoronary Optical Coherence Tomography and Histology at 1 Month and 2, 3,and 4 Years After Implantation of Everolimus-Eluting Bioresorbable Vascular Scaffolds in a Porcine Coronary Artery Model. An Attempt to Decipher the Human Optical Coherence Tomography Images in the ABSORB Trial. *Circulation*. 2010;122:2288-2300.
3. Oberhauser JP, Hossainy S, Rapoza RJ. Design principles and performance of bioresorbable polymeric vascular scaffolds. *EuroIntervention*. 2009;5:F15-F22.
4. Ormiston JA, Serruys PW, Regar E, Dudek D, Thuesen L, Webster MW, Onuma Y, Garcia-Garcia HM, McGreevy R, Veldhof S. A bioabsorbable everolimus-eluting coronary stent system for patients with single de-novo coronary artery lesions (ABSORB): a prospective open-label trial. *Lancet*. 2008;371: 899-907.
5. Suzuki Y, Ikeno F, Koizumi T, Tio F, Yeung AC, Yock PG, Fitzgerald PJ, Fearon WF. In vivo comparison between optical coherence tomography and intravascular ultrasound for detecting small degrees of in-stent neointima after stent implantation. *JACC Cardiovasc Interv*. 2008;1:168-173.
6. Deuse T, Erben RG, Ikeno F, Behnisch B, Boeger R, Connolly AJ, Reichenspurner H, Bergow C, Pelletier MP, Robbins RC, Schrepfer S. Introducing the first polymer-free leflunomide eluting stent. *Atherosclerosis*. 2008;200:126-134.
7. Prati F, Zimarino M, Stabile E, Pizzicannella G, Fouad T, Rabozzi R, Filippini A, Pizzicannella J, Cera M, De Caterina R. Does optical coherence tomography identify arterial healing after stenting? An in vivo comparison with histology, in a rabbit carotid model. *Heart*. 2008;94:217-221.
8. Murata A, Wallace-Bradley D, Tellez A, Alviar C, Aboodi M, Sheehy A, Coleman L, Perkins L, Nakazawa G, Mintz G, Kaluza GL, Virmani R, Granada JF. Accuracy of optical coherence tomography in the evaluation of neointimal coverage after stent implantation. *JACC Cardiovasc Imaging*. 2010;3:76-84.
9. Guagliumi G, Sirbu V. Optical coherence tomography: high resolution intravascular imaging to evaluate vascular healing after coronary stenting. *Catheter Cardiovasc Interv.* 2008;72:237-247.
10. Templin C, Meyer M, Muller MF, Djonov V, Hlushchuk R, Dimova I, Flueckiger S, Kronen P, Sidler M, Klein K, Nicholls F, Ghadri JR, Weber K, Paunovic D, Corti R, Hoerstrup SP, Luscher TF, Landmesser U. Coronary optical frequency domain imaging (OFDI) for in vivo evaluation of stent healing: comparison with light and electron microscopy. *Eur Heart J.* 2010;31:1792-1801.
11. Rossmann K, LUBBERTS G, Cleare H.M. Measurement of the Line Spread-Function of Radiographic Systems Containing Fluorescent Screens. *J Opt Soc Am.* 1964;54:187-189.
12. Serruys PW, Onuma Y, Ormiston JA, De Bruyne B, Regar E, Dudek D, Thuesen L, Smits PC, Chevalier B, McClean D, Koolen J, Windecker S, Whitbourn R, Meredith I, Dorange C, Veldhof S, Hebert KM, Rapoza RJ, Garcia-Garcia HM. Evaluation of the second generation of a bioresorbable everolimus drug-eluting vascular scaffold for treatment of de novo coronary artery stenosis: 6-month clinical and imaging outcomes. *Circulation.* 2010;122:2301-2312.
13. Bezerra HG, Costa MA, Guagliumi G, Rollins AM, Simon DI. Intracoronary optical coherence tomography: a comprehensive review clinical and research applications. JACC Cardiovasc Interv. 2009;2:1035-1046.
14. Prati F, Cera M, Ramazzotti V, Imola F, Giudice R, Giudice M, Propris SD, Albertucci M. From bench to bedside: a novel technique of acquiring OCT images. Circ J. 2008;72:839-843.

15. Davis CC. Lasers and electro-optics: fundamentals and engineering. New York, N.Y.: Cambridge University Press; 1996.
16. Yang Yr, Wanek J, Shahidi M. Representing the retinal line spread shape with mathematical functions. J Zhejiang Univ Sci B.2008;9:996-1002.
17. Peng Y, Lu R. Modeling multispectral scattering profiles for prediction of apple fruit firmness. Trans ASAE. 2005;48:235-242.
18. Amirav I, Kramer SS, Grunstein MM, Hoffman EA. Assessment of methacholine-induced airway constriction by ultrafast high-resolution computed tomography. J Appl Physiol. 1993;75:2239-2250.
19. Jang IK, Bouma BE, Kang DH, Park SJ, Park SW, Seung KB, Choi KB, Shishkov M, Schlendorf K, Pomerantsev E, Houser SL, Aretz HT, Tearney GJ. Visualization of coronary atherosclerotic plaques in patients using optical coherence tomography: comparison with intravascular ultrasound. J Am Coll Cardiol. 2002;39:604-609.
20. Finn AV, Joner M, Nakazawa G, Kolodgie F, Newell J, John MC, Gold HK, Virmani R. Pathological Correlates of Late Drug-Eluting Stent Thrombosis: Strut Coverage as a Marker of Endothelialization. Circulation. 2007;115:2435-2441.
21. Tearney GJ, Yabushita H, Houser SL, Aretz HT, Jang IK, Schlendorf KH, Kauffman CR, Shishkov M, Halpern EF, Bouma BE. Quantification of Macrophage Content in Atherosclerotic Plaques by Optical Coherence Tomography. Circulation. 2003;107:113-119.
22. MacNeill BD, Jang IK, Bouma BE, Iftimia N, Takano M, Yabushita H, Shishkov M, Kauffman CR, Houser SL, Aretz HT, DeJoseph D, Halpern EF, Tearney GJ. Focal and multi-focal plaque macrophage distributions in patients with acute and stable presentations of coronary artery disease. J Am Coll Cardiol. 2004;44:972-979.
23. Liu L, Gardecki JA, Nadkarni SK, Toussaint JD, Yagi Y, Bouma BE, Tearney GJ. Imaging the subcellular structure of human coronary atherosclerosis using micro-optical coherence tomography. Nat Med. 2011;17:1010-1014.

PART
II

Chapter 10

Six-Month Clinical Outcome Following the Implantation of the Bioresorbable Everolimus Eluting Vascular Scaffold in Vessels Smaller or Larger than 2.5 mm

Roberto Diletti, MD; Yoshinobu Onuma, MD; Vasim Farooq, MBChB, MRCP; Josep Gomez-Lara, MD; Salvatore Brugaletta, MD; Robert Jan van Geuns, MD PhD; Evelyn Regar, MD PhD; Bernard de Bruyne, MD; Dariusz Dudek, MD; Leif Thuesen, MD, FACC; Bernard Chevalier, MD; Dougal McClean, MD; Stephan Windecker, MD, PhD; Robert Whitbourn, MD;Pieter Smits, MD, PhD; Jacques Koolen, MD; Ian Meredith, MBBS, PhD, FACC; Dong Li, MSc; Susan Veldhof, RN; Richard Rapoza, PhD; Hector M. Garcia-Garcia, MD, PhD, FACC; John A. Ormiston, MBChB, PhD; Patrick W. Serruys, MD, PhD, FACC

J Am Coll Cardiol 2011 Jul 12;58(3):258-64

ABSTRACT

Objectives We investigate the six month clinical outcome after implantation of a second generation 3.0mm Bioresorbable Everolimus-eluting Vascular Scaffolds (BVS) in small coronary vessels (<2.5mm).

Background BVS are a novel approach to treating coronary lesions and are untested in small vessels.

Methods The ABSORB Cohort B Trial is a multicentre single-arm, prospective, open-label trial in which 101 patients were enrolled. The pre-procedural RVD was assessed by quantitative coronary angiography during post-hoc analysis. The vessel size was overestimated, by visual assessment, in 41 patients prior to implantation of a 3.0mm BVS in vessels with a pre-procedural reference vessel diameter (RVD) <2.5mm.

The study population was divided into two groups, group I (41 patients) with RVD <2.5mm and group II (60 patients) with RVD ≥2.5 mm. The composite endpoint of ischemia-driven major adverse cardiac events (ID-MACE), defined as ischemia-driven target lesion revascularization (ID-TLR), myocardial infarction (MI) or cardiac death, were assessed. Out of the 45 patients scheduled for 6 month coronary angiography, 42 patients had the procedure performed with IVUS undertaken in 40 of these patients.

Results At 6 months no significant differences in ID-MACE (3/41, 7.3% vs. 2/60 cases, 3.3% p=0.3933) were observed in the small and large vessel groups respectively. No cardiac deaths or episodes of in-scaffold thromboses were seen. Angiographic and IVUS follow-up demonstrated no differences in late lumen loss (0.16±0.18mm vs. 0.21±0.17mm, p=0.3525) or percentage lumen area stenosis (17.6±6.0% vs. 19.8±8.5%, p=0.3643).

Conclusion The second generation 3.0mm BVS appears to be safe in small vessels with similar clinical and angiographic outcomes compared to large vessels.

INTRODUCTION

Fully bioresorbable drug-eluting vascular scaffolds (BVS, Abbott Vascular, Santa Clara, CA, USA) are a novel approach to treating coronary lesions in that they provide transient vessel support and drug delivery to the vessel wall. The first generation BVS demonstrated slightly higher acute and late recoil when compared to conventional metallic stents. [1,2] To further enhance support of the vessel wall, the strut design and the manufacturing processes of the polymer were modified, leading to the BVS revision 1.1; this device was subsequently investigated in the ABSORB Cohort B trial. Because of the single size availability of the BVS (3.0 mm in diameter), the target lesions were required to be located in vessels with a visual estimated vessel diameter of ≥2.5 mm and ≤3.3 mm. However, during the clinical use of the BVS, more than one third of the scaffolds were found to have been deployed in vessels with a pre-procedural reference vessel diameter (RVD) <2.5 mm. This protocol violation has provided the opportunity to assess the performance of the 3.0 mm BVS device in these vessels.

The purpose of this substudy is therefore to investigate the clinical and angiographic outcomes after implantation of the new generation of BVS in small coronary vessels (RVD < 2.5 mm).

METHODS

Study design and population

The study design and device have previously been described [3]. In brief, a total of 101 patients were enrolled in the ABSORB Cohort B study and implanted with a 3mm BVS. Assessment of vessel size prior to BVS implantation was made by visual estimation of the operator. In the present post hoc analysis, the study population was divided into two groups based on the RVD prior to intervention. Group I included 41 patients (41 lesions) with a RVD <2.5mm and group II included 60 patients (61 lesions) with a RVD mm ≥2.5 mm. Out of the 45 patients initially scheduled for 6 and 24-month coronary angiography, 42 patients underwent the procedure at 6-month follow-up with IVUS analyses being performed in 40 cases.

QCA and IVUS analysis

In all patients, analyses were undertaken by quantitative coronary angiography (QCA) using the Coronary Angiography Analysis System (Pie Medical Imaging, Maastricht, Netherlands). The reference vessel diameter was obtained by the interpolated method.

[4] Post procedural and follow-up scaffold segments were analyzed with phased array intravascular ultrasound (IVUS) catheters (EagleEye; Volcano Corporation, Rancho Cordova, CA, USA), with an automated pullback of 0.5 mm per second. Images were analyzed off-line with semiautomatic contours detection provided by dedicated software, as previously reported. (3)

Statistical analysis

Categorical variables are presented as counts and percentages. Continuous variables are presented as means ± SD. P-values are calculated with Fisher's Exact test for binary variables and Wilcoxon's Rank Sum test for continuous variables. All p-values are calculated for descriptive purposes and do not form part of formal hypothesis tests. Statistical analyses were performed using SAS (version 9.1.3).

RESULTS

Baseline Characteristics and Procedural Outcome

In the ABSORB Cohort B Trial, 101 patients were enrolled and 102 lesions treated with implantation of a BVS. 41 lesions had a RVD <2.5 mm and 61 lesions a RVD ≥2.5 mm (Figure 1). In the small vessel group, 34 (83%) lesions were located in the mid or distal part of main coronary arteries or in secondary branches. No significant differences in baseline demographics or clinical and angiographic characteristics were seen in both groups (Tables 1-2). Comparable pre-procedural percentage diameter stenoses (57.0±9.3% vs. 60.3±10.3%, p =0.1000) and post-procedural acute gains (1.21±0.30 mm vs. 1.25mm±0.33 mm, p= 0.4946) were observed.

Clinical Outcomes

No statistically significant differences were observed in the incidences of both in-hospital (small vessel group: 2/41 cases, 4.9% and large vessel group 0/60 cases, 0%, p=0.1624) and 6 month (small vessel group: 3/41 cases, 7.3% and large vessel group 2/60 cases, 3.3%, p=0.3933) MACE in both groups (Table 3). At 6 months, the incidences of ischemia driven TLR (1/41 patients, 2.4% vs. 1/60 patients, 1.7%, p=1.0000), TVR (2.6% vs. 1.7%, p=1.0000), and myocardial infarction (2/41 patients, 4.9% vs. 1/60 patients, 1.7%, p=0.5645) were similar in both groups with no cardiac deaths observed. At 6 months no episodes of scaffold thromboses, as defined by the Academic research Consortium (ARC)[5] definition, were reported. One episode of a non-ischemic driven TLR event was seen in the large vessel group.

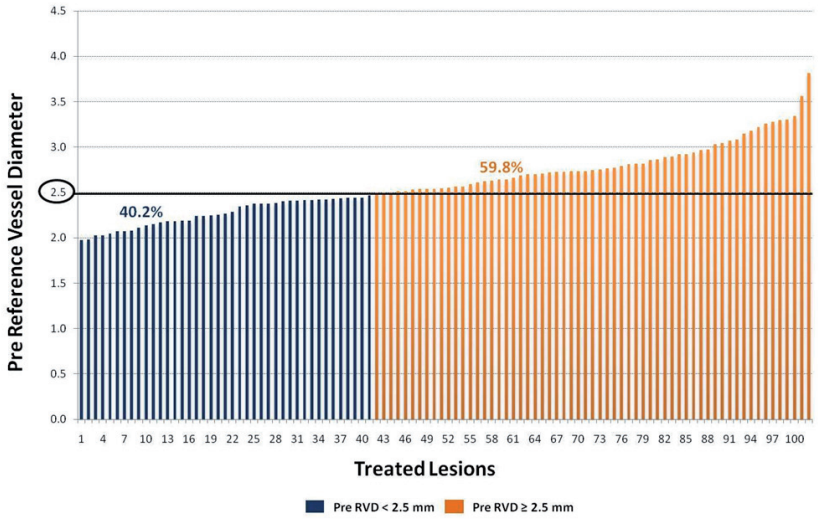

Figure 1. Distribution of Pre-Implantation RVD in ABSORB Cohort B Trial Population.
More than one-third of the treated lesions (40.2%) in the ABSORB Cohort B trial had a pre-implantation reference vessel diameter (RVD) 2.5 mm.

Table 1. Baseline characteristics in intention–to-treat (ITT) population.

	Small Vessels (<2.5mm) (N=41)	Large Vessels (>=2.5mm) (N=60)	P-value
Age (yrs)	62.4 ± 9.4 (41)	62.2 ± 8.7 (60)	0.9193
Male Gender	63.4% (26/41)	78.3% (47/60)	0.1169
Current Tobacco Use	22.0% (9/41)	13.6% (8/59)	0.2917
Diabetes	22.0% (9/41)	13.3% (8/60)	0.2875
Hypertension Requiring Medication	58.5% (24/41)	64.4% (38/59)	0.6757
Hypercholesterolemia Requiring Medication	85.4% (35/41)	73.3% (44/60)	0.2196
Family History of Coronary Artery Disease	60.5% (23/38)	50.8% (30/59)	0.4065
Prior PTCA	14.6% (6/41)	25.0% (15/60)	0.3180
Prior CABG	2.4% (1/41)	3.3% (2/60)	1.0000
Prior MI	17.5% (7/40)	30.0% (18/60)	0.2382
Target Vessel			
RCA	31.7% (13/41)	34.4% (21/61)	0.8326
LAD	46.3% (19/41)	41.0% (25/61)	0.6845
LCX	19.5% (8/41)	24.6% (15/61)	0.6332
American College of Cardiology/American Heart Association (ACC/AHA) Lesion Class			
A	0.0% (0/40)	1.7% (1/60)	1.0000
B1	52.5% (21/40)	56.7% (34/60)	0.6878
B2	45.0% (18/40)	36.7% (22/60)	0.4143
C	2.5% (1/40)	5.0% (3/60)	0.6479

Table 2. Baseline QCA characteristics pre and post procedure in intention–to-treat (ITT) population.

	Small Vessels (<2.5mm) (N=41)	Larg Vessels (>=2.5mm) (N=60)	Difference [95% CI]	P-value
Pre Procedure				
Reference Vessel Diameter (mm)	2.27 ± 0.15 (41)	2.83 ± 0.29 (61)	-0.56 [-0.65, -0.48]	<0.0001
Minimal Luminal Diameter (mm)	0.97 ± 0.20 (39)	1.12 ± 0.30 (59)	-0.15 [-0.25, -0.05]	0.0044
Percent Diameter Stenosis (%)	57.0 ± 9.3 (39)	60.3 ± 10.3 (59)	-3.3 [-7.3, 0.7]	0.1000
Post-Procedure				
In-Scaffold Minimal Luminal Diameter (mm)	2.17 ± 0.22 (41)	2.37 ± 0.23 (61)	-0.21 [-0.30, -0.12]	<0.0001
In-Scaffold Percent Diameter Stenosis (%)	13.8 ± 4.0 (41)	16.2 ± 6.7 (61)	-2.4 [-4.5, -0.3]	0.0280
In-Scaffold Acute Gain (mm)	1.21 ± 0.30 (39)	1.25 ± 0.33 (59)	-0.04 [-0.17, 0.08]	0.4946

Table 3. Adverse Events at 6-Month Follow-Up.

	Small Vessels (<2.5mm) (N=41)	Large Vessels (>=2.5mm) (N=60)	P-value
ID-MACE (Cardiac Death, MI, ID-TLR)	7.3% (3/41)	3.3% (2/60)	0.3933
Cardiac Death	0.0% (0/41)	0.0% (0/60)	NA
Myocardial Infarction (MI)	4.9% (2/41)	1.7% (1/60)	0.5645
QWMI	0.0% (0/41)	0.0% (0/60)	NA
NQWMI	4.9% (2/41)	1.7% (1/60)	0.5645
ID-TLR	2.4% (1/41)	1.7% (1/60)	1.0000
CABG	0.0% (0/41)	0.0% (0/60)	NA
PCI	2.4% (1/41)	1.7% (1/60)	1.0000
Non ID-TLR	0.0% (0/41)	0.0% (0/60)	NA
CABG	0.0% (0/41)	0.0% (0/60)	NA
PCI	0.0% (0/41)	1.7% (1/60)	1.0000

Table 4. QCA Analysis at Baseline and 6-Month Follow-Up.

	Small Vessels (<2.5mm) (N=20)	Large Vessels (>=2.5mm) (N=25)	Difference [95% CI]	P-value
Baseline QCA Analysis				
Pre-Procedure				
Reference Vessel Diameter (mm)	2.24 ± 0.17 (20)	2.96 ± 0.33 (25)	-0.72 [-0.88, -0.57]	<0.0001
Minimal Luminal Diameter (mm)	0.93 ± 0.22 (19)	1.15 ± 0.35 (25)	-0.22 [-0.40, -0.04]	0.0154
Percent Diameter Stenosis (%)	58.0 ± 11.1 (19)	60.8 ± 11.9 (25)	-2.8 [-9.9, 4.2]	0.4216
Post-Procedure				
In-Scaffold Acute Gain (mm)	1.23 ± 0.37 (19)	1.29 ± 0.35 (25)	-0.05 [-0.28, 0.17]	0.6269
6-Month QCA Analysis				
In-Scaffold Late-Loss (mm)	0.16 ± 0.18 (19)	0.21 ± 0.17 (23)	-0.05 [-0.16, 0.06]	0.3525
In-Scaffold Percent Diameter Stenosis (%)	18.1 ± 7.2 (19)	20.2 ± 8.0 (23)	-2.1 [-6.8, 2.6]	0.3736
In-Scaffold Binary Restenosis	0.0% (0/19)	0.0% (0/23)	0.00% [Assump. not met]	NA

Six-month angiographic and IVUS results

QCA analyses at six-month were available in 42 patients (small vessel group: n=19, large vessel group: n=23). No statistical differences in-scaffold percentage diameter stenosis (18.1±7.2% vs. 20.2±8.0%, p=0.3736) and in scaffold late loss (0.16±0.18 mm vs. 0.21±0.17 mm, p=0.3525) were observed between both groups. No cases of binary restenosis within the scaffold were evident in either group. (Table 4)

Grey-scale IVUS analysis (from 42 patients) demonstrated no statistically significant differences in the lumen area stenosis (17.6 ± 6.0 % vs. 19.8 ± 8.5 %, p=0.3643) or neointimal hyperplasia (NIH) area (0.06±0.12 mm^2 vs. 0.09±0.12 mm^2, p=0.4084) between the two groups. (Table 5).

However the comparison of IVUS results is limited by the small number of available data; a post-hoc power analysis showed that with this sample size, a difference in NIH area of 0.11 mm^2 could be detected with 80% power.

Table 5. IVUS Analysis at Baseline and 6-Month Follow-Up.

	Small Vessels (<2.5mm) (N=20)	Large Vessels (>=2.5mm) (N=25)	Difference [95% CI]	P-value
Baseline IVUS Analysis				
Average Vessel Area (mm^2)	11.85 ± 3.36 (18)	16.40 ± 2.87 (22)	-4.55 [-6.59, -2.52]	<0.0001
Average Lumen Area (mm^2)	5.84 ± 0.99 (18)	7.22 ± 0.96 (22)	-1.38 [-2.01, -0.75]	<0.0001
Average Scaffold Area (mm^2)	5.86 ± 0.98 (18)	7.16 ± 0.92 (22)	-1.30 [-1.91, -0.68]	0.0001
Average Plaque Area (mm^2)	6.01 ± 2.66 (18)	9.18 ± 2.29 (22)	-3.17 [-4.79, -1.55]	0.0003
6 Months IVUS Analysis				
Average Vessel Area (mm^2)	12.46 ± 3.26 (19)	16.28 ± 2.75 (21)	-3.82 [-5.76, -1.88]	0.0003
Average Lumen Area (mm^2)	5.79 ± 0.93 (19)	6.87 ± 0.96 (21)	-1.08 [-1.68, -0.47]	0.0009
Average Scaffold Area (mm^2)	5.84 ± 0.91 (19)	6.94 ± 0.94 (21)	-1.10 [-1.69, -0.51]	0.0006
Average Plaque Area (mm^2)	6.67 ± 2.53 (19)	9.41 ± 2.15 (21)	-2.74 [-4.26, -1.23]	0.0008
Minimal Lumen Area (mm^2)	4.78 ± 0.90 (19)	5.49 ± 0.87 (21)	-0.72 [-1.28, -0.15]	0.0143
Lumen Area Stenosis (%)	17.6 ± 6.0 (19)	19.8 ± 8.5 (21)	-2.1 [-6.8, 2.6]	0.3643
Area Obstruction (%)	1.1 ± 2.2 (19)	1.4 ± 1.9 (21)	-0.3 [-1.6, 1.0]	0.6363
Neointimal Hyperplasia Area (mm^2)	0.06 ± 0.12 (19)	0.09 ± 0.12 (21)	-0.03 [-0.11, 0.05]	0.4084

Case Descriptions of MACE and Non ID-TLR Events

In the small vessel group, 3 MACE events were reported. In the first patient (RVD 2.05 mm), six-month scheduled angiography disclosed a proximal edge stenosis in the mid RCA subsequently treated. Of note is that during the index procedure, the operator had deeply inserted the Amplatz guide catheter into the mid RCA; the possibility of endothelial denudation therefore cannot be excluded as a potential cause of the restenosis. In the second patient (RVD 2.15mm) predilatation of the lesion provoked a dissection which became occlusive after incomplete lesion coverage with the BVS. Subsequent bailout stenting was performed. The peak value of troponin was 0.8 µg/ml (ULN < 0.03 ng/ml), CK: 521 U/L (ULN < 180 U/L) and CK-MB: 48 U/L (ULN < 5 U/L) and was adjudicated as peri-

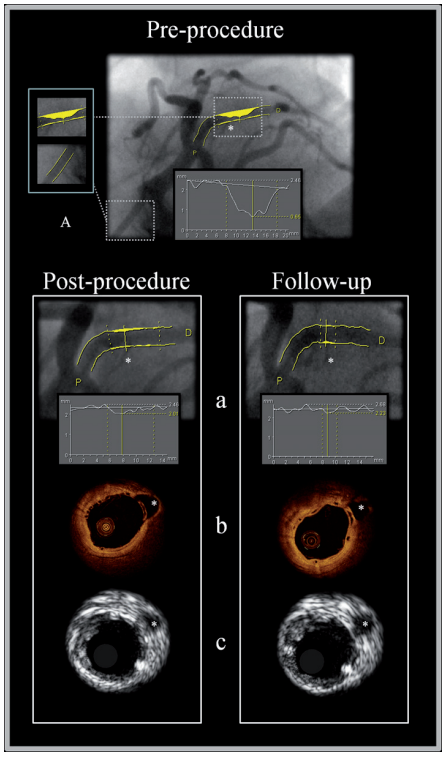

Figure 2. Small Vessel Treated With Implantation of BVS
Angiographic, optical coherence tomography (OCT), and intravascular ultrasound (IVUS) images before procedure, after procedure, and at 6-month follow-up are shown. The images show an example of a small vessel treated with a bioresorbable drug-eluting vascular scaffold (BVS) (pre-RVD 2.24 mm). (A) A visual comparison between the vessel-treated segment and a 6-Fr catheter (1.98 mm) is highlighted. Pre-procedural angiography and quantitative coronary angiography (QCA) analysis revealed a minimal lumen diameter (MLD) of 0.65 mm. Post-procedural angiography (left panel) and QCA analysis demonstrated an MLD of 2.01 mm. At the 6-month follow-up (right panel), the MLD was 2.23 mm. For illustrative purposes, the OCT (B) and IVUS (C) images are presented. These are corresponding frames taken from the MLD. A small side branch (*) located at the post-procedural MLD was used as a landmark for accurate matching of the images among different imaging modalities (angiography,

procedural NQMI. In the third patient (RVD 2.18 mm) a non-occlusive dissection occurred after lesion predilatation; the dissection was however fully covered with a BVS. The ECG remained unremarkable. Subsequent troponin, CK and CK-MB levels however peaked at 0.81 µg/L (ULN <0.03 µg/L), 667 U/L (ULN < 150 U/L) and 97.2 ng/ml (ULN < 4 ng/ml) respectively. In the large vessel group, 2 MACE were reported. In the first patient (RVD 2.51 mm) a BVS was implanted in the LAD with a myocardial bridge. Three months later, the patient presented with recurrent angina. Repeat coronary angiography demonstrated a diameter stenosis of 40% and 85% in diastole and systole respectively, resulting in the implantation

of a metallic everolimus-eluting stent. In the second patient (RVD 2.74 mm) an iatrogenic non Q-wave MI (CK 600 U/L, CK-MB 72 U/L, ≥2X upper limit of normal) was caused by thrombus formation following an IVUS examination during a failed attempt at imaging the vessel with OCT.

In a separate patient, a 3.0 mm BVS was post-dilated with a larger 3.5mm semi-compliant balloon to 16 atm (expected diameter: 3.96 mm). Post procedural OCT revealed several scaffold pattern irregularities but with a 20% diameter stenosis, consequently no further intervention was carried out. Thirty-three days later the patient was readmitted due to recurrent nocturnal chest pain. Coronary angiography demonstrated a non-significant diameter stenosis of 23%. OCT however revealed multiple scaffold pattern irregularities in the proximal half of the BVS with several strut cross sections appearing in the middle of the lumen. A 3.5 mm drug eluting stent was deployed in the proximal BVS with a satisfactory result. This event was adjudicated as being a non-ischaemic driven TLR by the Clinical Events Committee (CEC).

DISCUSSION

The present sub-study of ABSORB Cohort B is the first to report the use of a completely bioresorbable everolimus eluting scaffold in the setting of small vessel disease. The major findings of this sub-study are as follows: 1) patients who underwent BVS implantation in small vessels had 6-month clinical outcomes similar to patients who underwent the procedure in large vessels; 2) implantation of small vessels with a 3mm BVS was associated with an equivalent late luminal loss, percentage diameter stenosis and binary restenosis rates, compared to large vessels.

Small vessel coronary artery disease is a recognised challenging subset within the field of coronary artery intervention in that balloon angioplasty and bare metal stents have previously demonstrated unacceptable rates of restenosis and MACE. [6,7] The use of DES in this setting have however lead to more acceptable long-term results, although important differences in types of DES appear to exist. [8,9]

In the present study despite the implantation of larger (3.0mm) BVS in small vessels (<2.5 mm), no significant differences in clinical outcomes were observed in both groups at 6 months. In the small vessel group all 3 cases may possibly have been explained by procedural related complications and not due to device failure itself. However due to the small sample size and low incidence rate in this study, caution should be made in making firm conclusions with regards to the safety and efficacy.

A high degree of vessel stretch and injury, smaller post-procedural lumen area and a high

metal density have all previously been proposed as contributing factors to explain the poorer outcomes associated with small vessels [10]. Current consensus however is that the so called "bigger-is-better" paradigm [11] is likely to be the most plausible mechanism to explain the poorer outcomes associated with small vessel disease. Effectively, a smaller vessel size would be less able to accommodate the same absolute volume of NIH as a larger vessel, with the resultant increase in the rate of binary restenosis. The other potential concern is the thickness of the BVS struts (150 micrometers), as previous studies have suggested a link between thicker struts and an increased risk of restenosis; [12] these concerns however did not appear to be evident in this present study.

Vessels with RVD < 2.5 mm were treated with a 3.0 mm BVS scaffold pre-mounted on a 3.0 mm diameter balloon. This factor may have played a role in the similar angiographic and clinical outcomes observed between the two groups. Further study of this device is currently being undertaken in the multicentre, ABSORB Extend Single Arm Study where the introduction of a 2.5 mm BVS device is planned. This 2.5 mm BVS device is actually the same scaffold as the 3.0 mm but crimped onto a smaller 2.5 mm balloon and is intended for the treatment of vessels ≥2.0 mm and ≤3.0 mm. This may aid in further understanding as to whether the impact of a larger (3.0 mm) deployment balloon size played any significant role in the excellent outcomes seen with the device in small vessels.

It would therefore appear that the concerns of BVS implantation in small vessels may not be justified, whereas the risk of excessive post-dilatation of the BVS appears to be of more concern. Appropriate sizing of the vessel with QCA analysis and respect for the maximal diameter limits of the BVS are therefore currently required.

Study limitations

The present study is a post-hoc analysis and the number of patients is limited. Therefore *p* values presented are exploratory and should be interpreted with caution. Secondly, coronary angiography is limited to the detection of the lumen contour without taking into account the actual vessel size. IVUS allows assessment of the vessel size, this however was not performed prior to the BVS implantation in the present study.

CONCLUSION

The 3.0 mm bioresorbable vascular everolimus eluting scaffold appears to be safe and effective in small vessels, with similar clinical and angiographic outcomes observed when compared to large vessels.

REFERENCES

1. Tanimoto S, Serruys PW, Thuesen L, et al. Comparison of in vivo acute stent recoil between the bioabsorbable everolimus-eluting coronary stent and the everolimus-eluting cobalt chromium coronary stent: insights from the ABSORB and SPIRIT trials. Catheter Cardiovasc Interv 2007;70:515-23.
2. Tanimoto S, Bruining N, van Domburg RT, et al. Late stent recoil of the bioabsorbable everolimus-eluting coronary stent and its relationship with plaque morphology. J Am Coll Cardiol 2008;52:1616-20.
3. Serruys PW, Onuma Y, Ormiston JA, et al. Evaluation of the second generation of a bioresorbable everolimus drug-eluting vascular scaffold for treatment of de novo coronary artery stenosis: six-month clinical and imaging outcomes. Circulation;122:2301-12.
4. Reiber JH, Serruys PW. Quantitative Coronary Angiography: Methodologies. Quantitative Coronary Angiography. Dordrecht, The Netherlands: Kluwer Academic Publishers, 1991:98-102.
5. Cutlip DE, Windecker S, Mehran R, et al. Clinical end points in coronary stent trials: a case for standardized definitions. Circulation 2007;115:2344-51.
6. Elezi S, Kastrati A, Neumann FJ, Hadamitzky M, Dirschinger J, Schomig A. Vessel size and long-term outcome after coronary stent placement. Circulation 1998;98:1875-80.
7. Agostoni P, Biondi-Zoccai GG, Gasparini GL, et al. Is bare-metal stenting superior to balloon angioplasty for small vessel coronary artery disease? Evidence from a meta-analysis of randomized trials. Eur Heart J 2005;26:881-9.
8. Garg S, Serruys PW. Coronary stents: current status. J Am Coll Cardiol;56:S1-42.
9. Biondi-Zoccai G, Moretti C, Abbate A, Sheiban I. Percutaneous coronary intervention for small vessel coronary artery disease. Cardiovasc Revasc Med;11:189-98.
10. Briguori C, Sarais C, Pagnotta P, et al. In-stent restenosis in small coronary arteries: impact of strut thickness. J Am Coll Cardiol 2002;40:403-9.
11. Honda Y, Fitzgerald PJ. Stent expansion as a mechanical parameter to predict late stent patency: back to the basics. JACC Cardiovasc Interv 2009;2:1276-8.
12. Pache J, Kastrati A, Mehilli J, et al. Intracoronary stenting and angiographic results: strut thickness effect on restenosis outcome (ISAR-STEREO-2) trial. J Am Coll Cardiol 2003;41:1283-8.

PART
II

Chapter 11

Vascular Response of the Segments Adjacent to the Proximal and Distal Edges of the ABSORB Everolimus-Eluting Bioresorbable Vascular Scaffold: 6-Month and 1-Year Follow-Up Assessment

A Virtual Histology Intravascular Ultrasound Study From the First-in-Man ABSORB Cohort B Trial

Bill D. Gogas; Patrick W. Serruys; Roberto Diletti; Vasim Farooq; Salvatore Brugaletta; Maria D. Radu; Jung Ho Heo; Yoshinobu Onuma; Robert-Jan M. van Geuns; Evelyn Regar; Bernard De Bruyne; Bernard Chevalier; Leif Thuesen; Pieter C. Smits; Dariusz Dudek; Jacques Koolen; Stefan Windecker; Robert Whitbourn; Karine Miquel-Hebert; Cecile Dorange; Richard Rapoza; Hector M. Garcia-Garcia; Dougal McClean; John A. Ormiston

JACC Cardiovasc Interv 2012 Jun;5(6):656-65.

ABSTRACT

Objectives This study sought to investigate in vivo the vascular response at the proximal and distal edges of the second-generation ABSORB everolimus-eluting bioresorbable vascular scaffold (BVS).

Background The edge vascular response after implantation of the BVS has not been previously investigated.

Methods The ABSORB Cohort B trial enrolled 101 patients and was divided into B1 (n = 45) and B2 (n = 56) subgroups. The adjacent (5-mm) proximal and distal vessel segments to the implanted ABSORB BVS were investigated at either 6 months (B1) or 1 year (B2) with virtual histology intravascular ultrasound (VH-IVUS) imaging.

Results At the 5-mm proximal edge, the only significant change was modest constrictive remodeling at 6 months (Δ vessel cross-sectional area: -1.80% [-3.18; 1.30], $p < 0.05$), with a tendency to regress at 1 year (Δ vessel cross-sectional area: -1.53% [-7.74; 2.48], $p = 0.06$). The relative change of the fibrotic and fibrofatty (FF) tissue areas at this segment were not statistically significant at either time point. At the 5-mm distal edge, a significant increase in the FF tissue of 43.32% [-19.90; 244.28], ($p < 0.05$) 1-year post-implantation was evident. The changes in dense calcium need to be interpreted with caution since the polymeric struts are detected as "pseudo" dense calcium structures with the VH-IVUS imaging modality.

Conclusions The vascular response up to 1 year after implantation of the ABSORB BVS demonstrated some degree of proximal edge constrictive remodeling and distal edge increase in FF tissue resulting in nonsignificant plaque progression with adaptive expansive remodeling. This morphological and tissue composition behavior appears to not significantly differ from the behavior of metallic drug-eluting stents at the same observational time points. (J Am Coll Cardiol Intv 2012;5:656 – 65)

INTRODUCTION

The vascular response at the stent edges has been evaluated with first-generation drug-eluting stents and appears to be dependent on the implanted device and the periprocedural induced vascular trauma because of the geographic miss (GM) phenomenon [1]. The initial trial with the sirolimus- eluting stent - RAVEL (RAndomized study with the sirolimus-eluting VElocity balloon-expandable stent in the treatment of patients with de novo native coronary artery Lesions) - demonstrated no significant edge effect, presum- ably due to the exceptional stent/lesion ratio of 2:1, due to the sole availability of stent length (18 mm). A significant proximal edge lumen loss was, however, observed in the SIRIUS (Sirolimus-Coated Bx Velocity Balloon- Expandable Stent in the Treatment of De Novo Native Coronary Artery Lesions) trial, which evaluated the same stent platform as in RAVEL, but with several stent lengths and diameters of the device in a more complex population. In the first-in-man TAXUS I trial, no edge effect was demonstrated with the use of the slow-release polymer formulation of the paclitaxel-eluting stent; conversely, in the TAXUS II trial, the slow-release and moderate-release polymer formulations of the paclitaxel-eluting stent resulted in an edge lumen area loss (-0.54 ± 2.1 mm2 and -0.88 ± 1.9 mm^2, respectively) at both the proximal and distal stent edges [2,3]. In the BETAX (BEside TAXus) trial, using the Taxus Express drug-eluting stent, significant tissue compositional changes were observed, mainly due to an increase in the fibrofatty (FF) tissue component causing expansive remodeling at both stent edges [4]. Pre-clinical research has demonstrated that the tissue response after stent implantation is exclusively composed of proteoglycan-rich smooth muscle cells and fibrolipidic areas rich in collagen and reticular fibers [5]. This iatrogenic entity of neointimal hyperplasia has been demonstrated to be usually focal and most commonly located at the proximal stent edge [6]. The advent of scaffolds with bioresorbable properties and differing biological behavior compared with the currently used metallic devices, has prompted the re-evaluation of the edge vascular response using sound-based imaging modalities with tissue characterization properties. Such a modality is the virtual histology intravascular ultrasound (VH-IVUS), which allows for the evaluation of the vascular geometric changes and assessment of the atheromatous plaque progression/regression.

The purpose of this study is to investigate the edge effect after the implantation of the ABSORB bioresorbable vascular scaffold (BVS) in the assessment of the geometric and compositional changes of the segments adjacent to the 5-mm proximal and distal edges of the scaffolded vessel, in a population investigated at either 6 months or 1 year post scaffold implantation.

METHODS

Study design and population

The ABSORB Cohort B trial is a multicenter, ongoing, single- arm prospective, open-label trial assessing the safety and performance of the second-generation ABSORB BVS in the treatment of patients with a maximum of 2 de novo native coronary artery lesions. In total, 101 patients were enrolled and subdivided into 2 subgroups - Cohort B1 (n = 45) and Cohort B2 (n = 56) - according to the predefined study design. Both groups underwent invasive follow-up, Cohort B1 at 6 months and Cohort B2 at 1 year. Cohort B1 is currently undergoing a second VH-IVUS imaging of the scaffold edges at 2 -years and Cohort B2 will undergo the final VH-IVUS imaging evaluation at 3 years (Fig. 1).

In the present study, patients over the age of 18 years, who had either stable or unstable angina pectoris or silent ischemia, were suitable for inclusion. All treated lesions were de novo lesions in a native coronary artery with a maximum diameter of 3.0 mm, a length of <14 mm, a percent diameter stenosis >50% and <100%, and a Thrombolysis In Myocardial Infarction (TIMI) flow grade of >1. Major exclusion criteria were patients presenting with an acute myocardial infarction or unstable arrhythmias, or patients who had a left ventricular ejection fraction <30%, restenotic lesions, lesions located in the left main coronary artery, lesions involving an epicardial side branch >2 mm in diameter by visual assessment, and the presence of thrombus or another clinically significant stenosis in the target vessel.

The ethics committee at each participating institution approved the protocol, and each patient gave written in- formed consent before inclusion.

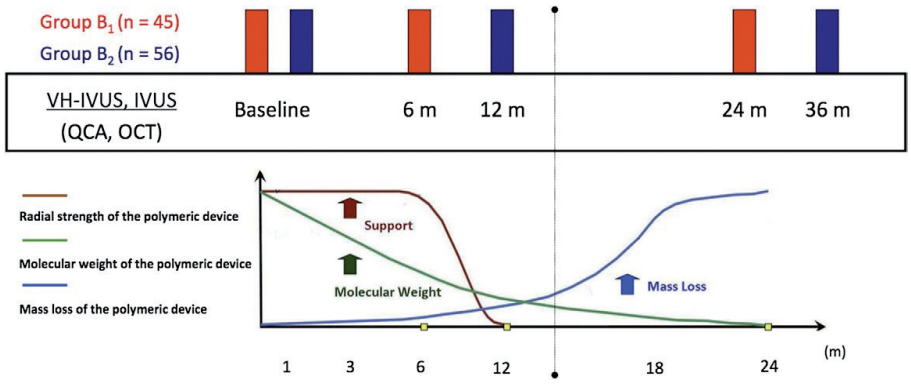

Figure 1. ABSORB Cohort B Study Design.
The study design of the ABSORB Cohort B trial with the respective biological behavior of the ABSORB bioresorbable vascular scaffold, at the different time frames that virtual histology intravascular ultrasound (VH-IVUS) imaging was performed (yellow points). OCT = optical coherence tomography; QCA = quantitative coronary angiography.

Treatment device

The ABSORB BVS (Abbott Vascular, Santa Clara, California) is a balloon-expandable device consisting of a polymer backbone of poly-L-lactide coated with a thin layer of a 1:1 mixture of poly-D,L-lactide. The polymer controls the release of the antiproliferative drug everolimus, and forms an amorphous drug-eluting coating matrix that contains 100 f.Lg of everolimus/cm2 of scaffold. According to bench studies, the ABSORB BVS device has shown a dynamic biological behavior at 6 months, 1 year, and 2 years, at which time the complete bioresorption of the polymer backbone is expected [7].

At 6 months, a gradual and steep loss of the device radial strength in parallel to the continuous decrease of the device molecular weight is observed because of the depolymerization and hydrolysis after implantation. The molecular weight of the polymeric platform continues to decrease until 1 year, when the radial strength is completely eliminated, and the device represents a passive structure without any supportive vascular properties. At 2 years, the ABSORB BVS is considered fully resorbed, having been metabolized into CO_2 and H_2O through the Krebs cycle (Fig. 1). This dynamic behavior of the polymeric device at the above- mentioned time points prompts the in vivo evaluation of the vascular response at the scaffold edges with VH-IVUS imaging in parallel to its evolving biological behavior [8].

Treatment procedure

Lesions were treated with routine interventional techniques that included mandatory pre- dilation with a balloon shorter and 0.5 mm smaller in diameter than the study device. The ABSORB BVS was implanted at a pressure not exceeding the rated burst pressure (16 atm). Post-dilation with a balloon shorter than the implanted device was allowed at the discretion of the operator, as was bailout treatment.

Quantitative IVUS and VH-IVUS analysis

Geometric parameters in the complete 5-mm proximal and distal segments derived from the grayscale IVUS and VH-IVUS acquisition were analyzed in each separate frame—that is, vessel area, lumen area, plaque area, and tissue composition parameters—as absolute values. Furthermore, percentages were assessed for each cross section in the same region of interest. Both the proximal and distal vessel segments were further divided into 1-mm subsegments, numbered from 1 (adjacent to the scaffold) to 5, and underwent similar imaging evaluation as for the complete segment.

The tissue compositional analysis was obtained with a phased-array 20-MHz intravascular ultrasound catheter (Eagle Eye, Volcano Corporation, Rancho Cordova, California) after intracoronary administration of 100 to 200 f.Lg of nitroglycerin, using automated pullback at 0.5 mm/ second (30 frames/s). The raw radiofrequency data were capture gated to the

R-wave. The main principle of the VH-IVUS imaging technique is that both the envelope amplitude of the reflected radiofrequency signals, as under- taken with standard grayscale IVUS analyses, and the underlying frequency content is used to analyze the tissue components present in coronary plaques. The combined information is subsequently processed using auto regressive models and thereafter categorized into a classification tree that determines the 4 basic plaque tissue components: 1) fibrous tissue - dark green; 2) FF - light green; 3) necrotic core (NC) - red; and 4) dense calcium (DC) - white [9]. All VH-IVUS analyses were performed offline using the pcVH 2.1 software (Volcano Corporation) by an independent clinical research organization (Cardialysis, Rotterdam, the Netherlands). At 6 months (Cohort B_1, n = 45), 23 proximal and 18 distal edge segments were suitable for analysis with grayscale IVUS and VH-IVUS imaging. At 1 year (Cohort B_2, n = 56), 25 proximal and 30 distal edge segments were analyzable.

The reasons for the reduced number of our final tested samples were: 1) the dropout of patients at follow-up (the attrition rate of the ABSORB Cohort B trial was ~ 20%) and exclusion of the unpaired samples from our final data; and 2) exclusion of cases, according to the standard operational procedure of the independent core laboratory (Cardialysis), with side-branch outgrowth of > 90° at the side of the scaffold edge that did not allow the analysis of the complete 5-mm segment and vessel wall out of the field of the view.

Statistical analysis

Discrete variables are presented as counts and percentages. Continuous variables are presented as medians and interquartile ranges. Comparison between baseline and follow-up was performed using the Wilcoxon signed rank test. Changes (differences) for each measurement were calculated as follow-up minus post- procedure values. Percent changes (differences) for each variable were calculated as follow-up post-rocedure/ post-procedure X100%. A p value <0.05 was considered statistically significant. Data analyses were performed with SAS version 9.1 software (SAS Institute, Cary, North Carolina).

RESULTS

The baseline clinical and lesion characteristics of the pa- tients are demonstrated in Table 1. The percent (%) changes (median [interquartile range]) of the vessel cross-sectional area (CSA), lumen CSA, and plaque CSA at the 5-mm proximal edge segment were at 6 months: -1.80% [-3.18;1.30], (p < 0.05), -4.10% [-11.61; 8.79], (p = 0.22), and - 4.04% [-10.65; 11.05] (p = 0.55); and at 1 year: - 1.53% [-7.74; 2.48], (p = 0.06), -5.32% [-12.36; 4.24], (p = 0.07), and - 2.03% [- 8.39; 7.76], (p = 0.72), respectively.

Table 1. Baseline Clinical and Lesion Characteristics.

	6 Months		1 Year	
	Proximal Edge (n = 23)	Distal Edge (n = 18)	Proximal Edge (n = 24)	Distal Edge (n = 29)
Age, yrs	62.41 ± 9.86	64.70 ± 9.83	59.21 ± 7.72	60.20 ± 7.72
Male	14 (61%)	12 (67%)	15 (63%)	20 (69.0%)
Current smoking	3 (13.0%)	1 (6%)	5 (21%)	2 (7%)
Diabetes	5 (22%)	3 (17%)	7 (29%)	6 (21%)
Hypertension	16 (70%)	13 (72%)	17 (74%)	19 (68%)
Hypercholesterolemia	22 (96%)	18 (100%)	18 (75%)	22 (76%)
Prior myocardial infarction	8 (35%)	7 (39%)	5 (21%)	3 (11%)
Unstable angina	3 (13%)	3 (17%)	4 (17%)	6 (21%)
Stable angina	16 (70%)	14 (78%)	14 (58%)	17 (59%)
Treated vessel				
Right coronary artery	9 (39%)	7 (39%)	9 (36%)	8 (27%)
Left anterior descending artery	6 (26%)	6 (33%)	10 (40%)	16 (53%)
Left circumflex artery	7 (30%)	4 (22%)	6 (24%)	6 (20%)
ACC/AHA lesion class:				
Type A	1 (4%)	1 (5%)	0 (0%)	0 (0%)
Type B1	10 (44%)	9 (50%)	17 (71%)	22 (73%)
Type B2	11 (48%)	8 (44%)	6 (25%)	7 (23%)
Type C	1 (4%)	0 (0%)	1 (4%)	1 (3%)
RVD before intervention, mm	2.56 ± 0.43	2.78 ± 0.45	2.61 ± 0.33	2.50 ± 0.28

Values are mean ± SD or n (%).
ACC/AHA = American College of Cardiology/American Heart Association; RVD = reference vessel diameter.

The % changes of the vessel CSA, lumen CSA, and plaque CSA at the 5-mm distal edge segment were at 6 months: - 0.59% [-3.74; 7.09], (p = 0.71), -0.32% [-7.71; 7.20], (p = 0.97), and 7.0% [-11.97; 18.36], (p = 0.50); and at 1 year: 3.45% [-2.08; 6.91], (p = 0.07), 0.95% [-7.56; 7.48], (p = 0.77), and 5.73% [-6.49; 5.47], (p = 0.09), respectively (Table 2). The absolute geometric and tissue composition changes and the subsegmental analysis at 1 year are tabulated in (Tables 3 and 4) and illustrated in Figs. 2, 3, and 4. The absolute tissue compositional changes at 6 months at both edges and the subsegmental analysis at the same time point are tabulated and illustrated in the Online Appendix.

The main findings of this study at the time point of 1-year post-implantation of the ABSORB BVS are as follows. Constrictive vascular remodeling at the proximal edge was evident without significant changes in tissue composition parameters. At the distal edge, tissue composition changes were evident with a significant increase in the FF tissue resulting in nonsignificant plaque progression and adaptive expansive remodeling (Fig. 2).

The edge effects following the implantation of either a metallic or a polymeric device have common etiological mechanisms, namely: 1) periprocedural or iatrogenic technical issues

Table 2. Summary of the % Changes of the Entire 5-mm Segment, at the Proximal and Distal Edges, Regarding Geometric and Plaque Composition Parameters 6 Months and 1 Year Following Implantation of the ABSORB BVS

	Vessel CSA (mm^2)	Lumen CSA (mm^2)	Plaque CSA (mm^2)
Proximal edge segment, (%) change			
6 months (n = 23)	-1.8 [-3.18; 1.30]	-4.1 [-11.61; 8.79]	-4.04 [-10.65; 11.05]
p value	**<0.05**	NS	NS
1 year (n = 25)	-1.53 [-7.74; 2.48]	-5.32 [-12.36; 4.24]	-2.03 [-8.39; 7.76]
p value	NS	NS	NS
Distal edge segment, (%) change			
6 months (n = 18)	-0.59 [-3.74; 7.09]	-0.32 [-7.71; 7.20]	7 [-11.97; 18.36]
p value	NS	NS	NS
1 year (n = 30)	3.45 [-2.08; 6.91]	0.95 [-7.56; 7.48]	5.73 [-6.49; 25.47]
p value	NS	NS	NS

	Dense Calcium (mm^2)	Fibrous (mm^2)	Fibrofatty (mm^2)	Necrotic Core (mm^2)
Proximal edge segment, (%) change				
6 months (n = 23)	12.02 [-31.62; 47.50]	4.44 [-16.83; 67.23]	10.3 [-46.38; 134.69]	
p value	NS	NS	NS	NS
1 year (n = 25)	-7.91 [-42.19; 17.26]	-2.58 [-20.03; 11.86]	-9 [-36.77; 87.41]	-4.35 [-31.23; 30.40]
p value	NS	NS	NS	NS
Distal edge segment, (%) change				
6 months (n = 18)	44.09 [22.81; 159.23]	4.07 [-18.83; 107.39]	8.21 [-37.77; 91.48]	23.59 [-19.89; 74.33]
p value	**<0.05**	NS	NS	NS
1 year (n = 30)	-20.57 [-50.22; 54.11]	18.87 [-11.14; 108.93]	43.32 [-19.90; 244.28]	-6.25 [-44.20; 81.94]
p value	NS	NS	**<0.05**	NS

p values in **bold** are statistically significant.
BVS _ bioresorbable vascular scaffold; CSA _ cross-sectional area; NS _ not significant.

affecting predominantly geometric parameters [1–11]; 2) tissue composition characteristics of the lesion [12]; and 3) local wall shear stress (WSS) conditions [13–15].

The GM phenomenon, associated with sirolimus-eluting stent implantation, was investigated in the STLLR (Stent Deployment Techniques on Clinical Outcomes of Patients Treated With the Cypher Stent) study and was reported to occur in nearly two-thirds (66.5%) of the study group; almost one-half of the patients (47.6%) experienced longitudinal GM, over one-third (35.2%) axial GM, and 16.5%, a combination of the 2 [1,10]. Hoffmann et al. [10] demonstrated within the E-SIRIUS (European, multi- center, randomized, double blind trial of the SIRolImUS-coated Bx-Velocity stent in the treatment

Table 3. Summary of the Proximal and Distal Edge Changes at 6 Months and 1 Year After Implantation of the ABSORB BVS

	Time After the Imaging Procedure					
	Vessel CSA (mm^2)	Lumen CSA (mm^2)	Plaque CSA (mm^2)	Vessel CSA (mm^2)	Lumen CSA (mm^2)	Plaque CSA (mm^2)
Proximal Edge		6 Months (n = 23)			1 Year (n = 25)	
Baseline	13.2 [10.81; 15.90]	7.15 [5.80; 8.65]	5.88 [4.22; 7.08]	13.89 [12.55; 17.24]	7.25 [6.44; 8.40]	7.02 [5.52; 7.80]
Follow-up	13.38 [10.26; 15.39]	7.15 [5.60; 8.41]	5.49 [3.86; 7.25]	13.71 [12.22; 16.11]	7 [6.14; 8.30]	7.08 [5.36; 8.38]
Median absolute difference	-0.25 [-0.54; 0.18]	-0.27 [-0.78; 0.67]	-0.25 [-0.63; 0.60]	-0.19 [-1.06; 0.33]	-0.35 [-0.77; 0.25]	-0.15 [-0.59; 0.37]
p value	**<0.05**	NS	NS	NS	NS	NS
Distal Edge		6 Months (n = 18)			1 Year (n = 30)	
Baseline	12.79 [10.17; 16.38]	7.27 [5.62; 7.90]	7.02 [4.15; 7.89]	10.28 [9.13; 13.46]	6.7 [5.63; 7.80]	4.47 [2.29; 5.61]
Follow-up	13.87 [10.42; 16.15]	6.85 [6.11; 8.44]	6.07 [4.90; 8.40]	10.49 [9.88; 13.33]	6.76 [5.56; 7.78]	4.46 [3.20; 6.61]
Median absolute difference	-0.07 [-0.51; 1.00]	-0.03 [-0.55; 0.58]	0.35 [-0.82; 0.97]	0.4 [-0.26; 0.63]	0.09 [-0.49; 0.43]	0.27 [-0.27; 0.97]
p value	NS	NS	NS	NS	NS	NS

p values in **bold** are statistically significant.
Abbreviations as in Table 2.

Table 4. Summary of the Tissue Composition Changes at the Proximal and Distal Edges, 1 Year After Implantation of the ABSORB BVS

	Dense Calcium (mm^2)	Dense Calcium (%)	Fibrous (mm^2)	Fibrous (%)	Fibrofatty (mm^2)	Fibrofatty (%)	Necrotic Core (mm^2)	Necrotic Core (%)
Proximal edge segment (n _ 25)								
Baseline	0.48 [0.24; 0.76]	12.55 [7.02; 20.20]	1.95 [1.01; 2.69]	55.08 [46.10; 63.52]	0.26 [0.11; 0.45]	7.34 [4.99; 10.36]	0.85 [0.40; 1.28]	19.63 [17.16; 29.81]
1-year follow-up	0.33 [0.24; 0.54]	11.97 [8.31; 17.94]	2.02 [1.37; 2.41]	53.62 [48.56; 59.95]	0.28 [0.09; 0.38]	8 [4.46; 11.39]	0.64 [0.42; 1.01]	20.49 [15.11; 29.02]
Median absolute difference	-0.02 [-0.20; 0.09]	-0.72 [-3.70; 4.65]	-0.04 [-0.33; 0.20]	-0.1 [-4.67; 5.71]	-0.01 [_0.10; 0.19]	0.03 [-3.08; 3.42]	-0.06 [-0.32; 0.23]	-2.05 [-5.58; 5.65]
p value	NS	NS	NS	NS	NS	NS	NS	NS
Distal edge segment (n _ 30)								
Baseline	0.18 [0.08; 0.57]	15.87 [10.17; 35.30]	0.91 [0.08; 1.61]	54.72 [35.05; 62.19]	0.06 [0.01; 0.17]	4.7 [2.49; 7.87]	0.4 [0.04; 0.72]	21.96 [17.58; 28.00]
1-year follow-up	0.19 [0.08; 0.31]	10.5 [6.93; 17.07]	0.9 [0.28; 1.52]	57.75 [51.27; 62.42]	0.1 [0.03; 0.28]	8.1 [4.23; 12.54]	0.3 [0.09; 0.64]	18.75 [14.65; 24.88]
Median absolute difference	-0.02 [-0.20; 0.07]	-4.22 [-12.18; 1.35]	0.09 [-0.07; 0.22]	1.83 [-4.36; 14.58]	0.02 [0.00; 0.09]	2.24 [0.48; 8.69]	-0.01 [-0.33; 0.09]	-2.82 [-7.26; 4.22]
p value	NS	**<0.05**	NS	NS	**<0.05**	**<0.05**	NS	NS

p values in **bold** are statistically significant.
Abbreviations as in Table 3.

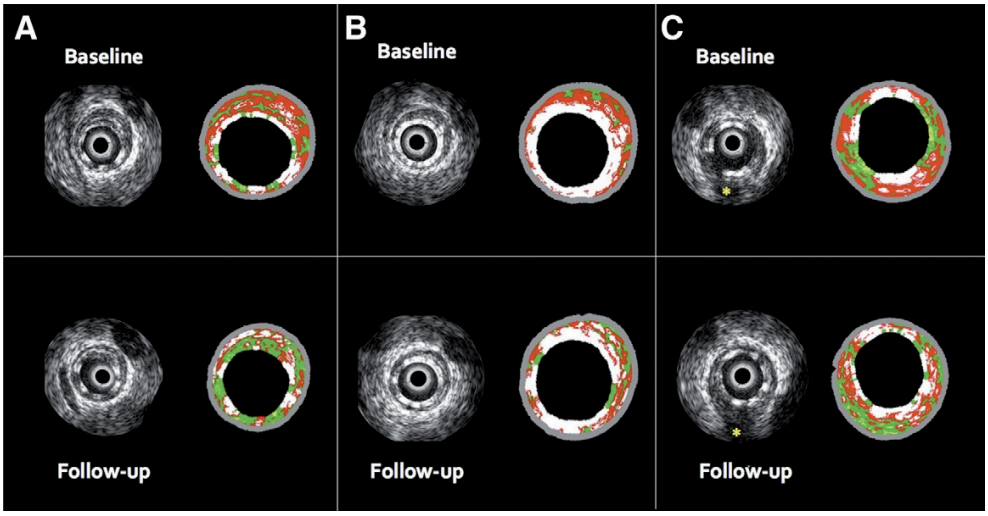

Figure 2. Grayscale IVUS and Corresponding VH-IVUS Still Frames at 1-Year After Implantation of the ABSORB BVS.

(**A**) Distal edge segment. At this segment a significant increase of the fibrofatty (FF) tissue was observed. VH-IVUS demonstrates at this frame a change in FF tis- sue area from 0.07 to 0.14 mm^2. Dense calcium (DC) and necrotic core tissue components changed from 2.39 mm^2 and 3.7 mm^2 to 2.07 mm^2 and 1.8 mm^2, respectively, as a consequence of the bioresorption process. (**B**) Scaffolded segment. The polymeric struts of the ABSORB BVS are detected as "pseudo" DC sur- rounded by a red, halo. (**C**) Proximal edge segment. At this segment some degree of proximal edge constrictive vascular remodeling was observed. Grayscale IVUS shows for this frame a change in the lumen area from 9.4 mm^2 to 8.4 mm^2 (The external elastic membrane has been extrapolated at the side of the side branch, [yellow asterisk]).

of patients with *de novo* coronary artery lesions)-IVUS substudy versus the SIRIUS-US (US, multicenter, ran- domized, double blind trial of the SIRolImUS-coated Bx-Velocity stent in the treatment of patients with de novo coronary artery lesions) trial, that both axial and longitudinal GM were reduced (from 5.9% to 2.1%) when periprocedural implantation parameters were taken into account, such as conservative pre-dilation, less forceful stent implantation (~16 atm), and selective postdilation with balloons shorter than the stent. Despite multiple technical guidelines regarding the ABSORB BVS delivery system to minimize the axial (burst pressure: 16 atm) and longitudinal (balloon shorter and 0.5 mm smaller than the implanted device) GM phenomena, a significant proximal edge constrictive response was demonstrated at 6 months, whereas at 1 year, the constrictive remodeling was only observed in the following proximal subsegments, starting from the scaffold edge (subsegment 1: Δ -0.96 mm^2, ($p < 0.05$); subsegment 2: Δ -0.71 mm^2, ($p < 0.05$); and subsegment 4: Δ -0.57($p < 0.05$) (Figs. 3 and 4). The changes in WSS distribution adjacent to the stent edges post device implantation appear to follow alterations in vessel curvature and angulation, and have been reported to result in step-up regions of low

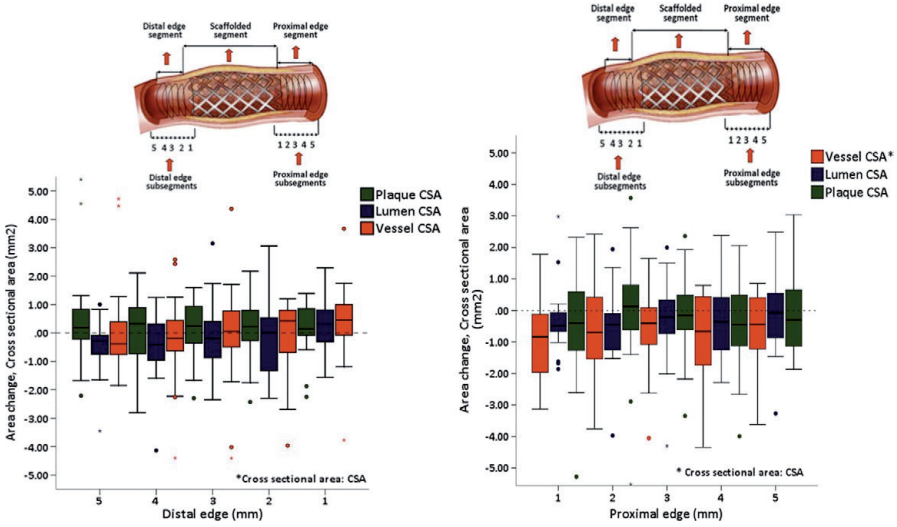

Figure 3. Subsegmental Analysis of the Geometric Changes at the Proximal and Distal Edges After Implantation of the ABSORB BVS. The analysis, per mm of the subsegments, was performed at 1-year follow-up. BVS = bioresorbable vascular scaffold.

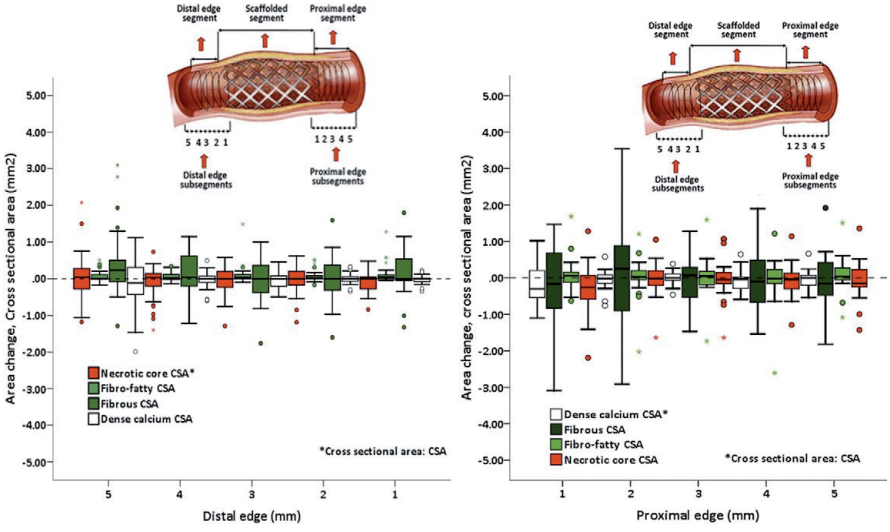

Figure 4. Subsegmental Analysis of the Tissue Composition Changes at the Proximal and Distal Edges After Implantation of the ABSORB BVS. The analysis, per mm of the subsegments, was performed at 1-year follow-up. BVS = bioresorbable vascular scaffold.

shear stress, prone to neointimal growth [13–15].

Metallic devices have a more accentuated effect on vessel curvature and angulation compared to the ABSORB BVS; however, despite the clinical benefits associated with better conformability [16] of the ABSORB BVS device, proximal constrictive remodeling was observed at 1-year after implantation, and further investigations are required to evaluate the changes of WSS at the scaffold edges or the in-scaffold area. Moreover, any of the initial flow–tissue interaction effects caused by the implantation of this bioresorbable device are expected to potentially subside after a 2-year period when the bioresorption process is expected to be complete and the polymeric platform is fully transformed to CO_2 and H_2O, with no consequent remaining compliance mismatch [8,16]. Samady et al. [17] recently demonstrated, in a cohort of 20 patients, that coronary segments with low WSS (step-up regions) are segments that develop constrictive remodeling, in contrast to the high-WSS segments that present excessive expansive remodeling with tissue composition changes, mainly due to an increase in DC and NC tissue components. These reported observations are in parallel with the present findings in this study regarding vessel geometry and tissue composition. The distal edge segment adjacent to the scaffold appeared to have major tissue composition changes with some degree of plaque progression, which caused a subsequent nonsignificant expansive remodeling. The VH-IVUS– derived tissue type that correlates with extracellular matrix is the FF tissue, which happens to be the one that increased the most [18]. The DC tissue component appeared to have a biphasic response at this segment after the ABSORB BVS implantation with a significant increase at 6 months and a trend toward a decrease at 1-year follow-up; conversely, the NC tissue changed nonsignificantly following sequential modifications of DC tissue.

The changes in DC and NC tissue components at follow-up should be interpreted with caution since the ABSORB BVS is made of bioresorbable polymeric material recognized as "pseudo" DC and NC, parameters that have previously been reported as surrogate markers of the bioresorption process [19,20]. In addition, the edges of the polymeric scaffold are not sharply demarcated since the vessel surrounding the imaging device are affected by the "to and fro" motion of the cardiac contraction, causing a "pseudoaxial" displacement of the IVUS catheter related to the arterial wall.

Indeed, the cardiac cycle can cause a mean axial displacement of the IVUS transducer of 1.5 mm with a maximum distortion up to 6.5 mm; however, the use of electrocardio- gram gating during IVUS data acquisition reduces the axial movement to a maximum of 0.8 mm [21–23] but does not fully prevent the imaging of the polymeric struts as "pseudo" DC in the adjacent edge of the implanted device. In keeping with the standard operational procedure of an independent core laboratory (Cardialysis), the quantification of the scaffold edges was initiated at the point where the visualization of the scaffold arc at each

frame was <360°, implying that the scaffold edge to some extent may include polymeric struts. The apparent increase in DC at 6 months, followed by a trend toward a reduction at 1 year, accompanied by the parallel behavior of the NC, are attributed to the introduction of the bioresorbable device during the procedure and subsequent bioresorption process long term. Other possible factors that may have influenced the NC tissue component are the locally eluted drug everolimus and the systemic use of HMG-CoA inhibitors. Verheye et al. [24] recently demonstrated that everolimus—an inhibitor of the mammalian target of rapamycin (m-TOR)— has autophagic capabilities on macrophages, with a subsequent effect of diminishing NC formation, inflammation, and thrombosis. Hong et al. [25] reported a significant 13% relative reduction in plaque necrotic core volume, and a significant 27% relative increase in plaque FF content with the administration of HMG-CoA inhibitors, assessed with VH-IVUS at 1-year follow-up. Coronary endothelial dysfunction has been previously associated with underlying plaque composition, in particular high content of DC and NC. Lavi et al. [26] have demonstrated impaired endothelial-dependent vasomotion in vessel segments with underlying NC-rich plaques. Our group has recently demonstrated that the restored normal vasodilatory response to acetylcholine in coronary segments that have previously undergone implantation with an AB-SORB BVS, is associated with a reduction of NC [27], implying the potential restoration of the vasomotor function of the treated vessel with reductions of specific tissue components. Whether the present findings are due to the combined effects of locally eliminated m-TOR inhibitor everolimus, with the systemic use of the HMG-CoA inhibitors, or the natural history of the bioresorbable process of the implanted device, remains to be elucidated in future studies, where a potential restoration of the vasomotor function at the scaffold edges would be highly expected with the sustained tissue composition changes observed at 1-year follow-up. Furthermore, the combination of continuous polymer degradation and elaboration of the treated vessel from its foreign material beyond 1 year, with the restoration of vessel biological behavior (vasomotor function) and the interplay with pharmacological intervention may potentially eliminate the risk of late stent thrombosis. The clinical outcome of the ABSORB Cohort B trial at 1-year post implantation of the ABSORB BVS revealed a hierarchical major adverse cardiac event rate of 6.9%, with no episodes of scaffold thrombosis (according to the protocol or Academic Research Consortium definitions). Pre-scaffolding VH-IVUS analysis can give an insight into the extent of plaque and NC within and beyond the intended scaffolded segment. This latter point is potentially important, since full coverage of the lesion by the implanted device is the desired goal of the interventionalist, as incomplete coronary plaque coverage has been reported to effect long-term clinical events, especially in the presence of NC-containing plaques [11].

Study limitations

The main limitation of our study is the small number of the investigated scaffold edges. The complete cohort (B1+B2) at the different time points without splitting the population would potentially have increased the sample size; this, however, was a predefined design of the study.

CONCLUSIONS

The edge vascular response, with the use of the ABSORB BVS device at 1-year post implantation, demonstrates a degree of proximal edge constrictive remodeling and distal edge plaque compositional changes, a biological behavior similar to that observed with the metallic devices. Full bioresorption of the device, expected to occur in approximately 2 years, will potentially allow for the evaluation and comparison of the exact biological composition of the treated vessel at the scaffold edges, utilizing the VH-IVUS imaging modality.

REFERENCES

1. Costa MA, Angiolillo DJ, Tannenbaum M, et al. Impact of stent deployment procedural factors on long-term effectiveness and safety of sirolimus-eluting stents (final results of the multicenter prospective STLLR trial). Am J Cardiol 2008;101:1704 –11.
2. Grube E, Silber S, Hauptmann KE, et al. TAXUS I: six- and twelve-month results from a randomized, double-blind trial on a slow-release paclitaxel-eluting stent for de novo coronary lesions. Circulation 2003;107:38 – 42.
3. Serruys PW, Degertekin M, Tanabe K, et al. Vascular responses at proximal and distal edges of paclitaxel-eluting stents: serial intravascu- lar ultrasound analysis from the TAXUS II trial. Circulation 2004;109: 627–33.
4. Garcıa-Garcıa HM, Gonzalo N, Tanimoto S, Meliga E, de Jaegere P, Serruys PW. Characterization of edge effects with paclitaxel-eluting stents using serial intravascular ultrasound radiofrequency data analysis: the BETAX (BEside TAXus) study. Rev Esp Cardiol 2008;61:1013–9.
5. Chieffo A, Foglieni C, Nodari RL, et al. Histopathology of clinical coronary restenosis in drug-eluting versus bare metal stents. Am J Cardiol 2009;104:1660 –7.
6. Byrne RA, Eberle S, Kastrati A, et al. Distribution of angiographic measures of restenosis after drug-eluting stent implantation. Heart 2009;95:1572– 8.
7. Onuma Y, Serruys PW, Perkins LE, et al. Intracoronary optical coherence tomography and histology at 1 month and 2, 3, and 4 years after implantation of everolimus-eluting bioresorbable vascular scaffolds in a porcine coronary artery model: an attempt to decipher the human optical coherence tomography images in the ABSORB trial. Circulation 2010;122:2288 –300.
8. Gogas BD, Radu M, Onuma Y, et al. Evaluation with in vivo optical coherence tomography and histology of the vascular effects of the everolimus-eluting bioresorbable vascular scaffold at two years following implantation in a healthy porcine coronary artery model: implications of pilot results for future pre-clinical studies. Int J Cardiovasc Imaging 2012;28:499 –516.
9. Gogas BD, Farooq V, Serruys PW, et al. Assessment of coronary atherosclerosis by IVUS and IVUS-based imaging modalities: progres sion and regression studies, tissue composition and beyond. Int J Cardiovasc Imaging 2011;27:225–37.
10. Hoffmann R, Guagliumi G, Musumeci G, et al. Vascular response to sirolimus-eluting stents delivered with a nonaggressive implantation technique: comparison of intravascular ultrasound results from the multicenter, randomized e-Sirius, and Sirius trials. Catheter Cardiovasc Interv 2005;66:499 –506.
11. Farb A, Burke AP, Kolodgie FD, Virmani R. Pathological mechanisms of fatal late coronary stent thrombosis in humans. Circulation 2003;108:1701– 6.
12. Wentzel JJ, Gijsen FJ, Stergiopulos N, Serruys PW, Slager CJ, Krams R. Shear stress, vascular remodeling and neointimal formation. J Biomech 2003;36:681– 8.
13. Wentzel JJ, Whelan DM, van der Giessen WJ, et al. Coronary stent implantation changes 3-d vessel geometry and 3-d shear stress distribution. J Biomech 2000;33:1287–95.
14. Thury A, Wentzel JJ, Vinke RV, et al. Images in cardiovascular medicine. Focal in-stent restenosis near step-up: roles of low and oscillating shear stress? Circulation 2002;105:e185–7.
15. Gomez-Lara J, Garcia-Garcia HM, Onuma Y, et al. A comparison of the conformability of everolimus-eluting bioresorbable vascular scaffolds to metal platform coronary stents. J Am Coll Cardiol Intv 2010;3:1190 – 8.
16. Tortoriello A, Pedrizzetti G. Flow-tissue interaction with compliance mismatch in a model stented artery. J Biomech 2004;37:1–11.

17. Samady H, Eshtehardi P, McDaniel MC, et al. Coronary artery wall shear stress is associated with progression and transformation of atherosclerotic plaque and arterial remodeling in patients with coronary artery disease. Circulation 2011;124:779 – 88.
18. Farb A, Kolodgie FD, Hwang JY, et al. Extracellular matrix changes in stented human coronary arteries. Circulation 2004;110:940 –7.
19. Kim SW, Mintz GS, Hong YJ, et al. The virtual histology intravascular ultrasound appearance of newly placed drug-eluting stents. Am J Cardiol 2008;102:1182– 6.
20. Bruining N, de Winter S, Roelandt JR, et al. Monitoring in vivo absorption of a drug-eluting bioabsorbable stent with intravascular ultrasound-derived parameters a feasibility study. J Am Coll Cardiol Intv 2010;3:449 –56.
21. Arbab-Zadeh A, DeMaria AN, Penny WF, Russo RJ, Kimura BJ, Bhargava V. Axial movement of the intravascular ultrasound probe during the cardiac cycle: implications for three-dimensional reconstruction and measurements of coronary dimensions. Am Heart J 1999;138:865–72.
22. von Birgelen C, de Vrey EA, Mintz GS, et al. ECG-gated three-dimensional intravascular ultrasound: feasibility and reproducibility of the automated analysis of coronary lumen and atherosclerotic plaque dimensions in humans. Circulation 1997;96:2944 –52.
23. Bruining N, von Birgelen C, de Feyter PJ, et al. ECG-gated versus nongated three-dimensional intracoronary ultrasound analysis: implications for volumetric measurements. Cathet Cardiovasc Diagn 1998; 43:254 – 60.
24. Verheye S, Martinet W, Kockx MM, et al. Selective clearance of macrophages in atherosclerotic plaques by autophagy. J Am Coll Cardiol 2007;49:706 –15.
25. Hong MK, Park DW, Lee CW, et al. Effects of statin treatments on coronary plaques assessed by volumetric virtual histology intravascular ultrasound analysis. J Am Coll Cardiol Intv 2009;2:679 – 88.
26. Lavi S, Bae JH, Rihal CS, et al. Segmental coronary endothelial dysfunction in patients with minimal atherosclerosis is associated with necrotic core plaques. Heart 2009;95:1525–30.
27. Brugaletta S, Heo HJ, Garcia-Garcia HM, et al. Endothelial-dependent vasomotion in coronary segment treated by ABSORB everolimus-eluting bioresorbable vascular scaffold system is related to plaque composition at the time of bioresorption of the polymer: indirect finding of vascular reparative therapy? Eur Heart J 2012 Apr 16 [E-pub ahead of print].

Chapter 12

Clinical and Intravascular Imaging Outcomes at 1 and 2 years after Implantation of Absorb Everolimus Eluting Bioresorbable Vascular Scaffolds in Small Vessels

Late Lumen Enlargement: Does Bioresorption Matter with Small Vessel Size? Insight from the ABSORB Cohort B Trial

Roberto Diletti, MD; Vasim Farooq, MBChB, MRCP; Chrysafios Girasis, MD; Christos Bourantas, MD, PhD; Yoshinobu Onuma MD; Jung He Heo, MD; Bill D. Gogas, MD; Robert Jan van Geuns, MD PhD; Evelyn Regar, MD PhD; Bernard de Bruyne, MD; Dariusz Dudek, MD; Leif Thuesen, MD, FACC; Bernard Chevalier, MD; Dougal McClean, MD; Stephan Windecker, MD; Robert Whitbourn, MD; Pieter Smits, MD, PhD; Jacques Koolen, MD; Ian Meredith, MBBS, PhD; Xiaolin Li, MSc; Karine Miquel-Hebert, PhD; Susan Veldhof, RN; Hector M. Garcia-Garcia, MD, PhD; John A. Ormiston, MBChB, PhD; Patrick W. Serruys, MD, PhD

Heart. 2013 Jan;99(2):98-105.

ABSTRACT

Background The long-term results after second generation everolimus eluting bioresorbable vascular scaffold (Absorb BVS) implantation in small vessels are unknown. We investigated the impact of vessel size on long-term outcomes, after BVS implantation.

Methods In ABSORB Cohort B Trial out of the total study population (101 patients), 45 patients were assigned to undergo 6-month and 2-year angiographic follow-up (Cohort B1) and 56 patients to have angiographic follow-up at 1-year (Cohort B2). The pre-RVD was < 2.5 mm (small-vessel group) in 41 patients and ≥ 2.5 mm (large-vessel group) in 60 patients. Outcomes were compared according to pre-RVD.

Results At 2-year angiographic follow-up no differences in late lumen loss (0.29±0.16 mm vs. 0.25±0.22 mm, p=0.4391), and in-segment binary restenosis (5.3% vs. 5.3% p=1.0000) were demonstrated. In the small-vessel group, IVUS analysis showed a significant increase in vessel area (12.25±3.47 mm^2 vs. 13.09±3.38 mm^2 p=0.0015), scaffold area (5.76±0.96 mm^2 vs. 6.41±1.30 mm^2 p=0.0008) and lumen area (5.71±0.98 mm^2 vs. 6.20±1.27 mm^2 p=0.0155) between 6-months and 2-year follow-up. No differences in plaque composition were reported between groups at either time point. At 2-year clinical follow-up, no differences in ID-MACE (7.3% vs. 10.2%, p=0.7335), MI (4.9% vs. 1.7%, p=0.5662) or ID-TLR (2.4% vs. 8.5%, p=0.3962) were reported between small and large vessels. No deaths or scaffold thrombosis were observed.

Conclusion Similar clinical and angiographic outcomes at 2-year follow-up were reported in small and large vessel groups. A significant late lumen enlargement and positive vessel remodeling were observed in small vessels.

INTRODUCTION

The first generation Absorb everolimus eluting bioresorbable vascular scaffold (Absorb BVS, Abbott Vascular, Santa Clara, CA, USA) has been previously tested in the First-In-Man ABSORB Cohort A study, in a series of 30 patients [1, 2] with excellent long-term clinical results reported up to 4 years.[3] In the second generation Absorb BVS, further modifications in the manufacturing processes and scaffold design resulted in a more durable and uniform support and drug delivery to the vessel wall. [4, 5] This second generation Absorb BVS has subsequently been tested in the ABSORB Cohort B trial, which enrolled 101 patients.

Due to the single size availability of this second generation scaffold (3.0 mm in diameter), in ABSORB Cohort B Trial the angiographic inclusion criteria were appropriately restrictive, in that the target lesion must have been located in a native coronary artery with pre-procedural reference vessel diameter (RVD) of 3.0 mm. However within the study, it was found that the visual estimation of the RVD was often incorrect, with a significant number of Absorb BVS being deployed in vessels with a pre-RVD smaller than 2.5 mm by quantitative coronary angiography (QCA). Among the 102 treated-lesions, 41 lesions had a RVD < 2.5 mm (small-vessel group) and 61 lesions had a RVD mm ≥ 2.5 mm (large-vessel group)[6]. Comparable clinical and angiographic outcomes in small and large vessels have been previously reported six months post implantation.[6]

A theoretical concern for the implantation of the BVS in small coronary arteries was the thick struts of this device, a characteristic that was reported in previous studies to be associated with an increased risk of restenosis especially with small vessel diameter.

In the present study we evaluate the impact of vessel size on clinical and angiographic outcomes at 1- and 2-year follow up after implantation of the second generation Absorb BVS. This follow-up time period is critical due to the expected loss of mechanical support of the Absorb BVS, the potential return of vasomotion properties of the treated vessel at 1 year,[7, 8] and the expected substantial scaffold polymer bioresorption at 2 years.[5]

METHODS

Study design and population

The study design and the study device have previously been described.[9] In brief, the ABSORB Cohort B Trial is a multicentre single-arm, prospective, open-label trial assessing the safety and performance of the Absorb BVS (Abbott Vascular, Santa Clara, CA, USA). All patients were older than 18 years, and had a diagnosis of stable or unstable angina, or silent ischemia. As per-protocol, treated-lesions were a maximum of two, de-novo lesions in separate native coronary arteries with a visually estimated diameter of 3.0 mm, a length shorter than 14 mm and a percentage diameter stenosis greater than or equal to 50% and less than 100%. Major exclusion criteria were patients presenting with an acute myocardial infarction or unstable arrhythmias, or those who had left ventricular ejection fraction less than 30%, restenotic lesions, lesions located in the left main coronary artery, lesions involving a side branch more than or equal to 2 mm in diameter, and the presence of thrombus or other clinically significant stenoses in the target vessel. The ethics committee at each participating institution approved the protocol and each patient gave written informed consent prior to inclusion. A total of 101 patients were enrolled in the ABSORB Cohort B study. Out of the total population, 45 patients (45 lesions) were assigned to undergo 6-month and 2-year angiographic follow-up (ABSORB Cohort B1), and 56 patients (57 lesions) 12-month angiographic follow-up (ABSORB Cohort B2). In the present investigation, evaluation of the impact of vessel size (RVD < 2.5 mm or RVD ≥ 2.5 mm) on angiographic outcomes was undertaken at 1 year in the ABSORB Cohort B2 population and at 2 years in ABSORB Cohort B1 population; at the same time points, clinical outcomes in the entire ABSORB Cohort B population (i.e. ABSORB Cohort B1 plus B2) were also evaluated.

QCA analysis

Quantitative coronary angiography (QCA) analyses were performed with the Coronary Angiography Analysis System (Pie Medical Imaging, Maastricht, Netherlands). The 37 µm platinum radio-markers located at each end of the Absorb BVS aided in the localization of the non-radio-opaque scaffold for QCA. The following QCA parameters were computed: pre-procedural reference vessel diameter (RVD) calculated with interpolated method, [10] minimal luminal diameter (MLD), percentage diameter stenosis (%DS), in-scaffold acute gain and binary restenosis. Late loss was defined as the difference between the post-procedural and follow-up minimal luminal diameter.

Furthermore, to adjust for the absolute change in MLD to the vessel size (pre-RVD) post-procedurally and at follow-up, the reporting of relative gain and relative loss – previously

demonstrated to be more representative of the real injury to the vessel wall and the subsequent neointimal response[11, 12] – were undertaken. The absolute net gain, the net gain index and the loss index were also computed.
Those parameters were defined as:

- Relative gain: (post-procedure MLD minus pre-procedure MLD) divided by vessel size.
- Relative loss: (post-procedure MLD minus MLD at follow-up) divided by vessel size.
- Absolute net gain: MLD at follow-up minus pre-procedure MLD.
- Net gain index: net gain normalized for the vessel size and calculated as (MLD at follow-up minus pre-procedure MLD) divided by vessel size.
- Loss index: this is the relation of late loss to acute gain and is calculated as (MLD at follow-up minus post-procedure MLD) divided by (post-procedure MLD minus pre-procedure MLD).

IVUS and IVUS-VH analysis

Scaffolded segments were analyzed post-procedurally and at follow-up with phased array intravascular ultrasound (IVUS) catheters (EagleEye; Volcano Corporation, Rancho Cordova, CA, USA). An automated pullback of 0.5 mm per second was utilized. IVUS images were analyzed off-line with semi-automatic contour detection provided by dedicated software. The vessel area, scaffold area, lumen area, plaque area, in-scaffold neointimal area and lumen area stenosis were measured using a computer based contour detection program. IVUS-VH provides tissue characterization using an autoregressive spectral analysis classification system. Each tissue component is quantified and color-coded as follow: fibrous tissue in green, fibrofatty in greenish yellow, necrotic core in red and calcium in white. For each frame the absolute and the percentage amount of each tissue component is assessed.

OCT analysis

As additional information an OCT data comparison between large and small vessels was performed in the subgroup of patients undergoing OCT imaging at baseline and follow-up. In ABSORB Cohort B Trial OCT imaging was performed at baseline and follow-up in selected centers as an optional investigation. The OCT M3 (Time Domain-OCT) and C7 (Fourier Domain-OCT) systems (LightLab Imaging Inc., Westford, MA, US) were used. The vessels were imaged using an automated pullback system at 20 mm/sec (C7XR system) and 3.0mm/sec (M3 system). During image acquisition, coronary blood was replaced by continuous flushing of contrast at 3.0-4.0 ml/sec. Cross-sectional images were acquired at 100 frames/sec for C7 and at 20 frames/sec for M3. The analysis of continuous cross-sections was performed at each 1 mm longitudinal interval within the treated segment. Quantitative measurements were performed as previously described [7, 9, 13, 14]

Definitions

The composite end point of ischemia-driven major adverse cardiovascular events (ID-MACE) comprised cardiac death, myocardial infarction (MI, classified as Q-wave and Non-Q wave) and ischemia-driven target lesion revascularization (ID-TLR) by CABG or PCI. Angiographic restenosis was defined as a diameter stenosis ≥50% at the treated site at follow-up angiography. Cardiac death was defined as any death in which a cardiac cause could not be excluded. A diagnosis of Q-wave MI was made with evidence of new pathological Q waves on electrocardiogram (ECG). A diagnosis of non-Q-wave MI was made with an elevation of the creatinine kinase (CK) greater than or equal to twice the upper limit of normal, with an elevated CK-MB and the absence of new pathological Q waves. Ischemia-driven target lesion revascularization (ID-TLR) was defined by either of the three following definitions: I) revascularization of the target lesion associated with a positive functional ischemia study, II) ischemia symptoms and angiographic minimal lumen diameter stenosis ≥ 50% by core laboratory assessed quantitative coronary angiography (QCA), III) revascularization of a target lesion with diameter stenosis ≥ 70% by core laboratory assessed QCA, without either ischemic symptoms or a positive functional study.
The ARC (Academic Research Consortium) definitions [15] for stent thrombosis were utilized for this study. The CEC (clinical events committee) reviewed and adjudicated all cases of safety endpoint events.

Funding source and contributors

Abbott Vascular funded the ABSORB Cohort B trial and the present sub-study. The Clinical Events Committee (CEC) comprised of qualified physicians (who were not investigators in the trial) was responsible for adjudicating all MACE-related endpoints. Imaging acquisitions were evaluated by an independent core laboratory (Cardialysis, Rotterdam, The Netherlands). RD and PWS interpreted the data and drafted the report, which was critically revised for important intellectual content by all other authors. SV, XL and KMH approved the final version of the manuscript.

STATISTICAL ANALYSIS

Categorical variables are reported as counts and percentages, continuous variables as mean ± standard deviation (SD). P-values were calculated with Fisher's Exact test for binary variables, Wilcoxon's Rank Sum test for continuous variables and Wilcoxon Signed Rank test for paired comparison between the different time points. A p value <0.05 was considered statistically significant. Statistical analyses were performed using SAS (version 9.1.3).

RESULTS

QCA analysis

Pre-procedural mean RVD was significantly smaller in vessels with RVD < 2.5 mm; percentage diameter stenosis was similar between large and small vessels (Table 1).
Post-procedural MLD was significantly greater in large vessels, however the mean acute gain was similar between groups. After adjustment for vessel size, the relative gain was found to be significantly greater in the small-vessel group.

Table1. Baseline QCA Analysis in ABSORB Cohort B1 and B2 (Intent-to-Treat Populations).

	Cohort B2			Cohort B1		
	Small Vessels (<2.5mm) (N=21) (L=21)	**Large Vessels (>=2.5mm) (N=35) (L=36)**	**P-value**	**Small Vessels (<2.5mm) (N=20) (L=20)**	**Larger Vessels (>=2.5mm) (N=25) (L=25)**	**P-value**
Baseline QCA Analysis						
Pre-Procedure						
RVD (mm)	2.29 ± 0.14 (21)	2.74 ± 0.21 (36)	<0.0001	2.24 ± 0.17 (20)	2.96 ± 0.33 (25)	<0.0001
MLD (mm)	1.01 ± 0.17 (20)	1.10 ± 0.26 (34)	0.1191	0.93 ± 0.22 (19)	1.15 ± 0.35 (25)	0.0492
% DS	56.1 ± 7.27 (20)	59.9 ± 9.20 (34)	0.1939	57.97 ± 11.09 (19)	60.80 ± 11.88 (25)	0.3804
Post-Procedure						
In-Scaffold MLD (mm)	2.16 ± 0.20 (21)	2.33 ± 0.23 (36)	0.0094	2.16 ± 0.24 (20)	2.44 ± 0.22 (25)	0.0007
In-Scaffold % DS	14.6 ± 5.17 (21)	15.6 ± 6.44 (36)	0.7096	13.23 ± 3.03 (20)	17.14 ± 7.02 (25)	0.0375
In-Scaffold Acute Gain (mm)	1.18 ± 0.22 (20)	1.22 ± 0.31 (34)	0.4792	1.23 ± 0.37 (19)	1.29 ± 0.35 (25)	0.6697
Relative Gain	0.51 ± 0.09 (20)	0.45 ± 0.11 (34	0.0542	0.55 ± 0.16 (19)	0.44 ± 0.12 (25)	0.0167

At 1- and 2-year follow-up no differences were reported in in-scaffold late loss, %DS and binary restenosis. Also after adjustment for vessel size, the relative loss, the absolute net gain, the net gain index and the loss index were similar between the small- and large-vessel groups.

Table 2. QCA Analysis ABSORB and B2 at 12-month Follow-Up Cohort B1 at 24-month Follow-Up (Intent-to-Treat Populations).

	Cohort B2 – 12-month follow-up -			Cohort B1 – 24-month follow-up -		
	Small Vessels (<2.5mm) (N=21) (L=21)	Large Vessels (>=2.5mm) (N=35) (L=36)	P-value	Small Vessels (< 2.5mm) (N=20) (L=20)	Larger Vessels (≥ 2.5mm) (N=25) (L=25)	P-value
In-Scaffold Late-Loss (mm)	0.27 ± 0.32 (20)	0.27 ± 0.32 (36)	0.8979	0.29 ± 0.16 (19)	0.25 ± 0.22 (19)	0.4391
In-Scaffold % DS	18.8 ± 10.5 (21)	22.5 ± 11.5 (36)	0.2114	20.72 ± 7.33 (19)	21.17 ± 8.11 (19)	0.7702
In-Scaffold Binary Restenosis	0.0% (0/21)	5.6% (2/36)	0.5263	0.0% (0/19)	0.0% (0/19)	NA
In-Segment Binary Restenosis	0.0% (0/21)	5.6% (2/36)	0.5263	5.3% (1/19)	5.3% (1/19)	1.0000
Relative Loss	0.10 ± 0.14 (21)	0.10 ± 0.13 (36)	0.9073	0.13 ± 0.07 (18)	0.09± 0.08 (19)	0.1489
The Absolute Net Gain	0.92 ± 0.42 (20)	0.96 ± 0.35 (34)	0.9926	0.97 ± 0.32 (18)	1.02 ± 0.47 (19)	0.7267
The Net Gain Index	0.41 ± 0.18 (20)	0.34 ± 0.12 (34)	0.0564	0.43 ± 0.14 (18)	0.35 ± 0.16 (19)	0.1040
The Loss Index	0.23 ± 0.32 (19)	0.20 ± 0.22 (34)	0.8311	0.21 ± 0.16 (18)	0.23 ± 0.22 (19)	0.7041

IVUS and IVUS-VH analysis

In the large vessel group, paired per lesion IVUS grey scale analysis demonstrated a constant vessel area growth at each time point that became significant at 2-year follow-up associated with a similar plaque area enlargement. Scaffold area also showed a significant enlargement between 6 months and 2 years. Lumen area numerically increased in ABSORB cohort B1 between 6-month and 2-year follow-up but without reaching any statistical significance; with a borderline significant decrease in ABSORB Cohort B2 between baseline and 1-year follow-up (Table 3).

In the small vessel group, vessel area was observed to grow from baseline to 6-month and 2-year follow-up and was associated with a parallel growth in plaque area over time (Table 3). The scaffold area at 6-month follow-up did not show any enlargement but was observed to grow significantly from 6-month to 2-year follow-up. The lumen area followed a similar evolution over time with a significant late lumen enlargement from 6-month to 2-year follow-up. (Table 3)

Comparison of small and large vessels at 1- and 2-year follow-up showed similar minimal lumen area, % lumen area stenosis and neointimal hyperplasia area between groups at each time point. (Table 3)

Paired per-lesion IVUS-VH analyses demonstrated a consistent reduction in dense calcium content over time that reached the significant level in the cohort B2 at 1-year follow-up

Table 3. Paired Per-Lesion IVUS Measurements at 1-year follow-up in Cohort B 2 and 2-year follow-up in Cohort B 1 and comparison small and large vessels at 1- and 2-year follow-up (Intent-to-Treat Populations).

Paired Per-Lesion Analysis								
	Cohort B2			**Cohort B1**				
	Post-Procedure (N=35) (L=36)	**1-Year (N=35) (L=36)**	**p-value**	**Post-Procedure (N=25) (L=25)**	**6-Month (N=25) (L=25)**	**2-Year (N=25) (L=25)**	**p-value[2] Post vs. 2Y**	**p-value[2] 6M vs. 2Y**
Large Vessels								
Average Vessel Area (mm^2)	14.78 ± 3.43 (34)	14.89 ± 3.22 (34)	0.6153	16.18 ± 2.74 (17)	16.51 ± 2.92 (17)	17.47 ± 3.49 (17)	0.0038	0.0003
Average Scaffold Area (mm^2)	6.48 ± 1.00 (34)	6.42 ± 0.97 (34)	0.1641	7.21 ± 1.04 (17)	7.04 ± 1.01 (17)	7.70 ± 1.89 (17)	0.2247	0.0154
Average Lumen Area (mm^2)	6.51 ± 1.05 (34)	6.40 ± 0.99 (34)	0.0541	7.22 ± 1.04 (17)	6.97 ± 1.03 (17)	7.47 ± 1.99 (17)	0.9724	0.2114
Average Plaque Area (mm^2)	8.27 ± 2.77 (34)	8.49 ± 2.61 (34)	0.0873	8.96 ± 2.08 (17)	9.53 ± 2.22 (17)	10.00 ± 2.36 (17)	0.0007	0.0076
Minimal Lumen Area (mm^2)	5.30 ± 1.04 (34)	5.13 ± 0.92 (34)	0.0620	5.97 ± 0.99 (17)	5.56 ± 0.91 (17)	5.54 ± 1.38 (17)	0.0887	0.8307
Neointimal Hyperplasia (NIH) Area (mm^2)	---	0.05 ± 0.09 (35)	---	---	0.10 ± 0.13 (17)	0.25 ± 0.29 (17)	---	0.0286
Small Vessels								
Average Vessel Area (mm^2)	12.74 ± 1.52 (20)	14.19 ± 2.79 (20)	0.0032	11.78 ± 3.50 (16)	12.25 ± 3.47 (16)	13.09 ± 3.38 (16)	< 0.0001	0.0015
Average Scaffold Area (mm^2)	5.96 ± 0.64 (20)	6.18 ± 1.00 (20)	0.4139	5.82 ± 1.01 (16)	5.76 ± 0.96 (16)	6.41 ± 1.30 (16)	0.0015	0.0008
Average Lumen Area (mm^2)	5.97 ± 0.64 (20	6.21 ± 1.46 (20)	0.8983	5.79 ± 1.01 (16)	5.71 ± 0.98 (16)	6.20 ± 1.27 (16)	0.1883	0.0155
Minimal Lumen Area (mm^2)	4.79 ± 0.73 (20)	4.72 ± 1.03 (20)	0.7306	4.88 ± 0.88 (16)	4.66 ± 0.91 (16)	4.69 ± 0.96 (16)	0.1553	0.7300
Average Plaque Area (mm^2)	6.77 ± 1.31 (20)	7.98 ± 1.84 (20)	< 0.0001	5.99 ± 2.79 (16)	6.54 ± 2.72 (16)	6.89 ± 2.56 (16)	< 0.0001	0.0562
NIH Area (mm^2)	---	0.16 ± 0.24 (21)	---	---	0.06 ± 0.13 (16)	0.25 ± 0.25 (16)	---	0.0009
Comparison small and large vessels								
	Cohort B2, 1-year follow-up			**Cohort B1, 2-year follow-up**				
	Small Vessels (<2.5mm) (N=21) (L=21)	**Large Vessels (>=2.5mm) (N=35) (L=36)**	**P-value**	**Small Vessels (< 2.5mm) (N=20) (L=20)**	**Large Vessels (≥ 2.5mm) (N=25) (L=25)**		**P-value**	
Minimal Lumen Area (mm^2)	4.66 ± 1.04 (21)	5.14 ± 0.91 (35)	0.1601	4.83 ± 0.97 (19)	5.51 ± 1.43 (19)		0.1611	
Lumen Area Stenosis (%)	23.85 ± 9.95 (21)	19.92 ± 5.34 (35)	0.2104	22.75 ± 8.30 (19)	26.19 ± 8.87 (19)		0.3069	
Neointimal Hyperplasia Area (mm^2)	0.16 ± 0.24 (21)	0.05 ± 0.09 (35)	0.0556	0.25 ± 0.26 (19)	0.23 ± 0.28 (19)		0.4813	

Table 4. OCT Comparison small and large vessels.

	Cohort B1+B2 post-procedure			Cohort B2, 1-year follow-up			Cohort B1, 2-year follow-up		
	Small Vessels (<2.5mm) (N=39) (L=39)	**Large Vessels (>=2.5mm) (N=58) (L=61)**	**P-value**	**Small Vessels (<2.5mm) (N=) (L=)**	**Large Vessels (>=2.5mm) (N=) (L=)**	**P-value**	**Small Vessels (< 2.5mm) (N=19) (L=19)**	**Large Vessels (≥ 2.5mm) (N=) (L=)**	**P-value**
Mean scaffold area, mm	7.02 ± 0.99 (20)	7.97 ± 1.02 (30)	0.0021	7.39 ± 1.10 (11)	7.47 ± 1.36 (18)	0.8667	7.27 ± 1.82 (12)	8.80 ± 1.76 (15)	0.0385
Minimal scaffold area	5.83 ± 1.04 (20)	6.56 ± 1.02 (30)	0.0185	5.78 ± 1.18 (11)	6.17 ± 1.10 (18)	0.3779	5.55 ± 1.26 (12)	6.90 ± 1.38 (15)	0.0142
Mean NH area (mm^2)	NA	NA	NA	1.42 ± 0.82 (11)	1.30 ± 0.69 (18)	0.7096	2.03 ± 0.57 (12)	2.06 ± 0.47 (15)	0.9006
Mean lumen area	6.81 ± 1.08 (20)	7.94 ± 1.16 (30)	0.0010	5.93 ± 1.86 (11)	6.01 ± 1.63 (18)	0.9072	5.09 ± 1.47 (12)	6.60 ± 1.71 (15)	0.0207
Minimal lumen area	5.57 ± 1.12 (20)	6.34 ± 1.01 (30)	0.0174	4.04 ± 1.36 (11)	4.55 ± 1.38 (18)	0.3457	3.58 ± 1.23 (12)	4.72 ± 1.46 (15)	0.0375
% Lumen Area Stenosis	18.50 ± 7.67 (20)	19.98 ± 7.57 (30)	0.5056	31.95 ± 9.83 (11)	25.66 ± 12.85 (18)	0.1502	29.42 ± 11.85 (12)	28.69 ± 10.07 (15)	0.8655
Uncovered struts, %	97.63 ± 5.12 (20)	97.77 ± 4.76 (30)	0.9238	2.36 ± 2.34 (11)	3.85 ± 3.28 (18)	0.1637	1.99 ± 3.41 (12)	1.12 ± 1.29 (15)	0.4170
Incomplete strut apposition (mm^2)	0.28 ± 0.30 (8)	0.37 ± 0.64 (25)	0.5711	1.57 ± 0.78 (3)	2.65 ± 1.77 (4)	0.3340	1.97 ± NA (1)	8.77 ± NA (1)	NA

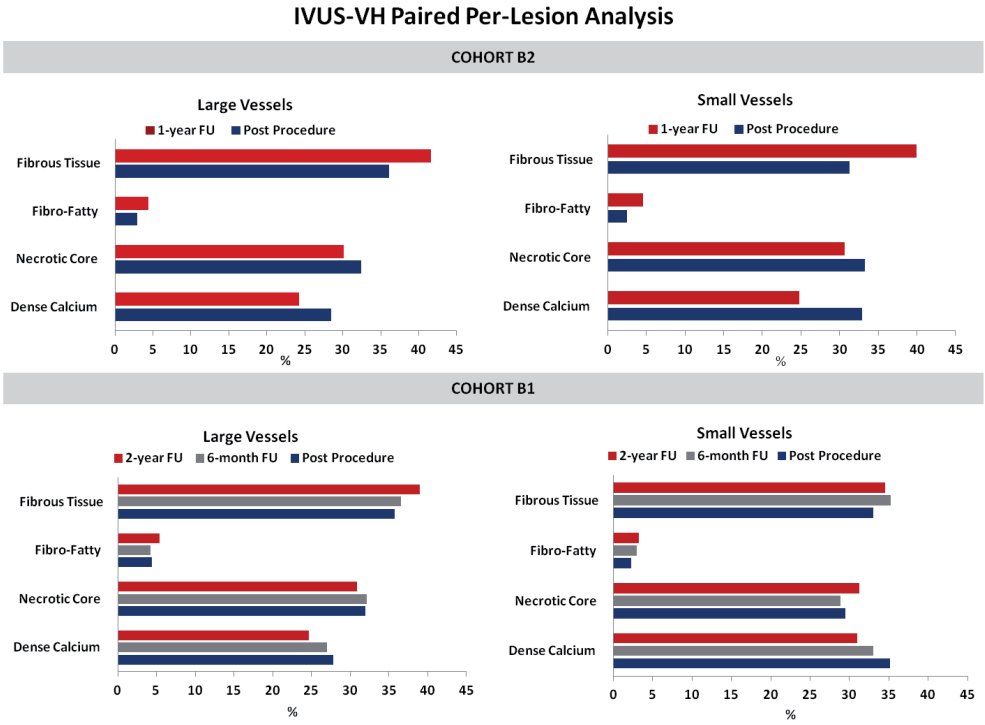

Figure 1. Serial changes in plaque composition in small and large vessels treated with second generation BVS. The dense calcium content (surrogate marker of scaffold bioresorption) decreased over time in both groups. No significant changes in necrotic core and a mild increase in fibro-fatty and fibrous tissue were consistently observed in both groups.

(large vessels 28.50 ± 9.05% vs 24.13 ± 7.84%, p=0.0041; small vessels 32.96 ± 11.65% vs 24.77 ± 7.75%, p=0.0047) but was not significant at 2-year in cohort B1. Fibrous and fibro-fatty tissue significantly increased at 1-year follow-up (Fibrous tissue: large vessels 36.14 ± 10.89% vs 41.52 ± 9.75% p=0.0148; small vessels 31.28 ± 10.01% vs 39.98 ± 9.25%, p=0.0104. Fibro-fatty large vessels 2.90 ± 2.40 % vs 4.35 ± 2.20 % p=0.0035; small vessels 2.50 ± 1.90 % vs 4.56 ± 2.79 %, p= 0.0120). No changes in percentage necrotic core were observed at either time point. No further differences in plaque compositional characteristics were detected between small and large vessels at 1-and 2-year follow-up. (Figure 1-2, Appendix Table 6)

OCT analysis

OCT data at baseline were available for the present analysis in 50 patients, 20 patients in the small vessel group and 30 in the large vessel group. Post-procedurally the incomplete stent apposition (ISA) area was similar in both groups. Mean scaffold area, minimal

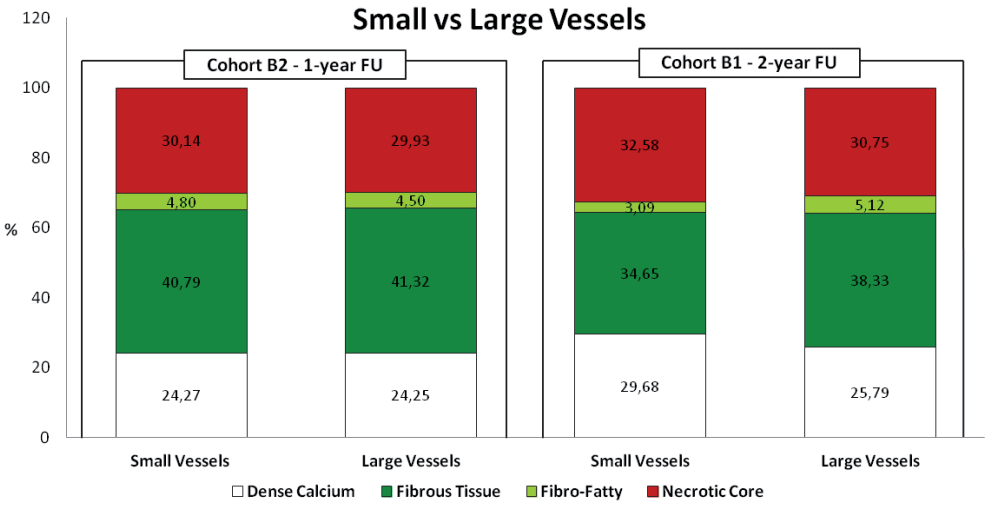

Figure 2. Comparison of plaque compositional findings between small and large vessels at 1- and 2-year follow-up. Small and large vessels showed similar plaque composition at both follow-up time points..

scaffold area, mean lumen area and minimal lumen area were significantly larger in the large vessel group and this was observed also at 2-year follow-up. No differences in % uncovered struts, % lumen area stenosis and mean neointimal hyperplasia (NH) area were observed over time. (Table 4)

Clinical Outcomes

At 1-year follow-up, comparisons of clinical outcomes between small and large vessels, demonstrated no differences in MACE (small-vessel group: 3/41 cases, 7.3% and large-vessel group 4/60 cases, 6.7%, p=1.0000), MI (small-vessel group: 2/41 cases, 4.9% and large-vessel group 1/60 cases, 1.7%, p=0.5645) or ischemia driven target lesion revascularization (TLR) (small-vessel group: 1/41 cases, 2.4%; large-vessel group 3/60, 5.0%, p=0.6445). (Table 5, Appendix Figure 3)

At 2-year follow-up only 2 further events were reported, namely 2 ischemia-driven TLR, both in the large vessels group. (Appendix Figure 4) Comparisons of clinical outcomes between small and large vessels, demonstrated no differences in MACE, MI or ischemia driven target lesion revascularization (TLR). No deaths were reported in either group up to 2 years. No episodes of definite, probable, or possible scaffold thrombosis were observed up to 2 years. (Table 5)

Table 5. Adverse Events at 12- and 24-Month Follow-Up in the entire population (Cohort B1 and B2) (Intent-to-Treat Population).

	Cohort B1 and B2 12-Month Follow-Up			Cohort B1 and B2 24-Month Follow-Up		
	Small Vessels (<2.5mm) (N=41)	Large Vessels (>=2.5mm) (N=60)	P-value	Small Vessels (<2.5mm) (N=41)	Large Vessels (>=2.5mm) (N=60)	P-value
MACE (Cardiac Death, MI, ID-TLR)	7.3% (3/41)	6.7% (4/60)	1.0000	7.3% (3/41)	10.2% (6/59)	0.7335
Cardiac Death	0.0% (0/41)	0.0% (0/60)	NA	0.0% (0/41)	0.0% (0/59)	NA
Myocardial Infarction (MI)	4.9% (2/41)	1.7% (1/60)	0.5645	4.9% (2/41)	1.7% (1/59)	0.5662
QMI	0.0% (0/41)	0.0% (0/60)	NA	0.0% (0/41)	0.0% (0/59)	NA
NQMI	4.9% (2/41)	1.7% (1/60)	0.5645	4.9% (2/41)	1.7% (1/59)	0.5662
ID-TLR (PCI)	2.4% (1/41)	5.0% (3/60)	0.6445	2.4% (1/41)	8.5% (5/59)	0.3962
Scaffold Thrombosis	0.0% (0/41)	0.0% (0/60)	NA	0.0% (0/41)	0.0% (0/60)	NA

DISCUSSION

The present study investigated the long-term clinical and angiographic outcomes following the implantation of the second generation Absorb everolimus eluting bioresorbable vascular scaffold in small and large vessels. The major findings are: I) similar angiographic results were observed up to 2-year follow-up and the significant larger relative gain attained in the small-vessel group at the index procedure, that did not translate into greater relative late lumen loss, percentage diameter stenosis or binary restenosis at 2 years; II) IVUS grey scale analyses in the small vessel group demonstrated expansive vessel remodeling associated with a significant late lumen enlargement; III) Both the small- and large- vessel groups, treated with a 3.0 mm Absorb BVS, showed a similar and low rate of cardiovascular events

Angiographic results

In the ABSORB Cohort B Trial, vessels with a RVD < or ≥ 2.5 mm were both treated with a 3.0 mm device. Both groups demonstrated a similar pre-procedural MLD and post-procedural in-scaffold acute gain. Following adjustment for vessel size, it was demonstrated that the relative gain was significantly greater in the small-vessel group compared to the large-vessel group.

In previous studies, a larger relative gain was observed to be an independent predictor of restenosis, with a direct relationship between relative gain and the subsequent relative loss at follow-up. [11, 16]

Schwartz et al [17] previously demonstrated that neointimal growth is proportional to the degree of vessel injury during the index procedure, and more specifically to the disruption of the internal elastic membrane. Consequently if we consider the relative gain as a surrogate measurement of the vessel injury induced by treatment, a greater luminal re-narrowing in vessels with a greater luminal relative gain is not surprising.[18]

Theoretically a similar relative gain and injury in small and large vessels would produce a similar quantitative neointimal response. In this situation small vessels would be less able to accommodate the same absolute amount of neointimal tissue compared to large vessels. [19, 20]

These considerations suggest that optimal acute and long-term outcomes after coronary interventions may result from the appropriate balance between luminal gain and vascular injury.

In the present study the implantation of a 3.0 mm Absorb BVS in vessels with RVD < 2.5 mm produced a significantly larger angiographic relative gain in small vessels compared to large vessels. At 1-and 2-year follow-up no differences in relative loss and percentage diameter stenosis were evident. Furthermore the net gain index (describing the outcome of intervention relating the pre MLD to the MLD at follow-up),[11] and the loss index (relating late loss to acute gain)[12] were also similar between the small- and large-vessel groups.

These data suggest that the slightly higher relative gain in the present series of small vessels, was associated with a favorable balance between vessel injury and luminal expansion, followed by comparable long-term clinical and angiographic outcomes between groups.

IVUS grey scale analyses

IVUS geometrical analyses demonstrated that at 1- and 2-year follow-up, minimal lumen area, percentage lumen area stenosis and neointimal hyperplasia area were similar between small and large vessels. Specifically, the neointimal hyperplasia area in both the small and large vessel groups and at both time points was limited and at the resolution limit of the imaging technique, [21] thus making even a statistically significant difference poorly relevant. IVUS analyses demonstrated also a consistent growth in vessel area over time irrespectively of vessel size; this observation was associated with an increase in plaque area but also with an increase in scaffold area, that was observed to occur in both large and small vessel at 2-year follow-up. These findings are consistent with the planned scaffold bioresorption process. During the first months after implantation the

Absorb BVS plays a role similar to conventional metallic DES, providing essentially a vessel mechanical scaffolding and drug elution. Between 6 months and 1 year the gradual polymer degradation leads to a progressive loss in scaffold structural integrity, and as recently demonstrated the return of the vasomotion properties of the treated segment at 12-month follow-up.[8]

Furthermore, whilst at 6-months lumen area slightly decreased as would be expected after conventional metallic stent implantation, at 2-year follow-up a late lumen enlargement was observed, that reached statistical significance in the small vessel group.

A largely accepted theory for the higher rates of restenosis and clinical events in small vessels is that a smaller lumen area is less able to accommodate the same amount of neointimal tissue compared to a larger lumen area. [19] Therefore, in this scenario a late lumen enlargement may play a key role in the prevention of restenosis in the small vessels lesions subset.

These data also suggest that the potential concern related to the implantation of the present thick strut BVS (strut thickness 157 μm) in vessels with small lumen area may be unfounded.

IVUS-VH analysis

The dense calcium content has been previously used as a surrogate marker of polymer bioresorption [22, 23, 24] and in the present study was observed to decrease in parallel to a mild increase in fibro-fatty and fibrous tissue over time in both groups reaching the statistically significant level at 1-year follow-up in the Cohort B2 population. Compositional analyses also disclosed no significant changes in necrotic core content in both groups over time, consistently with previous histological studies reporting no relevant inflammatory response associated with Absorb BVS implantation.[5] (Figure 1-2, Appendix table 6)

OCT analysis

The OCT analysis showed a larger mean scaffold area, minimal scaffold area, mean lumen area and minimal lumen area, in large vessels compared with small vessels with similar post-procedural % lumen area stenosis, demonstrating a larger stent deployment and vessels size in the large vessel group.

Notably at baseline the mean incomplete stent apposition (ISA) area was similar between the two groups reducing the possibility that the increased positive vessel remodeling in the small vessel group was due to an artificial improved stent apposition and drug elution in this population.

At 2-year follow-up similar neointimal growth was observed between small and large vessels and in only in one patient for each group was detectable incomplete stent apposition.

Clinical outcomes

A small vessel diameter is a well-recognized independent predictor of a higher rate of in-stent restenosis and poorer clinical outcomes [25, 26] with bare metal stents and first and second generation drug eluting stents.[27, 28, 29]

In the present study, the long-term clinical outcomes after implantation of the second generation Absorb BVS in small vessels were similar to that observed in large vessels, with low and comparable rates of MI and ischemia-driven TLR. Notably, no death or in-scaffold thrombosis events were reported at 2-year follow-up.

The two clinical events reported between 6 and 12 months and the further 2 between 1 and 2 years all occurred in the large vessel group. (Appendix Figure 3 and 4) Furthermore the three events that occurred in the small vessel group up to 6 months were likely to have been related to baseline procedural complications, rather than device failure *per se*.[6]

However, it should be highlighted that due to the limited patients population and low incidence rate in this study, caution should be made in making conclusions with regards to the safety.

In conclusion, treatment of small vessels with second generation Absorb BVS was observed in the present report to be associated with similar angiographic, IVUS and long-term clinical outcomes compared to large vessels. The expected loss of structural integrity of the Absorb BVS device, and the return of the vasomotor properties of the treated vessel, unhindered by a metallic cage, translated into further beneficial positive remodeling and late lumen enlargement, which was particularly relevant in the small vessel group.

Study limitations

The present study is a post-hoc analysis of the ABSORB Cohort B Trial. Due to the limited patient population, the *p* values were calculated for descriptive purposes and should be considered as exploratory and hypothesis generating. Further investigations are needed to fully investigate the impact of vessel size on clinical and angiographic outcomes after Absorb BVS implantation.

In Absorb Cohort B the bioresorbable vascular scaffold was implanted in discrete lesions located in native coronary arties excluding restenotic lesions, lesions located in the left main coronary artery, lesions involving a side branch more than 2 mm in diameter, and lesions with presence of thrombus or another clinically significant stenosis in the target vessel. We therefore cannot exclude that the implantation of BVS in different and more

complex lesions could have been associated with different results.
During the ABSORB Cohort B study only the 3 mm BVS was available. A novel BVS 2.5mm mm is currently under clinical evaluation in two separate studies (the multicenter ABSORB Extend Single-Arm Study and the ABSORB II Randomized Controlled Trial) possibly aiding in further understanding on the performance of this device in the small vessels scenario. Quantitative coronary angiography that in the present paper was used to define vessel size is characterized by the detection of the angiographic lumen contour without any evaluation of the actual vessel wall size.

CONCLUSION

In the present study the implantation of the 3.0 mm ABSORB everolimus eluting bioresorbable vascular scaffold in coronary arteries with RVD < 2.5 mm appears safe, with angiographic and clinical outcomes similar to those in large vessels at 1- and 2-year follow-up. A favourable balance between acute luminal gain and vascular injury and the observed significant late lumen enlargement may be the possible explanation for the encouraging long-term results in small vessels.

REFERENCES

1 Serruys PW, Ormiston JA, Onuma Y, et al. A bioabsorbable everolimus-eluting coronary stent system (ABSORB): 2-year outcomes and results from multiple imaging methods. *Lancet* 2009;373:897-910.

2 Onuma Y, Serruys PW, Ormiston JA, et al. Three-year results of clinical follow-up after a bioresorbable everolimus-eluting scaffold in patients with de novo coronary artery disease: the ABSORB trial. *EuroIntervention* 2010;6:447-53.

3 Dudek D, Onuma Y, Ormiston JA, et al. Four-year clinical follow-up of the ABSORB everolimus-eluting bioresorbable vascular scaffold in patients with de novo coronary artery disease: the ABSORB trial. *EuroIntervention : journal of EuroPCR in collaboration with the Working Group on Interventional Cardiology of the European Society of Cardiology* 2012;7:1060-1.

4 Okamura T, Garg S, Gutierrez-Chico JL, et al. In vivo evaluation of stent strut distribution patterns in the bioabsorbable everolimus-eluting device: an OCT ad hoc analysis of the revision 1.0 and revision 1.1 stent design in the ABSORB clinical trial. *EuroIntervention* 2010;5:932-8.

5 Onuma Y, Serruys PW, Perkins LE, et al. Intracoronary optical coherence tomography and histology at 1 month and 2, 3, and 4 years after implantation of everolimus-eluting bioresorbable vascular scaffolds in a porcine coronary artery model: an attempt to decipher the human optical coherence tomography images in the ABSORB trial. *Circulation* 2010;122:2288-300.

6 Diletti R, Onuma Y, Farooq V, et al. 6-month clinical outcomes following implantation of the bioresorbable everolimus-eluting vascular scaffold in vessels smaller or larger than 2.5 mm. *Journal of the American College of Cardiology* 2011;58:258-64.

7 Serruys PW, Onuma Y, Dudek D, et al. Evaluation of the second generation of a bioresorbable everolimus-eluting vascular scaffold for the treatment of de novo coronary artery stenosis: 12-month clinical and imaging outcomes. *Journal of the American College of Cardiology* 2011;58:1578-88.

8 Brugaletta S, Heo JH, Garcia-Garcia HM, et al. Endothelial-dependent vasomotion in a coronary segment treated by ABSORB everolimus-eluting bioresorbable vascular scaffold system is related to plaque composition at the time of bioresorption of the polymer: indirect finding of vascular reparative therapy? *European heart journal* 2012.

9 Serruys PW, Onuma Y, Ormiston JA, et al. Evaluation of the second generation of a bioresorbable everolimus drug-eluting vascular scaffold for treatment of de novo coronary artery stenosis: six-month clinical and imaging outcomes. *Circulation* 2010;122:2301-12.

10 Reiber JH, Serruys PW. Quantitative Coronary Angiography: Methodologies. *Quantitative Coronary Angiography*. Dordrecht, The Netherlands: Kluwer Academic Publishers 1991:98-102.

11 Serruys PW, Foley DP, de Feyter PJ. Restenosis after coronary angioplasty: a proposal of new comparative approaches based on quantitative angiography. *Br Heart J* 1992;68:417-24.

12 Violaris AG, Melkert R, Serruys PW. Long-term luminal renarrowing after successful elective coronary angioplasty of total occlusions. A quantitative angiographic analysis. *Circulation* 1995;91:2140-50.

13 Gomez-Lara J, Brugaletta S, Diletti R, et al. A comparative assessment by optical coherence tomography of the performance of the first and second generation of the everolimus-eluting bioresorbable vascular scaffolds. *European heart journal* 2011;32:294-304.

14 Gomez-Lara J, Radu M, Brugaletta S, et al. Serial analysis of the malapposed and uncovered struts of the new generation of everolimus-eluting bioresorbable scaffold with optical coherence tomography. *JACC Cardiovascular interventions* 2011;4:992-1001.

15 Cutlip DE, Windecker S, Mehran R, et al. Clinical end points in coronary stent trials: a case for standardized definitions. *Circulation* 2007;115:2344-51.

16 Rensing BJ, Hermans WR, Vos J, et al. Angiographic risk factors of luminal narrowing after coronary balloon angioplasty using balloon measurements to reflect stretch and elastic recoil at the dilation site. The CARPORT Study Group. *Am J Cardiol* 1992;69:584-91.

17 Schwartz RS, Huber KC, Murphy JG, et al. Restenosis and the proportional neointimal response to coronary artery injury: results in a porcine model. *J Am Coll Cardiol* 1992;19:267-74.

18 Beatt KJ, Serruys PW, Luijten HE, et al. Restenosis after coronary angioplasty: the paradox of increased lumen diameter and restenosis. *J Am Coll Cardiol* 1992;19:258-66.

19 Honda Y, Fitzgerald PJ. Stent expansion as a mechanical parameter to predict late stent patency: back to the basics. *JACC Cardiovasc Interv* 2009;2:1276-8.

20 Farooq V, Gogas BD, Serruys PW. Restenosis: delineating the numerous causes of drug-eluting stent restenosis. *Circ Cardiovasc Interv*;4:195-205.

21 Suzuki Y, Ikeno F, Koizumi T, et al. In vivo comparison between optical coherence tomography and intravascular ultrasound for detecting small degrees of in-stent neointima after stent implantation. *JACC Cardiovasc Interv* 2008;1:168-73.

22 Brugaletta S, Garcia-Garcia HM, Diletti R, et al. Comparison between the first and second generation bioresorbable vascular scaffolds: a six month virtual histology study. *EuroIntervention*;6:1110-6.

23 Garcia-Garcia HM, Gonzalo N, Pawar R, et al. Assessment of the absorption process following bioabsorbable everolimus-eluting stent implantation: temporal changes in strain values and tissue composition using intravascular ultrasound radiofrequency data analysis. A substudy of the ABSORB clinical trial. *EuroIntervention* 2009;4:443-8.

24 Sarno G, Onuma Y, Garcia Garcia HM, et al. IVUS radiofrequency analysis in the evaluation of the polymeric struts of the bioabsorbable everolimus-eluting device during the bioabsorption process. *Catheter Cardiovasc Interv*;75:914-8.

25 Kastrati A, Schomig A, Elezi S, et al. Predictive factors of restenosis after coronary stent placement. *J Am Coll Cardiol* 1997;30:1428-36.

26 Elezi S, Kastrati A, Neumann FJ, et al. Vessel size and long-term outcome after coronary stent placement. *Circulation* 1998;98:1875-80.

27 Agostoni P, Biondi-Zoccai GG, Gasparini GL, et al. Is bare-metal stenting superior to balloon angioplasty for small vessel coronary artery disease? Evidence from a meta-analysis of randomized trials. *Eur Heart J* 2005;26:881-9.

28 Biondi-Zoccai G, Moretti C, Abbate A, et al. Percutaneous coronary intervention for small vessel coronary artery disease. *Cardiovasc Revasc Med*;11:189-98.

29 Garg S, Serruys PW. Coronary stents: current status. *J Am Coll Cardiol* 2010;56:S1-42.

30 Gogas BD, Serruys PW, Diletti R, et al. Vascular Response of the Segments Adjacent to the Proximal and Distal Edges of the ABSORB Everolimus-Eluting Bioresorbable Vascular Scaffold: 6-Month and 1-Year Follow-Up Assessment: A Virtual Histology Intravascular Ultrasound Study From the First-in-Man ABSORB Cohort B Trial. *JACC Cardiovascular interventions* 2012;5:656-65.

APPENDIX I

Table 6. IVUS-VH Paired Per-Lesion Analysis Cohort B1 and B2 and comparison small and large vessels at 1- and 2-year follow-up (Intent-to-Treat Population).

Paired Per-Lesion Analysis								
	Cohort B2			**Cohort B1**				
	Post-Procedure (N=35) (L=36)	**1-year (N=35) (L=36)**	**p-value**	**Post-Procedure (N=20) (L=20)**	**6-Month (N=20) (L=20)**	**2-Year (N=16) (L=16)**	**P-value Post vs. 2Y**	**P-value 6M vs. 2Y**
Large vessels								
% Dense Calcium	28.50 ± 9.05 (30)	24.13 ± 7.84 (30)	0.0041	27.82 ± 9.85 (14)	27.04 ± 8.84 (14)	24.68 ± 7.28 (14)	0.0785	0.2412
% Necrotic Core	32.46 ± 7.39 (30)	29.99 ± 6.90 (30)	0.1274	31.98 ± 8.87 (14)	32.15 ± 6.46 (14)	30.91 ± 5.13 (14)	0.6257	0.2166
% Fibro-Fatty	2.90 ± 2.40 (30)	4.35 ± 2.20 (30)	0.0035	4.45 ± 6.10 (14)	4.25 ± 5.09 (14)	5.43 ± 3.77 (14)	0.0676	0.1040
% Fibrous tissue	36.14 ± 10.89 (30)	41.52 ± 9.75 (30)	0.0148	35.75 ± 12.01 (14)	36.56 ± 9.07 (14)	38.98 ± 7.16 (14)	0.2958	0.4631
Small Vessels								
% Dense Calcium of VH plaque	32.96 ± 11.65 (18)	24.77 ± 7.75 (18)	0.0047	35.16 ± 15.96 (12)	32.99 ± 11.70 (12)	30.98 ± 7.78 (12)	0.2334	0.4238
% Necrotic Core of VH plaque	33.26 ± 5.57 (18)	30.69 ± 6.20 (18)	0.2288	29.49 ± 6.89 (12)	28.82 ± 5.05 (12)	31.24 ± 3.81 (12)	0.0771	0.1763
% Fibro-Fatty of VH plaque	2.50 ± 1.90 (18)	4.56 ± 2.79 (18)	0.0120	2.29 ± 2.76 (12)	2.97 ± 1.86 (12)	3.23 ± 1.32 (12)	0.2334	0.4697
% Fibrous of VH plaque	31.28 ± 10.01 (18)	39.98 ± 9.25 (18)	0.0104	33.06 ± 16.67 (12)	35.21 ± 12.10 (12)	34.55 ± 7.78 (12)	0.7910	0.7910
Comparison small and large vessels								
	Cohort B2, 1-year follow-up			**Cohort B1, 2-year follow-up**				
	Small Vessels (<2.5mm) (N=21) (L=21)	**Large Vessels (>=2.5mm) (N=35) (L=36)**	**P-value**	**Small Vessels (< 2.5mm) (N=20) (L=20)**	**Large Vessels (≥ 2.5mm) (N=25) (L=25)**	**P-value**		
% Dense Calcium	24.27 ± 7.85 (19)	24.25 ± 7.97 (33)	0.9697	29.68 ± 7.18 (16)	25.79 ± 7.43 (16)	0.2351		
% Necrotic Core	30.14 ± 6.49 (19)	29.93 ± 7.11 (33)	0.9092	32.58 ± 4.42 (16)	30.75 ± 4.82 (16)	0.2206		
% Fibro-Fatty	4.80 ± 2.91 (19)	4.50 ± 2.33 (33)	0.9243	3.09 ± 1.20 (16)	5.12 ± 3.61 (16)	0.0863		
% Fibrous	40.79 ± 9.66 (19)	41.32 ± 9.60 (33)	0.7181	34.65 ± 6.84 (16)	38.33 ± 6.93 (16)	0.1935		

APPENDIX II

Case descriptions of clinical events

Events between 6- and 12-month follow-up

Between 6- and 12-month follow-ups, two new ID-TLRs were observed in the large-vessel group; no clinical events occurred in the small vessel group within this time period.

The first patient (RVD 2.81 mm) was a 76-year-old male, with treated hypercholesterolemia, family history of premature CAD, previous PTCA with metallic stent in the middle part of LAD (non-target lesion). The patient presented with stable angina, Canadian Cardiovascular Society Angina Classification Class III.

Initial coronary angiography revealed a significant lesion in the proximal LAD. After pre-dilatation with a semi-compliant balloon (2.5x12mm) to 16 ATM, a 3.0x18mm Absorb BVS was deployed in the proximal LAD to a maximal implantation pressure of 14 ATM. The % diameter stenosis was reduced to 12% post procedure. Post dilatation was not performed. On review of the cine-angiograms, it was also observed that the scaffold was deployed slightly distal to the segment pre-dilated with a modest geographical miss. (Appendix Figure 3)

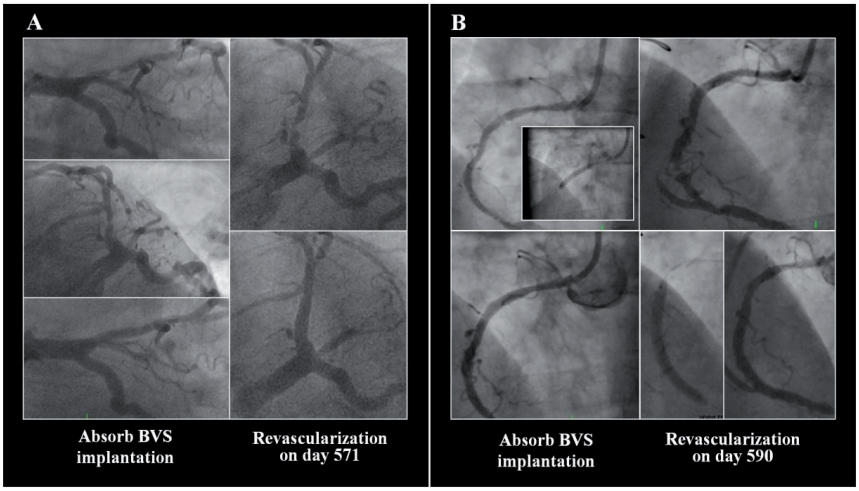

Figure 3. Clinical events between 6-month and 1-year follow-up.
Two target lesion revascularizations occurred both in large vessels (namely in the proximal left anterior descending artery). Of note in one case (A, left panel) the Absorb BVS was deployed slightly distally in the pre-dilated region (white line). Vascular response to vessel injury can therefore not be excluded as cause of restenosis at the proximal edge (platinum markers indicated by the white arrows). In the second case (B, right panel) restenosis developed in the mid segment of the BVS (B, upper panel). The magnified scaffolded segment (B, lower panel) shows the 2 platinum markers (black arrows) and the focal in-scaffold restenosis (white arrows).

On day 358, the patient was hospitalized due to unstable angina pectoris. ECG revealed sinus bradycardia (53/minute), normal axis and conduction. Angiography disclosed a scaffold proximal edge stenosis. Direct stenting in overlap with the area of the study device was performed with a metallic Xience V everolimus eluting stent 3.0x15 mm with a good angiographic result. The CEC adjudicated this event per protocol as ischemia driven target lesion revascularization. In this case geographical miss during scaffold deployment, and the subsequent vascular response to injury after predilatation, are the probable causes for repeat revascularization.

In the second case (RVD 2.64 mm), a 57-year old man with treated hypercholesterolemia, former tobacco use, history of ischemic cardiomyopathy and unstable angina, Braunwald class II, normal cardiac enzymes, was treated for a significant focal lesion in the proximal LAD. After pre-dilatation with a semi compliant balloon 2.5 x 10 mm (12 atm), a 3.0 x 18 mm Absorb BVS (12 atm) was implanted and post-dilated with a 3.0x10 mm non-compliant balloon (20 atm).

On day 353 the patient was readmitted due to chest pain with elevation of troponin (0.3µg/L, ULN=0.03µg/L), normal CK (89U/L, ULN=200U/L) and normal CK-MB (5.4µg/L, ULN=6.73µg/L). ECG showed an incomplete RBB and anteroseptal sub-epicardial ischemia. Cardiac ultrasound revealed anterior hypokinesis with a LVEF of 50%. Angiography was performed on day 354 revealing a significant in-scaffold restenosis (Figure 2) that was treated with a metallic Xience V everolimus eluting stent. Whether this restenosis resulted by an intrinsic patient's resistance to everolimus as antiproliferative drug or was secondary to a different mechanism [30] remains speculative. The CEC adjudicated the event per Protocol as ischemia-driven TLR.

Events between 1- and 2-year follow-up

The first case (RVD 2.72 mm) was a 63-year-old female with a medical history of hyperlipidemia and hypertension both requiring medication. She presented with a positive functional ischemia study due to two vessel disease and normal cardiac biomarkers.

After pre-dilatation with a 2.5 x 15 mm Monorail compliant balloon at 12 atm, one 3.0 x 18 mm Absorb BVS was deployed with an investigator assessed 80% DS lesion in the proximal RCA (CASS #1) with a maximal implantation pressure of 14 atm. Post-scaffold dilatation was performed with a 3.25 x 12 mm NC balloon at a maximal pressure of 16 atm. The investigator assessed DS was reduced from 80% to < 10 % post procedure. The patient was discharged on Day 4 and aspirin and clopidogrel were used during the index procedure per protocol.

On Day 363 the patient was hospitalized due to Braunwald Class II unstable angina. Cardiac biomarkers were within normal limits and the ECG demonstrated no signs of

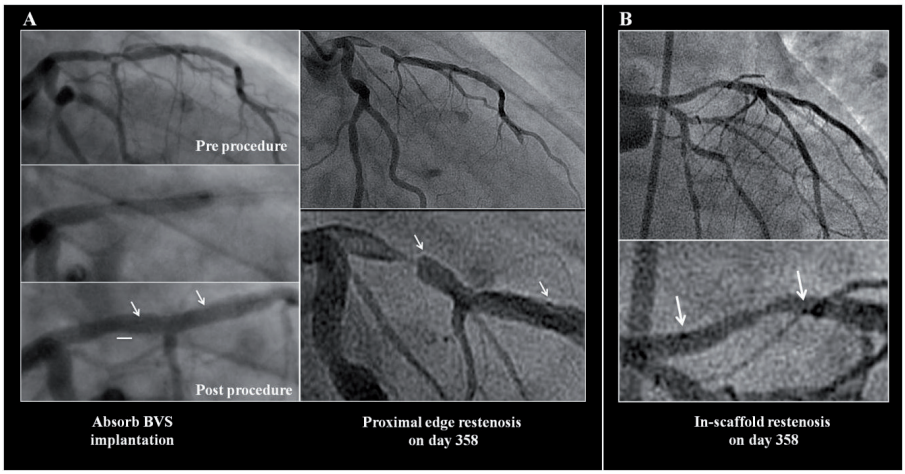

Figure 4. Clinical events between 1- and 2-year follow-up.
Two additional target lesion revascularizations occurred in large vessels, namely proximal left anterior descending artery (A, left panel) and proximal-mid right coronary artery (B, right panel).

ischemia. Coronary angiography revealed a patent study Absorb BVS with a core lab assessed 26% DS of target lesion, and an investigator assessed 60% DS lesion in the distal LMCA, an 80% DS ostial lesion of LCX and a 70% DS ostial lesion of RCA. The core lab assessed a bifurcation lesion at LMCA-LAD-LCX and bifurcation lesion at distal RCA-RPDA, and the lesion in the distal RCA as significant. The IVUS investigator assessment confirmed good index PCI result and critical LMCA and ostial RCA stenosis. No intervention was performed and the patient was referred for cardiac surgical follow-up. On Day 439 the patient underwent CABG revascularization with SVG to the distal RCA and proximal LCX, and LIMA to the mid LAD. In addition, a left ICA endarterectomy was performed for critical stenosis without symptoms. The patient's hospital course was unremarkable and she was discharged on Day 477. Aspirin and clopidogrel were ongoing at the time of this event. The investigator considered the event as not related to the study device or study procedure and not caused by a malfunction of the study device. The CEC adjudicated the event per protocol as ischemia-driven TVR by CABG and ischemia-driven NTVR x 2 by CABG. The CEC adjudicated the event per ARC as a clinically indicated TVR by CABG and clinically indicated NTVR x 2 by CABG.

On Day 590 the patient was hospitalized due to Braunwald Class II unstable angina with an elevated CK-MB of 25 U/L (ULN 24 U/L). Coronary angiogram revealed a core lab assessed 16% DS lesion in the proximal RCA and 60% DS lesion in the mid RCA. On Day 591, after pre-dilatation with a 2.5 x 15 mm balloon catheter at 12 atm, one 4.0 x 38 mm metallic DES was implanted across the lesion in the mid RCA (CASS # 2) on the edge of index Absorb

BVS (CASS #1) at 12 atm with good results confirmed by IVUS. The investigator assessed the event as not related to the study device or procedure and not caused by a malfunction of the study device. The patient was discharged on Day 591 and aspirin and clopidogrel were ongoing on the time of this event. The CEC adjudicated the event per protocol as ischemia-driven TLR by PCI.

The second patient (RVD 2.96 mm) was a 62 year old male former tobacco user with a history of hypertension requiring medication and COPD. He presented with CCS Class III stable angina due to single vessel disease with normal cardiac biomarkers. After pre-dilatation with a 2.5 x 12 mm compliant balloon catheter at 12 atm, one 3.0 x 18 mm Absorb BVS was deployed across an investigator assessed 90% DS lesion in the proximal LAD (CASS #12) with a maximum implantation pressure of 14 atm. Post-scaffold dilatation was performed with a 3.25 x 12 mm non-compliant balloon catheter at a maximal pressure of 16 atm followed by 3.5 x 8 mm proximal non compliant balloon catheter dilatation at a maximal pressure of 12 atm. OCT showed a good scaffold apposition and expansion apart from a rim of unopposed struts at the very proximal portion of the scaffold where the vessel was ectatic. There were no procedural complications and the patient was discharged on Day 1. Aspirin and clopidogrel were used during the index procedure per protocol.

Angiography performed on Day 346 revealed the study Absorb BVS in the proximal LAD to be widely patent with a mild area of disease noted in the mid LAD distal to the scaffolded segment. IVUS and OCT showed the scaffold to be well apposed and expanded with thin neo-intimal coverage. The proximal struts that were unapposed at the index procedure were noted to be covered with a thin rim of tissue.

On Day 564 the patient was hospitalized with Braunwald Class I unstable angina. Angiography performed on Day 567 revealed a corelab assessed 74% DS in-scaffold restenosis in the proximal LAD (CASS #12) with no thrombosis or occlusion. The troponin was elevated with a peak value of 1.66 ng/ml (ULN 0.04 ng/ml) with normal CK. On Day 571 the patient underwent PCI revascularization with one 3.0 x 18 mm Xience V everolimus eluting metallic DES successfully deployed across the lesion in the proximal LAD at 16 atm and post dilated with 3.5 x 8 mm non compliant balloon at 22 atm with good result. The investigator assessed the event as related to the study device and not caused by a malfunction of the study device. The patient was discharged on Day 572. Aspirin and clopidogrel were ongoing at the time of the event.

The CEC adjudicated the event per protocol as ischemia-driven TLR by PCI.

Chapter 13

ABSORB II Randomized Controlled Trial

A Clinical Evaluation to Compare the Safety, Efficacy and Performance of the Absorb Everolimus Eluting Bioresorbable Vascular Scaffold System Against the Xience Everolimus Eluting Coronary Stent System in the Treatment of Subjects with Ischemic Heart Disease caused by *De Novo* Native Coronary Artery Lesions: Rationale and Study Design

Roberto Diletti, MD; Patrick W. Serruys, MD, PhD; Vasim Farooq, MBChB, MRCP; Krishnankutty Sudhir, MD, PhD; Cecile Dorange, MSc; Karine Miquel-Hebert, PhD; Susan Veldhof, RN; Richard Rapoza, PhD; Yoshinobu Onuma, MD; Hector M. Garcia-Garcia, MD, PhD; Bernard Chevalier, MD

Am Heart J 2012 Nov;164(5):654-63

ABSTRACT

Background Currently no data are available on the direct comparison between the Absorb everolimus eluting bioresorbable vascular scaffold (Absorb BVS) and conventional metallic drug eluting stents.

Methods The ABSORB II Study is a randomized, active-controlled, single-blinded, multicenter clinical trial aiming to compare the second generation Absorb BVS with the XIENCE everolimus eluting metallic stent. Approximately 501 subjects will be enrolled on a 2:1 randomization basis (Absorb BVS: XIENCE) in approximately 40 investigational sites across Europe and New Zealand. Treated lesions will be up to 2 *de novo* native coronary artery lesions, each located in different major epicardial vessels, all with an angiographic maximal luminal diameter between 2.25 mm and 3.3 mm as estimated by on-line quantitative coronary angiography (QCA), and a lesion length of ≤48 mm. Clinical follow-up is planned at 30 days, 180 days and at 1, 2 and 3 years. All subjects will undergo coronary angiography, intravascular ultrasound (IVUS) and IVUS-virtual histology (IVUS-VH) at baseline (pre- and post-device implantation) and at 2-year angiographic follow-up. The primary end point is superiority of the Absorb BVS versus XIENCE in terms of vasomotor reactivity of the treated segment at 2 years- defined as the QCA quantified change in the mean lumen diameter pre- and post-nitrate administration. The co-primary endpoint is the non-inferiority (reflex to superiority) of the QCA derived minimum lumen diameter (MLD) at 2 years post nitrate minus MLD post procedure post nitrate by QCA. In addition all subjects allocated to the Absorb BVS group will undergo MSCT imaging at 3 years.

Conclusions The ABSORB II RCT (ClinicalTrials.gov NCT01425281) is designed to compare the safety, efficacy and performance of Absorb BVS against the XIENCE everolimus eluting stent in the treatment of *de novo* native coronary artery lesions.

INTRODUCTION

The Absorb everolimus eluting bioresorbable vascular scaffold (Absorb BVS) was developed to provide a novel approach to treating coronary artery lesions with transient vessel support and drug delivery.

Preclinical evaluation in animal model demonstrated substantial polymer degradation at 2-years post Absorb BVS implantation, with complete disappearance of the Absorb BVS strut 'footprint' in the vessel wall within a 4-year period, with no significant inflammatory response associated with BVS implantation at short or long-term follow-up[1]

The first generation Absorb BVS was tested in the ABSORB Cohort A Trial and demonstrated promising results with a low clinical event rate at 5 years follow-up.[2] The device was however limited by slightly higher late recoil compared to conventional metallic platform stents.(3,4) Improvements in design were therefore introduced in the second generation Absorb BVS, notably an enhanced mechanical strength, more durable support to the vessel wall, a reduced maximum circular unsupported surface area and a more uniform strut distribution and drug delivery. The performance of this next generation Absorb BVS was subsequently investigated in the ABSORB Cohort B Trial [5,6] which reported excellent clinical results up to 1-year follow-up. [7]

To date, the treatment of coronary artery disease with the second generation Absorb BVS has been investigated in a limited number of patients with relatively simple coronary lesion complexity. Furthermore no randomized comparison between the Absorb BVS and conventional metallic drug-eluting stent has yet been undertaken.

Therefore, the ABSORB II controlled randomized trial (ClinicalTrials.gov NCT01425281) comparing the metallic everolimus-eluting stent XIENCE with the Absorb BVS will be initiated and treatment will be expanded to include subjects with small target vessels diameter and long lesion length.

Investigational Device

The second generation Absorb BVS (Abbott Vascular, Santa Clara, CA, USA) is a balloon expandable device consisting of a polymer backbone of Poly-L lactide (PLLA) coated with a thin layer of a 1:1 mixture of an amorphous matrix of Poly-D, L lactide (PDLLA) polymer, and 100 micrograms/cm^2 of the anti-proliferative drug everolimus. Two platinum markers located at each Absorb BVS edge allow for accurate visualization of the radiolucent Absorb BVS during angiography or other imaging modalities. The PDLLA controls the release of everolimus, 80% of which is eluted within the first 30-days. Both PLLA and PDLLA are fully bioresorbable. The polymers are degraded via hydrolysis of the ester bonds and the resulting lactate and its oligomers are quickly transformed to pyruvate and metabolized in

the Krebs energy cycle. Small particles, less than 2 μm in diameter, have also been shown to be phagocytised and degraded by macrophages.[8] According to preclinical studies the time for complete bioresorption of the polymer backbone is 2 to 3 years.[1]

Control Device

The XIENCE (Abbott Vascular, Santa Clara, CA, USA) is a balloon expandable metallic platform stent manufactured from a flexible cobalt chromium alloy with a multicellular design, and coated with a thin (7.8 μm) non-adhesive, durable, biocompatible acrylic and fluorinated everolimus releasing copolymer.

The delivery system to be used in both arms of the trial will utilize the same principle of operation as other Abbott Vascular Rapid Exchange (RX) coronary stent systems and coronary dilation catheters.

Treatment Strategy

Quantitative assessment of target vessel diameter by on-line quantitative coronary angiography (QCA) is required at baseline after nitroglycerin for appropriate ABSORB BVS or XIENCE stent size selection. The required range for target vessel diameter is assessed in terms of the on-line QCA parameters distal Dmax and proximal Dmax, which refer to maximum lumen diameter evaluated prior to pre-dilatation up to 5-10 mm distal and proximal to the boundaries of the lesion length defined by QCA. A 3.5 mm ABSORB BVS or XIENCE should be used when both the proximal and distal mean lumen diameter are within the upper limit of 3.8 mm and the lower limit of 3.0 mm. A 3.0 mm ABSORB BVS or XIENCE stent must be used when both the proximal and distal mean lumen diameter are within the upper limit of 3.3 mm and the lower limit of 2.5 mm. A 2.5 mm ABSORB BVS or XIENCE stent must be used when both the proximal and distal mean lumen diameter are within the upper limit of 3.0 mm and the lower limit of 2.25 mm. Both the proximal mean lumen diameter and the distal mean lumen diameter need to be within the upper and lower limits specified for the scaffold/stent size. Overlap will be allowed. (Table 1)

Dual Antiplatelet Therapy

All subjects will receive ≥75 mg of aspirin daily after the index procedure and throughout the length of the clinical investigation. All subjects will be maintained at a minimum of 75 mg of clopidogrel daily or a minimum of 10 mg of prasugrel daily for a minimum of 180 days following the procedure leading to a dual antiplatelet therapy for a minimum of 180 days. If a subject develops sensitivity to clopidogrel or prasugrel, they may be switched to ticlopidine according to standard hospital practice.

Table 1. Device sizes to be used in the study according to the maximum lumen diameter (Dmax) by online QCA only.

Device		Lesion and Device Sizes	
		Dmax	Lesion Length
ABSORB BVS Scaffold diameter	2.5 mm	≥ 2.25 mm and ≤ 3.0 mm	≤ 48 mm Scaffold Length: 18, 28 mm
	3.0 mm	≥ 2.5 mm and ≤ 3.3 mm	≤ 48 mm Scaffold Length: 18, 28 mm
	3.5 mm	≥ 3.0 mm and ≤ 3.8 mm	≤ 48 mm Scaffold Length: 12, 18, 28 mm
XIENCE Stent diameter	2.5 mm	≥ 2.25 mm and ≤ 3.0 mm	≤ 48 mm Scaffold Length: 18, 28 mm
	3.0 mm	≥ 2.5 mm and ≤ 3.3 mm	≤ 48 mm Scaffold Length: 18, 28 mm
	3.5 mm	≥ 3.0 mm and ≤ 3.8 mm	≤ 48 mm Scaffold Length: 12, 18, 28 mm

The anti-platelet therapy can be halted for clinical indications if required, however must be resumed as soon as possible per-physician discretion.

Trial design and objective

The ABSORB II Randomized Controlled Trial (RCT) is intended to continue to evaluate the safety and efficacy of the Absorb BVS, and to directly compare it to the metallic drug-eluting stent XIENCE.

XIENCE stent and Absorb BVS share the same basic MULTI-LINK design and both devices are similar in terms of drug, drug dose density, and elution profile.

The ABSORB II RCT is a prospective, randomized, active-controlled, single-blinded, parallel two-arm, multi-center clinical trial. A total of approximately 501 subjects (334 in the Absorb BVS group and 167 in the XIENCE stent group) will be randomized in approximately 40 sites in Europe and New Zealand. The trial protocol allows the treatment of up to 2 *de novo* native coronary artery lesions, each located in different major epicardial vessels, with a maximal lumen diameter comprised between 2.25 mm and 3.8 mm as assessed by on-line quantitative coronary angiography (QCA), and a maximum lesion length ≤ 48 mm.

All subjects will be screened per the protocol inclusion and exclusion criteria prior to enrolment. Subjects will have clinical follow-up at 30 days, 180 days and at 1, 2 and 3 years. All subjects will undergo coronary angiography, intravascular ultrasound (IVUS) and IVUS-virtual histology (VH) imaging pre- and post- device implantation and at 2 years post index procedure.

Subjects from the Erasmus Medical Centre (MC) Rotterdam, The Netherlands will also undergo intravascular imaging with near infrared spectroscopy (Lipiscan) pre- and post-

device implantation and at 2 years post index procedure.
All subjects allocated to the Absorb BVS arm will undergo MSCT imaging at 3 years post index procedure. Subjects will be unblinded after completion of the 2-year follow-up for the co-primary endpoints.
The primary objective of the ABSORB II RCT is to compare the safety, efficacy and performance of Absorb BVS against the XIENCE stent in the treatment of subjects with ischemic heart disease caused by de novo native coronary artery lesions.
The ABSORB II RCT is intended to show superiority of Absorb BVS versus XIENCE stent, in terms of the primary endpoint of vasomotor reactivity as assessed by the change in mean lumen diameter pre- and post-nitrate and at 2-year invasive follow-up with QCA, and non-inferiority (reflex to superiority) in terms of the co-primary endpoint of angiographic late loss at 2-year follow-up (minimum lumen diameter (MLD) at 2 years post nitrate minus MLD post procedure post nitrate by QCA).
All invasive procedures may be deferred to 3 years depending on the results of the ABSORB Cohort B trial.
This trial will be conducted in accordance with the Clinical Investigational Plan, the Declaration of Helsinki, ISO 14155 standards and the appropriate local legislation(s). The conduct of the trial will be approved by the appropriate Ethics Committee (EC) of the respective clinical site and as specified by local regulations.

PATIENT SELECTION

Subjects enrolled into the clinical trial will be male or female derived from the general interventional cardiology population. The clinical trial will randomize up to approximately 501 subjects. Subjects meeting the general inclusion and exclusion criteria (Table 2, Table 3) will be asked to sign an informed consent. Non-routine laboratory assessments specific to the clinical investigation will not be performed before an informed consent has been signed.
Screening failures will be captured on a paper-screening log.
After successful pre-dilatation of the first target lesion, subject ID, randomization number and treatment arm will be assigned by a central allocation service (interactive voice / interactive web-based randomization service).
Subjects will be randomized in a 2:1 ratio to Absorb BVS versus XIENCE stent. Randomization will be further stratified by diabetes mellitus status and number of planned target lesions.

Table 2. Inclusion criteria.

General Inclusion Criteria
• Subject must be at least 18 years of age and less than 85 years of age. • Subject must agree not to participate in any other clinical investigation for a period of three years following the index procedure. This includes clinical trials of medication and invasive procedures. Questionnaire-based studies, or other studies that are non-invasive and do not require medication are allowed. • Subject is able to verbally confirm understanding of risks, benefits and treatment alternatives of receiving the ABSORB BVS and he/she or his/her legally authorized representative provides written informed consent prior to any Clinical Investigation related procedure, as approved by the appropriate Ethics Committee. • Subject must have evidence of myocardial ischemia (e.g., stable or unstable angina, silent ischemia). • Subject must be an acceptable candidate for coronary artery bypass graft (CABG) surgery • Subject must agree to undergo all clinical investigation plan-required follow-up visits, exercise testing, blood draw as well as adherence to ESC Guidelines and completion of quality of life questionnaires and of a subject diary to collect information including but not limited to tobacco usage, food intake, daily exercise and body weight.
Angiographic Inclusion Criteria
• One or two de novo native lesions each located in a different epicardial vessel. • If two treatable lesions meet the eligibility criteria, they must be in separate major epicardial vessels (LAD with septal and diagonal branches, LCX with obtuse marginal and/or ramus intermedius branches and RCA and any of its branches). • Lesion(s) must have a visually estimated diameter stenosis of ≥50% and <100% with a TIMI flow of ≥1. • Lesion(s) must be located in a native coronary artery with Dmax by on-line QCA of ≥2.25 mm and ≤3.3 mm. • Lesion(s) must be located in a native coronary artery with lesion(s) length by on-line QCA of ≤48 mm. • Percutaneous interventions for lesions in a non-target vessel are allowed if done ≥30 days prior to or if planned to be done 2 years after the index procedure. • Percutaneous intervention for lesions in the target vessel are allowed if done >6 months prior to or if planned to be done 2 years after the index procedure

Table 3. Exclusion criteria.

General Exclusion Criteria
• Known hypersensitivity or contraindication to aspirin, both heparin and bivalirudin, antiplatelet medication specified for use in the study (clopidogrel and prasugrel and ticlopidine, inclusive), everolimus, poly (L-lactide), poly (DL-lactide), cobalt, chromium, nickel, tungsten, acrylic and fluoro polymers or contrast sensitivity that cannot be adequately pre-medicated. • Subject has a known diagnosis of acute myocardial infarction (AMI) at any time preceding the index procedure and relevant cardiac enzymes (according to local standard hospital practice) have not returned within normal limits at the time of procedure. • Evidence of ongoing acute myocardial infarction in ECG prior to procedure • Subject has current unstable arrhythmias. • Left ventricular ejection fraction (LVEF) < 30%. • Subject has received a heart transplant or any other organ transplant or is on a waiting list for any organ transplant. • Subject is receiving or scheduled to receive chemotherapy for malignancy within 30 days prior to or after the procedure.

Table 3. Continued

General Exclusion Criteria
• Subject is receiving immunosuppressant therapy and/or has known immunosuppressive or autoimmune disease (e.g. human immunodeficiency virus, systemic lupus erythematosus, rheumatoid arthritis, severe asthma requiring immunosuppressive medication, etc.). • Subject is receiving chronic anticoagulation therapy that can not be stopped and restarted according to local hospital standard procedures. • Elective surgery is planned within 2 years after the procedure that will require discontinuing either aspirin, clopidogrel, prasugrel or ticlopidine. • Subject has a platelet count <100,000 cells/mm3 or >700,000 cells/mm3, a WBC of <3,000 cells/mm3, or documented or suspected liver disease (including laboratory evidence of hepatitis) • Known renal insufficiency (e.g., eGFR <60 ml/kg/m2 or serum creatinine level of >2.5 mg/dL, or subject on dialysis). • History of bleeding diathesis or coagulopathy or will refuse blood transfusions. • Subject has had a cerebrovascular accident (CVA) or transient ischemic neurological attack (TIA) within the past 6 months. • Pregnant or nursing subjects and those who plan pregnancy in the period up to 3 years following index procedure. (Female subjects of child-bearing potential must have a negative pregnancy test done within 28 days prior to the index procedure and contraception must be used during participation in this trial) • Other medical illness (e.g., cancer or congestive heart failure) or known history of substance abuse (alcohol, cocaine, heroin etc.) as per physician judgment that may cause non-compliance with the protocol or confound the data interpretation or is associated with a limited life expectancy. • Subject is already participating in another clinical investigation that has not yet reached its primary endpoint. • Subject is belonging to a vulnerable population (per investigator's judgment, e.g., subordinate hospital staff or sponsor staff) or subject unable to read or write
Angiographic Exclusion Criteria
• Target lesion which prevents adequate (residual stenosis at target lesion(s) is ≤ 40% by visual assessment) coronary pre-dilatation. • Target lesion in left main trunk. • Aorto-ostial target lesion (within 3 mm of the aorta junction). • Target lesion located within 2 mm of the origin of the LAD or LCX. • Target lesion located distal to a diseased (vessel irregularity per angiogram and >20% stenosed lesion) arterial or saphenous vein graft. • Target lesion involving a bifurcation lesion with side branch ≥2 mm in diameter, or with a side branch <2mm in diameter requiring guide wire protection or dilatation. • Total occlusion (TIMI flow 0), prior to wire crossing • Excessive tortuosity (≥ two 45° angles), or extreme angulation (≥90 °) proximal to or within the target lesion. • Restenotic from previous intervention • Heavy calcification proximal to or within the target lesion. • Target lesion involves myocardial bridge. • Target vessel contains thrombus as indicated in the angiographic images. • Additionally clinically significant lesion(s) (≥ 40% diameter stenosis by visual assessment) for which PCI may be required <2 years after the index procedure. • Subject has received brachytherapy in any epicardial vessel (including side branches) • Subject has a high probability that a procedure other than pre-dilatation and study device implantation and (if necessary) post-dilatation will be required at the time of index procedure for treatment of the target vessel

Follow-up schedule

Subjects will be followed for a 3-year period post index procedure with clinical and invasive imaging follow-up. (Figure 1)

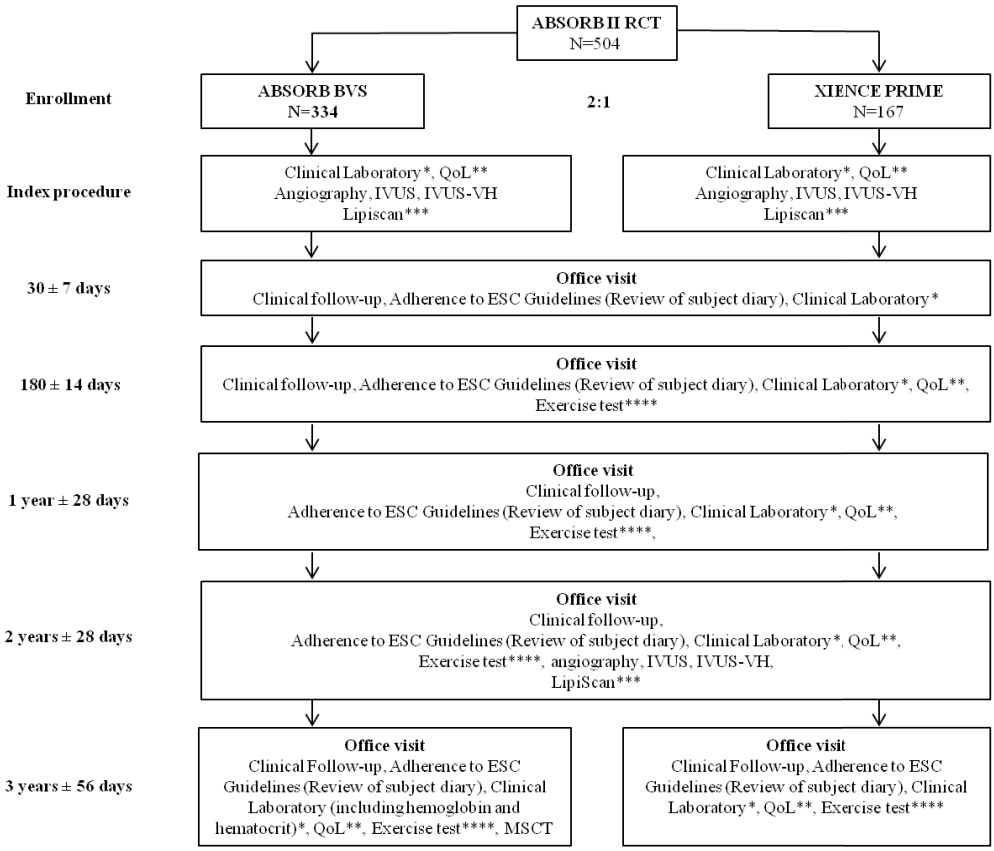

Figure 1. Clinical investigation flow chart.

*Clinical Laboratory: blood sample (to be obtained before exercise testing) to aid in the adjustment of medical treatment and adherence to ESC guidelines. **QoL: Quality of Life using the Seattle Angina Questionnaire (SAQ), the SF-12 Health Survey and the EuroQoL EQ-5D Health Survey. This information will be collected at the indicated time points. ***Lipiscan analysis will be done at the Erasmus MC only. ****Exercise test to be done prior to any required imaging procedure and after blood draws. The office imaging visit at 2 years (including exercise testing, coronary angiogram, IVUS, IVUS-VH, Lipiscan, SF12, EuroQoL EQ-5D and SAQ) may be changed to 3 years depending on cohort B 2 year imaging data. In that case the 2 year imaging visit would be replaced by an office visit where exercise testing, SF12, EuroQoL EQ-5D, SAQ, adherence to ESC Guidelines per protocol medication, concomitant medication and adverse events would be reviewed.

Clinical follow-up

Clinical visit follow-up including blood sampling will be performed in all patients at 30 days, 180 days, 1, 2 and 3 years days post-procedure. A central laboratory will be used for blood analysis of troponin, CK, CK-MB, fasting total cholesterol, fasting LDL cholesterol, fasting HDL cholesterol, fasting triglycerides, HbA1c, fasting blood glucose levels. These blood samples for central laboratory will be obtained before or at the time of the procedure; the results will not be reviewed at the procedure time.

Local analyses may be performed in parallel to any blood results that are relevant for appropriate protocol compliance, subject care and treatment optimization.

Exercise testing will be required at 180 days, 1, 2 and 3 years post-procedure, to be performed prior to any required imaging procedure and after blood sampling. Exercise tests will be performed at each investigational site according to local clinical practise.

All patients and treating physicians will be asked to adhere to the European Society of Cardiology (ESC) Guidelines[9] in terms of tobacco usage, exercise, healthy food intake, maintaining an adequate weight (body mass index) and waist circumference, achieving target blood lipid levels and blood pressure control. These parameters will be evaluated at pre-procedure, 30 days, 180 days, 1, 2 and 3 years post-procedure.

Quality of life questionnaires will be undertaken in the ABSORB II RCT to provide a complementary evaluation of the effectiveness of the Absorb BVS system. The questionnaires will be collected at pre-implantation, 180 days, 1, 2 and 3-year follow-up and will include both the overall health status, assessed using the SF-12 Health Survey and the EuroQoL EQ-5D survey and disease-specific quality of life, assessed using the Seattle Angina Questionnaire (SAQ)

Intravascular Imaging follow-up

Angiography

All subjects will undergo coronary angiography at pre- and post-device implantation and at 2-year follow-up

Grey Scale Intravascular Ultrasound (IVUS) - Virtual Histology (VH)

IVUS and IVUS-VH assessment will be performed in all patients after coronary angiography, at pre- and post-implantation and at 2-year follow-up. Pre-procedural IVUS and IVUS-VH will be performed before pre-dilatation of each target lesion. If not technically feasible, (i.e. the IVUS catheter cannot cross the lesion) pre-dilatation with a small balloon dilatation catheter is allowed for IVUS catheter access. IVUS and IVUS-VH are intended for documentary purposes only and not for vessel sizing, thus this will not impact on inclusion/

exclusion decision-making processes. In case of two target lesions, pre-procedural IVUS and IVUS-VH will be performed for the second lesion after the treatment of the first lesion.

Near Infrared Spectroscopy (Lipiscan)

A Near infrared spectroscopy sub-study will take place in Erasmus MC only. Analyses will be performed at pre- and post-device implantation and at 2-year follow-up. NIRS assessment will be performed after IVUS and IVUS-VH at each time point. All invasive imaging procedures at 2 years may be deferred to 3 years depending on the results of the ABSORB Cohort B 2-year imaging follow up data.

Multi Slice Computed Tomography (MSCT)

A MSCT scan is mandatory for all subjects in the Absorb BVS arm at 3 years follow-up.

Endpoints

Primary Endpoints and Rationale

The co-primary endpoints of the clinical trial are: 1) Vasomotion assessed by change in Mean Lumen Diameter between pre- and post-nitrate at 2 years by QCA (superiority) and 2) Minimum lumen diameter at 2 years post nitrate minus minimum lumen diameter post procedure, post nitrate by QCA (non-inferiority, reflex to superiority). (Table 4)
Secondary clinical and imaging endpoints are reported in Table 4.

STATISTICAL CONSIDERATIONS

Sample Size Calculations and Assumptions

The sample size calculation is based on the first co-primary endpoint (superiority for vasomotion assessed by change in mean lumen diameter between pre- and post-nitrate at 2 years by QCA). The following assumptions were considered:
1) Two-tailed superiority t-test; 2) $\alpha = 0.05$; 3) Power = 90%; 4) Randomization ratio 2:1 (Absorb BVS arm : XIENCE stent); 5) Based on previous vasomotion data at 2 years after BVS implantation,[10] The true change in mean lumen diameter between pre- and post-nitrate at 2-year follow-up is assumed to be 0.07 mm for Absorb BVS and 0 mm for XIENCE stent; 6) The standard deviation is assumed to be 0.20 mm.
Based on the above assumptions 260 lesions in the Absorb BVS arm and 130 lesions in the XIENCE stent arm will be required for the study. The attrition rate observed in ABSORB Cohort A and SPIRIT II at 2-year was 24%, we expect an additional loss of 5% for

Table 4. Clinical angiographic and imaging endpoints.

Clinical Endpoints

Acute success
- Device success (lesion based analysis)
- Procedural success (subject based analysis)

Clinical Endpoint (at 30 and 180 days, 1, 2, and 3 years follow-up)
- Component
  - Death (Cardiac, Vascular, Non-Cardiovascular)
  - Myocardial Infarction (MI: QMI and NQMI)*
  - Target Lesion Revascularization (TLR)
    Clinically-indicated TLR (CI-TLR)
    Not clinically-indicated TLR (NCI-TLR)
  - Target Vessel Revascularization (TVR)
    Clinically-indicated TVR (CI-TVR)
    Not clinically-indicated TVR (NCI-TVR)
  - Non-Target Vessel Revascularization (NTVR)
    Clinically-indicated NTVR (CI-NTVR)
    Not clinically-indicated NTVR (NCI-NTVR)
  - All coronary revascularization
- Composite Endpoints
  Death/All MI
  Cardiac Death/TV-MI/CI-TLR (Target Lesion Failure (TLF)) (Device-oriented endpoint)
  Cardiac Death/All MI/CI-TLR (Major Adverse Cardiac Events (MACE))
  Cardiac Death/All MI/CI-TVR (Target Vessel Failure (TVF))
  Death/All MI/All revascularization (DMR) (Subject-oriented endpoint)
- Scaffold/Stent Thrombosis
  Timing (acute, sub-acute, late and very late)
  Evidence (Definite, Probable and Possible)

Quality of Life (QoL) related Endpoints

- Health status will be assessed using the SF-12 Health Survey and the EuroQoL EQ-5D at pre-implantation, 180 days, 1, 2 and 3 years follow-up.
- Disease-specific QoL will be assessed using the Seattle Angina Questionnaire (SAQ) at pre-implantation, 180 days, 1, 2 and 3 years follow-up.

Angiographic Endpoints

- In-segment LL post-nitrate at 2* years;
- Proximal LL (proximal defined as within 5 mm of tissue proximal to scaffold/stent placement) post-nitrate at 2* years;
- Distal LL (distal defined as within 5 mm of tissue distal to scaffold/stent placement) post-nitrate at 2* years;
- In-scaffold/In-stent, in-segment, proximal and distal Minimum Luminal Diameter (MLD) post-nitrate post-procedure and at 2* years;
- In-scaffold/In-stent, in-segment, proximal and distal % Diameter Stenosis (DS) post-nitrate post-procedure and at 2* years;
- In-scaffold/In-stent, in-segment, proximal and distal Angiographic Binary Restenosis (ABR) rate post-nitrate at 2* years;
- In-scaffold/in-stent net gain (being the change in MLD between 2* years versus pre-implantation) post-nitrate;
- Change in Mean and Minimal lumen diameter at 2* years follow-up from pre-nitrate to post-nitrate by angiography
- In-scaffold/in-stent %Diameter Stenosis (DS) at 2* years pre- and post-nitrate by angiography
- Conformability assessed by change in curvature and angulation between pre-, post-procedure and follow-up

Table 4. Continued..

IVUS Endpoints
• Minimal Lumen Area (MLA) by IVUS post-nitrate at 2* years • Percentage of patients with late gain (IVUS MLA post procedure post-nitrate < IVUS MLA 2 years follow-up post-nitrate) without IVUS malapposition • Change of total plaque (tissue between lumen and external elastic membrane) within scaffold/stent by IVUS post-nitrate between post-implantation and 2* years • Mean/ Minimal Vessel diameter/area/volume pre-procedure, post-procedure and at 2* years; • Mean/ Minimal Scaffold/Stent diameter/area/volume pre-procedure, post-procedure and (if analyzable) at 2* years; • Mean/Minimal Lumen diameter/area/volume pre-procedure, post-procedure and at 2* years, including change in MLA between post-procedure and follow-up; • Plaque behind metallic stent area/volume post-procedure and at 2* years; • Plaque behind polymeric scaffold area/volume post-procedure and at 2* years (if analyzable); • Mean/ maximal neointima hyperplasia in the metallic stent area/volume/percentage at 2* years; • Mean/ maximal neointima hyperplasia in the polymeric scaffold area/volume/percentage at 2* years (if analyzable); • Incomplete apposition (post-implantation), persisting incomplete apposition, late acquired incomplete apposition and resolved incomplete apposition at 2* years (if analyzable); • Total Plaque area/volume pre-procedure, post-procedure and at 2* years, including change in total plaque between pre-procedure and follow-up;
IVUS-VH Endpoints
• Dense Calcium Volume, Area, % , pre-procedure, post procedure and at 2* years; • Necrotic Core Volume, Area, % , pre-procedure, post procedure and at 2* years; • Fibro-Fatty Volume, Area, % , pre-procedure, post procedure and at 2* years; • Fibrous Volume, Area, % , pre-procedure, post procedure and at 2* years;
Near Infrared Spectroscopy Endpoint (sub-study in Erasmus MC)
• Change in Lipid Core Burden index from pre-implantation to post-implantation and 2* years follow-up.
MSCT Endpoints (subjects in the ABSORB BVS arm only)
The following MSCT endpoints will be examined in the ABSORB BVS arm only • Descriptive analysis of vascular and scaffold morphology at 3 years • Measurement of lumen area and diameter (min, max, mean), %DS and % Area Stenosis (AS) at 3 years

unmatched pre and post nitrates and about 10% of patients with dual lesions. Therefore approximately 501 subjects will be randomized in ABSORB II, with approximately 334 in the Absorb BVS arm and 167 in the XIENCE stent arm.

Considering the 390 lesions available for QCA assessments, the study has more than 89% power to detect non-inferiority in the second co-primary endpoint of MLD at 2 years post nitrate minus MLD post procedure post nitrate by QCA (assuming the true means are equal in both groups with a standard deviation of 0.45 mm and a non-inferiority margin (δ) of 0.14mm).

The power calculations were performed using PASS 11 (Hintze, J. 2011).

Co-Primary Endpoints Analysis

The co-primary endpoints will be analyzed for the Intent-to-Treat (ITT) population, on a lesion basis. For the endpoint of vasomotion assessed by change in Mean Lumen Diameter between pre- and post-nitrate at 2 years by QCA, the comparison will be tested using a 2-sided t-test at the 0.05 significance level. For the endpoint of MLD at 2 years post nitrate minus MLD post procedure post nitrate by QCA, non-inferiority will be tested using a one-sided asymptotic test at the 0.05 significance level, considering the non-inferiority margin of 0.14mm. If non-inferiority is met with higher value in the Absorb BVS arm, then superiority will be tested using a 2-sided t-test at the 0.05 significance level. If the normality assumption is untenable, non-parametric tests may be considered. In order for the trial to be successful, the criteria for superiority should be met for the co-primary endpoint of vasomotion and the criteria for non-inferiority should be met for the co-primary endpoint of MLD at 2 years post nitrate minus MLD post procedure post nitrate. In addition, as a secondary analysis, the co-primary endpoints will be analyzed on the per treatment evaluable (PTE) population.

Secondary Endpoint Analyses

Analyses of other secondary endpoints will be descriptive and will be performed on both the ITT and PTE populations. For binary variables such as TVF, TLR, and clinical procedure success, counts, percentages, and exact 95% confidence intervals using Clopper-Pearson's method will be calculated. For continuous variables such as diameter stenosis, means, standard deviations, and 95% confidence intervals for the mean using the Gaussian approximation will be calculated.

Study management

The ABSORB II Trial is funded by Abbott Vascular. The Data Safety Monitoring Board (DSMB) will monitor the safety of subjects and/or efficacy throughout the subject enrolment and on an on-going basis. The Clinical Events Committee (CEC) will be comprised of qualified physicians who are not investigators in the trial. The CEC will be responsible for adjudicating all MACE-related endpoints. Central lab cardiac enzymes values will be used for event adjudication (in case central lab values would not be available, the local lab results will be used). Imaging acquisitions will be evaluated by an independent core laboratory (Cardialysis, Rotterdam, The Netherlands).

DISCUSSION

The introduction in the last decade of drug-eluting coronary stents marked an important progress in the field of coronary artery disease treatment. The inhibition of neointimal growth by locally delivering anti-proliferative drugs, translated into a reduction in intra-stent restenosis lowering the need for repeated revascularizations. [11,12]

However metallic stent placement is not devoid of important long-term limitations. The metallic implant results in a permanent caging of the vessel, preventing late lumen enlargement, jailing side branches, precluding non-invasive imaging and further surgical revascularization of stented segments.[13] Moreover, in spite of the beneficial effect of neointimal inhibition, the antiproliferative drug elution has been shown to interfere with the vascular healing processes thus providing the background for phenomena such as delayed strut coverage and persistent or acquired malapposition, implicated in causing late and very late stent thrombosis.[14,15]

Given this background the new everolimus eluting bioresorbable vascular scaffolds have been introduced in the attempt to overcome the above-mentioned limitations and in the ABSORB II trial will be compared to the current standard of metal DES in terms of vasomotion and late loss at 2-year follow-up.

Vasomotion plays an important role in the regulation of coronary blood flow, ensuring the maintenance of an appropriate coronary flow pressure and impaired vasomotor activity of coronary vessels has been shown to be associated with an increased risk of future cardiovascular events.[16-18] Restoration of vasomotor activity is therefore desirable after percutaneous revascularization, and is a suitable endpoint for the evaluation of coronary artery disease treatment with drug-eluting stents/scaffolds in randomized trials.

Minimum lumen diameter at 2 years minus post procedural minimum lumen diameter (late lumen loss) is a direct measurement of neointimal hyperplasia and the best mechanistic measurement of procedural-related hemodynamic narrowing. This endpoint is reported to be both theoretically and clinically correlated with binary restenosis and target vessel revascularization (TVR).[19] Late lumen loss has been also previously observed to be a reliable and powerful end point across drug-eluting stent platforms studies. [20,21] Consequently the MLD at 2 years minus the post implantation MLD at baseline is considered a suitable endpoint for evaluation of the performance of drug-eluting stents/scaffolds in the present randomized trial.

In addition to the theoretical advantages, namely the possibility for further surgical revascularization and a potential reduction in events such as late scaffold thrombosis after the complete scaffold bioresorption,[13] the implantation of the Absorb BVS has previously been demonstrated not to preclude the non-invasive imaging of the treated arteries at any

stage of patient follow-up, [10,22] and the restoration of coronary vasomotion was observed to return after 1 year post scaffold implantation. [7] Moreover the Absorb BVS placement has been associated with the formation of a neointimal layer that may potentially represent a *de novo* circumferential plaque thick cap - after scaffold bioresorption - with the potential function of plaque stabilization. [23]

From a physiological perspective, complete scaffold bioresorption exposes the vessel wall to the cyclical strain of blood pulsatility. Previous studies have suggested that the mechanical stimuli induced by a pulsatile blood flow increases the release of nitric oxide (NO) and prostacyclin [24] and is associated with a reduction of monocyte adhesion providing a fundamental atheroprotective effect.[25-28]

Biomechanical stimuli also modulate endothelial cell morphology, proliferation, apoptosis, [29,30] elongation and realignment, [31] extracellular matrix production[32] and inflammatory signals.[33]

Pulsatile flow and its mechanical action on vessel wall is associated with a down regulation of NADPH oxidase activity, present in the endothelium, vascular smooth muscle cells, fibroblasts, and monocytes [34,35] with a consequent reduction in reactive oxygen species formation. [36,37]

Previous reports have demonstrated that reactive oxygen species, such as superoxide and hydrogen peroxide inactivates nitric oxide and provokes the formation of oxidants that induces both low-density lipoprotein (LDL) oxidation and expression of monocyte chemo-attractant proteins on endothelial cells with subsequent monocyte binding and trans-endothelial migration, that are both fundamental processes in atherogenesis. [38-41]

The restoration of the beneficial cyclical strain, [7,42] and the consequent reduction in reactive oxygen species formation may therefore have an impact on both endothelium-dependent vasodilation and atherogenesis.

In addition, the above-mentioned phenomena will take place in a micro-environment treated with the mTOR (mammalian Target Of Rapamycin) inhibitor everolimus. The protein mTOR is a key serine-threonine kinase playing a central role in the regulation of cell growth, proliferation and survival. On a molecular level everolimus forms a complex with the cytoplasmic protein FKBP-12,[43] this complex binds to mTOR and inhibits its signalling function, thus inhibiting growth factor-stimulated proliferation of vascular smooth muscle cells which is triggered by injury to endothelial cells and leads to neointima formation. [44]

In the new scenario of a coronary vessel free of metallic caging, the concomitant scaffold drug elution at early stages, [45] medical therapy [46-48] and changes in life style [49,50] may all play a key additional role to facilitate phenomena such as plaque regression, expansive remodeling and late luminal enlargement.

An analysis of vasoreactivity in scaffolded segments at 12- and 24- month follow-up with

both endothelial-depend and -independ agents, has been recently reported, showing that endothelial dysfunction in those regions is correlated to the amount of plaque burden and necrotic core content. [51]

These data support the hypothesis that an improvement of plaque composition and plaque burden could have a beneficial impact also on post scaffolding vasomotion resembling the behaviour of native non-stented segments.

Consequently, in the ABSORB II RCT, special attention will be paid to the adherence to guidelines for the prevention of cardiovascular disease.[9] Patients enrolled will be followed regarding their life style habits and compliance to medical treatment and efforts will be made to aid subjects in following recommendations by notifying any non-satisfactory result in collaboration with their treating physician(s).

In conclusion, the present trial will provide a randomized direct comparison between the everolimus-eluting bioresorbable vascular scaffold and the everolimus-eluting metallic stent. In addition this study aims to present a new approach to coronary artery disease treatment that integrates transient mechanical revascularization, drug elution, medical treatment and life style changes into a single strategy to restore coronary blood flow and vessel physiology.

REFERENCES

1. Onuma Y, Serruys PW, Perkins LE et al. Intracoronary optical coherence tomography and histology at 1 month and 2, 3, and 4 years after implantation of everolimus-eluting bioresorbable vascular scaffolds in a porcine coronary artery model: an attempt to decipher the human optical coherence tomography images in the ABSORB trial. Circulation 2010;122:2288-300.
2. Dudek D, Onuma Y, Ormiston JA, Thuesen L, Miquel-Hebert K, Serruys PW. Four-year clinical follow-up of the ABSORB everolimus-eluting bioresorbable vascular scaffold in patients with denovo coronary artery disease: the ABSORB trial. EuroIntervention : journal of EuroPCR in collaboration with the Working Group on Interventional Cardiology of the European Society of Cardiology 2011;7:1060-1.
3. Tanimoto S, Serruys PW, Thuesen L et al. Comparison of in vivo acute stent recoil between the bioabsorbable everolimus-eluting coronary stent and the everolimus-eluting cobalt chromium coronary stent: insights from the ABSORB and SPIRIT trials. Catheterization and cardiovascular interventions : official journal of the Society for Cardiac Angiography & Interventions 2007;70:515-23.
4. Tanimoto S, Bruining N, van Domburg RT et al. Late stent recoil of the bioabsorbable everolimus-eluting coronary stent and its relationship with plaque morphology. Journal of the American College of Cardiology 2008;52:1616-20.
5. Serruys PW, Onuma Y, Ormiston JA et al. Evaluation of the second generation of a bioresorbable everolimus drug-eluting vascular scaffold for treatment of de novo coronary artery stenosis: six-month clinical and imaging outcomes. Circulation 2010;122:2301-12.
6. Gomez-Lara J, Brugaletta S, Diletti R et al. A comparative assessment by optical coherence tomography of the performance of the first and second generation of the everolimus-eluting bioresorbable vascular scaffolds. European heart journal 2011;32:294-304.
7. Serruys PW, Onuma Y, Dudek D et al. Evaluation of the second generation of a bioresorbable everolimus-eluting vascular scaffold for the treatment of de novo coronary artery stenosis: 12-month clinical and imaging outcomes. Journal of the American College of Cardiology 2011;58:1578-88.
8. Onuma Y, Serruys PW. Bioresorbable scaffold: the advent of a new era in percutaneous coronary and peripheral revascularization? Circulation 2011;123:779-97.
9. Graham I, Atar D, Borch-Johnsen K et al. European guidelines on cardiovascular disease prevention in clinical practice: executive summary: Fourth Joint Task Force of the European Society of Cardiology and Other Societies on Cardiovascular Disease Prevention in Clinical Practice (Constituted by representatives of nine societies and by invited experts). European heart journal 2007;28:2375-414.
10. Serruys PW, Ormiston JA, Onuma Y et al. A bioabsorbable everolimus-eluting coronary stent system (ABSORB): 2-year outcomes and results from multiple imaging methods. Lancet 2009;373:897-910.
11. Sousa JE, Costa MA, Abizaid A et al. Lack of neointimal proliferation after implantation of sirolimus-coated stents in human coronary arteries: a quantitative coronary angiography and three-dimensional intravascular ultrasound study. Circulation 2001;103:192-5.
12. Sousa JE, Costa MA, Abizaid AC et al. Sustained suppression of neointimal proliferation by sirolimus-eluting stents: one-year angiographic and intravascular ultrasound follow-up. Circulation 2001;104:2007-11.
13. Serruys PW, Garcia-Garcia HM, Onuma Y. From metallic cages to transient bioresorbable scaffolds: change in paradigm of coronary revascularization in the upcoming decade? European heart journal 2012;33:16-25.
14. Finn AV, Joner M, Nakazawa G et al. Pathological correlates of late drug-eluting stent thrombosis: strut coverage as a marker of endothelialization. Circulation 2007;115:2435-41.

15. Joner M, Finn AV, Farb A et al. Pathology of drug-eluting stents in humans: delayed healing and late thrombotic risk. Journal of the American College of Cardiology 2006;48:193-202.
16. Kitta Y, Obata JE, Nakamura T et al. Persistent impairment of endothelial vasomotor function has a negative impact on outcome in patients with coronary artery disease. Journal of the American College of Cardiology 2009;53:323-30.
17. Vita JA, Treasure CB, Nabel EG et al. Coronary vasomotor response to acetylcholine relates to risk factors for coronary artery disease. Circulation 1990;81:491-7.
18. von Mering GO, Arant CB, Wessel TR et al. Abnormal coronary vasomotion as a prognostic indicator of cardiovascular events in women: results from the National Heart, Lung, and Blood Institute-Sponsored Women's Ischemia Syndrome Evaluation (WISE). Circulation 2004;109:722-5.
19. Brener SJ, Prasad AJ, Khan Z, Sacchi TJ. The relationship between late lumen loss and restenosis among various drug-eluting stents: a systematic review and meta-regression analysis of randomized clinical trials. Atherosclerosis 2011;214:158-62.
20. Mauri L, Orav EJ, Candia SC, Cutlip DE, Kuntz RE. Robustness of late lumen loss in discriminating drug-eluting stents across variable observational and randomized trials. Circulation 2005;112:2833-9.
21. Mauri L, Orav EJ, Kuntz RE. Late loss in lumen diameter and binary restenosis for drug-eluting stent comparison. Circulation 2005;111:3435-42.
22. Bruining N, Tanimoto S, Otsuka M et al. Quantitative multi-modality imaging analysis of a bioabsorbable poly-L-lactic acid stent design in the acute phase: a comparison between 2- and 3D-QCA, QCU and QMSCT-CA. EuroIntervention : journal of EuroPCR in collaboration with the Working Group on Interventional Cardiology of the European Society of Cardiology 2008;4:285-91.
23. Brugaletta S, Radu MD, Garcia-Garcia HM et al. Circumferential evaluation of the neointima by optical coherence tomography after ABSORB bioresorbable vascular scaffold implantation: Can the scaffold cap the plaque? Atherosclerosis 2011.
24. Frangos JA, Huang TY, Clark CB. Steady shear and step changes in shear stimulate endothelium via independent mechanisms--superposition of transient and sustained nitric oxide production. Biochemical and biophysical research communications 1996;224:660-5.
25. Hsiai TK, Cho SK, Reddy S et al. Pulsatile flow regulates monocyte adhesion to oxidized lipid-induced endothelial cells. Arteriosclerosis, thrombosis, and vascular biology 2001;21:1770-6.
26. Ross R. Atherosclerosis is an inflammatory disease. American heart journal 1999;138:S419-20.
27. Gerrity RG. The role of the monocyte in atherogenesis: II. Migration of foam cells from atherosclerotic lesions. The American journal of pathology 1981;103:191-200.
28. Gerrity RG. The role of the monocyte in atherogenesis: I. Transition of blood-borne monocytes into foam cells in fatty lesions. The American journal of pathology 1981;103:181-90.
29. Kaiser D, Freyberg MA, Friedl P. Lack of hemodynamic forces triggers apoptosis in vascular endothelial cells. Biochemical and biophysical research communications 1997;231:586-90.
30. Karlon WJ, Hsu PP, Li S, Chien S, McCulloch AD, Omens JH. Measurement of orientation and distribution of cellular alignment and cytoskeletal organization. Annals of biomedical engineering 1999;27:712-20.
31. Hsiai TK, Cho SK, Honda HM et al. Endothelial cell dynamics under pulsating flows: significance of high versus low shear stress slew rates (d(tau)/dt). Annals of biomedical engineering 2002;30:646-56.
32. Galis ZS, Sukhova GK, Lark MW, Libby P. Increased expression of matrix metalloproteinases and matrix degrading activity in vulnerable regions of human atherosclerotic plaques. The Journal of clinical investigation 1994;94:2493-503.
33. Dirksen MT, van der Wal AC, van den Berg FM, van der Loos CM, Becker AE. Distribution of inflammatory cells in atherosclerotic plaques relates to the direction of flow. Circulation 1998;98:2000-3.

34. Hsieh HJ, Cheng CC, Wu ST, Chiu JJ, Wung BS, Wang DL. Increase of reactive oxygen species (ROS) in endothelial cells by shear flow and involvement of ROS in shear-induced c-fos expression. Journal of cellular physiology 1998;175:156-62.
35. Mollnau H, Wendt M, Szocs K et al. Effects of angiotensin II infusion on the expression and function of NAD(P)H oxidase and components of nitric oxide/cGMP signaling. Circulation research 2002;90:E58-65.
36. Irani K. Oxidant signaling in vascular cell growth, death, and survival : a review of the roles of reactive oxygen species in smooth muscle and endothelial cell mitogenic and apoptotic signaling. Circulation research 2000;87:179-83.
37. Hwang J, Ing MH, Salazar A et al. Pulsatile versus oscillatory shear stress regulates NADPH oxidase subunit expression: implication for native LDL oxidation. Circulation research 2003;93:1225-32.
38. Cushing SD, Berliner JA, Valente AJ et al. Minimally modified low density lipoprotein induces monocyte chemotactic protein 1 in human endothelial cells and smooth muscle cells. Proceedings of the National Academy of Sciences of the United States of America 1990;87:5134-8.
39. Berliner JA, Territo MC, Sevanian A et al. Minimally modified low density lipoprotein stimulates monocyte endothelial interactions. The Journal of clinical investigation 1990;85:1260-6.
40. Berliner JA, Navab M, Fogelman AM et al. Atherosclerosis: basic mechanisms. Oxidation, inflammation, and genetics. Circulation 1995;91:2488-96.
41. Sevanian A, Hwang J, Hodis H, Cazzolato G, Avogaro P, Bittolo-Bon G. Contribution of an in vivo oxidized LDL to LDL oxidation and its association with dense LDL subpopulations. Arteriosclerosis, thrombosis, and vascular biology 1996;16:784-93.
42. Resnick N, Yahav H, Shay-Salit A et al. Fluid shear stress and the vascular endothelium: for better and for worse. Progress in biophysics and molecular biology 2003;81:177-99.
43. van Rossum HH, Romijn FP, Smit NP, de Fijter JW, van Pelt J. Everolimus and sirolimus antagonize tacrolimus based calcineurin inhibition via competition for FK-binding protein 12. Biochemical pharmacology 2009;77:1206-12.
44. Guertin DA, Sabatini DM. The pharmacology of mTOR inhibition. Science signaling 2009;2:pe24.
45. Mueller MA, Beutner F, Teupser D, Ceglarek U, Thiery J. Prevention of atherosclerosis by the mTOR inhibitor everolimus in LDLR-/- mice despite severe hypercholesterolemia. Atherosclerosis 2008;198:39-48.
46. Serruys PW, Garcia-Garcia HM, Buszman P et al. Effects of the direct lipoprotein-associated phospholipase A(2) inhibitor darapladib on human coronary atherosclerotic plaque. Circulation 2008;118:1172-82.
47. Khera AV, Cuchel M, de la Llera-Moya M et al. Cholesterol efflux capacity, high-density lipoprotein function, and atherosclerosis. The New England journal of medicine 2011;364:127-35.
48. Jensen LO, Thayssen P, Pedersen KE, Stender S, Haghfelt T. Regression of coronary atherosclerosis by simvastatin: a serial intravascular ultrasound study. Circulation 2004;110:265-70.
49. Ornish D, Brown SE, Scherwitz LW et al. Can lifestyle changes reverse coronary heart disease? The Lifestyle Heart Trial. Lancet 1990;336:129-33.
50. Schuler G, Hambrecht R, Schlierf G et al. Regular physical exercise and low-fat diet. Effects on progression of coronary artery disease. Circulation 1992;86:1-11.
51. Brugaletta S, Heo JH, Garcia-Garcia HM et al. Endothelial-dependent vasomotion in a coronary segment treated by ABSORB everolimus-eluting bioresorbable vascular scaffold system is related to plaque composition at the time of bioresorption of the polymer: indirect finding of vascular reparative therapy? European heart journal 2012;33:1325-33.

PART III

BIORESORBABLE SCAFFOLDS FOR TREATMENT OF COMPLEX LESIONS AND PATIENTS WITH ACUTE CORONARY SYNDROMES

Chapter 14

Everolimus-eluting bioresorbable vascular scaffolds for treatment of patients presenting with ST-segment elevation myocardial infarction: BVS STEMI first study

Roberto Diletti; Antonios Karanasos; Takashi Muramatsu; Shimpei Nakatani; Nicolas M. Van Mieghem; Yoshinobu Onuma; Sjoerd T. Nauta; Yuki Ishibashi; Mattie J. Lenzen; Jurgen Ligthart; Carl Schultz; Evelyn Regar; Peter P. de Jaegere; Patrick W. Serruys; Felix Zijlstra; Robert Jan van Geuns

Eur Heart J. 2014 Mar;35(12):777-86

Aims We evaluated the feasibility and the acute performance of the everolimus-eluting bioresorbable vascular scaffolds (BVS) for the treatment of patients presenting with ST-segment elevation myocardial infarction (STEMI).

Methods and results The present investigation is a prospective, single-arm, single-centre study, reporting data after the BVS implantation in STEMI patients. Quantitative coronary angiography and optical coherence tomography (OCT) data were evaluated. Clinical outcomes are reported at the 30-day follow-up. The intent-to-treat population comprises a total of 49 patients. The procedural success was 97.9%. Pre-procedure TIMI-flow was0 in 50.0% of the patients; after the BVS implantation, a TIMI flow III was achieved in 91.7% of patients and the post-procedure percentage diameter stenosis was 14.7±8.2%. No patients had angiographically visible residual thrombus at the end of the procedure. Optical coherence tomography analysis performed in 31 patients showed that the post-procedure mean lumen area was 8.02±1.92 mm^2, minimum lumen
area 5.95±1.61 mm^2, mean incomplete scaffold apposition area 0.118±0.162 mm^2, mean intraluminal defect area 0.013±+0.017 mm^2, and mean percentage malapposed struts per patient 2.80±3.90%. Scaffolds with >5% malapposed struts were 7. At the 30-day follow-up, target-lesion failure rate was 0%. Non-target-vessel revascularization and target vessel myocardial infarction (MI)were reported. A non-target-vessel non-Q-wave MI occurred. No cases of cardiac death or scaffold thrombosis were observed.

INTRODUCTION

Primary percutaneous coronary intervention has been demonstrated to be superior to thrombolytic strategy and is currently the treatment of first choice for patients presenting with ST-segment elevation myocardial infarction (STEMI) in experienced centres with limited time delay.[1] First-generation drug-eluting stents (DES) have been shown to reduce the need for repeat revascularization compared with bare-metal stents (BMS),[2 – 4] and the newer-generation DE S with improved biocompatibility of polymers may lower the rate of clinical events also in acute patients.[5,6] However, the implantation of metal devices is not devoid of important limitations, such as permanent caging of the vessel with permanent impairment of coronary vasomotion, side branch jailing, impossibility of late lumen enlargement, non-invasive imaging and future surgical revascularization of stented segments.[7] Moreover, in spite of the beneficial effect of neointimal inhibition, the antiproliferative drug elution has been shown to interfere with the vascular healing processes providing the background for delayed strut coverage and persistent or acquired malapposition.[8,9] The above-mentioned limitations can be proposed for both stable and acute patients; however, primary stenting has additional specific characteristics that should be highlighted. Stent placement in acute thrombotic lesions has been reported to be an independent predictor of late stent malapposition after the BMS[10] or DES[11] implantation. Possible explanations for this phenomenon could be the thrombus sequestration behind the struts—which subsequently resolves—and the vasoconstriction during the acute phase. Both these factors may predispose to stent underdeployment, malapposition and finally to stent thrombosis. The everolimus-eluting bioresorbable vascular scaffold (BVS) has been designed to overcome the general limitations of the metallic stents and recently has been shown to provide excellent results for the treatment of stable patients.[12,13] However, so far very limited data are available on the use of this novel device in patients with acute coronary syndromes (ACS).[14,15] Given this background, a pilot study investigating the feasibility and acute performance of the BVS for the treatment of patients presenting with STEMI was initiated.

METHODS

Rationale

As of 1 September 2012, the BVS (ABSORB; Abbott Vascular, Santa Clara, CA, USA) has been commercially available in the Netherlands. Based on previous experience and available evidence, reported in ABSORB Cohort A and B Trial[13,16] our institution initiated the use of BVS for the treatment of patients presenting for PCI in everyday clinical practice, with a preference for patients with a good life expectancy as demonstrated by the presence of limited co-morbidities. As these patients might have more complex lesions compared with the ABSORB study patients[16,17] the BVS-EXPAND registry was initiated. The BVS-EXPAND also included patients with ACS (unstable angina or non-STEMI). After the first experience with ACS patients and an interim analysis, a decision was made to extend BVS utilization to the treatment of STEMI. As an additional measure for assessing the safety of a treatment approach with BVS in STEMI, optical coherence tomography (OCT) imaging was performed, according to clinical judgment, for a more comprehensive evaluation of the acute procedural outcome.

Study design

The present report is an investigator initiated, prospective, single arm, single-centre study to assess feasibility and performance of the second-generation everolimus-eluting BVS for the treatment of patients presenting with STEMI. Subjects enrolled were patients of ≥18-year-old admitted with STEMI, defined as at least 1 mm ST-segment elevation in two or more standard leads or at least 2 mm in two or more contiguous precordial leads or new left bundle branch block within 12 h after the onset of symptoms. Culprit lesions were located in vessels within the upper limit of 3.8 mm and the lower limit of 2.0 mm by online quantitative coronary angiography (QCA). The absorb BVS was implanted according to the manufacturer's indication on target vessel diameter ranges and absorb BVS diameters to be used. The absorb BVS with a nominal diameter of 2.5 mm was implanted in vessels ≥ 2.0 and ≤ 3.0 mm by online QCA; the 3.0 mm BVS was implanted in vessels ≥ 2.5 and ≤3.3 mm by online QCA; the 3.5 mm BVS was implanted in vessels ≥ 3.0 and ≤3.8 mm. Given the manufacturer's indication on maximum scaffold expansion, for each nominal diameter a further expansion of 0.5 mm was allowed. Enrolled subjects were willing to comply with specified follow-up evaluation and to be contacted by telephone. Exclusion criteria comprise pregnancy, known intolerance to contrast medium, uncertain neurological outcome after cardiopulmonary resuscitation, previous percutaneous coronary intervention with the implantation of a metal stent, left main (LM) disease previous coronary artery bypass grafting (CABG), age superior to 75

years, and participation to another investigational drug or device study before reaching the primary endpoints. The enrolment period started on 1November 2012 and ended on 30 March 2013. Dual antiplatelet therapy after the BVS implantation was planned to have a duration of 12 months. Baseline and post-BVS implantation QCA analysis, OCT analyses at post-BVS implantation, and clinical outcomes at the 30-day follow-up were evaluated.

Definitions

Success rates were defined as follows: device success was the attainment of <30% final residual stenosis of the segment of the culprit lesion covered by the BVS, by angiographic visual estimation. Procedure success was defined as device success and no major periprocedural complications (Emergent CABG, coronary perforation requiring pericardial drainage, residual dissection impairing vessel flow—TIMI-flow II or less). Clinical success was defined as procedural success and no in-hospital major adverse cardiac events (MACE). All deaths were considered cardiac unless an undisputed non-cardiac cause was identified. Myocardial infarction (MI) and scaffold thrombosis were defined according to the Academic Research Consortium definition.[18] Target-lesion revascularization (TLR) was defined as clinically driven if at repeat angiography the diameter stenosis was >70%, or if a diameter stenosis >50% was present in association with (i) presence of recurrent angina pectoris, related to the target vessel; (ii) objective signs of ischaemia at rest (ECG changes) or during exercise test, related to the target vessel; and (iii) abnormal results of any functional diagnostic test. The device-oriented endpoint target-lesion failure was defined as the composite of cardiac death, target-vessel MI, or ischaemia-driven TLR. Major adverse cardiac events defined as the composite of cardiac death, any re-infarction (Q- or non-Q-wave), emergent bypass surgery (CABG), or clinically driven TLR. Target-vessel failure (TVF) was defined as cardiac death, target-vessel MI, or clinically driven TVR.

Ethics

This is an observational study, performed according to the privacy policy of the Erasmus MC and to the Erasmus MC regulations for the appropriate use of data in patient-oriented research, which are based on international regulations, including the declaration of Helsinki. The BVS received the CE mark for clinical use, indicated for improving coronary lumen diameter in patients with ischaemic heart disease due to de novo native coronary artery lesions with no restriction in terms of clinical presentation. Therefore, the BVS can be currently used routinely in Europe in different settings comprising the acute MI without a specific written informed consent in addition to the standard informed consent to the procedure. Given this background, a waiver from the hospital Ethical Committee was obtained for written informed consent, as according to Dutch law written consent is not required, if patients are not subject to acts other than as part of their regular treatment.

Study device

The second-generation everolimus-eluting BVS is a balloon expandable device consisting of a polymer backbone of poly-L-lactide acid (PLLA) coated with a thin layer of amorphous matrix of poly-D and -L-lactide acid (PDLLA) polymer (strut thickness 157 μm). The PDLLA controls the release of the antiproliferative drug everolimus (100 μg/cm^2), 80% of which is eluted within the first 30 days. Both PLLA and PDLLA are fully bioresorbable. The polymers are degraded via hydrolysis of the ester bonds and the resulting lactate and its oligomers are metabolized by the Krebs cycles. Small particles (<2 μm in diameter) may be also phagocytized and degraded by macrophages.[19] According to preclinical studies, the time for complete bioresorption of the polymer backbone is ~2–3 years.[20] The BVS edges contain two platinum markers for accurate visualization during angiography or other imaging modalities.

Quantitative coronary angiography analysis

Quantitative coronary angiography (QCA) analyses were performed using the Coronary Angiography Analysis System (Pie Medical Imaging, Maastricht, Netherlands). Analyses were performed at pre-procedure, after thombectomy, after balloon dilatation, and after the BVS implantation with a methodology already reported.[21]

In case of thrombotic total occlusion, pre-procedure QCA analysis was performed as proximally as possible from the occlusion (in case of a side branch distally to the most proximal take off of the side branch). Intracoronary thrombus was angiographically identified and scored in five grades as previously described.[22] Thrombus grade was assessed before procedure and after thombectomy. The QCA measurements included reference vessel diameter (RVD)—calculated with interpolate method—percentage diameter stenosis, minimal lumen diameter (MLD), and maximal lumen diameter (Dmax). Acute gain was defined as post-procedural MLD minus pre-procedural MLD (MLD value equal to zero was applied when culprit vessel was occluded pre-procedurally). Complications occurring any time during the procedure, such as dissection, spasm, distal embolization, and no-reflow were reported. As additional information, MI SYNTAX I and MI SYNTAX II scores providing long-term risk stratification for mortality and MACE in patients presenting with STEMI were assessed.[23]

Optical coherence tomography image acquisition and analysis

Optical coherence tomography imaging after the BVS implantation was encouraged in all patients but was not mandatory, subordinated to device availability and left at the operator's discretion. Therefore, OCT imaging of the culprit lesion after treatment was performed in a subset of the population. The image acquisition was performed with

C7XR imaging console and the Dragonfly intravascular imaging catheter (both St. Jude Medical, St. Paul, MN, USA). Image acquisition has been previously described.[24] Briefly, after positioning the OCT catheter distally to the most distal scaffold marker, the catheter is pulled back automatically at 20 mm/s with simultaneous contrast infusion by a power injector (flush rate 3–4 mL/s). In cases where the entire scaffold region was not imaged in one pullback, a second more proximal pullback was performed for complete visualization. Images were stored and analyzed offline. Analysis of the OCT images was performed with the St Jude/Lightlab offline analysis software (St. Jude Medical), using previously described methodology for BVS analysis.[17] Analysis was performed in 1-mm longitudinal intervals within the treated culprit segment, after exclusion of frames with <75% lumen contour visibility. Lumen, scaffold, and incomplete scaffold apposition (ISA) area were calculated in accordance with standard methodology for analysis of bioresorbable scaffolds[17] (Figure 1A and B), while in sites with overlapping scaffolds, analysis was performed using previously suggested modifications[25] (Figure 1D). Specifically, the lumen contour is traced at the lumen border and in the abluminal (outer) side of apposed struts, while in the case of malapposed struts the contour is traced behind the malapposed struts. In cases where the scaffold struts are completely covered by tissue or thrombus, the lumen contour is traced above the prolapsing tissue (Figure 1C). The scaffold area is traced following interpolation of points located in the mid-point of the abluminal border of the black core in apposed struts and the mid-point of the abluminal strut frame border in malapposed or side branch-related struts, so that the scaffold area is identical to the lumen area in the absence of ISA and tissue prolapse. Incomplete scaffold apposition area is traced in the case of malapposed struts as the area delineated between the lumen and scaffold contours (Figure 1B). A special consideration should be mentioned concerning BVS analysis in MI with the presence of increased tissue prolapse and residual thrombus post-implantation [21,26] (Figures 1C and 2). Tissue prolapsed area can be quantified as the difference between the scaffold and the lumen area. For the calculation of prolapse area, in the case that one or more scaffold struts are completely covered by thrombus or tissue, the total black core area of these struts is also measured. Prolapse area is then calculated as [scaffold area + ISA area - lumen area - embedded black core area]. The area of non-attached intraluminal defects (e.g. thrombus) is also measured. Atherothrombotic area is then calculated as the sum of prolapse area and intraluminal defect area and normalized as a percent ratio of the scaffold area (atherothrombotic burden, ATB).[21,26] It should be noted that in the case of bioresorbable scaffolds where measurements of the scaffold area are performed using the abluminal side of the scaffold struts, ATB is overestimated compared with metal platform stents where measurements of the stent area are performed from the adluminal (inner) side of the struts. Additionally, flow area was assessed as [scaffold

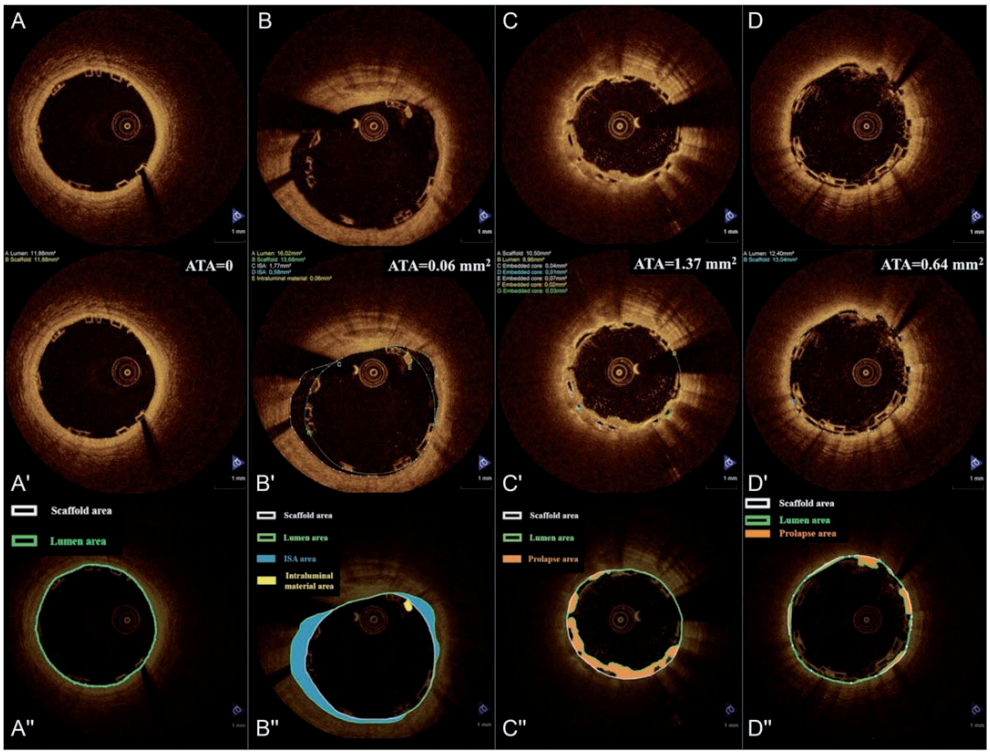

Figure 1. Flow-chart of the study.
From 1st November 2012 to 30th April 2013 a total of 267 patients presented with acute myocardial infarction. Twenty-one of those patients were treated percutaneously but without any stent implantation (thrombectomy or balloon dilatation alone). Seventy-four had a culprit lesion located in a coronary vessel with a vessel diameter out of the range availability of the BVS (i.e reference vessel diameter > 4.0 mm). The remaining 172 patients were treated in 123 cases with metal stents and 49 were enrolled in the present study. Out of those 172 patients only 125 were meeting the inclusion and exclusion criteria of the present study; thus the patients implanted with BVS constitute the 39% of the patients eligible for the present investigation

area + ISA area - atherothrombotic area - total strut area] and the minimal flow area was recorded. A scaffold strut is defined as incompletely apposed when there is no contact between the abluminal border of the strut and the vessel wall. This does not include struts located in front of side branches or their ostium (polygon of confluence region), which are defined as side branch-related struts. Intraluminal struts that are part of adjacent clusters of apposed struts in overlapping scaffolds are also not considered malapposed.[25] For illustrative proposes, OCT bi-dimensional images are reported by three-dimensional rendering by dedicated software (Intage Realia, KGT, Kyoto, Japan)[17] (Figures 2 and 3).

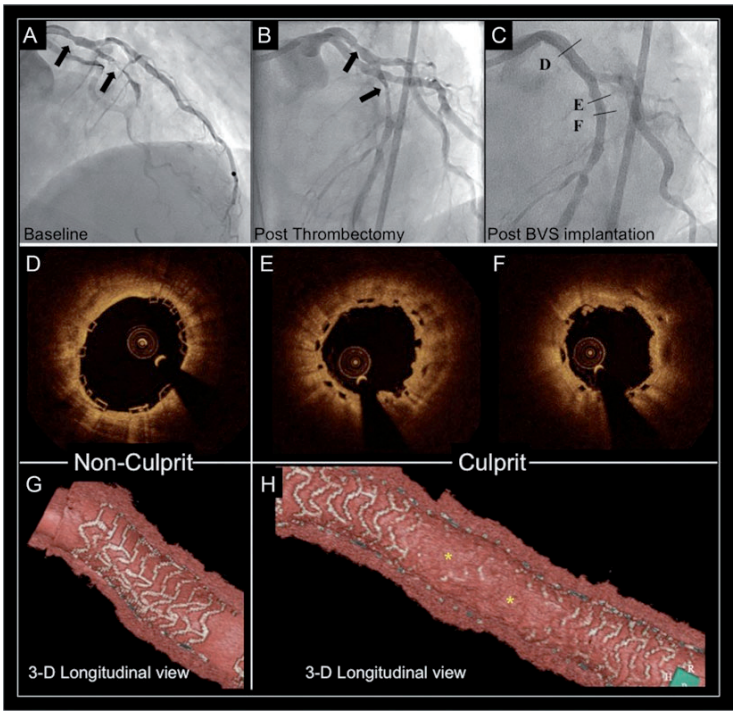

Figure 2. Methodology of OCT analysis.
A. Good scaffold apposition and absence of ISA or tissue prolapse; B. ISA; C. Sites with high tissue prolapse and struts completely covered by thrombus; D. Overlapping scaffolds. Upper panel shows baseline images, middle panel quantitative measurements, lower panel methodology for analysis. Abbreviations: ISA=incomplete scaffold apposition, ATA=atherothrombotic area

Statistical analysis

Continuous variables are presented as mean and standard deviation, and categorical variables are reported as count and percentages. Descriptive statistics was provided for all variables. The present study is intended to be a 'first experience investigation' evaluating feasibility and acute performance of the everolimus-eluting BVS for the treatment of patients presenting with STEMI. A patient population of at least 30 patients was planned to be included in the present study. Comparisons among multiple means were performed with analysis of variance (one-way ANOVA). Score (Wilson) confidence intervals were reported for measures of success. Type A intraclass correlation coefficients (ICCs) for absolute agreement were used for assessing intra- and interobserver agreement, while measurement error and 95% limits of agreement were assessed by Bland–Altman analysis. The ICCs were computed with a two-way random effects model (single measures). All statistical tests were performed with SPSS, version 15.0 for windows (IL, USA).

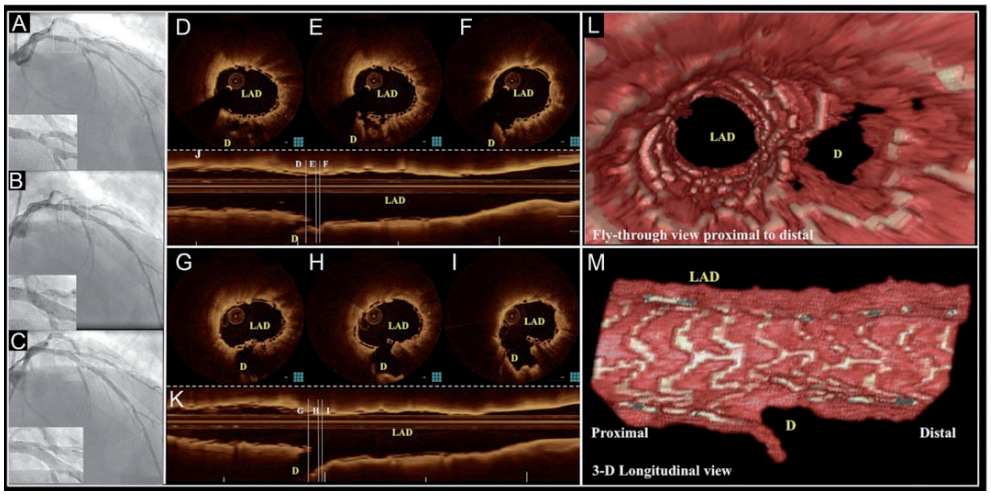

Figure 3. BVS implantation in a culprit and a non-culprit lesion in myocardial infarction.
A. Coronary angiography demonstrating a stenotic lesion in proximal LAD (proximal non-culprit lesion) and a total occlusion of the mid LAD (culprit lesion). B. Angiography following thrombus aspiration. C. Angiography following implantation of a 3.5x12mm BVS at the proximal LAD lesion and a 3.0x28mm BVS at the mid LAD lesion. D. OCT image from the proximal non-culprit lesion showing absence of tissue prolapse and thrombus in the 3.5x12mm scaffold. E. and F. OCT images from the culprit lesion showing complete coverage of the BVS by tissue prolapse and presence of small amount of intraluminal defect. G. Three-dimensional OCT rendering in the proximal non-culprit lesion with complete scaffold visualization indicating the absence of prolapsing material. H. Conversely, in the 3-dimensional rendering of the culprit lesion, the morphology of the BVS cannot be fully visualized due to high levels of tissue prolapse (*).

RESULTS

From 1 November 2012 to 30 April 2013, a total of 267 patients presented with acute MI. Twenty-one of those patients were treated percutaneously without any stent implantation (thrombectomy or balloon dilatation alone). Seventy-four had a culprit lesion located in a coronary vessel with a vessel diameter out of the range availability of the BVS (i.e. RVD >4.0 mm). Out of the remaining 172 patients, 125 were meeting the inclusion and none of the exclusion criteria of the present study (47 patients excluded for age, previous PCI or CABG, left main disease). Seventy-six of those patients were treated with metal stents and 49 cases (48 implanted with BVS) were enrolled in the present study (Figure 4, Table 1). Therefore, the patients implanted with BVS constitute the ~38% of the patients eligible for the present investigation. Baseline clinical characteristics of the 172 patients (49 patients included in the intent-to-treat population and 123 patients implanted with metal stents)

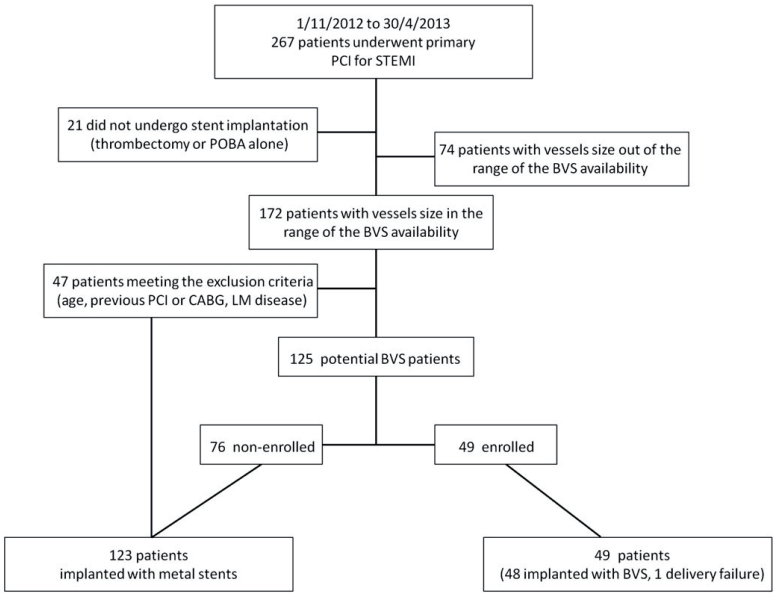

Figure 4. BVS implantation in a thrombotic bifurcation lesion treated with provisional approach.
Coronary angiography pre intervention. B. Angiography following BVS implantation in the LAD, showing pinching of the ostium of the diagonal (D). C. Final angiographic result following side-branch dilation with 2.0x15mm balloon. D. E. F. J. OCT cross-sectional images and I-mode after BVS implantation showing the compromise of the side-branch after implantation and presence of thrombus at the side-branch ostium. G. H. I. K. OCT cross-sectional images and I-mode after side-branch dilation, showing the opening of the carina of the side branch. L. M. Three-dimensional reconstructions confirm the opening of the side-branch ostium.

with vessels size in the range of the BVS availability are reported in Table 1. In the intent-to-treat population thirty-eight patients were male (77.6%), mean age was 58.9±10.5 years. Lesions were distributed as follows: left anterior descending [21] (42.9%), right coronary artery [22] (44.9%), and circumflex 6 (12.2%). Baseline clinical data of the enrolled patients were compared with the general population presenting with acute MI and implanted with a metal stent in vessels theoretically suitable for BVS implantation. Minimal differences were observed between the two groups. Namely, age 58.9±10.5 vs. 66.4±12.2, P <0.001 and previous PCI 0% vs. 12.2%, P = 0.007. All the other clinical characteristics of the two populations did not show any significant difference.

Mean door-to-balloon time was 31.3±19.5 min. All patients were treated with unfractionated heparin at the dose of 70–100 UI/kg and dual antiplatelet therapy (aspirin plus, prasugrel in 45 patients or clopidogrel in 4 patients). Manual thrombectomy was performed in 38 patients. In 16 cases, direct stenting was performed; a total of 65 scaffolds were implanted

(12 patients received overlapping scaffolds—overlap was systematically intended to be minimal). The scaffolds lengths used were 12, 18, and 28 mm, with scaffolds diameters 2.5, 3.0, and 3.5 mm. Mean scaffold length per-lesion was 26.40±13.86 mm, mean scaffold diameter per-lesion was 3.2±34 mm. A highly supportive wire was used in five cases and radial approach was performed in 26 patients (53.0%) (Table 2). The procedural success was 97.9% (48/49 patients); in one patient, the delivery of the BVS was unsuccessful (due to the remarkable vessel tortuosity was not possible to advance the BVS at the site of the lesion) and a metallic DES was implanted. Clinical success was 97.9% (48/49 patients).

Table 1. Baseline clinical characteristics intent-to-treat population and patients treated with metallic stent in the enrolment period.

Clinical characteristics	BVS (N=49)	Metal stents (N=123)	p value
Age (y)	58.9±10.5	66.4±12.2	<0.001
Male n. (%)	38 (77.6)	93 (75.6)	0.845
Hypertension n. (%)	19 (38.8)	53/105 (50.5)	0.225
Hypercholesterolemia n. (%)	11 (22.4)	30/100 (30.0)	0.435
Diabetes n. (%)	4 (8.2)	14/116 (12.1)	0.590
Smoke n. (%)	27 (69.2)	46/116 (39.7)	0.120
Family history of CAD n. (%)	12 (24.5)	31/95 (32.6)	0.343
Prior Cerebrovascular accident n. (%)	0 (0)	13 (10.6)	0.021
Peripheral vascular disease n. (%)	1 (2.0)	8 (6.5)	0.449
Kidney disease n. (%)	1 (2.0)	7 (5.7)	0.442
Prior MI n. (%)	1 (2.0)	14 (11.4)	0.070
Prior PCI n. (%)	0 (0.0)	15 (12.2)	0.007
Prior CABG n. (%)	0 (0.0)	3 (2.4)	0.559
COPD n. (%)	2 (4.1)	5 (4.1)	1.000
Culprit vessel			0.624
LM n. (%)	0 (0)	2 (1.6)	
LAD n. (%)	21 (42.9)	52 (42.3)	
RCA n. (%)	22 (44.9)	46 (37.4)	
LCX n. (%)	6 (12.2)	21 (17.1)	
SVG n. (%)	0 (0)	2 (1.6)	

Patients with vessels diameters not feasible for BVS implantation (i.e. reference vessel diameter larger than 4.0 mm) were excluded CAD=coronary artery disease; PCI=percutaneous coronary intervention; CABG=Coronary artery bypass graft; COPD=Chronic obstructive pulmonary disease; LAD=left anterior descending; RCA=right coronary artery; LCX=circumflex. Data are expressed as mean ± SD or number and proportion, n. (%).

Quantitative coronary angiography analysis

The QCA is reported only in patients implanted with BVS. In 50.0% of those patients, pre-procedure TIMI-flow was 0 and the RVD was 2.94±0.77 mm. In the non-totally occluded vessels, the RVD was 2.62±0.63 mm, with an MLD of 0.75±0.44 mm and a mean diameter stenosis of 70.8±12.5%. After thrombectomy and balloon dilatation, TIMI-flow grade 0 was present in 2.5 and 0.0% of patients, respectively, and TIMI-flow III in 52.5 and 59.3% of the cases, respectively. After the scaffold implantation, there were no cases of TIMI flow 0,

Table 2. Procedural data Intent-to-treat population.

Procedural data	N =49
Medications	
Aspirin n. (%)	49 (100)
Prasugrel n. (%)	45 (91.8)
Clopidogrel n. (%)	4 (8.2)
Glycoprotein IIb/IIIa antagonists n. (%)	17 (34.7)
Unfractionated heparin n. (%)	49 (100)
Mean door-to-balloon time (min)	31.3 ± 19.5
Manual Thrombectomy n. (%)	38 (77.5)
Direct stenting n. (%)	16 (32.7)
Pre-dilatation n. (%)	33 (67.3)
Mean pre-dilatation balloon diameter per-lesion (mm)	2.6±0.67
Post-dilatation n. (%)	10 (20.4)
Mean post-dilatation balloon diameter per-lesion (mm)	3.5±0.47
Overlapping n. (%)	12 (24.5)
Overlap scaffolds diameters 3.5 mm – 3.5 mm n. (%)	5 (10.2)
Overlap scaffolds diameters 3.5 mm – 3 mm n. (%)	5 (10.2)
Overlap scaffolds diameters 3.5 mm – 2.5 mm n. (%)	1 (2.0)
Overlap scaffolds diameters 3 mm – 2.5 mm n. (%)	1 (2.0)
Total number of scaffolds n.	65
Mean scaffolds per-lesion n.	1.35±0.60
Mean scaffold length per-lesion (mm)	26.40±13.86
Mean scaffold diameter per lesion (mm)	3.2±34
Supportive wire n. (%)	5 (10.2)
Radial approach n. (%)	26 (53.0)

Data are expressed as mean ± SD or number and proportion, n. (%).

Table 3. Angiographic analysis in patients implanted with BVS.

Angiographic data	N=48
Pre-procedure	
TIMI flow grade, %(n)	
0	50.0% (23/46)
1	15.2% (7/46)
2	21.7% (10/46)
3	13.0% (6/46)
Thrombus burden index, %(n)	
0	0.0% (0/46)
1	6.5% (3/46)
2	17.4% (8/46)
3	13.0% (6/46)
4	13.0% (6/46)
5	50.0% (23/46)
Total occlusion (n=23)	
RVD, mm	2.94 ± 0.77
Non-total occlusion (n=23)	
RVD, mm	2.62 ± 0.63
Minimal lumen diameter, mm	0.75 ± 0.44
Diameter stenosis, %	70.8 ± 12.5
After thrombectomy	
TIMI flow grade, %(n)	
0	2.5% (1/40)
1	7.5% (3/40)
2	37.5% (15/40)
3	52.5% (21/40)
Thrombus burden index, %(n)	
0	0.0% (0/40)
1	30.0% (12/40)
2	35.0% (14/40)
3	22.5% (9/40)
4	10.0% (4/40)
5	2.5% (1/40)
After pre-dilatation	
TIMI flow grade, %(n)	
0	0.0% (0/27)
1	7.4% (2/27)
2	33.3% (9/27)
3	59.3% (16/27)
Before BVS implantation	
RVD, mm	2.63 ± 0.53
Minimal lumen diameter, mm	1.21 ± 0.46
Diameter stenosis, %	53.2 ± 16.1
Dmax, mm	3.01 ± 0.52

Table 3. Continued.

Angiographic data	N=48
Post-procedure	
TIMI flow grade, %(n)	
0	0.0% (0/48)
1	0.0% (0/48)
2	8.3% (4/48)
3	91.7% (44/48)
In-scaffold	
RVD, mm	2.86 ± 0.52
Minimal lumen diameter, mm	2.44 ± 0.49
Diameter stenosis, %	14.7 ± 8.2
In-segment	
RVD, mm	2.74 ± 0.59
Minimal lumen diameter, mm	2.20 ± 0.53
Diameter stenosis, %	21.8 ± 12.0
MI syntax score I *	10.0 (7.0-15.0)
MI syntax score II *	7.0 (4.25-10.0)
Dominant right coronary artery, %(n)	93.8% (45/48)
Scaffold-to-artery ratio	1.19 ± 0.24
Complications, %(n)	
Dissection	6.3% (3/48)
Spasm	4.2% (2/48)
Distal embolism	14.6% (7/48)
No-reflow	2.1% (1/48)

Data are expressed as mean±SD or proportion (%). * MI syntax score I and II are expressed as median (interquartile range).

and a TIMI-flow III was achieved in 91.7% of patients, the mean post-procedure in-scaffold % diameter stenosis was 14.7±8.2%, in-scaffold MLD was 2.44±0.49 mm (Table 3). No angiographically visible residual thrombus was observed at post-procedure.

Optical coherence tomography findings

Optical coherence tomography analysis was performed in a subgroup of 31 patients implanted with BVS. Mean lumen area was 8.02±1.92 mm^2, minimum lumen area 5.95±1.61 mm^2, and minimum flow area 5.62±1.66 mm^2. Incomplete scaffold apposition (ISA) was observed in 20 patients with a mean ISA area of 0.118±0.162 mm^2 and a mean percentage of malapposed struts per patients equal to 2.80±3.90%. The mean prolapse area was 0.60±0.26 mm^2, and the mean intraluminal defect area was 0.013±0.017 mm^2. Scaffolds with >5% malapposed struts were 7 (Table 4). The OCT analysis stratified by scaffold size (5 BVS 2.5 mm, 13 BVS 3.0 mm, 24 BVS 3.5 mm) showed different lumen,

Table 4. OCT findings post-implantation in patients implanted with BVS .

OCT variables	N=31
Analyzed length, mm	28.16±13.29
Analyzed struts, n	245±135
Minimum lumen area, mm^2	5.95±1.61
Mean lumen area, mm^2	8.02±1.92
Lumen volume, mm^3	225.78±113.63
Minimum scaffold area, mm^2	6.69±1.94
Mean scaffold area, mm^2	8.54±1.97
Scaffold volume, mm^3	240.07±118.48
Minimum flow area, mm^2	5.62±1.66
ISA area, mm^2 (n=20)	0.118±0.162
Mean prolapse area, mm^2	0.60±0.26
Mean intraluminal defect area, mm^2	0.013±0.017
Maximum intraluminal defect area, mm^2	0.094±0.077
Mean atherothrombotic area, mm^2	0.61±0.27
Mean atherothrombotic burden, %	7.29±3.12
Malapposed struts per patient, %	2.80±3.90
Scaffolds with at least 1 malapposed strut, n (%)	20 (64.5)
Scaffolds with >5% malapposed struts, n (%)	7 (22.6)

ISA=incomplete scaffold apposition; Data are expressed as mean ± SD or number and proportion, n. (%).

Table 5. OCT findings post-implantation stratified by scaffold size in patients implanted with BVS

OCT variables				
Scaffold size	2.5mm (N=5)	3.0mm (N=13)	3.5mm (N=24)	p
Analyzed length, mm	18.80±1.30	22.23±6.46	21.33±7.38	0.628
Minimum lumen area, mm^2	4.08±0.24	5.60±0.93	7.18±1.58	0.001
Mean lumen area, mm^2	5.42±0.75	7.18±1.03	9.25±1.72	0.001
Minimum scaffold area, mm^2	4.53±0.51	6.13±1.02	8.06±1.82	0.001
Mean scaffold area, mm^2	5.62±0.28	7.66±0.88	9.82±1.70	0.001
Minimum flow area, mm^2	3.84±0.28	5.17±0.86	6.77±1.60	0.001
ISA area, mm^2 (n=25)	0.190±0.318 (n=3)	0.063±0.072 (n=10)	0.133±0.177 (n=12)	0.429
Mean prolapse area, mm^2	0.40±0.19	0.54±0.27	0.62±0.29	0.246
Mean intraluminal defect area, mm^2	0.007±0.008	0.016±0.021	0.012±0.018	0.628
Maximum intraluminal defect area, mm^2	0.072±0.081	0.102±0.086	0.068±0.065	0.096
Mean atherothrombotic area, mm^2	0.40±0.19	0.56±0.27	0.64±0.30	0.237
Mean atherothrombotic burden, %	6.00±4.66	7.42±3.79	6.20±3.39	0.594

ISA=incomplete scaffold apposition; Data are expressed as mean ± SD or number and proportion, n. (%).

scaffold, and flow areas, but similar amounts of incomplete stent apposition, plaque prolapse, and intraluminal mass areas (Table 5). In three cases, the observation of scaffold malapposition by OCT, guided an additional post-dilatation and in one patient the visualization of considerable intraluminal thrombus as assessed by OCT led to a repeated thrombus aspiration. Intra-observer variability was excellent. Intraclass correlation coefficients were 0.999 for lumen area and 0.999 for scaffold area, and the corresponding measurement errors and limits of agreement were 0.01 mm^2 (-0.12 to 0.15 mm^2) for lumen area and -0.01 mm^2 (-0.20 to 0.17 mm^2) for scaffold area. Similarly, inter-observer intraclass correlation coefficients were 0.997 for lumen area and 0.987 for scaffold area, and the corresponding measurement errors and limits of agreement were -0.01 mm^2 (-0.30 to 0.28 mm^2) for lumen area and -0.22 mm^2 (-0.68 to 0.24 mm^2) for scaffold area.

Clinical outcomes

At the 30-day follow-up, the rate of the device-oriented endpoint, target-lesion failure, was 0%. None of the patients experienced target-vessel re-infarction, emergent bypass surgery, or clinically driven TLR. No cases of cardiac death or scaffold thrombosis were reported. The MACE rate was 2.6% as one patient, after discharge developed a non-Q-wave MI related to a non-target-vessel lesion and underwent a non-target-vessel revascularization within the 30 days post-procedure. This was the only event reported in the studied population (Table 6).

Table 6. Clinical outcomes at 30-day follow-up Intent-to-treat population

Clinical events	N=49	95% CI
Target lesion failure	(0/49) 0%	(0-7.41)
Target vessel failure	(0/49) 0%	(0-7.41)
Cardiac death	(0/49) 0%	(0-7.41)
Target vessel myocardial infarction	(0/49) 0%	(0-7.41)
Q-Wave myocardial infarction	(0/49) 0%	(0-7.41)
Non Q-Wave myocardial infarction	(0/49) 0%	(0-7.41)
Clinically driven target vessel revascularization	(0/49) 0%	(0-7.41)
Any myocardial infarction	(1/49) 2.6%	(0-10.69)
Q-Wave myocardial infarction	(0/49) 0%	(0-7.41)
Non Q-Wave myocardial infarction	(1/49) 2.6%	(0-10.69)
Major Adverse Cardiac Events	(1/49) 2.6%	(0-10.69)
Non-target vessel revascularization	(1/49) 2.6%	(0-10.69)
Definite or probable scaffold thrombosis	(0/49) 0%	(0-7.41)

DISCUSSION

The everolimus-eluting BVS has been tested so far only in elective patients with stable, unstable angina, or silent ischaemia;[16,17,27–29]showing promising results up to 4-year follow-up30 for the first generation and up to 2 years for the second-generation BVS.[12,13,31] The present study represents an early investigation reporting clinical and angiographic data on the use of the second-generation BVS for the treatment of patients presenting with STEMI and evaluating acute results with high-resolution intracoronary imaging (OCT). A high device, procedural, and clinical success rates were observed with all the scaffolds achieving a residual stenosis <30% and no in-hospital MACE. Such data are supportive of feasibility and good acute performance of the BVS for the treatment of patients with acute MI.

Angiographic data

The everolimus-eluting BVS was implanted in patients presenting with ST-segment elevation and a thrombus burden 4 or 5 in 63.0% of the cases. A theoretical concern related to the implantation of the BVS in such thrombotic lesions is the fact that scaffold positioning and placement may need a more aggressive lesion preparation (predilatation) compared with standard metal devices, due to its slightly higher profile. We hypothesized that this strategy might be prone to an increase in distal embolization following balloon inflations, favouring no-reflow and reducing the rate of final TIMI-flow III. However, the analysis of the post-procedural angiographies revealed a TIMI-flow III in 91.7% of the cases; such results are in line with recently reported large trials evaluating the performance of metallic stents in patients presenting with acute MI.[5,6] Less thrombus embolization may result from a different pattern of thrombus dislodgment and compression to the arterial wall after deployment of a device with a larger strut width (157 mm) compared with currently available metallic stents. The percentage of vessel wall area covered by the BVS polymer (scaffold/vessel ratio) has been previously evaluated to be 26%,[32] a value considerably higher compared with what observed for conventional metallic DES (i.e. EES provides a percentage stent/vessel ratio equal to 12%).[32] This characteristic of the BVS might be associated to an increased capacity of capturing debris and thrombotic material behind the struts before embolization to distal microcirculation. This so-called snow racket concept (entrapment of thrombotic material between the stent and the vessel) is currently the basis for the design of novel devices and clinical studies.[33]

Optical coherence tomography findings

Given its high resolution, OCT allows the assessment of in vivo strut apposition and presence of thrombus.[24,34 – 36] The present analysis was performed at 1 mm intervals in the OCT pullback. Although, the possibility for a more strict assessment of OCT analysis in thrombotic lesion may be considered,[21] this methodology is the current standard applied in our institution for clinical studies, and the most commonly used in the literature. Previous reports defined a stent malapposed if at least 5% of struts were observed to be malapposed;[37,38] in the present investigation, only seven scaffolds (22.6%) investigated with OCT showed a strut malapposition of >5%, with an overall mean struts malapposition equal to 2.8±3.90%. A recently reported study using a similar methodology to investigate malapposition after metallic balloon expandable stent implantation in STEMI patients showed a total of 37.1% malapposed stents (stents with >5% malapposition) with a mean percentage of strut malapposition equal to 5.99±7.28%.[38] In addition, the mean ISA area was 0.118±0.162 mm^2, a value in line with data reported for metallic stent implantation in patients presenting with STEMI.[21,38] Similarly, the amount of intraluminal defect after scaffold implantation was minimal and comparable with what is observed in metallic stents.[21] Notably, these results were consistent among different scaffold sizes.

Clinical outcomes

In the present series, none of patients treated with BVS experienced a clinical event related to the treated vessel at the 30-day follow-up. These observations support the feasibility of BVS implantation in patients presenting with acute STEMI. Data showed in the present report with optimal acute performance in terms of final TIMI-flow and scaffold apposition may suggest that everolimus-eluting BVS could be considered for the treatment of patients presenting with STEMI, however, due to the limited number of patients and events, caution should be made in reaching firm conclusions. Further larger studies are needed to fully evaluate the performance of the present device in STEMI patients.

Limitations

The present study represents a feasibility study with a limited number of patients. The small sample size does not allow reaching conclusions in terms of clinical outcomes. The lack of a head-to-head comparison with the current standard of care is a major limitation of the present study. A longer follow-up is needed to fully evaluate the performance of this novel device in patients presenting with acute MI. During the enrolment period, the implantation of either metallic stent or BVS in STEMI patients was left to the operator's discretion; this methodology may be prone to selection bias. Therefore, these data should not stimulate at the current state of knowledge the use of BVS in patients presenting

with acute MI. Larger randomized studies are needed to confirm these preliminary observations.

CONCLUSION

In the present investigation, the implantation of the everolimus-eluting BVS was observed to be feasible in patients presenting with STEMI with optimal acute performance. These data are preliminary and need further confirmation in randomized controlled trials to define the true role of BVS for the treatment of patients presenting with acute myocardial infarction.

REFERENCES

1. Task Force on Myocardial Revascularization of the European Society of C, the European Association for Cardio-Thoracic S, European Association for Percutaneous Cardiovascular I, WijnsW, Kolh P, Danchin N, Di Mario C, Falk V, Folliguet T, Garg S, Huber K, James S, Knuuti J, Lopez-Sendon J, Marco J, Menicanti L, Ostojic M, Piepoli MF, Pirlet C, Pomar JL, Reifart N, Ribichini FL, Schalij MJ, Sergeant P, SerruysPW, Silber S, Sousa Uva M, Taggart D. Guidelines on myocardial revascularization. Eur Heart J 2010;31:2501–2555.
2. Spaulding C, Henry P, Teiger E, Beatt K, Bramucci E, Carrie D, Slama MS, Merkely B, Erglis A, Margheri M, Varenne O, Cebrian A, Stoll HP, Snead DB, Bode C, Investigators T. Sirolimus-eluting versus uncoated stents in acute myocardial infarction. N Engl J Med 2006;355:1093–1104.
3. Stone GW, Lansky AJ, Pocock SJ, Gersh BJ, Dangas G,Wong SC, Witzenbichler B, Guagliumi G, Peruga JZ, Brodie BR, Dudek D, Mockel M, Ochala A, Kellock A, Parise H, Mehran R, Investigators H-AT. Paclitaxel-eluting stents versus bare-metal stents in acute myocardial infarction. N Engl J Med 2009;360:1946–1959.
4. Brar SS, Leon MB, Stone GW, Mehran R, Moses JW, Brar SK, Dangas G. Use of drug-eluting stents in acute myocardial infarction: a systematic review and meta-analysis. J Am Coll Cardiol 2009;53:1677–1689.
5. Raber L, Kelbaek H, Ostojic M, BaumbachA, HegD, Tuller D, von Birgelen C, RoffiM, Moschovitis, Khattab AA, Wenaweser P, Bonvini R, Pedrazzini G, Kornowski R, Weber K, Trelle S, Luscher TF, Taniwaki M, Matter CM, Meier B, Juni P, Windecker S, InvestigatorsCAT. Effect of biolimus-eluting stents with biodegradable polymer vs bare-metal stents on cardiovascular events among patients with acute myocardial infarction: the COMFORTABLE AMI randomized trial. JAMA 2012; 308:777–787.
6. Sabate M, Cequier A, Iniguez A, Serra A, Hernandez-Antolin R, Mainar V, Valgimigli M, Tespili M, den Heijer P, Bethencourt A, Vazquez N, Gomez-Hospital JA, Baz JA, Martin-Yuste V, van Geuns RJ, Alfonso F, Bordes P, Tebaldi M, Masotti M, Silvestro A, Backx B, Brugaletta S, van Es GA, Serruys PW. Everolimus-eluting stent versus bare-metal stent in ST-segment elevation myocardial infarction (EXAMINATION): 1 year results of a randomised controlled trial. Lancet 2012;380:1482–1490.
7. Serruys PW, Garcia-Garcia HM, Onuma Y. From metallic cages to transient bioresorbable scaffolds: change in paradigm of coronary revascularization in the upcoming decade? Eur Heart J 2012;33:16–25b.
8. Finn AV, Joner M, Nakazawa G, Kolodgie F, Newell J, John MC, Gold HK, Virmani R. Pathological correlates of late drug-eluting stent thrombosis: strut coverage as a marker of endothelialization. Circulation 2007;115:2435–2441.
9. Joner M, Finn AV, Farb A, Mont EK, Kolodgie FD, Ladich E, Kutys R, Skorija K, Gold HK, Virmani R. Pathology of drug-eluting stents in humans: delayed healing and late thrombotic risk. J Am Coll Cardiol 2006;48:193–202.
10. Hong MK, Mintz GS, LeeCW, Kim YH, LeeSW, Song JM, Han KH, Kang DH, Song JK, Kim JJ, ParkSW, Park SJ. Incidence, mechanism, predictors, and long-termprognosis of late stent malapposition after bare-metal stent implantation. Circulation 2004;109:881–886.
11. Hong MK, Mintz GS, LeeCW, ParkDW, Park KM, Lee BK, Kim YH, Song JM, Han KH, Kang DH, Cheong SS, Song JK, Kim JJ, ParkSW, Park SJ. Late stent malapposition after drug-eluting stent implantation: an intravascular ultrasound analysis with long-term follow-up. Circulation 2006;113:414–419.
12. Ormiston JA, Serruys PW, Onuma Y, van Geuns RJ, de Bruyne B, Dudek D, Thuesen L, Smits PC, Chevalier B, McClean D, Koolen J, Windecker S, Whitbourn R, Meredith I, Dorange C, Veldhof S, Hebert KM, Rapoza R, Garcia-Garcia HM. First serial assessment at 6 months and 2 years of the second generation of absorb everolimus-eluting bioresorbable vascular scaffold: a multi-imaging modality study. Circ Cardiovasc Interv 2012;5:620–632.

13. Serruys PW, Onuma Y, Dudek D, Smits PC, Koolen J, Chevalier B, de Bruyne B, Thuesen L, McClean D, van Geuns RJ, Windecker S, Whitbourn R, Meredith I, Dorange C, Veldhof S, Hebert KM, Sudhir K, Garcia-Garcia HM, Ormiston JA. Evaluation of the second generation of a bioresorbable everolimus-eluting vascular scaffold for the treatment of de novo coronary artery stenosis: 12-month clinical and imaging outcomes. J Am Coll Cardiol 2011;58:1578–1588.
14. Kajiya T, Liang M, Sharma RK, Lee CH, Chan MY, Tay E, Chan KH, Tan HC, Low AF. Everolimus-eluting bioresorbable vascular scaffold (BVS) implantation in patients with ST-segment elevation myocardial infarction (STEMI). EuroIntervention 2013;9:501–504.
15. Kocka V, Lisa L, Tousek P, Budesinsky T, Widimsky P. ST elevation myocardial infarction treated with bioresorbable vascular scaffold: rationale and first cases. Eur Heart J 2013;34:2073.
16. Ormiston JA, Serruys PW, Regar E, Dudek D, Thuesen L,WebsterMW, Onuma Y, Garcia-Garcia HM,McGreevy R, Veldhof S.A bioabsorbable everolimus-eluting coronary stent system for patients with single de-novo coronary artery lesions (ABSORB): a prospective open-label trial. Lancet 2008;371:899–907.
17. Serruys PW, Onuma Y, Ormiston JA, de Bruyne B, Regar E, Dudek D, Thuesen L, Smits PC, Chevalier B, McClean D, Koolen J, Windecker S, Whitbourn R, Meredith I, Dorange C, Veldhof S, Miquel-Hebert K, Rapoza R, Garcia-Garcia HM. Evaluation of the second generation of a bioresorbable everolimus drug-eluting vascular scaffold for treatment of de novo coronary artery stenosis: six-month clinical and imaging outcomes. Circulation 2010;122:2301–2312.
18. Cutlip DE, Windecker S, Mehran R, Boam A, Cohen DJ, van Es GA, Steg PG, Morel MA, Mauri L, Vranckx P, McFadden E, Lansky A, Hamon M, Krucoff MW, Serruys PW, Academic Research C. Clinical end points in coronary stent trials: a case for standardized definitions. Circulation 2007;115:2344–2351.
19. Onuma Y, SerruysPW. Bioresorbable scaffold: the advent of a new era in percutaneous coronary and peripheral revascularization? Circulation 2011;123:779–797.
20. OnumaY, Serruys PW, Perkins LE ,Okamura T,Gonzalo N, Garcia-Garcia HM, Regar E, Kamberi M, Powers JC, Rapoza R, van Beusekom H, van der GiessenW, Virmani R. Intracoronary optical coherence tomography and histology at 1 month and 2, 3, and 4 years after implantation of everolimus-eluting bioresorbable vascular scaffolds in a porcine coronary arterymodel: an attempt to decipher the human optical coherence tomography images in the ABSORB trial. Circulation 2010;122:2288–2300.
21. Onuma Y, Thuesen L, van Geuns RJ, van der Ent M, Desch S, Fajadet J, Christiansen E, Smits P, Ramsing Holm N, Regar E, van Mieghem N, Borovicanin V, Paunovic D, Senshu K, van Es GA, Muramatsu T, Lee IS, Schuler G, Zijlstra F, Garcia-Garcia HM, Serruys PW, Investigators T. Randomized study to assess the effect of thrombus aspiration on flow area in patients with ST-elevation myocardial infarction: an optical frequency domain imaging study – TROFI trial. Eur Heart J 2013;34:1050–1060.
22. Sianos G, Papafaklis MI, Daemen J, Vaina S, van Mieghem CA, van Domburg RT, Michalis LK, Serruys PW. Angiographic stent thrombosis after routine use of drug-eluting stents in ST-segment elevation myocardial infarction: the importance of thrombus burden. J Am Coll Cardiol 007;50:573–583.
23. Magro M, Nauta S, Simsek C, Onuma Y, Garg S, van der Heide E, van der Giessen WJ, Boersma E, van Domburg RT, van Geuns RJ, Serruys PW. Value of the SYNTAX score in patients treated by primary percutaneous coronary intervention for acute ST-elevation myocardial infarction: The MI SYNTAXscore study. Am Heart J 2011;161:771–781.
24. Tearney GJ, Regar E, Akasaka T, Adriaenssens T, Barlis P, Bezerra HG, Bouma B, Bruining N, Cho JM, Chowdhary S, Costa MA, de Silva R, Dijkstra J, Di Mario C, Dudek D, Falk E, Feldman MD, Fitzgerald P, Garcia-Garcia HM, Gonzalo N, Granada JF, Guagliumi G, Holm NR, Honda Y, Ikeno F, Kawasaki M, Kochman J, Koltowski L, Kubo T, Kume T, Kyono H, Lam CC, Lamouche G, Lee DP, Leon MB, Maehara A, Manfrini O, Mintz GS, Mizuno K, Morel MA, Nadkarni S, Okura H, Otake H, Pietrasik A, Prati F, Raber L, Radu MD, Rieber J, Riga M, Rollins A, Rosenberg M, Sirbu V, Serruys PW, Shimada K, Shinke T, Shite J, Siegel E, Sonoda S, Suter M, Takarada S, Tanaka A, Terashima M, Thim T, Uemura S, Ughi GJ, van Beusekom HM, van der Steen

AF, van Es GA, van Soest G, Virmani R, Waxman S,Weissman NJ,Weisz G, International Working Group for Intravascular Optical Coherence T. Consensus standards for acquisition, measurement, and reporting of intravascular optical coherence tomography studies: a report from the International Working Group for Intravascular Optical Coherence Tomography Standardization and Validation. J Am Coll Cardiol 2012;59:1058–1072.

25. FarooqV, Onuma Y, Radu M, Okamura T, Gomez-Lara J, Brugaletta S, Gogas BD, van Geuns RJ, Regar E, Schultz C, Windecker S, Lefevre T, Brueren BR, Powers J, Perkins LL, Rapoza RJ, Virmani R, Garcia-GarciaHM,SerruysPW. Optical coherence tomography (OCT) of overlapping bioresorbable scaffolds: from benchwork to clinical application. EuroIntervention 2011;7:386–399.
26. Magro M, Regar E, Gutierrez-Chico JL, Garcia-Garcia H, Simsek C, Schultz C, Zijlstra F, Serruys PW, van Geuns RJ. Residual atherothrombotic material after stenting in acute myocardial infarction – an optical coherence tomographic evaluation. IntJ Cardiol 2013;167:656–663.
27. Serruys PW, Ormiston JA, Onuma Y, Regar E, Gonzalo N, Garcia-Garcia HM, Nieman K, Bruining N, Dorange C, Miquel-Hebert K, Veldhof S, Webster M, Thuesen L, Dudek D. A bioabsorbable everolimus-eluting coronary stent system (ABSORB): 2-year outcomes and results from multiple imaging methods. Lancet 2009;373:897–910.
28. Diletti R, Onuma Y, Farooq V, Gomez-Lara J, Brugaletta S, van Geuns RJ, Regar E, de Bruyne B, Dudek D, Thuesen L, Chevalier B, McClean D, Windecker S, Whitbourn R, Smits P, Koolen J, Meredith I, Li D, Veldhof S, Rapoza R, Garcia-Garcia HM, Ormiston JA, Serruys PW. 6-month clinical outcomes following implantation of the bioresorbable everolimus-eluting vascular scaffold in vessels smaller or larger than 2.5 mm. J Am Coll Cardiol 2011;58:258–264.
29. Diletti R, Serruys PW, Farooq V, Sudhir K, Dorange C, Miquel-Hebert K, Veldhof S, Rapoza R, Onuma Y, Garcia-Garcia HM, Chevalier B. ABSORB II randomized controlled trial: a clinical evaluation to compare the safety, efficacy, and performance of the absorb everolimus-eluting bioresorbable vascular scaffold system against the XIENCE everolimus-eluting coronary stent system in the treatment of subjects with ischemic heart disease caused by de novo native coronary artery lesions: rationale and study design. Am Heart J 2012;164:654–663.
30. Dudek D, Onuma Y, Ormiston JA, Thuesen L, Miquel-Hebert K, SerruysPW. Fouryear clinical follow-up of the ABSORB everolimus-eluting bioresorbable vascular scaffold in patients with de novo coronary artery disease: the ABSORB trial. EuroIntervention 2012;7:1060–1061.
31. Diletti R, Farooq V, Girasis C, Bourantas C, Onuma Y, Heo JH, Gogas BD, van Geuns RJ, Regar E, de Bruyne B, Dudek D, Thuesen L, Chevalier B, McClean D, Windecker S, Whitbourn RJ, Smits P, Koolen J, Meredith I, Li X, Miquel-Hebert K, Veldhof S, Garcia-Garcia HM, Ormiston JA, Serruys PW. Clinical and intravascular imaging outcomes at 1 and 2 years after implantation of absorb everolimus eluting bioresorbable vascular scaffolds in small vessels. Late lumen enlargement: does bioresorption matter with small vessel size? Insight from the ABSORB cohort B trial. Heart 2013;99:98–105.
32. Muramatsu T, Onuma Y, Garcia-Garcia HM, Farooq V, Bourantas CV, Morel MA, Li X, Veldhof S, Bartorelli A, Whitbourn R, Abizaid A, Serruys PW, Investigators A-E. Incidence and short-term clinical outcomes of small side branch occlusion after implantation of an everolimus-eluting bioresorbable vascular scaffold: an interim report of 435 patients in the ABSORB-EXTEND single-arm trial in comparison with an everolimus-eluting metallic stent in the SPIRIT first and II trials. JACC Cardiovasc Interv 2013;6:247–257.
33. Stone GW, Abizaid A, Silber S, Dizon JM, Merkely B, Costa RA, Kornowski R, Abizaid A,Wojdyla R, Maehara A, Dressler O, Brener SJ, Bar E, Dudek D. Prospective, randomized, multicenter evaluation of a polyethylene terephthalate micronet mesh-covered stent (MGuard) in ST-segment elevation myocardial infarction: the MASTER trial. J Am Coll Cardiol. 2012;60:1975–1984.
34. Otake H, Shite J, Ako J, Shinke T, Tanino Y, Ogasawara D, Sawada T, Miyoshi N, Kato H, Koo BK, Honda Y, Fitzgerald PJ, Hirata K. Local determinants of thrombus formation following sirolimus-eluting stent implantation assessed by optical coherence tomography. JACC Cardiovasc Interv 2009;2:459–466.

35. Prati F, Guagliumi G, Mintz GS, Costa M, Regar E, Akasaka T, Barlis P , Tearney GJ, Jang IK, Arbustini E, Bezerra HG, Ozaki Y, Bruining N, Dudek D, Radu M, Erglis A, Motreff P, Alfonso F, Toutouzas K, Gonzalo N, Tamburino C, Adriaenssens T, Pinto F, Serruys PW, Di Mario C, Expert's OCTRD. Expert review document part 2: methodology, terminology and clinical applications of optical coherence tomography for the assessment of interventional procedures. Eur Heart J 2012;33:2513–2520.
36. Prati F, Regar E, Mintz GS, Arbustini E, Di Mario C, Jang IK, Akasaka T, Costa M, Guagliumi G, Grube E, Ozaki Y, Pinto F, Serruys PW, Expert's OCTRD. Expert review document on methodology, terminology, and clinical applications of optical coherence tomography: physical principles, methodology of image acquisition, and clinical application for assessment of coronary arteries and atherosclerosis. Eur Heart J 2010;31:401–415.
37. Barlis P, Regar E, Serruys PW, Dimopoulos K, van der Giessen WJ, van Geuns RJ, Ferrante G, Wandel S, Windecker S, van Es GA, Eerdmans P, Juni P, di Mario C. An optical coherence tomography study of a biodegradable vs. durable polymer-coated limus-eluting stent: a LEADERS trial sub-study. Eur Heart J 2010; 31:165–176.
38. van Geuns RJ, Tamburino C, Fajadet J, Vrolix M, Witzenbichler B, Eeckhout E, Spaulding C, Reczuch K, La Manna A, Spaargaren R, Garcia-Garcia HM, Regar E, Capodanno D, Van Langenhove G, Verheye S. Self-expanding versus balloon-expandable stents in acute myocardial infarction: results from the APPOSITION II study: self-expanding stents in ST-segment elevation myocardial infarction. JACC Cardiovasc Interv 2012;5:1209–1219.

PART
III

Chapter 15

Percutaneous Coronary Interventions during ST-segment elevation Myocardial Infarction

Current Status and Future Perspectives

Roberto Diletti, MD; Tuncay Yetgin, MD; Olivier C. Manintveld, MD, PhD; Jurgen M.R. Ligthart, RT; Carlo Zivelonghi, MD; Felix Zijlstra, MD, PhD; Flavio Ribichini, MD

EuroIntervention. 2014 Aug;10 Suppl T:T13-22

ABSTRACT

The present article focuses on recent innovations and possible future perspectives in the reperfusion treatment of ST-segment elevation myocardial infarction (STEMI). Among these, the shift from the femoral to the radial vascular access, the recent availability of bioresorbable coronary scaffolds, other innovative forms of stents specifically designed for STEMI patients, the use of cardio-protective strategies, as well as the possibility of including autologous bone marrow stem cell transplantation as part of the treatment of patients with STEMI are described and commented as a glance into the future. This article integrates the supplement of EuroIntervention addressing specific topics related to reperfusion strategies during STEMI in dedicated chapters.

VASCULAR ACCESS

One of the most relevant changes introduced in the field of the primary percutaneous coronary interventions (PCI) compared to the initial experiences relates to the vascular access. The use of the radial artery instead of the femoral artery in the specific setting of STEMI translates into a significant reduction in mortality mostly due to the reduction of bleeding as investigated in the RIFFLE and the RIVAL Trials. [1, 2] Of note, the significant reduction of mortality offered by the radial vascular access was particularly evident in patients presenting with STEMI compared with other forms of acute coronary syndromes (ACS). These data were subsequently confirmed by a large post-hoc analysis[3] and several additional investigations. [4-6]

Although the femoral artery may be preferred in some patients, such as those with a very weak radial pulse, or patients needing left ventricular hemodynamic support, or right ventricular pacing during the primary PCI, the radial access should be probably embraced as default for STEMI patients after adequate training in elective cases. It is worthy mentioning that the use of dedicated femoral closure devices has not reduced the risk of complications associated to the femoral puncture.[7]

However, considering the fact that the rate of complications for expert femoral operators could be very low, the recommendation to develop radial access skills is mainly aimed at preparing a change for future generations of internationalists, rather than requiring a change in clinical practise to experts.

MECHANICAL REPERFUSION

Primary percutaneous coronary intervention is superior to fibrinolysis by reducing mortality, re-infarction, and stroke, also improving patency of the infarct-related artery, reducing the severity of the residual stenotic lesion, with an overall better left ventricular function.[8-10]

Furthermore, performing coronary angiography in STEMI allows the immediate and accurate risk stratification based on the knowledge of the degree of the coronary artery disease and invasive hemodynamic parameters. For all these reasons primary PCI is currently the recommended treatment of first choice for patients presenting with STEMI when performed in experienced centres and limited time delay.[11]

Nevertheless, fibrinolysis remains a first line approach in many areas of the world where primary PCI is not an option, or at least is not "the first option available".

Therefore, fibrinolysis, is common as treatment of choice in many developing Countries as

well as in some regions of developed Countries not covered by a permanent and effective primary PCI service.[12] The optimization of the social impact of reperfusion treatment will continue expanding such approach in many areas of the world before a systematic access to well trained cathlabs could become a reality, education and training of paramedics being the first step of this worldwide commitment.

PRIMARY PERCUTANEOUS CORONARY INTERVENTIONS

Balloon-expandable stents

Bare metal stent (BMS) implantation during primary PCI was initially associated with improved angiographic result and decreased need for target vessel revascularizations[13, 14] compared with balloon angioplasty but failed in adding a clear advantage in terms of mortality.

The introduction of the first generation drug eluting stents (DES) brought a further reduction of restenosis with a subsequent lower rate of repeat revascularizations but again without providing benefits on mortality and re-infarction[15] and the enthusiasm related to DES implantation in STEMI patients was tempered by the observation of higer rates of late and very late stent thrombosis.[16]

The high thrombotic burden and vessel vasoconstriction present in the acute phase leading to stent under-sizing and late malapposition in addition to polymer-related persistent inflammation and delayed vessel healing were identified as mechanisms involved in DES thrombosis[16]

Second generation DES with different drugs, biocompatible polymers, better stent designs and thinner struts, have overcome most of the limitations of first generation DES. The use of the second generation everolimus eluting stents (EES) with durable fluoro-polymer in STEMI reduced target lesion and target vessel revascularisation compared to BMS (2.1% vs 5.0%, p=0.003, and 3.7% vs 6.8%, p=0.0077, respectively) at 1-year follow-up with a lower incidence of stent thrombosis (definite stent thrombosis 0.5% vs 1.9%; definite or probable stent0.9% vs 2.5%, p=0.019).[17]

Biolimus A9 eluting stents with biodegradable polymer tested in comparison with BMS reduced the occurrence of the composite of cardiac death, target vessel-related re-infarction, and ischemia-driven target-lesion revascularization (4.3% vs 8.7%, p=0.004) at 1-year follow-up after primary PCI,[18] although the individual endpoints of death and re-infarction remained unchanged.

The introduction of next generation DES with thinner struts, and newer polymers, as well as the development of new stents dedicated to the treatment of STEMI patients may further improve the present clinical results.

Self-expanding stents

Self-expanding stents allowing low-pressure deployment were initially developed in the attempt to reduce the vessel injury and the neointimal response after stent implantation. In the specific setting of STEMI, the use of oversized balloons and high-pressure dilatation might trigger distal embolization and no-reflow with a reduction of myocardial savage. Therefore, the concept of gentle deployment and delayed self-expansion has been recently applied as an option for STEMI patients (Figure 1) and a thin struts self-expanding, nitinol, stent has been recently tested in patients presenting with acute myocardial infarction and compared with currently available balloon-expandable stents[19] showing less struts malapposition at 3 days after implantation as assessed by optical coherence tomography, with similar clinical outcomes at 6 months between the two study arms. Dedicated larger clinical studies are currently needed to further investigate the clinical value of this new technology.

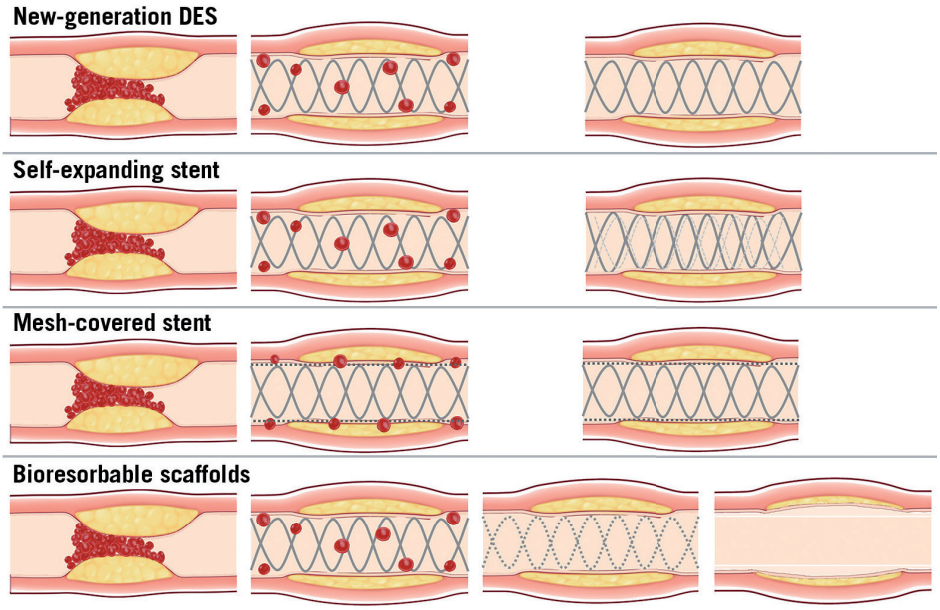

Figure 1. Different devices and mechanisms of revascularization.
New generation DES provides reduced incidence of target lesion revascularisation and very low rate of stent thrombosis. Self-expanding stents with gentle deployment and delayed self-expansion could allow for a theoretical reduction in distal embolization and less malapposition compared to balloon-expandable stents. Mesh-covered stents with the presence of a micronet mesh is intended to trap thrombotic material between the stent and the arterial wall thus potentially reducing the risk of distal embolization. The implantation of bioresorbable scaffolds provides revascularization, and after bioresorption, restoration of vasomotor function, vessel compliance and cyclic strain in response to pulsatile flow, re-establishing the coronary physiology, potentially allowing for positive remodeling and late lumen enlargement.

Mesh-Covered Stent

Microvascular dysfunction after primary PCI is associated with increased infarct size and worse clinical outcomes.[20-23]

Although many factors might promote such phenomenon, distal embolization of thrombotic debrides from the culprit lesions during the stent deployment seems to play a key role. Mechanical and pharmacological approaches have been previously tested to reduce the impact of thrombus embolization often with non-definitive results. However, despite the appealing concept of protecting the distal microcirculation with dedicated devices for distal or proximal capture of thrombo-emolic debris, randomized trials failed to demonstrate a relevant clinical advantage of these strategies.[24, 25]

Recently, a BMS covered with a polyethylene terephthalate micronet mesh was introduced in the clinical arena. The presence of a micronet mesh is intended to trap thrombotic material between the stent and the arterial wall thus theoretically reducing the risk of distal embolization. (Figure 1) Several reports showed safety and feasibility of this technology, and a randomized trial has been performed comparing the rate of complete (≥70%) ST-segment resolution measured at 60 to 90 min post-procedure, between mesh-covered stents and standard stents.[26]

This endpoint was significantly improved in patients treated with mesh-covered stents (57.8% vs. 44.7%; p = 0.008), with also superior rate of TIMI 3 flow (91.7% vs. 82.9%, p = 0.006) with equivalent myocardial blush grade 2 or 3 (83.9% vs. 84.7%, p = 0.81) compared with standard stents. Although a mesh-covered stent in STEMI could have interesting implications especially in relation with the reduction of thrombus dislodgment and embolization, its BMS nature and the presence of a permanent polyethylene micronet mesh, suggest the need for a careful assessment of the restenosis rate.

Bioresorbable vascular scaffolds (BVS)

Bioresorbable technologies represent a potential step forward in endovascular interventions. Its applicability in the STEMI setting (Figure 2) may provide additional benefit to that could be maximized in young patients with long life expectancy. Acute coronary syndromes (ACS) and STEMI are often the first clinical manifestation of coronary artery disease (CAD) in young subjects and the possibility of coronary artery treatment without permanent metallic implants, could have important implications in the long-term patient's perspective.

Two studies have been recently published reporting feasibility and safety of Absorb BVS implantation specifically in STEMI patients[27, 28] and few other investigations with small series of STEMI and NSTEMI [29]

Implantation of Absorb BVS in STEMI patients yielded high procedural success rate.

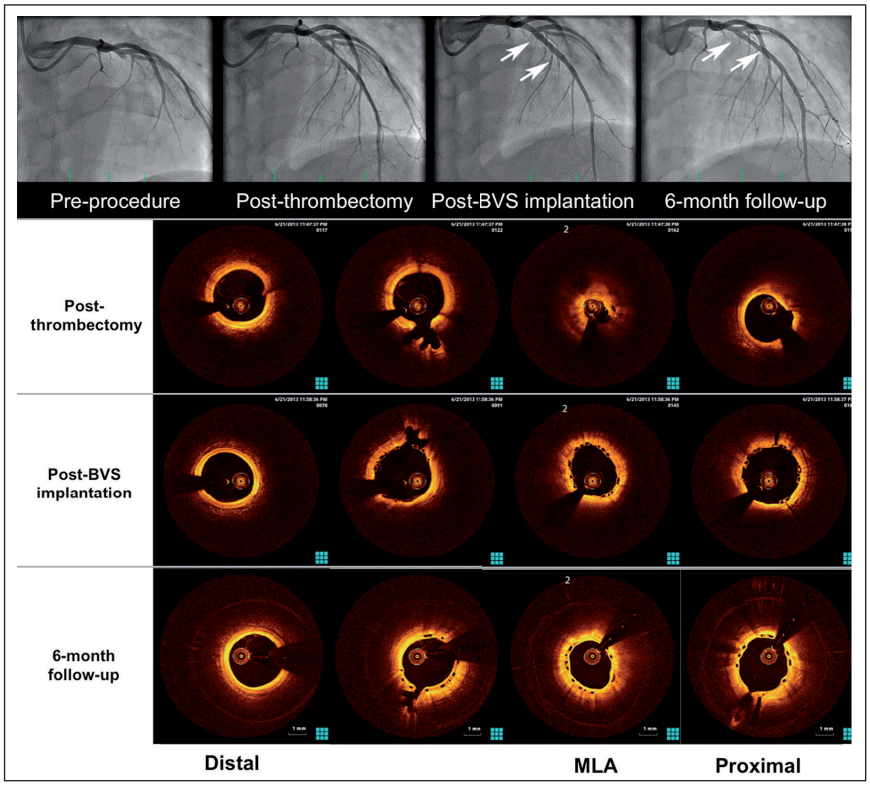

Figure 2. Treatment of an acute myocardial infarction with an Absorb BVS and 6-moth invasive follow-up.
Upper panel: angiographic images at the index procedure and at mid-term (6-month) follow-up showing optimal lumen patency.
Lower panel: Optical coherence images showing the presence residual thrombus after thrombus aspiration but not after BVS implantation supporting the concept of increased thrombus sequestration between the struts and the vessel wall due to BVS wider struts (snow shoes concept). At 6-month follow-up the scaffold appear patent and fully covered with a thin layer of neointimal tissue.

Thrombus aspiration and lesion preparation was performed in a high percentage of patients as recommended because of the higher profile of the scaffold compared with standard stents. A theoretical concern regarding Absorb BVS implantation in STEMI, is that a more extensive lesion preparation, could result in increased distal embolization and a higher risk of no-reflow. However this effect was not reported in none of the above-mentioned preliminary evaluations. The deployment of a device with a larger strut width (Absorb BVS 157μm) compared to metallic stents could induce a different pattern of thrombus dislodgment, with a percentage of vessel wall area paved by the BVS (scaffold/vessel ratio) reaching 26%, a higher value compared to metallic DES (i.e. EES provides a percentage stent/vessel ratio equal to 12%).[30] This characteristic might be associated

with an increased capacity of capturing thrombotic material behind the struts reducing distal embolization (snow-shoes concept).[27] The perspective of vessel healing without a permanent metallic cage is of particular interest as providing revascularization, and after bioresorption, restoration of vasomotor function, vessel compliance and cyclic strain in response to pulsatile flow, re-establishing a normal coronary physiology, potentially allowing for positive remodeling and late lumen enlargement. (Figure 1)
Given the very limited data on the clinical use of the Absorb BVS in acute patients several aspects need to be carefully evaluated, among them the incidence of scaffold thrombosis, and the optimal anti-platelet strategy.

CARDIO-PROTECTION: MYOCARDIAL CONDITIONING

Ischemic pre-conditioning (IPC)

Myocardial conditioning is a broad term used to describe the intriguing finding that brief, non-lethal episodes of myocardial ischemia and reperfusion applied to an organ or tissue render the heart resistant to a subsequent episode of sustained, lethal ischemia-reperfusion injury.[31] (Figure 3)
However, the requirement to implement the IPC stimulus before the onset of ischemia has restricted its clinical application to elective procedures in which the ischemic episode can be anticipated, such as cardiac surgery.
Interestingly, the IPC stimulus was found to be also effective when applied to an organ or tissue distant from the target organ requiring protection (remote ischemic conditioning). In fact, brief ischemic episodes of the circumflex artery significantly reduced myocardial infarct size following sustained occlusion of the left anterior descending artery in dogs (ie, remote intra-cardiac conditioning, and a 15-min period of small intestine or renal ischaemia was also capable of limiting infarct size (ie, remote inter-organ conditioning).[32, 33] The observation that transient ischaemia and reperfusion of the limb could also elicit remote inter-organ conditioning facilitated the translation of this endogenous cardio-protective phenomenon into the clinical field[34] and two clinical trials evaluated the effect of remote ischemic preconditioning in STEMI.[35] Bøtker et al. showed that four 5-minutes arm cuff inflations and deflations applied by ambulance personnel during transport to the hospital, was capable of increasing myocardial salvage and decreasing infarct size at 1 month[35] Importantly, the greatest advantage was observed in patients presenting with occlusion of the left anterior descending artery, suggesting that patients most likely to benefit are those sustaining large anterior infarctions. A subsequent trial has confirmed the protective effects of remote conditioning (three 3/4-minutes cycles of arm cuff

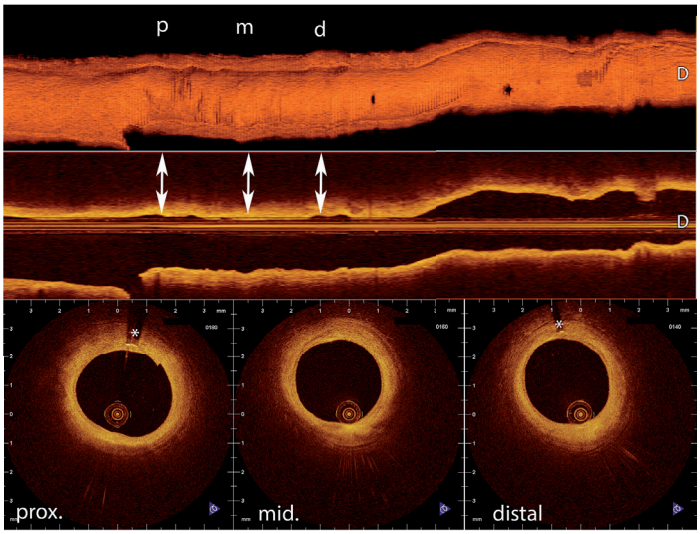

Figure 3. Timing of different conditioning strategies in relation to ischemia and reperfusion periods.
Panel A: Ischemic pre-conditioning (IPC) with episodes of myocardial ischemia and reperfusion applied before reperfusion. Ischemic post-conditioning (IPOC) with episodes of myocardial ischemia and reperfusion applied after reperfusion. Pharmacological conditioning (PharmaC) with drugs intended to mimic the cardio-protective effects of myocardial conditioning.
Panel B: Remote ischemic conditioning. Remote ischemic pre-conditioning (RIPC) with episodes of ischemia and reperfusion applied before reperfusion, to an organ or tissue distant from the target organ requiring protection (myocardium). Remote ischemic per-conditioning (RIPerC) with episodes of ischemia and reperfusion applied during reperfusion, to an organ or tissue distant from the myocardium. Remote ischemic (RIPoC) post-conditioning with episodes of ischemia and reperfusion applied after reperfusion, to an organ or tissue distant from the myocardium.

inflations and deflations) in patients undergoing primary PCI on myocardial infarct size as measured by serum levels of troponin I[36] and that the addition of morphine appeared to increase the beneficial effect of remote ischemic per-conditioning. Most importantly, the follow-up study of the trial by Bøtker et al. demonstrated that the reduction in infarct size obtained with remote ischemic per-conditioning before hospital admission translated into a significant reduction in major adverse cardiovascular events at five years, that was principally driven by a reduction of mortality.[37]

Ischemic post-conditioning

A further form of myocardial conditioning is ischemic post-conditioning.[38] (Figure 3) In 2003, Zhao et al. reported that brief interruptions of coronary blood flow at the onset of reperfusion were also able to induce cardio-protection in canine hearts. The investigators demonstrated that this technique resulted in a 43% reduction in myocardial infarct size following 60 min of left anterior descending artery occlusion[38] This concept provided a

new strategy of intervention that could be applied at the time of myocardial reperfusion for patients presenting with STEMI, and immediately sparked the interest of clinical investigators.

The first clinical application in patients with STEMI demonstrated that interrupting reperfusion (with four cycles of 1-minute low pressure inflations and deflations of the angioplasty balloon immediately after direct stenting of the infarct related artery) resulted in a 36% reduction in infarct size as assessed by creatine kinase release over 72h[39] However, recent trials provide inconsistent results.[40] The value of ischemic post-conditioning is currently being investigated among others in the DANAMI-3 Trials (ClinicalTrials.gov identifier NCT01435408). An overview of these clinical studies can be seen in Table 1.

Pharmacological conditioning

Over the last few decades, research into the mechanisms of myocardial conditioning has revealed the function of multiple receptors, signal transduction pathways, and end-effectors, all of which are amenable to pharmacological manipulation. These efforts enable drugs to be used to mimic the cardio-protective effects of the different forms of myocardial conditioning. Experimental observations showing that drugs are capable of limiting infarct size when administered just prior to or at the onset of reperfusion have resulted in several clinical studies evaluating these drugs. However, many investigations yielded negative results, largely due to a lack of consistent preclinical data, poor study design, or delayed drug administration, as previously suggested[41]

The signal transduction pathways involved in both pre- and post-conditioning seem to converge at the mitochondria and studies with agents that are known to preserve mitochondrial function are currently ongoing. (CIRCUS and the CYCLE, both involving ciclosporin; ClinicalTrials.gov identifiers NCT01502774 and NCT01650662 respectively, and EMBRACE (involving Bendavia; ClinicalTrials.gov identifiers NCT01572909) and MitoCare (involving TR040303; European Commission FP7 project number 261034). The results of these studies are eagerly awaited to validate the smaller pilot trials conducted so far.

Future perspectives

In brief, there might be a role of ischemic conditioning as strategy with potential for preserving cell viability after a prolonged ischemic insult. Although scientifically appealing, the available evidence related to pharmacologic interventions to preconditioning is still insufficient to envision its imminent clinical applicability. The invasive nature of the mechanic post-conditioning interventions, on the other hand, limits their use to patients

Table 1. Ischemic postconditioning in patients with STEMI

Study	*N*	Ischemic Time (min)	Postconditioning protocol (cycles x duration)	Result
Laskey et al.(50) (2005)	17	342	2 x 90s	↔ peak CK; ↑ CBF and STR
Staat et al.(39) (2005)	30	318	4 x 60s	↓ 72-h AUC CK (36%); ↑ MBG
Ma et al.(51) (2006)	94	396	3 x 30s	↓ peak CK (28%); ↑ wall motion score index at 8 wks
Yang et al.(52) (2007)	41	288	3 x 30s	↓ peak CK (28%); ↓ IS (27%) at 1 wk (SPECT)
Thibault et al.(53) (2008)	38	282	4 x 60s	↓ 72-h AUC CK (40%); ↓ IS (39%) at 6 mo (SPECT); 7% increase LVEF at 1 y
Laskey et al.(54) (2008)	24	225	2 x 90s	↓ peak CK (19%); ↑ CBF and STR
Zhao et al.(55) (2009)	75	348 / 432	3 x 30s / 3 x 60s	↓ TnI at 1 wk; ↑ LVEF at 1 wk (60s>30s>control)
Lønborg et al.(56) (2010)	118	248	4 x 30s	↓ IS (19%) at 3 mo (CMR); 31% increase MSI
Sörensson et al.(57) (2010)	76	175	4 x 60s	↔ 48-h AUC CK-MB/TnT; ↔ MSI at 1 wk (CMR); significant increase MSI when risk zone >30% of left ventricle
Garcia et al.(58) (2010)	43	267	4 x 30s	↓ peak CK (11%) and CK-MB (20%); ↑ MBG
Xue et al.(59) (2010)	43	285	4 x 60s	↓ 72-h AUC CK-MB (26%); ↓ IS (46%) at 1 wk (SPECT); ↑ STR
Freixa et al.(40) (2012)	79	328	4 x 60s	↔ IS at 1 wk or 6 mo (CMR); worse MSI at 1 wk
Thuny et al.(60) (2012)	50	252	4 x 60s	↓ peak/AUC CK; ↓ IS and edema at 3 d (CMR)
Tarantini et al.(61) (2012)	78	203	4 x 60s	Trend toward increased IS at 1 mo (CMR)
Engstrøm et al.(62) (2012)	2,000	NA	4 x 30s	Ongoing phase 3 study investigating the effect of IPOC on death and hospitalization for heart failure
Mewton et al.(63) (2013)	50	289	4 x 60s	↓ IS and MVO at 3 d (CMR)
Dwyer et al.(64) (2013)	102	150	4 x 30s	↔ IS and trend towards increased MSI at 3 d (CMR)
Hahn et al.(65) (2013)	700	196	4 x 60s	↔ STR >70% or MBG
Roubille et al.(66) (2014)	90	263	4 x 60s	↔ peak/AUC CK or TnI; ↔ IS or MVO at 5 d (CMR)
Limalanathan et al.(67) (2014)	272	198	4 x 60s	↔ peak TnT; ↔ MBG or STR; ↔ IS or MSI at 4 mo (CMR)
Bodi et al.(68) (2014)	101	190	4 x 60s	↔ peak CK-MB; ↔ MBG or STR; ↔ IS or MVO at 1 wk (CMR)

↔ denotes neutral effect; ↑, improved; ↓, reduced; AUC, area under the curve; CBF, coronary blood flow; CK, creatine kinase; CK-MB, creatine kinase-myocardial band; CMR, cardiac magnetic resonance; IS, infarct size; LVEF, left ventricular ejection fraction; MBG, myocardial blush grade; MSI, myocardial salvage index; MVO, microvascular obstruction; NA, not admissible; SPECT, single photon emission computed tomography; STR, ST-segment resolution; TnI, troponin I; and TnT, troponin T.

undergoing invasive reperfusion, but the potential of mechanical remote ischemic preconditioning as obtained with the simple compression of the arm using a pressure cuffing may provide relevant clinical implications.

CELL THERAPY

If enlarging treatment availability to the largest possible number of STEMI patients should be the start-point of efforts to improve reperfusion treatment and survival worldwide, the regeneration of myocardial tissue after cellular death represents the ultimate end-point; an option that may dramatically transform the natural history of the ischemic heart disease.

Two different forms of cell treatment have been envisioned and developed in this setting. One is the implantation of bone marrow stem cells during or early after primary PCI, the other is that of implanting the cells during the chronic phase of the disease in patients who have evolved into advanced forms of chronic heart failure after myocardial infarction.

The demonstration of continued cell division within the adult heart following myocardial infarction[42] and the capability of bone marrow-derived progenitor/stem cells (BMSCs) to trans-differentiate into cardiomyocytes, improving left ventricle (LV) function after STEMI was demonstrated in the mouse model at the end of the nineties[43] Such an amazing finding fuelled continuous research, followed by a substantial number of human clinical trials in the last decade.

Initial studies yielded promising results, in particular data from the first human trial by Strauer et al. [44] Subsequently, only a modest or no increase in LV function and reduction in the infarct size were observed.[45-47]

Today, none of the published trials has been able to replicate the magnitude of the functional improvement observed in the animal experiments. Autologous BMSCs, which consist of haematopoietic stem cells (HSCs), mesenchymal stem cells (MSCs) and endothelial progenitor cells (EPCs), account for the most studied adult stem cells; these are obtained through a bone marrow aspiration under local anesthesia, isolated and cultivated, using variable protocols in the different trials. Upcoming trials are testing the efficacy of allogeneic MSCs, thus not requiring cells isolation and re-implantation (AMICI trial, number NCT01781390; Prochymal-2 trial, number NCT 00877903), according to some promising results derived from animal experiments. Other possible source accounting for the variability of the clinical results derives from the different techniques for percutaneous delivering of the BMSCs into the infarcted area of the left ventricle, with consequent variable retention rates. Cell delivery has been performed by the simple anterograde

intracoronary injection, by peri-adventitial administration, by retrograde trans-venous and endo-ventricular catheters. Such technical differences may account for a large part of the diverging findings in these studies. Moreover, other procedural factors have been brought into question such as the timing of cells delivery (ranging from 1 to 18 days after the acute event), the kinetics of the delivery (from continuous infusion to multiple injections), the cells processing protocols and the dose of the cells administered.

Moreover, other cells types such as autologous or allogeneic mesenchymal stem cells, adipose tissue–derived regenerative cells, or cardiosphere-derived cells have also been tested in the STEMI setting with some benefits, but these results are strongly limited by the small number of treated patients. In addition, systemic administration of a haematopoietic cytokine, the granulocyte colony-stimulating factor (G-CSF), has been tested in this setting, for its effect of enhanced translocation of BMSCs to the infarcted region post-STEMI. Despite the solid molecular demonstration of the activity of this cytokine, trials involving its use in patients with acute myocardial infarction have shown discrepancy in results, with poor or no improvement in LV function.

Cell delivery immediately after reopening the occluded artery actually bares the interesting perspective of using stem cells derived from young and healthy donors that can be stored in a shelf, readily available directly after primary PCI, and administered in an allogeneic setting, with the obvious logistic simplification. To date, the intracoronary infusion of bone marrow-derived mononuclear cell although safe, did not enhance cardiac function on MRI-derived parameters, nor did it improve clinical outcome, as recently demonstrated in a meta-analysis of 22 randomized studies[48] Conversely, the elective implantation of autologous adult bone marrow-derived stem cells as a treatment for chronic ischemic heart disease and heart failure provided beneficial clinical effect in terms of mortality and long-term performance status in patients suffering from chronic ischemic heart disease and heart failure. Cell therapy in this setting has been investigated with similar techniques and methodology as was done in STEMI patients. Intracoronary delivery of BMSCs was tested in the STAR-Heart study, which confirmed the beneficial effects of cell therapy in 191 patients with chronic heart failure in terms of improved LV function, improved patients' exercise capacity and decreased in long-term mortality when compared with a control group of 200 patients who declined to undergo active intervention at 5 years follow-up[49] Similarly, the trans-endocardial injection of BMSCs has also been shown to be safe with potential beneficial effects, as well as the subcutaneous G-CSF administration.

Results of cell therapy in patients with chronic heart failure after STEMI maintain are currently of high interest due to relevant therapeutic perspectives. The currently ongoing intensive investigation in this field will probably add in further understanding on the future real role of stem cells in the therapeutic horizon of STEMI patients.

REFERENCES

1. Jolly SS, Yusuf S, Cairns J, Niemela K, Xavier D, Widimsky P, et al. Radial versus femoral access for coronary angiography and intervention in patients with acute coronary syndromes (RIVAL): a randomised, parallel group, multicentre trial. Lancet. 2011;377(9775):1409-20.
2. Romagnoli E, Biondi-Zoccai G, Sciahbasi A, Politi L, Rigattieri S, Pendenza G, et al. Radial versus femoral randomized investigation in ST-segment elevation acute coronary syndrome: the RIFLE-STEACS (Radial Versus Femoral Randomized Investigation in ST-Elevation Acute Coronary Syndrome) study. Journal of the American College of Cardiology. 2012;60(24):2481-9.
3. Mamas MA, Ratib K, Routledge H, Neyses L, Fraser DG, de Belder M, et al. Influence of arterial access site selection on outcomes in primary percutaneous coronary intervention: are the results of randomized trials achievable in clinical practice? JACC Cardiovascular interventions. 2013;6(7):698-706.
4. Bernat I, Horak D, Stasek J, Mates M, Pesek J, Ostadal P, et al. ST-segment elevation myocardial infarction treated by radial or femoral approach in a multicenter randomized clinical trial: the STEMI-RADIAL trial. Journal of the American College of Cardiology. 2014;63(10):964-72.
5. Baklanov DV, Kaltenbach LA, Marso SP, Subherwal SS, Feldman DN, Garratt KN, et al. The prevalence and outcomes of transradial percutaneous coronary intervention for ST-segment elevation myocardial infarction: analysis from the National Cardiovascular Data Registry (2007 to 2011). Journal of the American College of Cardiology. 2013;61(4):420-6.
6. Mehta SR, Jolly SS, Cairns J, Niemela K, Rao SV, Cheema AN, et al. Effects of radial versus femoral artery access in patients with acute coronary syndromes with or without ST-segment elevation. Journal of the American College of Cardiology. 2012;60(24):2490-9.
7. Biancari F, D'Andrea V, Di Marco C, Savino G, Tiozzo V, Catania A. Meta-analysis of randomized trials on the efficacy of vascular closure devices after diagnostic angiography and angioplasty. American heart journal. 2010;159(4):518-31.
8. Weaver WD, Simes RJ, Betriu A, Grines CL, Zijlstra F, Garcia E, et al. Comparison of primary coronary angioplasty and intravenous thrombolytic therapy for acute myocardial infarction: a quantitative review. JAMA : the journal of the American Medical Association. 1997;278(23):2093-8.
9. Keeley EC, Boura JA, Grines CL. Primary angioplasty versus intravenous thrombolytic therapy for acute myocardial infarction: a quantitative review of 23 randomised trials. Lancet. 2003;361(9351):13-20.
10. Zijlstra F, de Boer MJ, Hoorntje JC, Reiffers S, Reiber JH, Suryapranata H. A comparison of immediate coronary angioplasty with intravenous streptokinase in acute myocardial infarction. The New England journal of medicine. 1993;328(10):680-4.
11. Task Force on the management of STseamiotESoC, Steg PG, James SK, Atar D, Badano LP, Blomstrom-Lundqvist C, et al. ESC Guidelines for the management of acute myocardial infarction in patients presenting with ST-segment elevation. European heart journal. 2012;33(20):2569-619.
12. Danchin N, Puymirat E, Steg PG, Goldstein P, Schiele F, Belle L, et al. Five-year survival in patients with ST-segment-elevation myocardial infarction according to modalities of reperfusion therapy: the French Registry on Acute ST-Elevation and Non-ST-Elevation Myocardial Infarction (FAST-MI) 2005 Cohort. Circulation. 2014;129(16):1629-36.
13. Grines CL, Cox DA, Stone GW, Garcia E, Mattos LA, Giambartolomei A, et al. Coronary angioplasty with or without stent implantation for acute myocardial infarction. Stent Primary Angioplasty in Myocardial Infarction Study Group. The New England journal of medicine. 1999;341(26):1949-56.
14. Stone GW, Grines CL, Cox DA, Garcia E, Tcheng JE, Griffin JJ, et al. Comparison of angioplasty with stenting, with or without abciximab, in acute myocardial infarction. The New England journal of medicine. 2002;346(13):957-66.

15. Stone GW, Lansky AJ, Pocock SJ, Gersh BJ, Dangas G, Wong SC, et al. Paclitaxel-eluting stents versus bare-metal stents in acute myocardial infarction. The New England journal of medicine. 2009;360(19):1946-59.
16. Webster MW, Ormiston JA. Drug-eluting stents and late stent thrombosis. Lancet. 2007;370(9591):914-5.
17. Sabate M, Cequier A, Iniguez A, Serra A, Hernandez-Antolin R, Mainar V, et al. Everolimus-eluting stent versus bare-metal stent in ST-segment elevation myocardial infarction (EXAMINATION): 1 year results of a randomised controlled trial. Lancet. 2012;380(9852):1482-90.
18. Raber L, Kelbaek H, Ostojic M, Baumbach A, Heg D, Tuller D, et al. Effect of biolimus-eluting stents with biodegradable polymer vs bare-metal stents on cardiovascular events among patients with acute myocardial infarction: the COMFORTABLE AMI randomized trial. JAMA : the journal of the American Medical Association. 2012;308(8):777-87.
19. van Geuns RJ, Tamburino C, Fajadet J, Vrolix M, Witzenbichler B, Eeckhout E, et al. Self-expanding versus balloon-expandable stents in acute myocardial infarction: results from the APPOSITION II study: self-expanding stents in ST-segment elevation myocardial infarction. JACC Cardiovascular interventions. 2012;5(12):1209-19.
20. Kitabata H, Kubo T, Ishibashi K, Komukai K, Tanimoto T, Ino Y, et al. Prognostic value of microvascular resistance index immediately after primary percutaneous coronary intervention on left ventricular remodeling in patients with reperfused anterior acute ST-segment elevation myocardial infarction. JACC Cardiovascular interventions. 2013;6(10):1046-54.
21. van de Hoef TP, Bax M, Meuwissen M, Damman P, Delewi R, de Winter RJ, et al. Impact of coronary microvascular function on long-term cardiac mortality in patients with acute ST-segment-elevation myocardial infarction. Circulation Cardiovascular interventions. 2013;6(3):207-15.
22. Fearon WF, Low AF, Yong AS, McGeoch R, Berry C, Shah MG, et al. Prognostic value of the Index of Microcirculatory Resistance measured after primary percutaneous coronary intervention. Circulation. 2013;127(24):2436-41.
23. Anderson TJ, Charbonneau F, Title LM, Buithieu J, Rose MS, Conradson H, et al. Microvascular function predicts cardiovascular events in primary prevention: long-term results from the Firefighters and Their Endothelium (FATE) study. Circulation. 2011;123(2):163-9.
24. Stone GW, Webb J, Cox DA, Brodie BR, Qureshi M, Kalynych A, et al. Distal microcirculatory protection during percutaneous coronary intervention in acute ST-segment elevation myocardial infarction: a randomized controlled trial. JAMA : the journal of the American Medical Association. 2005;293(9):1063-72.
25. Gick M, Jander N, Bestehorn HP, Kienzle RP, Ferenc M, Werner K, et al. Randomized evaluation of the effects of filter-based distal protection on myocardial perfusion and infarct size after primary percutaneous catheter intervention in myocardial infarction with and without ST-segment elevation. Circulation. 2005;112(10):1462-9.
26. Stone GW, Abizaid A, Silber S, Dizon JM, Merkely B, Costa RA, et al. Prospective, Randomized, Multicenter Evaluation of a Polyethylene Terephthalate Micronet Mesh-Covered Stent (MGuard) in ST-Segment Elevation Myocardial Infarction: The MASTER Trial. Journal of the American College of Cardiology. 2012.
27. Diletti R, Karanasos A, Muramatsu T, Nakatani S, Van Mieghem NM, Onuma Y, et al. Everolimus-eluting bioresorbable vascular scaffolds for treatment of patients presenting with ST-segment elevation myocardial infarction: BVS STEMI first study. European heart journal. 2014;35(12):777-86.
28. Kocka V, Maly M, Tousek P, Budesinsky T, Lisa L, Prodanov P, et al. Bioresorbable vascular scaffolds in acute ST-segment elevation myocardial infarction: a prospective multicentre study 'Prague 19'. European heart journal. 2014;35(12):787-94.
29. Gori T, Schulz E, Hink U, Wenzel P, Post F, Jabs A, et al. Early outcome after implantation of Absorb bioresorbable drug-eluting scaffolds in patients with acute coronary syndromes. EuroIntervention : journal of EuroPCR in collaboration with the Working Group on Interventional Cardiology of the European Society of Cardiology. 2014;9(9):1036-41.

30. Muramatsu T, Onuma Y, Garcia-Garcia HM, Farooq V, Bourantas CV, Morel MA, et al. Incidence and short-term clinical outcomes of small side branch occlusion after implantation of an everolimus-eluting bioresorbable vascular scaffold: an interim report of 435 patients in the ABSORB-EXTEND single-arm trial in comparison with an everolimus-eluting metallic stent in the SPIRIT first and II trials. JACC Cardiovascular interventions. 2013;6(3):247-57.
31. Murry CE, Jennings RB, Reimer KA. Preconditioning with ischemia: a delay of lethal cell injury in ischemic myocardium. Circulation. 1986;74(5):1124-36.
32. Przyklenk K, Bauer B, Ovize M, Kloner RA, Whittaker P. Regional ischemic 'preconditioning' protects remote virgin myocardium from subsequent sustained coronary occlusion. Circulation. 1993;87(3):893-9.
33. Gho BC, Schoemaker RG, van den Doel MA, Duncker DJ, Verdouw PD. Myocardial protection by brief ischemia in noncardiac tissue. Circulation. 1996;94(9):2193-200.
34. Yetgin T, Manintveld OC, Groen F, Tas B, Kappetein AP, van Geuns RJ, et al. The emerging application of remote ischemic conditioning in the clinical arena. Cardiology in review. 2012;20(6):279-87.
35. Botker HE, Kharbanda R, Schmidt MR, Bottcher M, Kaltoft AK, Terkelsen CJ, et al. Remote ischaemic conditioning before hospital admission, as a complement to angioplasty, and effect on myocardial salvage in patients with acute myocardial infarction: a randomised trial. Lancet. 2010;375(9716):727-34.
36. Rentoukas I, Giannopoulos G, Kaoukis A, Kossyvakis C, Raisakis K, Driva M, et al. Cardioprotective role of remote ischemic periconditioning in primary percutaneous coronary intervention: enhancement by opioid action. JACC Cardiovascular interventions. 2010;3(1):49-55.
37. Sloth AD, Schmidt MR, Munk K, Kharbanda RK, Redington AN, Schmidt M, et al. Improved long-term clinical outcomes in patients with ST-elevation myocardial infarction undergoing remote ischaemic conditioning as an adjunct to primary percutaneous coronary intervention. European heart journal. 2014;35(3):168-75.
38. Zhao ZQ, Corvera JS, Halkos ME, Kerendi F, Wang NP, Guyton RA, et al. Inhibition of myocardial injury by ischemic postconditioning during reperfusion: comparison with ischemic preconditioning. American journal of physiology Heart and circulatory physiology. 2003;285(2):H579-88.
39. Staat P, Rioufol G, Piot C, Cottin Y, Cung TT, L'Huillier I, et al. Postconditioning the human heart. Circulation. 2005;112(14):2143-8.
40. Freixa X, Bellera N, Ortiz-Perez JT, Jimenez M, Pare C, Bosch X, et al. Ischaemic postconditioning revisited: lack of effects on infarct size following primary percutaneous coronary intervention. European heart journal. 2012;33(1):103-12.
41. Dirksen MT, Laarman GJ, Simoons ML, Duncker DJ. Reperfusion injury in humans: a review of clinical trials on reperfusion injury inhibitory strategies. Cardiovascular research. 2007;74(3):343-55.
42. Beltrami AP, Urbanek K, Kajstura J, Yan SM, Finato N, Bussani R, et al. Evidence that human cardiac myocytes divide after myocardial infarction. The New England journal of medicine. 2001;344(23):1750-7.
43. Orlic D, Kajstura J, Chimenti S, Jakoniuk I, Anderson SM, Li B, et al. Bone marrow cells regenerate infarcted myocardium. Nature. 2001;410(6829):701-5.
44. Strauer BE, Brehm M, Zeus T, Kostering M, Hernandez A, Sorg RV, et al. Repair of infarcted myocardium by autologous intracoronary mononuclear bone marrow cell transplantation in humans. Circulation. 2002;106(15):1913-8.
45. Surder D, Manka R, Lo Cicero V, Moccetti T, Rufibach K, Soncin S, et al. Intracoronary injection of bone marrow-derived mononuclear cells early or late after acute myocardial infarction: effects on global left ventricular function. Circulation. 2013;127(19):1968-79.
46. Traverse JH, Henry TD, Pepine CJ, Willerson JT, Zhao DX, Ellis SG, et al. Effect of the use and timing of bone marrow mononuclear cell delivery on left ventricular function after acute myocardial infarction: the TIME randomized trial. JAMA : the journal of the American Medical Association. 2012;308(22):2380-9.

47. Assmus B, Leistner DM, Schachinger V, Erbs S, Elsasser A, Haberbosch W, et al. Long-term clinical outcome after intracoronary application of bone marrow-derived mononuclear cells for acute myocardial infarction: migratory capacity of administered cells determines event-free survival. European heart journal. 2014;35(19):1275-83.
48. de Jong R, Houtgraaf JH, Samiei S, Boersma E, Duckers HJ. Intracoronary stem cell infusion after acute myocardial infarction: a meta-analysis and update on clinical trials. Circulation Cardiovascular interventions. 2014;7(2):156-67.
49. Strauer BE, Yousef M, Schannwell CM. The acute and long-term effects of intracoronary Stem cell Transplantation in 191 patients with chronic heARt failure: the STAR-heart study. European journal of heart failure. 2010;12(7):721-9.
50. Laskey WK. Brief repetitive balloon occlusions enhance reperfusion during percutaneous coronary intervention for acute myocardial infarction: a pilot study. Catheter Cardiovasc Interv. 2005;65(3):361-7.
51. Ma X, Zhang X, Li C, Luo M. Effect of postconditioning on coronary blood flow velocity and endothelial function and LV recovery after myocardial infarction. J Interv Cardiol. 2006;19(5):367-75.
52. Yang XC, Liu Y, Wang LF, Cui L, Wang T, Ge YG, et al. Reduction in myocardial infarct size by postconditioning in patients after percutaneous coronary intervention. J Invasive Cardiol. 2007;19(10):424-30.
53. Thibault H, Piot C, Staat P, Bontemps L, Sportouch C, Rioufol G, et al. Long-term benefit of postconditioning. Circulation. 2008;117(8):1037-44.
54. Laskey WK, Yoon S, Calzada N, Ricciardi MJ. Concordant improvements in coronary flow reserve and ST-segment resolution during percutaneous coronary intervention for acute myocardial infarction: a benefit of postconditioning. Catheter Cardiovasc Interv. 2008;72(2):212-20.
55. Zhao WS, Xu L, Wang LF, Zhang L, Zhang ZY, Liu Y, et al. A 60-s postconditioning protocol by percutaneous coronary intervention inhibits myocardial apoptosis in patients with acute myocardial infarction. Apoptosis. 2009;14(10):1204-11.
56. Lonborg J, Kelbaek H, Vejlstrup N, Jorgensen E, Helqvist S, Saunamaki K, et al. Cardioprotective effects of ischemic postconditioning in patients treated with primary percutaneous coronary intervention, evaluated by magnetic resonance. Circ Cardiovasc Interv. 2010;3(1):34-41.
57. Sorensson P, Saleh N, Bouvier F, Bohm F, Settergren M, Caidahl K, et al. Effect of postconditioning on infarct size in patients with ST elevation myocardial infarction. Heart. 2010;96(21):1710-5.
58. Garcia S, Henry TD, Wang YL, Chavez IJ, Pedersen WR, Lesser JR, et al. Long-term follow-up of patients undergoing postconditioning during ST-elevation myocardial infarction. J Cardiovasc Transl Res. 2011;4(1):92-8.
59. Xue F, Yang X, Zhang B, Zhao C, Song J, Jiang T, et al. Postconditioning the human heart in percutaneous coronary intervention. Clin Cardiol. 2010;33(7):439-44.
60. Thuny F, Lairez O, Roubille F, Mewton N, Rioufol G, Sportouch C, et al. Post-conditioning reduces infarct size and edema in patients with ST-segment elevation myocardial infarction. J Am Coll Cardiol. 2012;59(24):2175-81.
61. Tarantini G, Favaretto E, Marra MP, Frigo AC, Napodano M, Cacciavillani L, et al. Postconditioning during coronary angioplasty in acute myocardial infarction: the POST-AMI trial. Int J Cardiol. 2012.
62. Pell TJ, Baxter GF, Yellon DM, Drew GM. Renal ischemia preconditions myocardium: role of adenosine receptors and ATP-sensitive potassium channels. Am J Physiol. 1998;275(5 Pt 2):H1542-7.
63. Mewton N, Thibault H, Roubille F, Lairez O, Rioufol G, Sportouch C, et al. Postconditioning attenuates no-reflow in STEMI patients. Basic Res Cardiol. 2013;108(6):383.
64. Dwyer NB, Mikami Y, Hilland D, Aljizeeri A, Friedrich MG, Traboulsi M, et al. No Cardioprotective Benefit of Ischemic Postconditioning in Patients With ST-Segment Elevation Myocardial Infarction. J Interv Cardiol. 2013;26(5):482-90.

65. Hahn JY, Song YB, Kim EK, Yu CW, Bae JW, Chung WY, et al. Ischemic Postconditioning During Primary Percutaneous Coronary Intervention: The Effects of Postconditioning on Myocardial Reperfusion in Patients With ST-Segment Elevation Myocardial Infarction (POST) Randomized Trial. Circulation. 2013;128(17):1889-96.
66. Roubille F, Mewton N, Elbaz M, Roth O, Prunier F, Cung TT, et al. No post-conditioning in the human heart with thrombolysis in myocardial infarction flow 2-3 on admission. Eur Heart J. 2014;35(25):1675-82.
67. Limalanathan S, Andersen GO, Klow NE, Abdelnoor M, Hoffmann P, Eritsland J. Effect of ischemic postconditioning on infarct size in patients with ST-elevation myocardial infarction treated by primary PCI results of the POSTEMI (POstconditioning in ST-Elevation Myocardial Infarction) randomized trial. J Am Heart Assoc. 2014;3(2):e000679.
68. Bodi V, Ruiz-Nodar JM, Feliu E, Minana G, Nunez J, Husser O, et al. Effect of ischemic postconditioning on microvascular obstruction in reperfused myocardial infarction. Results of a randomized study in patients and of an experimental model in swine. Int J Cardiol. 2014;175(1):138-46.

PART
III

Chapter 16

Self-correction Property a Novel Feature of Bioresorbable Coronary Scaffolds

Roberto Diletti, MD; Jurgen M.R. Ligthart, RT; Rakesh Ramdhan, RT;
Nicolas M. Van Mieghem, MD, PhD

International Journal of Cardiology 214 (2016) 417–418

TO THE EDITOR

Bioresorbable scaffolds represent a novel paradigm for coronary artery treatment, providing transient vessel scaffolding and drug elution. These devices were developed to overcome the limitations of metallic stents such as permanent caging of the artery, impaired vasomotion and jailing of side-branches while allowing non-invasive imaging of the treated segment and preserving the option for surgical revascularizations after resorption.

On the other hand the current bioresorbable technology is not devoid from limitations. The polymeric nature of the scaffold makes this device prone to structural fractures if expanded over a certain limit.[1] In addition the larger struts thickness could be associated with a delayed vascular healing and scaffold coverage especially at the overlapping segments, thus theoretically facilitating the occurrence of scaffold thrombosis.[2]

Malapposition may also be a relevant issue. Malapposed thick struts could trigger thrombus formation and should be corrected by high pressure post-dilatation, yet at the risk of scaffold disruption.

Recently a novel bioresorbable coronary scaffold eluting novolimus (DESolve Novolimus-Eluting Bioresorbable Coronary Scaffold Elixir Medical Corporation, Sunnyvale, California) has been introduced in the clinical arena. An interesting feature of this device is the so-called "self-correction" property. In case of under-expansion and malapposition the scaffold will self-expand up to its nominal diameter, theoretically allowing for a gentle correction of the malapposition without post-dilatation.[3]

We tested this feature in vitro deploying a 3.25 x 18 mm scaffold in a 3.5 mm diameter silicon coronary phantom (when choosing the diameters we took into account the 2x150 µm strut thickness) within saline solution at 37 °C. We intentionally deployed the scaffold at 4 atm displaying initial under-expansion. An optical coherence tomography (OCT) catheter was immediately advanced into the under-expanded scaffold and the OCT signal continuously recorded.

The scaffold showed a progressive expansion in diameter and correction for malapposition with an improvement that was evident already after 15 minutes and that proceeded for the following hour with a nearly complete resolution of both under-expansion and malapposition. (Figure 1, Video 1) The scaffold area showed a progressive enlargement, reaching a 21% increase at the end of the process. This bench test represents the first clear evidence of the self-correction process in the novolimus eluting coronary scaffold.

The self-correcting property could have relevant clinical implications with respect to the incidence of scaffold malapposition and subsequent thrombosis. This feature could be valuable in 1) tapered vessels where a low-pressure deployment could ensure correct

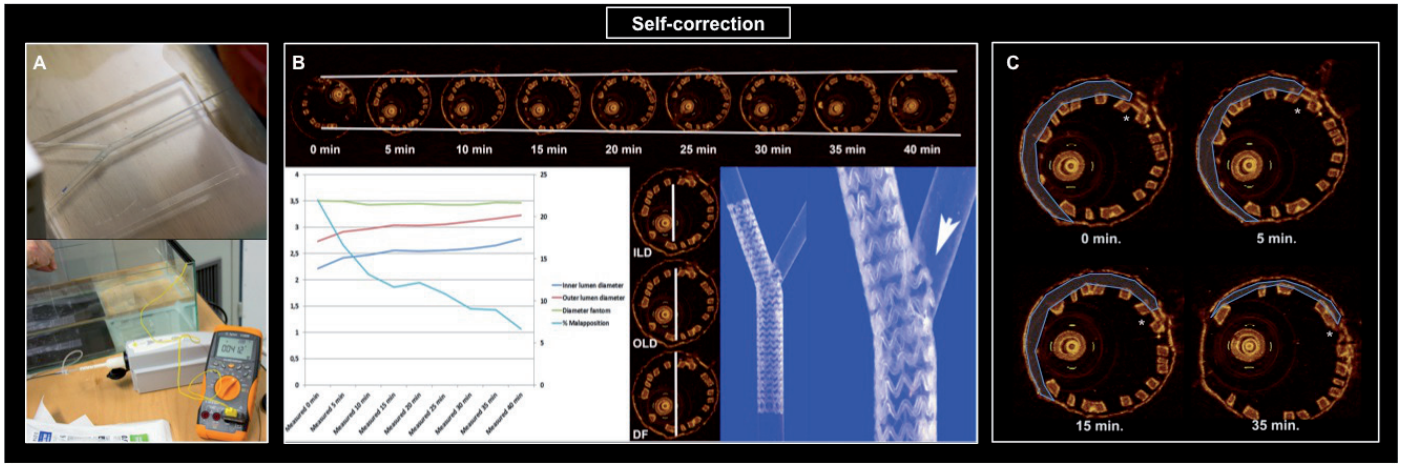

Figure 1. A: in the upper panel the bifurcation phantom in the basin with the scaffold and the OCT catheter in situ. In the lower panel an overview of the test stand: the basin with warm water (35 – 41 °C, the test was performed at ~ 37 °C) containing the phantom with the Elixir test scaffold, the OCT interface and a multimeter to monitor the water temperature.
B: Test results, the upper panel shows a cross-section of the scaffold every 5 minutes from the start of imaging. The lines indicate the outer side of the scaffold and indicate the gradual increase of the diameter over time. The graph indicates the inner lumen diameter (ILD), the outer lumen diameter (OLD) and the phantom diameter (FD) of the scaffold over time showing the increase in scaffold diameters. The % malapposition shows the decrease in malapposition over time from 22 to 5%. The photograph shows the scaffold in the phantom at the end of the experiment, with the scaffold "enlarging" into the side-branch. (arrow).
C: self-correction of the malapposition at different time points. Optical coherence tomography appearance of the scaffold immediately after deployment (upper panel left) after 5 minutes (upper panel right), after 15 minutes (lower panel left) and after 35 minutes (lower panel right). The scaffold shows a progressive enlargement with a reduction of the malapposition area. A scaffold landmark (*) is used to show serial images of the same cross-section.

apposition at both the distal edge with minimal risk of edge dissection and at the larger proximal edge by relying on the self-correction; 2) in bifurcation lesions to preclude the need for proximal optimisation (POT); 3) thrombotic lesions, where the presence of vasoconstriction and thrombus are recognized factors facilitating stent under-sizing and malapposition.

REFERENCES

1. Onuma Y, Serruys PW, Muramatsu T, Nakatani S, van Geuns RJ, de Bruyne B, et al. Incidence and Imaging Outcomes of Acute Scaffold Disruption and Late Structural Discontinuity After Implantation of the Absorb Everolimus-Eluting Fully Bioresorbable Vascular Scaffold: Optical Coherence Tomography Assessment in the ABSORB Cohort B Trial (A Clinical Evaluation of the Bioabsorbable Everolimus Eluting Coronary Stent System in the Treatment of Patients With De Novo Native Coronary Artery Lesions). JACC Cardiovascular interventions. 2014;7:1400-11.
2. Farooq V, Serruys PW, Heo JH, Gogas BD, Onuma Y, Perkins LE, et al. Intracoronary optical coherence tomography and histology of overlapping everolimus-eluting bioresorbable vascular scaffolds in a porcine coronary artery model: the potential implications for clinical practice. JACC Cardiovascular interventions. 2013;6:523-32.
3. Verheye S, Ormiston JA, Stewart J, Webster M, Sanidas E, Costa R, et al. A next-generation bioresorbable coronary scaffold system: from bench to first clinical evaluation: 6- and 12-month clinical and multimodality imaging results. JACC Cardiovascular interventions. 2014;7:89-99.

Chapter 17

Expanded clinical use of everolimus eluting bioresorbable vascular scaffolds for treatment of coronary artery disease

The BVS-Expand Study

Roberto Diletti, MD; Yuki Ishibashi, MD, PhD; Cordula Felix MD; Yoshinobu Onuma, MD; Shimpei Nakatani, MD; Nicolas M Van Mieghem, MD; Evelin Regar, MD, PhD; Marco Valgimigli, MD, PhD; Pieter P. de Jaegere MD, PhD; Nienke van Ditzhuijzen, MD; Jiang Ming, Fam, MBBS; Jurgen M.R. Ligthart, RT; Mattie J. Lenzen, PhD; Patrick W. Serruys MD, PhD; Felix Zijlstra, MD, PhD; Robert Jan van Geuns, MD, PhD

Submitted

ABSTRACT

Background Limited data are currently available on the performance of everolimus eluting bioresorbable vascular scaffold (BVS) for treatment of coronary lesions representative of daily practice.

Methods This is a prospective, mono-center, single-arm study. Patients were presenting with stable, unstable angina, or non-ST segment elevation myocardial infarction caused by de novo stenotic lesions in native coronary arteries. No restrictions were applied to lesion complexity. Procedural results and 6-manth clinical outcomes were reported.

Results A total of 180 patients have been evaluated in the present study, with 249 treated coronary lesions. Device Success per lesion was 99.2%. A total of 119 calcified lesions were treated with results comparable among severe, moderate and non-calcified lesions in term of percentage diameter stenosis (%DS) (20.3±10.5%, 17.8±7.7%, 16.8±8.6%; p=0.112) and acute gain (1.36±0.41mm, 1.48±0.44mm, 1.56±0.54 mm; p=0.109). A total of 54 bifurcations were treated, side-branch ballooning after main vessel treatment was often performed (33.3%). The rate of side-branch impairment was low and comparable to metallic stents (9.3%). Total occlusions were 29, after BVS implantation %DS was not different from other lesion types (17.2±9.4%, vs 17.7±8.6%; p=0.780). At one year, all-cause mortality was reported in 3 cases. A total of 5 target lesion revascularizations and 4 non-target vessel revascularisations were reported. Four cases of definite scaffold thrombosis occurred; none of them was acute or subacute.

Conclusions The implantation of the everolimus eluting bioresorbable vascular scaffold in an expanded range of coronary lesion types and clinical presentations was observed to be viable with promising angiographic results and mid-term clinical outcomes.

INTRODUCTION

The everolimus eluting bioresorbable vascular scaffolds (BVS) represent a novel approach for treatment of coronary artery disease. Similarly to conventional metal stents the absorb BVS provide acute lumen gain, vessel scaffolding and drug elution to the vessel wall immediately after implantation.[1] However, at variance of standard stents, the polymeric structure of this device allows a gradual bioresorption of the implant over time.[2] Complete scaffold bioresorption is hypothesized to offer several advantages over permanent metal devices comprising re-acquirement of physiological vasomotion, late lumen enlargement, non-invasive imaging and future treatment with bypass grafting.(3-5) In addition the absence of a foreign body could avoid phenomena such as permanent side-branch jailing, late acquired malapposition and the occurrence of late and very late stent thrombosis.[5]

The absorb BVS has been initially tested in humans in two cohort studies, both showing promising results in terms of surrogate and clinical endpoints.[6-9] However, being those studies an early evaluation of this technology, they were characterized by a patient population showing stable coronary artery disease and relatively simple lesions. The first randomized data in very selected patients (Absorb II, Absorb Japan) supported the further development of this technique.

At the current state of the art, very limited data are available on BVS performance in real-world patients, including those presenting with acute coronary syndromes and complex coronary lesions. A lack of information is especially evident when considering important lesion subsets such as calcified plaques, long lesions, bifurcations, and total occlusions.

Given this background, the present study aims to reports angiographic and clinical data after an expanded clinical use of the second generation BVS, implanted in patients admitted with different clinical presentations including acute coronary syndromes and having a broad range of coronary lesion types.

METHODS

This is an investigator initiated, prospective, single-centre, single-arm post market study, aiming to evaluate the feasibility safety and performance of the absorb BVS for treatment of patients with coronary artery disease in routine clinical practice. Enrolled patients were subjects presenting with stable, unstable angina, or non-ST segment elevation myocardial infarction caused by *de novo* stenotic lesions in native coronary arteries. No restrictions were applied to lesion complexity. Due to the absorb BVS size availability, a Dmax (proximal and distal mean lumen diameter) within the upper limit of 3.8 mm and the lower limit of 2.0 mm by online QCA was required. Exclusion criteria were minimal and comprised allergies or contraindications to antiplatelet medication, female patient with childbearing potential or currently breastfeeding, acute ST segment elevation myocardial infarction and post CABG patients. As per hospital policy patients with a previously implanted metal DES in the intended target vessel were also excluded. Also, although old age was not an exclusion criterion, BVS were in general reserved for younger patients, and left to operator's interpretation of biological age. A hybrid approach combining BVS with small DES or large DES where necessary was also not recommended.
All patients were treated with DAPT according to current guidelines. DAPT was prescribed for one year after PCI. Prasugrel was standard therapy for ACS presenting patients while Clopidogrel was initiated for Stable angina patients only.

Ethics

This is an observational study, performed according to the privacy policy of the Erasmus MC, and to the Erasmus MC regulations for the appropriate use of data in patient-oriented research, which are based on international regulations, including the declaration of Helsinki. The BVS received the CE mark for clinical use, indicated for improving coronary lumen diameter in patients with ischemic heart disease due to de novo native coronary artery lesions with no restriction in terms of clinical presentation. Therefore the BVS can be currently used routinely in Europe in different settings without a specific written informed consent in addition to the standard informed consent prior to the procedure. Therefore, a waiver from the hospital Ethical Committee was obtained for written informed consent, as according to Dutch law written consent is not required, if patients are not subject to acts other than as part of their regular treatment. Specific written informed consent post procedure was asked for a detailed follow-up program.

Study device

The device used in the present study is the second generation Absorb BVS (Abbott Vascular, Santa Clara, CA, USA); a balloon expandable scaffold with a polymer backbone of Poly-L lactide Acid (PLLA) coated with a thin layer of a 1:1 mixture of an amorphous matrix of Poly-D and L lactide acid (PDLLA) polymer, controlling the realise of 100 micrograms/cm^2 of the anti-proliferative drug everolimus. Two platinum markers located at each Absorb BVS edge allowing for accurate visualization of the radiolucent Absorb BVS during angiography or other imaging modalities. Approximately 80% of the drug is eluted within the first 30-days. Both PLLA and PDLLA are fully bioresorbable. The polymers are degraded mainly via hydrolysis resulting oligomers of lactate metabolized by Krebs cycle. Small particles, less than 2 μm in diameter, have also been shown to be phagocytised and degraded by macrophages.

Definitions

Device Success was defined as the attainment of <30% final in segment residual stenosis after absorb BVS implantation, by angiographic visual estimation. Procedure Success was defined as device success and no major peri-procedural complications (Emergent CABG, coronary perforation requiring pericardial drainage, residual dissection impairing vessel flow – TIMI-flow II or less -). Clinical success was defined as procedural success and no in-hospital major adverse cardiac events (MACE). All deaths were considered cardiac unless an undisputed non-cardiac cause was identified. Myocardial infarction (MI) and scaffold thrombosis were defined according to the Academic Research Consortium (ARC) definition. Any Target lesion revascularization (TLR) was defined as clinically driven if at repeat angiography a diameter stenosis >70% was observed, or if a diameter stenosis >50% was present in association with recurrent angina pectoris; objective signs of ischaemia (ECG changes) at rest or during exercise test, likely to be related to the target vessel; abnormal results of any invasive functional diagnostic test.

Target lesion failure was defined as the composite of cardiac death, target vessel myocardial infarction, or ischemia driven target lesion revascularization. Major adverse cardiac events (MACE), defined as the composite of cardiac death, any re-infarction (Q or Non Q-Wave), emergent bypass surgery (CABG), or clinically driven target lesion revascularization (TLR). Target vessel failure (TVF) was defined as cardiac death, target vessel myocardial infarction (MI), or clinically driven target vessel revascularization (TVR). Delivery failure was defined as opening of scaffold from its cover and insertion into the guiding-catheter without final implantation.

All potential events were adjudicated by a local independent Clinical Events Committee (CEC).

Quantitative coronary angiography

Quantitative coronary angiography (QCA) analyses were performed using the Coronary Angiography Analysis System (Pie Medical Imaging, Maastricht, Netherlands).

The QCA measurements we performed pre and post BVS implantation. The 37 µm platinum radio-markers located at each end of the Absorb BVS aided in the localisation of the non-radio-opaque scaffold for QCA. Analysed parameters included reference vessel diameter (RVD) - calculated with interpolate method - percentage diameter stenosis (%DS) and minimal lumen diameter (MLD). Acute gain was defined as post-procedural MLD minus pre-procedural MLD. The angiographic analysis were performed by three investigators (YI, YO and RD) who where extensively trained in an experienced core-lab (Cardialysis BV, Rotterdam, The Netherlands)

A calcified coronary culprit lesion was defined as already reported[10] 'readily apparent densities noted within the apparent vascular wall at the site of the stenosis.' By qualitative assessment of the angiograms, target lesions were classified as severe ('radioopacities noted without cardiac motion prior to contrast injection generally involving both sides of the arterial wall'), moderate ('densities noted only during the cardiac cycle prior to contrast injection'), or none/mild (lesions other than severe and moderate calcified lesions). The Inter- and intra-observer variability in the qualitative analysis of coronary calcium on coronary angiograms have been already reported. [11]

To provide insights on the coronary bifurcation treatment with BVS we performed a full analysis of techniques and material used and we reported the occurrence of side-branch impairment, an end-point already reported in the literature as "side-branch trouble"[12] and defined as follow: at least 1 of the following procedural parameters: 1) Side-branch TIMI flow grade <3 after main vessel stenting; 2) need of guide-wire(s) different from the workhorse wire to rewire side-branch after main vessel scaffolding; 3) failure to rewire the side-branch after main vessel scaffolding; or 4) failure to dilate the side-branch after main vessel scaffolding and side-branch rewiring.

Statistical analysis

Categorical variables are reported as counts and percentages, continuous variables as mean ± standard deviation; p values were calculated with Fisher's Exact test for binary variables, Wilcoxon's Rank Sum test for continuous variables. Comparisons among multiple means were performed with analysis of variance (1-way ANOVA). A p value<0.05 was considered statistically significant. Statistical analyses were performed using SPSS, version 15.0 for windows (IL,US).

RESULTS

From September 2012 to July 2013 a total of 1529 percutaneous coronary interventions were performed in our center. A total of 180 patients have been enrolled in the present study, with 249 treated coronary lesions. A total of 1157 patients were treated with standard second generation drug eluting stents. The remaining cases were treated with bare metal stents, dedicated bifurcation stents, balloon angioplasty only or thrombectomy only. Baseline clinical characteristics of the patients implanted with bioresorbable devices compared with those of the patients implanted with second generation drug eluting metal stents are reported in Table 1. We observed that patients treated with bioresorbable devices were overall younger, more frequently smokers, and had a lower rate of prior myocardial infarction, PCI and CABG. Therefore, this patient population is slightly different from the general population treated with percutaneous coronary intervention in everyday practice. However, the observed differences are in line with the predefined exclusion criteria.

Table 1. Baseline clinical characteristics.

Clinical characteristics	N = 180	N=1157	
Age	60.6 ± 10.6	66.1 ± 11.7	<0.001
Male n. (%)	134 (74.4%)	850 (73.5%)	0.69
Hypertension n. (%)	94 (52.2%)	661 (57.1%)	0.54
Hypercholesterolemia n. (%)	84 (46.7%)	504 (43.6%)	0.18
Diabetes n. (%)	32 (17.8%)	231 (19.9%)	0.80
Smoke n. (%)	99 (55.0%)	481 (41.6%)	< 0.001
Peripheral vascular disease n. %	19 (10.6%)	101 (8.7%)	0.32
CVA n. (%)	14 (7.8%)	87 (7.5%)	0.73
Kidney disease n. (%)	11 (6.1%)	122 (10.5%)	0.06
Prior MI n. (%)	30 (16.7%)	305 (26.3%)	0.01
Prior PCI n. (%)	17 (9.4%)	358 (30.9%)	< 0.001
Prior CABG n. (%)	0 (0.0%)	118 (10.2%)	< 0.001
COPD n. (%)	11 (6.1%)	71 (6.1%)	0.81
History of heart failure n. (%)	10 (5.6%)	70 (6.0%)	0.74

CVA= cerebrovascular accident; PCI = percutaneous coronary intervention; CABG = coronary artery bypass graft; COPD = chronic obstructive pulmonary disease. Data are expressed as mean ± standard deviation or number and proportion.

Seventy-three patients (40.6%) showed multivessel disease. A total of 109 lesions (43.8%) were classified as type B2 or C, mean lesion length was 25.86 mm, bifurcation lesions with side-branch ≥ 2 mm were 54, a total of 119 lesion were defined with severe or moderate calcification and in 29 case was present a total occlusion. (Table 2)

Table 2. Lesion characteristics.

Lesion characteristics	N = 180, L= 249
Number of Diseased Vessel	
One vessel disease	107 / 180 (59.4%)
Two vessel disease	61 / 180 (33.9%)
Three vessel disease	12 / 180 (6.7%)
Number of Treated Lesions per vessel (%)	
0 lesion	1/ 249 (0.4%)
1 lesion	189 / 249 (75.9%)
2 lesions	54 / 249 (21.7%)
3 lesions	4 / 249 (1.6%)
4 lesions	1 / 249 (0.4%)
Lesion Location (%)	
LAD	120 / 249 (48.2%)
LCX	55 / 249 (22.1%)
RCA	66 / 249 (26.5%)
DIAGONAL	7 / 249 (2.8%)
LMCA/Ramus	1 / 249 (0.4%)
AHA/ACC Lesion Classification (%)	
A	38 / 249 (15.3%)
B1	103 / 249 (41.4%)
B2	63 / 249 (25.3%)
C	46 / 249 (18.5%)
Lesion Length (mm)	25.86 ± 13.64
Range min, max (mm)	5.32 - 80.01
Bifurcation Lesion n. (%)	54 / 249 (21.7%)
Total Occlusion (%)	29 / 249 (11.6%)
Calcification Lesion (%)	119/ 249 (47.8%)

Data are expressed as mean ± standard deviation or number and proportion.

Lesion preparation was performed in a large part of the cases mainly through balloon predilatation (89.2%); rotational atherectomy was necessary in 4.8% of cases. Multiple scaffold implantation per lesion was allowed and often performed, (31.7%) up to the implantation of 5 scaffolds.

No scaffold dislodgment was reported.

Bailout with drug eluting metal stents was performed in only 2 cases. Balloon post-dilatation was performed in a remarkable percentage of cases (45.0%) with often a balloon/scaffold ratio > 1.0 (41.8%). (Table 3)

The overall device, procedure and clinical success rates per lesion, were respectively 99.2%, 98.8% and 98.8%.

Table 3. Procedural data per-lesion analysis.

Lesion characteristics	L= 249
Number of Scaffold or stent – per lesion (%)	
Average	1.41± 0.75
0 scaffold or stent	1 / 249 (0.4%)
1 scaffold or stent	169 / 249 (67.9%)
2 scaffolds or stents	61 / 249 (24.5%)
3 scaffolds or stents	10 / 249 (4.0%)
4 scaffolds or stents	7 / 249 (2.8%)
5 scaffolds or stents	1 / 249 (0.4%)
Overlapping	78
Overlapping BVS-BVS	76
Overlap scaffolds diameters 3.5mm-3.5mm,n (%)	20 (26.3%)
Overlap scaffolds diameters 3.5mm-3.0mm,n (%)	15 (19.7%)
Overlap scaffolds diameters 3.5mm-2.5mm,n (%)	3 (3.9%)
Overlap scaffolds diameters 3.0mm-3.0mm,n (%)	15(19.7%)
Overlap scaffolds diameters 3.0mm-2.5mm,n (%)	15 (19.7%)
Overlap scaffolds diameters 2.5mm-2.5mm,n (%)	8 (10.5%)
Overlapping BVS-Metal	2 (2.6%)
Bailout scaffold/stent (%) – per lesion	
with BVS	8 / 249 (3.2%)
with Metallic stent	2 / 249 (0.8%)
Pre dilatation (%)	222 / 249 (89.2%)
Type of predilatation balloon*	
Non-compliant	16 / 203 (7.9%)
Semi-compliant	187 / 203 (92.1%)
The usage of scoring (scoreflex or cutting)	9 / 219 (4.1%)
Average size of balloon	2.52 ± 0.36
Balloon / artery (pre RVD) Ratio < 1 (excluding total occlusion before procedure)	100 / 184 (54.3%)
Balloon / scaffold ratio ≤1	198 / 202 (98.0%)
Balloon 0.5mm smaller ≤ scaffold size	172/202 (85.1%)
Max pressure	13.95 ± 2.86

Table 3. Continued.

Lesion characteristics	L= 249
Use of other devices for lesion preparation	
Rotational Atherectomy	12 / 249 (4.8%)
Manual Thrombectomy	11 / 249 (4.4%)
Daughter Catheter	5 / 249 (2.0%)
Buddy wire	18 / 249 (7.2%)
Post dilatation (%)	112 / 249 (45.0%)
Type of postdilatation balloon**	
Compliant	32 / 110 (29.1%)
Noncompliant	78 / 110 (70.9%)
Average size of balloon	3.27 ± 0.46 mm
Max pressure	15.58± 3.46
Balloon / Artery < 1	25 / 110 (22.7%)
Balloon > Scaffold size	46 / 110 (41.8%)
Balloon > Scaffold size+0.25mm	15 / 110 (13.6%)
Device Success per lesion (%)	247 / 249 (99.2%)
Procedure Success per lesion (%)	246 / 249 (98.8%)
Clinical Success per lesion	246 / 249 (98.8%)

*Type of predilatation balloon is reported in a subgroup of 203 patients. ** Type of posdilatation balloon is reported in a subgroup of 110 patients. Data are expressed as mean ± standard deviation or number and proportion.

Table 4. Quantitative coronary angiography analysis (QCA).

QCA data	N = 180, L = 249
QCA pre-procedure	
RVD (mm)	2.63 ± 0.43
MLD (mm)	0.90 ± 0.35
% DS (%)	64.8 ± 14.5
Proximal Dmax (mm)	3.92 ± 8.28
Distal Dmax (mm)	2.89 ± 2.31
QCA Post-procedure In-scaffold	
RVD (mm)	2.89 ± 0.42
DS (%)	17.6 ± 8.65
MLD (mm)	2.41 ± 0.41
Scaffold length	29.44± 15.71
Acute gain (mm)	1.51 ± 0.49
TIMI grade 2	2 / 249 (0.8%)
TIMI grade 3	247 / 249 (99.2%)

Data are expressed as mean ± standard deviation or number and proportion.

QCA analysis

The mean pre-procedure reference vessel diameter (RVD) was 2.63 ± 0.43 mm, with a mean percentage diameter stenosis (%DS) of 64.8 ± 14.5% and a mean minimal lumen diameter (MLD) equal to 0.90 ± 0.35 mm. Post-procedure %DS was 17.60 ± 8.65 % with a mean MLD equal to 2.41 ± 0.41 mm reflecting a mean acute gain of 1.51 ± 0.49 mm. TIMI 3 flow was observed in 99.2% of the final angiograms. (Table 4, Figure 1)

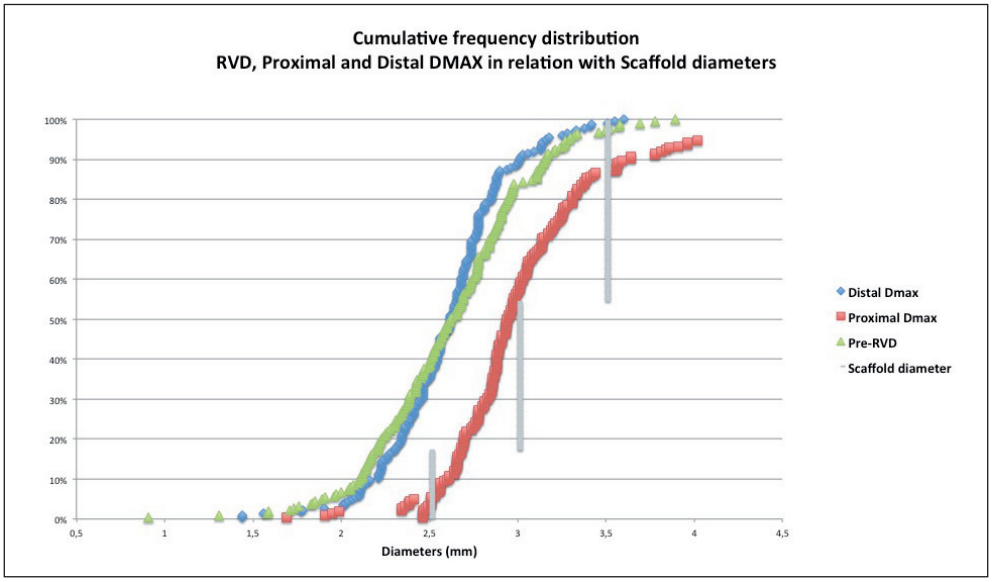

Figure 1. Vessel and scaffold diameters.
Cumulative frequency distribution of the reference vessel diameter the proximal end distal diameter in relation with the scaffold nominal size implanted.

Bifurcation Lesions

A total of 54 lesions were located at the site of a bifurcation with a side-branch ≥ 2.0 mm. In 51 cases a provisional side branch technique was used, in addition 1 T stenting, 1 culotte, 1 T-stenting with small protrusion techniques were performed. In 18 cases branch wire protection was used, pre-dilatation and post-dilatation of the main vessel was often performed. Side branch dilatation post MV stenting was necessary in 18 lesions. A final TIMI flow <3 in the main vessels (MV) was observed in only one case, at the side-branch this was reported in 3 lesions. Failure to re-wire the side-branch was never reported but in one case the operator was unable to re-cross the scaffold with a small balloon of 1.5 mm in diameter. (Table 5) The overall of rate of side-branch impairment was 9.3% (5/54)

Table 5. BVS implantation in Bifurcation lesions.

Procedural characteristics	L=54
LAD	38
CX	12
RCA	4
Involvement of both SB and MV (Medina 111, 101, 011)	15 (27.8%)
1 Scaffold Technique	51 (94.4%)
Provisional T	51 (94.4%)
T-stenting	1 (1.8%)
Culotte	1 (1.8%)
TAP	1 (1.8%)
MV pre-dilatation	44 (81.4%)
MV post-dilatation	26 (44.4%)
SB pre-dilatation	6 (11.1%)
SB dilatation post MV Scaffolding	18 (33.3%)
Kissing balloon	3 (5.6%)
Proximal optimization technique	26 (44.4%)
Final MV TIMI flow <3	1 (1.8%)
Side-branch Timi flow <3	3 (5.6%)
Failure to rewire the SB	0 (0%)
Different wire from the workhorse to rewire SB after MV scaffolding	2 (3.7%)
Failure to dilate SB	1 (1.8%)
Composite of side-branch impairment	5 (9.3%)

Data are expressed as mean ± standard deviation or number and proportion.

Calcified lesions

A total of 119 calcified lesions were treated with BVS ,33 with severe calcification, 86 with moderate calcification, (Figure 2) and compared with non-calcified lesions. Given a non significant difference in pre-procedure RVD, MLD and %DS no differences were observed after treatment between calcified and non calcified lesions in terms of MLD (Severe calcified 2.38 ± 0.38 mm, moderate calcified 2.41 ± 0.39 mm, non-calcified 2.42 ± 0.43 mm; p=0.889), %DS (Severe calcified 20.3 ± 10.5 %, moderate calcified 17.8 ± 7.7%, non-calcified 16.8 ± 8.6%; p=0.112) and acute gain (Severe calcified 1.36 ± 0.41mm, moderate calcified 1.48 ± 0.44 mm, non-calcified 1.56 ± 0.54 mm; p=0.109). These results were achieved with an overall higher use of buddy wires in calcified lesions (severe calcified 18.2%, moderate calcified 9.3%, non-calcified 3.0%; p=0.016)

Lesion preparation was more aggressive in calcified lesions with a higher use of rotational atherectomy (Severe calcified 18.2%, moderate calcified 4.7%, non-calcified 1.5%; p<0.001) and scoring balloons (Severe calcified 15 .2%, moderate calcified 3.5%, non-calcified 0.8%; p=0.001). Success rates were high in calcified vessels showing no significant differences when compare do non-calcified ones. Device success in severe calcified lesions was 97.0%, in moderate calcified 100% and in non-calcified 99.2%; p=0.251. (Table 6)

Table 6. BVS implantation in calcified lesions.

Procedural characteristics	Severe calcification (L = 33)	Moderate calcification (L =86)	No calcification (L =130)	P value
Lesion preparation				
Rotational Atherectomy ,% (n)	18.2% (6/33)	4.7% (4/86)	1.5% (2/130)	<0.001
Scoring balloon ,% (n)	15.2% (5/33)	3.5% (3/86)	0.8% (1/130)	0.001
Daughter catheter ,% (n)	3.0% (1/33)	2.3% (2/86)	1.5% (2/130)	0.886
Buddy wire,% (n)	18.2% (6/33)	9.3% (8/86)	3.0% (4/130)	0.016
Average size of balloon	2.48 ± 0.38	2.55 ± 0.35	2.52 ± 0.36	0.702
Non-compliant balloon ,% (n)	13.3% (4/30)	9.5% (7/74)	5.1% (5/99)	0.276
QCA pre-procedure				
RVD (mm)	2.51 ± 0.35	2.66 ± 0.43	2.64 ± 0.46	0.256
MLD (mm)	0.97 ± 0.40	0.92 ± 0.36	0.87 ± 0.34	0.358
% DS (%)	62.3 ± 13.5	65.0 ± 12.6	65.3 ± 15.7	0.592
Lesion length	36.11 ± 2.34	27.99 ± 1.54	22.11 ± 1.16	<0.001
QCA post-procedure				
RVD (mm)	2.97 ± 0.38	2.93 ± 0.39	2.85 ± 0.46	0.244
MLD (mm)	2.38 ± 0.38	2.41 ± 0.39	2.42 ± 0.43	0.889
% DS	20.3 ± 10.5	17.8 ± 7.7	16.8 ± 8.6	0.112
Acute gain (mm)	1.36 ± 0.41	1.48 ± 0.44	1.56 ± 0.54	0.109
Device Success per lesion, % (n)	97.0% (32/33)	100% (86/86)	99.2% (129/130)	0.251
Procedure Success per lesion, % (n)	97.0% (32/33)	98.8% (85/86)	99.2% (129/130)	0.571
Clinical Success (per lesion), % (n)	97.0% (32/33)	98.8% (85/86)	99.2% (129/130)	0.571

Data are expressed as mean ± standard deviation or number and proportion.

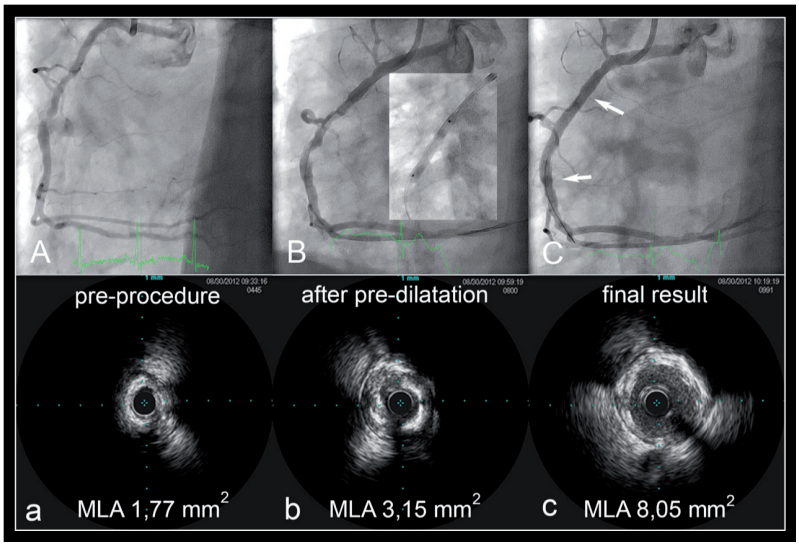

Figure 2. Calcified lesion.
Angiogram showing a long lesion in the RCA (panel A). IVUS pre-procedure (Panel a) shows at the MLA more than 180 degrees superficial calcium (*). Panel B shows the angiogram after pre-dilatation (semi-compliant balloon 3.0 x 20mm). IVUS (panel b) shows clear "cracks" in the calcium (arrowheads), reducing the plaque resistance, thus sufficiently prepared for BVS implantation. Panels C and c show respectively the result on angiogram and on IVUS after implanting a BVS 3.5 x 28mm.

Table 7. BVS implantation in Total occlusions.

	Occluded (L =29)	Non-occluded (L = 220)	P value
QCA post-procedure			
RVD (mm)	3.01 ± 0.47	2.88 ± 0.41	0.103
MLD (mm)	2.51 ± 0.53	2.40 ± 0.39	0.163
% DS (%)	17.2 ± 9.4	17.7 ± 8.6	0.780
Acute gain (mm)	-	1.51 ± 0.49	-
Procedural characteristics			
Daughter catheter, % (n)	3.4% (1/29)	1.8% (4/220)	0.465
Buddy wire, % (n)	10.3% (3/29)	6.8% (15/220)	0.449
Type of first wire (after recanalization)			
Supportive	54.2% (13/ 24)	2.1% (4/195)	<0.001
Non-supportive	45.8% (11/24)	97.9% (191/195)	<0.001
Device Success after disobstruction per lesion, % (n)	100% (29/29)	99.1% (218/220)	1.0
Procedure Success after disobstruction per lesion, % (n)	100% (29/29)	98.6% (217/220)	1.0
Clinical Success after disobstruction per lesion, % (n)	100% (29/29)	98.6% (217/220)	1.0

Data are expressed as mean ± standard deviation or number and proportion.

Total Occlusions

Vessels showing a total occlusion were 29. After vessel desobstruction total occluded vessel were treated with BVS achieving a final MLD and %DS not different from other lesion types (MLD: 2.51 ± 0.53 mm vs 2.40 ± 0.39; p=0.163; %DS: 17.2 ± 9.4% vs 17.7 ± 8.6%; p=0.780), with a high rate of final device success (96.6% vs 98.2%; p=0.465) and procedure success (96.6% vs 98.6%; p=0.393). To reach those results supportive wires were used much more frequently in occluded vessels (54.2% vs 2.1%; p<0.001). (Table 7, Figure 3)

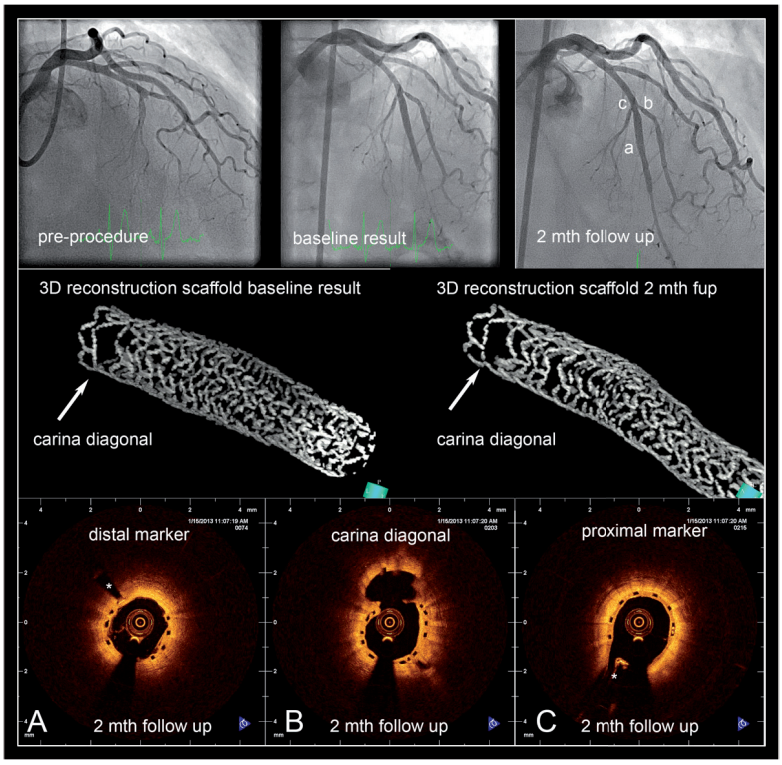

Figure 3. Chronic total occlusion and bifurcation.
Top panels show from left to right the angiograms pre-procedure, after recanalization and scaffold implantation (BVS 3.0 x 28mm with the sequential post dilatation of the diagonal and the scaffold in the main branch) and 2-month follw-up with partial distal vessel positive remodeling. Characters a-c indicate the positions of the OCT cross-sections. OCT (St.Jude Lightlab Dragonfly™) post procedure show distal a well deployed scaffold (Panel A), an well opened carina with the diagonal branch (Panel B *) and the overlap of the proximal marker with the septal branch (Panel C *). The 3D reconstruction (Intage realia™, Cybersystems, Tokyo, Japan) shows the opening of the struts at the carina with the diagonal branch. (Arrowhead bottom panel).

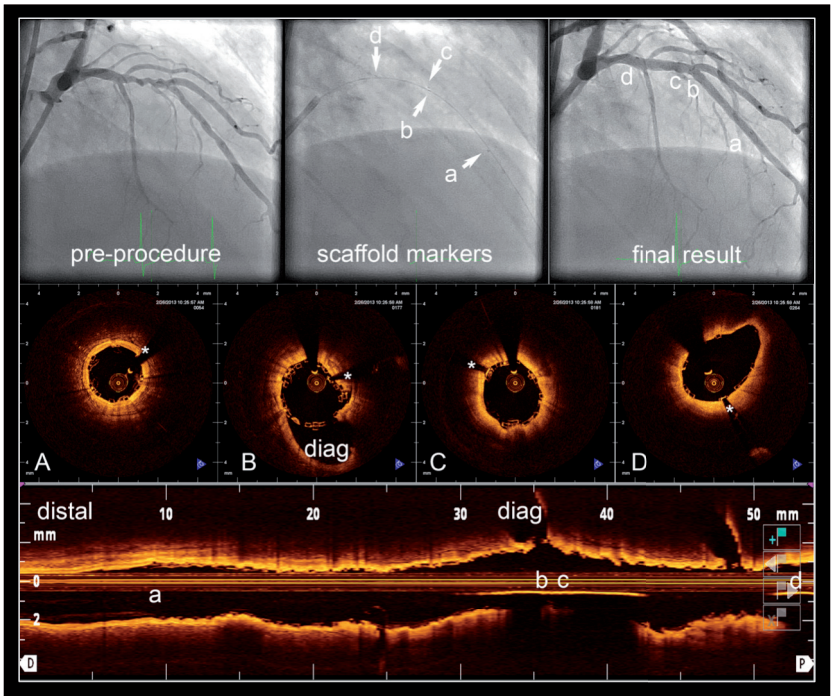

Figure 4. Chronic total occlusion and bifurcation.
The angiogram top left shows the long lesion in the LAD. The mid-panel shows the markers of the two overlapping scaffolds (a & c distal BVS 3.0 x 28mm and b & d proximal BVS 3.5 x 18mm). The top right shows the final result with the OCT cross-section positions indicated by a to d). OCT (St.Jude Lightlab Dragonfly™) shows a well deployed scaffold. Panels B & C show the markers of respectively the proximal and distal scaffolds (*), indicating an overlap of approximately 1 mm.

Long Lesions

In a total of 79 lesions (31.7%) more than one device was implanted (Figure 4). The mean lesion length treated with BVS was 25.86 ± 13.64 mm. The maximum lesion length covered by BVS was 80.01 mm. Overlapping of BVS with BVS was often performed with a total of 76 overlapping scaffolds. The great majority (96%, 73/76) were performed using scaffold of the same diameter or with a maximum of 0.5 mm difference in nominal diameter. In 3 cases a 3.5 mm scaffold was placed in overlap with a 2.5 mm device.

Clinical outcomes

Survival data at 12 months after the procedure were available for 99.4 % of patients. A questionnaire was sent to all living patients with specific queries on re-hospitalization and cardiovascular events. For patients who suffered an adverse event at another center,

medical records or discharge letters from the other institutions were systematically reviewed. General practitioners and referring physicians were contacted for additional information if necessary.

At 12-month follow-up all cause-death was reported in 3 cases. A total of 5 target lesion revascularizations and 4 non-target vessel revascularisations were reported. Four definite, scaffold thrombosis (ST) occurred within one year after index procedure; none of them was acute or sub-acute. Of note, one of those cases was meeting the ARC criteria for ST but no clear thrombus was observed by optical coherence tomography (OCT). In the remaining 3 cases, severe calcification, bifurcation lesion and long overlap were observed but BVS underexpansion was the factor that was present in all of them.

DESCRIPTION OF THE SCAFFOLD THROMBOSIS CASES

Case 1

A 59-year old male patient, smoker, with history of cerebrovascular accident and stable angina pectoris, was treated after predilatation on long lesion involving the ostial left anterior descending (LAD) and the bifurcation with the first diagonal (D1), using a BVS 3.5 x 28mm. Despite a postdilatation was performed with a 3.5 non-complaint (NC) balloon at high pressure, the BVS remained under-expanded with an impaired flow in the first diagonal. At the day 111 post PCI the patient was re-admitted with NSTEMI, while being on DAPT, and angiographically was observed a total re-occlusion of the LAD beginning from the ostium. After predilatation a DES 3.5 x32mm was implanted. Of note, at day 81 after the second PCI the patients was again re-admitted for instable angina pectoris caused by a re-occlusion also of the metal stent in the proximal LAD. The patients was treated with CABG.

Lesion key characteristics: ***Ostial lesion, long lesion, bifurcation, impaired side-branch TIMI flow and BVS underexpansion***

Case 2

A 69-year old male with history of dyslipidaemia and hypertension was admitted with NSTEMI. Angiographically was observed a long, severely calcified, chronic total occlusion (CTO) of the proximal and mid LAD with severe calcification and involvement of D1. After Predilatation, 2x 3.5 x 18mm BVS were implanted. The procedure was complicated by pinching of D1 and thrombus formation. Additional ballooning of the ostium of the side-branch was performed, but at the end of the procedure remained BVS underexpansion and haziness in the mid LAD. Despite continued DAPT usage the patient developed at day

47 a non-Q wave MI due to definite scaffold thrombosis in the proximal LAD, which was treated with thrombectomy and DES implantation.
Lesion key characteristics: ***CTO, long lesion, bifurcation, severe calcification, thrombus formation and BVS underexpansion***

Case 3

A 65-year old male patient, smoker, with history of hypertension was admitted with NSTEMI, due to a sub-occlusive lesion in the LAD located at the site of a tortuous trifurcation with the first and second diagonal. The initial TIMI flow was 1. After predilatation, a 3.0 x 18mm BVS was implanted and after postdilatation a TIMI III flow was achieved. At day 142 on DAPT the patient was re-admitted with NSTEMI. Angiographically a proximal BVS edge sub-total restenosis was observed with a distal TIMI flow 1. A DES stent 3.5 x38mm was deployed covering the BVS and a large proximal segment. Of note, this case was meeting the ARC criteria for stent thrombosis and was adjudicated as such by the CEC, but should be mentioned that an OCT performed before predilatation did not showed any clear intraluminal thrombus.
Lesion key characteristics: ***tortuous trifurcation (no thrombus by OCT)***

Case 4

A 70-year old male, with severe peripheral vascular disease, diabetes mellitus, dyslipidaemia, hypertension, and reduced left ventricular function was admitted with stable angina pectoris. Angiography revealed, a long and severely calcified lesion mid LAD involving two bifurcations (D1 and D2). Aggressive preparation was performed with rotational atherectomy and high-pressure dilatations with NC and cutting balloons. Two overlapping BVS were placed with a quite long segment of overlap (5 mm). Despite extensive postdilatation under-expansion remained at the end of the procedure. Five months after index PCI, the patient underwent non-cardiac surgery. The antiplatelet therapy was interrupted (both aspirin and clopidogrel) and the patient developed a NSTEMI due to a scaffold thrombosis that was treated with balloon dilatation and eptifibatide. Unfortunately, the patient died few days later because of heart failure.
Lesion key characteristics: ***Severe calcification, bifurcation, long overlap, no antiplatelet therapy and BVS underexpansion***

DISCUSSION

The present investigation represents en evaluation of the feasibility of BVS implantation in everyday clinical practise reflected by in a wide range of coronary lesions subsets including bifurcations, calcified vessels, chronic total occlusions and long lesion in patients with stable coronary artery disease and acute coronary syndromes. At variance of previous reports we also aimed to provide a detailed description of procedural data en techniques that were used to allow the use of this novel device in challenging subsets.

Bifurcation lesions

A common concern regarding this technology is the fact that implantation of the BVS in bifurcation lesions might result into side-branch compromise due to the thick strut nature of this device. In keeping with this concept, a recent study performed by our group showed that BVS deployment could be associated with an increased small (≤0.5 mm) side-branch occlusion and a consequent increase of enzymes release after procedure.[13]

However, in the present report the effect of BVS implantation in what is commonly considered a bifurcation lesion (with a side branch ≥ 2 mm) was specifically investigated. Rewiring of the side-branch in those cases and consequent ballooning (mainly with small balloon 1.5-2 mm in diameter) of the SB ostium is feasible as we already reported[13] and safe also in terms of scaffold geometry and fracture.(14,15) In the present study side-branch ballooning was performed in one third of the patients (33%, 18/54) with promising results. In majority of the cases this was done with sequential ballooning and proximal optimization technique (POT), kissing balloon only in 3 cases.

Taking into consideration the rates of TIMI flow < 3 in the main vessel or in the side-branch, the rate of failure to rewire the side-branch and failure to dilate the side-branch, the BVS performed at least as good as metallic stents according to historical data. [12]

In addition the rate of the composite endpoint of side-branch impairment (9.3%) was observed to be encouraging especially when compared with data recently reported by Burzotta et al. with rates of side-branch impairment in sirolimus and everolimus eluting stents respectively 16% and 11%. [12] These data are supportive of the concept that BVS could be used safely in bifurcation lesions with side-branch ≥ 2.0 mm with a single scaffold approach and could provide results similar to metallic stents.

Calcified lesions

A total of 119 calcified lesions with a considerable percentage of heavily calcified plaques, were treated with BVS. A large number of those lesions were located in diffusely diseased vessels with an overall mean treated lesion length of more than 36 mm (severe calcified

group). QCA analysis showed final MLD, %DS, acute gain and device, procedural and clinical success not different from non-calcified lesions. These results were obtained at the cost of a more aggressive lesion preparation with a considerable use of rotational atherectomy and scoring balloons.
Such approach is needed to facilitate the delivery of the scaffold given its slightly higher profile compared with second generation DES. In addition appropriate lesion preparation could avoid scaffold under-expansion or need for aggressive post-dilatation. This strategy could be relevant also when using metallic stents. [16] Our data might suggest feasibility of BVS implantation in calcified vessels with optimal results given an adequate lesion preparation.
On the other hand, should be mentioned that many of the advantages proposed for BVS namely the restoration of the vasomotion and vessel physiology could be minimized in artery at a very advanced stage of the atherosclerosis process even considering the fact that patients with diffused calcified vessels have also a multivessel disease,[17] that might benefit from a temporary implant allowing future surgical treatments.

Total occlusions

Successful re-canalization of total occlusions has been previously associated with a significant improvement in angina symptoms [18,19] and complete coronary revascularization was demonstrated to have an important impact on long-term clinical outcomes.[20]
Vessels with total occlusions have peculiar characteristics in terms of vascular remodeling; this is a dynamic process involving regulation of vascular cell migration and mitosis and apoptosis rates in response to several factors comprising blood flow and pressure, shear stress, circumferential stretch and wall tension.[21] Reduction or even more absence of blood flow in totally occluded vessels might promote negative remodeling and plaque growth; on the other hand restoration of flow could have an opposite effect.
Recently, Park J.J. and colleagues reported, at 6-month follow-up after successful total occlusion revascularization, a flow-dependent vascular remodeling process in human coronary arteries, associated with increases in lumen diameter, lumen area and external elastic membrane area.[22] This process was observed in a large part of treated vessels (69%) with a mean lumen diameter increase of 0.40 ± 0.34 mm. IVUS analysis of those vessels revealed that the amount of incomplete stent apposition increased significantly during 6 months in patients with positive remodeling and lumen area increase but not in those without lumen area increase.
In this scenario choosing a metal stent based on the vessel diameter at the index procedure might lead to stent under-sizing.
Given this background a theoretical advantage of BVS implantation in patients with total

occlusion is the fact that it might allow at mid-term follow-up, after the loss of scaffold mechanical integrity, late lumen enlargement without late acquired malapposition, as at that time the remnants of the bioresorbable implant can follow the vessel remodeling.

Long lesions and overlap

In the present series several lesions were treated with more than one scaffold up to a maximum of 5 scaffolds for a maximum lesion length of 80 mm. Operators were advised to minimize the extension of overlapping segment using a marker-to-marker technique. In the metal stent era, long segments treatment has been associated to an increased risk of stent thrombosis,[23-25] and could results in prevention of future surgical revascularisations. Both these issues could be overcome with the use of bioresorbable technologies and the introduction in the near future of bioresorbable scaffold with thinner struts could mitigate the effect of overlap on delayed vascular healing.

Clinical outcomes

The mid-term clinical outcomes of this study revealed a relatively reassuring safety profile of the BVS when used in a large range of lesion type and in patients with either stable symptoms or acute coronary syndromes. The event rate in this study is only minimal higher compared to the results in non-complex patients as treated in the randomized Absorb II and Absorb Japan studies [26,27]. In other European registries like GHOST-EU and AMC registries [28,29] initial event rate is in general higher compared to the selected patients studies, although results seem to be better in more recent registries like the Milan registry [30] and ASSURE BVS [31] where more BVS specific implantation protocols where applied. Regarding the occurrence of scaffold thrombosis (ST), at variance of previous reports no acute or sub-acute STs were observed in the present investigation. This datum could be related to procedural characteristics including a meticulous lesion preparation pre BVS implantation and an advanced stage in learning curve of the operators in terms of BVS implantation. The revision of the cases with ST revealed that several factors might be associated with such event comprising severe lesion calcification, the presence of bifurcations, long overlap and antiplatelet therapy discontinuation. However, the factor that was particularly consistent was scaffold under-expansion. Previous investigations described stent underexpansion as an important predictor of ST with both bare metal stents and DES,[32-36] with an impact on the occurrence of ST that was hypostasized to be superior to stent malapposition.[37] The mechanisms behind these findings could be the fact that stent underexpansion translates into an abnormal shear stress. In particular increased radial transport of blood components and low wall shear stress, were described to promote platelet-dependent thrombosis.[38] In addition the impact of underexpansion

on shear stress could be potentiated by the presence of the BVS thick struts.[39]
Although, given the small number of patients and event reported in the present study it is not possible to reach firm conclusions, our findings suggest that optimal BVS expansion, with lesion preparation and appropriate scaffold postdilatation, should be pursued given the possible relevant clinical implications.

Limitations

The present report is an investigator initiated, single center, single arm study. The choice for BVS implantation was left to operator discretion, this could be source of selection bias. The absence of a comparator arm is limiting the interpretation of our data. The limited number of patients does not allow reaching firm conclusions on clinical outcomes. The mid-term follow-up is preventing the availability of information on long-term safety and efficacy.

CONCLUSION

The implantation of the everolimus eluting bioresorbable vascular scaffold in an expanded range of coronary lesion types and clinical presentations was observed to be viable with promising angiographic results and mid-term clinical outcomes. Larger studies with longer follow-up and a direct comparison with currently available metallic drug eluting stents are needed to fully evaluate the possible additional value of the bioresorbable technologies an all comers setting.

Acknowledgments

This study was supported by an unrestricted grant from Abbott Vascular.
The authors want to thank Isabella Kardys, Johannes Schaar and Martijn Akkerhuis, for their contribution in the event adjudication.

REFERENCES

1. Serruys PW, Onuma Y, Ormiston JA et al. Evaluation of the second generation of a bioresorbable everolimus drug-eluting vascular scaffold for treatment of de novo coronary artery stenosis: six-month clinical and imaging outcomes. Circulation 2010;122:2301-12.
2. Onuma Y, Serruys PW, Perkins LE et al. Intracoronary optical coherence tomography and histology at 1 month and 2, 3, and 4 years after implantation of everolimus-eluting bioresorbable vascular scaffolds in a porcine coronary artery model: an attempt to decipher the human optical coherence tomography images in the ABSORB trial. Circulation 2010;122:2288-300.
3. Onuma Y, Serruys PW. Bioresorbable scaffold: the advent of a new era in percutaneous coronary and peripheral revascularization? Circulation 2011;123:779-97.
4. Diletti R, Farooq V, Girasis C et al. Clinical and intravascular imaging outcomes at 1 and 2 years after implantation of absorb everolimus eluting bioresorbable vascular scaffolds in small vessels. Late lumen enlargement: does bioresorption matter with small vessel size? Insight from the ABSORB cohort B trial. Heart 2013;99:98-105.
5. Serruys PW, Garcia-Garcia HM, Onuma Y. From metallic cages to transient bioresorbable scaffolds: change in paradigm of coronary revascularization in the upcoming decade? European heart journal 2012;33:16-25b.
6. Serruys PW, Ormiston JA, Onuma Y et al. A bioabsorbable everolimus-eluting coronary stent system (ABSORB): 2-year outcomes and results from multiple imaging methods. Lancet 2009;373:897-910.
7. Onuma Y, Dudek D, Thuesen L et al. Five-year clinical and functional multislice computed tomography angiographic results after coronary implantation of the fully resorbable polymeric everolimus-eluting scaffold in patients with de novo coronary artery disease: the ABSORB cohort A trial. JACC Cardiovascular interventions 2013;6:999-1009.
8. Serruys PW, Onuma Y, Garcia-Garcia HM et al. Dynamics of vessel wall changes following the implantation of the absorb everolimus-eluting bioresorbable vascular scaffold: a multi-imaging modality study at 6, 12, 24 and 36 months. EuroIntervention : journal of EuroPCR in collaboration with the Working Group on Interventional Cardiology of the European Society of Cardiology 2014;9:1271-84.
9. Diletti R, Onuma Y, Farooq V et al. 6-month clinical outcomes following implantation of the bioresorbable everolimus-eluting vascular scaffold in vessels smaller or larger than 2.5 mm. Journal of the American College of Cardiology 2011;58:258-64.
10. Onuma Y, Tanimoto S, Ruygrok P et al. Efficacy of everolimus eluting stent implantation in patients with calcified coronary culprit lesions: two-year angiographic and three-year clinical results from the SPIRIT II study. Catheterization and cardiovascular interventions : official journal of the Society for Cardiac Angiography & Interventions 2010;76:634-42.
11. Herrman JP, Azar A, Umans VA, Boersma E, von Es GA, Serruys PW. Inter- and intra-observer variability in the qualitative categorization of coronary angiograms. International journal of cardiac imaging 1996;12:21-30.
12. Burzotta F, Trani C, Todaro D et al. Prospective randomized comparison of sirolimus- or everolimus-eluting stent to treat bifurcated lesions by provisional approach. JACC Cardiovascular interventions 2011;4:327-35.
13. Muramatsu T, Onuma Y, Garcia-Garcia HM et al. Incidence and short-term clinical outcomes of small side branch occlusion after implantation of an everolimus-eluting bioresorbable vascular scaffold: an interim report of 435 patients in the ABSORB-EXTEND single-arm trial in comparison with an everolimus-eluting metallic stent in the SPIRIT first and II trials. JACC Cardiovascular interventions 2013;6:247-57.
14. Dzavik V, Colombo A. The absorb bioresorbable vascular scaffold in coronary bifurcations: insights from bench testing. JACC Cardiovascular interventions 2014;7:81-8.

15. Ormiston JA, Webber B, Ubod B, Webster MW, White J. Absorb everolimus-eluting bioresorbable scaffolds in coronary bifurcations: a bench study of deployment, side branch dilatation and post-dilatation strategies. EuroIntervention : journal of EuroPCR in collaboration with the Working Group on Interventional Cardiology of the European Society of Cardiology 2014.
16. Abdel-Wahab M, Baev R, Dieker P et al. Long-term clinical outcome of rotational atherectomy followed by drug-eluting stent implantation in complex calcified coronary lesions. Catheterization and cardiovascular interventions : official journal of the Society for Cardiac Angiography & Interventions 2013;81:285-91.
17. Genereux P, Madhavan MV, Mintz GS et al. Ischemic outcomes after coronary intervention of calcified vessels in acute coronary syndromes. Pooled analysis from the HORIZONS-AMI (Harmonizing Outcomes With Revascularization and Stents in Acute Myocardial Infarction) and ACUITY (Acute Catheterization and Urgent Intervention Triage Strategy) TRIALS. Journal of the American College of Cardiology 2014;63:1845-54.
18. Stone GW, Kandzari DE, Mehran R et al. Percutaneous recanalization of chronically occluded coronary arteries: a consensus document: part I. Circulation 2005;112:2364-72.
19. Stone GW, Reifart NJ, Moussa I et al. Percutaneous recanalization of chronically occluded coronary arteries: a consensus document: part II. Circulation 2005;112:2530-7.
20. Farooq V, Serruys PW, Garcia-Garcia HM et al. The negative impact of incomplete angiographic revascularization on clinical outcomes and its association with total occlusions: the SYNTAX (Synergy Between Percutaneous Coronary Intervention with Taxus and Cardiac Surgery) trial. Journal of the American College of Cardiology 2013;61:282-94.
21. Langille BL. Arterial remodeling: relation to hemodynamics. Canadian journal of physiology and pharmacology 1996;74:834-41.
22. Park JJ, Chae IH, Cho YS et al. The recanalization of chronic total occlusion leads to lumen area increase in distal reference segments in selected patients: an intravascular ultrasound study. JACC Cardiovascular interventions 2012;5:827-36.
23. Park DW, Park SW, Park KH et al. Frequency of and risk factors for stent thrombosis after drug-eluting stent implantation during long-term follow-up. The American journal of cardiology 2006;98:352-6.
24. Moreno R, Fernandez C, Hernandez R et al. Drug-eluting stent thrombosis: results from a pooled analysis including 10 randomized studies. Journal of the American College of Cardiology 2005;45:954-9.
25. Suh J, Park DW, Lee JY et al. The relationship and threshold of stent length with regard to risk of stent thrombosis after drug-eluting stent implantation. JACC Cardiovascular interventions 2010;3:383-9.
26. Serruys PW, Chevalier B, Dudek D et al. A bioresorbable everolimus-eluting scaffold versus a metallic everolimus-eluting stent for ischaemic heart disease caused by de-novo native coronary artery lesions (ABSORB II): an interim 1-year analysis of clinical and procedural secondary outcomes from a randomised controlled trial. Lancet 2015;385:43-54.
27. Kimura T, Kozuma K, Tanabe K et al. A randomized trial evaluating everolimus-eluting Absorb bioresorbable scaffolds vs. everolimus-eluting metallic stents in patients with coronary artery disease: ABSORB Japan. European heart journal 2015.
28. Capodanno D, Gori T, Nef H et al. Percutaneous coronary intervention with everolimus-eluting bioresorbable vascular scaffolds in routine clinical practice: early and midterm outcomes from the European multicentre GHOST-EU registry. EuroIntervention : journal of EuroPCR in collaboration with the Working Group on Interventional Cardiology of the European Society of Cardiology 2015;10:1144-53.
29. Kraak RP, Hassell ME, Grundeken MJ et al. Initial experience and clinical evaluation of the Absorb bioresorbable vascular scaffold (BVS) in real-world practice: the AMC Single Centre Real World PCI Registry. EuroIntervention : journal of EuroPCR in collaboration with the Working Group on Interventional Cardiology of the European Society of Cardiology 2015;10:1160-8.

30. Costopoulos C, Latib A, Naganuma T et al. Comparison of early clinical outcomes between ABSORB bioresorbable vascular scaffold and everolimus-eluting stent implantation in a real-world population. Catheterization and cardiovascular interventions : official journal of the Society for Cardiac Angiography & Interventions 2015;85:E10-5.
31. Wohrle J, Naber C, Schmitz T et al. Beyond the early stages: insights from the ASSURE registry on bioresorbable vascular scaffolds. EuroIntervention : journal of EuroPCR in collaboration with the Working Group on Interventional Cardiology of the European Society of Cardiology 2015;11:149-56.
32. Fujii K, Carlier SG, Mintz GS et al. Stent underexpansion and residual reference segment stenosis are related to stent thrombosis after sirolimus-eluting stent implantation: an intravascular ultrasound study. Journal of the American College of Cardiology 2005;45:995-8.
33. Cheneau E, Leborgne L, Mintz GS et al. Predictors of subacute stent thrombosis: results of a systematic intravascular ultrasound study. Circulation 2003;108:43-7.
34. Kasaoka S, Tobis JM, Akiyama T et al. Angiographic and intravascular ultrasound predictors of in-stent restenosis. Journal of the American College of Cardiology 1998;32:1630-5.
35. Sonoda S, Morino Y, Ako J et al. Impact of final stent dimensions on long-term results following sirolimus-eluting stent implantation: serial intravascular ultrasound analysis from the sirius trial. Journal of the American College of Cardiology 2004;43:1959-63.
36. Uren NG, Schwarzacher SP, Metz JA et al. Predictors and outcomes of stent thrombosis: an intravascular ultrasound registry. European heart journal 2002;23:124-32.
37. Liu X, Doi H, Maehara A et al. A volumetric intravascular ultrasound comparison of early drug-eluting stent thrombosis versus restenosis. JACC Cardiovascular interventions 2009;2:428-34.
38. Sukavaneshvar S, Rosa GM, Solen KA. Enhancement of stent-induced thromboembolism by residual stenoses: contribution of hemodynamics. Annals of biomedical engineering 2000;28:182-93.
39. Bourantas CV, Papafaklis MI, Kotsia A et al. Effect of the endothelial shear stress patterns on neointimal proliferation following drug-eluting bioresorbable vascular scaffold implantation: an optical coherence tomography study. JACC Cardiovascular interventions 2014;7:315-24.

Chapter 18

Bioresorbable Scaffolds for Treatment of Coronary Bifurcation Lesions

Critical Appraisal and Future Perspectives

Roberto Diletti, MD; Didier Tchetche, MD; Emanuele Barbato, MD, PhD;
Azeem Latib, MD; Bruno Farah, MD; Robert-Jan van Geuns, MD, PhD;
Antonio Colombo, MD; Jean Fajadet, MD; Nicolas M. van Mieghem, MD, PhD

Catheter Cardiovasc Interv. 2016, In press

ABSTRACT

Bioresorbable vascular scaffolds have been recently introduced as a novel paradigm for coronary artery disease treatment allowing temporary vessel support and drug delivery without long term coronary caging, potentially reducing the long-term limitation of metallic stents.

The scientific community have rapidly embraced this concept and bioresorbable devices have been introduced in clinical practice.

However, despite the fact that bifurcation lesions represent a large and challenging subset in the field of interventional cardiology, this subgroup of lesions have been avoided in the initial experience with bioresorbable scaffolds and clear recommendations on methodological approaches are lacking.

In the present report we describe the various techniques for bifurcation treatment with bioresorbable scaffolds and the theoretical advantages and disadvantages of this technology in different scenarios, with a glimpse to challenging subsets and possible complications.

Therefore, we aim to provide experience based insights and practical guidance for bioresorbable scaffold implantation in bifurcation lesions.

INTRODUCTION

Bifurcation lesions represent a technically challenging subset of percutaneous coronary interventions (PCI) accounting for 15-20% of all procedures (1,2). Despite the several technological revolutions in stent designs, PCI for bifurcation lesions is associated with worse clinical outcomes compared with non-bifurcation lesions[3]. Bare metal stents (BMS) were associated with high restenosis rates irrespectively of the bifurcation technique adopted.(4-10) Drug eluting stent technology significantly reduced neointimal proliferation, restenosis rate and target lesion revascularization, yet clinical results remained inferior to non-bifurcations lesions.

In particular, the ostium of the side-branch was identified as the site most frequently affected by increased atherogenesis and restenosis.[11,12] In addition, bifurcation treatment was reported to be associated with an higher risk of stent thrombosis,[13,14] probably triggered by delayed vascular healing and incomplete neointimal coverage[15]

Bioresorbable scaffolds were recently introduced as a novel paradigm for coronary artery disease treatment, potentially reducing the long-term limitation of metallic stents, such as vessel caging, permanent side-branch jailing and impairment of vasomotion.[16] The scientific community rapidly embraced and introduced this bioresorbable concept into clinical practice.

However, bifurcation lesions have been avoided in the initial experience with bioresorbable scaffolds and clear recommendations on methodological approaches are lacking.

The present report aims to provide experience based insights and practical guidance for bioresorbable scaffold implantation in bifurcation lesions.

APPROACH TO BIFURCATION TREATMENT, ONE- OR TWO-SCAFFOLD STRATEGY

The provisional 1-stent approach is the technique of first choice in the current era of bifurcation stenting. The main vessel is stented first and only if needed subsequent ballooning and stenting of the side-branch (SB) is performed [17-22]

Dedicated research will reveal whether the same paradigm holds for the second-generation everolimus eluting bioresorbable vascular scaffold (BVS). In principle at least for the first 6 months, the current BVS technology behaves like other metallic devices (revascularization, drug elution and vessels scaffolding), therefore supporting a generalization of metal stents results in bifurcation lesions also to this novel device. On the other hand, the strut thickness and the polymeric nature of the device allowing full bioresorption over time, differentiate the BVS from the latest generation drug eluting metal stents (DES).

The large BVS strut thickness (157 μm) results in a higher device profile, reduced deliverability and may predispose to more scaffold thrombosis. From a technical perspective, it may be more difficult to rewire through a previously deployed thicker strut device. Furthermore a two-stent technique typically requires final kissing balloon (FKB) inflation to optimize stent deployment and apposition and obtain adequate carina coverage. FKB may impose excessive mechanical stress to the polymeric scaffold that could eventually damage its integrity and impair long-term clinical outcome. All these considerations could suggest the provisional T-stenting as first choice also when implanting a BVS in bifurcation lesions.

On the other hand, particular anatomical substrates such as large SB diameter with significant narrowing may justify a 2 stent/scaffold technique. This hypothesis, applied to metal stents, was tested in the recently presented Nordic Baltic IV study evaluating provisional approach vs 2 stent technique (mainly culotte) in bifurcations with SB ≥ 2.75 mm and showing a trend towards improved short term outcomes in the 2 stent arm.[23] A similar concept was reported in the DKCRUSH-II study[24] evaluating true bifurcation lesions with a reference vessel diameter comprised between 2.5 and 4.0 in both branches and comparing double kissing crush (DK crush) or provisional stenting techniques, with a significant reduction of target lesion revascularization (TLR) and target vessel revascularization (TVR) in the DK crush group. An additional trial, the EBC II study comparing culotte vs provisional stenting in bifurcation with SB≥2.5 mm and significant disease is currently ongoing and could add further to our understanding on the indication for a complex approach in bifurcation lesions.

In conclusion, a simple provisional T-scaffolding approach (Figure 1) could be the most appropriate in the majority of the bifurcation lesions (similarly as for metal stents). In selected cases with large side-branches, a 2-scaffold technique could be considered.

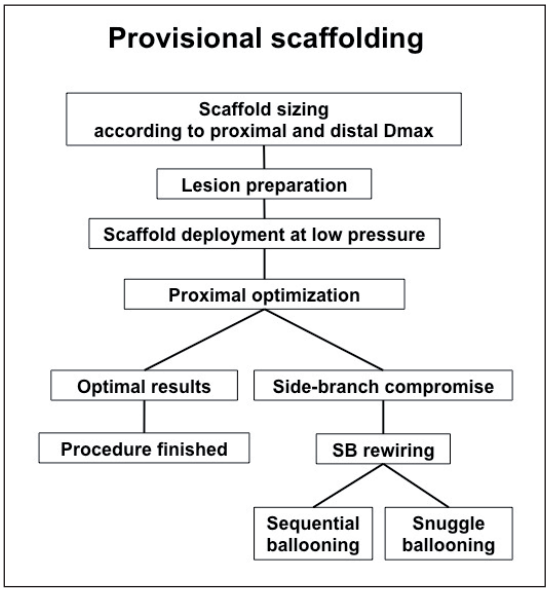

Figure 1. Flow chart of the Provisional T-scaffolding.

One-scaffold strategy

In a one-scaffold strategy (provisional T-scaffolding) only the main vessel is treated with BVS implantation. Meticulous lesion preparation has an important role in facilitating an easy delivery of the device and optimal deployment; in the specific setting of BVS use, the adoption of predilatation with non-compliant balloons with a nominal size equal to the intended BVS and inflated at high pressure, may be a reasonable strategy.

Predilatation of the side-branch gives the obvious advantage of an increased SB ostium lumen before scaffolding and could reduce the diameter stenosis after scaffolding lowering the need for rewiring and ballooning. On the other hand predilatation of the SB may lead to ostial damage and dissection with an increased risk for bailout SB scaffolding. Currently available data on this topic report conflicting results with SB predilatation probably increasing the overall rate of target lesion failure[25] but potentially having some benefit in case of true bifurcation lesions.[26]

When choosing the size of the BVS in bifurcation lesions, several models may be applied to understand the degree of distal diameter reduction in relation to the side-branch size and guide optimal BVS size selection [27-30].

The maximum diameter proximal to the bifurcation requires particular attention [31]. To ensure adequate apposition in the proximal part of the bifurcation, the size of the BVS

should allow safe expansion up to the estimated proximal maximal diameter (Dmax). Given the reported long term safety and efficacy of minimal under-expansion of slightly oversized BVS in small vessels,[32,33], a low-pressure inflation of a BVS sized on the basis of the proximal Dmax, planning a subsequent proximal optimization (POT) could be a reasonable strategy. When using this approach initial low-pressure scaffold deployment should be considered a key factor to avoid distal edge dissection and bailout interventions. On this regard distal Dmax could be considered for scaffold sizing in case of minimal mismatch between the proximal and distal bifurcation segment, taking into account the possibility for an additional POT using up to 0.5 mm bigger balloons.

The proximal optimization technique, [34] a concept already reported for bifurcation stenting with metal devices, could have additional advantages with a thick strut device like the BVS. Reduction of proximal malapposition could lower the occurrence of scaffold thrombosis at the bifurcation site, in addition as the wider BVS strut might be associated with difficult SB re-wiring and ballooning, the oblique BVS shape after POT at the site of the SB ostium could facilitate re-crossing.

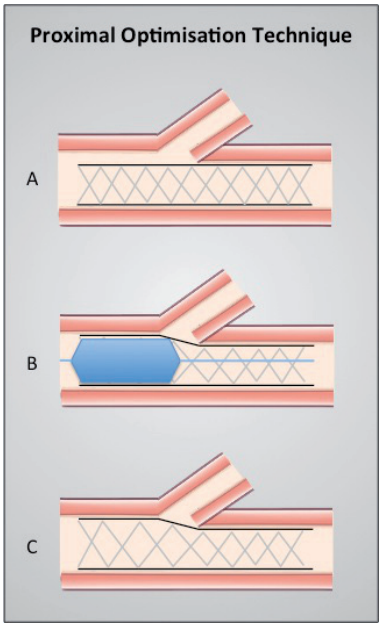

Figure 2. Proximal optimization technique (POT). Upper panel (A) a low pressure inflation of a BVS sized on the basis of the proximal Dmax ensure distal optimal apposition e low risk of distal dissection. Middle panel (B) proximal optimization with a non complaint balloon inflated on the basis of the proximal Dmax. Lower panel (C) final result after POT with an oblique BVS shape at the site of the side branch possibly facilitating re-crossing.

Side-branch ballooning and Sequential ballooning

In case of side-branch compromise, re-wiring the SB through the BVS struts should be attempted. Ideally such manoeuvre should be performed after the POT to minimize the chances of wire placement behind malapposed struts. The feasibility of side branch re-wiring and side-branch ostium ballooning through the BVS struts has been previously reported.[35,36]

In a bifurcation phantom model, Ormiston et al.[37] deployed a 3.0 and 3.5 mm BVS in the main branch, and after rewiring inflated 2.0, 2.5 and 3.0 mm balloons up to 14 atm at the ostium of the SB. In those experiments, the 2.0 mm balloon did not cause any fracture. The 2.5 mm balloon was associated with a 13% scaffold fracture and the 3.0 mm balloon 19%. In the same report SB dilatations with a 3.0 mm non-compliant balloon in a 3.0 mm scaffold up to 10 atm pressure were not likely to cause fractures whilst a similar strategy but with higher SB balloon pressures was associated with scaffold structure discontinuity.[37]

Also as expected with metal stents, the inflation of a balloon in the ostium of the SB could be associated with main vessel (MV) scaffold distortion and consequent malapposition opposite to the SB ostium and MV scaffold narrowing immediately distal to the SB.

Therefore it is recommended to perform a second MV post dilatation in a sequential manner after SB ballooning (sequential ballooning).

Kissing Balloons

The strain created by the overlapping kissing balloons can fracture the BVS circular rings potentially extending to the entire length of the scaffold segment where the 2 balloons are overlapping translating into a relevant scaffold fracture (scaffold "unzipping"). [38]

An alternative strategy is the adoption of a mini kissing balloon post dilatation (mini-KBPD) approach also named "snuggle balloon dilatation".[39] With this technique, the final optimization of the bifurcation is performed with simultaneous dilatation of the 2 balloons but with a minimal protrusion in the MV of the SB balloon.

Practically the snuggle technique requires placement of the proximal marker of the SB balloon in the MV just proximal to the SB ostium.[37] The SB balloon is inflated first. This technique may safely enlarge the SB ostium with minimal MV scaffold distortion. Of note, the risk of BVS fracture increased exponentially for pressures higher than 5 atm [37].

In aggregate, we suggest to avoid true kissing balloon inflations whenever possible and prefer POT in combination with sequential ballooning and recommend confirmation of the final result with intravascular imaging.

Need for bailout SB Scaffolding/stenting

Both metallic stents and additional BVS can be considered for bail-out techniques such as T-stenting or T-stenting and small protrusion (TAP). BVS has a higher profile compared to contemporary metallic DES, which may affect crossing the BVS towards the SB and mandate aggressive SB ostium dilatation with increased risk of MV BVS damage.
Meticulous sizing and BVS positioning in the SB is crucial to avoid excessive strut protrusion in the MV. Interestingly, TAP with BVS may have the unique advantage of a complete coverage of the SB ostium with a complete disappearance of the protruding struts over time.
In conclusion in case of bailout SB stenting with reverse T-stenting or TAP, complete bifurcation coverage with BVS may be challenging and sometimes use of metal DES may technically be the ultimate solution.

TWO-SCAFFOLD APPROACH

A 2-scaffold technique may be needed in selected bifurcation anatomies.
The same principles that are valid for metallic stents could be applied to the bioresorbable technology (BVS) with some important caveats.

Culotte technique

The culotte technique has been fully described previously.[2] In brief the SB is scaffolded first, followed by rewiring the MB through the scaffold and performing balloon inflation. Subsequently a 2nd scaffold is inflated through the first scaffold into the MB. The SB is then rewired and the case is completed with kissing balloon inflations.
The Culotte technique implies double scaffold coverage in the proximal segment of the main vessel and in principle results in complete carina coverage.[40] The culotte technique fits best when there is only a limited size mismatch between the branches.
This technique performed with metal stents has been evaluated in several studies. ([17,40-43]
Feasibility of the culotte technique with BVS has been shown.[44] Theoretically BVS could be appealing with this technique since over time the scaffolds will resorb, avoiding a permanent multilayer of metal in the coronary artery, leaving a smooth carina and virtually eliminating persistent device-malapposition or delayed healing at the side branch ostium. However, from a purely technical point of view the implantation procedure per se could be hindered by the relatively high crossing profile of the BVS, reasonably requiring an optimal back-up guide catheter, highly supportive wires and a relatively aggressive lesion preparation and initial scaffold dilatation. In addition although a strategy of "mini-culotte"

should be applied, the proximal part of the vessel will be covered by 2 layer of a thick strut polymeric material that could increase the risk of delayed vessel healing and scaffold thrombosis.

Finally the kissing balloon recommended when performing culotte with metal stents, will determine cells opening, distortion and mechanical stretch of both implanted devices increasing the probability of scaffold fracture.

Given these considerations and in absence of solid clinical data, the culotte technique with the current generation of bioresorbable devices is not recommended and should be performed only if strctly necessary with extreme caution. We recommend meticulous case preparation including 1) appropriate supportive guiding catheters and guidewires; 2) aggressive lesion preparation with the use of adequately sized balloons in main and side branches; 3) Minimization of the proximal overlap 4) POT; 5) sequential final ballooning avoiding classical FKB (snuggle technique can be a valid alternative, avoiding high pressures); 6) Confirmation of the final result with intravascular imaging such as optical coherence tomography.

Figure 3. Culotte technique performed with bioresorbable vascular scaffolds in a chronically occluded vessel.

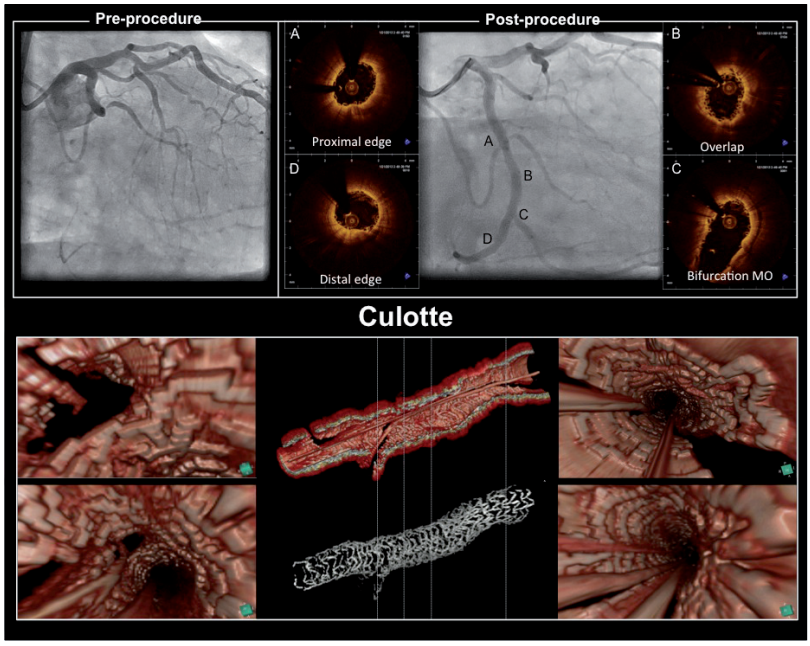

Crush techniques

The crush technique has been extensively evaluated with metal stents, with various procedural modifications like double crush, mini-crush and double kissing crush techniques.

The common denominator is the crushing and deformation of the proximal protruding segment of the side branch scaffold, that is implanted first, followed by a second scaffold implantation in the main vessel.

Thereafter, the side branch needs to be rewired through the cells of the two devices to complete the procedure with a final kissing balloon (Figure 4). Currently, even with metals stents, a mini-crash approach is largely recommended over the classic crush to minimize the extent of multiple layers in the main vessel. In the context of BVS, the impact of crushing the polymeric struts has been preliminary explored in bench testing showing technical feasibility of this approach.[45]

Figure 4. Crush technique performed with bioresorbable vascular scaffolds.

However, the crush technique implies the presence of 3 overlapping layers of 157 μm each in the proximal vessel, a condition that is prompt to malapposition, underexpansion, long-term uncoverage and increased risk of thrombosis. This background could be even worsened by the possible occurrence of areas of malapposition between the carina and the 2 scaffolds mainly due to the geometrical deformation of the SB scaffold.[45]

The use of a mini-crush technique would reduce the amount of polymeric material crushed against the vessel wall and it should be preferred to a classical crush.

The DK-crush has never been reported with BVS. Although this technique could bring some advantages when performed with metal stents (easier re-crossing and expanded

SB ostial area) with BVS the following issues arise; 1) the above mentioned limitation of crush per se, 2) the mechanical stress of the kissing balloon with theoretical increased risk of scaffold fracture.
Given those considerations, at the current status of the art in bioresorbable technologies there is common agreement among authors not to favour crush techniques with BVS.

T-stenting

The T-stenting technique provides a good solution in case of bifurcation with angle close to 90 degrees. A fundamental aspect of this technique is to precisely deploy the side-branch scaffold to ensure optimal SB ostial coverage.
To achieve such results, radiopaque markers at each scaffold edge could be used as reference [43].

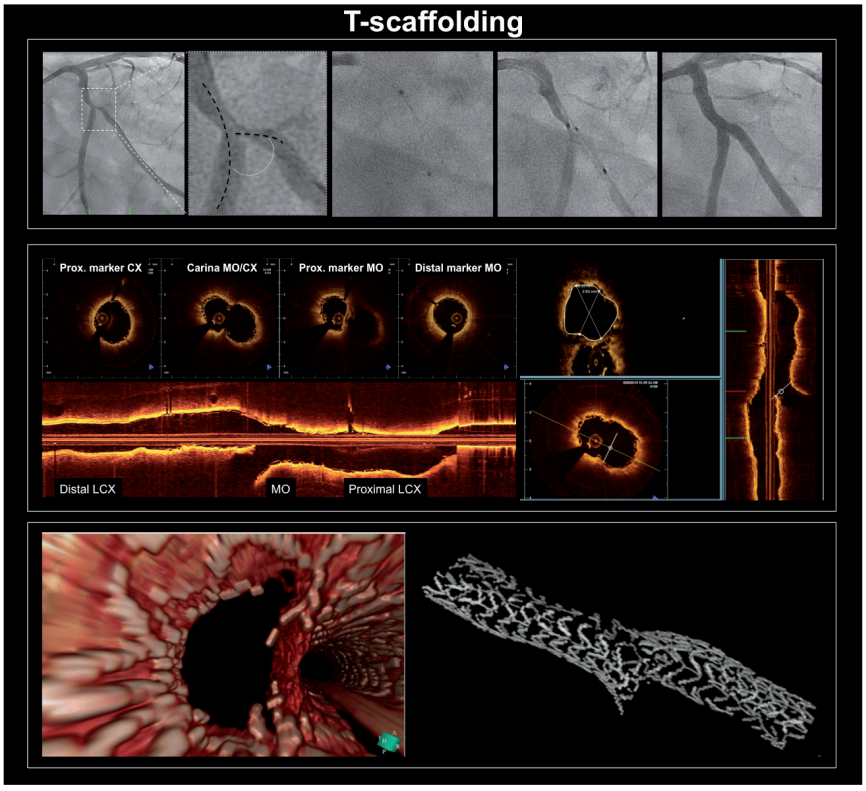

Figure 5. T-scaffolding performed in a bifurcation lesion with a favourable angle.

(In the everolimus eluting bioresorbable vascular scaffold, the proximal polymeric ring of a 3.5-mm BVS protrudes 1.4 mm from the proximal radiopaque platinum marker when crimped and 1mm when the scaffold is deployed).
A practical approach would be to align the proximal marker to the carina. This will warrant sufficient protrusion into the main branch to allow for complete coverage of the bifurcation and avoiding excessive protrusion into the main vessels that would convert the technique into a mini-crush.[46] The final result should be optimized by POT. Intravascular imaging might be indicated to confirm results.

V-stenting

The V-technique implies the delivery and simultaneous implantation of two devices. One scaffold is advanced in the side branch, the other in the main branch creating a new proximal carina.[47-49]
The V-technique is particularly suitable for bifurcations with medina classification 0,1,1 and classically regarded as appropriate for bifurcations with a very proximal location in the coronary tree (i.e. ostial left anterior descending and circumflex). Bifurcation angles less than 90 degrees are preferable for this approach given the fact that the 2 scaffolds are forming a new carina. When this new carina is considerably (≥ 5 mm) extended proximally, this technique has been named as simultaneous kissing stents/scaffolds [50]

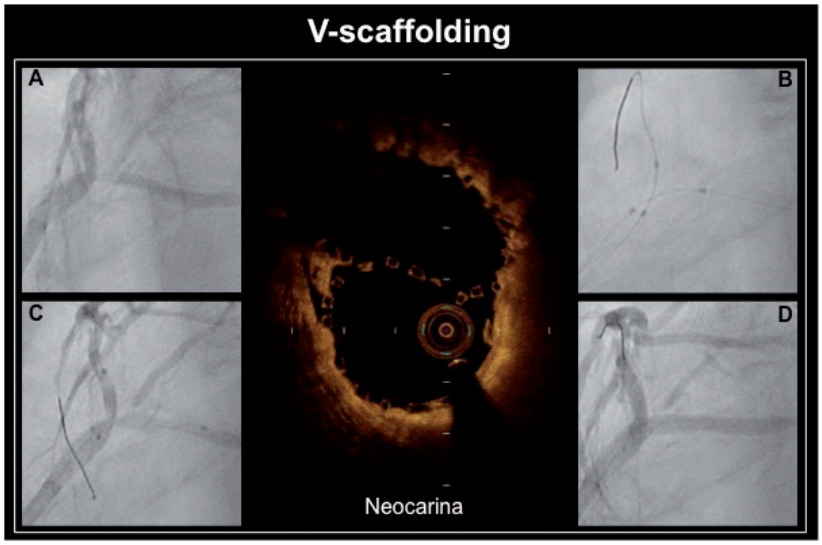

Figure 6. Left main bifurcation lesion treated with V-scaffolding technique. Distal left main lesion (A), predilatation (B), simultaneous kissing Scafoold implantation (C), final result (D). Optical coherence appearance of the polymeric neocarina (mid panel).

If executed in a medina 0,1,1 lesion, struts will not jail the access to either of the two branches with no need for strut re-crossing. Intravascular imaging might be indicated to confirm results.

THE ROLE OF INTRAVASCULAR IMAGING

Intravascular imaging, both IVUS and OCT contributed to our understanding of the mechanisms of side-branch compromise after bifurcation stenting.[51-54] OCT with its higher resolution may have a specific role in guiding bifurcation treatment with bioresorbable technologies.[55,56]

Invasive imaging may provide detailed insights on plaque morphology and distribution pre intervention[57] and may elucidate the concept of carina shift.

OCT may guide SB rewiring, a classification system was introduced taking into account the different compartments the ostium of the SB could be divided into when implanting BVS with potential implications on neointimal growth and strut coverage and providing a detailed guide for optimal SB re-wiring specifically when using BVS.[58] After main vessel treatment, OCT guidance for distal stent/scaffold cell re-crossing towards the SB has

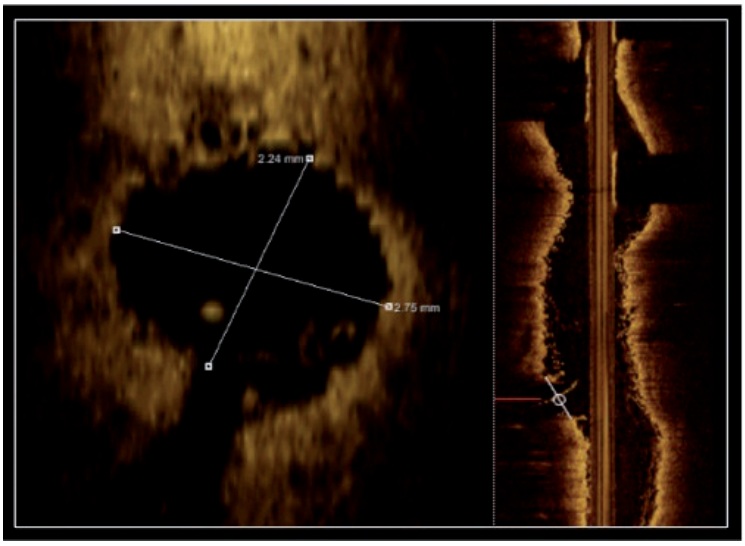

Figure 7. Accurate assessment of SB ostia from one single MB pullback obtained with a reconstruction of the cross-sections perpendicular to the SB centreline.

been demonstrated to be feasible and to reduce the rate of strut malapposition at the SB ostium.[59] In addition, the recent development of software for three-dimensional (3D) OCT reconstruction enables formal spatial characterisation of the strut position at the site of the SB ostium.[52,60]

Post scaffold implantation OCT is a reliable tool to assess malapposition, underexpansion, scaffold fractures, struts protrusion in the MB and the need for additional manoeuvres (i.e post dilatation, POT, etc.).

Although the use of intravascular imaging should not be considered mandatory, we recommend invasive imaging to achieve optimal results, especially during the initial phase of the BVS implantation learning curve, or in case of complex procedures involving 2-scaffold techniques. It should be acknowledged that OCT imaging might disclose defects in implantation such as scaffold fractures that are not yet clearly codified in terms of management.

Ideally, a comprehensive evaluation of bifurcation treatment with a 2-scaffold technique implies OCT pullbacks from both branches. The QAngioOCT 1.0 (Medis Specials Bv, Leiden, the Netherlands) is a new software tool to reconstruct the cross-sections perpendicular to the SB centreline to obtain more accurate assessment of SB ostia from one single MB pullback [61,62]

CHALLENGING SUBSETS

Left main

Limited data exists on the use of everolimus eluting vascular scaffolds implantation in the left main (LM) coronary artery.[63-65]. The current limited size availability of BVS with the largest device being a 3.5 mm with a maximal postdilatation limit at 4.0 mm has drastically limited the use of this scaffold for left main disease. In addition the potential need for SB dilatation with large balloons ≥2.5 mm (i.e. towards the LCX artery), might translate into scaffold disruption.

Furthermore, a 2-scaffold strategy could imply the presence of multi-layered thick scaffold struts or their protrusion in the distal LM (in case of TAP), with a theoretical increased risk of thrombosis.

As previously hypothesized,[66] a LM lesion not involving the ostium of the LCX may be more suitable for BVS implantation.

Intravascular imaging should be considered to elucidate size, plaque burden and distribution in both MB and SB .[66]

The introduction of novel devices such as the novolimus eluting coronary scaffold [67] with a wider safety margin for expansion and thinner struts and/or the next generation BVS could improve the usage and the treatment options with bioresorbable technologies in left main coronary artery disease.

In-stent restenosis

Limited data are currently available on the use of bioresorbable devices for treatment of in-stent restenosis (ISR).[68-70]

Conceptually the implantation of a bioresorbable scaffold in such lesions could be appealing, as it would ensure a higher vessel scaffolding and longer drug delivery compared with simple balloon or drug eluting balloon angioplasty, avoiding at the same time the permanent multiple layer of metal in the coronary artery. For this indication we would recommend proper pre-dilatation and meticulous scaffold evaluation after implantation by invasive imaging.

Thrombotic lesions

Intracoronary thrombus, with the concomitant presence of a relevant side branch at the lesion site, is not an unusual finding during acute coronary syndromes and the feasibility of BVS implantation in thrombotic lesions has been recently reported.[71-73] Initial thrombectomy may improve visualization of the target vessel and thus sizing. Again a single-scaffold provisional approach should be the first choice. Bioresorbable scaffolds may have particular features appealing for thrombotic lesions: 1) Wider struts may reduce thrombus dislodgment and distal embolization;[71] 2) The so-called self-correction property of the recently introduced novolimus eluting coronary scaffold [67] could limit under-sizing and malapposition.

COMPLICATIONS

Abrupt side-branch closure

Initial concerns were raised regarding the fact that implantation of bioresorbable scaffolds in bifurcation lesions might result into a higher side-branch impairment, compared to metallic stents, due to the presence of thick struts in front of the SB ostium. In keeping with this concept, BVS deployment seemed to be associated with more small (≤0.5 mm) side-branch occlusions and consequent cardiac enzyme release after the procedure. [74] Whether this finding also holds when applied to what is commonly considered a bifurcations lesion (with a side branch ≥ 2 mm) is unsettled.

Rewiring of the side-branch in those cases and consequent ballooning (mainly with an undersized balloon 1.5-2 mm in diameter) of the SB ostium is feasible and safe also in terms of scaffold geometry and fracture.[37,45]

Scaffold fracture

Although the structural discontinuity of the polymeric struts at a later stage is a programmed fate of the scaffold as part of the bioresorption process, scaffold disruption during the index procedure is an iatrogenic phenomenon that is associated with clinical events.

The identified reason for scaffold fracture during implantation is the overexpansion beyond the safety limits of the device. Therefore postdilatation with bioresorbable scaffolds should be performed with a balloon no larger than 0.5 mm above the nominal scaffold diameter. Dilatation of the SB ostium can be safely performed with 1.5 mm or 2.0 mm balloon. The risk of scaffold damage increases with 2.5 mm and 3.0 mm balloons at high pressure.[37] Kissing balloon techniques might lead to relevant scaffold damage.

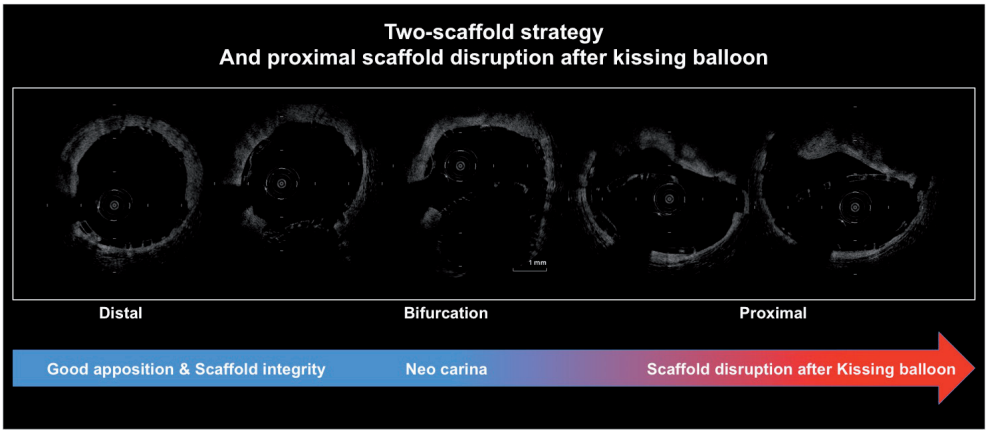

Figure 8. Scaffold fracture after kissing balloon.

Sequential ballooning and the snuggle technique may be more appropriate with bioresorbable scaffolds.

The clinical impact of scaffold fracture and how to approach it when discovered is unclear. In a recent post hoc analysis of the ABSORB Cohort B study, the reported incidence of acute scaffold disruption was low, (2 cases, 3.9%), yet associated with a target lesion revascularization (TLR) at 1 month in 1 patient.[75]

Scaffold disruption diminishes its local support to the vessel wall and the presence of struts floating in the lumen could induce flow disturbance triggering small thrombus formation.[75,76] Novel bioresorbable devices with wider safety limits in terms of overexpansion are currently being tested.[67]

Dissections

Main vessel dissection Bioresorbable scaffolds implantation demands appropriate lesion preparation, which may predispose to coronary dissection due to balloon dilatation. Optimal scaffold coverage of the dissected segment is thus mandatory. In particular remaining edge dissections after stenting have been associated with an increased risk of stent thrombosis in the early phases after implantation.

Side branch dissection When treating bifurcation lesion a common complication is side-branch impairment after provisional scaffolding of the main vessel. Subsequent SB ballooning may be associated with SB dissection prompting a bailout treatment (T-stenting or T-stenting and small protrusion). The high BVS profile may impair proper SB access with additional bioresorbable scaffolds. In such cases a hybrid approach with a metallic stent in the side-branch could be considered.

FUTURE PROSPECTIVE

Implantation of bioresorbable devices in coronary bifurcation lesions results in the formation of a smooth neointimal membranous neocarina and complete strut disappearance facing the SB ostium over time [77]. However, the presence of struts at the ostium of the SB can also lead to the formation of endoluminal neointimal bridges as results of strut coverage. Concerns about long-term SB patency[58] were refuted as these tissue bridges progressively thinned over time suggesting a probable benign nature of those formations.[78] This concept also holds true for 2-scaffold techniques implying the presence of struts in the vessel lumen such us the TAP technique.

Future improvements in the bioresorbable technology are thinner struts with less polymeric material at the site of the SB ostia, with easier scaffold delivery and potentially improved vascular healing.

CONCLUSION

A one-scaffold strategy, namely provisional T-scaffolding with meticulous lesion preparation and proximal optimization should be considered the strategy of choice for the vast majority of the cases. In selected cases, a two-scaffold approach could be considered with intravascular imaging representing a useful tool for procedural optimization. Future technical improvement of the bioresorbable scaffolds could facilitate the expanded use of these devices in bifurcation lesions.

Sources of Funding
Thoraxcenter receives unrestricted grants from the Abbott Vascular

Disclosures
The Authors have no conflicts of interest to disclose

REFERENCES

1. Sarno G, Lagerqvist B, Frobert O, Nilsson J, Olivecrona G, Omerovic E, Saleh N, Venetzanos D, James S. Lower risk of stent thrombosis and restenosis with unrestricted use of 'new-generation' drug-eluting stents: a report from the nationwide Swedish Coronary Angiography and Angioplasty Registry (SCAAR). Eur Heart J 2012;33(5):606-13.
2. Lassen JF, Holm NR, Stankovic G, Lefevre T, Chieffo A, Hildick-Smith D, Pan M, Darremont O, Albiero R, Ferenc M and others. Percutaneous coronary intervention for coronary bifurcation disease: consensus from the first 10 years of the European Bifurcation Club meetings. EuroIntervention 2014;10(5):545-60.
3. Diletti R, Garcia-Garcia HM, Bourantas CV, van Geuns RJ, Van Mieghem NM, Vranckx P, Zhang YJ, Farooq V, Iqbal J, Wykrzykowska JJ and others. Clinical outcomes after zotarolimus and everolimus drug eluting stent implantation in coronary artery bifurcation lesions: insights from the RESOLUTE All Comers Trial. Heart 2013;99(17):1267-74.
4. Yamashita T, Nishida T, Adamian MG, Briguori C, Vaghetti M, Corvaja N, Albiero R, Finci L, Di Mario C, Tobis JM and others. Bifurcation lesions: two stents versus one stent--immediate and follow-up results. J Am Coll Cardiol 2000;35(5):1145-51.
5. Sheiban I, Albiero R, Marsico F, Dharmadhikari A, Tzifos V, Pagnotta P, Montorfano M, Leonardo F, Saba P, Di Mario C and others. Immediate and long-term results of "T" stenting for bifurcation coronary lesions. Am J Cardiol 2000;85(9):1141-4, A9.
6. Lefevre T, Louvard Y, Morice MC, Dumas P, Loubeyre C, Benslimane A, Premchand RK, Guillard N, Piechaud JF. Stenting of bifurcation lesions: classification, treatments, and results. Catheter Cardiovasc Interv 2000;49(3):274-83.
7. Karvouni E, Di Mario C, Nishida T, Tzifos V, Reimers B, Albiero R, Corvaja N, Colombo A. Directional atherectomy prior to stenting in bifurcation lesions: a matched comparison study with stenting alone. Catheter Cardiovasc Interv 2001;53(1):12-20.
8. Al Suwaidi J, Berger PB, Rihal CS, Garratt KN, Bell MR, Ting HH, Bresnahan JF, Grill DE, Holmes DR, Jr. Immediate and long-term outcome of intracoronary stent implantation for true bifurcation lesions. J Am Coll Cardiol 2000;35(4):929-36.
9. Thuesen L, Kelbaek H, Klovgaard L, Helqvist S, Jorgensen E, Aljabbari S, Krusell LR, Jensen GV, Botker HE, Saunamaki K and others. Comparison of sirolimus-eluting and bare metal stents in coronary bifurcation lesions: subgroup analysis of the Stenting Coronary Arteries in Non-Stress/Benestent Disease Trial (SCANDSTENT). Am Heart J 2006;152(6):1140-5.
10. Colombo A, Al-Lamee R. Bifurcation lesions: an inside view. Circ Cardiovasc Interv 2010;3(2):94-6.
11. Colombo A, Moses JW, Morice MC, Ludwig J, Holmes DR, Jr., Spanos V, Louvard Y, Desmedt B, Di Mario C, Leon MB. Randomized study to evaluate sirolimus-eluting stents implanted at coronary bifurcation lesions. Circulation 2004;109(10):1244-9.
12. Tanabe K, Hoye A, Lemos PA, Aoki J, Arampatzis CA, Saia F, Lee CH, Degertekin M, Hofma SH, Sianos G and others. Restenosis rates following bifurcation stenting with sirolimus-eluting stents for de novo narrowings. Am J Cardiol 2004;94(1):115-8.
13. Farb A, Boam AB. Stent thrombosis redux--the FDA perspective. N Engl J Med 2007;356(10):984-7.
14. Iakovou I, Schmidt T, Bonizzoni E, Ge L, Sangiorgi GM, Stankovic G, Airoldi F, Chieffo A, Montorfano M, Carlino M and others. Incidence, predictors, and outcome of thrombosis after successful implantation of drug-eluting stents. JAMA 2005;293(17):2126-30.
15. Farb A, Burke AP, Kolodgie FD, Virmani R. Pathological mechanisms of fatal late coronary stent thrombosis in humans. Circulation 2003;108(14):1701-6.

16. Serruys PW, Garcia-Garcia HM, Onuma Y. From metallic cages to transient bioresorbable scaffolds: change in paradigm of coronary revascularization in the upcoming decade? Eur Heart J 2012;33(1):16-25b.
17. Hildick-Smith D, de Belder AJ, Cooter N, Curzen NP, Clayton TC, Oldroyd KG, Bennett L, Holmberg S, Cotton JM, Glennon PE and others. Randomized trial of simple versus complex drug-eluting stenting for bifurcation lesions: the British Bifurcation Coronary Study: old, new, and evolving strategies. Circulation 2010;121(10):1235-43.
18. Ferenc M, Gick M, Kienzle RP, Bestehorn HP, Werner KD, Comberg T, Kuebler P, Buttner HJ, Neumann FJ. Randomized trial on routine vs. provisional T-stenting in the treatment of de novo coronary bifurcation lesions. Eur Heart J 2008;29(23):2859-67.
19. Colombo A, Bramucci E, Sacca S, Violini R, Lettieri C, Zanini R, Sheiban I, Paloscia L, Grube E, Schofer J and others. Randomized study of the crush technique versus provisional side-branch stenting in true coronary bifurcations: the CACTUS (Coronary Bifurcations: Application of the Crushing Technique Using Sirolimus-Eluting Stents) Study. Circulation 2009;119(1):71-8.
20. Behan MW, Holm NR, Curzen NP, Erglis A, Stables RH, de Belder AJ, Niemela M, Cooter N, Chew DP, Steigen TK and others. Simple or complex stenting for bifurcation coronary lesions: a patient-level pooled-analysis of the Nordic Bifurcation Study and the British Bifurcation Coronary Study. Circ Cardiovasc Interv 2011;4(1):57-64.
21. Maeng M, Holm NR, Erglis A, Kumsars I, Niemela M, Kervinen K, Jensen JS, Galloe A, Steigen TK, Wiseth R and others. Long-term results after simple versus complex stenting of coronary artery bifurcation lesions: Nordic Bifurcation Study 5-year follow-up results. J Am Coll Cardiol 2013;62(1):30-4.
22. Louvard Y, Thomas M, Dzavik V, Hildick-Smith D, Galassi AR, Pan M, Burzotta F, Zelizko M, Dudek D, Ludman P and others. Classification of coronary artery bifurcation lesions and treatments: time for a consensus! Catheter Cardiovasc Interv 2008;71(2):175-83.
23. I K. Randomized comparison of provisional side-branch stenting versus a 2-stent strategy for treatment of true coronary bifurcation lesions involving a large side branch. 2-year results in the Nordic-Baltic Bifurcation Study IV. EuroPCR; May 21, 2015; Paris, France 2015.
24. Chen SL, Santoso T, Zhang JJ, Ye F, Xu YW, Fu Q, Kan J, Paiboon C, Zhou Y, Ding SQ and others. A randomized clinical study comparing double kissing crush with provisional stenting for treatment of coronary bifurcation lesions: results from the DKCRUSH-II (Double Kissing Crush versus Provisional Stenting Technique for Treatment of Coronary Bifurcation Lesions) trial. J Am Coll Cardiol 2011;57(8):914-20.
25. Song PS, Song YB, Yang JH, Hahn JY, Choi SH, Choi JH, Koo BK, Seung KB, Park SJ, Gwon HC. The Impact of Side Branch Predilatation on Procedural and Long-term Clinical Outcomes in Coronary Bifurcation Lesions Treated by the Provisional Approach. Rev Esp Cardiol (Engl Ed) 2014;67(10):804-12.
26. Pan M, Medina A, Romero M, Ojeda S, Martin P, Suarez de Lezo J, Segura J, Mazuelos F, Novoa J, Suarez de Lezo J. Assessment of side branch predilation before a provisional T-stent strategy for bifurcation lesions. A randomized trial. Am Heart J 2014;168(3):374-80.
27. Murray CD. The Physiological Principle of Minimum Work Applied to the Angle of Branching of Arteries. J Gen Physiol 1926;9(6):835-41.
28. Finet G, Gilard M, Perrenot B, Rioufol G, Motreff P, Gavit L, Prost R. Fractal geometry of arterial coronary bifurcations: a quantitative coronary angiography and intravascular ultrasound analysis. EuroIntervention 2008;3(4):490-8.
29. Kamiya A, Togawa T. Optimal branching structure of the vascular tree. Bull Math Biophys 1972;34(4):431-8.
30. Huo Y, Finet G, Lefevre T, Louvard Y, Moussa I, Kassab GS. Optimal diameter of diseased bifurcation segment: a practical rule for percutaneous coronary intervention. EuroIntervention 2012;7(11):1310-6.

31. Gomez-Lara J, Diletti R, Brugaletta S, Onuma Y, Farooq V, Thuesen L, McClean D, Koolen J, Ormiston JA, Windecker S and others. Angiographic maximal luminal diameter and appropriate deployment of the everolimus-eluting bioresorbable vascular scaffold as assessed by optical coherence tomography: an ABSORB cohort B trial sub-study. EuroIntervention 2012;8(2):214-24.
32. Diletti R, Onuma Y, Farooq V, Gomez-Lara J, Brugaletta S, van Geuns RJ, Regar E, de Bruyne B, Dudek D, Thuesen L and others. 6-month clinical outcomes following implantation of the bioresorbable everolimus-eluting vascular scaffold in vessels smaller or larger than 2.5 mm. J Am Coll Cardiol 2011;58(3):258-64.
33. Diletti R, Farooq V, Girasis C, Bourantas C, Onuma Y, Heo JH, Gogas BD, van Geuns RJ, Regar E, de Bruyne B and others. Clinical and intravascular imaging outcomes at 1 and 2 years after implantation of absorb everolimus eluting bioresorbable vascular scaffolds in small vessels. Late lumen enlargement: does bioresorption matter with small vessel size? Insight from the ABSORB cohort B trial. Heart 2013;99(2):98-105.
34. Hildick-Smith D, Lassen JF, Albiero R, Lefevre T, Darremont O, Pan M, Ferenc M, Stankovic G, Louvard Y, European Bifurcation C. Consensus from the 5th European Bifurcation Club meeting. EuroIntervention 2010;6(1):34-8.
35. van Geuns RJ, Gogas BD, Farooq V, Regar E, Serruys PW. 3-Dimensional reconstruction of a bifurcation lesion with double wire after implantation of a second generation everolimus-eluting bioresorbable vascular scaffold. Int J Cardiol 2011;153(2):e43-5.
36. Gogas BD, van Geuns RJ, Farooq V, Regar E, Heo JH, Ligthart J, Serruys PW. Three-dimensional reconstruction of the post-dilated ABSORB everolimus-eluting bioresorbable vascular scaffold in a true bifurcation lesion for flow restoration. JACC Cardiovasc Interv 2011;4(10):1149-50.
37. Ormiston JA, Webber B, Ubod B, Webster MW, White J. Absorb everolimus-eluting bioresorbable scaffolds in coronary bifurcations: a bench study of deployment, side branch dilatation and post-dilatation strategies. EuroIntervention 2014.
38. Di Mario C, Foin N, Colombo A. Kissing vanishing stents: are we trading ephemeral benefit for permanent damage? EuroIntervention 2013;9(7):777-9.
39. Seth A, Sengottuvelu G, Ravisekar V. Salvage of side branch by provisional "TAP technique" using Absorb bioresorbable vascular scaffolds for bifurcation lesions: first case reports with technical considerations. Catheter Cardiovasc Interv 2014;84(1):55-61.
40. Adriaenssens T, Byrne RA, Dibra A, Iijima R, Mehilli J, Bruskina O, Schomig A, Kastrati A. Culotte stenting technique in coronary bifurcation disease: angiographic follow-up using dedicated quantitative coronary angiographic analysis and 12-month clinical outcomes. Eur Heart J 2008;29(23):2868-76.
41. Tiroch K, Mehilli J, Byrne RA, Schulz S, Massberg S, Laugwitz KL, Vorpahl M, Seyfarth M, Kastrati A, Investigators I-LMS. Impact of coronary anatomy and stenting technique on long-term outcome after drug-eluting stent implantation for unprotected left main coronary artery disease. JACC Cardiovasc Interv 2014;7(1):29-36.
42. Kervinen K, Niemela M, Romppanen H, Erglis A, Kumsars I, Maeng M, Holm NR, Lassen JF, Gunnes P, Stavnes S and others. Clinical outcome after crush versus culotte stenting of coronary artery bifurcation lesions: the Nordic Stent Technique Study 36-month follow-up results. JACC Cardiovasc Interv 2013;6(11):1160-5.
43. Chen SL, Xu B, Han YL, Sheiban I, Zhang JJ, Ye F, Kwan TW, Paiboon C, Zhou YJ, Lv SZ and others. Comparison of double kissing crush versus Culotte stenting for unprotected distal left main bifurcation lesions: results from a multicenter, randomized, prospective DKCRUSH-III study. J Am Coll Cardiol 2013;61(14):1482-8.
44. Ruzsa Z, van der Linden M, Van Mieghem NM, Regar E, Ligthart JM, Serruys P, van Geuns RJ. Culotte stenting with bioabsorbable everolimus-eluting stents. Int J Cardiol 2013;168(2):e35-7.
45. Dzavik V, Colombo A. The absorb bioresorbable vascular scaffold in coronary bifurcations: insights from bench testing. JACC Cardiovasc Interv 2014;7(1):81-8.

46. van Mieghem N, Wilschut JJ, Ligthart J, Witberg K, van Geuns RJ, Regar E. Modified T-technique with bioresorbable scaffolds ensures complete carina coverage: an optical coherence tomography study. JACC Cardiovasc Interv 2014;7(8):e109-10.
47. Iakovou I, Ge L, Colombo A. Contemporary stent treatment of coronary bifurcations. J Am Coll Cardiol 2005;46(8):1446-55.
48. Schampaert E, Fort S, Adelman AG, Schwartz L. The V-stent: a novel technique for coronary bifurcation stenting. Cathet Cardiovasc Diagn 1996;39(3):320-6.
49. Colombo A, Gaglione A, Nakamura S, Finci L. "Kissing" stents for bifurcational coronary lesion. Cathet Cardiovasc Diagn 1993;30(4):327-30.
50. Sharma SK, Choudhury A, Lee J, Kim MC, Fisher E, Steinheimer AM, Kini AS. Simultaneous kissing stents (SKS) technique for treating bifurcation lesions in medium-to-large size coronary arteries. Am J Cardiol 2004;94(7):913-7.
51. Karanasos A, Tu S, van der Heide E, Reiber JH, Regar E. Carina shift as a mechanism for side-branch compromise following main vessel intervention: insights from three-dimensional optical coherence tomography. Cardiovasc Diagn Ther 2012;2(2):173-7.
52. Farooq V, Serruys PW, Heo JH, Gogas BD, Okamura T, Gomez-Lara J, Brugaletta S, Garcia-Garcia HM, van Geuns RJ. New insights into the coronary artery bifurcation hypothesis-generating concepts utilizing 3-dimensional optical frequency domain imaging. JACC Cardiovasc Interv 2011;4(8):921-31.
53. Koo BK, Waseda K, Kang HJ, Kim HS, Nam CW, Hur SH, Kim JS, Choi D, Jang Y, Hahn JY and others. Anatomic and functional evaluation of bifurcation lesions undergoing percutaneous coronary intervention. Circ Cardiovasc Interv 2010;3(2):113-9.
54. Suarez de Lezo J, Medina A, Martin P, Novoa J, Suarez de Lezo J, Pan M, Caballero E, Melian F, Mazuelos F, Quevedo V. Predictors of ostial side branch damage during provisional stenting of coronary bifurcation lesions not involving the side branch origin: an ultrasonographic study. EuroIntervention 2012;7(10):1147-54.
55. Di Mario C, Iakovou I, van der Giessen WJ, Foin N, Adrianssens T, Tyczynski P, Ghilencea L, Viceconte N, Lindsay AC. Optical coherence tomography for guidance in bifurcation lesion treatment. EuroIntervention 2010;6 Suppl J:J99-J106.
56. Karanasos A, Tu S, van der Linden M, van Weenen S, Ligthart J, Regar E. Online 3-dimensional rendering of optical coherence tomography images for the assessment of bifurcation intervention. Can J Cardiol 2012;28(6):759 e1-3.
57. Diletti R, Garcia-Garcia HM, Gomez-Lara J, Brugaletta S, Wykrzykowska JJ, van Ditzhuijzen N, van Geuns RJ, Regar E, Ambrosio G, Serruys PW. Assessment of coronary atherosclerosis progression and regression at bifurcations using combined IVUS and OCT. JACC Cardiovasc Imaging 2011;4(7):774-80.
58. Okamura T, Onuma Y, Garcia-Garcia HM, Regar E, Wykrzykowska JJ, Koolen J, Thuesen L, Windecker S, Whitbourn R, McClean DR and others. 3-Dimensional optical coherence tomography assessment of jailed side branches by bioresorbable vascular scaffolds: a proposal for classification. JACC Cardiovasc Interv 2010;3(8):836-44.
59. Alegria-Barrero E, Foin N, Chan PH, Syrseloudis D, Lindsay AC, Dimopolous K, Alonso-Gonzalez R, Viceconte N, De Silva R, Di Mario C. Optical coherence tomography for guidance of distal cell recrossing in bifurcation stenting: choosing the right cell matters. EuroIntervention 2012;8(2):205-13.
60. Farooq V, Gogas BD, Okamura T, Heo JH, Magro M, Gomez-Lara J, Onuma Y, Radu MD, Brugaletta S, van Bochove G and others. Three-dimensional optical frequency domain imaging in conventional percutaneous coronary intervention: the potential for clinical application. Eur Heart J 2013;34(12):875-85.
61. Tu S, Holm NR, Christiansen EH, Reiber JH. First presentation of 3-dimensional reconstruction and centerline-guided assessment of coronary bifurcation by fusion of X-ray angiography and optical coherence tomography. JACC Cardiovasc Interv 2012;5(8):884-5.

62. Karanasos A, Tu S, van Ditzhuijzen NS, Ligthart JM, Witberg K, Van Mieghem N, van Geuns RJ, de Jaegere P, Zijlstra F, Reiber JH and others. A novel method to assess coronary artery bifurcations by OCT: cut-plane analysis for side-branch ostial assessment from a main-vessel pullback. Eur Heart J Cardiovasc Imaging 2015;16(2):177-89.
63. Grundeken MJ, Kraak RP, de Bruin DM, Wykrzykowska JJ. Three-dimensional optical coherence tomography evaluation of a left main bifurcation lesion treated with ABSORB(R) bioresorbable vascular scaffold including fenestration and dilatation of the side branch. Int J Cardiol 2013;168(3):e107-8.
64. Sato K, Latib A, Panoulas VF, Naganuma T, Miyazaki T, Colombo A. A case of true left main bifurcation treated with bioresorbable everolimus-eluting stent v-stenting. JACC Cardiovasc Interv 2014;7(8):e103-4.
65. Sengottuvelu G, Dattagupta A. Optical coherence tomographic image of dynamic left main coronary artery compression caused by intramural haematoma due to spontaneous coronary artery dissection - degloved artery managed with bioresorbable vascular scaffold. EuroIntervention 2014.
66. Miyazaki T, Panoulas VF, Sato K, Naganuma T, Latib A, Colombo A. Bioresorbable vascular scaffolds for left main lesions; a novel strategy to overcome limitations. Int J Cardiol 2014;175(1):e11-3.
67. Verheye S, Ormiston JA, Stewart J, Webster M, Sanidas E, Costa R, Costa JR, Jr., Chamie D, Abizaid AS, Pinto I and others. A next-generation bioresorbable coronary scaffold system: from bench to first clinical evaluation: 6- and 12-month clinical and multimodality imaging results. JACC Cardiovasc Interv 2014;7(1):89-99.
68. Ielasi A, Latib A, Naganuma T, Cortese B, Sato K, Miyazaki T, Panoulas VF, Tespili M, Colombo A. Early results following everolimus-eluting bioresorbable vascular scaffold implantation for the treatment of in-stent restenosis. Int J Cardiol 2014;173(3):513-4.
69. Grasso C, Attizzani GF, Patane M, Ohno Y, Capodanno D, Tamburino C. First-in-human description of everolimus-eluting bioabsorbable vascular scaffold implantation for the treatment of drug-eluting stent failure: insights from optical coherence tomography. Int J Cardiol 2013;168(4):4490-1.
70. Naganuma T, Costopoulos C, Latib A, Sato K, Miyazaki T, Colombo A. Feasibility and efficacy of bioresorbable vascular scaffolds use for the treatment of in-stent restenosis and a bifurcation lesion in a heavily calcified diffusely diseased vessel. JACC Cardiovasc Interv 2014;7(5):e45-6.
71. Diletti R, Karanasos A, Muramatsu T, Nakatani S, Van Mieghem NM, Onuma Y, Nauta ST, Ishibashi Y, Lenzen MJ, Ligthart J and others. Everolimus-eluting bioresorbable vascular scaffolds for treatment of patients presenting with ST-segment elevation myocardial infarction: BVS STEMI first study. Eur Heart J 2014;35(12):777-86.
72. Kocka V, Maly M, Tousek P, Budesinsky T, Lisa L, Prodanov P, Jarkovsky J, Widimsky P. Bioresorbable vascular scaffolds in acute ST-segment elevation myocardial infarction: a prospective multicentre study 'Prague 19'. Eur Heart J 2014;35(12):787-94.
73. Brugaletta S, Gori T, Low AF, Tousek P, Pinar E, Gomez-Lara J, Scalone G, Schulz E, Chan MY, Kocka V and others. Absorb Bioresorbable Vascular Scaffold Versus Everolimus-Eluting Metallic Stent in ST-Segment Elevation Myocardial Infarction: 1-Year Results of a Propensity Score Matching Comparison: The BVS-EXAMINATION Study (Bioresorbable Vascular Scaffold-A Clinical Evaluation of Everolimus Eluting Coronary Stents in the Treatment of Patients With ST-segment Elevation Myocardial Infarction). JACC Cardiovasc Interv 2015;8(1 Pt B):189-97.
74. Muramatsu T, Onuma Y, Garcia-Garcia HM, Farooq V, Bourantas CV, Morel MA, Li X, Veldhof S, Bartorelli A, Whitbourn R and others. Incidence and short-term clinical outcomes of small side branch occlusion after implantation of an everolimus-eluting bioresorbable vascular scaffold: an interim report of 435 patients in the ABSORB-EXTEND single-arm trial in comparison with an everolimus-eluting metallic stent in the SPIRIT first and II trials. JACC Cardiovasc Interv 2013;6(3):247-57.

75. Onuma Y, Serruys PW, Muramatsu T, Nakatani S, van Geuns RJ, de Bruyne B, Dudek D, Christiansen E, Smits PC, Chevalier B and others. Incidence and imaging outcomes of acute scaffold disruption and late structural discontinuity after implantation of the absorb Everolimus-Eluting fully bioresorbable vascular scaffold: optical coherence tomography assessment in the ABSORB cohort B Trial (A Clinical Evaluation of the Bioabsorbable Everolimus Eluting Coronary Stent System in the Treatment of Patients With De Novo Native Coronary Artery Lesions). JACC Cardiovasc Interv 2014;7(12):1400-11.
76. Onuma Y, Serruys PW, Ormiston JA, Regar E, Webster M, Thuesen L, Dudek D, Veldhof S, Rapoza R. Three-year results of clinical follow-up after a bioresorbable everolimus-eluting scaffold in patients with de novo coronary artery disease: the ABSORB trial. EuroIntervention 2010;6(4):447-53.
77. Okamura T, Serruys PW, Regar E. Cardiovascular flashlight. The fate of bioresorbable struts located at a side branch ostium: serial three-dimensional optical coherence tomography assessment. Eur Heart J 2010;31(17):2179.
78. Karanasos A, Simsek C, Gnanadesigan M, van Ditzhuijzen NS, Freire R, Dijkstra J, Tu S, Van Mieghem N, van Soest G, de Jaegere P and others. OCT Assessment of the Long-Term Vascular Healing Response 5 Years After Everolimus-Eluting Bioresorbable Vascular Scaffold. J Am Coll Cardiol 2014;64(22):2343-56.

PART
III

Chapter 19

Everolimus Eluting Bioresorbable Vascular Scaffold for Treatment of Complex Chronic Total Occlusions

Jiang Ming Fam, MD; Soledad Ojeda, MD, PhD, Azeem Latib, MD; Marcella De Paolis, MD; Roberto Garbo, MD; Robert Jan van Geuns MD, PhD; Beatriz Vaquerizo, MD; Georgios J. Vlachojannis MD, PhD; Hiroyoshi Kawamoto, MD; Jors van der Sijde, MD; Cordula Felix, MD; Manuel Pan MD, PhD; Roberta Serdoz MD; Babu Ezhumalai, MD; Giacomo Giovanni Boccuzzi, MD; Boukhris Marouane, MD; Gennaro Sardella, MD; Alessio La Manna, MD; Corrado Tamburino MD, PhD; Pieter C. Smits MD, PhD; Nicolas M. van Mieghem MD, PhD; Carlo Di Mario MD, PhD; Ashok Seth, MD; Antonio Serra MD; Antonio Colombo MD; Alfredo R. Galassi, MD; Patrick Serruys MD, PhD; Felix Zijlstra MD, PhD; Roberto Diletti, MD

Submitted

ABSTRACT

Aims The bioresorbable vascular scaffolds (BVS) represent a novel therapeutic option for the treatment of coronary artery diseases. The objective of this study is to evaluate the feasibility and clinical outcomes following BVS deployment in complex chronic coronary total occlusions (CTO).

Methods and Results The present report is a multi-centre registry evaluating results after BVS implantation in challenging CTOs lesion defined as J-CTO score≥2 (difficult or very difficult).

A total of 105 patients were included in the present analysis. The mean J-CTO score was 2.61 (difficult 52.4%, very difficult 47.6%). Device-success and procedural-success were 98.1% and 97.1% respectively. Retrograde approach was used in 25.7% of the cases. After wire-crossing predilatation was performed in all cases with a mean predilatation balloon diameter of 2.69 ± 0.32 mm. The mean scaffold length was 59.75±25.85 mm, with postdilatation performed in 89.5 % of the cases and a mean postdilatation balloon diameter of 3.35±0.44 mm. Post-PCI minimal lumen diameter was 2.50±0.51 mm, percentage diameter stenosis was 14.53±10.31 %. Multislice CT scan was performed in a subgroup of patients (32.4 %) at 6-month post index-procedure and only in 2 cases was observed scaffold restenosis. At 6-month follow-up the MACE rate was 3.1%, with one case of late scaffold thrombosis at 47 days after index procedure. No case of mortality occurred.

Conclusions The present report suggests feasibility of BVS implantation in complex CTO lesion, given adequate lesion preparation and post-dilatation, with good acute angiographic results and mid-term clinical outcomes.

INTRODUCTION

Successful recanalization of chronic total occlusions (CTO) by percutaneous coronary intervention (PCI) has been associated with angina relief, improved left ventricular function,[1-3] reduction in the rate of myocardial infarction and coronary artery bypass grafting with an overall improved patient survival,[4-10] even in patients with well-developed collateral circulation.[10]

However, despite the recent advancement in techniques and materials, success rate for PCI in CTO is significantly lower compared to other lesion subsets[11, 12] and although the presence of CTO have been reported in a remarkable percentage of the patients with coronary artery disease undergoing elective angiography[13, 14] this lesion subset represents only a minority of the target lesion treated with PCI.[14, 15] In addition, CTOs are often long lesions requiring the implantation of multiple metallic stents resulting in a "full metal jacket" treated artery,[16] potentially increasing the risk of thrombosis and restenosis.[17]

Furthermore, many patients with CTO show extensive coronary disease, requiring multivessel revascularization,[5, 6, 8, 18] potentially benefiting from bypass graft surgery.

Given this background, the introduction of bioresorbable vascular scaffolds provides a novel therapeutic option for the treatment of chronic total occlusions, allowing revascularization without permanent caging of long coronary segments, potentially reducing the long term events related to the presence of metallic stents and maintaining the option for future surgical revascularizations.

Bioresorbable technologies have shown so far promising results in relatively simple coronary lesions,[19, 20] but there are very limited data and experience on the use of BVS in complex scenarios, especially in CTO lesions. Initial experience in this subgroup was reported in limited cohorts[21-23] with no specific evaluation of BVS performance in challenging CTO lesions.

Therefore, the objective of the present study is to evaluate the feasibility and mid-term BVS performance after implantation in coronary chronic occluded vessels presenting characteristics likely to make the procedure challenging according to the J-CTO score.[24]

METHODS

This is a multicentre single arm study conducted to evaluate the feasibility, procedural results and mid-term performance of the Absorb BVS (Abbott Vascular, Santa Clara, CA, USA) for the treatment of patients with complex CTO lesions.

Enrolled patients were male or female subjects presenting with silent ischemia, stable

angina pectoris or acute coronary syndromes, candidates for percutaneous treatment of coronary CTO lesions. Lesion difficulty was graded according to the J-CTO score, lesions defined as to be "easy" (J-CTO score 0) or at intermediate difficulty (J-CTO score 1) were excluded from the analysis and only complex cases defined as those with J-CTO score of ≥2 (difficult or very difficult)[24] were evaluated. Exclusion criteria comprised contraindications to antiplatelet medication, maximal vessel diameter > 4 mm, female patient with childbearing potential or currently breastfeeding and acute ST-segment elevation myocardial infarction.

Study device

The study device is the second generation Absorb BVS which is a balloon expandable scaffold with a polymer backbone of Poly-L lactide Acid (PLLA) coated with a thin layer of a 1:1 mixture of an amorphous matrix of Poly-D and L lactide acid (PDLLA) polymer, eluting 100 micrograms/cm2 of everolimus. Approximately 80% of the drug is eluted within the first 30-days. Two radiopaque platinum markers positioned at the ends of the scaffold allow for accurate visualization of the radiolucent Absorb BVS during angiography. Both PLLA and PDLLA are fully bioresorbable. The polymers are degraded via hydrolysis of the ester bonds, and the resulting lactate and its oligomers are quickly transformed to pyruvate and metabolized in the Krebs energy cycle. Small particles, less than 2μm in diameter, have also been shown to be phagocytized and degraded by macrophages. According to preclinical studies, the time for complete bioresorption of the polymer backbone is 2 to 3 years.

Study Procedure

All patients underwent PCI according to standard practice.[25, 26] Vascular access and either antegrade or retrograde approach (Figure 1, Figure 2,) were determined depending on anatomy and at operator discretion. Vessel sizing pre BVS implantation was conducted after intracoronary injection of nitroglycerine and only after confirmation of successful wire crossing into the true lumen either by contrast injection or intravascular ultrasound (IVUS). The Absorb BVS was deployed gradually in stepwise increments of 2 atm every 5 seconds.[27] If more than one BVS was necessary, they were implanted from the distal to the proximal part of the target vessel in a minimal marker-to-marker overlapping manner. IVUS was performed mainly for procedural guidance. After implantation, optical coherence tomography (OCT) was performed in a patient subgroup of 10 patients to assess scaffold expansion and incomplete strut apposition (ISA).

All patients were placed on a treatment regime of dual antiplatelet therapy for at least 12 months followed by lifelong aspirin.

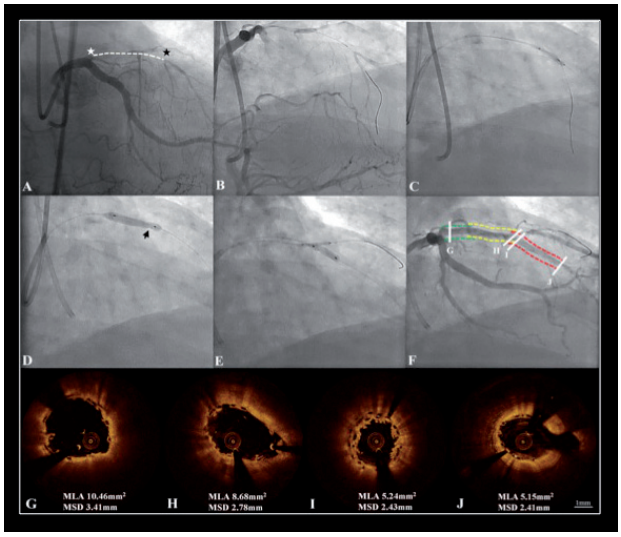

Figure 1. Successful implantation of bioresorbable vascular scaffolds using an antegrade strategy.
Occlusion length was 29.7mm and J-CTO score was 3. The lesion had a blunt stump (white star) with good distal landing zone (black star) (Panel A). Successful crossing was achieved with antegrade approach and confirmed with antegrade contrast injection (Panel B). Predilation (Panel C) was performed with a non-compliant 3.0mm balloon. Two BVS 3,5 x 18 mm and one 3.0 x 28mm were implanted in overlap (Black arrow) (Panel D). Final snuggle kissing balloon dilation was performed at the bifurcation (Panel E) with good angiographic result (Panel F). Optimal scaffold expansion and apposition was seen on Optical Coherence Tomograpy (OCT) post deployment. MLA- Minimal lumen area; MSD- Minimum scaffold diameter.

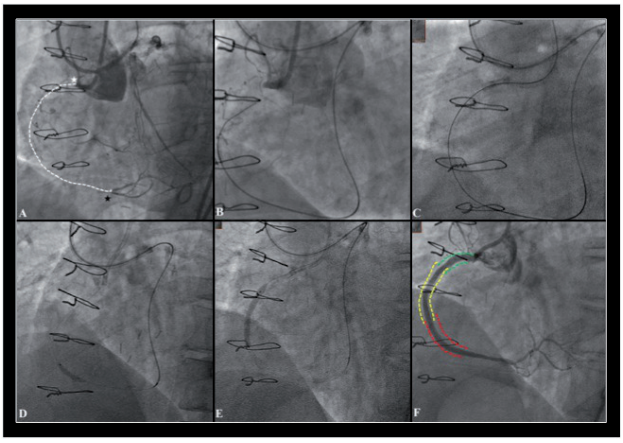

Figure 2. Successful implantation of bioresorbable vascular scaffolds in a right coronary artery with a chronic total occlusion using a retrograde strategy.
The lesion had a blunt stump (white star) with good distal landing zone (black star) (Panel A). Good septal collaterals were seen from contralateral contrast injection. Successful crossing was achieved with a Conquest ProTM wire on CorsairTM microcatheter support (Panel B and C). Predilation (Panel D) was performed before scaffolds deployment (two BVS 3,5 x 28mm and one 3.0 x 28mm in an overlap) (Panel E) with good angiographic result (Panel F).

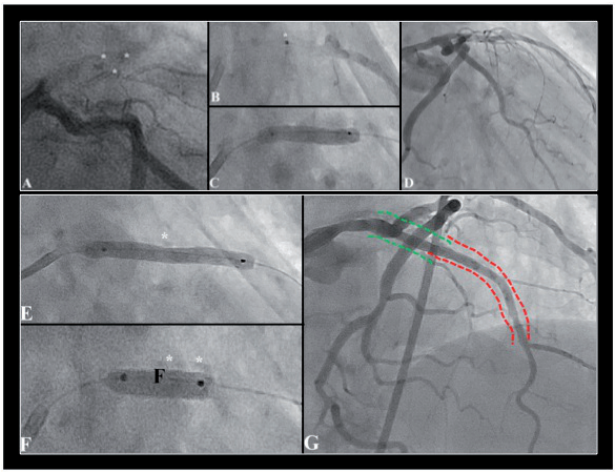

Figure 3. BVS implantation in a calcified chronic total occlusion using an antegrade strategy.
The lesion had a blunt proximal stump and multiple calcifications (marked *) (Panel A). J-CTO score was 2. Successful wire crossing was achieved with antegrade approach and confirmed with antegrade contrast injection (Panel B). Predilation was performed with a 3.0 x 20 mm semi-compliant balloon at maximum inflation pressure of 16 atm (Panel C). Panel D shows the left anterior descending artery after predilation BVS before implantation. Two scaffolds (BVS 3.5 x 28mm and 2.5 x 28mm were deployed in overlap) and postdilated with a non-compliant balloon 3.5 x 12mm (Panel F) with good final angiographic result (Panel G- dashed lines indicating scaffolds location)

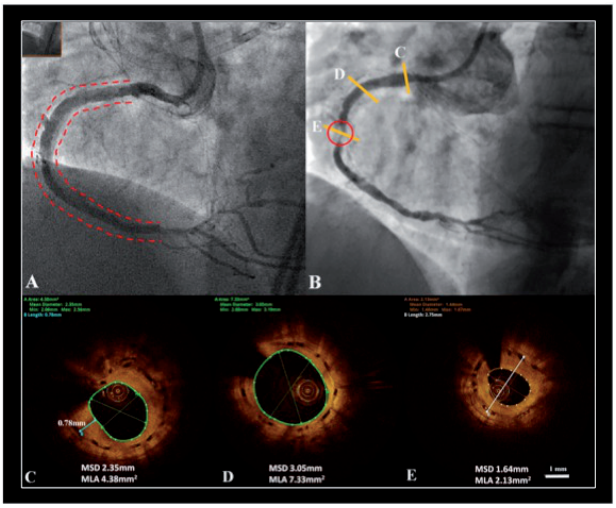

Figure 4. Subintimal BVS implantation.
Final result at the index procedure after subintimal tracking, true lumen re-entry and subintimal BVS implantation (Panel A). 2-year angiographic appearance (Panel B) with an in-scaffold restenosis (circled area). Panel D and E long-term vascular healing after BVS subintimal implantation. Panel C in-scaffold restenosis. MSD- Mean scaffold Diameter MLA- Mean lumen area.

Quantitative coronary angiography

Quantitative coronary angiography (QCA) analyses were performed using the Coronary Angiography Analysis System (Pie Medical Imaging, Maastricht, Netherlands). The QCA measurements we performed pre and post BVS implantation. Angiographic views with minimal foreshortening of the lesion and limited overlap with other vessels were used. Pre-procedure QCA analysis was performed as proximally as possible from the occlusion (in case of a side branch, distally to the most proximal take off of the side branch) as already described.[28] For each lesion, the following QCA parameters were measured in diastole: minimal lumen diameter (MLD), reference vessel diameter (RVD), percentage of area stenosis, and occlusion length. For each lesion, was computed the J-CTO score which has been shown to correlate well with lesion complexity and procedural outcomes.

OCT image acquisition and analysis

The C7 system or the Ilumien Optis system and the corresponding DragonFly or DragonFly Duo imaging catheters (St. Jude Medical, St Paul, Minneapolis, Minnesota) were used for image acquisition. The OCT catheter was advanced distal to the treated segment, and an automated pullback was performed at 20mm/s with simultaneous contrast injection at a rate of 3 to 4 ml/s using a power injector. Two sequential pullbacks were performed to enable assessment of the entire scaffolded/ stented segment when required.

The OCT measurements were performed offline using the QCU-CMS software, (Medis Medical Imaging Systems, Leiden, The Netherlands). Analysis was performed at 1-mm intervals within the entire scaffolded segment and proximal and distal edge segments. Lumen and scaffold area and diameter measurements were performed in the region of interest, as appropriate, (Figure 4) using standard methodology for the analysis of bioresorbable scaffolds.[28-30] Eccentricity index and Symmetry index were additionally calculated as previously reported.[31-33]

Study definitions

Device Success was defined as successful BVS implantation with the attainment of <30% final in segment residual stenosis by angiographic visual estimation after Absorb BVS implantation. Procedure Success was defined as device success and no major peri-procedural complications (Emergent CABG, coronary perforation requiring pericardial drainage, residual dissection impairing vessel flow – TIMI-flow II or less). Clinical success was defined as procedural success and no in-hospital major adverse cardiac events (MACE). All deaths were considered cardiac unless an undisputed non-cardiac cause was identified. Myocardial infarction (MI) and scaffold thrombosis were defined according to the Academic Research Consortium (ARC) definition.[34] Any Target lesion revascularization

(TLR) was defined as clinically driven if at repeat angiography a diameter stenosis >70% was observed, or if a diameter stenosis >50% was present in association with recurrent angina pectoris; objective signs of ischaemia (ECG changes) at rest or during exercise test, likely to be related to the target vessel; abnormal results of any invasive functional diagnostic test.
Major adverse cardiac events (MACE) was defined as the composite of cardiac death, any re-infarction (Q or Non Q-Wave), emergent bypass surgery (CABG), or clinically driven target lesion revascularization (TLR).

Statistical Analysis

Categorical variables are reported as counts and percentages and continuous variables are reported as mean ± standard deviation. Statistical analyses were performed using SPSS, version 20.0 for Windows (IL,US).

RESULTS

Patient demographics

Baseline demographics of the patients (n=105) are presented in Table 1. Mean age was 59.40 ± 8.96, 89.5 % of the patients were male, 33.3% had diabetes mellitus, 68.6 % presented with stable angina.

Angiographic and lesion characteristics

The most frequently treated vessel was the right coronary artery (44.8%), 35.2% of the CTO were located at the proximal/ostial coronary segment, 28.6% cases involved a bifurcation lesion with aside branch ≥ 2 mm and 56.2% of the cases showed a multivessel disease, 74.3% of the lesions had occlusion length ≥ 20 mm and 43.8% bridging collaterals at the level of the occlusion. Rentrop grade 3 collaterals were present in 29.5% of the lesions.
The mean J-CTO score was 2.61 with nearly half (47.6 %) of the CTO lesions being very difficult (J-CTO score ≥3). (Table 2)
Quantitative coronary angiography showed a Pre-treatment reference vessel diameter of 2.71 ± 0.55 mm, Post-PCI mean MLD of 2.50 ± 0.51 mm with a percentage diameter stenosis of 14.53 ± 10.31%. (Table 2)

Procedural Characteristics

Procedural characteristics are shown in Table 3. The majority of the cases (62.9%) were performed with a bi-femoral approach with a frequent use of contralateral injection.

Table 1. Baseline Demographic and Clinical Characteristics.

	n=105
Age, yrs	59.40 ± 8.96
Male gender %	89.5
History of smoking%	48.6
Diabetes mellitus%	33.3
Dyslipidemia%	72.4
Hypertension%	69.5
Family History of CAD%	21.9
Myocardial Infarct%	29.5
Prior PCI%	46.7
Prior CABG%	2.9
Silent ischemia%	5.7
Stable angina%	68.6
Acute coronary syndrome%	23.8
Congestive cardiac failure%	1.9

Values specified as percentages or mean with standard deviation. CAD=coronary artery disease, PCI=percutaneous coronary intervention, CABG= coronary artery bypass graft

Table 2. Baseline Lesion and Angiographic Characteristics.

	n=105
Left anterior descending artery%	41.9
Left circumflex/ marginal%	12.4
Right coronary artery%	44.8
Ostial-proximal %	35.2
Mid%	61.9
Distal%	2.8
Bifurcation %	28.6
Single vessel disease%	43.8
Two-vessel disease%	40.0
Three-vessel disease%	16.2
Severe tortuosity%	26.7
Blunt stump%	60.0
Calcification present%	70.5
Bending > 45 degrees%	49.5
Occlusion ≥ 20mm%	74.3
Retry lesion%	11.4
(Any) Side branch present%	65.7

Table 2. Continued.

	n=105
(Any) Bridge collateral present%	43.8
Rentrop grade 3 collateral%	29.5
Bad landing zone%	34.3
Bad distal vessel%	26.7
CTO J-score%	2.61 ± 0.75
Easy (J-CTO score 0) %	0
Intermediate (J-CTO score 1) %	0
Difficult (J-CTO score 2) %	52.4
Very Difficult (J-CTO score ≥3) %	47.6
J-CTO score 3	37.1
J-CTO score 4	7.6
J-CTO score 5	2.9
Pretreatment reference vessel diameter, mm	2.71 ± 0.55
Pretreatment Diameter stenosis, %	100,0
Post-treatment minimal lumen diameter, mm	2.50 ± 0.51
Post-treatment reference vessel diameter, mm	2.88 ± 0.51
Post-treatment diameter stenosis, %	14.53 ± 10.31

Values specified as percentages or mean with standard deviation.

Successful lesion crossing with retrograde strategy occurred in 25.7% of the procedures. Predilatation was performed in every lesion with a mean predilatation balloon diameter of 2.69 ± 0.32 mm. Guide-wires used for successful crossing included the Conquest Pro 9/12 (12.4%), Gaia First/ Second/ Third (11.4%), Miracle Bros 3/6 (8.6%) and Pilot 150/200 (19.0%). A total of 256 BVS were implanted with a mean number of scaffolds implanted per lesion equal to 2.44 ± 1.12, with 79 overlaps, a total scaffold length per lesion of 59.75 ± 25.85 mm and a mean scaffold diameter per lesion of 3.00 ± 0.31 mm. Postdilation was performed in 89.5% of the cases.

OCT measurements Post scaffold deployment

Post scaffold deployment imaging of the scaffolds with the use of OCT was performed in 10 cases (18.2%). Mean lumen area was 7.31± 1.28 mm^2, with a minimum lumen area 5.35 ±1.53 mm^2 and residual area stenosis of 6.83 ± 26.44%. Mean ISA area was 0.03 ± 0.04 mm^2. Mean eccentricity index 0.86 ± 0.04 and symmetry index was 0.37 ±0.10. (Table 4)

Clinical Outcomes

Device success and procedural success were 98.1% and 97.1% respectively. During the index procedure two patients required bailout stenting with metal stents and in one case was observed a final TIMI II flow. No other major peri-procedural complications such as

Table 3. Procedural Characteristics.

	n=105
Vascular access	
Single access, femoral	22.8
Single access, radial	9.5
Double access, femoral and radial	4.8
Double access, both femoral	62.9
Contralateral injection	63.8
Intravascular imaging	
Intravascular ultrasound	55.2
Optical coherence tomography	9.5
Successsful antergrade strategy	74.3
Successsful Retrograde strategy	25.7
Number of guidewires used per lesion	3.27 ± 1.69
Guidewire or CTO Devices used for crossing	
Conquest Pro 9/12	12.4
Fielder XT-R/FC	23.8
Gaia First/ Second/ Third	11.4
Miracle Bros 3/6	8.6
Pilot 150/200	19.0
Sion/Sion Black/ Sion Blue	6.7
Ultimate Bro	5.7
BMW	1.9
CrossIT 100/200 XT/ Progress	8.6
Whisper	1.9
Predilation performed	100
Use of OTW balloon	8.6
Microcatheters used	85.7
Cutting balloon/ rotation artherectomy (11/1)	11.4
Maximum predilation balloon diameter, mm	2.73 ± 0.43
Maximum predilation pressure, atm	14.97 ± 2.72
Total number of scaffolds imganted	256
Number of scaffolds per lesion	2.44± 1.12
Overlapping scaffolds	79.0
Total scaffold length per lesion, mm	59.75 ± 25.85
Mean scaffold diameter per lesion, mm	3.00 ± 0.31
Maximum scaffold implantation pressure, atm	13.82 ± 2.93
Postdilation performed	89.5
Maximum postdilation balloon diameter, mm	3.35 ± 0.44

Table 3. Continued.

	n=105
Procedure time, min	167.06 ± 78.28
Fluroscopy time, min	60.95 ± 35.16
Contrast volume, mls	334.63 ± 138.01
Antiplatelet therapy	
Aspirin	100.0
Clopidogrel	47.6
Prasugrel	28.6
Ticagrelor	23.8

OTW- over the wire. Values specified as percentages or mean with standard deviation.

Table 4. Optical Coherence Tomography Measurements post scaffold deployment.

	n=10
Analyzed length/mm	36.64 ±11.64
Reference lumen area/mm^2	6.00 ± 1.88
Minimum lumen area/mm^2	5.35 ±1.53
Mean lumen area/mm^2	7.31 ±1.28
Lumen volume/mm^3	254.02 ± 79.47
Maximum scaffold diameter/mm	3.85 ± 0.45
Minimum scaffold diameter/mm	2.42 ± 0.32
MSA/mm^2	5.84 ±1.31
Mean scaffold area/mm^2	7.71 ±1.37
Scaffold volume/mm^3	268.81 ± 93.51
RAS/%	6.83 ± 26.44
EI	0.86 ± 0.04
EI at MSA	0.84 ±0.06
SI	0.37 ±0.10
Device with ISA detected	6
Mean ISA area/mm^2	0.03 ± 0.04
Total struts	3,387
Malapposed struts	39
Mean prolapse area/mm^2	0.53 ± 0.42
Edge Dissection	8 (80.0)

EI-Eccentricity index
ISA-Incomplete strut apposition
MSA- Minimum scaffold area
RAS-Residual area stenosis
SI- Symmetricity index
Values are expressed as mean ± standard deviation.

scaffold thrombosis were reported. No episodes of severe in hospital adverse events were observed.

The 6-month follow up was completed in 91.4% of the cases. One patient developed late scaffold thrombosis at 47 days post-procedure. The patient had 3 Absorb BVS scaffolds (3.0 x 28mm; 3.5 x 18mm and 3.5 x 18mm in an overlapping manner) implanted in the left anterior descending artery CTO (J-CTO score 3). The lesion was predilated with a 3.0mm balloon and postdilated with a 3.5mm noncompliant balloon. He presented with a Non ST-segment Elevation Myocardial Infarct, the coronary angiogram showed scaffold thrombosis involving the treated artery and further PCI was performed (thrombectomy, implantation of a drug eluting metal stent and intravenous infusion of eptifibatide). Two additional clinically driven target lesion revascularisations were reported, one of those was performed after observation by CT scan of re-occlusion of the 3.0 x 28mm Absorb BVS scaffold previously implanted in the left circumflex artery the patient was symptomatic and a treatment was carried out at 6 months post-procedure with a metallic drug eluting stent. No cases of mortality were seen. The overall MACE rate was therefore 3.1%

Computed Tomography scans were performed at 6 months in 34 patients, only in two cases was observed scaffold restenosis. After clinical re-evaluation of these two patients, 1 case (above-mentioned) underwent TLR whereas the other case give the absence of symptoms and of inducible ischemia was managed conservatively.

DISCUSSION

Coronary chronic total occlusions are classically regarded as a challenging subset burdened by low procedural success and poorer clinical outcomes when compared to other lesion types. Even though the introduction of drug eluting stents has reduced the rate of in-stent restenosis, the adoption of these devices is not devoid of limitations especially in chronically occluded vessels.

Treatment of CTOs often implies stenting of long coronary segments with permanent vessel caging of large part of the artery. This is not only associated with a possible increased risk of restenosis and stent thrombosis, but is also precluding future surgical revascularizations in patients that often show diffuse and multivessel atherosclerosis as also confirmed in the present report with 56.2% of the patients having multivessel disease. In addition after recanalization of CTOs, a flow-dependent positive vascular remodeling process has been reported and has been associated with progressive increase in lumen diameter, external elastic membrane (EEM) diameter, lumen area and EEM area.[35-37] Park and colleagues[35] reported that this increase in lumen dimensions is followed by an

increased incomplete stent apposition at 6-month follow-up in patients treated for CTO lesions. Theoretically, the bioresorption process could eliminate this limitation as the scaffold remnants can follow the vessel wall motion already between six months and one year after implantation.[20]

Recently, small series of CTOs treated with BVS with slightly lower lesion complexity has been reported, with outcomes comparable to ours.[21-23] The present investigation focused specifically on complex chronically occluded coronary lesions, excluding all cases scored as easy or intermediately difficult according to de J-CTO score, with nearly half of the occlusions defined as very difficult. Our data suggests feasibility of BVS implantation also in the challenging subset of complex CTO lesions, with optimal acute scaffold expansion and apposition given an appropriate lesion preparation and a high rate of final postdilatation. The final angiographic results showed a post-PCI minimal lumen diameter of 2.50 ± 0.55 with a very low percentage diameter stenosis (14.53 ± 10.31 %) associated with a final TIMI 3 flow achieved practically in the entire population. Such promising acute results are in line with angiographic data obtained in previous reports evaluating the BVS as well as metallic DES implantation in CTO lesions[21, 23, 38]

These data were obtained after an aggressive lesion predilatation with maximum balloon diameter close to the reference vessel diameter and to the nominal scaffold diameter. Postdilatation was performed in a large number of cases with balloons bigger than the nominal scaffold diameter (up to 0.5 mm exceeding the scaffold diameter). This approach translated also into an optimal device apposition with a very low incomplete scaffold apposition area as assessed by OCT and facilitated optimal scaffold expansion. On this regard, a common concern when hypothesising the use of BVS in CTO lesion is the fact that the presence of diffusely diseased vessels with extensive calcifications may affect the scaffold expansion. In the present investigation was observed a mean scaffold eccentricity and symmetry index resembling results previously reported for BVS and for metal DES in non-chronically occluded vessels.[31-33] These findings suggest that the concern on BVS optimal expansion in CTO lesions might not be justified if an appropriate lesion preparation and scaffold postdilatation is performed. (Figure 3)

The encouraging angiographic results were followed by mid-term clinical outcomes showing an overall survival and target lesion revascularisation comparable the everolimus eluting stent in CTO lesions.[39] However, given the limited number of patients and the low event rate this data should be considered as simply descriptive and hypothesis generating. A current limitation of the bioresorbable technology is the high strut thickness that could be associated with a delayed vascular healing and endothelialisation especially at the site of the overlap. In addition the larger profile of this device compared with last generation metallic DES could represent an important obstacle when approaching tortuous, calcified

vessels. Technical scaffold improvement such as new delivery systems, reduction in strut thickness and in the crossing profile, are awaited for an improvement of the current device performance.
Our results support feasibility of BVS implantation in CTO lesion even in complex scenarios, the theoretical advantages of this new technology need to be evaluated in further larger studies focused on direct comparison with standard metal drug eluting stents and analysing angiographic, intravascular imaging and clinical results at long-term follow-up.

Limitations

This is a single arm retrospective study, as such procedural and clinical outcomes cannot be directly compared with lesions treated with drug eluting metallic stents. Given the limited number of patients and the low rate of events clinical outcomes data should be considered as purely descriptive and hypothesis generating. The BVS was used as per operator discretion, this methodology may be source of selection bias. The number of OCT performed in the present study is very limited and results should be considered as descriptive and hypothesis generating.

CONCLUSION

The findings provided by the present investigation suggest feasibility of BVS implantation for treatment of complex CTO lesions. In this setting, good procedural and mid term clinical outcomes may be achieved given adequate lesion preparation and scaffold postdilatation.

Clinical Implications

Our seminal observations suggest feasibility of bioresorbable scaffold implantation in patients with chronic total occlusion and complex anatomies supporting an expansion of the BVS use also in this setting, potentially extending the theoretical advantages of this novel technology. Optimal antiplatelet regimen, accurate comparison with the current generation metallic DES and long-term performance remain to be evaluated.

REFERENCES

1. Sirnes PA, Myreng Y, Molstad P, Bonarjee V, Golf S. Improvement in left ventricular ejection fraction and wall motion after successful recanalization of chronic coronary occlusions. Eur Heart J 1998;19(2):273-81.
2. Chung CM, Nakamura S, Tanaka K, Tanigawa J, Kitano K, Akiyama T, Matoba Y, Katoh O. Effect of recanalization of chronic total occlusions on global and regional left ventricular function in patients with or without previous myocardial infarction. Catheter Cardiovasc Interv 2003;60(3):368-74.
3. Chadid P, Markovic S, Bernhardt P, Hombach V, Rottbauer W, Wohrle J. Improvement of regional and global left ventricular function in magnetic resonance imaging after recanalization of true coronary chronic total occlusions. Cardiovasc Revasc Med 2015.
4. George S, Cockburn J, Clayton TC, Ludman P, Cotton J, Spratt J, Redwood S, de Belder M, de Belder A, Hill J, Hoye A, Palmer N, Rathore S, Gershlick A, Di Mario C, Hildick-Smith D, British Cardiovascular Intervention S, National Institute for Cardiovascular Outcomes R. Long-term follow-up of elective chronic total coronary occlusion angioplasty: analysis from the U.K. Central Cardiac Audit Database. J Am Coll Cardiol 2014;64(3):235-43.
5. Hoye A, van Domburg RT, Sonnenschein K, Serruys PW. Percutaneous coronary intervention for chronic total occlusions: the Thoraxcenter experience 1992-2002. Eur Heart J 2005;26(24):2630-6.
6. Suero JA, Marso SP, Jones PG, Laster SB, Huber KC, Giorgi LV, Johnson WL, Rutherford BD. Procedural outcomes and long-term survival among patients undergoing percutaneous coronary intervention of a chronic total occlusion in native coronary arteries: a 20-year experience. J Am Coll Cardiol 2001;38(2):409-14.
7. Aziz S, Stables RH, Grayson AD, Perry RA, Ramsdale DR. Percutaneous coronary intervention for chronic total occlusions: improved survival for patients with successful revascularization compared to a failed procedure. Catheter Cardiovasc Interv 2007;70(1):15-20.
8. Valenti R, Migliorini A, Signorini U, Vergara R, Parodi G, Carrabba N, Cerisano G, Antoniucci D. Impact of complete revascularization with percutaneous coronary intervention on survival in patients with at least one chronic total occlusion. Eur Heart J 2008;29(19):2336-42.
9. Christakopoulos GE, Christopoulos G, Carlino M, Jeroudi OM, Roesle M, Rangan BV, Abdullah S, Grodin J, Kumbhani DJ, Vo M, Luna M, Alaswad K, Karmpaliotis D, Rinfret S, Garcia S, Banerjee S, Brilakis ES. Meta-analysis of clinical outcomes of patients who underwent percutaneous coronary interventions for chronic total occlusions. Am J Cardiol 2015;115(10):1367-75.
10. Jang WJ, Yang JH, Choi SH, Song YB, Hahn JY, Choi JH, Kim WS, Lee YT, Gwon HC. Long-term survival benefit of revascularization compared with medical therapy in patients with coronary chronic total occlusion and well-developed collateral circulation. JACC Cardiovasc Interv 2015;8(2):271-9.
11. Abbott JD, Kip KE, Vlachos HA, Sawhney N, Srinivas VS, Jacobs AK, Holmes DR, Williams DO. Recent trends in the percutaneous treatment of chronic total coronary occlusions. Am J Cardiol 2006;97(12):1691-6.
12. Prasad A, Rihal CS, Lennon RJ, Wiste HJ, Singh M, Holmes DR, Jr. Trends in outcomes after percutaneous coronary intervention for chronic total occlusions: a 25-year experience from the Mayo Clinic. J Am Coll Cardiol 2007;49(15):1611-8.
13. Fefer P, Knudtson ML, Cheema AN, Galbraith PD, Osherov AB, Yalonetsky S, Gannot S, Samuel M, Weisbrod M, Bierstone D, Sparkes JD, Wright GA, Strauss BH. Current perspectives on coronary chronic total occlusions: the Canadian Multicenter Chronic Total Occlusions Registry. J Am Coll Cardiol 2012;59(11):991-7.
14. Christofferson RD, Lehmann KG, Martin GV, Every N, Caldwell JH, Kapadia SR. Effect of chronic total coronary occlusion on treatment strategy. Am J Cardiol 2005;95(9):1088-91.

15. Kahn JK. Angiographic suitability for catheter revascularization of total coronary occlusions in patients from a community hospital setting. Am Heart J 1993;126(3 Pt 1):561-4.
16. Sharp AS, Latib A, Ielasi A, Larosa C, Godino C, Saolini M, Magni V, Gerber RT, Montorfano M, Carlino M, Michev I, Chieffo A, Colombo A. Long-term follow-up on a large cohort of "full-metal jacket" percutaneous coronary intervention procedures. Circ Cardiovasc Interv 2009;2(5):416-22.
17. Moreno R, Fernandez C, Hernandez R, Alfonso F, Angiolillo DJ, Sabate M, Escaned J, Banuelos C, Fernandez-Ortiz A, Macaya C. Drug-eluting stent thrombosis: results from a pooled analysis including 10 randomized studies. J Am Coll Cardiol 2005;45(6):954-9.
18. Olivari Z, Rubartelli P, Piscione F, Ettori F, Fontanelli A, Salemme L, Giachero C, Di Mario C, Gabrielli G, Spedicato L, Bedogni F, Investigators T-G. Immediate results and one-year clinical outcome after percutaneous coronary interventions in chronic total occlusions: data from a multicenter, prospective, observational study (TOAST-GISE). J Am Coll Cardiol 2003;41(10):1672-8.
19. Serruys PW, Chevalier B, Dudek D, Cequier A, Carrie D, Iniguez A, Dominici M, van der Schaaf RJ, Haude M, Wasungu L, Veldhof S, Peng L, Staehr P, Grundeken MJ, Ishibashi Y, Garcia-Garcia HM, Onuma Y. A bioresorbable everolimus-eluting scaffold versus a metallic everolimus-eluting stent for ischaemic heart disease caused by de-novo native coronary artery lesions (ABSORB II): an interim 1-year analysis of clinical and procedural secondary outcomes from a randomised controlled trial. Lancet 2015;385(9962):43-54.
20. Serruys PW, Onuma Y, Dudek D, Smits PC, Koolen J, Chevalier B, de Bruyne B, Thuesen L, McClean D, van Geuns RJ, Windecker S, Whitbourn R, Meredith I, Dorange C, Veldhof S, Hebert KM, Sudhir K, Garcia-Garcia HM, Ormiston JA. Evaluation of the second generation of a bioresorbable everolimus-eluting vascular scaffold for the treatment of de novo coronary artery stenosis: 12-month clinical and imaging outcomes. J Am Coll Cardiol 2011;58(15):1578-88.
21. Vaquerizo B, Barros A, Pujadas S, Bajo E, Estrada D, Miranda-Guardiola F, Rigla J, Jimenez M, Cinca J, Serra A. Bioresorbable everolimus-eluting vascular scaffold for the treatment of chronic total occlusions: CTO-ABSORB pilot study. EuroIntervention 2014.
22. Wiebe J, Liebetrau C, Dorr O, Most A, Weipert K, Rixe J, Bauer T, Mollmann H, Elsasser A, Hamm CW, Nef HM. Feasibility of everolimus-eluting bioresorbable vascular scaffolds in patients with chronic total occlusion. Int J Cardiol 2015;179:90-4.
23. Ojeda S, Pan M, Romero M, Suarez de Lezo J, Mazuelos F, Segura J, Espejo S, Morenate C, Blanco M, Martin P, Medina A, Suarez de Lezo J. Outcomes and Computed Tomography Scan Follow-Up of Bioresorbable Vascular Scaffold for the Percutaneous Treatment of Chronic Total Coronary Artery Occlusion. Am J Cardiol 2015.
24. Morino Y, Abe M, Morimoto T, Kimura T, Hayashi Y, Muramatsu T, Ochiai M, Noguchi Y, Kato K, Shibata Y, Hiasa Y, Doi O, Yamashita T, Hinohara T, Tanaka H, Mitsudo K, Investigators JCR. Predicting successful guidewire crossing through chronic total occlusion of native coronary lesions within 30 minutes: the J-CTO (Multicenter CTO Registry in Japan) score as a difficulty grading and time assessment tool. JACC Cardiovasc Interv 2011;4(2):213-21.
25. Authors/Task Force m, Windecker S, Kolh P, Alfonso F, Collet JP, Cremer J, Falk V, Filippatos G, Hamm C, Head SJ, Juni P, Kappetein AP, Kastrati A, Knuuti J, Landmesser U, Laufer G, Neumann FJ, Richter DJ, Schauerte P, Sousa Uva M, Stefanini GG, Taggart DP, Torracca L, Valgimigli M, Wijns W, Witkowski A. 2014 ESC/EACTS Guidelines on myocardial revascularization: The Task Force on Myocardial Revascularization of the European Society of Cardiology (ESC) and the European Association for Cardio-Thoracic Surgery (EACTS) Developed with the special contribution of the European Association of Percutaneous Cardiovascular Interventions (EAPCI). Eur Heart J 2014;35(37):2541-619.
26. Di Mario C, Werner GS, Sianos G, Galassi AR, Buttner J, Dudek D, Chevalier B, Lefevre T, Schofer J, Koolen J, Sievert H, Reimers B, Fajadet J, Colombo A, Gershlick A, Serruys PW, Reifart N. European perspective in the recanalisation of Chronic Total Occlusions (CTO): consensus document from the EuroCTO Club. EuroIntervention 2007;3(1):30-43.

27. Tamburino C, Latib A, van Geuns RJ, Sabate M, Mehilli J, Gori T, Achenbach S, Pan Alvarez M, Nef H, Lesiak M, Di Mario C, Colombo A, Naber CK, Caramanno G, Capranzano P, Brugaletta S, Geraci S, Araszkiewicz A, Mattesini A, Pyxaras SA, Rzeszutko L, Depukat R, Diletti R, Boone E, Capodanno D, Dudek D. Contemporary practice and technical aspects in coronary intervention with bioresorbable scaffolds: a European perspective. EuroIntervention 2015;10(10).
28. Diletti R, Karanasos A, Muramatsu T, Nakatani S, Van Mieghem NM, Onuma Y, Nauta ST, Ishibashi Y, Lenzen MJ, Ligthart J, Schultz C, Regar E, de Jaegere PP, Serruys PW, Zijlstra F, van Geuns RJ. Everolimus-eluting bioresorbable vascular scaffolds for treatment of patients presenting with ST-segment elevation myocardial infarction: BVS STEMI first study. Eur Heart J 2014;35(12):777-86.
29. Serruys PW, Onuma Y, Ormiston JA, de Bruyne B, Regar E, Dudek D, Thuesen L, Smits PC, Chevalier B, McClean D, Koolen J, Windecker S, Whitbourn R, Meredith I, Dorange C, Veldhof S, Miquel-Hebert K, Rapoza R, Garcia-Garcia HM. Evaluation of the second generation of a bioresorbable everolimus drug-eluting vascular scaffold for treatment of de novo coronary artery stenosis: six-month clinical and imaging outcomes. Circulation 2010;122(22):2301-12.
30. Garcia-Garcia HM, Serruys PW, Campos CM, Muramatsu T, Nakatani S, Zhang YJ, Onuma Y, Stone GW. Assessing bioresorbable coronary devices: methods and parameters. JACC Cardiovasc Imaging 2014;7(11):1130-48.
31. Mattesini A, Secco GG, Dall'Ara G, Ghione M, Rama-Merchan JC, Lupi A, Viceconte N, Lindsay AC, De Silva R, Foin N, Naganuma T, Valente S, Colombo A, Di Mario C. ABSORB biodegradable stents versus second-generation metal stents: a comparison study of 100 complex lesions treated under OCT guidance. JACC Cardiovasc Interv 2014;7(7):741-50.
32. Brugaletta S, Gomez-Lara J, Diletti R, Farooq V, van Geuns RJ, de Bruyne B, Dudek D, Garcia-Garcia HM, Ormiston JA, Serruys PW. Comparison of in vivo eccentricity and symmetry indices between metallic stents and bioresorbable vascular scaffolds: insights from the ABSORB and SPIRIT trials. Catheter Cardiovasc Interv 2012;79(2):219-28.
33. Shaw E, Allahwala UK, Cockburn JA, Hansen TC, Mazhar J, Figtree GA, Hansen PS, Bhindi R. The effect of coronary artery plaque composition, morphology and burden on Absorb bioresorbable vascular scaffold expansion and eccentricity - A detailed analysis with optical coherence tomography. Int J Cardiol 2015;184:230-6.
34. Cutlip DE, Windecker S, Mehran R, Boam A, Cohen DJ, van Es GA, Steg PG, Morel MA, Mauri L, Vranckx P, McFadden E, Lansky A, Hamon M, Krucoff MW, Serruys PW, Academic Research C. Clinical end points in coronary stent trials: a case for standardized definitions. Circulation 2007;115(17):2344-51.
35. Park JJ, Chae IH, Cho YS, Kim SW, Yang HM, Seo JB, Kim SY, Oh IY, Yoon CH, Suh JW, Park KW, Chung WY, Youn TJ, Choi DJ, Kim HS. The recanalization of chronic total occlusion leads to lumen area increase in distal reference segments in selected patients: an intravascular ultrasound study. JACC Cardiovasc Interv 2012;5(8):827-36.
36. Gomez-Lara J, Teruel L, Homs S, Ferreiro JL, Romaguera R, Roura G, Sanchez-Elvira G, Jara F, Brugaletta S, Gomez-Hospital JA, Cequier A. Lumen enlargement of the coronary segments located distal to chronic total occlusions successfully treated with drug-eluting stents at follow-up. EuroIntervention 2014;9(10):1181-8.
37. Galassi AR, Tomasello SD, Crea F, Costanzo L, Campisano MB, Marza F, Tamburino C. Transient impairment of vasomotion function after successful chronic total occlusion recanalization. J Am Coll Cardiol 2012;59(8):711-8.
38. Colmenarez HJ, Escaned J, Fernandez C, Lobo L, Cano S, del Angel JG, Alfonso F, Jimenez P, Banuelos C, Gonzalo N, Garcia E, Hernandez R, Macaya C. Efficacy and safety of drug-eluting stents in chronic total coronary occlusion recanalization: a systematic review and meta-analysis. J Am Coll Cardiol 2010;55(17):1854-66.

39. Kandzari DE, Kini AS, Karmpaliotis D, Moses JW, Tummala PE, Grantham JA, Orr C, Lombardi W, Nicholson WJ, Lembo NJ, Popma JJ, Wang J, Larracas C, Rutledge DR. Safety and Effectiveness of Everolimus-Eluting Stents in Chronic Total Coronary Occlusion Revascularization: Results From the EXPERT CTO (Evaluation of the XIENCE Coronary Stent, Performance, and Technique in Chronic Total Occlusions) Multicenter Trial. JACC Cardiovasc Interv 2015.

Summary & Conclusions

ASSESSMENT OF CORONARY ATHEROSCLEROSIS WITH INTRAVASCULAR IMAGING

The understanding of the atherosclerotic process is fundamental to achieve an adequate treatment of the coronary artery disease. The first part of the present thesis is focused on the characterisation of the coronary plaques using intravascular imaging; the use of such technologies allows us to assess the plaques characteristics and composition. In particular the combination of different imaging modalities (i.e. intravascular ultrasound virtual histology and optical coherence tomography) could be appropriate to fully investigate lesion vulnerability.

Plaque rupture and subsequent activation of the clotting cascade resulting in sudden intraluminal

thrombosis are thought to be the most frequent cause of acute coronary syndromes.[1, 2]

In pathology, precursor lesions, known as thin-cap fibroatheromas (TCFA), are characterized by a large pool of necrotic core covered by a thin fibrous cap <65 μm^3. The resolution of current intravascular ultrasound (IVUS) systems (100 to 200 μm) constitutes an important limitation of this technique for the measurement of fibrous cap thickness. On the other hand, optical coherence tomography (OCT), has higher resolution (10 to 20 μm) but low signal penetration.[4] Therefore, combining the two imaging modalities might provide a more accurate method to investigate TCFAs[5, 6]

In addition the full understanding of the plaque morphology and composition may guide the appropriate strategy when treating coronary lesions. The presence of a large amount of circumferential calcium could be the underlying reason to initiate a coronary intervention with an aggressive lesion preparation approach (i.e. rotablation, cutting balloon, high pressure non compliant ballooning). Such information maybe of paramount importance especially when implanting bioresorbable devices, as an optimal lesion preparation and scaffold deployment has been identified as key factors to facilitate good angiographic results and clinical outcomes.

Continuous developments in invasive and non-invasive imaging allow a detailed visualization of coronary pathology, considerably increasing our knowledge about plaque growth and rupture while prospective natural history of atherosclerosis studies observed a link between plaque morphology and future clinical outcomes.[7]

However, the invasive treatment of a potential culprit lesion in asymptomatic patients can be justified only if stent implantation is completely safe. Initial reports demonstrated an unacceptable high risk of complications in non flow limiting lesions treated with balloon angioplasty or bare metal stents, whereas the new developments in stent design may have reduced the risk of complications, but they have not eradicated them.[8]

The alteration of vessel wall physiology as well as the risk of neoatherosclerosis and inflammatory reaction to a permanent foreign body remains considerable pitfalls of metallic stents.

Bioresorbable scaffold is a recent technology introduced to address the above-mentioned drawbacks. These devices have the ability to dissolve after restoring the patency of the vessel allowing the coronary artery to maintain its physiologic integrity.[9]

Recent reports demonstrated that the neointimal tissue developed postimplantation of a bioresorbable scaffold can seal the underlying plaques, whereas studies in animal models showed that the neointimal tissue has features associated with plaque stability.[10, 11]

These initial reports may support the use of bioresorbable scaffolds for paving diseased coronary segments with vulnerable plaques, but long-term follow-up data are required to elucidate this prospective.

At the current state of the art, given our inability to accurately predict which of the detected vulnerable plaques will rupture, when this will occur, and whether this event will have clinical implications an invasive sealing of potential culprit lesions cannot be justified.

However, the revolution occurring in invasive and non-invasive imaging and the advances in molecular biology are expected to provide additional information about atherosclerotic disease progression/regression, probably allowing us to predict with a higher accuracy events and plaque ruptures. Although, few years ago, the early detection and invasive passivation of future culprit lesions appeared as an unrealistic dream, it is currently regarded as a future potentiality.

INITIAL EXPERIENCE WITH BIORESORBABLE SCAFFOLDS

The everolimus eluting bioresorbable vascular scaffold (BVS) consists of a backbone of poly-L-lactide (PLLA) coated with poly-D,L-lactide (PDLLA) that contains and controls the release of the antiproliferative drug everolimus. It has been initially evaluated in humans in a small cohort study, the Absorb Cohort A trial enrolling 30 patients[12] and showing feasibility of implantation of this novel technology, with an acceptable in-stent late loss at 6-month follow-up (0.44 ±0.35 mm).

The first generation of BVS showed a slightly higher acute recoil compared with conventional metallic platform stents,[13] and at 6 months, an 11.8% reduction in scaffold area and a 24.3% decrease in minimal luminal area were documented and defined "late recoil."[12, 14]

Although the short- and long-term results of the ABSORB cohort A trial were favourable,

reinforcement of the mechanical performance of the device and prolongation of its mechanical integrity up to 6 months were regarded as potential improvements of this technology.

To enhance the mechanical strength of the struts and to reduce immediate and late recoil,[14] the strut design and the manufacturing process of the polymer were modified in the revised version, BVS 1.1. The new design has in-phase zigzag hoops linked by bridges that allow a more uniform

strut distribution, reduce maximum circular unsupported surface area, and provide more uniform vessel wall support and drug release.[15] In addition, a modified manufacturing process has resulted in a lower hydrolysis (in vivo degradation) rate of the polymer, thus preserving its mechanical integrity for a longer period of time.[10] The BVS revision 1.1 was tested in 101 patients of the ABSORB cohort B study.

The Part II of the present thesis represents an overview of initial investigations performed in the very early phase of our knowledge on this technology.

We learned, that the late shrinkage and the performance of the second generation BVS improved by changing the manufacturing process of the polymer, reducing the maximum circular unsupported surface area[16], and modifying the bioresorption profile.

We assessed such improvement in the bioresorption process with IVUS-Virtual histology (VH).

IVUS-VH misrepresents polymeric struts as dense calcium and necrotic core so that their presence and disappearance could be used as potential artifactual surrogate of bioresorption[17]

The particular polymeric composition of the scaffold lead to slightly different geometrical properties of this device compared with metal when implanted in coronary arteries, particularly in terms of lower eccentricity index and a higher symmetry index[18] without apparently affecting clinical outcomes.

The bioresorbable vascular scaffold is a totally novel paradigm for coronary artery treatment and a novel approach for implantation should be considered, in particular an initial concern raised from the possibility of fracturing the scaffold by over-expanding it. The appropriate sizing of the vessels before implantation was regarded as a key point for an optimal implantation and the adoption of the proximal and distal maximal lumen diameters (DMAX) as reverences added in important information on how to perform an optimal deployment.

The polymeric nature of the device was also associated to a novel way to display stent contours when performing intravascular imaging, with the consequent need for a deep understanding of the new images. In particular the assessment of strut coverage became more challenging with the standard optical coherence tomography (OCT).

Strut coverage after implantation is expressing endothelialisation and the overall vascular healing and could be related to future events like scaffold thrombosis.
Struts imaged with OCT post-implantation typically appear as a box-shaped highly reflective frame that marks the refractive index change at the lumen-polymer and polymer-tissue interfaces.[10, 19] Unlike metallic stents, the assessment of coverage with BVS is more challenging, because the backscattering from thin neointimal layers mixes with that from the polymer interface and can be difficult to discern in a conventional analysis of the log-transformed OCT signal. On the other hand fitting the raw OCT backscattering signal to a Gaussian line spread functions (LSF) facilitates identification of the interfaces between BVS polymer and lumen or tissue. Such analysis enables more precise measurement of the strut thickness and an objective assessment of coverage. A similar concept has been recently used in randomized trials comparing BVS with metal stents.[20]
The initial experience with bioresorbable vascular scaffold implantation in humans showed promising results also in terms of clinical and angiographic outcomes when considering relatively challenging scenarios such as small vessels[21] with a vascular response similar to what observed in metal stents.[22]
Given this background a randomized trial was initiated to compare BVS with current generation metallic drug eluting stents and also aiming to present a new approach to coronary artery disease treatment that integrates transient mechanical revascularization, drug elution, medical treatment and life style changes into a single strategy to restore coronary blood flow and vessel physiology.

BIORESORBABLE SCAFFOLDS FOR TREATMENT OF COMPLEX LESIONS AND PATIENTS WITH ACUTE CORONARY SYNDROMES

After the introduction of BVS and the preliminary results in relatively simple lesions and stable patients the devices received the CE mark for clinical use, indicated for improving coronary lumen diameter in patients with ischemic heart disease due to de novo native coronary artery lesions with no restriction in terms of clinical presentation. Therefore the BVS can be currently used routinely in Europe in different settings comprising complex lesions and the acute myocardial infarction without a specific written informed consent in addition to the standard informed consent to the procedure. Our institution was the first simultaneously with the group of Prague to report results after BVS implantation in acute myocardial infarction.[23, 24]
And both analyses showed very similar results supporting feasibility the BVS implantation

in patients presenting with acute myocardial infarction, with high rate of final TIMI-flow III and good scaffold apposition.
These evidences not only diffused the idea, within the scientific community, that acute thrombotic lesions could be treated with bioresorbable devices but some authors identified the soft ruptured plaques as an appealing subset for the implantation of polymeric devices given the easily distensibility of such lesions.[25]
At the current state of the art the implantation of this device in the entire spectrum of complex lesions encountered during the daily practice is still matter of debate.
In particular the implantation technique has been profoundly changed since the initial experience when most of the operator were reluctant to the idea of an aggressive postdilatation.
Accumulating data on the expanded use of the bioresorbable technology in daily practice suggest the importance of an appropriate lesion preparation and even more an adequate postdilatation to optimize deployment and expansion.
This evolution of the implantation technique allowed us to implant this device in real challenging subsets like calcified lesions, bifurcations and total occlusions.
In particular thank to the collaboration of many expert in chronic total occlusion (CTO) treatment we were able to report promising data after implantation of this novel device also in complex CTO that probably represent the most challenging subset in interventional cardiology.

CONCLUSIONS

The bioresorbable technologies represent a novel concept for treatment of coronary artery disease providing revascularization with transient vascular support and drug delivery. This novel therapy has been termed as vascular restoration therapy as after bioresorption the coronary vessel will be able to re-acquire the physiological vasomotion, without metallic caging, exposed to the pulsatile blood flow and potentially free to have positive remodeling and late lumen enlargement.
Given the peculiar mechanical properties and the polymeric nature of this device, it should not be considered just another stent in the clinical arena but a separated way of treating patients. This implies that a dedicated technique of implantation should be adopted with a meticulous lesion preparation, particular attention to the expansion limits and high pressure postdilation in the majority of the cases.

The theoretical advantages of these novel technologies could be potentially beneficial for every patient but the implantation of bioresorbable scaffold should be probably primarily considered in those subjects where these advantages could be maximized. In particular, young patients who could benefit from having coronaries free of metal for many years, patients with multivessel disease that could in future be candidate for surgical revascularisations and acute patients were vasoconstriction could be associated with stent undersizing and very long-term malapposition.

The current bioresorbable devices are not devoid of limitations. The higher profile of the second generation BVS make the scaffold delivery slightly more challenging than standard metal stents especially in tortuous calcified vessels. The higher strut thickness might delay the endothelialisation and coverage facilitating platelet aggregation and the occurrence of thrombotic events.

However, this technology is probably in a very early phase of its development and similar clinical outcomes compared to metals DES that have been optimised for more than fifteen years should be considered already a great achievement. Technical improvements of the scaffold with the introduction of thinner struts more similar to those of the current generation DES, a wider range of available sizes and less strict expansion limits are currently awaited. Such improvements could reduce the technical gap between bioresorbable and metal and facilitate a larger adoption of this technology in clinical practice.

REFERENCES

1. Virmani R, Kolodgie FD, Burke AP, Farb A, Schwartz SM. Lessons from sudden coronary death: a comprehensive morphological classification scheme for atherosclerotic lesions. Arterioscler Thromb Vasc Biol 2000;20(5):1262-75.
2. Burke AP, Farb A, Malcom GT, Liang YH, Smialek J, Virmani R. Coronary risk factors and plaque morphology in men with coronary disease who died suddenly. N Engl J Med 1997;336(18):1276-82.
3. Virmani R, Burke AP, Farb A, Kolodgie FD. Pathology of the vulnerable plaque. J Am Coll Cardiol 2006;47(8 Suppl):C13-8.
4. Manfrini O, Mont E, Leone O, Arbustini E, Eusebi V, Virmani R, Bugiardini R. Sources of error and interpretation of plaque morphology by optical coherence tomography. Am J Cardiol 2006;98(2):156-9.
5. Sawada T, Shite J, Garcia-Garcia HM, Shinke T, Watanabe S, Otake H, Matsumoto D, Tanino Y, Ogasawara D, Kawamori H, Kato H, Miyoshi N, Yokoyama M, Serruys PW, Hirata K. Feasibility of combined use of intravascular ultrasound radiofrequency data analysis and optical coherence tomography for detecting thin-cap fibroatheroma. Eur Heart J 2008;29(9):1136-46.
6. Gonzalo N, Garcia-Garcia HM, Regar E, Barlis P, Wentzel J, Onuma Y, Ligthart J, Serruys PW. In vivo assessment of high-risk coronary plaques at bifurcations with combined intravascular ultrasound and optical coherence tomography. JACC Cardiovasc Imaging 2009;2(4):473-82.
7. Stone GW, Maehara A, Lansky AJ, de Bruyne B, Cristea E, Mintz GS, Mehran R, McPherson J, Farhat N, Marso SP, Parise H, Templin B, White R, Zhang Z, Serruys PW, Investigators P. A prospective natural-history study of coronary atherosclerosis. N Engl J Med 2011;364(3):226-35.
8. Mercado N, Maier W, Boersma E, Bucher C, de Valk V, O'Neill WW, Gersh BJ, Meier B, Serruys PW, Wijns W. Clinical and angiographic outcome of patients with mild coronary lesions treated with balloon angioplasty or coronary stenting. Implications for mechanical plaque sealing. Eur Heart J 2003;24(6):541-51.
9. Serruys PW, Garcia-Garcia HM, Onuma Y. From metallic cages to transient bioresorbable scaffolds: change in paradigm of coronary revascularization in the upcoming decade? Eur Heart J 2012;33(1):16-25b.
10. Onuma Y, Serruys PW, Perkins LE, Okamura T, Gonzalo N, Garcia-Garcia HM, Regar E, Kamberi M, Powers JC, Rapoza R, van Beusekom H, van der Giessen W, Virmani R. Intracoronary optical coherence tomography and histology at 1 month and 2, 3, and 4 years after implantation of everolimus-eluting bioresorbable vascular scaffolds in a porcine coronary artery model: an attempt to decipher the human optical coherence tomography images in the ABSORB trial. Circulation 2010;122(22):2288-300.
11. Brugaletta S, Radu MD, Garcia-Garcia HM, Heo JH, Farooq V, Girasis C, van Geuns RJ, Thuesen L, McClean D, Chevalier B, Windecker S, Koolen J, Rapoza R, Miquel-Hebert K, Ormiston J, Serruys PW. Circumferential evaluation of the neointima by optical coherence tomography after ABSORB bioresorbable vascular scaffold implantation: can the scaffold cap the plaque? Atherosclerosis 2012;221(1):106-12.
12. Ormiston JA, Serruys PW, Regar E, Dudek D, Thuesen L, Webster MW, Onuma Y, Garcia-Garcia HM, McGreevy R, Veldhof S. A bioabsorbable everolimus-eluting coronary stent system for patients with single de-novo coronary artery lesions (ABSORB): a prospective open-label trial. Lancet 2008;371(9616):899-907.
13. Tanimoto S, Serruys PW, Thuesen L, Dudek D, de Bruyne B, Chevalier B, Ormiston JA. Comparison of in vivo acute stent recoil between the bioabsorbable everolimus-eluting coronary stent and the everolimus-eluting cobalt chromium coronary stent: insights from the ABSORB and SPIRIT trials. Catheter Cardiovasc Interv 2007;70(4):515-23.
14. Tanimoto S, Bruining N, van Domburg RT, Rotger D, Radeva P, Ligthart JM, Serruys PW. Late stent recoil of the bioabsorbable everolimus-eluting coronary stent and its relationship with plaque morphology. J Am Coll Cardiol 2008;52(20):1616-20.
15. Okamura T, Garg S, Gutierrez-Chico JL, Shin ES, Onuma Y, Garcia-Garcia HM, Rapoza RJ, Sudhir K, Regar E, Serruys PW. In vivo evaluation of stent strut distribution patterns in the bioabsorbable everolimus-

eluting device: an OCT ad hoc analysis of the revision 1.0 and revision 1.1 stent design in the ABSORB clinical trial. EuroIntervention 2010;5(8):932-8.

16. Gomez-Lara J, Brugaletta S, Diletti R, Garg S, Onuma Y, Gogas BD, van Geuns RJ, Dorange C, Veldhof S, Rapoza R, Whitbourn R, Windecker S, Garcia-Garcia HM, Regar E, Serruys PW. A comparative assessment by optical coherence tomography of the performance of the first and second generation of the everolimus-eluting bioresorbable vascular scaffolds. Eur Heart J 2011;32(3):294-304.
17. Brugaletta S, Garcia-Garcia HM, Diletti R, Gomez-Lara J, Garg S, Onuma Y, Shin ES, van Geuns RJ, de Bruyne B, Dudek D, Thuesen L, Chevalier B, McClean D, Windecker S, Whitbourn R, Dorange C, Veldhof S, Rapoza R, Sudhir K, Bruining N, Ormiston JA, Serruys PW. Comparison between the first and second generation bioresorbable vascular scaffolds: a six month virtual histology study. EuroIntervention 2011;6(9):1110-6.
18. de Jaegere P, Mudra H, Figulla H, Almagor Y, Doucet S, Penn I, Colombo A, Hamm C, Bartorelli A, Rothman M, Nobuyoshi M, Yamaguchi T, Voudris V, DiMario C, Makovski S, Hausmann D, Rowe S, Rabinovich S, Sunamura M, van Es GA. Intravascular ultrasound-guided optimized stent deployment. Immediate and 6 months clinical and angiographic results from the Multicenter Ultrasound Stenting in Coronaries Study (MUSIC Study). Eur Heart J 1998;19(8):1214-23.
19. Serruys PW, Ormiston JA, Onuma Y, Regar E, Gonzalo N, Garcia-Garcia HM, Nieman K, Bruining N, Dorange C, Miquel-Hebert K, Veldhof S, Webster M, Thuesen L, Dudek D. A bioabsorbable everolimus-eluting coronary stent system (ABSORB): 2-year outcomes and results from multiple imaging methods. Lancet 2009;373(9667):897-910.
20. Sabate M, Windecker S, Iniguez A, Okkels-Jensen L, Cequier A, Brugaletta S, Hofma SH, Raber L, Christiansen EH, Suttorp M, Pilgrim T, Anne van Es G, Sotomi Y, Garcia-Garcia HM, Onuma Y, Serruys PW. Everolimus-eluting bioresorbable stent vs. durable polymer everolimus-eluting metallic stent in patients with ST-segment elevation myocardial infarction: results of the randomized ABSORB ST-segment elevation myocardial infarction-TROFI II trial. Eur Heart J 2016;37(3):229-40.
21. Diletti R, Onuma Y, Farooq V, Gomez-Lara J, Brugaletta S, van Geuns RJ, Regar E, de Bruyne B, Dudek D, Thuesen L, Chevalier B, McClean D, Windecker S, Whitbourn R, Smits P, Koolen J, Meredith I, Li D, Veldhof S, Rapoza R, Garcia-Garcia HM, Ormiston JA, Serruys PW. 6-month clinical outcomes following implantation of the bioresorbable everolimus-eluting vascular scaffold in vessels smaller or larger than 2.5 mm. J Am Coll Cardiol 2011;58(3):258-64.
22. Gogas BD, Serruys PW, Diletti R, Farooq V, Brugaletta S, Radu MD, Heo JH, Onuma Y, van Geuns RJ, Regar E, De Bruyne B, Chevalier B, Thuesen L, Smits PC, Dudek D, Koolen J, Windecker S, Whitbourn R, Miquel-Hebert K, Dorange C, Rapoza R, Garcia-Garcia HM, McClean D, Ormiston JA. Vascular response of the segments adjacent to the proximal and distal edges of the ABSORB everolimus-eluting bioresorbable vascular scaffold: 6-month and 1-year follow-up assessment: a virtual histology intravascular ultrasound study from the first-in-man ABSORB cohort B trial. JACC Cardiovasc Interv 2012;5(6):656-65.
23. Diletti R, Karanasos A, Muramatsu T, Nakatani S, Van Mieghem NM, Onuma Y, Nauta ST, Ishibashi Y, Lenzen MJ, Ligthart J, Schultz C, Regar E, de Jaegere PP, Serruys PW, Zijlstra F, van Geuns RJ. Everolimus-eluting bioresorbable vascular scaffolds for treatment of patients presenting with ST-segment elevation myocardial infarction: BVS STEMI first study. Eur Heart J 2014;35(12):777-86.
24. Kocka V, Maly M, Tousek P, Budesinsky T, Lisa L, Prodanov P, Jarkovsky J, Widimsky P. Bioresorbable vascular scaffolds in acute ST-segment elevation myocardial infarction: a prospective multicentre study 'Prague 19'. Eur Heart J 2014;35(12):787-94.
25. Brugaletta S, Gori T, Low AF, Tousek P, Pinar E, Gomez-Lara J, Scalone G, Schulz E, Chan MY, Kocka V, Hurtado J, Gomez-Hospital JA, Munzel T, Lee CH, Cequier A, Valdes M, Widimsky P, Serruys PW, Sabate M. Absorb bioresorbable vascular scaffold versus everolimus-eluting metallic stent in ST-segment elevation myocardial infarction: 1-year results of a propensity score matching comparison: the BVS-EXAMINATION Study (bioresorbable vascular scaffold-a clinical evaluation of everolimus eluting coronary stents in the treatment of patients with ST-segment elevation myocardial infarction). JACC Cardiovasc Interv 2015;8(1 Pt B):189-97.

Samenvatting & Conclusies

KARAKTERISERING VAN CORONAIRE ATHEROSCLEROSE MET INTRAVASCULAIRE IMAGING

Het begrip van het atherosclerotisch proces is fundamenteel voor het bereiken van een adequate behandeling van coronaire hartziekte. Het eerste deel van dit proefschrift is gericht op de karakterisering van de coronaire plaques met gebruikmaking van intravasculaire beeldvorming; het gebruik van dergelijke technologieën stelt ons in staat de karakterisering en samenstelling van de plaques te beoordelen. Met name de combinatie van verschillende beeldvormingsmodaliteiten (d.w.z. intravasculaire ultrasound, virtuele histologie en optische coherentietomografie) zou geschikt zijn voor een volledig onderzoek van de laesiekwetsbaarheid.

Plaqueruptuur en daaropvolgende activering van de stollingscascade leidend tot plotse intraluminale trombose, vormen naar men denkt de vaakst voorkomende oorzaak van acute coronaire syndromen.[1, 2]

In de pathologie worden precursorlaesies, bekend als thin-cap fibroatheromas (TCFA) gekarakteriseerd door een grote pool van necrotische kern, bedekt door een dunne fibreuze kap < 65 µm[3]. De resolutie van de huidige intravasculaire ultrasoundsystemen (IVUS) (100 tot 200 µm) vormt een belangrijke beperking van deze techniek voor de meting van de dikte van de fibreuze kap. Anderzijds heeft optische coherentietomografie (OCT) een hogere resolutie (10 tot 20 µm) maar een lage signaalpenetratie.[4] Daarom zou combinatie van de twee beeldvormingsmodaliteiten een nauwkeurige methode kunnen bieden voor het onderzoeken van TCFA's[5, 6]

Bovendien kan volledig begrip van de plaquemorfologie en -samenstelling een leidraad zijn voor de juiste strategie bij de behandeling van coronaire laesies. De aanwezigheid van een grote hoeveelheid omringend calcium zou de onderliggende reden kunnen zij voor het initiëren van een coronaire interventie met een agressieve laesiepreparatiebenadering (d.w.z. rotablatie, snijballon, high pressure non compliant ballooning). Dergelijke informatie kan van zeer groot belang zijn, met name bij de implantatie van bioresorbeerbare stents, omdat is vastgesteld dat optimale laesiepreparatie en scaffoldgebruik de belangrijkste factoren zijn voor het vergemakkelijken van goede angiografische resultaten en klinische uitkomsten.

Continue ontwikkelingen op het gebied van de invasieve en non-invasieve beeldvorming maken een gedetailleerde visualisatie mogelijk van coronaire pathologie, wat een aanzienlijke vermeerdering betekent van onze kennis over plaquegroei en -ruptuur, terwijl de prospectieve natuurlijke voorgeschiedenis van atherosclerose-onderzoeken een koppeling aangaf tussen plaquemorfologie en toekomstige klinische uitkomsten.[7]

De invasieve behandeling van een potentiële culprit laesie bij asymptomatische

patiënten kan echter alleen gerechtvaardigd zijn als stent-implantatie geheel veilig is. De eerste meldingen toonden een onaanvaardbaar hoog risico op complicaties in niet-flowbeperkende laesies behandeld met ballonangioplastiek of bare-metal-stents, terwijl de nieuwe ontwikkelingen op het gebied van stent-ontwerp het risico op complicaties verminderd hebben maar niet doen verdwijnen.[8]

De verandering van de vaatwandfysiologie en het risico op neoatherosclerose en ontstekingsreactie op een permanent vreemd lichaam blijven een aanzienlijk nadeel van metalen stents.

Bioresorbeerbare scaffold is een recente technologie die is geïntroduceerd om de bovengenoemde bezwaren aan te pakken. Deze stents hebben het vermogen om op te lossen na het herstellen van de doorgankelijkheid van het vat, waardoor de coronairarterie zijn fysiologische integriteit behoudt.[9]

Recente rapporten toonden dat het neo-intimale weefsel dat wordt ontwikkeld na implantatie van een bioresorbeerbare scaffold de onderliggende plaques kan verzegelen, terwijl onderzoeken in diermodellen toonden dat het neo-intimale weefsel kenmerken heeft die zijn geassocieerd met plaquestabiliteit.[10, 11]

Deze eerste rapporten kunnen het gebruik van bioresorbeerbare scaffolds voor zieke coronaire segmenten met kwetsbare plaques ondersteunen, maar langetermijnfollow-upgegevens zijn vereist om deze verwachting te verklaren.

Bij de huidige stand van de techniek zal, gegeven ons onvermogen om nauwkeurig te voorspellen welke van de kwetsbare plaques zullen scheuren, wanneer dit zal gebeuren en of dat voorval klinische implicaties zal hebben een invasieve sealing van mogelijke culprit laesies niet zijn gerechtvaardigd.

De revolutie die gaande is op het gebied van invasieve en non-invasieve beeldvorming en de vooruitgang in de moleculaire biologie zal echter naar verwachting aanvullende informatie opleveren over progressie/regressie van atherosclerotische ziekte, waardoor wij waarschijnlijk met grotere nauwkeurigheid voorvallen en plaquerupturen kunnen voorspellen. Hoewel een aantal jaren geleden de vroege detectie en invasieve passivering van toekomstige culprit laesies een onrealistische droom leek, wordt dit momenteel gezien als een mogelijkheid voor de toekomst.

EERSTE ERVARING MET BIORESORBEERBARE STENTS

De everolimus-eluderende bioresorbeerbare vasculaire scaffold (BVS) bestaat uit een backbone van poly-L-lactide (PLLA) bekleed met poly-D,L-lactide (PDLLA) dat het antiproliferatieve geneesmiddel everolimus bevat en dat afgeeft. Het is in eerste instantie

beoordeeld bij mensen in een klein cohortonderzoek, het Absorb Cohort A-onderzoek waarin 30 patiënten werden ingeschreven[12] en dat de haalbaarheid aantoonde van implantatie van deze nieuwe technologie, met een aanvaardbare in-stent late loss bij follow-up na 6 maanden (0,44 ±0,35 mm).

De eerste generatie BVS toonde een iets hogere acute recoil vergeleken met conventionele metalen platformstents,[13] en na 6 maanden werden een 11,8% reductie in het scaffoldgebied en een 24,3% afname in het minimale luminale gebied gedocumenteerd en gedefinieerd als "late recoil".[12, 14]

Hoewel de kortetermijn- en de langetermijnresultaten van het ABSORB cohort A-onderzoek gunstig waren, werden versterking van de mechanische prestaties van het implantaat en verlenging van de mechanische integriteit ervan tot 6 maanden gezien als mogelijke verbeteringen van deze technologie.

Om de mechanische sterkte van de steunen te vergroten en onmiddellijke en late recoil te verminderen,[14] werden het steun-ontwerp en het fabricageproces van het polymeer gewijzigd in de herziene versie, BVS 1.1. Het nieuwe ontwerp heeft in-fase zigzag hoops gekoppeld door bruggen die een uniformere steunverdeling mogelijk maken, het maximale circulaire niet-ondersteunde vlak verkleinen en uniformere vaatwandondersteuning en geneesmiddelafgifte bieden.[15] Bovendien heeft een gewijzigd fabricageproces geleid tot een lager hydrolysepercentage (afbraak in vivo) van de polymeer, waardoor de mechanische integriteit daarvan langer behouden blijft.[10] De BVS-revisie 1.1 werd getest bij 101 patiënten uit het ABSORB cohort B onderzoek.

Deel II van dit proefschrift geeft een overzicht van de eerste onderzoeken uitgevoerd in de zeer vroege fase van onze kennis over deze technologie.

We hebben ontdekt dat de late krimping en de prestaties van de tweede generatie BVS verbeterden door het veranderen van het fabricageproces van de polymeer, wat een vermindering betekent van het maximale circulaire niet-ondersteunde vlak[16] en het veranderen van het bioresorptieprofiel.

We beoordeelden een dergelijke verbetering in het bioresorptieproces met IVUS-Virtuele Histologie (VH).

IVUS-VH geeft een verkeerde voorstelling van polymerische steunen als dichte calcium en necrotische kern zodat hun aanwezigheid en verdwijning zou kunnen worden gebruikt als potentieel artifactueel surrogaat van bioresorptie[17]

De specifieke polymerische samenstelling van de scaffold leidt tot verschillende geometrische eigenschappen van deze stent vergeleken met metaal bij implantatie in coronairarteriën, met name in termen van een lagere eccentriciteitsindex en een hogere symmetrie-index[18] zonder kennelijk invloed te hebben op de klinische uitkomsten.

De bioresorbeerbare vasculaire scaffold is een geheel nieuw paradigma voor coronaire-

arteriebehandeling en een nieuwe benadering voor implantatie zou overwogen moeten worden, met name een initieel punt van zorg gelet op de mogelijkheid van breuk van de scaffold door deze te sterk te expanderen. De juiste maatvoering van de vaten voorafgaand aan implantatie werd beschouwd als een zeer belangrijk punt voor een optimale implantatie en het gebruik van de proximale en distale maximale lumendiameters (DMAX) wordt toegevoegd aan belangrijke informatie over hoe optimaal gebruik kan worden bereikt.

De polymerische aard van het implantaat werd ook in verband gebracht met een nieuwe manier voor het weergeven van de stentcontouren bij het uitvoeren van intravasculaire beeldvorming, met de daaruit voortvloeiende behoefte aan een diepgaand begrip van de nieuwe beelden. Met name de beoordeling van steuncoverage werd moeilijker met de standaard optische coherentietomografie (OCT).

Steuncoverage na implantatie geeft endothelialisatie en totale vasculaire genezing aan en zou gerelateerd kunnen zijn aan toekomstige voorvallen zoals scaffoldtrombose.

Steunen waarvan beelden worden gemaakt met OCT post-implantatie worden meestal weergegeven als een doosvormig uiterst reflectief frame dat de refractieve indexverandering bij de lumen-polymeer en polymeerweefselinterfaces weergeeft.[10, 19] In tegenstelling tot metalen stents is de beoordeling van coverage met BVS moeilijker, omdat de backscattering uit dunne neo-intimale lagen wordt vermengd met die uit de polymeerinterface en moeilijk te onderscheiden kan zijn in een conventionele analyse van het log-getransformeerde OCT-signaal. Anderzijds vergemakkelijkt het passen van het ruwe OCT backscatteringsignaal bij een Gaussian line spread functions (LSF) identificatie van de interfaces tussen BVS-polymeer en lumen of weefsel. Een dergelijke analyse maakt nauwkeuriger meting mogelijk van de steundikte en een objectieve beoordeling van de coverage. Een soortgelijk concept is reeds gebruikt in gerandomiseerde onderzoeken ter vergelijking van BVS met metalen stents.[20]

De eerste ervaring met bioresorbeerbare vasculaire scaffold-implantatie bij de mens toonde veelbelovende resultaten, ook in termen van klinische en angiografische uitkomsten bij het overwegen van relatief moeilijke scenario's zoals kleine vaten[21] met een vasculaire respons soortgelijk aan die die is waargenomen bij metalen stents.[22]

Gegeven deze achtergrond werd een gerandomiseerd onderzoek gestart ter vergelijking van BVS met de huidige generatie metalen drug-eluting stents ook gericht op het presenteren van een nieuwe benadering van behandeling van ziekte van de coronairarterie die voorbijgaande mechanische revascularisatie, geneesmiddelafgifte, medische behandeling en leefstijlveranderingen integreert in één enkele strategie om de coronaire bloedstroom en de vaatfysiologie te herstellen.

BIORESORBEERBARE SCAFFOLDS VOOR BEHANDELING VAN COMPLEXE LAESIES EN PATIËNTEN MET ACUTE CORONAIRE SYNDROMEN

Na de introductie van BVS en de voorlopige resultaten in relatief eenvoudige laesies en bij stabiele patiënten kregen de stents een CE-markering voor klinisch gebruik, geïndiceerd voor verbetering van de coronaire lumendiameter bij patiënten met ischemische hartziekte als gevolg van de novo native coronairarterielaesies zonder beperking in termen van klinische presentatie. Daarom kan de BVS momenteel als routine worden gebruikt in Europa in verschillende settings bestaande uit complexe laesies en acuut myocardinfarct zonder een specifieke schriftelijke geïnformeerde toestemming naast de standaard geïnformeerde toestemming voor de procedure. Onze instelling was tegelijk met de groep uit Praag de eerste die resultaten rapporteerde na BVS-implantatie bij acuut myocardinfarct.[23, 24]

En beide analyses toonden zeer soortgelijke resultaten ter ondersteuning van de haalbaarheid van de BVS-implantatie bij patiënten met acuut myocardinfarct, met een hoge uiteindelijke TIMI-flow III en goede scaffold-appositie.

Deze bewijzen deden het idee binnen de wetenschappelijke gemeenschap vervagen dat acute trombotische laesies behandeld zouden kunnen worden met bioresorbeerbare stents, maar sommige auteurs identificeerden de zachte gescheurde plaques als een aantrekkelijke subset voor de implantatie van polymerische implantaten, gegeven de gemakkelijke uitzetbaarheid van dergelijke laesies.[25] Bij de huidige stand van de techniek is de implantatie van deze stent in het gehele spectrum van complexe laesies die men tegenkomt in de dagelijkse praktijk nog steeds een punt van discussie.

Met name de implantatietechniek is sterk veranderd sinds de eerste ervaring toen de meeste operateurs terughoudend waren wat betreft het idee van een agressieve postdilatatie.

Verzamelde gegevens over het uitgebreide gebruik van de bioresorbeerbare technologie in de dagelijkse praktijk suggereren het belang van een passende laesiepreparatie en nog meer een adequate postdilatatie om plaatsing en expansie te optimaliseren.

Deze ontwikkeling van de implantatietechniek heeft ons in staat gesteld tot het implanteren van deze stent in werkelijk moeilijke subsets zoals verkalkte laesies, bifurcaties en totale occlusies.

Met name dankzij de medewerking van veel deskundigen op het gebied van behandeling van chronische totale occlusie (CTO) konden we veelbelovende data melden na implantatie van dit nieuwe implantaat, ook bij complexe CTO die waarschijnlijk de moeilijkste subset in de interventiecardiologie vertegenwoordigen.

CONCLUSIES

De bioresorbeerbare technologieën vertegenwoordigen een nieuw concept voor de behandeling van coronairarterielijden dat revascularisatie biedt met tijdelijke vasculaire ondersteuning en geneesmiddeltoediening. Deze nieuwe behandeling wordt vasculaire restauratietherapie genoemd omdat na bioresorptie het coronairvat weer fysiologische vasomotie kan verkrijgen, zonder metalen caging, blootgesteld aan de pulserende bloedstroom en potentieel vrij voor positieve hermodellering en late lumenvergroting.
Gegeven de bijzondere mechanische eigenschappen en de polymerische aard van deze stent moet deze niet worden gezien als gewoon een andere stent in de klinische arena maar als een afzonderlijke manier om patiënten te behandelen. Dit impliceert dat een speciale implantatietechniek moet worden toegepast met een zeer nauwgezette laesiepreparatie, specifieke aandacht voor de expansiegrenzen en in de meeste gevallen hoge druk na dilatatie.
De theoretische voordelen van deze nieuwe technologieën zouden mogelijk gunstig kunnen zijn voor elke patiënt, maar de implantatie van bioresorbeerbare scaffolds zou waarschijnlijk primair kunnen worden overwogen bij die proefpersonen bij wie het meeste uit deze voordelen gehaald zou kunnen worden. Met name jonge patiënten die jarenlang zouden kunnen profiteren van kransslagaders zonder metaal, patiënten met ziekte van meerdere vaten die in de toekomst in aanmerking zouden kunnen komen voor chirurgische revascularisaties en acute patiënten bij wie vasoconstrictie in verband gebracht zou kunnen worden met een te kleine stent en zeer langdurige slechte appositie.
De huidige bioresorbeerbare stents zijn niet zonder beperkingen. Het hogere profiel van de tweede generatie BVS maakt de scaffoldplaatsing iets moeilijker dan die van standaard metalen stents, met name in tortueuze verkalkte vaten. De grotere steundikte zou de endothelialisatie en de coverage kunnen vertragen, wat bloedplaatjesaggregatie en het optreden van trombotische voorvallen vergemakkelijkt.
Deze technologie bevindt zich waarschijnlijk in een zeer vroege fase van ontwikkeling en soortgelijke klinische uitkomsten vergeleken met metalen DES die gedurende meer dan vijftien jaar steeds beter zijn geworden moeten al als een uitstekend resultaat worden beschouwd. Technische verbeteringen van de scaffold met de introductie van dunnere steunen die meer lijken op die van de huidige generatie DES, een breder assortiment beschikbare maten en minder strikte expansiegrenzen worden momenteel verwacht. Dergelijke verbeteringen zouden de technische kloof tussen bioresorbeerbare en metalen stents kunnen verkleinen en een breder gebruik van deze technologie in de klinische praktijk vergemakkelijken.

REFERENTIES

1. Virmani R, Kolodgie FD, Burke AP, Farb A, Schwartz SM. Lessons from sudden coronary death: a comprehensive morphological classification scheme for atherosclerotic lesions. Arterioscler Thromb Vasc Biol 2000;20(5):1262-75.
2. Burke AP, Farb A, Malcom GT, Liang YH, Smialek J, Virmani R. Coronary risk factors and plaque morphology in men with coronary disease who died suddenly. N Engl J Med 1997;336(18):1276-82.
3. Virmani R, Burke AP, Farb A, Kolodgie FD. Pathology of the vulnerable plaque. J Am Coll Cardiol 2006;47(8 Suppl):C13-8.
4. Manfrini O, Mont E, Leone O, Arbustini E, Eusebi V, Virmani R, Bugiardini R. Sources of error and interpretation of plaque morphology by optical coherence tomography. Am J Cardiol 2006;98(2):156-9.
5. Sawada T, Shite J, Garcia-Garcia HM, Shinke T, Watanabe S, Otake H, Matsumoto D, Tanino Y, Ogasawara D, Kawamori H, Kato H, Miyoshi N, Yokoyama M, Serruys PW, Hirata K. Feasibility of combined use of intravascular ultrasound radiofrequency data analysis and optical coherence tomography for detecting thin-cap fibroatheroma. Eur Heart J 2008;29(9):1136-46.
6. Gonzalo N, Garcia-Garcia HM, Regar E, Barlis P, Wentzel J, Onuma Y, Ligthart J, Serruys PW. In vivo assessment of high-risk coronary plaques at bifurcations with combined intravascular ultrasound and optical coherence tomography. JACC Cardiovasc Imaging 2009;2(4):473-82.
7. Stone GW, Maehara A, Lansky AJ, de Bruyne B, Cristea E, Mintz GS, Mehran R, McPherson J, Farhat N, Marso SP, Parise H, Templin B, White R, Zhang Z, Serruys PW, Investigators P. A prospective natural-history study of coronary atherosclerosis. N Engl J Med 2011;364(3):226-35.
8. Mercado N, Maier W, Boersma E, Bucher C, de Valk V, O'Neill WW, Gersh BJ, Meier B, Serruys PW, Wijns W. Clinical and angiographic outcome of patients with mild coronary lesions treated with balloon angioplasty or coronary stenting. Implications for mechanical plaque sealing. Eur Heart J 2003;24(6):541-51.
9. Serruys PW, Garcia-Garcia HM, Onuma Y. From metallic cages to transient bioresorbable scaffolds: change in paradigm of coronary revascularization in the upcoming decade? Eur Heart J 2012;33(1):16-25b.
10. Onuma Y, Serruys PW, Perkins LE, Okamura T, Gonzalo N, Garcia-Garcia HM, Regar E, Kamberi M, Powers JC, Rapoza R, van Beusekom H, van der Giessen W, Virmani R. Intracoronary optical coherence tomography and histology at 1 month and 2, 3, and 4 years after implantation of everolimus-eluting bioresorbable vascular scaffolds in a porcine coronary artery model: an attempt to decipher the human optical coherence tomography images in the ABSORB trial. Circulation 2010;122(22):2288-300.
11. Brugaletta S, Radu MD, Garcia-Garcia HM, Heo JH, Farooq V, Girasis C, van Geuns RJ, Thuesen L, McClean D, Chevalier B, Windecker S, Koolen J, Rapoza R, Miquel-Hebert K, Ormiston J, Serruys PW. Circumferential evaluation of the neointima by optical coherence tomography after ABSORB bioresorbable vascular scaffold implantation: can the scaffold cap the plaque? Atherosclerosis 2012;221(1):106-12.
12. Ormiston JA, Serruys PW, Regar E, Dudek D, Thuesen L, Webster MW, Onuma Y, Garcia-Garcia HM, McGreevy R, Veldhof S. A bioabsorbable everolimus-eluting coronary stent system for patients with single de-novo coronary artery lesions (ABSORB): a prospective open-label trial. Lancet 2008;371(9616):899-907.
13. Tanimoto S, Serruys PW, Thuesen L, Dudek D, de Bruyne B, Chevalier B, Ormiston JA. Comparison of in vivo acute stent recoil between the bioabsorbable everolimus-eluting coronary stent and the everolimus-eluting cobalt chromium coronary stent: insights from the ABSORB and SPIRIT trials. Catheter Cardiovasc Interv 2007;70(4):515-23.
14. Tanimoto S, Bruining N, van Domburg RT, Rotger D, Radeva P, Ligthart JM, Serruys PW. Late stent recoil of the bioabsorbable everolimus-eluting coronary stent and its relationship with plaque morphology. J Am Coll Cardiol 2008;52(20):1616-20.
15. Okamura T, Garg S, Gutierrez-Chico JL, Shin ES, Onuma Y, Garcia-Garcia HM, Rapoza RJ, Sudhir K, Regar E, Serruys PW. In vivo evaluation of stent strut distribution patterns in the bioabsorbable everolimus-eluting

device: an OCT ad hoc analysis of the revision 1.0 and revision 1.1 stent design in the ABSORB clinical trial. EuroIntervention 2010;5(8):932-8.

16. Gomez-Lara J, Brugaletta S, Diletti R, Garg S, Onuma Y, Gogas BD, van Geuns RJ, Dorange C, Veldhof S, Rapoza R, Whitbourn R, Windecker S, Garcia-Garcia HM, Regar E, Serruys PW. A comparative assessment by optical coherence tomography of the performance of the first and second generation of the everolimus-eluting bioresorbable vascular scaffolds. Eur Heart J 2011;32(3):294-304.
17. Brugaletta S, Garcia-Garcia HM, Diletti R, Gomez-Lara J, Garg S, Onuma Y, Shin ES, van Geuns RJ, de Bruyne B, Dudek D, Thuesen L, Chevalier B, McClean D, Windecker S, Whitbourn R, Dorange C, Veldhof S, Rapoza R, Sudhir K, Bruining N, Ormiston JA, Serruys PW. Comparison between the first and second generation bioresorbable vascular scaffolds: a six month virtual histology study. EuroIntervention 2011;6(9):1110-6.
18. de Jaegere P, Mudra H, Figulla H, Almagor Y, Doucet S, Penn I, Colombo A, Hamm C, Bartorelli A, Rothman M, Nobuyoshi M, Yamaguchi T, Voudris V, DiMario C, Makovski S, Hausmann D, Rowe S, Rabinovich S, Sunamura M, van Es GA. Intravascular ultrasound-guided optimized stent deployment. Immediate and 6 months clinical and angiographic results from the Multicenter Ultrasound Stenting in Coronaries Study (MUSIC Study). Eur Heart J 1998;19(8):1214-23.
19. Serruys PW, Ormiston JA, Onuma Y, Regar E, Gonzalo N, Garcia-Garcia HM, Nieman K, Bruining N, Dorange C, Miquel-Hebert K, Veldhof S, Webster M, Thuesen L, Dudek D. A bioabsorbable everolimus-eluting coronary stent system (ABSORB): 2-year outcomes and results from multiple imaging methods. Lancet 2009;373(9667):897-910.
20. Sabate M, Windecker S, Iniguez A, Okkels-Jensen L, Cequier A, Brugaletta S, Hofma SH, Raber L, Christiansen EH, Suttorp M, Pilgrim T, Anne van Es G, Sotomi Y, Garcia-Garcia HM, Onuma Y, Serruys PW. Everolimus-eluting bioresorbable stent vs. durable polymer everolimus-eluting metallic stent in patients with ST-segment elevation myocardial infarction: results of the randomized ABSORB ST-segment elevation myocardial infarction-TROFI II trial. Eur Heart J 2016;37(3):229-40.
21. Diletti R, Onuma Y, Farooq V, Gomez-Lara J, Brugaletta S, van Geuns RJ, Regar E, de Bruyne B, Dudek D, Thuesen L, Chevalier B, McClean D, Windecker S, Whitbourn R, Smits P, Koolen J, Meredith I, Li D, Veldhof S, Rapoza R, Garcia-Garcia HM, Ormiston JA, Serruys PW. 6-month clinical outcomes following implantation of the bioresorbable everolimus-eluting vascular scaffold in vessels smaller or larger than 2.5 mm. J Am Coll Cardiol 2011;58(3):258-64.
22. Gogas BD, Serruys PW, Diletti R, Farooq V, Brugaletta S, Radu MD, Heo JH, Onuma Y, van Geuns RJ, Regar E, De Bruyne B, Chevalier B, Thuesen L, Smits PC, Dudek D, Koolen J, Windecker S, Whitbourn R, Miquel-Hebert K, Dorange C, Rapoza R, Garcia-Garcia HM, McClean D, Ormiston JA. Vascular response of the segments adjacent to the proximal and distal edges of the ABSORB everolimus-eluting bioresorbable vascular scaffold: 6-month and 1-year follow-up assessment: a virtual histology intravascular ultrasound study from the first-in-man ABSORB cohort B trial. JACC Cardiovasc Interv 2012;5(6):656-65.
23. Diletti R, Karanasos A, Muramatsu T, Nakatani S, Van Mieghem NM, Onuma Y, Nauta ST, Ishibashi Y, Lenzen MJ, Ligthart J, Schultz C, Regar E, de Jaegere PP, Serruys PW, Zijlstra F, van Geuns RJ. Everolimus-eluting bioresorbable vascular scaffolds for treatment of patients presenting with ST-segment elevation myocardial infarction: BVS STEMI first study. Eur Heart J 2014;35(12):777-86.
24. Kocka V, Maly M, Tousek P, Budesinsky T, Lisa L, Prodanov P, Jarkovsky J, Widimsky P. Bioresorbable vascular scaffolds in acute ST-segment elevation myocardial infarction: a prospective multicentre study 'Prague 19'. Eur Heart J 2014;35(12):787-94.
25. Brugaletta S, Gori T, Low AF, Tousek P, Pinar E, Gomez-Lara J, Scalone G, Schulz E, Chan MY, Kocka V, Hurtado J, Gomez-Hospital JA, Munzel T, Lee CH, Cequier A, Valdes M, Widimsky P, Serruys PW, Sabate M. Absorb bioresorbable vascular scaffold versus everolimus-eluting metallic stent in ST-segment elevation myocardial infarction: 1-year results of a propensity score matching comparison: the BVS-EXAMINATION Study (bioresorbable vascular scaffold-a clinical evaluation of everolimus eluting coronary stents in the treatment of patients with ST-segment elevation myocardial infarction). JACC Cardiovasc Interv 2015;8(1 Pt B):189-97.

Acknowledgements

Just few years ago I was a young cardiologist in training and I would have never thought to settle in another country, finalize a PhD at the Thoraxcenter and become an interventional cardiologist in one of the most prestigious institution in the world.
This evolution in my life and career was possible because of my family and many extraordinary people I met during my journey.

First of all I would like to thank the person who has been a role model that guided me since my very first days, my father. You were intelligent, determined, brave, thoughtful and fun. You supported me in my important decisions, helpful when I was in troubles and happy for my little successes. I never went away from home for long periods than I came in Holland for my fellowship after a couple of months I came back to visits you and I found you strangely slim. I will have always the thought that if I would have stayed I could have recognised earlier the disease. I remember the day I received the communication I was awarded with the EAPCI grant. I immediately called you and you said "congratulations I am so happy for you". But that day I heard for the first time your voice so weak. The pain I felt was so intense that I tried to speak as less as possible to hide it. I would give back whatever award, my job, everything I have to hear your voice again strong as it was. One and half month later I received that grant and the only thing I was able to say in public was "I hope that the most important person in my life is looking from the sky into this room and he is proud of his son".
I have the same feeling also today and I hope that during my thesis defence you will be there proud of me. But most of all I hope you are proud of me for my everyday life, for how I work, for the family I am trying to build up, for the man I am. I hope to be able to be for my son what you have been for me. You known he looks like you in many ways.

Mamma, you have been the most sweet loving person in my life. You always surrounded me with love and you put me before everything. I felt secure in my childhood and so I feel now. You gave a great strength letting me understand that the only real things that matter is to have around you the few people who care about you and that you love. All the rest is secondary.

My little great sister Sara, you are a force of the nature, you are really great, strong, smart, determined, you planned targets in life and you achieved them one after the other, I am so proud of you. You are already a great lawyer, and I hope you will became soon judge as you wish. Despite having very busy days you were always able to help your brother who is calling you form Holland with every sort of issue or document needed at the very last moment (you know, I am not very well organized like you), and you always had to

run to fix everything. I can only thank you. Most of all I thank you for being my wonderful beloved little sister.

My love, my wife Sara, we have been together for the greatest part of our lives, we met when we were seventeen and we are still together but for me is like only one day has passed. You have been with me every moment, we grew together. Maybe it is for this reasons that we are so similar and you know me so well. I would not have done this thesis without you, actually I would not have done medicine without you. I was considering being en engineer but you really thought I was done to be a doctor, (by the way I was not that good in mathematics) and I cannot remember anything important I did without you being there, sometimes helping in the shadow (often literally, for this thesis you made the style corrections in the night). I think it was not easy to stay with me all these years, I am definitely not perfect but I also have the feeling that whatever happening we will be always together and this gives me a great strength. You make me think to the saying "behind a great man there is always a great woman", in our case I am not a great man but you are certainly a great woman.
During all these years, in every occasion you put me, my needs and my happiness first before thinking about you, from the very small things to the very important ones. For you it looks like natural but for me it is extraordinary. Many people seem to have a self-centered mind trying to emerge and to show to others they are special, but you not, you just want me to be happy, (and now also Riccardo), you make us feel loved and this makes you truly special, special for us.

Not only my family helped and supported me but also many great friends colleagues and highly qualified professionals who had an enormus impact on my reaserch, career and medical growth.

This thesis has two promoters, reflecting my activities and my experience, from full time research fellow to clinical fellow to senior interventional cardiologist.
I remember the first time I contacted Prof. Patrick W. Serruys via mail, respectfully asking for an interview with him, a living monument of interventional cardiology and research, he immediately replied positively and two weeks later I was in Rotterdam in his office.
I introduced myself, I explained my aspirations and ambitions and I showed him my CV with my 2 publications in a small Italian journal with no impact factor. After reading carefully every line of my CV, Prof. Serruys looked at me and told me: "Well… Roberto… actually you do not have a CV…" I was a little bit intimidated by him, but I firmly replied: "That is why I am here for, to build up my CV and career". He smiled and said: "then you definitely have to come…" and we started collaborating.

The first thing I wrote in Rotterdam was a case report with serial OCT imaging showing the healing process of a coronary dissection resulting in an intimal scar. A very small paper. I gave to Professor Serruys. The day after I was by chance passing by the meeting room in Cardialysis where at that moment was taking place the writing session for the RESOLUTE all comers Trial (lately published on the New England journal of Medicine) he saw me, he interrupted the session and he came out of the room to give me his comment and suggestions on the case report. I was impressed, it was a demonstration of great consideration and that day I learned that probably is not really important what you are working on (a NEJM paper or a case report) but is the commitment, the abnegation, and the integrity you put in your work to qualify you.
Few months later, during my research fellowship, I experienced the worse and saddest moment in my life, I had to stop my fellowship and come back to Italy. I still remember the support of Prof. Serruys and of all the people I had met in Rotterdam. One of my papers was left unfinished, Professor Serruys picked it up and wrote himself the missing parts.
The period I spent under the supervision of Professor Serruys was one of the most extraordinary of my life, a continuous flow of stimulating information and experiences that changed my way of looking at science and medicine thanks to one of the most intelligent, brilliant and illuminated mentor I could ever dream of.

After spending months in Cardialysis I realised that research was only part of the picture and that it could only be completed by a parallel clinical work. I decided to ask for a clinical fellowship at the Thoraxcenter.
I met for the first time Professor Zijlstra. I was excited of being interviewed by one of the person that gave a so great and decisive contribution to interventional cardiology and to our clinical practice. As a person truly engaged in patients treatment he received me in the office of the Cathlab. I was immediately impressed by his professionalism, his real interest in my potentiality, his unique way of leading the discussion.
That day I had my second great chance, I was accepted for a clinical fellowship at the Thoraxcenter.
During my very first Cathlab-day we had an acute case, a man with anterior infarction and in cardiogenic shock. The procedure was a complex one and required the positioning of intra-aortic balloon pump. I was not really familiar with the device, I was too slow. The procedure was successful but I knew I was the one slowing down the treatment that day. I promised myself to become extremely familiar with all possible action required and to perform them every time very fast so that the next time I would have been ready.
Few days later I was working with Professor Zijlstra and he saw me doing my job and rushing to do it as quickly as possible. He told me that the really good internationalist

should be calm and relaxed while doing fast the largest amount of manoeuvres and taking the time to precisely perform the few key actions that make a procedure successful. I started observing him and I learned when to be fast when to be precise, I learned how to approach a procedure and give a good treatment to the patient.
The interventional cardiologists are often tempted to focus on the coronaries, as this was the central and unique issue related to the patient.
Every time I was working with Professor Zijlstra I participated to a patient treatment, not just to a coronary artery treatment, evaluating the person in the global clinic situation and tailoring the intervention to the specific case. That is the way I am trying to follow in my daily practice.
One day I was not able even to engage the left coronary artery with the diagnostic catheter (one of the simplest things in interventional cardiology) Professor Zijlstra took over and he made the manoeuvre in about 2 seconds, then he left me continue. I was a bit disappointed with myself and I said: " I do not deserve it.." the reply I got was: " I have many more years of experience. I can do it because I also have the same experience before". I started again the case. In the same procedure we performed a CTO treatment, it was challenging but Professor Zijlstra guided me step by step; at the end we got blocked and our wire was not proceeding any more. He suggested using a wire I was not even considering and when I reached the lesion with that wire I was able to cross it immediately.
The nurse was impressed and immediately congratulated us for the success, but Professor Zijlstra said "It is not me, I did nothing, It was Roberto", (of course it was all due to him I would not ever had fished the procedure and everybody knew in the room).
That day I learned that stimulating the enthusiasm and the self confidence of a young is one of the greatest thing a mentor can do and secondly that great men do not need to show or highlight their qualities, if they are real they are just evident.
I could mention thousands of similar episodes from my everyday life. Professor Zijlstra has been and he is now a mentor for my profession and for my life I admire his way of approaching medicine, colleagues and life. He is a great example to follow and I will always remember every single time he supported me.

Nicholas van Mieghem is the co-promoter of this thesis. He was one of the first persons I met in the Thoraxcenter, I was immediately fascinated by his energetic enthusiasm, his ambition and his continuous flow of interesting ideas, mixed to an uncommon clinical competence and maturity.
I definitely enjoyed being trained by him. I feel in him my same passion for our profession that brought us to spend innumerable evenings performing cases. I learned from him to be methodical, to have a mental scheme of my procedure before performing it, to be

disciplined in my movements and actions. In the years of my training when I was working with him I had the feeling not to be with a colleague but with an older brother giving god advices to the youngest.
I remember that in the last year of my fellowship he was letting me do every single case, I guess it was terribly boring for him, but he guided me in every situation.
He was one of the persons that supported me the most, he was the first to mention me the idea of remaining in The Netherlands working in the Thoraxcentrum and he was the one together with Professor Zijlstra that primarily supported me to become an interventional cardiologist in this great institution. I would not be what I am now without him.

Professor De Jaegere is real guide for work and life. Every time I worked with him I grew as an interventional cardiologist, every time I talked with him I grew as a person. Because of his extraordinary clinical and scientific experience he was always able to give me the right suggestions in difficult situations and this was true also for non patients related issues.
While joking he often defined himself an "old Muppet", but during these years you have been a solid and fundamental guide for young interventionalists, generating in all our minds respect and admiration.

I would like to thank Professor Robert Jan van Geuns he was the person who introduced me in the Thoraxcenter, he trained me and we worked together on one of my favourite research topic, the bioresorbable technologies for treatment of coronary artery disease. He favoured the important transition for me from being a fellow, to guide fellows in research. I learned from him how to interpret the clinical evidences and he always gave me additional viewpoints to better understand reality.

Evelyn Regar was the first person to interview me among senior interventional cardiologists when I was applying for the clinical fellowship, she was immediately friendly and she explained me in details the organization of the daily work, none of us was imaging that we would have done that work together for years. I learned from her how to interpret intravascular imaging and that what we see with simple angiograms is only a small part of the reality. I understood how clinical events and complications often need a deep investigation and understanding of the underlying intravascular mechanisms to have a correct treatment. We have now quite a tradition with the live cases during the Optics in Cardiology meeting an some were so successful that companies put the live cases on their internet home page, such results were possible only thanks to an excellent teamwork and the appropriate use of cutting edge technologies.

Joost Daemen we are sharing the pleasure and the burden of being young interventional cardiologists in one of the most prestigious center in the world. We are also sharing similar experience with our private live building up a family. I wish you all the best in the profession and in your life.

I would like to thank all the colleagues of the cardiology department for the way we professionally collaborate everyday and for the amazing personal relation we established.

I would like to thank my Paranymphs Yoshinobu and Jurgen. Yoshi you have been always very helpful since when I arrived in Rotterdam, you are a great scientist and physician, I am sure you will be one of the most relevant opinion leaders in our field in the future.
Jurgen you are a real expert of intravascular imaging you sheared your knowledge with generations of fellows. We always collaborated with great results and with a lot of fun. Our live cases were meticulous prepared and successfully performed, our images were most of the time at the same time beautiful and meaningful.

Since my first day in the Cathlab, I was always supported by an extraordinary team of nurses and technicians. I know I have around me prepared persons, able to combine high professionalism with friendly attitude, creating a productive but confortable environment. This is something really uncommon and that I consider a great and precious value to preserve.

I would like to thank Anja, when she saw the deadline for the thesis defence and the organization of the symposium, she was skeptical about our chances to be able to do everything. But after a lot of work we made it. We made it.

Hanny, I have been calling you at any time during the day and also in the evening with often long questions and the need for quick answers and solutions. You have been always kindly available and helpful, I sincerely thank you.

Rakesh thank you for all the time we collaborated you have been always extremely professional and at the same time flexible to adapt to every situation, you are a great value for our department.

I would like to especially thank Salvatore Brugaletta and Josep Gomez-Lara, I learned a lot from you and you were my guidance at the very beginning of my experience here. We created a nice working team I will not forget those days.

In addition I would like to thank all the people I met in Cardialysis, they friendly accepted me since the beginning and we established a great professional and productive collaboration in particular Gerrit-Anne van Es, Marie-angèle Morel and Hector Garcia-Garcia have been fundamental for me.

I would like to also thank all the fellows and the young cardiologist in training that are working in our cathlab. It is a joy for me to be able to share with you what I know about our wonderful profession. While I ma teaching you, you make me a better operator, because I always try to give you the best example to follow, the most updated knowledge, the most appropriate way of approaching patients. You are the future, I wish you the best.

Finally I would like to thank my son Riccardo, you are my most profound joy. All my daily problems vanish immediatley when I come back home and I see you smiling and running (actually crewling) to me. I hope I will be a good father for you. You are the true meaning of my life.

Curriculum vitae

ROBERTO DILETTI

PERSONAL DATA

Full Name and Title: Roberto Diletti, MD
Place & Date of Birth: Rieti, Italy, May 31st, 1980
Istitution: Department of Interventional Cardiology, Thoraxcenter Erasmus MC, Rotterdam, the Netherlands
E-mail : r.diletti@erasmusmc.nl
Addresses: Westzeedijk 200, 3016 AM Rotterdam, the Netherlands

EDUCATION

2011 Cardiology Specialization Degree at Perugia University, School of Medicine. Summa cum Laude.

Since 2010 Research and clinical fellow interventional Cardiology at Thoraxcenter Erasmus MC Rotterdam, The Netherlands

2007 Residency training program in Cardiology – Santa Maria Hospital - Terni - University of Perugia.

2006 Italian Medical licensure examination (License number: 1585-Rieti).

2006 Graduated in Medicine at Perugia University School of Medicine -Summa cum Laude.

1999 Grammar High School, "Liceo Scientifico C.Jucci"- Rieti.

CLINICAL EXPERIENCE AND TRAINING

Since 2013 *Senior interventional cardiologist Thoraxcenter Erasmus MC Rotterdam, the Netherlands*

2012-13 Clinical fellowship Interventional Cardiology at Thoraxcenter Erasmus MC, Rotterdam the Netherlands

2010-12 Research Fellowship Interventional Cardiology at Thoraxcenter Erasmus MC, Rotterdam the Netherlands.

2008-2009 Interventional Cardiology Laboratory - Division of cardiology - Santa Maria Hospital - Terni *(Residency training program in Cardiology - University of Perugia)*.

2007 Intensive care unit and Echocardiography Laboratory - Division of cardiology - Santa Maria Hospital – Terni *(Residency training program in Cardiology - University of Perugia)*.

2006 Division of General Surgery.
2005-2006 Heart failure unit - Division of Cardiology - Santa Maria Della Misericordia Hospital - Perugia- Italy.
2005 Intensive care unit - Division of Cardiology – Hospital Virgen de la Arrixaca - University of Murcia (Spain).
2004 Department of Internal Medicine - University of Perugia.
2003 Laboratory of Human Physiology - University of Perugia.
2002 Laboratory of cell and molecular biology – University of Perugia.

MEMBERSHIPS

- Member of European Society of Cardiology (ESC)
- Member of the European Association of Percutaneous Cardiovascular Interventions **(EAPCI)**
- Member of the European Working Group on Atherosclerosis and Vascular Biology
- Member of the European Working Group on Acute Cardiac Care
- Member of the Italian Society of Cardiology **(SIC)**
- Member of the Italian Resuscitation Council **(IRC)**
- Member of the revision committee, "Future in research"- Italian Ministry of Education, University and Research.

REVIEWER

- Circulation
- Journal American College of cardiology
- European Heart journal
- JACC: Cardiovascular Interventions
- Circulation: Cardiovascular Interventions
- EuroIntervention
- International Journal of Cardiology
- Journal Interventional Cardiology
- Minerva Cardioangiologica
- Heart and Vessels
- Journal of Cardiovascular Medicine

AWARDS

1 Winner of the European Association of Percutaneous Cardiovascular Interventions (EAPCI) research award
Research project entitled: "OCT Light Intensity Analysis:A New Tool for the Detection of Bioresorbable Vascular Scaffold Tissue Coverage"
EuroPCR Paris 2011

2 Award for the Best Thesis in Cardiology 2011. Italian Society of Cardiology (SIC)
SIC Rome 2012

3 Winner of the Italian society of cardiology (SIC) research grant
Research project entitled: Platelet Reactivity and Clinical Outcomes In Patients Treated with Ticagrelor as Single Antiplatelet Therapy after Second Generation Drug Eluting Stent Implantation
SIC Rome 2012

April 2015

List of publications

LIST OF PUBLICATIONS

1. Ischemic postconditioning after routine thrombus aspiration during primary percutaneous coronary intervention: Rationale and design of the POstconditioning Rotterdam trial
   Yetgin T, van Kranenburg M, Ten Cate T, Duncker DJ, de Boer MJ, Diletti R, van Geuns RM, Zijlstra F, Manintveld OC.
   Catheter Cardiovasc Interv. 2015 Sep 10.

2. Safety of optical coherence tomography in daily practice: a comparison with intravascular ultrasound.
   van der Sijde JN, Karanasos A, van Ditzhuijzen NS, Okamura T, van Geuns RJ, Valgimigli M, Ligthart JM, Witberg KT, Wemelsfelder S, Fam JM, Zhang B, Diletti R, de Jaegere PP, van Mieghem NM, van Soest G, Zijlstra F, van Domburg RT, Regar E.
   Eur Heart J Cardiovasc Imaging. 2016 Mar 18.

3. The Rotterdam Radial Access Research: Ultrasound-Based Radial Artery Evaluation for Diagnostic and Therapeutic Coronary Procedures.
   Costa F, van Leeuwen MA, Daemen J, Diletti R, Kauer F, van Geuns RJ, Ligthart J, Witberg K, Zijlstra F, Valgimigli M, Van Mieghem NM.
   Circ Cardiovasc Interv. 2016 Feb;9(2):e003129.

4. Effectiveness of a novel biodegradable polymer, sirolimus-eluting stent platform in percutaneous coronary intervention.
   Dominici M, Arrivi A, Bazzucchi M, DE Paolis M, Milici C, Bock C, Placanica A, Lazzari L, Diletti R, Boschetti E.
   Minerva Cardioangiol. 2016 Feb;64(1):1-8. Epub 2015 Oct 7.

5. Primary PCI with or without Thrombectomy.
   Diletti R, van Mieghem NM, Zijlstra F.
   N Engl J Med. 2015 Aug 13;373(7):680.

6. Rapid exchange ultra-thin microcatheter using fibre-optic sensing technology for measurement of intracoronary fractional flow reserve.
   Diletti R, Van Mieghem NM, Valgimigli M, Karanasos A, Everaert BR, Daemen J, van Geuns RJ, de Jaegere PP, Zijlstra F, Regar E.
   EuroIntervention. 2015 Aug;11(4):428-32.

7. Angiographic and optical coherence tomography insights into bioresorbable scaffold thrombosis: single-center experience.
   Karanasos A, Van Mieghem N, van Ditzhuijzen N, Felix C, Daemen J, Autar A, Onuma Y, Kurata M, Diletti R, Valgimigli M, Kauer F, van Beusekom H, de Jaegere P, Zijlstra F, van Geuns RJ, Regar E.
   Circ Cardiovasc Interv. 2015 May;8(5

8. Early and late optical coherence tomography findings following everolimus-eluting bioresorbable vascular scaffold implantation in myocardial infarction: a preliminary report.
   Karanasos A, Muramatsu T, Diletti R, Nauta S, Onuma Y, Lenzen M, Nakatani S, Van Mieghem NM, Schultz C, De Jaegere PP, Serruys PW, Zijlstra F, Regar E, van Geuns RJ.
   Hellenic J Cardiol. 2015 Mar-Apr;56(2):125-35.

9. Impact of body mass index on long-term clinical outcomes after second-generation drug eluting stent implantation: Insights from the international global RESOLUTE program.
   Diletti R, Garcia-Garcia HM, Bourantas C, Van Mieghem NM, van Geuns RJ, Muramatsu T, Zhang YJ, Mauri L, Belardi J, Silber S, Widimsky P, Leon M, Windecker S, Meredith I, Neumann FJ, Yeung AC, Saito S, Liu M, van Leeuwen F, Serruys PW.
   Catheter Cardiovasc Interv. 2015 May;85(6):952-8.

10. Current status of clinically available bioresorbable scaffolds in percutaneous coronary interventions.
    Felix C, Everaert B, Diletti R, Van Mieghem N, Daemen J, Valgimigli M, de Jaegere PP, Zijlstra F, Regar E, Simsek C, Onuma Y, van Geuns RJ.
    Neth Heart J. 2015 Mar;23(3):153-60

11. Appropriate use of bioresorbable vascular scaffolds in percutaneous coronary interventions: a recommendation from experienced users : A position statement on the use of bioresorbable vascular scaffolds in the Netherlands.
    Everaert B, Felix C, Koolen J, den Heijer P, Henriques J, Wykrzykowska J, van der Schaaf R, de Smet B, Hofma S, Diletti R, Van Mieghem N, Regar E, Smits P, van Geuns RJ.
    Neth Heart J. 2015 Mar;23(3):161-5.

12. Contemporary practice and technical aspects in coronary intervention with bioresorbable scaffolds: a European perspective.
    Tamburino C, Latib A, van Geuns RJ, Sabate M, Mehilli J, Gori T, Achenbach S, Alvarez MP, Nef H, Lesiak M, Di Mario C, Colombo A, Naber CK, Caramanno G, Capranzano P, Brugaletta S, Geraci S, Araszkiewicz A, Mattesini A, Pyxaras SA, Rzeszutko L, Depukat R, Diletti R, Boone E, Capodanno D, Dudek D.
    EuroIntervention. 2015 May;11(1):45-52.

13. Bioresorbable vascular scaffold treatment induces the formation of neointimal cap that seals the underlying plaque without compromising the luminal dimensions: a concept based on serial optical coherence tomography data.
    Bourantas CV, Serruys PW, Nakatani S, Zhang YJ, Farooq V, Diletti R, Ligthart J, Sheehy A, van Geuns RJ, McClean D, Chevalier B, Windecker S, Koolen J, Ormiston J, Whitbourn R, Rapoza R, Veldhof S, Onuma Y, Garcia-Garcia HM.
    EuroIntervention. 2015 Nov;11(7):746-56.

14. Percutaneous coronary interventions during ST-segment elevation myocardial infarction: current status and future perspectives.
Diletti R, Yetgin T, Manintveld OC, Ligthart JM, Zivelonghi C, Zijlstra F, Ribichini F.
EuroIntervention. 2014 Aug;10 Suppl T:T13-22.

15. The 'Young Acute Cardiovascular Care Association group' of the Acute Cardiovascular Care Association.
Young ACCA Group, Diletti R, Krychtiuk K, Pöss J, Rubini-Gimenez M, Tejedor AV.
Eur Heart J. 2014 Jul 14;35(27):1770-1.

16. Impact of biodegradable versus durable polymer drug-eluting stents on clinical outcomes in patients with coronary artery disease: a meta-analysis of 15 randomized trials.
Zhang Y, Tian N, Dong S, Ye F, Li M, Bourantas CV, Iqbal J, Onuma Y, Muramatsu T, Diletti R, Garcia-Garcia HM, Xu B, Serruys PW, Chen S.
Chin Med J (Engl). 2014;127(11):2159-66.

17. Progress in treatment by percutaneous coronary intervention: the stent of the future.
Muramatsu T, Onuma Y, Zhang YJ, Bourantas CV, Kharlamov A, Diletti R, Farooq V, Gogas BD, Garg S, García-García HM, Ozaki Y, Serruys PW.
Rev Esp Cardiol (Engl Ed). 2013 Jun;66(6):483-96.

18. 1-year clinical outcomes of diabetic patients treated with everolimus-eluting bioresorbable vascular scaffolds: a pooled analysis of the ABSORB and the SPIRIT trials.
Muramatsu T, Onuma Y, van Geuns RJ, Chevalier B, Patel TM, Seth A, Diletti R, García-García HM, Dorange CC, Veldhof S, Cheong WF, Ozaki Y, Whitbourn R, Bartorelli A, Stone GW, Abizaid A, Serruys PW; ABSORB Cohort B Investigators; ABSORB EXTEND Investigators; SPIRIT FIRST Investigators; SPIRIT II Investigators; SPIRIT III Investigators; SPIRIT IV Investigators.
JACC Cardiovasc Interv. 2014 May;7(5):482-93.

19. First observation of acute coronary syndrome triggered by calcified nodules. Angiographic and optical coherence assessment.
Rodríguez-Olivares R, García-Touchard A, Diletti R, Oteo JF, Fernández-Díaz JA, Domínguez-Domínguez JR, Ruigómez JG.
Int J Cardiol. 2014 May 15;173(3):e70-1.

20. Thrombus aspiration during myocardial infarction.
Diletti R, Serruys PW.
N Engl J Med. 2014 Feb 13;370(7):675.

21. Comparison of acute gain and late lumen loss after PCI with bioresorbable vascular scaffolds versus everolimus-eluting stents: an exploratory observational study prior to a randomised trial.
Zhang YJ, Bourantas CV, Muramatsu T, Iqbal J, Farooq V, Diletti R, Campos CA, Onuma Y, Garcia-Garcia HM, Serruys PW.
EuroIntervention. 2014 Oct;10(6):672-80

22. Fusion of optical coherence tomographic and angiographic data for more accurate evaluation of the endothelial shear stress patterns and neointimal distribution after bioresorbable scaffold implantation: comparison with intravascular ultrasound-derived reconstructions.
Bourantas CV, Papafaklis MI, Lakkas L, Sakellarios A, Onuma Y, Zhang YJ, Muramatsu T, Diletti R, Bizopoulos P, Kalatzis F, Naka KK, Fotiadis DI, Wang J, Garcia Garcia HM, Kimura T, Michalis LK, Serruys PW.
Int J Cardiovasc Imaging. 2014 Mar;30(3):485-94.

23. Three-dimensional optical coherence tomography for guidance of complex percutaneous coronary interventions.
Ligthart JM, Diletti R, Witberg K, Schultz C.
JACC Cardiovasc Interv. 2014 Jan;7(1):102-3.

24. Short- and long-term implications of a bioresorbable vascular scaffold implantation on the local endothelial shear stress patterns.
Bourantas CV, Papafaklis MI, Garcia-Garcia HM, Farooq V, Diletti R, Muramatsu T, Zhang Y, Kalatzis FG, Naka KK, Fotiadis DI, Onuma Y, Michalis LK, Serruys PW.
JACC Cardiovasc Interv. 2014 Jan;7(1):100-1. doi: 10.1016/j.jcin.2013.01.139. No abstract available.

25. Everolimus-eluting bioresorbable vascular scaffolds for treatment of patients presenting with ST-segment elevation myocardial infarction: BVS STEMI first study.
Diletti R, Karanasos A, Muramatsu T, Nakatani S, Van Mieghem NM, Onuma Y, Nauta ST, Ishibashi Y, Lenzen MJ, Ligthart J, Schultz C, Regar E, de Jaegere PP, Serruys PW, Zijlstra F, van Geuns RJ.
Eur Heart J. 2014 Mar;35(12):777-86.

26. Impact of 3-dimensional bifurcation angle on 5-year outcome of patients after percutaneous coronary intervention for left main coronary artery disease: a substudy of the SYNTAX trial (synergy between percutaneous coronary intervention with taxus and cardiac surgery).
Girasis C, Farooq V, Diletti R, Muramatsu T, Bourantas CV, Onuma Y, Holmes DR, Feldman TE, Morel MA, van Es GA, Dawkins KD, Morice MC, Serruys PW.
JACC Cardiovasc Interv. 2013 Dec;6(12):1250-60.

27. Clinical and angiographic characteristics of patients likely to have vulnerable plaques: analysis from the PROSPECT study.
Bourantas CV, Garcia-Garcia HM, Farooq V, Maehara A, Xu K, Généreux P, Diletti R, Muramatsu T, Fahy M, Weisz G, Stone GW, Serruys PW.
JACC Cardiovasc Imaging. 2013 Dec;6(12):1263-72.

28. Intimal flaps detected by optical frequency domain imaging in the proximal segments of native coronary arteries: an innocent bystander? Insights from the TROFI Trial.
Muramatsu T, García-García HM, Onuma Y, Zhang YJ, Bourantas CV, Diletti R, Iqbal J, Radu MD,

Ozaki Y, Serruys PW; TROFI investigators.
Circ J. 2013;77(9):2327-33.

29. Complete revascularization is not a prerequisite for success in current transcatheter aortic valve implantation practice.
Van Mieghem NM, van der Boon RM, Faqiri E, Diletti R, Schultz C, van Geuns RJ, Serruys PW, Kappetein AP, van Domburg RT, de Jaegere PP.
JACC Cardiovasc Interv. 2013 Aug;6(8):867-75.

30. Assessment of plaque evolution in coronary bifurcations located beyond everolimus eluting scaffolds: serial intravascular ultrasound virtual histology study.
Lee IS, Bourantas CV, Muramatsu T, Gogas BD, Heo JH, Diletti R, Farooq V, Zhang Y, Onuma Y, Serruys PW, Garcia-Garcia HM.
Cardiovasc Ultrasound. 2013 Jul 20;11:25.

31. Prediction of 1-year mortality in patients with acute coronary syndromes undergoing percutaneous coronary intervention: validation of the logistic clinical SYNTAX (Synergy Between Percutaneous Coronary Interventions With Taxus and Cardiac Surgery) score.
Farooq V, Vergouwe Y, Généreux P, Bourantas CV, Palmerini T, Caixeta A, Garcìa-Garcìa HM, Diletti R, Morel MA, McAndrew TC, Kappetein AP, Valgimigli M, Windecker S, Dawkins KD, Steyerberg EW, Serruys PW, Stone GW.
JACC Cardiovasc Interv. 2013 Jul;6(7):737-45.

32. In vivo assessment of the three-dimensional haemodynamic micro-environment following drug-eluting bioresorbable vascular scaffold implantation in a human coronary artery: fusion of frequency domain optical coherence tomography and angiography.
Papafaklis MI, Bourantas CV, Farooq V, Diletti R, Muramatsu T, Zhang Y, Fotiadis DI, Onuma Y, Garcia Garcia HM, Michalis LK, Serruys PW.
EuroIntervention. 2013 Nov;9(7):890.

33. Clinical outcomes after zotarolimus and everolimus drug eluting stent implantation in coronary artery bifurcation lesions: insights from the RESOLUTE All Comers Trial.
Diletti R, Garcia-Garcia HM, Bourantas CV, van Geuns RJ, Van Mieghem NM, Vranckx P, Zhang YJ, Farooq V, Iqbal J, Wykrzykowska JJ, de Vries T, Swart M, Teunissen Y, Negoita M, van Leeuwen F, Silber S, Windecker S, Serruys PW; RESOLUTE All Comers Investigators.
Heart. 2013 Sep;99(17):1267-74.

34. Intimal Flaps Detected by Optical Frequency Domain Imaging in the Proximal Segments of Native Coronary Arteries.
Muramatsu T, García-García HM, Onuma Y, Zhang YJ, Bourantas CV, Diletti R, Iqbal J, Radu MD, Ozaki Y, Serruys PW; on behalf of the TROFI investigators.
Circ J. 2013 Jun 15.

35. Early detection and invasive passivation of future culprit lesions: a future potential or an unrealistic pursuit of chimeras?
Bourantas CV, Garcia-Garcia HM, Diletti R, Muramatsu T, Serruys PW.
Am Heart J. 2013 Jun;165(6):869-881.e4.

36. Intracoronary optical coherence tomography and histology of overlapping everolimus-eluting bioresorbable vascular scaffolds in a porcine coronary artery model: the potential implications for clinical practice.
Farooq V, Serruys PW, Heo JH, Gogas BD, Onuma Y, Perkins LE, Diletti R, Radu MD, Räber L, Bourantas CV, Zhang Y, van Remortel E, Pawar R, Rapoza RJ, Powers JC, van Beusekom HM, Garcìa-Garcìa HM, Virmani R.
JACC Cardiovasc Interv. 2013 May;6(5):523-32.

37. Clinical and angiographic outcomes following first-in-man implantation of a novel thin-strut low-profile fixed-wire stent: the Svelte Coronary Stent Integrated Delivery System first-in-man trial.
Diletti R, Garcia-Garcia HM, Bourantas CV, van Geuns RJ, Van Mieghem NM, Agostoni P, Muramatsu T, Farooq V, Spencer R, De Schepper J, Pomeranz M, Stella P, Serruys PW.
EuroIntervention. 2013 May 20;9(1):125-34.

38. Bioresorbable scaffolds in the treatment of coronary artery disease.
Zhang Y, Bourantas CV, Farooq V, Muramatsu T, Diletti R, Onuma Y, Garcia-Garcia HM, Serruys PW.
Med Devices (Auckl). 2013 Mar 12;6:37-48.

39. The edge vascular response following implantation of the Absorb everolimus-eluting bioresorbable vascular scaffold and the XIENCE V metallic everolimus-eluting stent. First serial follow-up assessment at six months and two years: insights from the first-in-man ABSORB Cohort B and SPIRIT II trials.
Gogas BD, Bourantas CV, Garcia-Garcia HM, Onuma Y, Muramatsu T, Farooq V, Diletti R, van Geuns RJ, De Bruyne B, Chevalier B, Thuesen L, Smits PC, Dudek D, Koolen J, Windecker S, Whitbourn R, McClean D, Dorange C, Miquel-Hebert K, Veldhof S, Rapoza R, Ormiston JA, Serruys PW.
EuroIntervention. 2013 Oct;9(6):709-20.

40. Operator exposure to x-ray in left and right radial access during percutaneous coronary procedures: OPERA randomised study.
Dominici M, Diletti R, Milici C, Bock C, Placanica A, D'Alessandro G, Arrivi A, Italiani M, Buono E, Boschetti E.
Heart. 2013 Apr;99(7):480-4.

41. The negative impact of incomplete angiographic revascularization on clinical outcomes and its association with total occlusions: the SYNTAX (Synergy Between Percutaneous Coronary Intervention with Taxus and Cardiac Surgery) trial.
Farooq V, Serruys PW, Garcia-Garcia HM, Zhang Y, Bourantas CV, Holmes DR, Mack M, Feldman T, Morice MC, Ståhle E, James S, Colombo A, Diletti R, Papafaklis MI, de Vries T, Morel MA, van Es GA, Mohr FW, Dawkins KD, Kappetein AP, Sianos G, Boersma E.
J Am Coll Cardiol. 2013 Jan 22;61(3):282-94

42. From first to second generation drug eluting stents for treatment of coronary bifurcations: are we making progress?
Diletti R, Serruys P.
Catheter Cardiovasc Interv. 2012 Dec 1;80(7):1171-2.

43. ABSORB II randomized controlled trial: a clinical evaluation to compare the safety, efficacy, and performance of the Absorb everolimus-eluting bioresorbable vascular scaffold system against the XIENCE everolimus-eluting coronary stent system in the treatment of subjects with ischemic heart disease caused by de novo native coronary artery lesions: rationale and study design.
Diletti R, Serruys PW, Farooq V, Sudhir K, Dorange C, Miquel-Hebert K, Veldhof S, Rapoza R, Onuma Y, Garcia-Garcia HM, Chevalier B.
Am Heart J. 2012 Nov;164(5):654-63.

44. Clinical and intravascular imaging outcomes at 1 and 2 years after implantation of absorb everolimus eluting bioresorbable vascular scaffolds in small vessels. Late lumen enlargement: does bioresorption matter with small vessel size? Insight from the ABSORB cohort B trial.
Diletti R, Farooq V, Girasis C, Bourantas C, Onuma Y, Heo JH, Gogas BD, van Geuns RJ, Regar E, de Bruyne B, Dudek D, Thuesen L, Chevalier B, McClean D, Windecker S, Whitbourn RJ, Smits P, Koolen J, Meredith I, Li X, Miquel-Hebert K, Veldhof S, Garcia-Garcia HM, Ormiston JA, Serruys PW.
Heart. 2013 Jan;99(2):98-105.

45. Incidence and multivariable correlates of long-term mortality in patients treated with surgical or percutaneous revascularization in the synergy between percutaneous coronary intervention with taxus and cardiac surgery (SYNTAX) trial.
Farooq V, Serruys PW, Bourantas C, Vranckx P, Diletti R, Garcia Garcia HM, Holmes DR, Kappetein AP, Mack M, Feldman T, Morice MC, Colombo A, Morel MA, de Vries T, van Es GA, Steyerberg EW, Dawkins KD, Mohr FW, James S, Ståhle E.
Eur Heart J. 2012 Dec;33(24):3105-13

46. Serial 2- and 3-dimensional visualization of side branch jailing after metallic stent implantation: to kiss or not to kiss...?
Diletti R, Farooq V, Muramatsu T, Gogas BD, Garcia-Garcia HM, van Geuns RJ, Serruys PW.
JACC Cardiovasc Interv. 2012 Oct;5(10):1089-90.

47. Combined anatomical and clinical factors for the long-term risk stratification of patients undergoing percutaneous coronary intervention: the Logistic Clinical SYNTAX score.
Farooq V, Vergouwe Y, Räber L, Vranckx P, Garcia-Garcia H, Diletti R, Kappetein AP, Morel MA, de Vries T, Swart M, Valgimigli M, Dawkins KD, Windecker S, Steyerberg EW, Serruys PW.
Eur Heart J. 2012 Dec;33(24):3098-104.

48 Vascular response of the segments adjacent to the proximal and distal edges of the ABSORB everolimus-eluting bioresorbable vascular scaffold: 6-month and 1-year follow-up assessment: a virtual histology intravascular ultrasound study from the first-in-man ABSORB cohort B trial.
Gogas BD, Serruys PW, Diletti R, Farooq V, Brugaletta S, Radu MD, Heo JH, Onuma Y, van Geuns RJ, Regar E, De Bruyne B, Chevalier B, Thuesen L, Smits PC, Dudek D, Koolen J, Windecker S, Whitbourn R, Miquel-Hebert K, Dorange C, Rapoza R, Garcia-Garcia HM, McClean D, Ormiston JA.
JACC Cardiovasc Interv. 2012 Jun;5(6):656-65.

49. Plaque sealing and passivation with a mechanical self-expanding low outward force nitinol vShield device for the treatment of IVUS and OCT-derived thin cap fibroatheromas (TCFAs) in native coronary arteries: report of the pilot study vShield Evaluated at Cardiac hospital in Rotterdam for Investigation and Treatment of TCFA (SECRITT).
Wykrzykowska JJ, Diletti R, Gutierrez-Chico JL, van Geuns RJ, van der Giessen WJ, Ramcharitar S, Duckers HE, Schultz C, de Feyter P, van der Ent M, Regar E, de Jaegere P, Garcia-Garcia HM, Pawar R, Gonzalo N, Ligthart J, de Schepper J, van den Berg N, Milewski K, Granada JF, Serruys PW.
EuroIntervention. 2012 Dec 20;8(8):945-54.

50. ST-elevation during surgery in a young male: who would bet on inverted takotsubo syndrome?
Diletti R, Dominici M, Patella MM, Citro R, Boschetti E.
Int J Cardiol. 2012 Dec 15;162(1):e6-7.

51. Angiographic and histological results following implantation of a novel stent-on-a-wire in the animal model.
Diletti R, Garcia-Garcia HM, van Geuns RJ, Farooq V, Bailey L, Rousselle S, Kopia G, Easterbrook W, Pomeranz M, Serruys PW.
EuroIntervention. 2012 Jul 20;8(3):390-9.

52. Left radial versus right radial approach for coronary artery catheterization: a prospective comparison.
Dominici M, Diletti R, Milici C, Bock C, Garg S, De Paolis M, Ambrosio G, Boschetti E.
J Interv Cardiol. 2012 Apr;25(2):203-9. doi: 10.1111/j.1540-8183.2011.00689.x. Epub 2012 Jan 25.

53. In vivo characterisation of bioresorbable vascular scaffold strut interfaces using optical coherence tomography with Gaussian line spread function analysis.
Sheehy A, Gutiérrez-Chico JL, Diletti R, Oberhauser JP, Glauser T, Harrington J, Kossuth MB, Rapoza RJ, Onuma Y, Serruys PW.
EuroIntervention. 2012 Feb;7(10):1227-35.

54. Head-to-head comparison of the neointimal response between metallic and bioresorbable everolimus-eluting scaffolds using optical coherence tomography.
Gomez-Lara J, Brugaletta S, Farooq V, Onuma Y, Diletti R, Windecker S, Thuesen L, McClean D, Koolen J, Whitbourn R, Dudek D, Smits PC, Chevalier B, Regar E, Veldhof S, Rapoza R, Ormiston JA, Garcia-Garcia HM, Serruys PW.
JACC Cardiovasc Interv. 2011 Dec;4(12):1271-80.

55. Spatial distribution and temporal evolution of scattering centers by optical coherence tomography in the poly(L-lactide) backbone of a bioresorbable vascular scaffold.
Gutiérrez-Chico JL, Radu MD, Diletti R, Sheehy A, Kossuth MB, Oberhauser JP, Glauser T, Harrington J, Rapoza RJ, Onuma Y, Serruys PW.
Circ J. 2012;76(2):342-50.

56. Angiographic maximal luminal diameter and appropriate deployment of the everolimus-eluting bioresorbable vascular scaffold as assessed by optical coherence tomography: an ABSORB cohort B trial sub-study.
Gomez-Lara J, Diletti R, Brugaletta S, Onuma Y, Farooq V, Thuesen L, McClean D, Koolen J, Ormiston JA, Windecker S, Whitbourn R, Dudek D, Dorange C, Veldhof S, Rapoza R, Regar E, Garcia-Garcia HM, Serruys PW.
EuroIntervention. 2012 Jun 20;8(2):214-24.

57. Tools & techniques: risk stratification and diagnostic tools in left main stem intervention.
Farooq V, Heo JH, Räber L, Brugaletta S, Radu M, Gogas BD, Diletti R, Onuma Y, Garcia-Garcia HM, Serruys PW.
EuroIntervention. 2011 Oct 30;7(6):747-53.

58. In vivo visualisation by three-dimensional optical coherence tomography of stress crazing of a bioresorbable vascular scaffold implanted for treatment of human coronary stenosis.
Radu MD, Onuma Y, Rapoza RJ, Diletti R, Serruys PW.
EuroIntervention. 2012 Apr;7(12):1461-3.

59. Serial analysis of the malapposed and uncovered struts of the new generation of everolimus-eluting bioresorbable scaffold with optical coherence tomography.
Gomez-Lara J, Radu M, Brugaletta S, Farooq V, Diletti R, Onuma Y, Windecker S, Thuesen L, McClean D, Koolen J, Whitbourn R, Dudek D, Smits PC, Regar E, Veldhof S, Rapoza R, Ormiston JA, Garcia-Garcia HM, Serruys PW.
JACC Cardiovasc Interv. 2011 Sep;4(9):992-1001

60. CRosser As First choice for crossing Totally occluded coronary arteries (CRAFT Registry): focus on conventional angiography and computed tomography angiography predictors of success.
García-García HM, Brugaletta S, van Mieghem CA, Gonzalo N, Diletti R, Gomez-Lara J, Airoldi F, Carlino M, Tavano D, Chieffo A, Montorfano M, Michev I, Colombo A, van der Ent M, Serruys PW.
EuroIntervention. 2011 Aug;7(4):480-6.

61. Assessment of coronary atherosclerosis progression and regression at bifurcations using combined IVUS and OCT.
Diletti R, Garcia-Garcia HM, Gomez-Lara J, Brugaletta S, Wykrzykowska JJ, van Ditzhuijzen N, van Geuns RJ, Regar E, Ambrosio G, Serruys PW.
JACC Cardiovasc Imaging. 2011 Jul;4(7):774-80.

62. 6-month clinical outcomes following implantation of the bioresorbable everolimus-eluting vascular scaffold in vessels smaller or larger than 2.5 mm.
Diletti R, Onuma Y, Farooq V, Gomez-Lara J, Brugaletta S, van Geuns RJ, Regar E, de Bruyne B, Dudek D, Thuesen L, Chevalier B, McClean D, Windecker S, Whitbourn R, Smits P, Koolen J, Meredith I, Li D, Veldhof S, Rapoza R, Garcia-Garcia HM, Ormiston JA, Serruys PW.
J Am Coll Cardiol. 2011 Jul 12;58(3):258-64. doi: 10.1016/j.jacc.2011.02.052.

63. NIRS and IVUS for characterization of atherosclerosis in patients undergoing coronary angiography.
Brugaletta S, Garcia-Garcia HM, Serruys PW, de Boer S, Ligthart J, Gomez-Lara J, Witberg K, Diletti R, Wykrzykowska J, van Geuns RJ, Schultz C, Regar E, Duckers HJ, van Mieghem N, de Jaegere P, Madden SP, Muller JE, van der Steen AF, van der Giessen WJ, Boersma E.
JACC Cardiovasc Imaging. 2011 Jun;4(6):647-55.

64. Healing of a coronary artery dissection detected by intravascular ultrasound and optical coherence tomography.
Diletti R, Garcia-Garcia HM, Brugaletta S, Lara JG, Serruys PW, Regar E.
EuroIntervention. 2011 Jun;7(2):288-9.

65. Comparison of in vivo eccentricity and symmetry indices between metallic stents and bioresorbable vascular scaffolds: insights from the ABSORB and SPIRIT trials.
Brugaletta S, Gomez-Lara J, Diletti R, Farooq V, van Geuns RJ, de Bruyne B, Dudek D, Garcia-Garcia HM, Ormiston JA, Serruys PW.
Catheter Cardiovasc Interv. 2012 Feb 1;79(2):219-28.

66. Agreement and reproducibility of gray-scale intravascular ultrasound and optical coherence tomography for the analysis of the bioresorbable vascular scaffold.
Gómez-Lara J, Brugaletta S, Diletti R, Gogas BD, Farooq V, Onuma Y, Gobbens P, Van Es GA, García-García HM, Serruys PW.
Catheter Cardiovasc Interv. 2012 May 1;79(6):890-902.

67. Comparison between the first and second generation bioresorbable vascular scaffolds: a six month virtual histology study.
Brugaletta S, Garcia-Garcia HM, Diletti R, Gomez-Lara J, Garg S, Onuma Y, Shin ES, van Geuns RJ, de Bruyne B, Dudek D, Thuesen L, Chevalier B, McClean D, Windecker S, Whitbourn R, Dorange C, Veldhof S, Rapoza R, Sudhir K, Bruining N, Ormiston JA, Serruys PW.
EuroIntervention. 2011 Apr;6(9):1110-6.

68. Evaluation with in vivo optical coherence tomography and histology of the vascular effects of the everolimus-eluting bioresorbable vascular scaffold at two years following implantation in a healthy porcine coronary artery model: implications of pilot results for future pre-clinical studies.
Gogas BD, Radu M, Onuma Y, Perkins L, Powers JC, Gomez-Lara J, Farooq V, Garcia-Garcia HM, Diletti R, Rapoza R, Virmani R, Serruys PW.
Int J Cardiovasc Imaging. 2012 Mar;28(3):499-511.

69. Morphology of coronary artery lesions assessed by virtual histology intravascular ultrasound tissue characterization and fractional flow reserve.
Brugaletta S, Garcia-Garcia HM, Shen ZJ, Gomez-Lara J, Diletti R, Sarno G, Gonzalo N, Wijns W, de Bruyne B, Alfonso F, Serruys PW.
Int J Cardiovasc Imaging. 2012 Feb;28(2):221-8.

70. Comparison of plaque prolapse in consecutive patients treated with Xience V and Taxus Liberte stents.
Shen ZJ, Brugaletta S, Garcia-Garcia HM, Ligthart J, Gomez-Lara J, Diletti R, Sarno G, Witberg K, Serruys PW.
Int J Cardiovasc Imaging. 2012 Jan;28(1):23-31.

71. A comparative assessment by optical coherence tomography of the performance of the first and second generation of the everolimus-eluting bioresorbable vascular scaffolds.
Gomez-Lara J, Brugaletta S, Diletti R, Garg S, Onuma Y, Gogas BD, van Geuns RJ, Dorange C, Veldhof S, Rapoza R, Whitbourn R, Windecker S, Garcia-Garcia HM, Regar E, Serruys PW.
Eur Heart J. 2011 Feb;32(3):294-304

72. Temporal changes of coronary artery plaque located behind the struts of the everolimus eluting bioresorbable vascular scaffold.
Brugaletta S, Garcia-Garcia HM, Garg S, Gomez-Lara J, Diletti R, Onuma Y, van Geuns RJ, McClean D, Dudek D, Thuesen L, Chevalier B, Windecker S, Whitbourn R, Dorange C, Miquel-Hebert K, Sudhir K, Ormiston JA, Serruys PW.
Int J Cardiovasc Imaging. 2011 Jul;27(6):859-66.

PhD Portfolio

PhD Portfolio

PHD TRAINING

In-depth courses	Date	ECTS
NIHES Course "Introduction to Data-analysis"	2010	1.5
NIHES Course "Modern Statistical Methods"	2010	1.5

International Conferences & Simposia (0.3 ECTS points/day)	Date and Location	ECTS
Vulnerable plaque meeting	Cascais, 18-22 June 2011	1.2
EuroPCR 2011	Paris, 17-20 May 2011	1.2
EuroPCR 2012	Paris, 15-18 May 2012	1.2
EuroPCR 2013	Paris, 21-24 May 2013	1.2
EuroPCR 2014	Paris, 20-23 May 2013	1.2
EuroPCR 2015	Paris, 17-20 May 2013	1.2
TCT 2011	San Francisco, 7-11 November 2011	1.5
TCT 2012	Miami, 22-26 October 2012	1.5
Optics in Cardiology	Rotterdam 11-13 March 2015	0.9
ESC 2015	London, 29 Aug-02 Sept 2015	1.5
Bioresorbable Vascular Scaffold Course 2014	Boston, 25-26 July 2014	0.6
ACCA Congress	Geneva, 18-20 October 2014	0.9
PCR Focus Group 2012	Rotterdam, 08-09 March 2012	0.6
GISE 2010 - The Italian Society of Invasive Cardiology Congress	Genoa, 19-22 October 2010	1.2
GISE 2011 - The Italian Society of Invasive Cardiology Congress	Genoa, 11-14 October 2011	1.2
GISE 2012 - The Italian Society of Invasive Cardiology Congress	Genoa, 3-5 October 2012	0.9
GISE 2013 - The Italian Society of Invasive Cardiology Congress	Genoa, 9-11 October 2013	0.9
GISE 2015 - The Italian Society of Invasive Cardiology Congress	Genoa, 27-30 October 2015	1.2
SIC 2014 - The Italian Society of Cardiology Congress	Rome, 13-15 December 2014	0.9
SIC 2013 - The Italian Society of Cardiology Congress	Rome, 14-16 December 2013	0.9
SIC 2012 - The Italian Society of Cardiology Congress	Rome, 15-17 December 2012	0.9
SIC 2011 - The Italian Society of Cardiology Congress	Rome, 10-12 December 2011	0.9
BVS Meeting	Cordova, 20-21 April 2015	0.6
CTO Summit	Turin, 14-15 April 2015	0.6
Euro CTO Club	Istanbul, 18-19 September 2015	0.6
Chronic Total Occlusion Summit	New York, 23-24 February 2016	0.6
DRES 2015	Nijkerk, 11-12 June 2015	0.6
Taiwan Absorb Symposium	Taiwan, 5 July 2014	0.3

TEACHING ACTIVITIES

Lecturing	Date and Location	ECTS
Zorgacademie Bijscholing "PCI bifurcatie en hoofdstam"	Rotterdam, 16 April 2016l	0.3
Zorgacademie Bijscholing "Bio - absorbeerbare stents (BVS) en pericardvocht"	Rotterdam, 09 December 2014	0.3
Zorgacademie Bijscholing "DAPT"	Rotterdam, 24 April 2014	0.3
Zorgacademie Bijscholing	Rotterdam, 18 December 2013	0.3

Conference Presentations/Lectures	Date and Location	ECTS
EuroPCR 2011 (1 oral presentation)	Paris, 17-20 May 2011	0.6
EuroPCR 2012 (3 oral presentations)	Paris, 15-18 May 2012	1.8
EuroPCR 2013 (2 oral presentations)	Paris, 21-24 May 2013	1.2
EuroPCR 2014 (1 oral presentation)	Paris, 20-23 May 2013	0.6
EuroPCR 2015 (1 oral presentation)	Paris, 17-20 May 2013	0.6
TCT 2011 (1 oral presentation)	San Francisco, 7-11 November 2011	0.6
TCT 2012 (1 oral presentation)	Miami, 22-26 October 2012	0.6
Optics in Cardiology (1 oral presentation)	Rotterdam 11-13 March 2015	0.6
ESC 2015 (1 oral presentation)	London, 29 Aug-02 Sept 2015	0.6
Bioresorbable Vascular Scaffold Course 2014 (4 oral presentations)	Boston, 25-26 July 2014	2.4
PCR Focus Group 2012 (3 oral presentations)	Rotterdam, 08-09 March 2012	1.8
GISE 2010 - The Italian Society of Invasive Cardiology Congress (1 oral presentation)	Genoa, 19-22 October 2010	0.6
GISE 2011 - The Italian Society of Invasive Cardiology Congress (2 oral presentations)	Genoa, 11-14 October 2011	1.2
GISE 2012 - The Italian Society of Invasive Cardiology Congress (1 oral presentation)	Genoa, 3-5 October 2012	0.6
GISE 2013 - The Italian Society of Invasive Cardiology Congress (1 oral presentation)	Genoa, 9-11 October 2013	0.6
GISE 2015 - The Italian Society of Invasive Cardiology Congress (3 oral presentations)	Genoa, 27-30 October 2015	1.8
SIC 2014 - The Italian Society of Cardiology Congress (1 oral presentation)	Rome, 13-15 December 2014	0.6
SIC 2013 - The Italian Society of Cardiology Congress (1 oral presentation)	Rome, 14-16 December 2013	0.6
SIC 2012 - The Italian Society of Cardiology Congress (4 oral presentatios)	Rome, 15-17 December 2012	2.4
SIC 2011 - The Italian Society of Cardiology Congress (1 oral presentation)	Rome, 10-12 December 2011	0.6
BVS Meeting (1 oral presentation)	Cordova, 20-21 April 2015	0.6
CTO Summit (1 oral presentation)	Turin, 14-15 April 2015	0.6
DRES 2015 (1 oral presentation)	Nijkerk, 11-12 June 2015	0.6
Taiwan Absorb Symposium (4 oral presentations)	Taiwan, 5 July 2014	2.4